A.Yu. Ishlinskii

Mechanics
of Gyroscopic Systems

TRANSLATED FROM RUSSIAN

A. Yu. ISHLINSKII

MECHANICS OF

GYROSCOPIC SYSTEMS

(Mekhanika giroskopicheskikh sistem)

Translated from Russian

Translated by A. Barouch, M. Sc.
Edited by Dipl. -Ing. T. Pelz, M. Sc.

VIII/18

TABLE OF CONTENTS

FOREWORD

This book discusses a fairly wide range of problems in mechanics connected with the practical application of gyroscopes.

The classical studies of A.N. Krylov and B.V. Bulgakov on the theory of gyroscopes are insufficient for solving the problems encountered in the development of new gyroscopic systems. Stricter standards of accuracy have made it necessary to take into account factors formerly neglected and to explain previously undetected experimental facts. New problems in kinematics, the applied theory of elasticity, the theory of oscillations and stability, and the theory of gyroscopes proper have thus arisen.

The material of this book is naturally diverse.

The first chapter deals with the solution of the geometric problems of the kinematics of gimbal systems. Important, practical problems are discussed such as the errors caused by the application of simplified schemes or by the imperfect coordination of gimbal systems operating together, and the stabilization errors caused by inaccurate mounting of the instruments. Definitions are given of the pitch and roll angles of the ship and of its course as functions of the angles recorded by the gyroscopic instruments. The theory of small rotations of a rigid body is applied to the determination of the stabilization errors. A particular problem in the theory of finite rotations is treated in a simplified manner. The treatment given differs from that of A.N. Krylov, B.I. Kudrevich, and G.V. Chekhovich in that spherical trigonometry is not used. The problem of the so-called gimbal error is solved purely analytically.

The second chapter deals, likewise analytically, with the geometric problems connected with the accuracy of the orientation of objects having heel and trim, solves the problem of the orientation of the German V-2 missile in the case of alignment errors, makes general remarks on the methods of solving problems on finite rotations of rigid bodies, and ends by considering the motion of gyroscopic devices from the point of view of the mechanics of systems with nonholonomic constraints. This last leads to some interesting practical conclusions.

The third chapter illustrates the importance of making the components of gyroscopic systems and gimbals sufficiently rigid. Components which superficially seem extremely rigid suffer frequently excessive deformations when the tolerances in the manufacture of assemblies for high-accuracy gyroscopic systems are taken into account. The problems discussed are the displacement of the gyros' center of gravity due to rotor deformation by centrifugal forces, the deformation of gimbal rings and bows, the misalignment of housings during mounting, and the influence of the rigidity of the gimbals on the frequency of nutations. The theory of the discontinuous motion of kinematic transmissions caused by insufficient rigidity is developed. The

1

chapter ends with general considerations on the rigidity of shock absorbers (dampers) of gyroscopic and other instruments installed on moving objects, and on the advisability of damping in general.

The fourth chapter begins with an exposition of the methods for establishing the equations of gyroscopic systems. The method proposed here for deriving the equations of motion of the gyro from Euler's dynamic equations seems to be the simplest and most obvious method. Its simplicity is obtained by renouncing the use of Euler angles and his kinematic equations as unsuited for the theory of gyroscopes, and by adopting Krylov's angles.

This chapter deals mainly with the theory of certain characteristic gyroscopic devices whose behavior can be described by means of linear differential equations. A new theory is given of the gyrovertical with air suspension. Means for reducing the error of the instrument during rolling, and methods for compensating the influence of maneuvers and drift on the instrument are given.

A theory, similar in many respects to the preceding, is developed for gyroscopic systems consisting of two gyros: one with a vertical axis and constant speed of rotation, the second with a horizontal axis and a speed of rotation varying in proportion to the ship's linear speed. The theory of this last device takes into account Coulomb friction and the operation of the follow-up system.

The idea of separating the system of differential equations into two quasi-independent subsystems is carried out for a relatively simple gyroscopic device used for equalizing the heel of moving objects. Deriving the equations of motion of this device by the Lagrange method is too tedious. The application of the angular momentum theorem necessitates fairly precise calculations of the interplay of forces in the gyro gimbals. This method for the derivation of the equations is given in the text.

The chapter ends by giving the general theory of the double-gyro frame, which is the principal element of many gyroscopic devices.

The fifth chapter treats more thoroughly a number of problems mentioned in the preceding chapter, taking into account the nonlinear character of the forces acting on gyroscopic systems. As a result, new facts are exposed, both in the behavior of gyroscopic systems and in the assessment of the influence of many parameters on the accuracy and stability.

The development of the theory of heel equalizers leads to the study of a new kind of motion in the phase plane, the so-called sliding motion.

Two approximative methods of solution are given in this chapter: the energy method and the method of successive approximations.

The first method is applied to the study of the gyro frame stability, and also, in the course of its development, to the solution of many other problems of the oscillations of electromechanical systems. In particular the influence of certain parameters, not appearing explicitly in the stability condition derived in the preceding chapter (which was based on the linear theory), on the damping of the gyro frame oscillations is made clear.

The second method is applied to the study of forced oscillations of the gyro frame and to the calculation of the errors of a directional-gyro scheme.

The sixth and last chapter of the book deals with a number of separate problems arising during the study of the behavior of gyroscopic devices under laboratory conditions.

One of these is the problem of the wander of the gyrohorizon during rolling when the method of contact control by the corrective pendulum is applied. It is solved with the help of probability considerations.

The problem of the influence of yaw on gyrohorizon accuracy was solved in collaboration with V. I. Kuznetsov. Lack of knowledge of its solution has frequently led to erroneous conclusions, in spite of its simplicity and obviousness.

The problem of the top bow represents an interesting example of applying the general theorems of mechanics to explaining a phenomenon not easily understood.

In addition this chapter discusses several small problems whose solutions necessitate taking into account seemingly secondary facts, such as the vibrational rigidity of the gyro suspension and the accuracy of mounting the contact instruments.

The chapter ends with the study of a follow-up system having a relatively large amplifier time-constant. An approximative treatment of the problems along the lines of Chapter V shows clearly the change in the conditions of free-oscillations and leads to the establishment of simple stability conditions.

It should be added in conclusion that the formulation of most of the problems treated in the book is the result of the author's contact with the late outstanding Soviet engineer N. N. Ostryakov (1904 — 1946) and with his gifted pupils and collaborators.

*   *   *

Several new papers on the theory of gyroscopic systems have been published by the author since this book was written (the present monograph is a second slightly revised edition of the book which was first printed in 1952 in a limited issue). Three of them are given here as appendixes.

The first appendix develops methods for writing the equations of motion of complex gyroscopic systems by applying the angular momentum theorem to the gyroscopic system as a whole and to its components. This makes it possible to obtain these equations in the simplest manner. The usual method of obtaining these equations by applying the Euler-Lagrange method involves laborious calculations.

An essential feature of the method given is the introduction of the so-called basic reference frame (which has a translational motion) and the auxiliary reference frame. The first is used for calculating the inertia forces and the angular velocities, while the second serves for writing the equations themselves in the most convenient form.

The second appendix contains the exact theory of the spatial gyrocompass, proposed by Geckeler. The equations of motion of this instrument are considerably simplified by introducing as initial system of coordinates a moving Darboux trihedron on a stationary sphere enclosing the Earth. The accuracy of the results of the theory of the spatial gyrocompass is improved, and the differential equations of small oscillations of the sensitive elements are solved for an arbitrary motion of the compass on the Earth.

The author uses the method of introducing a moving trihedron and a non-revolving sphere in many papers, in particular in establishing the mathematical bases to the theory of inertial navigation. The third appendix deals with this case.

This appendix gives, apparently for the first time, the equations determining the position of an object moving arbitrarily on the Earth. Small oscillations of the stabilized platform of the device are investigated. Inertial navigation during the object's motion at varying altitudes above the Earth's surface is also studied.

GEOMETRY AND KINEMATICS OF
GYROSCOPIC SYSTEMS

§ 1. Geometry of gimbal suspension systems.
Determination of a ship's pitch and roll angles and its course.
Gimbal error. Bicardan suspensions

   Gimbal systems (Cardan suspensions) (Figure 1) are an integral part
of gyro assemblies and of many other instruments. They are used in par-
ticular to create an artificial horizontal platform on a rolling ship. To
that end, the inner gimbal ring is confined to the horizontal plane, either
directly by means of gyroscopes, or by using a forced tilting of the outer
gimbal ring relative to the ship's body and of the inner ring relative to the
outer one through angles specified by special gyroscopic devices.
   Consider simultaneously two gimbal systems whose inner rings are
stabilized in the horizontal plane. Let the axis of the outer gimbal ring of
the first system be parallel to the ship's longitudinal axis (Figure 1), and
the axis of the outer gimbal ring of the second system be parallel to the
ship's transversal axis (Figure 2) or, which is the same, perpendicular to
its plane of symmetry.
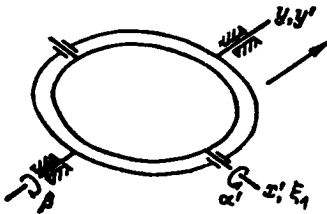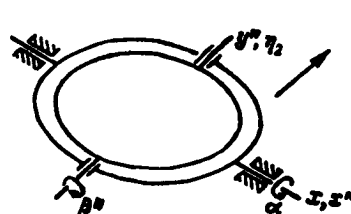
FIGURE 1   FIGURE 2

   The planes of the outer gimbal rings of the two systems usually form
some angle with the deck of the rolling ship. The angle of tilting of the outer
gimbal ring of the first system relative to the deck is called the ship's
a n g l e o f r o l l and is denoted by β. It is considered as positive when it
corresponds to a counterclockwise tilting of the gimbal ring relative to the
deck, as observed from the ship's bow (as is easily seen, this corresponds
to heel to port)*.

* In nautical language, the heel of the ship to starboard is called positive heel, and is frequently denoted
   by θ. The angles θ and β are obviously connected by the relationship $\theta = -\beta$.
      The heel is sometimes understood to mean not the angles of tilting of the outer gimbal ring relative
   to the deck, but the angle θ' which the ship's transversal axis forms with the horizontal plane. In this
   case $\text{tg } \theta' = -\text{tg } \beta \cos \alpha$, where α = the angle of pitch (cf. below). Neglecting the sign, the heel is then
   identical with the tilting angle β'' of the inner gimbal ring, relative to the outer one of the second system.

The angle of tilting of the outer gimbal ring of the second system relative to the deck is called the ship's a n g l e o f p i t c h and is denoted by α. It is considered as positive when it corresponds to a counterclockwise tilting of the gimbal ring relative to the deck, as observed from starboard (this corresponds to trim by the bow, or positive trim, in which case the stern is raised relative to the bow)*.

The ship's course will be defined later.

Five reference frames will be used: the xyz system fixed to the ship (the x-axis is directed to starboard parallel to the ship's transversal axis, the y-axis is directed to the bow parallel to the ship's longitudinal axis, and the z-axis is directed upward perpendicular to the deck); two systems $x'y'z'$ and $x''y''z''$ fixed to the outer gimbal rings of the first and second systems respectively; and two systems $\xi_1\eta_1\zeta_1$ and $\xi_2\eta_2\zeta_2$ fixed to the inner gimbal rings of the two systems. The axes of the last four systems are so oriented that all coincide for $\alpha = \beta = 0$ (i.e., when the deck plane xy is horizontal), except in the location of the origin of the xyz system.

The y'-axis of the $x'y'z'$ coordinate system fixed to the outer ring of the first gimbal system is parallel to the ship's longitudinal axis y (Figures 1 and 3). The ring itself is tilted through an angle β (roll angle) about the y'-axis.

The direction cosines of the $x'y'z'$ system relative to the xyz system are:

	x	y	z	
x'	$\cos\beta$	0	$-\sin\beta$	(1)
y'	0	1	0	
z'	$\sin\beta$	0	$\cos\beta$	

The x'-axis is simultaneously the ξ_1-axis of the $\xi_1\eta_1\zeta_1$ coordinate system fixed to the inner ring of the same gimbal system. The x'-axis (or, which is the same, the ξ_1-axis) is horizontal, since the inner gimbal ring is stabilized in the horizontal plane, and the $\xi_1\eta_1$ plane is therefore horizontal.

We denote by α' the tilting angle of the inner gimbal ring of the first system in relation to the outer ring (Figure 3). The tilting takes place about the ξ_1-axis (or, which is the same, about the x'-axis). It will be considered as positive $(\alpha' > 0)$ if the tilting is counterclockwise when observed from the positive direction of the axis $\xi_1 (x')$, that is from starboard. The direction cosines of the $\xi_1\eta_1\zeta_1$ system relative to the $x'y'z'$ system are:

	x'	y'	z'	
ξ_1	1	0	0	
η_1	0	$\cos\alpha'$	$\sin\alpha'$	(2)
ζ_1	0	$-\sin\alpha'$	$\cos\alpha'$	

The direction cosines of the $\xi_1\eta_1\zeta_1$ system relative to the xyz system can now be found. The following formula is obtained by using the well-known theorem of analytical geometry on the cosine of the angle between two straight lines in space:

$$\cos\xi_1 y = \cos\xi_1 x' \cos yx' + \cos\xi_1 y' \cos yy' + \cos\xi_1 z' \cos yz'.$$

---

* The term "trim" is sometimes also applied to the angle ψ which the ship's longitudinal axis makes with the horizontal plane. This angle coincides with the angle of tilting α' of the inner gimbal ring of the first system relative to the outer ring (Figure 1) and

$$\text{tg } \psi = \text{tg } \alpha \cos \beta.$$

.Analogous formulas are valid for the other angles. We finally obtain:

	x	y	z	
ξ_1	$\cos\beta$	0	$-\sin\beta$	
η_1	$\sin\alpha'\sin\beta$	$\cos\alpha'$	$\sin\alpha'\cos\beta$	(3)
ζ_1	$\cos\alpha'\sin\beta$	$-\sin\alpha'$	$\cos\alpha'\cos\beta$	

After a certain amount of practice, it is obviously easy to derive directly, by projecting on the axes x, y, and z unit lengths lying on the axes ξ_1, η_1, and ζ_1 (Figure 3).
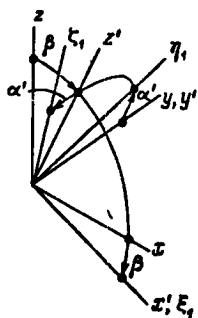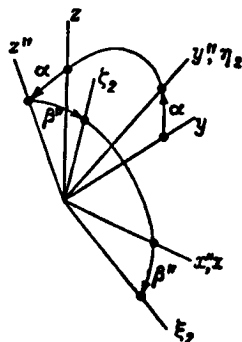
FIGURE 3   FIGURE 4

Consider now the second gimbal system. The x''-axis of the outer gimbal ring (Figures 2 and 4) is parallel to the ship's transversal axis, i.e., perpendicular to the ship's plane of symmetry. The ring itself is tilted through an angle α (pitch angle) about the x''-axis, the tilting being counterclockwise for $\alpha > 0$ [viewed from starboard].

The direction cosines of the $x''y''z''$ system relative to the xyz system are:

	x	y	z	
x''	1	0	0	
y''	0	$\cos\alpha$	$\sin\alpha$	(4)
z''	0	$-\sin\alpha$	$\cos\alpha$	

The inner gimbal ring is tilted relative to the outer ring about the η_2-axis or, which is the same, about the y''-axis (which coincides with the η_2-axis). We denote by β'' the tilting angle of the inner ring relative to the outer ring (Figure 4); this angle will be considered as positive when the inner ring is tilted counterclockwise when observed from the side of the positive η_2-axis (or, which is the same, of the positive y''-axis), that is, from the bow.

Since the inner ring is horizontally stabilized according to our assumptions, the $\xi_2\eta_2$ plane is horizontal, and therefore the y''-axis, which coincides with the η_2-axis, is also horizontal.

The direction cosines of the $\xi_2\eta_2\zeta_2$ system relative to the $x''y''z''$ system are:

	x''	y''	z''	
ξ_2	$\cos\beta''$	0	$-\sin\beta''$	
η_2	0	1	0	(5)
ζ_2	$\sin\beta''$	0	$\cos\beta''$	

7

The direction cosines of the $\xi_2\eta_2\zeta_2$ system relative to the *xyz* system can be found from (4) and (5):

	x	y	z
ξ_2	$\cos\beta''$	$\sin\alpha\sin\beta''$	$-\cos\alpha\sin\beta''$
η_2	0	$\cos\alpha$	$\sin\alpha$
ζ_2	$\sin\beta''$	$-\sin\alpha\cos\beta''$	$\cos\alpha\cos\beta''$

(6)

The $\xi_1\eta_1$ and $\xi_2\eta_2$ planes are horizontal according to our assumptions, and the axes ζ_1 and ζ_2 are therefore vertical. It follows that the axes ζ_1 and ζ_2 are parallel, and that their direction cosines relative to the *xyz* system are respectively equal. Three equations are therefore obtained from (3) and (6):

$$\cos\alpha'\sin\beta = \sin\beta'',$$
$$-\sin\alpha' = -\sin\alpha\cos\beta'', \qquad (7)$$
$$\cos\alpha'\cos\beta = \cos\alpha\cos\beta''.$$

Each of these equalities follows from the other two. The following two formulas are obtained by dividing both the second and first equations by the third:

$$\operatorname{tg}\alpha' = \operatorname{tg}\alpha\cos\beta, \qquad (8)$$
$$\operatorname{tg}\beta'' = \operatorname{tg}\beta\cos\alpha. \qquad (9)$$

These formulas are independent; they are important in the calculation and plotting of the tilting angles of the inner rings of the first and second gimbal systems relative to their outer rings.

It follows from these formulas that

$$\cos\alpha' = \frac{1}{\sqrt{1+\operatorname{tg}^2\alpha\cos^2\beta}} = \frac{\cos\alpha}{\sqrt{1-\sin^2\alpha\sin^2\beta}},$$
$$\sin\alpha' = \operatorname{tg}\alpha\cos\beta\,\frac{\cos\alpha}{\sqrt{1-\sin^2\alpha\sin^2\beta}} = \frac{\sin\alpha\cos\beta}{\sqrt{1-\sin^2\alpha\sin^2\beta}} \qquad (10)$$

and

$$\cos\beta'' = \frac{1}{R}\cos\beta,$$
$$\sin\beta'' = \frac{1}{R}\cos\alpha\sin\beta, \qquad (11)$$

where

$$R = \sqrt{1-\sin^2\alpha\sin^2\beta}. \qquad (12)$$

The value of the radical R is very near to unity for small values of the angles α and β. If, for instance, $\alpha = 7°$ and $\beta = 15°$, then

$$R = \sqrt{1-0.122^2\cdot 0.259^2} = 0.99950,$$

i.e., R differs from unity by only 0.0005.

Using formulas (10), (11), and (12), the trigonometric functions of the angles α' and β'' can be eliminated from (3) and (6), transforming them into:

	x	y	z
ξ_1	$\cos\beta$	0	$-\sin\beta$
η_1	$\frac{1}{R}\sin\alpha\cos\beta\sin\beta$	$\frac{1}{R}\cos\alpha$	$\frac{1}{R}\sin\alpha\cos^2\beta$
ζ_1	$\frac{1}{R}\cos\alpha\sin\beta$	$-\frac{1}{R}\sin\alpha\cos\beta$	$\frac{1}{R}\cos\alpha\cos\beta$

(13)

8

and

	x	y	z
ξ_2	$\dfrac{1}{R}\cos\beta$	$\dfrac{1}{R}\cos\alpha\sin\alpha\sin\beta$	$-\dfrac{1}{R}\cos^2\alpha\sin\beta$	
η_2	0	$\cos\alpha$	$\sin\alpha$	(14)
ζ_2	$\dfrac{1}{R}\cos\alpha\sin\beta$	$-\dfrac{1}{R}\sin\alpha\cos\beta$	$\dfrac{1}{R}\cos\alpha\cos\beta$	

Table (13) is most important.

It follows from (3) and (6) (or, which is the same, (13) and (14)) that when α and β differ from zero the coordinate systems $\xi_1\eta_1\zeta_1$ and $\xi_2\eta_2\zeta_2$ are differently oriented in relation to the ship, and therefore also in space. Since the axes ζ_1 and ζ_2 of these coordinate systems are parallel, this difference in the orientation reduces to a relative rotation of the parallel planes $\xi_1\eta_1$ and $\xi_2\eta_2$ in which the inner rings of the two gimbal systems lie. We denote this rotation by γ (Figure 5), and consider it as positive when the system $\xi_2\eta_2\zeta_2$ rotates counterclockwise relative to the system $\xi_1\eta_1\zeta_1$ when observed from the positive direction of the ζ_1-axis (or, which is the same, of the ζ_2-axis), i.e., from above.
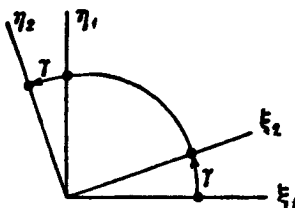
FIGURE 5

It is easily seen that

$$\sin\gamma = -\cos\xi_1\eta_2.$$

Also, since

$$\cos\xi_1\eta_2 = \cos\xi_1 x\,\cos\eta_2 x + \cos\xi_1 y\,\cos\eta_2 y + \cos\xi_1 z\,\cos\eta_2 z,$$

it follows from (3) and (6) (or, which is the same, from (13) and (14)) that the angle γ is given by

$$\sin\gamma = \sin\alpha\sin\beta. \qquad (15)$$

For small values of α and β this formula can be replaced by the approximation

$$\gamma = \alpha\beta. \qquad (16)$$

It follows from (15) that

$$\cos\gamma = \sqrt{1 - \sin^2\alpha\sin^2\beta} = R. \qquad (17)$$

It is thus seen that if the two gimbal systems are so mounted that the pivots of the outer ring of the first system are parallel to the ship's longitudinal axis while the pivots of the outer ring of the second system are perpendicular to the ship's plane of symmetry, and if the inner rings are then

9

stabilized by any method in the horizontal plane, the relative rotation of the inner rings during the ship's rolling will be determined by (15).

For a pitch angle $\alpha = 7°$ and a roll angle $\beta = 15°$ this formula yields:

$$\sin \gamma = 0.122 \cdot 0.259 = 0.0316, \quad \gamma = 1°48',$$

while the approximate formula (16) gives

$$\gamma = 0.122 \cdot 0.262 = 0.0320, \quad (1°50').$$

It is seen from this example that the angle γ may in many cases be very large. In order to avoid errors this fact should be taken into account when any azimuth direction is fixed relative to the inner gimbal rings.

Mount, for instance, on the stabilized inner ring of the first gimbal system a directional gyro oriented along the north-south line, and let the η_1-axis (the course line) form a certain angle $\varkappa$ with the directional gyro axle (the ship's course). Reproduce, by means of follow-up systems (servomechanisms), this angle in the second gimbal system as the angle between the η_2-axis and the horizontal optical axis of the sight mounted on this ring. The ship rolling will be accompanied by a movement of this optical axis in the horizontal plane. The axis will make an angle γ with the north-south line; the value of this angle is given by (15).

The fact that the stabilized rings of differently mounted gimbal systems rotate relative to each other was detected at the end of the thirties and received the name gimbal error (Chekhovich).

The problem of the gimbal error will later be examined more generally when the pivots of the outer gimbal rings of the two systems are not directed along the deck axes and form an arbitrary angle.

In order to avoid gimbal errors, the outer gimbal rings of the systems, which serve to stabilize the inner ring in the horizontal plane, are usually so disposed that their pivots are parallel to the ship's longitudinal axis (as was the case with the first of the above-considered two gimbal systems).

The η_1-axis, fixed to the inner ring of this gimbal system, is called the ship's c o u r s e l i n e. This axis is parallel to the projection of the ship's longitudinal axis on the horizontal plane; in the case of zero pitch angle α, it is parallel to the ship's longitudinal axis. The angle between the north direction and the ship's course line is called the s h i p ' s c o u r s e and is denoted by $\varkappa$ (Figure 6). An increase of the angle $\varkappa$ corresponds to a veering of the ship to starboard (a clockwise rotation when observed from above)*. The angle $\varkappa$ is measured and indicated on the repeaters of the ship's gyrocompasses.

The system of angles $\alpha, \beta, \varkappa$ defines uniquely, for a given ship location, the orientation of the ship as a rigid body in its rotational motion relative to the Earth.

Gyroscopic instruments such as the gyroazimuthhorizon measure and reproduce by means of follow-up systems (servo loops) all three angles $\alpha, \beta, \varkappa$, with the one exception that the angle $\varkappa$ is measured from some

---

* The ship's course has also been differently defined, e.g., as the angle between the north direction of the line formed by the intersection of the horizontal plane and the ship's plane of symmetry. It is easily seen that this last angle coincides with the angle between the north direction and the η_2-axis fixed to the inner ring of the second gimbal system (the pivots of whose outer ring are perpendicular to the ship's plane of symmetry), and therefore differs from the course definition given in the text by the value of the gimbal error γ.

10

gyro-determined direction in the horizontal plane, and not from the north-south line. Instruments such as the gyrovertical, also used in practice, only measure and reproduce the angles α and β.

The gimbal assemblies of instruments such as the gyroazimuthhorizon (without gyroazimuth) and the gyrovertical represent in many cases a combination of two simple gimbal systems: the ordinary gimbal system, with the outer ring directed, as a rule, parallel to the ship's longitudinal axis, and a gimbal system of different design (Figure 7), in which a carriage K slides along a bow B, and rod C, rigidly connected with the inner ring of the basic gimbal system, is inserted into the bearing P of the carriage. The bow B, whose pivots are perpendicular to the pivots of the basic gimbal system's outer ring, replaces the outer ring of the second gimbal system, while the carriage K replaces its inner ring. The need for the bearing P thus becomes clear, since during the ship's rolling the carriage K and the basic gimbal system's ring will rotate relative to each other through an angle equal to the gimbal error.
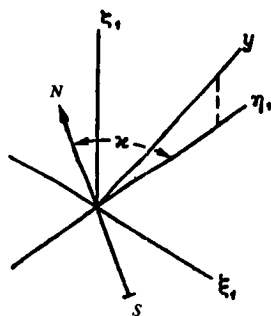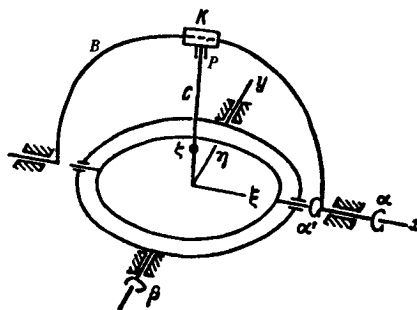
FIGURE 6   FIGURE 7

Similar gimbal systems* are met, in various design variants, in most control instruments (gyroverticals, coordinate transformers, etc.); they are called b i c a r d a n s u s p e n s i o n s.

The bow pivot axis (Figure 7) will be denoted by x, and the pivot axis of the outer gimbal ring of the basic system by y. The coordinate system xyz is therefore fixed to the instrument housing. The pivot axis of the inner gimbal ring of the basic system will be denoted by ξ, and the axis perpendicular to it and lying in the plane of the inner ring by η. The coordinate system $\xi\eta\zeta$ is thus fixed to the inner gimbal ring of the basic system. The position of the bow and the outer gimbal ring at which the planes $\xi\eta$ and xy coincide will be called the initial position. The counterclockwise tilting of the bow (when observed from the positive direction of the x-axis) will be defined as positive and denoted by α. The counterclockwise tilting of the outer gimbal ring (when observed from the positive direction of the y-axis) will be defined as positive and denoted by β.

If the bicardan suspension housing is so disposed that the xy plane is parallel to the deck plane and the y-axis parallel to the ship's longitudinal axis, it follows that if the $\xi\eta$ plane is stabilized in the horizontal plane the angle α

_____
* Some other types of gimbal systems will be described in § 4 of this chapter.

11

represents the ship's pitch angle, and the angle β the ship's roll angle, in the sense in which these angles were defined above (pp. 5 and 6).

In this case the η-axis represents the ship's course line; the angle $\varkappa$ between the η-axis and the north-south line is by definition the ship's course (cf. p.10).

If for $\alpha = \beta = 0$, the ship's direction points north, then $\varkappa = 0$; if it points east, then $\varkappa = 90°$.

It follows from the above that the direction cosines of the system $\xi\eta\zeta$, fixed to the inner gimbal ring, relative to the system xyz fixed to the housing are given in Table (13), which gives the direction cosines of the system $\xi_1\eta_1\zeta_1$ fixed to the inner gimbal ring relative to the system xyz fixed to the ship (in that case the y-axis is the pivot axis of the outer gimbal ring — cf. Figure 1).

Since this table is of great importance for many subsequent studies, it is repeated here:

	x	y	z	
ξ	$\cos\beta$	0	$-\sin\beta$	
η	$\frac{1}{R}\sin\alpha\cos\beta\sin\beta$	$\frac{1}{R}\cos\alpha$	$\frac{1}{R}\sin\alpha\cos^2\beta$	(18)
ζ	$\frac{1}{R}\cos\alpha\sin\beta$	$-\frac{1}{R}\sin\alpha\cos\beta$	$\frac{1}{R}\cos\alpha\cos\beta$	

Another table which will be helpful later on is

	x	y	z	
ξ	$\cos\beta$	0	$-\sin\beta$	
η	$\sin\alpha'\sin\beta$	$\cos\alpha'$	$\sin\alpha'\cos\beta$	(19)
ζ	$\cos\alpha'\sin\beta$	$-\sin\alpha'$	$\cos\alpha'\cos\beta$	

In this table, which is in fact Table (3), α' denotes the tilting of the inner gimbal ring of the bicardan suspension relative to the outer ring (Figure 7); it is considered as positive if the inner ring is tilted counterclockwise when observed from the positive direction of the ξ-axis.

Note that the orientation of the outer gimbal-ring pivot axis (whether parallel to the ship's longitudinal axis or perpendicular to its plane of symmetry), is unimportant for a gyrovertical without gyroazimuth. In fact, α and β, the angles of tilting of the bow and of the outer ring are symmetrical in the expressions given in Table (18) for the direction cosines of the ζ-axis relative to the x, y, z system.

Accordingly, if any instrument is stabilized in the horizontal plane by means of a synchronous link with a gyrovertical and is suspended in a bicardan suspension similar to that of the gyrovertical, then the mutual disposition of the bows of these suspensions, whether parallel or perpendicular to each other, is immaterial.

§ 2. Relative rotation of two stabilized systems
during ship's rolling

It was shown in the preceding section that if two gimbal systems are mounted on a rolling ship in such a way that the pivots of their outer rings

. . are parallel to the deck and perpendicular to each other, while the planes of the inner rings are stabilized in the horizontal plane, then during the ship's rolling the inner rings will rotate relative to each other through an angle determined exactly by (15) and approximately by (16).

This section deals with the more general case when the pivots of the outer rings form an arbitrary angle φ; the problem is solved with an accuracy sufficient for technical needs.

It will be assumed that two bicardan suspensions of the type shown in Figure 7 are mounted on the ship. The pivots of their outer gimbal rings and of the bows are parallel to the deck, their direction in the deck plane being arbitrary (it is of course also possible to dispose them parallel to any other plane fixed in the ship, such as the plane of the ship's frames).

We denote (in accordance with Figure 7) by x_1, y_1, z_1 the axes of the coordinate system fixed to the housing of the first bicardan suspension, by x_2, y_2, z_2 the axes of the coordinate system fixed to the housing of the second bicardan suspension ($x_{1,2}$ denotes the bow pivot axis, $y_{1,2}$ the outer gimbal-ring pivot axis), and by ξ_1, η_1, ζ_1 the axes of the coordinate system fixed to the inner gimbal ring of the first bicardan suspension; the axes ξ_1, η_1, ζ_1 coincide respectively with the axes x_1, y_1, z_1 when the plane of the inner ring is parallel to the deck plane (or, which is the same, to the $x_1 y_1$ plane).

We denote by α_1 and β_1 the angles of tilting of the first bicardan suspension bow and outer gimbal ring from their mid-positions. The bow plane passes in its mid-position through the z_1-axis, while the plane of the outer ring is in its mid-position perpendicular to this axis, i.e., it passes through the x_1-axis. The angle α_1 will be taken as positive when the bow is tilted counterclockwise when observed from the positive direction of the x_1-axis; the angle β_1 will be taken as positive when the outer ring is tilted counterclockwise when observed from the positive direction of the y_1-axis.

The direction cosines of the system $\xi_1 \eta_1 \zeta_1$ relative to the system $x_1 y_1 z_1$ can be found from Table (18) by suitably changing the notation:

	x_1	y_1	z_1
ξ_1	$\cos \beta_1$	0	$-\sin \beta_1$
η_1	$\dfrac{1}{R_1} \sin \alpha_1 \cos \beta_1 \sin \beta_1$	$\dfrac{1}{R_1} \cos \alpha_1$	$\dfrac{1}{R_1} \sin \alpha_1 \cos^2 \beta_1$
ζ_1	$\dfrac{1}{R_1} \cos \alpha_1 \sin \beta_1$	$-\dfrac{1}{R_1} \sin \alpha_1 \cos \beta_1$	$\dfrac{1}{R_1} \cos \alpha_1 \cos \beta_1$

$$\text{(20)}$$

where

$$R_1 = \sqrt{1 - \sin^2 \alpha_1 \sin^2 \beta_1}.$$

An analogous notation will be used for the second bicardan suspension: $x_2 y_2 z_2$ for the coordinate system fixed to its housing, $\xi_2 \eta_2 \zeta_2$ for the coordinate system fixed to its inner gimbal ring, and α_2 and β_2 for the angles of tilting of its bow and outer gimbal ring. The following table is then obtained by analogy with (20) for the direction cosines of the system $\xi_2 \eta_2 \zeta_2$ relative to the system $x_2 y_2 z_2$:

	x_2	y_2	z_2
ξ_2	$\cos \beta_2$	0	$-\sin \beta_2$
η_2	$\dfrac{1}{R_2} \sin \alpha_2 \cos \beta_2 \sin \beta_2$	$\dfrac{1}{R_2} \cos \alpha_2$	$\dfrac{1}{R_2} \sin \alpha_2 \cos^2 \beta_2$
ζ_2	$\dfrac{1}{R_2} \cos \alpha_2 \sin \beta_2$	$-\dfrac{1}{R_2} \sin \alpha_2 \cos \beta_2$	$\dfrac{1}{R_2} \cos \alpha_2 \cos \beta_2$

$$\text{(21)}$$

13

where

$$R_2 = \sqrt{1 - \sin^2\alpha_2 \sin^2\beta_2}.$$

The $x_1 y_1$ and $x_2 y_2$ planes are parallel in accordance with the above, and the angle between the axes x_1 and x_2 (or, which is the same, between the axes y_1 and y_2) is equal to some given value φ (Figure 8). The direction cosines of the system $x_2 y_2 z_2$ relative to the system $x_1 y_1 z_1$ are therefore:

	x_1	y_1	z_1	
x_2	$\cos\varphi$	$\sin\varphi$	0	
y_2	$-\sin\varphi$	$\cos\varphi$	0	(22)
z_2	0	0	1	

According to the conditions of the problem the planes of the inner gimbal rings of the two suspensions are also parallel. We denote by χ the unknown angle between the axes ξ_1 and ξ_2 (Figure 9).
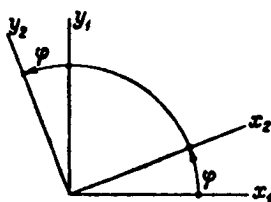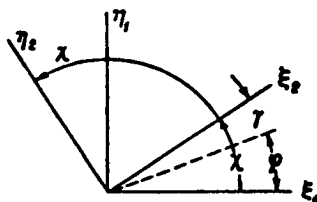

FIGURE 8   FIGURE 9

The direction cosines of the system $\xi_2\eta_2\zeta_2$ relative to the system $\xi_1\eta_1\zeta_1$ are analogous to those given in (22):

	ξ_1	η_1	ζ_1	
ξ_2	$\cos\chi$	$\sin\chi$	0	
η_2	$-\sin\chi$	$\cos\chi$	0	(23)
ζ_2	0	0	1	

Obviously, if $\alpha_1 = \beta_1 = 0$, then $\chi = \varphi$ and $\alpha_2 = \beta_2 = 0$, since in this case the coordinate system $x_1 y_1 z_1$ and $\xi_1\eta_1\zeta_1$, and also $x_2 y_2 z_2$ and $\xi_2\eta_2\zeta_2$, are respectively parallel.

If the angles α_1 and β_1 are different from zero, the angle χ will not be equal to φ, and their difference, $\gamma = \chi - \varphi$, will represent the magnitude of the rotation of the inner gimbal ring of the second suspension relative to its housing.

An analytical expression has now to be found for γ as a function of the angles α_1, β_1, φ. Such an expression can then if required be easily transformed into a function of the angles α_2, β_2, φ, since the angles α_1 and β_1 can be defined as functions of the variables α_2, β_2, and φ.

In order to solve this problem, the direction cosines of the system $x_2 y_2 z_2$ relative to the system $\xi_1\eta_1\zeta_1$ will be determined in two different ways, based respectively on Tables (20) and (22), and (21) and (23).

The first gives

$$\cos y_2\eta_1 = \cos y_2 x_1 \cos \eta_1 x_1 + \cos y_2 y_1 \cos \eta_1 y_1 + \cos y_2 z_1 \cos \eta_1 z_1 =$$
$$= -\frac{1}{R_1} \sin\alpha_1 \cos\beta_1 \sin\beta_1 \sin\varphi + \frac{1}{R_1} \cos\alpha_1 \cos\varphi,$$

14

· the second

$$\cos y_2\eta_1 = \cos y_2\xi_2 \cos \eta_1\xi_2 + \cos y_2\eta_2 \cos \eta_1\eta_2 + \cos y_2\zeta_2 \cos \eta_1\zeta_2 =$$
$$= \frac{1}{R_2} \cos \alpha_2 \cos \chi.$$

The required direction cosines are obtained in the following two forms:

	ξ_1	η_1	ζ_1
x_2	$\cos \beta_1 \cos \varphi$	$\frac{1}{R_1} \sin \alpha_1 \cos \beta_1 \sin \beta_1 \cos \varphi + $	$\frac{1}{R_1} \cos \alpha_1 \sin \beta_1 \cos \varphi - $
		$+ \frac{1}{R_1} \cos \alpha_1 \sin \varphi$	$- \frac{1}{R_1} \sin \alpha_1 \cos \beta_1 \sin \varphi$
y_2	$-\cos \beta_1 \sin \varphi$	$- \frac{1}{R_1} \sin \alpha_1 \cos \beta_1 \sin \beta_1 \sin \varphi + $	$- \frac{1}{R_1} \cos \alpha_1 \sin \beta_1 \sin \varphi - $
		$+ \frac{1}{R_1} \cos \alpha_1 \cos \varphi$	$- \frac{1}{R_1} \sin \alpha_1 \cos \beta_1 \cos \varphi$
z_2	$-\sin \beta_1$	$\frac{1}{R_1} \sin \alpha_1 \cos^2 \beta_1$	$\frac{1}{R_1} \cos \alpha_1 \cos \beta_1$

(24)

and

	ξ_1	η_1	ζ_1
x_2	$\cos \beta_2 \cos \chi - $	$\cos \beta_2 \sin \chi + $	$\frac{1}{R_2} \cos \alpha_2 \sin \beta_2$
	$- \frac{1}{R_2} \sin \alpha_2 \cos \beta_2 \sin \beta_2 \sin \chi$	$+ \frac{1}{R_2} \sin \alpha_2 \cos \beta_2 \sin \beta_2 \cos \chi$	
y_2	$- \frac{1}{R_2} \cos \alpha_2 \sin \chi$	$\frac{1}{R_2} \cos \alpha_2 \cos \chi$	$- \frac{1}{R_2} \sin \alpha_2 \cos \beta_2$
z_2	$- \sin \beta_2 \cos \chi - $	$- \sin \beta_2 \sin \chi + $	
	$- \frac{1}{R_2} \sin \alpha_2 \cos^2 \beta_2 \sin \chi$	$+ \frac{1}{R_2} \sin \alpha_2 \cos^2 \beta_2 \cos \chi$	$\frac{1}{R_2} \cos \alpha_2 \cos \beta_2$

(25)

where
$$R_1 = \sqrt{1 - \sin^2\alpha_1 \sin^2\beta_1} \quad \text{and} \quad R_2 = \sqrt{1 - \sin^2\alpha_2 \sin^2\beta_2}.$$

The following three equations are obtained by equating the expressions for the direction cosines of the ζ_1-axis relative to the system $x_2 y_2 z_2$ in (24) and (25):

$$\frac{1}{R_1} \cos \alpha_1 \sin \beta_1 \cos \varphi - \frac{1}{R_1} \sin \alpha_1 \cos \beta_1 \sin \varphi = \frac{1}{R_2} \cos \alpha_2 \sin \beta_2;$$

$$-\frac{1}{R_1} \cos \alpha_1 \sin \beta_1 \sin \varphi - \frac{1}{R_1} \sin \alpha_1 \cos \beta_1 \cos \varphi = -\frac{1}{R_2} \sin \alpha_2 \cos \beta_2; \quad (26)$$

$$\frac{1}{R_1} \cos \alpha_1 \cos \beta_1 = \frac{1}{R_2} \cos \alpha_2 \cos \beta_2.$$

Each of these equalities follows from the other two.

Assume that the angles α_1 and β_1 (and therefore also the angles α_2 and β_2) are first-order infinitesimals, and neglect all terms of higher order than the second; it then follows that the radicals R_1 and R_2 can be replaced by unity, since they differ from it only by fourth-order infinitesimals.

The first two equations of (26) can now be replaced by the following approximate formulas:

$$\beta_2 = -\alpha_1 \sin \varphi + \beta_1 \cos \varphi;$$
$$\alpha_2 = \alpha_1 \cos \varphi + \beta_1 \sin \varphi,$$

(27)

which will be accurate up to and including second-order infinitesimals.

The following equation is obtained by equating the cosines of the angle between the axes y_2 and ξ_1 in Tables (24) and (25):

$$-\cos \beta_1 \sin \varphi = -\frac{1}{R_2} \cos \alpha_2 \sin \chi.$$

(28)

The ratio of the cosines in this expression can be expanded in series and equals, in a second-order approximation.

$$\frac{\cos \beta_1}{\cos \alpha_2} = \frac{1 - \frac{1}{2}\beta_1^2}{1 - \frac{1}{2}\alpha_2^2} = 1 - \frac{1}{2}\beta_1^2 + \frac{1}{2}\alpha_2^2.$$

Using this expression, formula (28) reduces to the approximate equation:

$$\sin \chi = \left(1 - \frac{1}{2}\beta_1^2 + \frac{1}{2}\alpha_2^2\right) \sin \varphi.$$

(29)

It is seen from (29) that the angle χ differs from the angle φ by second-order infinitesimals only. Since $\gamma = \chi - \varphi$, the following approximate expression can be written:

$$\sin \chi = \sin (\varphi + \gamma) = \sin \varphi + \gamma \cos \varphi.$$

(30)

This expression is accurate up to second-order terms in $\alpha_1, \beta_1, \alpha_2,$ and β_2.

The following relationship is obtained by equating (29) and (30):

$$\gamma \cos \varphi = \frac{\alpha_2^2 - \beta_1^2}{2} \sin \varphi.$$

Inserting the second of equations (27) gives, after obvious simplifications.

$$\gamma = \frac{1}{4}(\alpha_1^2 - \beta_1^2) \sin 2\varphi + \alpha_1\beta_1 \sin^2 \varphi.$$

(31)

This last formula gives the solution to our problem.

For instance, let $\alpha_1 = -7°$, $\beta_1 = 15°$, $\varphi = 45°$. Then

$$\gamma = -\frac{1}{4}(0.262^2 - 0.122^2) - 0.262 \cdot 0.122 \cdot \frac{1}{2} = -0.0294.$$

This is a setting of the suspensions which was once popular.

For $\varphi = \frac{\pi}{2}$, i.e., when the axes of the outer gimbal rings of the two bicardan suspensions form a right angle, (31) reduces to

$$\gamma = \alpha_1\beta_1.$$

This formula coincides, as was to be expected, with the gimbal-error formula (16).

16

§ 3. Stabilization errors caused by inaccurate mounting of the gimbal systems (geometry of two bicardan suspensions)

The combined working of several stabilized devices on the same ship can be accompanied by errors due to additional rotations of the stabilized elements. Such rotations are caused by the absence of strict parallelism between the principal axes of the gimbal systems, by nonidentical kinematics of the gimbal systems, and by inaccurate stabilization in the horizontal plane.

The influence on the combined working of two bicardan suspensions of nonparallelism between the pivot axes of the outer gimbal rings or of the bows, will be examined in this section. The influence of the other factors mentioned above (nonidentical kinematics of the suspensions and inaccurate stabilization in the horizontal plane) will be treated in §§ 4 and 5 of this chapter.

Let two bicardan suspensions be mounted on the ship (Figure 7), and let their inner gimbal rings be accurately stabilized in the horizontal plane. Due to inaccuracies in the mounting of the suspensions housings, the pivot axes of their respective outer gimbal rings and bows will form small angles (since the housing of one suspension is rotated through a small angle in relation to the housing of the other suspension).

We will use the same notation as in the preceding section. The coordinate systems $x_1 y_1 z_1$ and $\xi_1 \eta_1 \zeta_1$ will be considered as fixed to the housing and to the inner gimbal ring of the first bicardan suspension respectively, while the systems $x_2 y_2 z_2$ and $\xi_2 \eta_2 \zeta_2$ will be fixed to the housing and the inner gimbal ring of the second suspension respectively. The letters α_1 and β_1 will respectively denote the angles of tilting of the outer gimbal ring and of the bow of the first suspension, the letters α_2 and β_2 the corresponding angles for the second suspension. The angles α_1 and α_2, and likewise the angles β_1 and β_2, are not equal because of the nonparallelism of the axes of the coordinate systems $x_1 y_1 z_1$ and $x_2 y_2 z_2$ (due to the inaccurate mounting of the suspensions housings).
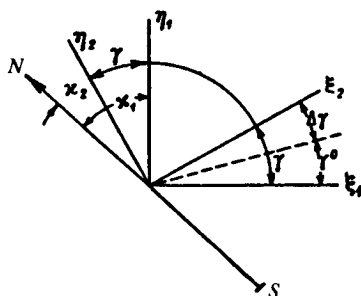
FIGURE 10

The angles $\varkappa_1$ and $\varkappa_2$, formed respectively by the axes η_1 and η_2 with the north-south line (or with any other fixed direction in the horizontal plane), are likewise not equal (Figure 10). In particular, the difference

$$\gamma = \varkappa_1 - \varkappa_2,$$ (32)

representing the angle between the axes η_1 and η_2 (or between the axes ξ_1 and ξ_2), is not zero.

Let α^0, β^0, γ^0 be the values of the angles α_2, β_2, γ for $\alpha_1 = \beta_1 = 0$ (i.e., when the $x_1 y_1$ plane coincides with the horizontal plane, or which is the same, with the $\xi_1 \eta_1$ and $\xi_2 \eta_2$ planes). We denote by α_2^*, β_2^*, $\varkappa_2^*$ the values obtained by subtracting respectively α^0, β^0, γ^0 from α_2, β_2, $\varkappa_2$.

If α_1, β_1, $\varkappa_1$ denote respectively the pitch angle, the roll angle, and the ship's course, then α_2^*, β_2^*, $\varkappa_2^*$ denote the same angles as measured on the second bicardan suspension after the so-called coordination of the latter's scales with those of the first suspension.

If the pitch and roll angles, α_1 and β_1, differ from zero, the angles α_2^*, β_2^*, $\varkappa_2^*$ will differ from the angles α_1, β_1, $\varkappa_1$ by the small magnitude $\Delta\alpha$, $\Delta\beta$, $\Delta\gamma$.

$$\alpha_2 = \alpha_2^* + \alpha^0 = \alpha_1 + \Delta\alpha + \alpha^0,$$
$$\beta_2 = \beta_2^* + \beta^0 = \beta_1 + \Delta\beta + \beta^0, \qquad (33)$$
$$\varkappa_2 = \varkappa_2^* + \gamma^0 = \varkappa_1 + \Delta\gamma + \gamma^0.$$

The stabilization errors $\Delta\alpha$, $\Delta\beta$, $\Delta\gamma$ become zero when $\alpha_1 = \beta_1 = 0$ independently of the value of α^0, β^0, γ^0; they also become zero when $\alpha^0 = \beta^0 = \gamma^0 = 0$ independently of the value of α_1 and β_1 (this corresponds to the case when the axes of the coordinate systems $x_1 y_1 z_1$ and $x_2 y_2 z_2$ fixed to the housings of the bicardan suspensions are perfectly in parallel).

It follows that the first nonzero terms in the expansions of $\Delta\alpha$, $\Delta\beta$, $\Delta\gamma$ in series as functions of the variables α_1, β_1, α^0, β^0, γ^0 must contain products of the variables α_1 and β_1 by α^0, β^0, and γ^0 (in other words, the expansions contain no free terms). If the angles α_1 and β_1 lie within the usual limits (much smaller than 90°), $\Delta\alpha$, $\Delta\beta$, and $\Delta\gamma$, can be considered as of the same order of magnitude as α^0, β^0, γ^0 or less.
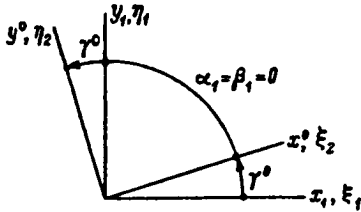
The squares and products of the angles α^0, β^0, γ^0, and also of $\Delta\alpha$, $\Delta\beta$, $\Delta\gamma$, will accordingly be neglected in comparison with first-order magnitudes. The expressions containing the angles α_1 and β_1 will be expanded up to and including second-order terms (squares and products of α_1 and β_1).

FIGURE 11

We must now obtain analytical expressions for the errors $\Delta\alpha$, $\Delta\beta$, $\Delta\varkappa$ as functions of the pitch and roll angles α_1, β_1, and the coordination-error angles α^0, β^0, γ^0, in order to form an idea on the accuracy with which the housing of one of the instruments must be mounted in relation to the other.

We now introduce a new coordinate system $x^0 y^0 z^0$ fixed to the second bicardan-suspension housing and directed so that its axes coincide respectively with those of the coordinate system $\xi_2 \eta_2 \zeta_2$, fixed to the inner gimbal ring, if the outer gimbal ring is tilted through an angle β^0 and the hoop through an angle α^0 from their mid-positions.

When $\alpha_1 = \beta_1 = 0$ (Figure 11), the axes of the coordinate system $\xi_1 \eta_1 \zeta_1$ coincide with those of the coordinate system $x_1 y_1 z_1$, and the axes of the coordinate system $\xi_2 \eta_2 \zeta_2$ coincide with those of the coordinate system $x^0 y^0 z^0$ (in accordance with the definition of the latter). The $\xi_1 \eta_1$ and $\xi_2 \eta_2$ planes are both horizontal and thus parallel; it follows that the $x_1 y_1$ and $x^0 y^0$ planes are also parallel. The angle between the ξ_1- and ξ_2-axes is equal to γ^0 for $\alpha_1 = \beta_1 = 0$; it follows that the angle between the x_1- and x^0-axes is likewise

18

equal to γ^0 (Figure 11). The direction cosines of the system $x^0y^0z^0$ relative to the system $x_1y_1z_1$ are therefore:

$$
\begin{array}{cccc}
 & x_1 & y_1 & z_1 \\
x^0 & \cos\gamma^0 & \sin\gamma^0 & 0 \\
y^0 & -\sin\gamma^0 & \cos\gamma^0 & 0 \\
z^0 & 0 & 0 & 1
\end{array}
\tag{34}
$$

In view of the smallness of the angle γ^0, (34) can also be written in the form:

$$
\begin{array}{cccc}
 & x_1 & y_1 & z_1 \\
x^0 & 1 & \gamma^0 & 0 \\
y^0 & -\gamma^0 & 1 & 0 \\
z^0 & 0 & 0 & 1
\end{array}
\tag{35}
$$

in which terms of higher order than the first have been neglected in the expansions of $\cos\gamma^0$ and $\sin\gamma^0$.

The direction cosines of the system $\xi_1\eta_1\zeta_1$ relative to the system $x_1y_1z_1$ are identical with those in Table (20) of the preceding section:

$$
\begin{array}{cccc}
 & x_1 & y_1 & z_1 \\
\xi_1 & \cos\beta_1 & 0 & -\sin\beta_1 \\
\eta_1 & \dfrac{1}{R_1}\sin\alpha_1\cos\beta_1\sin\beta_1 & \dfrac{1}{R_1}\cos\alpha_1 & \dfrac{1}{R_1}\sin\alpha_1\cos^2\beta_1 \\
\zeta_1 & \dfrac{1}{R_1}\cos\alpha_1\sin\beta_1 & -\dfrac{1}{R_1}\sin\alpha_1\cos\beta_1 & \dfrac{1}{R_1}\cos\alpha_1\cos\beta_1
\end{array}
$$

where
$$R_1 = \sqrt{1 - \sin^2\alpha_1\sin^2\beta_1}.$$

The direction cosines of the system $x^0y^0z^0$ relative to the system $\xi_1\eta_1\zeta_1$ are obtained from (20) and (35):

$$
\begin{array}{cccc}
 & \xi_1 & \eta_1 & \zeta_1 \\
x^0 & \cos\beta_1 & \dfrac{1}{R_1}\sin\alpha_1\cos\beta_1\sin\beta_1 + \gamma^0\dfrac{1}{R_1}\cos\alpha_1 & \dfrac{1}{R_1}\cos\alpha_1\sin\beta_1 - \gamma^0\dfrac{1}{R_1}\sin\alpha_1\cos\beta_1 \\
y^0 & -\gamma^0\cos\beta_1 & -\gamma^0\dfrac{1}{R_1}\sin\alpha_1\cos\beta_1\sin\beta_1 + \dfrac{1}{R_1}\cos\alpha_1 & -\gamma^0\dfrac{1}{R_1}\cos\alpha_1\sin\beta_1 - \dfrac{1}{R_1}\sin\alpha_1\cos\beta_1 \\
z^0 & -\sin\beta_1 & \dfrac{1}{R_1}\sin\alpha_1\cos^2\beta_1 & \dfrac{1}{R_1}\cos\alpha_1\cos\beta_1
\end{array}
\tag{36}
$$

We find now the direction cosines of the system $x^0y^0z^0$ relative to the system $x_2y_2z_2$. From Table (21) of the preceding section:

$$
\begin{array}{cccc}
 & x_2 & y_2 & z_2 \\
\xi_2 & \cos\beta_2 & 0 & -\sin\beta_2 \\
\eta_2 & \dfrac{1}{R_2}\sin\alpha_2\cos\beta_2\sin\beta_2 & \dfrac{1}{R_2}\cos\alpha_2 & \dfrac{1}{R_2}\sin\alpha_2\cos^2\beta_2 \\
\zeta_2 & \dfrac{1}{R_2}\cos\alpha_2\sin\beta_2 & -\dfrac{1}{R_2}\sin\alpha_2\cos\beta_2 & \dfrac{1}{R_2}\cos\alpha_2\cos\beta_2
\end{array}
$$

where

$$R_2 = \sqrt{1 - \sin^2 \alpha_2 \sin^2 \beta_2}.$$

Since the coordinate systems $x^0 y^0 z^0$ and $\xi_2 \eta_2 \zeta_2$ coincide when $\alpha_2 = \alpha^0$ and $\beta_2 = \beta^0$, the direction cosines of the system $x^0 y^0 z^0$ relative to the system $x_2 y_2 z_2$ are obtained from Table (21) by replacing α_2 and β_2 by α^0 and β^0 respectively:

	x_2	y_2	z_2	
x^0	$\cos \beta^0$	0	$-\sin \beta^0$	
y^0	$\dfrac{1}{R^0} \sin \alpha^0 \cos \beta^0 \sin \beta^0$	$\dfrac{1}{R^0} \cos \alpha^0$	$\dfrac{1}{R^0} \sin \alpha^0 \cos^2 \beta^0$	(37)
z^0	$\dfrac{1}{R^0} \cos \alpha^0 \sin \beta^0$	$-\dfrac{1}{R^0} \sin \alpha^0 \cos \beta^0$	$\dfrac{1}{R^0} \cos \alpha^0 \cos \beta^0$	

where

$$R^0 = \sqrt{1 - \sin^2 \alpha^0 \sin^2 \beta^0}.$$

The angles α^0 and β^0 are assumed to be small, and their squares and products are therefore negligible compared to unity. Table (37) can therefore be written as:

	x_2	y_2	z_2	
x^0	1	0	$-\beta^0$	
y^0	0	1	α^0	(38)
z^0	β^0	$-\alpha^0$	1	

The direction cosines of the system $x^0 y^0 z^0$ relative to the system $\xi_2 \eta_2 \zeta_2$ are obtained from (21) and (38):

	ξ_2	η_2	ζ_2	
x^0	$\cos \beta_2 + \beta^0 \sin \beta_2$	$\dfrac{1}{R_2} \sin \alpha_2 \cos \beta_2 \sin \beta_2 - {}$ $- \beta^0 \dfrac{1}{R_2} \sin \alpha_2 \cos^2 \beta_2$	$\dfrac{1}{R_2} \cos \alpha_2 \sin \beta_2 - {}$ $- \beta^0 \dfrac{1}{R_2} \cos \alpha_2 \cos \beta_2$	
y^0	$-\alpha^0 \sin \beta_2$	$\dfrac{1}{R_2} \cos \alpha_2 + \alpha^0 \dfrac{1}{R_2} \sin \alpha_2 \cos^2 \beta_2$	$-\dfrac{1}{R_2} \sin \alpha_2 \cos \beta_2 + {}$ $+ \alpha^0 \dfrac{1}{R_2} \cos \alpha_2 \cos \beta_2$	(39)
z^0	$\beta^0 \cos \beta_2 - \sin \beta_2$	$\beta^0 \dfrac{1}{R_2} \sin \alpha_2 \cos \beta_2 \sin \beta_2 - {}$ $- \alpha^0 \dfrac{1}{R_2} \cos \alpha_2 + {}$ $+ \dfrac{1}{R_2} \cos^2 \beta_2 \sin \alpha_2$	$\beta^0 \dfrac{1}{R_2} \cos \alpha_2 \sin \beta_2 + {}$ $+ \alpha^0 \dfrac{1}{R_2} \sin \alpha_2 \cos \beta_2 + {}$ $+ \dfrac{1}{R_2} \cos \alpha_2 \cos \beta_2$	

Tables (36) and (39) are important for the subsequent calculations.

Since the axes ζ_1 and ζ_2 are parallel, their direction cosines relative to the system $x^0 y^0 z^0$ must be equal. The following three equalities are therefore obtained from Tables (36) and (39):

$$\frac{1}{R_1} \cos \alpha_1 \sin \beta_1 - \gamma^0 \frac{1}{R_1} \sin \alpha_1 \cos \beta_1 =$$
$$= \frac{1}{R_2} \cos \alpha_2 \sin \beta_2 - \beta^0 \frac{1}{R_2} \cos \alpha_2 \cos \beta_2; \qquad (40)$$

$$-\gamma^0 \frac{1}{R_1} \cos \alpha_1 \sin \beta_1 - \frac{1}{R_1} \sin \alpha_1 \cos \beta_1 =$$

$$= - \frac{1}{R_2} \sin \alpha_2 \cos \beta_2 + \alpha^0 \frac{1}{R_2} \cos \alpha_2 \cos \beta_2;$$

$$\frac{1}{R_1} \cos \alpha_1 \cos \beta_1 = \beta^0 \frac{1}{R_2} \cos \alpha_2 \sin \beta_2 +$$

$$+ \alpha^0 \frac{1}{R_2} \sin \alpha_2 \cos \beta_2 + \frac{1}{R_2} \cos \alpha_2 \cos \beta_2 \qquad (40)$$

Each of these equations follows from the other two with an accuracy up to first-order terms in α^0, β^0, and γ^0.

Using (40), the angles α_2 and β_2 can be found if α_1, β_1, α^0, β^0, and γ^0 are given. This solves the problem of determining the errors in the stabilization of the inner gimbal ring of the second bicardan suspension in the horizontal plane, since $\Delta\alpha$ and $\Delta\beta$ can be obtained from (33) for known α_2 and β_2.

In order to obtain formulas for the direct determination of $\Delta\alpha$ and $\Delta\beta$, we expand the trigonometric functions of α^0 and β^0 in series. Using (33), the following expressions are obtained as a first-order approximation:

$$\cos \alpha_2 = \cos \alpha_1 - (\alpha^0 + \Delta\alpha) \sin \alpha_1,$$

$$\sin \alpha_2 = \sin \alpha_1 + (\alpha^0 + \Delta\alpha) \cos \alpha_1,$$

$$\cos \beta_2 = \cos \beta_1 - (\beta^0 + \Delta\beta) \sin \beta_1, \qquad (41)$$

$$\sin \beta_2 = \sin \beta_1 + (\beta^0 + \Delta\beta) \cos \beta_1$$

and

$$\frac{1}{R_2} = \frac{1}{\sqrt{1 - \sin^2 \alpha_2 \sin^2 \beta_2}} = \frac{1}{\sqrt{1 - \sin^2 \alpha_1 \sin^2 \beta_1}} +$$

$$+ (\alpha^0 + \Delta\alpha) \frac{\partial}{\partial \alpha_1} \frac{1}{\sqrt{1 - \sin^2 \alpha_1 \sin^2 \beta_1}} +$$

$$+ (\beta^0 + \Delta\beta) \frac{\partial}{\partial \beta_1} \frac{1}{\sqrt{1 - \sin^2 \alpha_1 \sin^2 \beta_1}} \qquad (42)$$

or

$$\frac{1}{R_2} = \frac{1}{R_1} + (\alpha^0 + \Delta\alpha) \frac{\cos \alpha_1 \sin \alpha_1 \sin^2 \beta_1}{R_1^3} +$$

$$+ (\beta^0 + \Delta\beta) \frac{\sin^2 \alpha_1 \cos \beta_1 \sin \beta_1}{R_1^3} . \qquad (43)$$

The substitution of (41) and (43) into the first two equations of (40) yields

$$\frac{1}{R_1} \cos \alpha_1 \sin \beta_1 - \gamma^0 \frac{1}{R_1} \sin \alpha_1 \cos \beta_1 = \frac{1}{R_1} \cos \alpha_1 \sin \beta_1 +$$

$$+ \frac{(\alpha^0 + \Delta\alpha)\cos \alpha_1 \sin \alpha_1 \sin^2 \beta_1 + (\beta^0 + \Delta\beta)\sin^2 \alpha_1 \cos \beta_1 \sin \beta_1}{R_1^3} \cos \alpha_1 \sin \beta_1 -$$

$$- \frac{1}{R_1} (\alpha^0 + \Delta\alpha) \sin \alpha_1 \sin \beta_1 + (\beta^0 + \Delta\beta) \frac{1}{R_1} \cos \alpha_1 \cos \beta_1 -$$

$$- \beta^0 \frac{1}{R_1} \cos \alpha_1 \cos \beta_1 , \qquad (44)$$

21

$$-\gamma^0 \frac{1}{R_1} \cos \alpha_1 \sin \beta_1 - \frac{1}{R_1} \sin \alpha_1 \cos \beta_1 = -\frac{1}{R_1} \sin \alpha_1 \cos \beta_1 -$$

$$- \frac{(\alpha^0 + \Delta\alpha) \cos \alpha_1 \sin \alpha_1 \sin^2 \beta_1 + (\beta^0 + \Delta\beta) \sin^2 \alpha_1 \cos \beta_1 \sin \beta_1}{R_1^3} \sin \alpha_1 \cos \beta_1 -$$

$$- (\alpha^0 + \Delta\alpha) \frac{1}{R_1} \cos \alpha_1 \cos \beta_1 + (\beta^0 + \Delta\beta) \frac{1}{R_1} \sin \alpha_1 \sin \beta_1 +$$

$$+ \alpha^0 \frac{1}{R_1} \cos \alpha_1 \cos \beta_1.$$

These equations are of the same order of accuracy as (41) and (43). They can be simplified to

$$-\gamma^0 \sin \alpha_1 \cos \beta_1 =$$

$$= \frac{(\alpha^0 + \Delta\alpha) \cos \alpha_1 \sin \beta_1 + (\beta^0 + \Delta\beta) \sin \alpha_1 \cos \beta_1}{1 - \sin^2 \alpha_1 \sin^2 \beta_1} \cos \alpha_1 \sin \alpha_1 \sin^2 \beta_1 -$$

$$- (\alpha^0 + \Delta\alpha) \sin \alpha_1 \sin \beta_1 + \Delta\beta \cos \alpha_1 \cos \beta_1,$$

$$\tag{45}$$

$$-\gamma^0 \cos \alpha_1 \sin \beta_1 =$$

$$= - \frac{(\alpha^0 + \Delta\alpha) \cos \alpha_1 \sin \beta_1 + (\beta^0 + \Delta\beta) \sin \alpha_1 \cos \beta_1}{1 - \sin^2 \alpha_1 \sin^2 \beta_1} \sin^2 \alpha_1 \cos \beta_1 \sin \beta_1 -$$

$$- \Delta\alpha \cos \alpha_1 \cos \beta_1 + (\beta^0 + \Delta\beta) \sin \alpha_1 \sin \beta_1.$$

We now expand the trigonometric functions of α_1 and β_1 appearing in (45) into power series and neglect all terms of higher order than the second. Equations (45) then become

$$-\gamma^0 \alpha_1 = -(\alpha^0 + \Delta\alpha) \alpha_1 \beta_1 + \Delta\beta \left(1 - \frac{1}{2} \alpha_1^2 - \frac{1}{2} \beta_1^2\right),$$

$$-\gamma^0 \beta_1 = -\Delta\alpha \left(1 - \frac{1}{2} \alpha_1^2 - \frac{1}{2} \beta_1^2\right) + (\beta^0 + \Delta\beta) \alpha_1 \beta_1.$$

$$\tag{46}$$

These can be simplified still further by taking into account the fact already mentioned (cf. p.18) that the expansions of $\Delta\alpha$ and $\Delta\beta$ in power series of α_1 and β_1 contain no free terms, and by neglecting the products of $\Delta\alpha$ and $\Delta\beta$ as second-order terms in α_1 and β_1. The following final formulas result:

$$\Delta\beta = -\gamma^0 \alpha_1 + \alpha^0 \alpha_1 \beta_1,$$

$$\Delta\alpha = \gamma^0 \beta_1 + \beta^0 \alpha_1 \beta_1.$$

$$\tag{47}$$

Formulas (47) give the value of the errors in the stabilization of the inner gimbal ring of the second suspension in the horizontal plane during the ship's rolling. It is seen that these errors depend mainly on γ^0, i.e., the rotation about the z_1-axis during mounting of the second bicardan suspension relative to the first.

Assume for instance

$$\alpha^0 = \beta^0 = \gamma^0 = 0.008 \ (\cong 0.5°); \quad \alpha_1 = 0.122 \ (7°); \quad \beta_1 = 0.262 \ (15°).$$

Then:

$$\Delta\alpha = \gamma^0\beta_1 + \beta^0\alpha_1\beta_1 = 0.0021 + 0.0003 \quad (7' + 1'),$$

$$\Delta\beta = -\gamma^0\alpha_1 + \alpha^0\alpha_1\beta_1 = -0.0010 + 0.0003 \quad (-3' + 1').$$

The value of $\Delta\gamma$, giving the azimuth error in the stabilization of the inner gimbal ring of the second suspension, will now be calculated. It is seen from Figure 10 that

$$\cos \xi_2\eta_1 = \sin (\gamma^0 + \Delta\gamma) \cong \gamma^0 + \Delta\gamma. \tag{48}$$

On the other hand it follows from (36) and (39) (which give the direction cosines of the system $x^0y^0z^0$ relative to the systems $\xi_1\eta_1\zeta_1$ and $\xi_2\eta_2\zeta_2$ respectively) that:

$$\cos \xi_2\eta_1 = \cos \xi_2 x^0 \cos \eta_1 x^0 + \cos \xi_2 y^0 \cos \eta_1 y^0 + \cos \xi_2 z^0 \cos \eta_1 z^0 =$$

$$= \left(\frac{1}{R_1} \sin \alpha_1 \cos \beta_1 \sin \beta_1 + \gamma^0 \frac{1}{R_1} \cos \alpha_1\right)(\cos \beta_2 + \beta^0 \sin \beta_2) +$$

$$+ \left(-\gamma^0 \frac{1}{R_1} \sin \alpha_1 \cos \beta_1 \sin \beta_1 + \frac{1}{R_1} \cos \alpha_1\right)(-\alpha^0 \sin \beta_2) +$$

$$+ \frac{1}{R_1} \sin \alpha_1 \cos^2 \beta_1 (\beta^0 \cos \beta_2 - \sin \beta_2). \tag{49}$$

Expanding the right-hand side of (49) in power series, neglecting all terms of higher order than the first in α^0, β^0, and γ^0, and equating it to the right-hand side of (48), we obtain

$$\gamma^0 + \Delta\gamma = \frac{1}{R_1} \sin \alpha_1 \cos \beta_1 \sin \beta_1 \cos \beta_2 + \gamma^0 \frac{1}{R_1} \cos \alpha_1 \cos \beta_2 +$$

$$+ \beta^0 \frac{1}{R_1} \sin \alpha_1 \cos \beta_1 \sin \beta_1 \sin \beta_2 - \alpha^0 \frac{1}{R_1} \cos \alpha_1 \sin \beta_2 +$$

$$+ \beta^0 \frac{1}{R_1} \sin \alpha_1 \cos^2 \beta_1 \cos \beta_2 - \frac{1}{R_1} \sin \alpha_1 \cos^2 \beta_1 \sin \beta_2. \tag{50}$$

Inserting (41), and neglecting all terms of higher order than the first in α^0 and β^0, yields

$$\gamma^0 + \Delta\gamma = \frac{1}{R_1} [\sin \alpha_1 \cos^2 \beta_1 \sin \beta_1 - (\beta^0 + \Delta\beta) \sin \alpha_1 \cos \beta_1 \sin^2 \beta_1 +$$

$$+ \gamma^0 \cos \alpha_1 \cos \beta_1 + \beta^0 \sin \alpha_1 \cos \beta_1 \sin^2 \beta_1 - \alpha^0 \cos \alpha_1 \sin \beta_1 +$$

$$+ \beta^0 \sin \alpha_1 \cos^3 \beta_1 - \sin \alpha_1 \cos^2 \beta_1 \sin \beta_1 -$$

$$- (\beta^0 + \Delta\beta) \sin \alpha_1 \cos^3 \beta_1], \tag{51}$$

which can be simplified to

$$\Delta\gamma = -\gamma^0 + \frac{1}{R_1} [\gamma^0 \cos \alpha_1 \cos \beta_1 - \Delta\beta \sin \alpha_1 \cos \beta_1 -$$

$$- \alpha^0 \cos \alpha_1 \sin \beta_1]. \tag{52}$$

Formula (52), which determines $\Delta\gamma$, can be considerably simplified by neglecting all terms of higher order than the second in α_1 and β_1:

$$\Delta\gamma = -\gamma^0 \frac{\alpha_1^2 + \beta_1^2}{2} - \alpha^0\beta_1 - \Delta\beta\alpha_1. \tag{53}$$

23

Inserting the expression for $\Delta\beta$ from (47), and neglecting terms of higher order, lead to the following final formula:

$$\Delta\gamma = -\alpha^0\beta_1 + \gamma^0 \frac{\alpha_1^2 - \beta_1^2}{2}. \tag{54}$$

This formula gives the azimuth error in the stabilization of the inner gimbal ring of the second suspension during the ship's rolling. It is seen that this error depends mainly on α^0, i.e., on the inclination of the housing of the second suspension (i.e., of the z_2-axis) referred to the plane x_1z_1.

Assume as above $\alpha^0 = \beta^0 = \gamma^0 = 0.008$ ($\cong 0.5°$), $\alpha_1 = 0.122$ (7°), $\beta_1 = 0.262$ (15°), then

$$\Delta\gamma = -\alpha^0\beta_1 + \gamma^0 \frac{\alpha_1^2 - \beta_1^2}{2} = -0.0021 - 0.0002 \ (-7' - 1').$$

The stabilization errors of the roll and pitch angles and of the course mounting of the [second] bicardan suspension housing are therefore, according to (47) and (54),

$$\Delta\alpha = \gamma^0\beta_1 + \beta^0\alpha_1\beta_1;$$

$$\Delta\beta = -\gamma^0\alpha_1 + \alpha^0\alpha_1\beta_1; \tag{55}$$

$$\Delta\gamma = -\alpha^0\beta_1 + \gamma^0 \frac{\alpha_1^2 - \beta_1^2}{2}.$$

It is seen from this that the influence on the stabilization accuracy of the inclination of the second suspension housing (i.e., of the z_2-axis), referred to the ship's plane of symmetry (the angle β^0) is negligible.

§ 4. Horizontal stabilization errors of combinations of different types of gimbal systems

If two kinematically different gimbal systems are mounted on the ship and their inner rings are stabilized in the horizontal plane, the values of the roll and pitch angles indicated on the scales of the two gimbal systems can differ, due to the difference in the geometric determination of these angles.

In a bicardan suspension, for instance (Figure 7), the tilting angle α of the bow is taken as the pitch angle, and the tilting angle β of the outer gimbal ring as the roll angle.

In the initial position, the plane of the outer gimbal ring is parallel to the xy plane, while the bow plane is perpendicular to it (x = bow pivot axis, y = outer gimbal-ring pivot axis; the xy plane is parallel to the deck plane, the y-axis being parallel to the ship's longitudinal axis).

In the simplest gimbal system on the other hand (Figure 1), the tilting angle α' of the inner ring relative to the outer ring is taken as the pitch angle, and the tilting angle β of the outer ring relative to the deck plane is taken as the roll angle (the outer ring pivot axis y is parallel to the ship's longitudinal axis).

It is therefore seen that, while the roll angle is identically defined in the two cases, different definitions are used for the pitch angle. In the first case, the pitch angle α is the bihedral angle between the bow plane $x\zeta$ (the vertical plane containing the x-axis) and the plane xz perpendicular to the

24

· ship's longitudinal axis (the *z*-axis is parallel to the ship's mast; the *xz* plane is parallel to the transversal plane or plane of the ship's frames). In the second case, the pitch angle α' is the bihedral angle between the vertical plane passing through the inner gimbal-ring pivot axis ξ_1 and the same *xz* plane perpendicular to the ship's longitudinal axis (this plane contains also the ξ_1-axis).

The angles α and α' are equal only for roll angle $\beta = 0$, i.e., when the inner ring pivot axis ξ_1 of the simplest gimbal system is parallel to the deck plane (and therefore to the bow pivot axis *x*). For roll angles differing from zero, the difference between the pitch angles α and α' indicated by the bicardan suspension and the simplest gimbal system respectively can be considerable.

The difference between the two angles can be calculated in the given case from formula (8):

$$\operatorname{tg} \alpha' = \operatorname{tg} \alpha \cos \beta,$$

which was derived in § 1 and which links the tilting angle α' of the inner gimbal ring relative to the outer ring to the tilting angle α of the bow plane and the tilting angle β of the outer gimbal ring cf the bicardan suspension relative to the deck.

This formula can be approximated by the formula (accurate up to third-order terms in α and β):

$$\operatorname{tg} \alpha' = \alpha - \frac{\alpha \beta^2}{2} + \frac{\alpha^3}{3}. \tag{56}$$

On the other hand, $\operatorname{tg} \alpha'$ can be expanded in the series:

$$\operatorname{tg} \alpha' = \alpha' + \frac{\alpha'^3}{3} + \cdots$$

It follows that the angle α' differs from the angle α by third-order terms in α and β. It is easily seen that, with the same accuracy:

$$\alpha' = \alpha - \frac{\alpha \beta^2}{2}. \tag{57}$$

It follows that if the inner gimbal ring of the bicardan suspension is perfectly stabilized in the horizontal plane, and if the pitch and roll angles α and β indicated by this suspension are accurately reproduced by means of follow-up systems as pitch and roll angles α' and β on the simplest gimbal system, the inner ring of the latter will not be horizontal. According to (57) the so-called stabilization error will be equal to

$$\Delta \alpha' = \alpha' - \alpha = - \frac{\alpha \beta^2}{2}.$$

This formula gives the amount by which the angle α' must be increased (or decreased, if $\Delta \alpha' < 0$) so that the inner ring of the simplest gimbal system is horizontal.

For $\alpha = 0.122$ (7°) and $\beta = 0.262$ (15°), this formula gives

$$\Delta \alpha' = - \frac{\alpha \beta^2}{2} = - 0.0042 \ (14.5'),$$

which is a relatively large error.

The difference between the pitch or roll angles indicated by kinematically different gimbal systems having perfectly horizontal inner gimbal rings

obviously gives the measure of the horizontal-stabilization error for the combination of these gimbal systems. It is of course assumed that the gimbal system housings have been mounted so accurately that the stabilization errors dealt with in § 3 can be neglected.

Two types of gimbal systems have been examined so far: the bicardan suspension and the simplest gimbal system. Some gimbal systems designed according to other kinematic schemes will now be considered (Figures 12−14).

The first of these gimbal systems (Figure 12) has been used in many instruments and devices, in particular for the horizontal stabilization of the gyrocompass follow-up sphere. This gimbal system will be denoted by *A*.
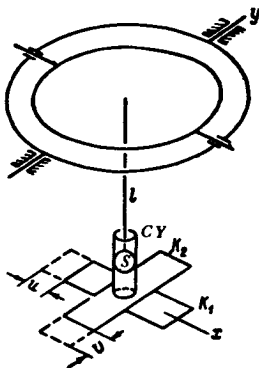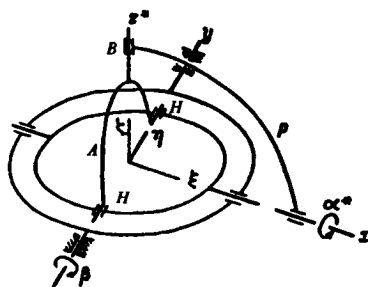

FIGURE 12   FIGURE 13

Another gimbal system, encountered in two different design variants in some instruments, is shown in Figures 13 and 14. It will be denoted by *G*.

The bicardan suspension (Figure 7), which is the type of gimbal system most frequently used in instruments and devices, will be denoted by *B*; lastly, the simplest gimbal system (Figure 1) will be denoted by *E*. The gimbal system *E* is remarkable in that the pitch and roll angles indicated by it form, together with the angle [of rotation about the ζ-axis] measured in the plane of the inner gimbal ring, a set of Euler angles.

In this section we determine the horizontal stabilization error for the combination of any two of the above gimbal systems, *B*, *E*, *A*, and *G*.

We consider the gimbal system *B* as basic, and find the relationships between the pitch and roll angles α and β indicated by this gimbal system, and by the gimbal systems *A* and *G*. The corresponding relationships for the gimbal system *E* have already been found and are expressed by formulas (8) and (57).

Consider first the gimbal system *A* (Figure 12). The pitch and roll angles are taken as the ratios of the displacements *u* and *v* of the slides K_1 and K_2 to the length *l* of the rod rigidly connected to the inner gimbal ring.

The rod ends in the sphere *S*, which slides freely inside the hollow cylinder *CY*, connected rigidly to the upper slide.

26

The upper slide moves the distance v in the direction of the ship's longitudinal axis relative to the lower slide; the lower slide moves the distance u in the transverse direction, parallel to the deck (the inverse position of the slides is also possible). The outer gimbal ring is parallel to the ship's longitudinal axis. For $u=v=0$ the plane of the inner ring is parallel to the deck plane. The ratios

$$\bar{\alpha}=-\frac{v}{l}, \quad \bar{\beta}=\frac{u}{l}$$

represent in the gimbal system A the ship's pitch and roll angles.

<div style="display:flex">
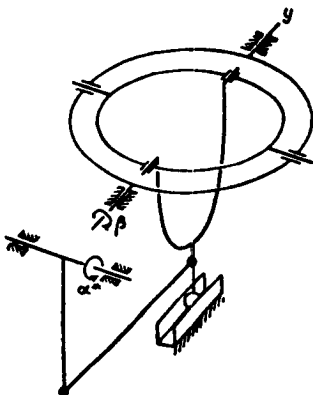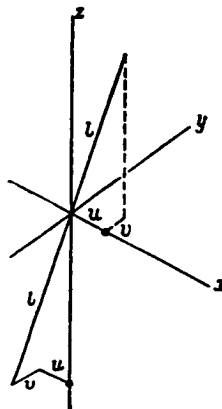<div>FIGURE 14</div>
<div>FIGURE 15</div>
</div>

It is easily seen (Figure 15) that the ratios $\frac{u}{l}$ and $\frac{v}{l}$ represent the cosines of the angles which the rod makes with the axes x and y (the x-axis is perpendicular to the ship's plane of symmetry, the y-axis is parallel to the ship's longitudinal axis). Since the rod is oriented perpendicular to the plane of the inner ring, which is assumed to be stabilized in the horizontal plane, $\bar{\alpha}$ and $\bar{\beta}$ should be equated respectively to the cosines of the angles formed by the ζ-axis of the bicardan suspension B with the same axes. The following relationships are obtained from (18):

$$\bar{\alpha}=\frac{1}{R}\sin\alpha\cos\beta,$$

$$\bar{\beta}=\frac{1}{R}\cos\alpha\sin\beta,$$

$$\tag{58}$$

where

$$R=\sqrt{1-\sin^2\alpha\sin^2\beta}.$$

We expand the right-hand sides of (58) in power series in α and β, and neglect all terms in these variables of higher order than the third. The following approximations are thus obtained:

$$\bar{\alpha}=\alpha-\frac{\alpha\beta^2}{2},$$

$$\bar{\beta}=\beta-\frac{\alpha^2\beta}{2}.$$

$$\tag{59}$$

It follows that the horizontal-stabilization errors for the combination of the gimbal systems *A* and *B* are expressed by the formulas

$$\Delta \bar{\alpha} = \bar{\alpha} - \alpha = -\frac{\alpha \beta^2}{2},$$

$$\Delta \bar{\beta} = \bar{\beta} - \beta = -\frac{\alpha^2 \beta}{2}. \qquad (60)$$

We consider now the gimbal system *G* (Figure 13 or 14). The roll angle is determined here, in the same way as in the bicardan suspension *B*, as the angle of tilting of the outer ring relative to the ship's deck (about the *y*-axis, parallel to the ship's longitudinal axis).

The pitch angle, which will be denoted by α^*, is defined here as the angle of tilting of the bow *P* about the *x*-axis which is perpendicular to the ship's plane of symmetry (Figure 13).

The bow *P* moves the arc *A*, connected to it by the bearing *B*; the axis of the bearing *B*, which will be denoted by z^*, is perpendicular to the *x*-axis and lies in the same plane.

The arc *A* moves in its turn the inner gimbal ring, to which it is connected by means of two hinges *H*.

The hinges *H* lie in the plane of the inner gimbal ring on the ship's course line (the η-axis), i.e., on the line perpendicular to the axis of tilting ξ of the inner ring relative to the outer ring.

FIGURE 16

The axis of the bearing *B* (the z^*-axis) is perpendicular to the ship's course line (the η-axis). According to (18), the direction cosines of the η-axis relative to the coordinate system *xyz* are respectively

$$\cos \eta x = \frac{1}{R} \sin \alpha \cos \beta \sin \beta,$$

$$\cos \eta y = \frac{1}{R} \cos \alpha, \qquad (61)$$

$$\cos \eta z = \frac{1}{R} \sin \alpha \cos^2 \beta.$$

On the other hand the z^*-axis forms an angle α^* with the *z*-axis and lies in the *yz* plane (Figure 16). The direction cosines of the z^*-axis relative to the *xyz* system are therefore:

$$\cos z^* x = \quad 0,$$

$$\cos z^* y = -\sin \alpha^*, \qquad (62)$$

$$\cos z^* z = \quad \cos \alpha^*.$$

The condition of orthogonality of the two axes η and z^* is defined in analytical geometry in the following way:

$$\cos \eta x \cos z^* x + \cos \eta y \cos z^* y + \cos \eta z \cos z^* z = 0.$$

Inserting the corresponding cosines from (61) and (62) we obtain

$$-\frac{1}{R} \cos \alpha \sin \alpha^* + \frac{1}{R} \sin \alpha \cos^2 \beta \cos \alpha^* = 0, \qquad (63)$$
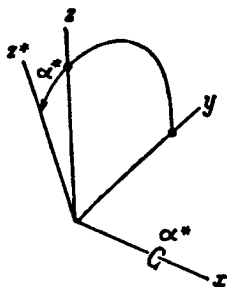
28

.whence
$$\text{tg}\,\alpha^* = \text{tg}\,\alpha\,\cos^2\beta. \tag{64}$$

The last formula is the required relationship between the pitch angle α^* indicated by the gimbal system G and the pitch and roll angles α and β indicated by the bicardan suspension B. This formula can be approximated by the following expression, accurate up to and including third-order terms in α and β:

$$\text{tg}\,\alpha\,\cos^2\beta = \left(\alpha + \frac{\alpha^3}{3}\right)\left(1 - \frac{\beta^2}{2}\right)^2 = \alpha + \frac{\alpha^3}{3} - \alpha\beta^2. \tag{65}$$

The following formula is obtained by following the same procedure as in the derivation of (57):

$$\text{tg}\,\alpha^* = \alpha^* + \frac{(\alpha^*)^3}{3} = \alpha + \frac{\alpha^3}{3} - \alpha\beta^2, \tag{66}$$

whence, with the same accuracy:

$$\alpha^* = \alpha - \alpha\beta^2. \tag{67}$$

It is thus seen that, when the gimbal system G and the bicardan suspension B act in conjunction, there is a horizontal stabilization error in the pitch angle only, and its value is given by

$$\Delta\alpha^* = \alpha^* - \alpha = -\alpha\beta^2. \tag{68}$$

The horizontal stabilization errors when the bicardan suspension B acts in conjunction with any of the gimbal systems E, A, or G can therefore be tabulated as follows

Gimbal system type	B	E	A	G	
Pitch angle error	0	$-\dfrac{\alpha\beta^2}{2}$	$-\dfrac{\alpha\beta^2}{2}$	$-\alpha\beta^2$	(69)
Roll angle error	0	0	$-\dfrac{\alpha^2\beta}{2}$	0	

The horizontal stabilization error for the combination of any two of the three gimbal systems E, A, G is obviously equal to the difference between the values given in the corresponding columns of this table. The pitch angle error for the combination of gimbal systems A and E is thus zero (more exactly, its magnitude is of an order higher than the third in α and β), while the roll angle error is equal to $-\dfrac{\alpha^2\beta}{2}$. This means that if the pitch and roll angles of the gimbal system E, whose inner ring is accurately stabilized in the horizontal plane, are reproduced by means of follow-up systems as pitch and roll angles in the gimbal system A, then the error $-\dfrac{\alpha^2\beta}{2}$ should be added to the pitch angle in order that the inner ring of gimbal system A be horizontal.

Within the above limits of accuracy, the pitch and roll angles indicated by any of the gimbal systems B, E, A, and G can be assumed to be α and β.

§ 5. Variation of the polar coordinates of a fixed point
caused by horizontal stabilization errors
(analytical treatment)

Consider two gimbal systems the axes of whose outer gimbal rings are parallel to the ship's longitudinal axis. Let the inner ring of the first gimbal system be accurately stabilized in the horizontal plane, while the inner ring of the second gimbal system is stabilized at a certain pitch angle error $\Delta\alpha$ and a certain roll angle error $\Delta\beta$.

We denote by ε_1 and ϕ_1 the polar coordinates of a given point S relative to the first gimbal system's inner ring, accurately stabilized in the horizontal plane. The coordinate ε_1 (Figure 17) is the so-called elevation angle, i.e., the angle between the line v_1 connecting the center of the gimbal system with the point S, and the plane of the first gimbal system's inner ring (or, in other words, the angle between the line v_1 and its projection g_1 on the plane of the inner ring).
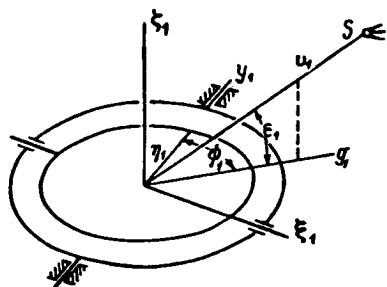
The coordinate ϕ_1 is the so-called course angle of point S, i.e., the angle between the ship's course line η_1 and the line g_1 (or, in other words, the angle between the ship's course line η_1 and the plane containing the point S and the center of the gimbal system, perpendicular to the plane of the inner ring).

FIGURE 17

The ship's course line η_1 has already been defined (§ 1, p. 10) as the line lying in the plane of the inner gimbal ring and parallel to the ship's longitudinal axis at zero pitch angle (i.e., when the planes of the inner and outer gimbal rings coincide).

The course angle ϕ_1 is measured clockwise from the course line η_1. For $\phi_1 = 90°$, for instance, the point S is situated on the ship's starboard.

The polar coordinates of the same point S, referred to the inner ring of the second gimbal system (which is inaccurately stabilized in the horizontal plane), will be denoted by ε_2 and ϕ_2.

It will be assumed that the point S is situated at such a distance that the lines connecting this point with the centers of the gimbal systems can be considered as parallel.

Our aim is to determine, with an accuracy sufficient for practical needs, the differences

$$\Delta\varepsilon = \varepsilon_2 - \varepsilon_1, \qquad \Delta\phi = \phi_2 - \phi_1 \tag{70}$$

for given values of the pitch and roll angles α and β, the horizontal stabilization errors $\Delta\alpha$ and $\Delta\beta$, and the polar coordinates ε_1 and ϕ_1.

The analytical solution of this problem (its geometric solution will be given in § 6) requires knowledge of the direction cosines of the coordinate system $\xi_1\eta_1\zeta_1$ (fixed to the inner ring of the first gimbal system) relative to the coordinate system $\xi_2\eta_2\zeta_2$ (fixed to the inner ring of the second gimbal system). It will be assumed that the axes of these systems, and likewise the axes of the systems $x_1y_1z_1$ and $x_2y_2z_2$ fixed to the gimbal system housings,

are oriented in the same way as in § 2, and that the axes of the systems $x_1 y_1 z_1$ and $x_2 y_2 z_2$ are respectively parallel.

The direction cosines of the system $\xi_1 \eta_1 \zeta_1$ relative to the system $x_1 y_1 z_1$ are identical with (20) of § 2:

	x_1	y_1	z_1
ξ_1	$\cos \beta_1$	0	$-\sin \beta_1$
η_1	$\dfrac{1}{R_1} \sin \alpha_1 \cos \beta_1 \sin \beta_1$	$\dfrac{1}{R_1} \cos \alpha_1$	$\dfrac{1}{R_1} \sin \alpha_1 \cos^2 \beta_1$
ζ_1	$\dfrac{1}{R_1} \cos \alpha_1 \sin \beta_1$	$-\dfrac{1}{R_1} \sin \alpha_1 \cos \beta_1$	$\dfrac{1}{R_1} \cos \alpha_1 \cos \beta_1$

where

$$R_1 = \sqrt{1 - \sin^2 \alpha_1 \sin^2 \beta_1}.$$

The direction cosines of the system $\xi_2 \eta_2 \zeta_2$ relative to the system $x_2 y_2 z_2$ are identical with (21):

	x_2	y_2	z_2
ξ_2	$\cos \beta_2$	0	$-\sin \beta_2$
η_2	$\dfrac{1}{R_2} \sin \alpha_2 \cos \beta_2 \sin \beta_2$	$\dfrac{1}{R_2} \cos \alpha_2$	$\dfrac{1}{R_2} \sin \alpha_2 \cos^2 \beta_2$
ζ_2	$\dfrac{1}{R_2} \cos \alpha_2 \sin \beta_2$	$-\dfrac{1}{R_2} \sin \alpha_2 \cos \beta_2$	$\dfrac{1}{R_2} \cos \alpha_2 \cos \beta_2$

where

$$R_2 = \sqrt{1 - \sin^2 \alpha_2 \sin^2 \beta_2}.$$

Since the angles α_2 and β_2 differ from the angles α_1 and β_1 by the small errors $\Delta \alpha$ and $\Delta \beta$:

$$\begin{aligned} \alpha_2 &= \alpha_1 + \Delta \alpha, \\ \beta_2 &= \beta_1 + \Delta \beta. \end{aligned} \tag{71}$$

it follows that the corresponding elements in (20) and (21) differ only slightly. The following expressions are obtained, accurate up to the first-order terms in the stabilization errors and up to and including second-order terms in α_1 and β_1:

$$\begin{aligned} \cos \beta_2 &= \cos \beta_1 - \Delta \beta \sin \beta_1 = \cos \beta_1 - \Delta \beta \cdot \beta_1, \\ \sin \beta_2 &= \sin \beta_1 + \Delta \beta \cos \beta_1 = \sin \beta_1 + \Delta \beta \left(1 - \tfrac{1}{2} \beta_1^2\right). \end{aligned} \tag{72}$$

$$\begin{aligned} \cos \alpha_2 &= \cos \alpha_1 - \Delta \alpha \cdot \alpha_1, \\ \sin \alpha_2 &= \sin \alpha_1 + \Delta \alpha \left(1 - \tfrac{1}{2} \alpha_1^2\right). \end{aligned} \tag{73}$$

The following formula is obtained in the same way as (43):

$$\frac{1}{R_2} = \frac{1}{R_1} + \Delta \alpha \frac{\partial}{\partial \alpha_1} \left(\frac{1}{R_1}\right) + \Delta \beta \frac{\partial}{\partial \beta_1} \left(\frac{1}{R_1}\right) = $$
$$= \frac{1}{R_1} + \Delta \alpha \frac{\cos \alpha_1 \sin \alpha_1 \sin^2 \beta_1}{R_1^3} + \Delta \beta \frac{\sin^2 \alpha_1 \cos \beta_1 \sin \beta_1}{R_1^3}. \tag{74}$$

This formula is simplified by neglecting third-order terms in α_1 and β_1:

$$\frac{1}{R_2} \cong \frac{1}{R_1} \cong 1. \tag{75}$$

The following expressions are obtained from (72) and (73) with the same accuracy:

$$\sin\alpha_2 \cos\beta_2 \sin\beta_2 = \sin\alpha_1 \cos\beta_1 \sin\beta_1 +$$

$$+ \Delta\alpha\left(1 - \frac{1}{2}\alpha_1^2\right)\cos\beta_1 \sin\beta_1 - \Delta\beta \cdot \beta_1 \sin\alpha_1 \sin\beta_1 +$$

$$+ \Delta\beta\left(1 - \frac{1}{2}\beta_1^2\right)\sin\alpha_1 \cos\beta_1 \cong \sin\alpha_1 \cos\beta_1 \sin\beta_1 + \Delta\alpha \cdot \beta_1 + \Delta\beta \cdot \alpha_1, \quad (76)$$

$$\sin\alpha_2 \cos^2\beta_2 = \sin\alpha_1 \cos^2\beta_1 + \Delta\alpha\left(1 - \frac{1}{2}\alpha_1^2\right)\cos^2\beta_1 - 2\Delta\beta \cdot \beta_1 \sin\alpha_1 \cong$$

$$\cong \sin\alpha_1 \cos^2\beta_1 + \Delta\alpha\left(1 - \frac{1}{2}\alpha_1^2 - \beta_1^2\right) - 2\Delta\beta \cdot \alpha_1\beta_1;$$

and

$$\cos\alpha_2 \sin\beta_2 = \cos\alpha_1 \sin\beta_1 - \Delta\alpha \cdot \alpha_1\beta_1 + \Delta\beta\left(1 - \frac{1}{2}\alpha_1^2 - \frac{1}{2}\beta_1^2\right),$$

$$\sin\alpha_2 \cos\beta_2 = \sin\alpha_1 \cos\beta_1 + \Delta\alpha\left(1 - \frac{1}{2}\alpha_1^2 - \frac{1}{2}\beta_1^2\right) - \Delta\beta \cdot \alpha_1\beta_1, \quad (77)$$

$$\cos\alpha_2 \cos\beta_2 = \cos\alpha_1 \cos\beta_1 - \Delta\alpha \cdot \alpha_1 - \Delta\beta \cdot \beta_1.$$

Inserting formulas (72)—(77) into (21), we obtain

	x_2	y_2	z_2
ξ_2	$\cos\beta_1 - \Delta\beta \cdot \beta_1$	0	$-\sin\beta_1 - \Delta\beta\left(1 - \frac{1}{2}\beta_1^2\right)$
η_2	$\sin\alpha_1 \cos\beta_1 \sin\beta_1 + \Delta\alpha \cdot \beta_1 + \Delta\beta \cdot \alpha_1$	$\cos\alpha_1 - \Delta\alpha \cdot \alpha_1$	$\sin\alpha_1 \cos^2\beta_1 + \Delta\alpha\left(1 - \frac{\alpha_1^2 + 2\beta_1^2}{2}\right) - 2\Delta\beta \cdot \alpha_1\beta_1$
ζ_2	$\cos\alpha_1 \sin\beta_1 - \Delta\alpha \cdot \alpha_1\beta_1 + \Delta\beta\left(1 - \frac{\alpha_1^2 + \beta_1^2}{2}\right)$	$-\sin\alpha_1 \cos\beta_1 + \Delta\beta \cdot \alpha_1\beta_1 - \Delta\alpha\left(1 - \frac{\alpha_1^2 + \beta_1^2}{2}\right)$	$\cos\alpha_1 \cos\beta_1 - \Delta\alpha \cdot \alpha_1 - \Delta\beta \cdot \beta_1$

$$(78)$$

The axes of the coordinate systems $x_2y_2z_2$ and $x_1y_1z_1$ are respectively parallel. The direction cosines of the system $\xi_2\eta_2\zeta_2$ relative to the system $\xi_1\eta_1\zeta_1$ are therefore obtained from (20) and (78), by using the well-known formulas of analytical geometry of the type

$$\cos^2\xi x + \cos^2\xi y + \cos^2\xi z = 1,$$

$$\cos\xi x \cos\eta x + \cos\xi y \cos\eta y + \cos\xi z \cos\eta z = 0, \quad (79)$$

and by neglecting third-order terms in α_1 and β_1:

	ξ_1	η_1	ζ_1
ξ_2	1	$-\Delta\beta \cdot \alpha_1$	$-\Delta\beta\left(1 - \frac{1}{2}\alpha_1^2\right)$
η_2	$\Delta\beta \cdot \alpha_1$	1	$\Delta\alpha\left(1 - \frac{1}{2}\beta_1^2\right) - \Delta\beta \cdot \alpha_1\beta_1$
ζ_2	$\Delta\beta\left(1 - \frac{1}{2}\alpha_1^2\right)$	$-\Delta\alpha\left(1 - \frac{1}{2}\beta_1^2\right) + \Delta\beta \cdot \alpha_1\beta_1$	1

$$(80)$$

It will be shown in the next section, how (80) can be derived more simply by using the formulas of small rotations of a rigid body.

Consider now a unit length of the line v_1 which connects the point $\mathcal{B}$ with the center of the first gimbal system (Figure 18). Its projections on the axes of the $\xi_1\eta_1\zeta_1$ system are

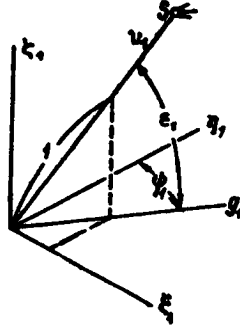$$\cos\epsilon_1\sin\psi_1, \quad \cos\epsilon_1\cos\psi_1, \quad \sin\epsilon_1. \tag{81}$$

FIGURE 18

The projections of the same length (or, which is the same, of a unit length of line v_2, parallel to v_1) on the axes of the $\xi_2\eta_2\zeta_2$ systems are given similarly by

$$\cos\epsilon_2\sin\psi_2 \quad \cos\epsilon_2\cos\psi_2, \quad \sin\epsilon_2. \tag{82}$$

These same projections can, however, be found in another way. The projection of a unit length of the line v_1 on the ξ_2-axis is the sum of the projections on this axis of three lengths lying on the axes ξ_1, η_1, and ζ_1 respectively, representing the projections on these axes of the unit length of the line v_1, i.e.,

$$\cos\epsilon_2\sin\psi_2 = \cos\epsilon_1\sin\psi_1\cos\xi_1\xi_2 +$$
$$+ \cos\epsilon_1\cos\psi_1\cos\eta_1\xi_2 + \sin\epsilon_1\cos\zeta_1\xi_2 \tag{83}$$
etc.

Using (80), these formulas become

$$\cos\epsilon_2\sin\psi_2 = \cos\epsilon_1\sin\psi_1 - \cos\epsilon_1\cos\psi_1\Delta\beta\cdot\alpha_1 - \sin\epsilon_1\Delta\beta\left(1 - \tfrac{1}{2}\alpha_1^2\right),$$

$$\cos\epsilon_2\cos\psi_2 = \cos\epsilon_1\sin\psi_1\Delta\beta\cdot\alpha_1 + \cos\epsilon_1\cos\psi_1 +$$
$$+ \sin\epsilon_1\left[\Delta\alpha\left(1 - \tfrac{1}{2}\beta_1^2\right) - \Delta\beta\cdot\alpha_1\beta_1\right],$$

$$\sin\epsilon_2 = \cos\epsilon_1\sin\psi_1\Delta\beta\left(1 - \tfrac{1}{2}\alpha_1^2\right) + \sin\epsilon_1 + \tag{84}$$
$$+ \cos\epsilon_1\cos\psi_1\left[-\Delta\alpha\left(1 - \tfrac{1}{2}\beta_1^2\right) + \Delta\beta\cdot\alpha_1\beta_1\right].$$

Since $\epsilon_2 = \epsilon_1$ and $\psi_2 = \psi_1$ for $\Delta\alpha = \Delta\beta = 0$, the expansions of the differences

$$\Delta\epsilon = \epsilon_2 - \epsilon_1, \quad \Delta\psi = \psi_2 - \psi_1$$

33

in powers of $\Delta\alpha$ and $\Delta\beta$ contain no free terms. The terms containing powers and products of these differences should therefore be neglected in the calculations, since only first-order terms in $\Delta\alpha$ and $\Delta\beta$ were retained. This yields

$$\cos\epsilon_2 \sin\phi_2 = \cos\epsilon_1 \sin\phi_1 - \sin\epsilon_1 \sin\phi_1\Delta\epsilon + \cos\epsilon_1 \cos\phi_1\Delta\phi,$$

$$\cos\epsilon_2 \cos\phi_2 = \cos\epsilon_1 \cos\phi_1 - \sin\epsilon_1 \cos\phi_1\Delta\epsilon - \cos\epsilon_1 \sin\phi_1\Delta\phi, \qquad (85)$$

$$\sin\epsilon_2 = \sin\epsilon_1 + \cos\epsilon_1\Delta\epsilon.$$

The following three equations are obtained for $\Delta\epsilon$ and $\Delta\phi$ by comparing (85) and (84) and simplifying:

$$-\sin\epsilon_1 \sin\phi_1\Delta\epsilon + \cos\epsilon_1 \cos\phi_1\Delta\phi = -\cos\epsilon_1 \cos\phi_1\Delta\beta \cdot \alpha_1 -$$

$$- \sin\epsilon_1\Delta\beta\left(1 - \frac{1}{2}\alpha_1^2\right);$$

$$-\sin\epsilon_1 \cos\phi_1\Delta\epsilon - \cos\epsilon_1 \sin\phi_1\Delta\phi = \cos\epsilon_1 \sin\phi_1\Delta\beta \cdot \alpha_1 +$$

$$+ \sin\epsilon_1\left[\Delta\alpha\left(1 - \frac{1}{2}\beta_1^2\right) - \Delta\beta \cdot \alpha_1\beta_1\right]; \qquad (86)$$

$$\cos\epsilon_1\Delta\epsilon = \cos\epsilon_1 \sin\phi_1\Delta\beta\left(1 - \frac{1}{2}\alpha_1^2\right) +$$

$$+ \cos\epsilon_1 \cos\phi_1\left[-\Delta\alpha\left(1 - \frac{1}{2}\beta_1^2\right) + \Delta\beta \cdot \alpha_1\beta_1\right].$$

Each of these equations follows from the other two. Multiplying the first by $\cos\phi_1$ and the second by $-\sin\phi_1$ and adding term by term, yields

$$\cos\epsilon_1\Delta\phi = -\cos\epsilon_1\Delta\beta \cdot \alpha_1 - \sin\epsilon_1\left\{\cos\phi_1\Delta\beta\left(1 - \frac{1}{2}\alpha_1^2\right) +\right.$$

$$\left. + \sin\phi_1\left[\Delta\alpha\left(1 - \frac{1}{2}\beta_1^2\right) - \Delta\beta \cdot \alpha_1\beta_1\right]\right\}, \qquad (87)$$

whence

$$\Delta\phi = -\Delta\beta \cdot \alpha_1 - \mathrm{tg}\,\epsilon_1\left\{\cos\phi_1\Delta\beta\left(1 - \frac{1}{2}\alpha_1^2\right) +\right.$$

$$\left. + \sin\phi_1\left[\Delta\alpha\left(1 - \frac{1}{2}\beta_1^2\right) - \Delta\beta \cdot \alpha_1\beta_1\right]\right\}. \qquad (88)$$

The third equation of (86) becomes

$$\Delta\epsilon = \sin\phi_1\Delta\beta\left(1 - \frac{1}{2}\alpha_1^2\right) - \cos\phi_1\left[\Delta\alpha\left(1 - \frac{1}{2}\beta_1^2\right) - \Delta\beta \cdot \alpha_1\beta_1\right]. \quad (89)$$

These last two formulas give the required solution. If the terms containing squares and products of the variables α_1 and β_1 are neglected, (88) and (89) become:

$$\Delta\epsilon = -\Delta\alpha \cos\phi_1 + \Delta\beta \sin\phi_1;$$

$$\Delta\phi = -\Delta\beta \cdot \alpha_1 - \mathrm{tg}\,\epsilon_1(\Delta\beta \cos\phi_1 + \Delta\alpha \sin\phi_1). \qquad (90)$$

Formulas (90) are usually sufficiently accurate.

If, for instance, $\Delta\alpha = \Delta\beta = 0.008$, $\phi_1 = 30°$, $\epsilon_1 = 60°$,

$$\alpha_1 = 0.122\,(7°), \quad \beta_1 = 0.262\,(15°),$$

then by (88) and (89):

$$\Delta\epsilon = -0.0025 \ (9'),$$
$$\Delta\psi = -0.0194 \ (1°7'),$$

while by (90)

$$\Delta\epsilon = -0.0029 \ (10'),$$
$$\Delta\psi = -0.0199 \ (1°8').$$

It was assumed above that the gimbal systems are mounted with a high accuracy relative to each other. If this is not so, the horizontal-stabilization errors and the azimuth-stabilization errors given by (55) (cf. § 3 of this chapter) should be taken into account in the derivation of (88) and (89).

§ 6. Geometric determination of the stabilization errors by the theory of infinitesimal rotations of a rigid body

Some of the problems treated in the preceding sections can be solved geometrically using the simplest principles of the theory of infinitesimal rotations of rigid bodies.

Infinitesimal rotations of a rigid body can be represented by vectors directed along the corresponding axes of rotation. A sequence of infinitesimal rotations of a rigid body about axes intersecting in one point can be replaced by a single rotation, represented by a vector equal to the geometric sum of the vectors of the given rotations, independently of the order in which they are carried out.

This can be extended to include small rotations of a rigid body. F i n i t e rotations are in fact noncommutative, but for small rotations the non-commutativity is of the second order. Consider two bodies subjected to equal small rotations in different sequences: in order to bring them into the same position it is then sufficient to rotate one of them about a suitably selected axis through an angle of the second-order referred to the angles of the small rotations.

FIGURE 19

Small finite rotations of a rigid body can therefore also be represented by vectors, oriented along the corresponding axes of rotation. Let the body undergo a rotation whose vector is the geometric sum of the vectors of given small rotations.

The position of the body will then differ by a small rotation of the second-order from the position which it would have occupied had it been subjected to all these small rotations in an arbitrary sequence. The same applies to the case when the vector of the small rotation is separated into components.

Consider as a first example the direction cosines of the coordinate system $x_1y_1z_1$ relative to the system $x_2y_2z_2$ obtained by rotating the first system through a small angle φ about an arbitrary axis (Figure 19). Let $\varphi_x, \ \varphi_y, \ \varphi_z$
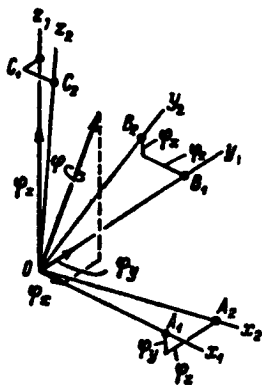
35

be the components of the vector φ along the axes x_1, y_1, z_1 and let OA_1, OB_1, OC_1 be unit lengths on these axes. Let A_2, B_2, C_2 be the positions which points A_1, B_1, C_1 occupy as a result of this small rotation. As can easily be seen from Figure 19, the coordinates of points A_2, B_2, C_2 in the coordinate system $x_1 y_1 z_1$ are, to a first-order approximation in φ_x, φ_y, φ_z,

$$
\begin{array}{llll}
A_2(& 1, & \varphi_z, & -\varphi_y); \\
B_2(-\varphi_z, & 1, & \varphi_x); \\
C_2(& \varphi_y, & -\varphi_x, & 1).
\end{array}
\tag{91}
$$

For instance, the point A_1 remains in place as a result of the rotation through a small angle φ_x about the x_1-axis; it moves a distance φ_y in the negative direction of the z_1-axis as a result of the counterclockwise rotation through a small angle φ_y about the y_1-axis; and it moves a distance φ_z in the positive direction of the y_1-axis as a result of the counterclockwise rotation through a small angle φ_z about the z_1-axis.

In accordance with (91) OA_2, OB_2, and OC_2 are unit lengths; thus, to a second-order approximation:

$$OA_2 = \sqrt{1 + \varphi_z^2 + \varphi_y^2} \cong 1.
\tag{92}$$

The coordinates of points A_2, B_2, and C_2 can therefore be considered as the direction cosines of the vectors OA_2, OB_2, and OC_2, i.e., of the axes x_2, y_2, z_2 relative to the system $x_1 y_1 z_1$. These direction cosines will therefore be

	x_1	y_1	z_1
x_2	1	φ_z	$-\varphi_y$
y_2	$-\varphi_z$	1	φ_x
z_2	φ_y	$-\varphi_x$	1

$$\tag{93}$$

The Table (80) of the direction cosines of the coordinate system $\xi_2\eta_2\zeta_2$ relative to the coordinate system $\xi_1\eta_1\zeta_1$, fixed respectively to the inner gimbal rings of two bicardan suspensions, having parallel outer ring and bow pivot axes, was derived in the preceding section. It was assumed there that the values β_1 and β_2 of the tilting angles of the outer gimbal rings of these suspensions relative to their suspension housings differ by the small angle $\Delta\beta$, and the values of the tilting angles α_1 and α_2 of the bows from their mid-positions by the small angle $\Delta\alpha$.

By the theory of small rotations of a rigid body the position of the coordinate system $\xi_2\eta_2\zeta_2$ can be considered to result from two successive rotations of the system $\xi_1\eta_1\zeta_1$, first through the angle $\Delta\beta$ about the y_1-axis and then through the angle $\Delta\alpha'$ about the ξ_2-axis (α' = angle of tilting of the inner gimbal ring relative to the outer ring).

According to (8):

$$\text{tg } \alpha' = \text{tg } \alpha_1 \cos \beta_1,
\tag{94}$$

from which it follows, to a first-order approximation in $\Delta\alpha$ and $\Delta\beta$:

$$\frac{\Delta\alpha'}{\cos^2 \alpha'} = \frac{\Delta\alpha}{\cos^2 \alpha_1} \cos \beta_1 - \Delta\beta \text{ tg } \alpha_1 \sin \beta_1.
\tag{95}$$

It follows from (10) and (12) that

$$\cos \alpha' = \frac{1}{R_1} \cos \alpha_1, \quad R_1 = \sqrt{1 - \sin^2 \alpha_1 \sin^2 \beta_1}.
\tag{96}$$

36

Inserting (96) into (95) gives

$$\Delta\alpha' = \frac{1}{R_1^2}\,(\Delta\alpha\cos\beta_1 - \Delta\beta\cos\alpha_1\sin\alpha_1\sin\beta_1). \tag{97}$$

According to (20) the y_1-axis, about which the inner ring is tilted through a small angle $\Delta\beta$, has the following direction cosines relative to the system $\xi_1\eta_1\zeta_1$:

$$0, \qquad \frac{1}{R_1}\cos\alpha_1, \qquad -\frac{1}{R_1}\sin\alpha_1\cos\beta_1.$$

The small rotation $\Delta\beta$ can therefore be separated into two rotations:
1) about the η_1-axis by the angle

$$\Delta\beta\,\frac{1}{R_1}\cos\alpha_1;$$

2) about the ζ_1-axis by the angle

$$-\Delta\beta\,\frac{1}{R_1}\sin\alpha_1\cos\beta_1.$$

The other small tilting of the inner ring through an angle $\Delta\alpha'$ is performed about the ξ_1-axis. The components in the system ξ_1, η_1, ζ_1 of the resulting tilting of the inner ring are therefore, for small variations of the angles α_1 and β_1 equal to

$$\varphi_\xi = \Delta\alpha' = \frac{1}{R_1^2}\,(\Delta\alpha\cos\beta_1 - \Delta\beta\cos\alpha_1\sin\alpha_1\sin\beta_1),$$

$$\varphi_\eta = \Delta\beta\,\frac{1}{R_1}\cos\alpha_1, \tag{98}$$

$$\varphi_\zeta = -\Delta\beta\,\frac{1}{R_1}\sin\alpha_1\cos\beta_1.$$

If the right-hand sides of these equations are expanded in powers of the variables α_1 and β_1 up to and including terms of the second order, the following formulas are obtained:

$$\varphi_\xi = \quad \Delta\alpha\Big(1 - \tfrac{1}{2}\beta_1^2\Big) - \Delta\beta\cdot\alpha_1\beta_1$$

$$\varphi_\eta = \quad \Delta\beta\Big(1 - \tfrac{1}{2}\alpha_1^2\Big), \tag{99}$$

$$\varphi_\zeta = -\Delta\beta\cdot\alpha_1.$$

The direction cosines of the system $\xi_2\eta_2\zeta_2$ relative to the system $\xi_1\eta_1\zeta_1$ can now be obtained by altering the symbols in (93) and using (99):

	ξ_1	η_1	ζ_1
ξ_2	1	$-\Delta\beta\cdot\alpha_1$	$-\Delta\beta\Big(1 - \tfrac{1}{2}\alpha_1^2\Big)$
η_2	$\Delta\beta\cdot\alpha_1$	1	$\Delta\alpha\Big(1 - \tfrac{1}{2}\beta_1^2\Big) - \Delta\beta\cdot\alpha_1\beta_1$
ζ_2	$\Delta\beta\Big(1 - \tfrac{1}{2}\alpha_1^2\Big)$	$-\Delta\alpha\Big(1 - \tfrac{1}{2}\beta_1^2\Big) + \\ + \Delta\beta\cdot\alpha_1\beta_1$	1

This same table was obtained in § 5 by purely analytical considerations (cf. Table 80).

When small rotations are considered, it is important to remember which of the given kinematically linked bodies undergoes any particular rotation. Otherwise errors are easily made. Thus, in the case just considered it would have been possible to consider erroneously that the small rotation of the inner ring consists of two small rotations: $\Delta\beta$ about the outer ring pivot axis y_1, and $\Delta\alpha$ about the bow pivot axis x_1. Using (20), the following incorrect formulas are then obtained for the components of the small tilting of the inner ring (instead of the correct ones (98)):

$$\varphi_\xi = \Delta\alpha \cos\beta_1;$$

$$\varphi_\eta = \Delta\alpha \frac{1}{R_1} \sin\alpha_1 \cos\beta_1 \sin\beta_1 + \Delta\beta \frac{1}{R_1} \cos\alpha_1;$$

$$\varphi_\zeta = \Delta\alpha \frac{1}{R_1} \cos\alpha_1 \sin\beta_1 - \Delta\beta \frac{1}{R_1} \sin\alpha_1 \cos\beta_1.$$

Actually, it is the bow, and not the inner ring which is tilted about the α_1-axis when β_1 varies while x_1 remains constant; the inner ring pivot axis of rotation coincides with that of the bow only for $\beta_1 = 0$, similarly, the inner and outer gimbal rings of the bicardan suspension are not tilted about the same axis when β_1 varies with α_1 constant (except when $\alpha_1 = 0$).

Consider now the problem of the variation of the polar coordinates of point S as a result of inaccurate horizontal stabilization. This problem was solved analytically in § 5.
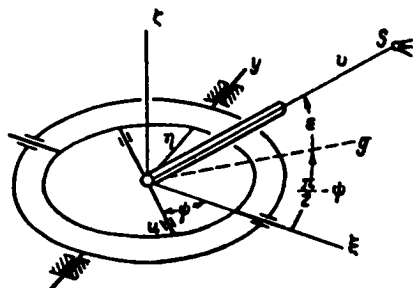

FIGURE 20

We mount a sight on the inner gimbal ring of the bicardan suspension, and aim its optical axis at the far-away point S (Figure 20). The angle ε between the optical axis and the plane of the inner ring is the angle of elevation, in accordance with the definitions of § 5; the angle φ between the sight's bearing axis u, located in the plane of the inner ring and the inner ring pivot axis ξ, is the course angle. This angle is equal to the angle between the projection g of the optical axis on the plane of the inner ring, and the ship's course line (the η-axis).

We alter by a small magnitude $\Delta\alpha$ the angle α_1 of the deviation of the bicardan-suspension bow (not shown in Figure 20) from its mid-position, and by a small magnitude $\Delta\beta$ the angle β_1 of the deviation of the outer gimbal ring from its mid-position, thus disturbing the horizontal stabilization of the inner ring. In order to bring back the optical axis to its original position, it is necessary to rotate the sight platform by a certain angle $\Delta\psi$ about

the ζ-axis (perpendicular to the plane of the inner ring) and, by rotating the sight about its bearing axis u, to alter the angle of elevation ε by $\Delta\varepsilon$. The angles $\Delta\varepsilon$ and $\Delta\phi$ represent the variation of the polar coordinates ε and ϕ of point S resulting from the disturbance by the angles $\Delta\alpha$ and $\Delta\beta$ of the horizontal stabilization of the inner gimbal ring.

We fix a uvw reference frame to the sight, and let u be the sight's bearing axis, v, its optical axis, and w, an axis perpendicular to both u and v and forming together with them a right-handed coordinate system.

Consider now the angular displacement of the sight produced by the variation of the angles α_1, β_1, ε, and ϕ.

Formulas (99), reduced (for simplicity's sake) to a first-order approximation in α_1 and β_1 become;

$$\varphi_\xi = \Delta\alpha,$$
$$\varphi_\eta = \Delta\beta,$$
$$\varphi_\zeta = -\alpha_1\Delta\beta. \tag{100}$$

The angular displacement of the sight caused by varying only the angles α and β will obviously equal that of the inner gimbal ring. The u, v, and w components of this angular displacement are equal (as can be seen from Figure 21), to

$$\varphi_\xi \cos\psi - \varphi_\eta \sin\psi = \Delta\alpha \cos\psi - \Delta\beta \sin\psi$$
$$(\varphi_\xi \sin\psi + \varphi_\eta \cos\psi)\cos\varepsilon + \varphi_\zeta \sin\varepsilon =$$
$$= (\Delta\alpha \sin\psi + \Delta\beta \cos\psi)\cos\varepsilon - \alpha_1\Delta\beta \sin\varepsilon, \tag{101}$$
$$-(\varphi_\xi \sin\psi + \varphi_\eta \cos\psi)\sin\varepsilon + \varphi_\zeta \cos\varepsilon =$$
$$= -(\Delta\alpha \sin\psi + \Delta\beta \cos\psi)\sin\varepsilon - \alpha_1\Delta\beta \cos\varepsilon.$$

A small variation of the angle ψ causes a rotation of the sight about the axis of its platform, i.e., about the ζ-axis; a small variation of the angle ε causes a rotation of the sight about its bearing axis, i.e., about the u-axis.
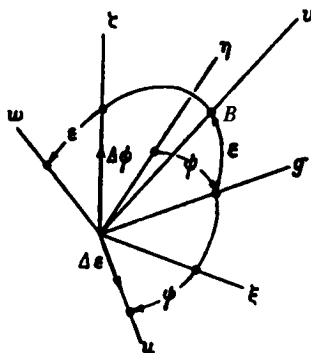

FIGURE 21

The u, v, w components of the angular displacement of the sight caused by the variation of the angles ε and ϕ will therefore be (taking into account that $\Delta\phi < 0$ for a counterclockwise rotation, as viewed from the positive ζ direction):

$$\Delta\varepsilon, \quad -\Delta\phi \sin\varepsilon, \quad -\Delta\phi \cos\varepsilon. \tag{102}$$

The vector of the resultant angular displacement of the sight caused by the variation of all the angles (α_1, β_1, ε, ψ), will equal the geometric sum of the vectors of the separate rotations. The u, v, and w components of this resultant rotation are:

$$\varphi_u = \Delta\alpha \cos\psi - \Delta\beta \sin\psi + \Delta\varepsilon,$$

$$\varphi_v = (\Delta\alpha \sin\psi + \Delta\beta \cos\psi) \cos\varepsilon - \alpha_1 \Delta\beta \sin\varepsilon - \Delta\psi \sin\varepsilon, \qquad (103)$$

$$\varphi_w = -(\Delta\alpha \sin\psi + \Delta\beta \cos\psi) \sin\varepsilon - \alpha_1 \Delta\beta \cos\varepsilon - \Delta\psi \cos\varepsilon.$$

The displacements of point B on the v-axis (OB is of unit length) in the directions of the axes u, v, and w (Figure 21), are by (91):

$$-\varphi_w, \qquad 0, \qquad \varphi_u. \qquad (104)$$

The optical axis of the sight will therefore remain in place if the components φ_u and φ_w of the resultant rotation are zero, i.e., if the following equations are satisfied (according to (103)):

$$\Delta\alpha \cos\psi - \Delta\beta \sin\psi + \Delta\varepsilon = 0,$$

$$(\Delta\alpha \sin\psi + \Delta\beta \cos\psi) \sin\varepsilon + \alpha_1 \Delta\beta \cos\varepsilon + \Delta\psi \cos\varepsilon = 0. \qquad (105)$$

The variations of the polar coordinates of the point S are, by (105):

$$\Delta\varepsilon = -\Delta\alpha \cos\psi + \Delta\beta \sin\psi,$$

$$\Delta\psi = -\alpha_1 \Delta\beta - (\Delta\alpha \sin\psi + \Delta\beta \cos\psi) \, \mathrm{tg}\,\varepsilon.$$

These expressions are identical with (90) of § 5.

The component φ_v in (103) represents the small angle of rotation of the sight about its optical axis v, caused by the disturbance of the horizontal stabilization and the variation of the angles ε and ψ. When conditions (105) are satisfied, i.e., when the sight's optical axis remains at rest, the angle $\Delta\psi$ can be eliminated from the expression for φ_v by means of the second equation (90). The rotation of the sight about its optical axis then becomes

$$\varphi_v = \frac{\Delta\alpha \sin\psi + \Delta\beta \cos\psi}{\cos\varepsilon}. \qquad (106)$$

This derivation is based entirely on a geometric consideration.

§ 7. Variation of the ship's roll and pitch angles
and of its course caused by a finite rotation of the
ship about an arbitrary axis

Laboratory tests of gyroscopic devices such as the gyroazimuthhorizon are frequently carried out by rotating the housings of these devices through finite angles about an inclined axis. If gyroscopes stabilize the inner ring of the bicardan suspension (Figure 7) in the horizontal plane and stabilize in addition a certain direction in this plane, then, when the housing is rotated, the suspension scales will indicate the pitch and roll angles α and β, while the inner ring will indicate the variation of the angle γ between the course line and the stabilized direction in the horizontal plane.

We must now determine the magnitudes of the angles α, β, γ from the specified rotation of the bicardan suspension housing from its initial position (at which $\alpha = \beta = 0$) and from the specified disposition of the axis of this rotation relative to the housing.

This problem is equivalent to the problem of determining the variation of the ship's pitch and roll angles and course for a finite angular displacement of the ship from one position to another one. In fact, according to a well-known theorem of kinematics, such a displacement can be obtained by means of a single finite rotation of the ship (neglecting translatory motion) about a suitable axis. Conversely, the pitch and roll angles and the course determine uniquely the orientation in space of a ship whose location is given.
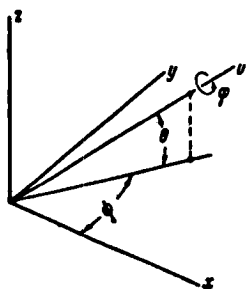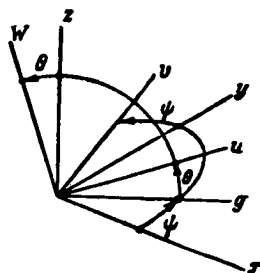

FIGURE 22   FIGURE 23

It should be noted that the replacement of a specific motion of a gyro-system housing by some other simplified motion may in many other cases lead to errors: this will be discussed in Chapter II, § 3.

Using the notation of § 1 (Figure 7), we assume a coordinate system xyz to be fixed to the bicardan suspension housing, with the x-axis directed along the bow pivot axis, the y-axis along the pivot axis of the outer gimbal ring, and the z-axis perpendicular to these two and directed upward.

We denote by u (Figure 22) the axis about which the housing of the bicardan suspension can rotate together with the system xyz. We further denote by θ the angle between the u-axis and the xy plane, and by ϕ the angle between the x-axis and the projection of the u-axis on this plane.

Consider now an auxiliary coordinate system uvw (Figure 23), in which the u-axis is, as above, the axis about which the bicardan suspension housing can rotate; the v-axis lies in the xy plane and is perpendicular to the projection of the u-axis on this plane; the w-axis is perpendicular to the axes u and v and forms together with them a right-handed coordinate system. The angle between the axes w and z is obviously equal to θ.

It is seen from Figure 23 that the direction cosines of the system xyz relative to the system uvw are:

	x	y	z	
u	$\cos\theta\cos\phi$	$\cos\theta\sin\phi$	$\sin\theta$	
v	$-\sin\phi$	$\cos\phi$	0	(107)
w	$-\sin\theta\cos\phi$	$-\sin\theta\sin\phi$	$\cos\theta$	

41

Assume, in accordance with the formulation of the problem, that the xy plane was horizontal before the rotation of the suspension housing about the u-axis. Introduce two fixed coordinate systems $x^0y^0z^0$ and $u^0v^0w^0$, whose axes coincide respectively with the axes of the coordinate systems xyz and uvw before the rotation of the housing. The x^0y^0 plane is thus horizontal.
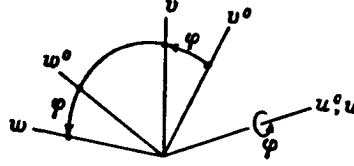

FIGURE 24

The direction cosines of the system $x^0y^0z^0$ relative to the system $u^0v^0w^0$ are obviously identical to the direction cosines of the system xyz relative to the system uvw, given by (107):

	x^0	y^0	z^0	
u^0	$\cos\theta\cos\phi$	$\cos\theta\sin\phi$	$\sin\theta$	
v^0	$-\sin\phi$	$\cos\phi$	0	(108)
w^0	$-\sin\theta\cos\phi$	$-\sin\theta\sin\phi$	$\cos\theta$	

After the rotation of the housing through an angle φ about the u-axis (Figure 24), which remains identical with the u^0-axis, the direction cosines of the system uvw relative to the system $u^0v^0w^0$ will be:

	u^0	v^0	w^0	
u	1	0	0	
v	0	$\cos\varphi$	$\sin\varphi$	(109)
w	0	$-\sin\varphi$	$\cos\varphi$	

The direction cosines of the system uvw relative to the system $x^0y^0z^0$ are found from (108) and (109):

$$\cos x^0v = \cos x^0u^0\cos vu^0 + \cos x^0v^0\cos vv^0 + \cos x^0w^0\cos vw^0 =$$
$$= -\sin\psi\cos\varphi - \sin\theta\cos\phi\sin\varphi.$$

The direction cosines are:

	x^0	y^0	z^0	
u	$\cos\theta\cos\phi$	$\cos\theta\sin\phi$	$\sin\theta$	
v	$-\sin\phi\cos\varphi -$ $-\sin\theta\cos\phi\sin\varphi$	$\cos\phi\cos\varphi -$ $-\sin\theta\sin\phi\sin\varphi$	$\cos\theta\sin\varphi$	(110)
w	$\sin\phi\sin\varphi -$ $-\sin\theta\cos\phi\cos\varphi$	$-\cos\psi\sin\varphi -$ $-\sin\theta\sin\phi\cos\varphi$	$\cos\theta\cos\varphi$	

42

Tables (107) and (110) determine the direction cosines of the system *uvw* relative to the systems *xyz* and $x^0y^0z^0$. The direction cosines of the system *xyz* relative to the system $x^0y^0z^0$ can therefore be obtained from them:

	x^0	y^0	z^0
x	$\mu \cos\theta \cos^2\psi + \cos\varphi$	$\mu \cos\theta \cos\psi \sin\psi + \sin\theta \sin\varphi$	$\mu \sin\theta \cos\psi - \cos\theta \sin\psi \sin\varphi$
y	$\mu \cos\theta \cos\psi \sin\psi - \sin\theta \sin\varphi$	$\mu \cos\theta \sin^2\psi + \cos\varphi$	$\mu \sin\theta \sin\psi + \cos\theta \cos\psi \sin\varphi$
z	$\mu \sin\theta \cos\psi + \cos\theta \sin\psi \sin\varphi$	$\mu \sin\theta \sin\psi - \cos\theta \cos\psi \sin\varphi$	$(1 - \cos\varphi)\sin^2\theta + \cos\varphi$

(111)

where

$$\mu = (1 - \cos\varphi) \cos\theta.$$

Table (111) gives the direction cosines between two coordinate systems obtained from each other by means of a finite rotation through an angle φ about an axis passing through their origin.

The inner ring of the bicardan suspension is stabilized in the horizontal plane. The ζ-axis which is perpendicular to the plane of the inner ring coincides therefore with the z^0-axis which is perpendicular to the horizontal plane; their direction cosines relative to the axes *x*, *y*, *z* are respectively equal.

The direction cosines of the system $\xi\eta\zeta$ (fixed to the inner ring of the bicardan suspension) relative to the coordinate system *xyz* are given by (18):

	x	y	z
ξ	$\cos\beta$	0	$-\sin\beta$
η	$\frac{1}{R} \sin\alpha \cos\beta \sin\beta$	$\frac{1}{R} \cos\alpha$	$\frac{1}{R} \sin\alpha \cos^2\beta$
ζ	$\frac{1}{R} \cos\alpha \sin\beta$	$-\frac{1}{R} \sin\alpha \cos\beta$	$\frac{1}{R} \cos\alpha \cos\beta$

where

$$R = \sqrt{1 - \sin^2\alpha \sin^2\beta}.$$

The following equations, obtained from (18) and (111), express the equality of the direction cosines of the axes ζ and z^0 relative to the axes *x*, *y*, *z*:

$$\frac{1}{R} \cos\alpha \sin\beta = (1 - \cos\varphi) \cos\theta \sin\theta \cos\psi - \cos\theta \sin\psi \sin\varphi;$$

$$-\frac{1}{R} \sin\alpha \cos\beta = (1 - \cos\varphi) \cos\theta \sin\theta \sin\psi + \cos\theta \cos\psi \sin\varphi; \quad (112)$$

$$\frac{1}{R} \cos\alpha \cos\beta = (1 - \cos\varphi) \sin^2\theta + \cos\varphi.$$

Each of these equations follows from the other two.

Using equations (112), the angles of tilting α and β of the bow and the outer ring relative to the housing can be found for given angles ψ, θ, φ.

If the angles θ and φ are assumed to be small, the first two equations of (112) become, to a second-order approximation in θ and φ:

$$\alpha = -\varphi \cos\psi, \quad \beta = -\varphi \sin\psi. \quad (113)$$

43

Formulas (113) become more accurate if we retain third-order terms in θ and φ in the expansions of the right-hand sides of (112), and insert (113) into the terms of higher order in α and β in the expansions of the left-hand sides of (112):

$$\alpha = -\varphi \cos\psi - \frac{\theta\varphi^2}{2}\sin\psi + \frac{\theta^2\varphi}{2}\cos\psi - \frac{\varphi^3}{2}\cos\psi\sin^2\psi,$$

$$\beta = -\varphi\sin\psi + \frac{\theta\varphi^2}{2}\cos\phi + \frac{\theta^2\varphi}{2}\sin\psi - \frac{\varphi^3}{2}\cos^2\phi\sin\phi. \tag{114}$$

The coordinate systems $\xi\eta\zeta$, xyz, and $x^0y^0z^0$ coincide for $\varphi = 0$; when $\varphi \neq 0$, the coordinate system $\xi\eta\zeta$ is rotated about the ζ-axis relative to the fixed coordinate system $x^0y^0z^0$ by a certain angle γ (Figure 25). The following relationship is obtained from (18) and (111):

$$\sin\gamma = \cos\xi y^0 = \cos\xi x \cos y^0 x + \cos\xi y \cos y^0 y + \cos\xi z \cos y^0 z =$$

$$= \cos\beta\,[(1 - \cos\varphi)\cos^2\theta\cos\psi\sin\psi + \sin\theta\sin\varphi] -$$

$$- \sin\beta\,[(1 - \cos\varphi)\cos\theta\sin\theta\sin\psi - \cos\theta\cos\psi\sin\varphi]. \tag{115}$$

Equation (115) defines the angle γ of the rotation of the inner ring about the ζ-axis for finite rotations of the housing about the u-axis. The rotation
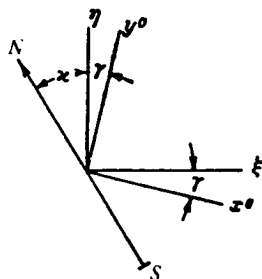

FIGURE 25

is counterclockwise for $\gamma > 0$ (when observed from above); the course, i.e., the angle $\varkappa$ between the north-south line and the η-axis, is therefore reduced by γ when the housing is inclined (Figure 25).

Equation (115) becomes, to a second-order approximation in θ and φ:

$$\gamma = \theta\varphi + \frac{1}{2}\varphi^2\cos\phi\sin\phi + \beta\varphi\cos\phi. \tag{116}$$

Inserting the second equation of (113) yields

$$\gamma = \theta\varphi - \frac{1}{2}\varphi^2\cos\phi\sin\phi. \tag{117}$$

A more accurate formula for γ can be obtained by retaining in the expansions of the right-and left-hand sides of (115) terms of higher order than the second in θ, φ, and γ.

Tiltings of the housing through the same angle but in opposite directions about the u-axis cause different rotations from the initial position ($\varphi = 0$) in the horizontal plane of the inner gimbal ring.

Numerical example. Let the suspension housing undergo oscillations of amplitude $\varphi_a = 0.300\ (17°11')$ about the u-axis, let the u-axis form

44

an angle $\theta = 0.200$ (11°28') with the horizontal plane, and let the projection of this axis on the xy plane bisect the angle between the bow pivot axis x and the outer gimbal-ring pivot axis y ($\phi = 45°$).

The approximation formulas (113) and (117) yield:

1) for $\varphi = +0.300$

$$\alpha = -\varphi \cos \phi = -0.212 \,(12°9'),$$

$$\beta = -\varphi \sin \phi = -0.212 \,(12°9'),$$

$$\gamma = \theta\varphi - \frac{1}{2} \varphi^2 \cos \phi \sin \phi = 0.0600 - 0.0225 = 0.0375 \,(2°9');$$

2) for $\varphi = -0.300$

$$\alpha = +0.212 \,(12°9'),$$

$$\beta = +0.212 \,(12°9'),$$

$$\gamma = -0.0600 - 0.0225 = -0.0825 \,(4°43').$$

On the other hand the accurate formulas (112) and (115) yield:

1) for $\varphi = +0.300$

$$\alpha = -0.217, \quad \beta = -0.205, \quad \gamma = 0.0381;$$

2) for $\varphi = -0.300$

$$\alpha = +0.205, \quad \beta = +0.217, \quad \gamma = 0.0820.$$

The approximate formulas (113) and (117) are accurate up to the second figure after the decimal point for α and β, and up to the third figure after the decimal point for γ. Formulas (114) for α and β are accurate to the third figure after the decimal point; they yield:

$$\text{for } \varphi = +0.300 \quad \alpha = -0.217, \quad \beta = -0.205;$$

$$\text{for } \varphi = -0.300 \quad \alpha = +0.205, \quad \beta = +0.217.$$

The angular velocities of the bow and the outer ring relative to the housing and the inner ring relative to an object fixed in space can be obtained by differentiating the approximate equations (113) and (117). Assume, for instance, that the law of variation with time of φ is expressed by

$$\varphi = \varphi_a \sin \omega t. \tag{118}$$

Inserting this expression into (113) and (117) gives

$$\alpha = -\varphi_a \cos \phi \sin \omega t,$$

$$\beta = -\varphi_a \sin \phi \sin \omega t,$$

$$\gamma = \theta\varphi_a \sin \omega t - \frac{1}{2} \varphi_a^2 \cos \phi \sin \phi \sin^2 \omega t = \tag{119}$$

$$= -\frac{1}{4} \varphi_a^2 \cos \phi \sin \phi + \theta\varphi_a \sin \omega t + \frac{1}{4} \varphi_a^2 \cos \phi \sin \phi \cos 2\omega t,$$

whence

$$\frac{d\alpha}{dt} = -\omega\varphi_a \cos \phi \cos \omega t,$$

$$\frac{d\beta}{dt} = -\omega\varphi_a \sin \phi \cos \omega t, \tag{120}$$

$$\frac{d\gamma}{dt} = \omega\theta\varphi_a \cos \omega t - \frac{1}{2} \omega\varphi_a^2 \cos \phi \sin \phi \sin 2\omega t.$$

In this case the motion of the inner gimbal ring represents a superposition of two harmonic oscillations, with frequencies ω and 2ω about the vertical ζ-axis.

45

Chapter II

ORIENTATION OF GYRO-CONTROLLED OBJECTS

§ 1. The orientation accuracy of an object launched
from an inclined base

The problem of the orientation of an object moving in steady motion shortly after being launched from an inclined base is similar to the problems treated in Chapter I.

We denote by ϑ_1 and ψ_1 the heel and trim of the base at the moment the object starts moving, and by ϑ and ψ the heel and trim of the object during steady motion.

As in Chapter I, § 1, the trim is defined as the angle formed by the longitudinal axis of the base or object with the horizontal plane; it is positive when the base or object are inclined forward. The heel is defined as the bihedral angle between the plane of symmetry of the base or object and the vertical plane containing their longitudinal axis; it is positive when the base or object are inclined to the right.

Let the object be launched from a starting device whose axis is parallel to the base plane and forms a small angle δ with the latter's longitudinal axis. It will be assumed that the gyroscopic device (top) is started simultaneously with the launching of the object, and that at the start the top axis is either parallel to the longitudinal axis of the object or perpendicular to its plane of symmetry, depending on the instrument design. In the latter case it will be assumed that when the object is on the carrying base its plane of symmetry is perpendicular to the plane of the base.

Since the time required for the object's motion to become steady is relatively short, it can be assumed that the top axis has at the beginning of the steady motion the same orientation as at the start.

The pivot axis of the outer gimbal ring of the top's gimbal system lies in the plane of symmetry of the object, and is perpendicular to its longitudinal axis. It will be assumed that the instrument is installed very accurately, so that mounting errors can be neglected. Throughout the motion the controlling instrument maintains the object in a position in which the latter's longitudinal axis is either perpendicular to the plane of the outer ring or parallel to it, depending upon the instrument design.

The small oscillatory motions of the object, and in particular its yaw can therefore be neglected in the calculations, and it can be assumed that during steady motion the angle which the object's longitudinal axis forms with the perpendicular to the plane of the outer gimbal ring is either zero or a right angle. The angle between the top axis and the perpendicular to the plane of the outer gimbal ring will be denoted by β. In technical language this angle is called the t o p   i n c l i n a t i o n (cf. Chapter VI, § 3).

We denote by x_1 the course of the base at the instant the object is started, and by x the course of the object during steady motion, the course being defined as the angle between the north-south line and the projection of the longitudinal axis of the base or the object on the horizontal plane (cf. Chapter I, § 1).

It is easily seen that if the heel and trim of both base and object are zero, then

$$x = x_1 + \delta, \tag{121}$$

i.e., the longitudinal axis of the object remains parallel to the position which the axis of the starting device occupied at the start*.

In the general case

$$x = x_1 + \delta + \gamma. \tag{122}$$

The angle γ is the error in the orientation of the object caused by the heel and trim of the base (ϑ_1, ψ_1) at the start and by the heel and trim of the object itself (ϑ, ψ) during its steady motion.

We are trying to find a relationship $\gamma = f(\vartheta_1, \psi_1, \vartheta, \psi; \delta)$ between the angle γ and the angles ϑ_1, ψ_1, ϑ, ψ for given values of the angle δ.
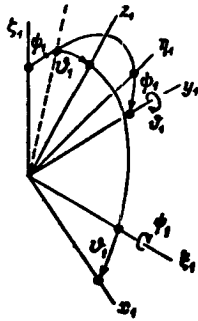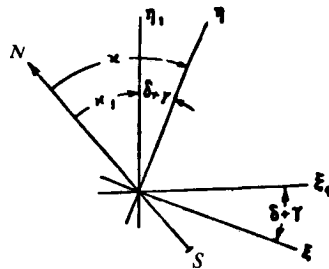

FIGURE 26   FIGURE 27

We introduce a coordinate system $\xi_1 \eta_1 \zeta_1$ (Figure 26), whose η_1-axis is the projection on the horizontal plane of the longitudinal axis y_1 of the base, and whose ζ_1-axis is vertical and directed upward. The angle x_1 (Figure 27) between the η_1-axis and the north-south line defines the course of the base. We introduce also a coordinate system $x_1 y_1 z_1$ fixed to the base (Figure 26), with the z_1-axis perpendicular to the plane of the base and directed upward, and the y_1-axis coinciding (as already mentioned above) with the longitudinal axis of the base.

It is easily seen that the direction cosines of the coordinate system $x_1 y_1 z_1$ relative to the system $\xi_1 \eta_1 \zeta_1$ are as follows:

	ξ_1	η_1	ζ_1	
x_1	$\cos \vartheta_1$	$-\sin \psi_1 \sin \vartheta_1$	$-\cos \phi_1 \sin \vartheta_1$	
y_1	0	$\cos \phi_1$	$-\sin \phi_1$	(123)
z_1	$\sin \vartheta_1$	$\sin \psi_1 \cos \vartheta_1$	$\cos \phi_1 \cos \vartheta_1$	

* We consider here the case in which angular adjustment of the gyroscopic instrument is made to compensate for the angle δ. The latter case will be considered later.

We also introduce a coordinate system $\xi\eta\zeta$, whose η-axis is the projection on the horizontal plane of the longitudinal axis y of the object, and whose ζ-axis is vertical (Figure 28). The angle x between the η-axis and the north-south line is the course of the moving object (Figure 27).

It follows from (122) that the angle between the axes η and η_1 (or, which is the same, between the axes ξ and ξ_1) is equal to $\delta+\gamma$. The direction cosines of the coordinate system $\xi_1\eta_1\zeta_1$ relative to the system $\xi\eta\zeta$, are therefore

$$
\begin{array}{cccc}
 & \xi & \eta & \zeta \\
\xi_1 & \cos(\gamma+\delta) & \sin(\gamma+\delta) & 0 \\
\eta_1 & -\sin(\gamma+\delta) & \cos(\gamma+\delta) & 0 \\
\zeta_1 & 0 & 0 & 1
\end{array}
\tag{124}
$$

The direction cosines of the system $x_1y_1z_1$ relative to the system $\xi\eta\zeta$ are finally obtained from (123) and (124):

$$
\begin{array}{cccc}
 & \xi & \eta & \zeta \\
x_1 & \begin{aligned}&\cos\vartheta_1\cos(\gamma+\delta)+\\&+\sin\psi_1\sin\vartheta_1\sin(\gamma+\delta)\end{aligned} & \begin{aligned}&\cos\vartheta_1\sin(\gamma+\delta)-\\&-\sin\psi_1\sin\vartheta_1\cos(\gamma+\delta)\end{aligned} & -\cos\psi_1\sin\vartheta_1 \\
y_1 & -\cos\psi_1\sin(\gamma+\delta) & \cos\psi_1\cos(\gamma+\delta) & -\sin\psi_1 \\
z_1 & \begin{aligned}&\sin\vartheta_1\cos(\gamma+\delta)-\\&-\sin\psi_1\cos\vartheta_1\sin(\gamma+\delta)\end{aligned} & \begin{aligned}&\sin\vartheta_1\sin(\gamma+\delta)+\\&+\sin\psi_1\cos\vartheta_1\cos(\gamma+\delta)\end{aligned} & \cos\psi_1\cos\vartheta_1
\end{array}
\tag{125}
$$

Consider first the design of a gyroscopic control instrument with the top axis parallel to the object's longitudinal axis at the start, and therefore parallel to the axis of the starting device.
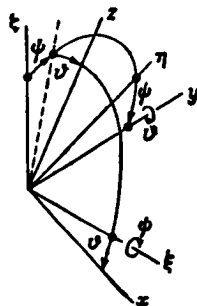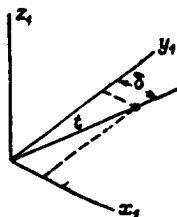

FIGURE 28   FIGURE 29

The projection of a unit length t of this axis on the axes x_1, y_1, and z_1 fixed to the base are equal to (Figure 29):

$$
\begin{aligned}
t_{x_1} &= \sin\delta, \\
t_{y_1} &= \cos\delta, \\
t_{z_1} &= 0.
\end{aligned}
\tag{126}
$$

The projections of this unit length on the axes ξ, η, and ζ can now be found by the well-known formula of analytical geometry:

$$
t_\xi = t_{x_1}\cos x_1\xi + t_{y_1}\cos y_1\xi + t_{z_1}\cos z_1\xi.
$$

48

The following expressions are obtained:

$$t_\xi = \quad [\cos \vartheta_1 \cos (\gamma + \delta) + \sin \psi_1 \sin \vartheta_1 \sin (\gamma + \delta)] \sin \delta -$$
$$- \cos \psi_1 \sin (\gamma + \delta) \cos \delta,$$

$$t_\eta = \quad [\cos \vartheta_1 \sin (\gamma + \delta) - \sin \psi_1 \sin \vartheta_1 \cos (\gamma + \delta)] \sin \delta + \qquad (127)$$
$$+ \cos \psi_1 \cos (\gamma + \delta) \cos \delta,$$

$$t_\zeta = -\cos \psi_1 \sin \vartheta_1 \sin \delta - \sin \psi_1 \cos \delta.$$

Since the top axis maintains its direction in space, formulas (127) are also true for the projections of a unit length of the top axis on these same axes.

Consider the projections of this unit length on the axes of the system xyz fixed to the moving object. The longitudinal axis of the object is perpendicular to the plane of the outer gimbal ring. It follows (Figure 30) that the top axis H lies in the plane of symmetry of the moving object and forms an unknown angle β with the longitudinal axis (top inclination). The projections of unit length t on the axes of the coordinate system xyz are equal to

$$t_x = \quad 0,$$
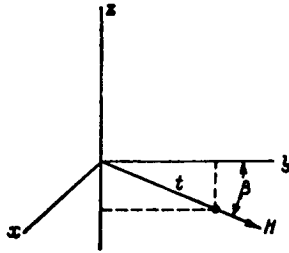$$t_y = \quad \cos \beta, \qquad (128)$$
$$t_z = -\sin \beta.$$

FIGURE 30

The direction cosines of the system xyz relative to the system $\xi\eta\zeta$ are identical with the direction cosines of the system $x_1y_1z_1$ relative to the system $\xi_1\eta_1\zeta_1$ given by (123),

	ξ	η	ζ
x	$\cos \vartheta$	$-\sin \psi \sin \vartheta$	$-\cos \psi \sin \vartheta$
y	0	$\cos \psi$	$-\sin \psi$
z	$\sin \vartheta$	$\sin \psi \cos \vartheta$	$\cos \psi \cos \vartheta$

(129)

The projections of unit length t on the axes ξ, η, and ζ can now be found from (129) and (128):

$$t_\xi = -\sin \vartheta \sin \beta,$$
$$t_\eta = \quad \cos \psi \cos \beta - \sin \psi \cos \vartheta \sin \beta, \qquad (130)$$
$$t_\zeta = -\sin \psi \cos \beta - \cos \psi \cos \vartheta \sin \beta.$$

49

Formulas (127) were previously obtained for the same projections. The following three relationships are obtained by equating the right-hand sides of (127) and (130):

$$[\cos \vartheta_1 \cos (\gamma + \delta) + \sin \psi_1 \sin \vartheta_1 \sin (\gamma + \delta)] \sin \delta -$$
$$- \cos \psi_1 \sin (\gamma + \delta) \cos \delta = -\sin \vartheta \sin \beta;$$

$$[\cos \vartheta_1 \sin (\gamma + \delta) - \sin \psi_1 \sin \vartheta_1 \cos (\gamma + \delta)] \sin \delta + \qquad (131)$$
$$+ \cos \psi_1 \cos (\gamma + \delta) \cos \delta = \cos \psi \cos \beta - \sin \psi \cos \vartheta \sin \beta;$$

$$-\cos \psi_1 \sin \vartheta_1 \sin \delta - \sin \psi_1 \cos \delta = -\sin \psi \cos \beta - \cos \psi \cos \vartheta \sin \beta.$$

Only two out of these three relationships are independent. The unknowns are the angles β and γ, and the angles ϑ_1, ψ_1, ϑ, ψ, δ must be given.

For $\delta = 0$ and $\psi = 0$ (i.e., when the axis of the starting device is parallel to the longitudinal axis of the base, and the trim of the object is zero), (131) becomes

$$-\cos \psi_1 \sin \gamma = -\sin \vartheta \sin \beta,$$
$$\cos \psi_1 \cos \gamma = \cos \beta, \qquad (132)$$
$$-\sin \psi_1 = -\cos \vartheta \sin \beta.$$

Dividing both sides of the first of equations (132) by the respective sides of the third of these equations, we obtain

$$\sin \gamma = \operatorname{tg} \vartheta \operatorname{tg} \psi_1. \qquad (133)$$

This formula gives the angle γ for $\delta = 0$, $\psi = 0$.
For $\psi_1 = 4°$ and $\vartheta = 10°$,

$$\sin \gamma = 0.0123; \quad \gamma = 42'.$$

Formula (133) could be obtained more simply by assuming from the beginning that the trim of the moving object is zero and that the axis of its starting device is parallel to the longitudinal axis of the base. It then becomes clear why the value of the base heel angle ϑ_1 has in this case (and also in the case $\delta = 0$, $\psi \neq 0$) no influence on the value of the error γ in the course of the moving object and therefore does not appear in (133).

We assume that the angle δ between the axis of the starting device and the longitudinal axis of the base, and the object trim ψ are of the order of several degrees. The numerical example using formula (133) shows that the deviation γ of the object from the course caused by the heel of the object and the trim of the base is also small. The angles δ, ψ, and γ will therefore be considered so small that their squares and products can be neglected. The expansion of the right- and left-hand sides of equations (131) neglecting all terms of higher order than the first in δ, ψ, γ yields:

$$\delta \cos \vartheta_1 - (\gamma + \delta) \cos \psi_1 = -\sin \vartheta \sin \beta,$$
$$-\delta \sin \psi_1 \sin \vartheta_1 + \cos \psi_1 = \cos \beta - \psi \cos \vartheta \sin \beta, \qquad (134)$$
$$-\delta \cos \psi_1 \sin \vartheta_1 - \sin \psi_1 = -\psi \cos \beta - \cos \vartheta \sin \beta.$$

Multiplying the second equation of (134) by ψ, adding to the third equation of (134), and neglecting second-order terms in δ and ψ, yields:

$$-\delta \cos \psi_1 \sin \vartheta_1 + \psi \cos \psi_1 - \sin \psi_1 = -\cos \vartheta \sin \beta. \qquad (135)$$

50

Dividing both sides of the first equation (134) by the corresponding sides of equation (135) gives, after some simplifications, the required formula:

$$\tau = \operatorname{tg} \psi_1 \operatorname{tg} \vartheta + \left(\frac{\cos \vartheta_1}{\cos \psi_1} + \sin \vartheta_1 \operatorname{tg} \vartheta - 1 \right) \delta - \phi \operatorname{tg} \vartheta. \qquad (136)$$

Numerical example. Let

$$\vartheta_1 = 8^\circ, \quad \psi_1 = 4^\circ, \quad \vartheta = 10^\circ, \quad \phi = -2^\circ, \quad \delta = 6^\circ,$$

then

$$\tau = 0.0123 + 0.0017 + 0.0062 = 0.0202 \quad (1^\circ 10').$$

Formula (136) and the numerical example show how important it is for orientation accuracy to obtain as small a steady-motion heel angle ϑ of the moving object as possible. This applies to a gyroscopic instrument in which the top axis coincides, at the beginning of the motion, with the longitudinal axis of the object.

Consider now an instrument whose top is started in a position in which its axis is perpendicular to the object's plane of symmetry. It was assumed above that the object's plane of symmetry is perpendicular to the base plane when the object is still in the starting device. The projections
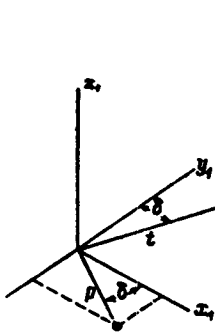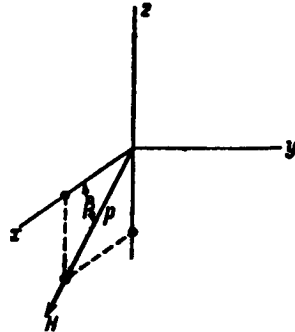

FIGURE 31   FIGURE 32

of a unit length p of the top axis on the axes of the coordinate system $x_1 y_1 z_1$ fixed to the base are (Figure 31):

$$\begin{aligned} p_{x_1} &= \cos \delta, \\ p_{y_1} &= -\sin \delta, \\ p_{z_1} &= 0. \end{aligned} \qquad (137)$$

The projections of this unit length on the axes of the coordinate system $\xi \eta \zeta$ can be found by using Table (125) of the direction cosines of the system $x_1 y_1 z_1$ relative to the system $\xi \eta \zeta$:

$$p_\xi = [\cos \vartheta_1 \cos(\tau + \delta) + \sin \psi_1 \sin \vartheta_1 \sin(\tau + \delta)] \cos \delta +$$
$$+ \cos \psi_1 \sin(\tau + \delta) \sin \delta;$$

$$p_\eta = [\cos \vartheta_1 \sin(\tau + \delta) - \sin \psi_1 \sin \vartheta_1 \cos(\tau + \delta)] \cos \delta - \qquad (138)$$
$$- \cos \psi_1 \cos(\tau + \delta) \sin \delta;$$

$$p_\zeta = -\cos \psi_1 \sin \vartheta_1 \cos \delta + \sin \psi_1 \sin \delta.$$

We now find the same projections as functions of the angles ϑ, ψ, and β referred to the moving object. Due to the action of the control system the longitudinal axis of the object lies in the plane of the outer gimbal ring and is therefore parallel to the pivot axis of the inner gimbal ring. The projections of p on the axes of the coordinate system xyz fixed to the moving object are (Figure 32):

$$p_x = \cos\beta,$$
$$p_y = 0, \qquad\qquad (139)$$
$$p_z = -\sin\beta.$$

The following expressions are now obtained from (129) for the projections of p on the axes of the coordinate system $\xi\eta\zeta$:

$$p_\xi = \cos\vartheta\cos\beta - \sin\vartheta\sin\beta;$$
$$p_\eta = -\sin\phi\sin\vartheta\cos\beta - \sin\psi\cos\vartheta\sin\beta; \qquad (140)$$
$$p_\zeta = -\cos\phi\sin\vartheta\cos\beta - \cos\psi\cos\vartheta\sin\beta.$$

Three equations, each of which follows from the other two, are obtained by equating the right-hand sides of (138) and (140):

$$[\cos\vartheta_1\cos(\gamma+\delta) + \sin\psi_1\sin\vartheta_1\sin(\gamma+\delta)]\cos\delta +$$
$$+ \cos\psi_1\sin(\gamma+\delta)\sin\delta = \cos\vartheta\cos\beta - \sin\vartheta\sin\beta;$$
$$[\cos\vartheta_1\sin(\gamma+\delta) - \sin\psi_1\sin\vartheta_1\cos(\gamma+\delta)]\cos\delta -$$
$$- \cos\psi_1\cos(\gamma+\delta)\sin\delta = -\sin\psi\sin\vartheta\cos\beta - \sin\psi\cos\vartheta\sin\beta; \qquad (141)$$
$$- \cos\psi_1\sin\vartheta_1\cos\delta + \sin\psi_1\sin\delta =$$
$$= -\cos\phi\sin\vartheta\cos\beta - \cos\psi\cos\vartheta\sin\beta.$$

The unknowns in (141) are the angles β and γ.

Dividing both sides of the second equation (141) by the corresponding sides of the third equation gives:

$$\frac{[\cos\vartheta_1\sin(\gamma+\delta) - \sin\psi_1\sin\vartheta_1\cos(\gamma+\delta)]\cos\delta - \cos\psi_1\cos(\gamma+\delta)\sin\delta}{-\cos\psi_1\sin\vartheta_1\cos\delta + \sin\psi_1\sin\delta} =$$
$$= \mathrm{tg}\,\phi. \qquad (142)$$

It follows that the error γ in the course of the moving object is in this case (top axis perpendicular at the start to the object's plane of symmetry) independent of the object's heel ϑ. This is easily understood, since the inner gimbal-ring pivot axis of the top is parallel to the object's longitudinal axis during steady motion of the latter.

For $\phi = 0$ (the object has no trim) (142) becomes

$$\mathrm{tg}(\gamma+\delta) = \frac{\sin\psi_1\sin\vartheta_1 + \cos\psi_1\,\mathrm{tg}\,\delta}{\cos\vartheta_1}. \qquad (143)$$

If, in addition, $\delta = 0$ (the axis of the starting device is parallel to the longitudinal axis of the base), then (143) is simplified to

$$\mathrm{tg}\,\gamma = \sin\psi_1\,\mathrm{tg}\,\vartheta_1. \qquad (144)$$

Formula (144) can also be obtained more simply by assuming from the beginning that the angles δ and ϕ are zero.

52

In the general case $(\phi \neq 0, \, \delta \neq 0)$ the angles ϕ, δ, and γ will be assumed to be small. Equation (142) can then be written, with an accuracy of up to first-order terms in ϕ, δ, and γ, in the form:

$$(\gamma + \delta) \cos \vartheta_1 - \sin \phi_1 \sin \vartheta_1 - \delta \cos \phi_1 = -\phi \cos \phi_1 \sin \vartheta_1, \quad (145)$$

whence

$$\gamma = \sin \phi_1 \, tg \, \vartheta_1 + \left(\frac{\cos \phi_1}{\cos \vartheta_1} - 1\right)\delta - \phi \cos \phi_1 \, tg \, \vartheta_1. \quad (146)$$

Consider a numerical example for the same angles as before:

$$\vartheta_1 = 8°; \quad \phi_1 = 4°; \quad \phi = -2°; \quad \vartheta = 10°; \quad \delta = 6°.$$

In this case the course error of the moving object is:

$$\gamma = 0.0098 + 0.0008 + 0.0049 = 0.0155 \, (52').$$

We now return to the first design variant and consider the case of the so-called angular setting of the instrument at an angle δ to the left. The instrument must have some device causing the control system to bring the object to a position such that the perpendicular y' to the plane of the top's outer gimbal ring forms an angle δ with the longitudinal axis y of the object (Figure 34). As a result, the object turns through an angle δ after leaving the base, so that the course of its steady motion will be identical with the course of the base at the start. We again denote by γ the error in the moving object's course.
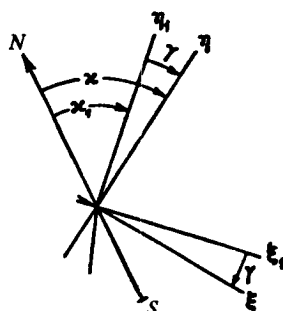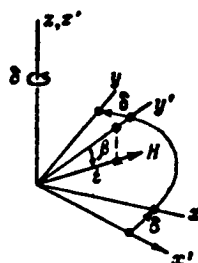

FIGURE 33   FIGURE 34

In this case (Figure 33), the angle γ will be the angle between the axes ξ and ξ_1 or, which is the same, between the axes η and η_1 of the coordinate systems $\xi\eta\zeta$ and $\xi_1\eta_1\zeta_1$. The direction cosines between the axes of these two coordinate systems must be of the form:

	ξ	η	ζ
ξ_1	$\cos \gamma$	$\sin \gamma$	0
η_1	$-\sin \gamma$	$\cos \gamma$	0
ζ_1	0	0	1

$$(147)$$

This result is obtained from (124) by replacing the angle $\gamma + \delta$ by the angle γ.

In the same way we obtain directly from (127) the projections of t on the axes of the coordinate system, $\xi\eta\zeta$, without having to find the direction

cosines of the system $x_1 y_1 z_1$ relative to the system $\xi \eta \zeta$:

$$t_\xi = (\cos \vartheta_1 \cos \gamma + \sin \phi_1 \sin \vartheta_1 \sin \gamma) \sin \delta - \cos \phi_1 \sin \gamma \cos \delta;$$

$$t_\eta = (\cos \vartheta_1 \sin \gamma - \sin \phi_1 \sin \vartheta_1 \cos \gamma) \sin \delta + \cos \phi_1 \cos \gamma \cos \delta; \qquad (148)$$

$$t_\zeta = -\cos \phi_1 \sin \vartheta_1 \sin \delta - \sin \phi_1 \cos \delta.$$

We now introduce the coordinate system $x'y'z'$ fixed to the outer ring of the top's gimbal system (Figure 34). The z'-axis of this system coincides with the z-axis of the system xyz fixed to the moving object; the x'-axis is the pivot axis of the inner ring of the top's gimbal system. The direction cosines of the system $x'y'z'$ relative to the system xyz are

	x	y	z
x'	$\cos \delta$	$-\sin \delta$	0
y'	$\sin \delta$	$\cos \delta$	0
z'	0	0	1

(149)

since during steady motion of the object the angle between the axes y and y' equals δ.

The top axis H lies in the $y'z'$ plane and forms an angle β with the y'-axis (Figure 34). The projections of unit length t of the rotor axis H on the axes of the coordinate system $x'y'z'$ are

$$t_{x'} = 0,$$

$$t_{y'} = \cos \beta, \qquad (150)$$

$$t_{z'} = -\sin \beta.$$

The projections of t on the axes of the coordinate system xyz are

$$t_x = \cos \beta \sin \delta;$$

$$t_y = \cos \beta \cos \delta; \qquad (151)$$

$$t_z = -\sin \beta.$$

This follows either from (149) or directly from Figure 34.

The projections of t on the axes of the coordinate system $\xi \eta \zeta$ are therefore

$$t_\xi = \cos \vartheta \cos \beta \sin \delta - \sin \vartheta \sin \beta;$$

$$t_\eta = -\sin \phi \sin \vartheta \cos \beta \sin \delta + \cos \psi \cos \beta \cos \delta - \sin \psi \cos \vartheta \sin \beta; \qquad (152)$$

$$t_\zeta = -\cos \phi \sin \vartheta \cos \beta \sin \delta - \sin \phi \cos \beta \cos \delta - \cos \phi \cos \vartheta \sin \beta.$$

This follows from (151) and (129).

The following three equations (only two of which are independent) for the unknowns β and γ, are obtained by equating (152) to (148):

$$(\cos \vartheta_1 \cos \gamma + \sin \phi_1 \sin \vartheta_1 \sin \gamma) \sin \delta - \cos \phi_1 \sin \gamma \cos \delta =$$

$$= \cos \vartheta \cos \beta \sin \delta - \sin \vartheta \sin \beta;$$

$$(\cos \vartheta_1 \sin \gamma - \sin \phi_1 \sin \vartheta_1 \cos \gamma) \sin \delta + \cos \phi_1 \cos \gamma \cos \delta =$$

$$= -\sin \phi \sin \vartheta \cos \beta \sin \delta + \cos \phi \cos \beta \cos \delta - \sin \phi \cos \vartheta \sin \beta;$$

$$-\cos \phi_1 \sin \vartheta_1 \sin \delta - \sin \phi_1 \cos \delta =$$

$$= -\cos \phi \sin \vartheta \cos \beta \sin \delta - \sin \phi \cos \beta \cos \delta - \cos \phi \cos \vartheta \sin \beta.$$

If all terms of higher order than the first in γ, δ, and ϕ are neglected,

these equations become

$$\delta \cos \vartheta_1 - \gamma \cos \psi_1 = \delta \cos \vartheta \cos \beta - \sin \vartheta \sin \beta,$$
$$-\delta \sin \psi_1 \sin \vartheta_1 + \cos \psi_1 = \cos \beta - \phi \cos \vartheta \sin \beta, \qquad (153)$$
$$-\delta \cos \psi_1 \sin \vartheta_1 - \sin \psi_1 = -\delta \sin \vartheta \cos \beta - \phi \cos \beta - \cos \vartheta \sin \beta.$$

We multiply the second equation of (153) by $-\delta \cos \vartheta$ and add it to the first; we also multiply the second equation by $\phi + \delta \sin \vartheta$ and add it to the third. Neglecting terms of higher order than the first in δ and ψ, we obtain:

$$\delta \cos \vartheta_1 - \gamma \cos \psi_1 - \delta \cos \psi_1 \cos \vartheta = -\sin \vartheta \sin \beta,$$
$$-\delta \cos \psi_1 \sin \vartheta_1 - \sin \psi_1 + \cos \psi_1 (\phi + \delta \sin \vartheta) = -\cos \vartheta \sin \beta. \qquad (154)$$

Dividing the first of these equations by the second yields:

$$\frac{\delta \cos \vartheta_1 - \gamma \cos \psi_1 - \delta \cos \psi_1 \cos \vartheta}{-\delta \cos \psi_1 \sin \vartheta_1 - \sin \psi_1 + \cos \psi_1 (\psi + \delta \sin \vartheta)} = \mathrm{tg}\, \vartheta. \qquad (155)$$

This equation contains only the unknown γ, and its solution is

$$\gamma = \mathrm{tg}\, \psi_1 \, \mathrm{tg}\, \vartheta + \left(\frac{\cos \vartheta_1}{\cos \psi_1} + \sin \vartheta_1 \, \mathrm{tg}\, \vartheta - \frac{1}{\cos \vartheta} \right) \delta - \phi \, \mathrm{tg}\, \vartheta. \qquad (156)$$

This formula differs only slightly from (136) obtained for the case when the moving object starts with zero angular setting. Using the same values of the angles,

$$\vartheta_1 = 8°, \quad \psi_1 = 4°, \quad \vartheta = 10°, \quad \psi = -2°,$$

equation (156) gives

$$\gamma = 0.0123 + 0.0001 + 0.0062 = 0.0186 \ (1°4').$$

Formulas (136) and (156) show the importance of obtaining as small an object-heel angle as possible, for accurate orientation, in the case of the first design variant of the gyroscopic instrument (top axis parallel to the object's longitudinal axis at the start). For zero heel angle ϑ the error γ is of the order of two to five minutes of an arc.

When the object starts from a horizontal base, $\vartheta_1 = 0$, $\psi_1 = 0$, $\delta = 0$, and therefore, according to (136):

$$\gamma = -\phi \, \mathrm{tg}\, \vartheta \approx -\phi\vartheta. \qquad (157)$$

If the object has a trim $\psi < 0$ during steady motion, the angle γ will be negative for $\vartheta < 0$ (heel to the left), which corresponds to a deviation of the object to the left of the specified direction. For a heel to the right, the object will deviate to the right during steady motion.

The value of this deviation can be considerable. Thus, for $\psi = -2°$ and $\vartheta = -10°$:

$$\gamma = -0.035 \cdot 0.175 = -0.0061 \ (21').$$

§ 2. Deviation of a self-guiding missile from the specified direction during flight

Problems similar to those discussed above are met in missile flight theory. We solve one of these problems in this section.

As an example consider the German **V-2** rocket in which flight control is by two free gyroscopes. The pivot axes y' and x'' of the outer gimbal rings of the gyroscopes are set perpendicular both to the axis of symmetry z of the rocket and to each other (Figure 35).
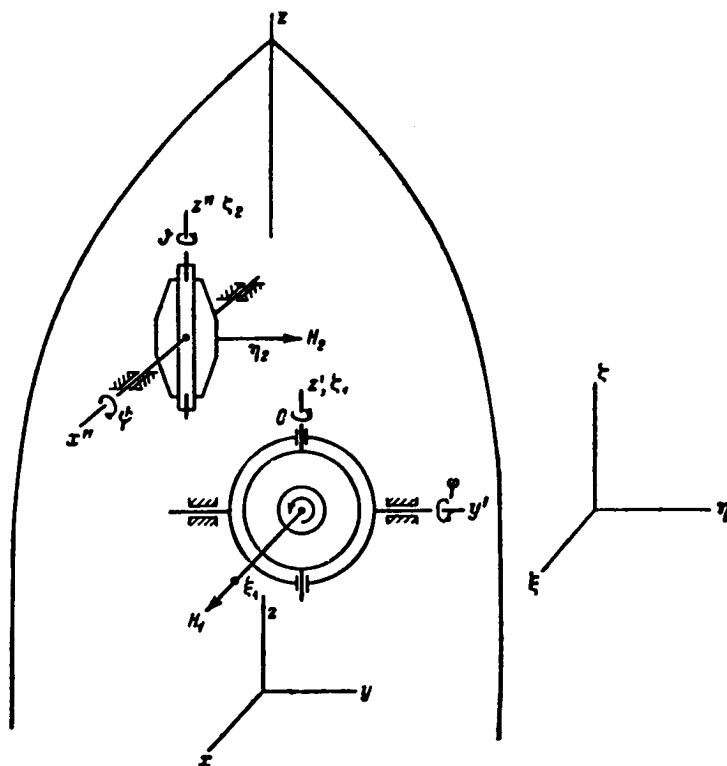

FIGURE 35

The rocket is placed vertically on the launching pad, and the y'-axis (the pivot axis of the outer gimbal ring of the so-called gyro-verticant) is aimed at the target by rotating the rocket about the vertical. As a result the x''-axis (the pivot axis of the outer gimbal ring of the so-called gyrohorizon) becomes perpendicular to the vertical plane $\eta\zeta$ (Figure 35) which contains the straight line connecting the rocket-launching pad with the target.

The axes of the gyro housings or, which is the same kinematically, the pivot axes ζ_1 and ζ_2 of their inner gimbal rings, are set on the launching pad parallel to the axis of symmetry z of the rocket and are therefore vertical.

The rotor top axis ξ_1 of the gyro-verticant is set on the launching pad perpendicular to the $\eta\zeta$ plane and maintains this orientation throughout the rocket flight (if instrument errors of the gyro are neglected). The axis η_2 of the gyrohorizon rotor is oriented parallel to the horizontal axis η and

remains parallel to this direction throughout the flight (again neglecting instrument errors). The Earth's rotation is neglected.

Consider the following coordinate systems:

1) a coordinate system $\xi\eta\zeta$ whose ζ-axis is vertical and whose η-axis is aimed at the target. This coordinate system is at rest relative to the Earth;

2) a coordinate system xyz fixed to the rocket body. The z-axis of this system is the axis of symmetry of the rocket, the x-axis is parallel to the x''-axis of the outer gimbal ring of the gyrohorizon, and the y-axis is parallel to the axis y' of the outer gimbal ring of the gyro-verticant;

3) a coordinate system $x'y'z'$ fixed to the outer gimbal ring of the gyroverticant. The $y'z'$ plane of this coordinate system contains the outer gimbal-ring pivot axis y' and the axis ζ_1 of the gyro-verticant housing, which coincides with the z'-axis:

4) a coordinate system $\xi_1\eta_1\zeta_1$ fixed to the gyro-verticant housing, the ξ_1-axis being identical with the rotor axis of the gyro, the ζ_1-axis being, as just mentioned, the axis of tilting of the gyro housing relative to the outer gimbal ring;

5) a coordinate system $x''y''z''$ fixed to the outer gimbal ring of the gyrohorizon. The x''-axis of this coordinate system is the pivot axis of the outer gimbal ring of the gyrohorizon and is parallel to the x-axis of the coordinate system xyz fixed to the rocket body; the y''-axis coincides with the η_2-axis;

6) a coordinate system $\xi_2\eta_2\zeta_2$ fixed to the gyrohorizon housing. The axis of the gyrohorizon rotor coincides with the η_2-axis; the housing can be tilted relative to the outer gimbal ring about the ζ_2-axis.

The corresponding axes of all these systems either coincide or are parallel while the rocket is on the launching pad.

The following angles, related to the gimbal systems of the gyros, are recorded during flight:

1) the angle φ between the z- and z'-axes (or, which is the same, between the axes x and x'). The angle φ is the angle of tilting about the y'-axis (i.e., about the y-axis) of the rocket body relative to the outer gimbal ring of the gyro-verticant (Figures 35 and 37);
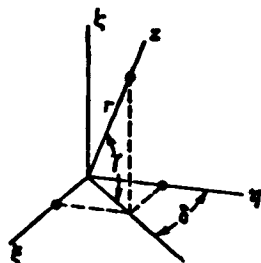

FIGURE 36

2) the angle θ between the axes y' and η_1 (or, which is the same, between the axes z' and ξ_1), i.e., the angle of tilting about the ζ_1-axis of the outer gimbal ring of the gyro-verticant relative to the gyro housing (Figures 35 and 38);

3) the angle ψ between the axes z and z'' (or between the axes y and y''), i.e., the angle of tilting about the x''-axis of the rocket body relative to the outer gimbal ring of the gyrohorizon (Figures 35 and 40).

The rocket is guided so as to make the angles φ and θ zero and the angle ψ vary as a given function of time, corresponding to the so-called flight program.

Our problem can be stated as follows: let the angles φ and θ recorded by the gyro-verticant, and ψ recorded by the gyrohorizon, be known. Calculate the angle δ giving the deviation from the η-direction of the projection of the rocket axis z on the horizontal plane $\xi\eta$ (Figure 36).

Consider unit length r of the rocket axis z (Figure 36); its projections on the axes of the coordinate system $\xi\eta\zeta$ are respectively

$$r_\xi = \cos z\xi = \cos\gamma \sin\delta,$$
$$r_\eta = \cos z\eta = \cos\gamma \cos\delta, \tag{158}$$
$$r_\zeta = \cos z\zeta = \sin\gamma,$$

where γ is the angle between the rocket axis and the $\xi\eta$ horizontal plane.

It is obvious (Figure 36) that

$$\text{tg}\,\delta = \frac{r_\xi}{r_\eta} = \frac{\cos z\xi}{\cos z\eta}. \tag{159}$$

It follows that to determine the angle δ we must know the direction cosines of the rocket axis z relative to the fixed axes ξ and η in terms of the angles φ, θ, and ψ.

To do this we find the direction cosines of the system xyz relative to the system $\xi\eta\zeta$ in two different ways: first, through the angles related to the gyro-verticant (the angles φ and θ in particular), and then through the angles related to the gyrohorizon (the angle ψ in particular), and compare the results.

The direction cosines of the system $x'y'z'$ relative to the system xyz (Figure 37) are

	x	y	z
x'	$\cos\varphi$	0	$\sin\varphi$
y'	0	1	0
z'	$-\sin\varphi$	0	$\cos\varphi$

(160)

For $\varphi > 0$, the system xyz (fixed to the rocket body) is rotated counterclockwise about the y'-axis (parallel to the y-axis relative to the system $x'y'z'$
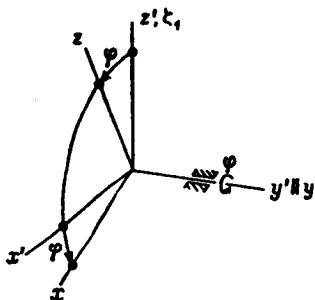

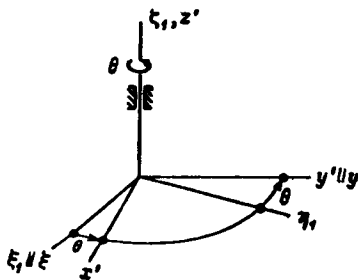FIGURE 37   FIGURE 38

(fixed to the outer gimbal ring of the gyro-verticant) if viewed from the positive direction of the y'-axis.

The direction cosines of the system $\xi_1\eta_1\zeta_1$ relative to the system $x'y'z'$ (Figure 38) are

	x'	y'	z'
ξ_1	$\cos\theta$	$-\sin\theta$	0
η_1	$\sin\theta$	$\cos\theta$	0
ζ_1	0	0	1

(161)

58

For $\theta > 0$, the system $x'y'z'$ (fixed to the outer gimbal ring of the gyro-vertical) is rotated counterclockwise about the ζ_1-axis (which coincides with the z'-axis) relative to the system $\xi_1\eta_1\zeta_1$ (fixed to the gyro-verticant housing) if viewed from the positive direction of the ζ_1-axis.

The direction cosines of the system $\xi_1\eta_1\zeta_1$ relative to the system xyz can now be found from (160) and (161) by using the methods of Chapter I, § 1:

	x	y	z	
ξ_1	$\cos\varphi\cos\theta$	$-\sin\theta$	$\sin\varphi\cos\theta$	
η_1	$\cos\varphi\sin\theta$	$\cos\theta$	$\sin\varphi\sin\theta$	(162)
ζ_1	$-\sin\varphi$	0	$\cos\varphi$	

Finally, the direction cosines of the system $\xi_1\eta_1\zeta_1$ (fixed to the gyro-verticant housing) relative to the fixed coordinate system $\xi\eta\zeta$ are determined (Figure 39). We denote by ψ^* the angle between the axes η and η_1 (or, which is the same, between the axes ζ and ζ_1).
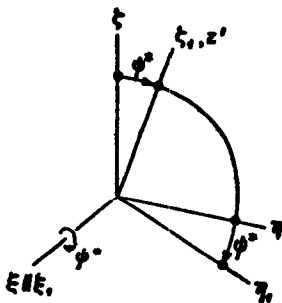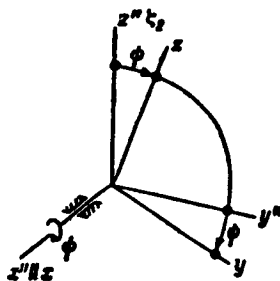
FIGURE 39   FIGURE 40

Assume that for $\psi^*>0$ the system $\xi_1\eta_1\zeta_1$, fixed to the gyro-verticant housing, is rotated clockwise about the gyro-verticant rotor axis relative to its initial position when the rocket is on the launching pad. The angle ψ^* cannot be indicated by the gyro-verticant, and must be considered as unknown. The required direction cosines are:

	ξ	η	ζ	
ξ_1	1	0	0	
η_1	0	$\cos\psi^*$	$-\sin\psi^*$	(163)
ζ_1	0	$\sin\psi^*$	$\cos\psi^*$	

The gyro-verticant rotor axis ξ_1 remains, as already mentioned, parallel to the horizontal axis ξ throughout the rocket flight, since it is assumed that there are no instrument errors in the gyros and that the Earth's rotation is negligible.

The direction cosines of the system xyz relative to the system $\xi\eta\zeta$ are found from (162) and (163):

	ξ	η	ζ	
x	$\cos\varphi\cos\theta$	$\cos\varphi\sin\theta\cos\psi^* - \sin\varphi\sin\psi^*$	$-\cos\varphi\sin\theta\sin\psi^* - \sin\varphi\cos\psi^*$	
y	$-\sin\theta$	$\cos\theta\cos\psi^*$	$-\cos\theta\sin\psi^*$	(164)
z	$\sin\varphi\cos\theta$	$\sin\varphi\sin\theta\cos\psi^* + \cos\varphi\sin\psi^*$	$-\sin\varphi\sin\theta\sin\psi^* + \cos\varphi\cos\psi^*$	

The direction cosines are given here as functions of the angles φ, θ, and ψ^* related only to the gyro-verticant. It remains now to determine these same direction cosines as functions of the angles ϕ, ϑ, and φ^* (cf. below) related to the gyrohorizon only.

The direction cosines of the coordinate system $x''y''z''$ (fixed to the outer gimbal ring of the gyrohorizon) relative to the system xyz (fixed to the rocket body) (Figure 40) are:

	x	y	z
x''	1	0	0
y''	0	$\cos\phi$	$\sin\phi$
z''	0	$-\sin\phi$	$\cos\phi$

$$(165)$$

For $\phi>0$, the coordinate system xyz is rotated clockwise about the x''-axis (the pivot axis of the gyrohorizon's outer gimbal ring, parallel to the x-axis) relative to the system $x''y''z''$, if viewed from the positive direction of the x''-axis.

The direction cosines of the system $\xi_2\eta_2\zeta_2$ (fixed to the gyrohorizon housing) relative to the system $x''y''z''$ (fixed to the outer gimbal ring of the gyrohorizon) (Figure 41) are:

	x''	y''	z''
ξ_2	$\cos\vartheta$	$-\sin\vartheta$	0
η_2	$\sin\vartheta$	$\cos\vartheta$	0
ζ_2	0	0	1

$$(166)$$

The coordinate system $x''y''z''$ is rotated counterclockwise through an angle ϑ about the gyro housing axis ζ_2 relative to the coordinate system $\xi_2\eta_2\zeta_2$. The angle ϑ is usually not indicated and must therefore be considered as unknown.
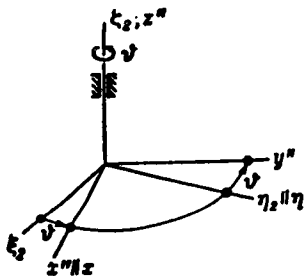

FIGURE 41   FIGURE 42
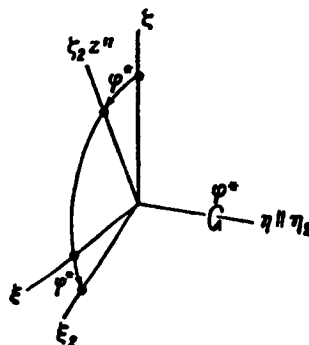
The direction cosines of the system $\xi_2\eta_2\zeta_2$ relative to the system xyz can now be determined from (165) and (166):

	x	y	z
ξ_2	$\cos\vartheta$	$-\cos\phi\sin\vartheta$	$-\sin\phi\sin\vartheta$
η_2	$\sin\vartheta$	$\cos\phi\cos\vartheta$	$\sin\phi\cos\vartheta$
ζ_2	0	$-\sin\phi$	$\cos\phi$

$$(167)$$

60

We finally determine the direction cosines of the coordinate system $\xi_2\eta_2\zeta_2$, fixed to the gyrohorizon housing, relative to the fixed coordinate system $\xi\eta\zeta$ (Figure 42). According to our assumptions, the axis of rotation of the gyrohorizon rotor η_2 maintains its direction in space throughout the flight, and is therefore always parallel to the fixed horizontal axis η We denote by φ^* the angle between the axes ζ and ζ_2 (or, which is the same, between the axes ξ and ξ_2), and consider it as positive if the coordinate system $\xi_2\eta_2\zeta_2$ is rotated counterclockwise relative to the coordinate system $\xi\eta\zeta$ if viewed from the positive direction of the η_2-axis. The angle φ^* cannot be indicated, and must therefore be considered as unknown.

The required direction cosines are therefore:

	ξ	η	ζ
ξ_2	$\cos\varphi^*$	0	$-\sin\varphi^*$
η_2	0	1	0
ζ_2	$\sin\varphi^*$	0	$\cos\varphi^*$

(168)

The direction cosines of the system xyz relative to the system $\xi\eta\zeta$ are obtained from (167) and (168) as functions of the angles ψ, ϑ, and φ^*, related to the gyrohorizon only:

	ξ	η	ζ
x	$\cos\vartheta\cos\varphi^*$	$\sin\vartheta$	$-\cos\vartheta\sin\varphi^*$
y	$-\cos\psi\sin\vartheta\cos\varphi^* - \sin\psi\sin\varphi^*$	$\cos\psi\cos\vartheta$	$\cos\psi\sin\vartheta\sin\varphi^* - \sin\psi\cos\varphi^*$
z	$-\sin\psi\sin\vartheta\cos\varphi^* + \cos\psi\sin\varphi^*$	$\sin\psi\cos\vartheta$	$\sin\psi\sin\vartheta\sin\varphi^* + \cos\psi\cos\varphi^*$

(169)

The angle δ (the angle of deviation from the axis η, aimed at the target, of the projection of the rocket axis z on the horizontal plane) is found most simply from (159), taking the value of $\cos z\xi$ from (164) and that of $\cos z\eta$ from (169):

$$\operatorname{tg}\delta = \frac{\cos z\xi}{\cos z\eta} = \frac{\sin\varphi\cos\vartheta}{\sin\psi\cos\vartheta}.$$ (170)

To obtain the angle ϑ as function of the angles φ, ϑ, and ψ, we equate the values given in (164) and (169) for the direction cosines of the ξ-axis relative to the coordinate system xyz. This yields the following three equations:

$$\cos x\xi = \cos\varphi\cos\vartheta = \cos\vartheta\cos\varphi^*,$$
$$\cos y\xi = -\sin\vartheta = -\cos\psi\sin\vartheta\cos\varphi^* - \sin\psi\sin\varphi^*,$$ (171)
$$\cos z\xi = \sin\varphi\cos\vartheta = -\sin\psi\sin\vartheta\cos\varphi^* + \cos\psi\sin\varphi^*,$$

each of which follows from the other two.

Multiplying the second equation of (171) by $-\cos\psi$, the third by $-\sin\psi$, and adding, we obtain

$$\cos\psi\sin\vartheta - \sin\psi\sin\varphi\cos\vartheta = \sin\vartheta\cos\varphi^*.$$ (172)

Dividing this equation by the first of equations (171) yields:

$$\operatorname{tg}\vartheta = \frac{\cos\psi}{\cos\varphi}\operatorname{tg}\vartheta - \operatorname{tg}\varphi\sin\psi,$$ (173)

which determines the angle ϑ as a function of the angles φ, ϑ, and ψ indicated by the gyroscopic instruments of the rocket.

61

We also have

$$\frac{1}{\cos\vartheta} = \sqrt{1+\operatorname{tg}^2\vartheta} = \sqrt{1+\left(\frac{\cos\psi}{\cos\varphi}\operatorname{tg}\theta - \operatorname{tg}\varphi\sin\psi\right)^2}. \qquad (174)$$

Inserting this into (170) yields:

$$\operatorname{tg}\delta = \frac{\cos\theta\sin\varphi}{\sin\psi}\sqrt{1+\left(\frac{\cos\psi}{\cos\varphi}\operatorname{tg}\theta - \operatorname{tg}\varphi\sin\psi\right)^2}, \qquad (175)$$

which is simplified to the following final formula for the angle δ:

$$\operatorname{tg}\delta = \frac{\operatorname{tg}\varphi}{\sin\psi}\sqrt{\cos^2\varphi\cos^2\theta + (\sin\varphi\sin\psi\cos\theta - \sin\theta\cos\psi)^2}. \qquad (176)$$

From this formula we find that $\delta = \frac{\pi}{2}$ for the limiting case $\psi = 0$ and $\varphi \neq 0$. In fact, for $\psi = 0$ (Figure 35), the rocket axis z is parallel to the z''-axis which coincides with the axis of rotation of the gyrohorizon housing ζ_2, which in its turn is perpendicular to the rotor axis η_2, and therefore also to the fixed axis η. It follows that for $\psi = 0$ the rocket axis z, and its projection on the horizontal plane $\xi\eta$, are perpendicular to the axis η aimed at the target, i.e., $\delta = \frac{\pi}{2}$.

For $\psi = \frac{\pi}{2}$, (176) becomes

$$\operatorname{tg}\delta = \operatorname{tg}\varphi\cos\theta. \qquad (177)$$

This simple formula can also be derived directly.

Taking $\theta = 0$ in (177), we find that $\delta = \varphi$. It is easily seen that in this case the rocket axis z lies in the horizontal plane. In fact, for $\theta = 0$ the $y(y')$-axis lies in the vertical plane, perpendicular to the ξ_1-axis (Figure 38); on the other hand, for $\psi = \frac{\pi}{2}$ the y-axis lies in another vertical plane, perpendicular to the $\eta_2(y'')$-axis. The y-axis is therefore parallel to the vertical axis ζ, and the z-axis is parallel to the horizontal plane $\xi\eta$.

§ 3. Some general considerations on methods for solving problems on the geometry of stabilization systems

It is evident that the determination of the direction cosines between different reference frames is of much importance. Every problem was usually reduced to a comparison of the direction cosines of two given reference frames obtained in two different ways. It is therefore important to simplify this process as far as possible in order to avoid lengthy and repetitive operations which may introduce errors.

The two specified reference frames usually represent the initial and final positions of a trihedron, which performs finite rotations about one or another of its axes (edges) in a specified order.

It is easily seen that if this trihedron performs successively three finite rotations, one about each of its axes, then only two essentially different sequences of such rotations are possible. The problem therefore reduces to obtaining once and for all two essentially different tables of the cosines

of the angles between the trihedron axes in their initial and their final positions.

We denote the axes of the trihedron by a, b, and c, the initial positions of these axes by x, y, and z, and their final position by ξ, η, and ζ. Let the axes a, b, and c form a right-handed coordinate system (Figure 43). We denote by α the angle of rotation of the trihedron abc about the a-axis, by β the angle of its rotation about the b-axis, and by γ the angle of its rotation about the c-axis. These angles are positive when the rotation is counterclockwise. The displacement of the trihedron abc from position xyz to position $\xi\eta\zeta$ by successive rotations, namely, through an angle α about the a-axis, an angle β about the b-axis, and an angle γ about the c-axis is called a right-hand displacement or a displacement of the first kind.
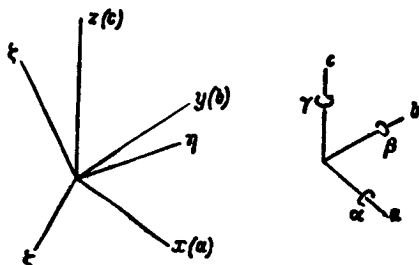
FIGURE 43

The displacement of the trihedron abc from position xyz to position $\xi\eta\zeta$ by successive rotations, namely, through an angle β about the b-axis, an angle α about the a-axis, and an angle γ about the c-axis is called a left-hand displacement or a displacement of the second kind.

It is easily seen that any other displacement of the trihedron composed of three finite rotations, one about each of its axes, can be reduced to one of the two displacements described above, provided the trihedron axes are suitably denoted by a, b, and c, and the angles of its rotations about these axes by α, β, and γ.

Let the trihedron uvw, whose axes form a right-handed coordinate system, undergo a displacement from the initial position $u^0v^0w^0$ to the final position $u^*v^*w^*$ by means of a rotation through an angle $\varkappa$ about the w-axis followed by a rotation through an angle ϵ about the v-axis, and finally by a rotation through an angle δ about the u-axis. We denote the v-axis by a, the w-axis by b, the u-axis by c, and the angles as follows:

$$\epsilon = \alpha, \ \varkappa = \beta, \ \delta = \gamma.$$

It is seen that the trihedron abc is right-handed (i.e., the axes a, b, and c form a right-handed coordinate system), and that the sequence of rotations is about the axes b, a, c. This example thus corresponds to a rotation of the second kind.

The displacement of a rigid body determined by the classical Euler angles ψ, θ, and φ (Figure 44) does not belong to the class of displacements considered here, since it consists of a rotation of the trihedron abc through an angle ψ about the axis $c(z_0)$, followed by a rotation through an angle θ

63

about the axis $a(x')$, and then again through an angle φ about the axis $c(z)$. This is also the reason for the inconvenience of using the classical Euler angles in the study of small displacements of a rigid body. Such displacements usually correspond to large angles ψ and φ whose difference is small.

We now obtain the direction cosines of the system xyz relative to the system $\xi\eta\zeta$ for right- and left-hand displacements of the trihedron abc.

For displacements of the first kind, the first rotation is through an angle α about the axis $a(x)$. This rotation brings the trihedron abc from the position xyz into a position $x'y'z'$ (Figure 45). The direction cosines of the system $x'y'z'$ relative to the system xyz are

	x	y	z
x'	1	0	0
y'	0	$\cos\alpha$	$\sin\alpha$
z'	0	$-\sin\alpha$	$\cos\alpha$

$$(178)$$

The next rotation is through an angle β about the axis $b(y')$; it brings the trihedron abc from the position $x'y'z'$ into a position $\xi_1\eta_1\zeta_1$ (Figure 46).
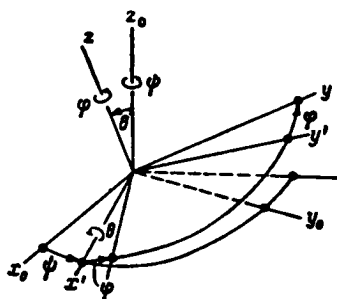
FIGURE 44
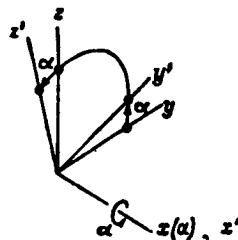
FIGURE 45

The direction cosines of the system $\xi_1\eta_1\zeta_1$ relative to the system $x'y'z'$, are

	x'	y'	z'
ξ_1	$\cos\beta$	0	$-\sin\beta$
η_1	0	1	0
ζ_1	$\sin\beta$	0	$\cos\beta$

$$(179)$$

The direction cosines of the system $\xi_1\eta_1\zeta_1$ relative to the system xyz are from (178) and (179):

	x	y	z
ξ_1	$\cos\beta$	$\sin\alpha\sin\beta$	$-\cos\alpha\sin\beta$
η_1	0	$\cos\alpha$	$\sin\alpha$
ζ_1	$\sin\beta$	$-\sin\alpha\cos\beta$	$\cos\alpha\cos\beta$

$$(180)$$

The last rotation of the trihedron abc, that is the rotation through the angle γ about the axis $c(\zeta_1)$, corresponds to bringing the trihedron from position $\xi_1\eta_1\zeta_1$ into the final position $\xi\eta\zeta$ (Figure 47).

The direction cosines of the system $\xi_1\eta_1\zeta_1$ relative to the system $\xi\eta\zeta$ are:

	ξ	η	ζ
ξ_1	$\cos\gamma$	$-\sin\gamma$	0
η_1	$\sin\gamma$	$\cos\gamma$	0
ζ_1	0	0	1

(181)

The direction cosines of the system xyz relative to the system $\xi\eta\zeta$, which define a displacement of the first kind (consisting of consecutive rotations of the trihedron abc about the axes a, b, and c), can now be obtained from (180) and (181). These direction cosines constitute a table of the first kind. It has the form:

	ξ	η	ζ
x	$\cos\beta\cos\gamma$	$-\cos\beta\sin\gamma$	$\sin\beta$
y	$\sin\alpha\sin\beta\cos\gamma+$ $+\cos\alpha\sin\gamma$	$-\sin\alpha\sin\beta\sin\gamma+$ $+\cos\alpha\cos\gamma$	$-\sin\alpha\cos\beta$
z	$-\cos\alpha\sin\beta\cos\gamma+$ $+\sin\alpha\sin\gamma$	$\cos\alpha\sin\beta\sin\gamma+$ $+\sin\alpha\cos\gamma$	$\cos\alpha\cos\beta$

(182)

We now determine the same direction cosines for a displacement of the second kind. In this case the first rotation of the trihedron abc is about the axis $b(y)$ through an angle β (Figure 48). As a result the trihedron abc
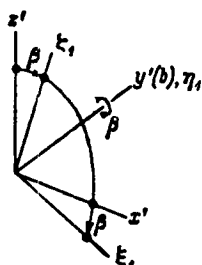
FIGURE 46
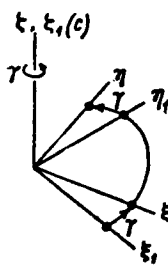
FIGURE 47

is brought from the initial position xyz into a position $x''y''z''$. The direction cosines of the system $x''y''z''$ relative to the system xyz are:

	x	y	z
x''	$\cos\beta$	0	$-\sin\beta$
y''	0	1	0
z''	$\sin\beta$	0	$\cos\beta$

(183)

The next rotation of the trihedron abc is through an angle α about the axis $a(x'')$ This brings the trihedron from the position $x''y''z''$ into a position $\xi_2\eta_2\zeta_2$ (Figure 49). The direction cosines of the system $\xi_2\eta_2\zeta_2$ relative to the

65

system $x''y''z'$ are

	x''	y''	z'
ξ_2	1	0	0
η_2	0	$\cos \alpha$	$\sin \alpha$
ζ_2	0	$-\sin \alpha$	$\cos \alpha$

(184)

The direction cosines of the system $\xi_2\eta_2\zeta_2$ relative to the system xyz can now be found from (183) and (184):

	x	y	z
ξ_2	$\cos \beta$	0	$-\sin \beta$
η_2	$\sin \alpha \sin \beta$	$\cos \alpha$	$\sin \alpha \cos \beta$
ζ_2	$\cos \alpha \sin \beta$	$-\sin \alpha$	$\cos \alpha \cos \beta$

(185)

The last rotation through an angle γ about the axis $c\,(\zeta_2)$ brings the trihedron abc from position $\xi_2\eta_2\zeta_2$ into the final position $\xi\eta\zeta$ (Figure 50). The
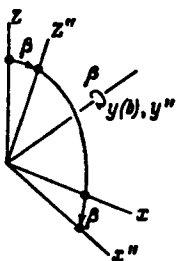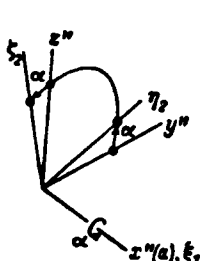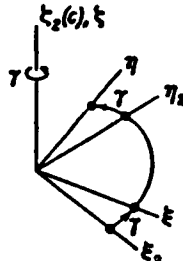
FIGURE 48   FIGURE 49   FIGURE 50

corresponding direction cosines are similar to those in (181), i.e.,

	ξ	η	ζ
ξ_2	$\cos \gamma$	$-\sin \gamma$	0
η_2	$\sin \gamma$	$\cos \gamma$	0
ζ_2	0	0	1

(186)

The direction cosines of the system xyz relative to the system $\xi\eta\zeta$ can now be found from (185) and (186):

	ξ	η	ζ
x	$\cos \beta \cos \gamma +$ $+ \sin \beta \sin \alpha \sin \gamma$	$-\cos \beta \sin \gamma +$ $+ \sin \beta \sin \alpha \cos \gamma$	$\sin \beta \cos \alpha$
y	$\cos \alpha \sin \gamma$	$\cos \alpha \cos \gamma$	$-\sin \alpha$
z	$-\sin \beta \cos \gamma +$ $+ \cos \beta \sin \alpha \sin \gamma$	$\sin \beta \sin \gamma +$ $+ \cos \beta \sin \alpha \cos \gamma$	$\cos \beta \cos \alpha$

(187)

This will be called a table of the second kind. It defines a left-handed displacement of the trihedron abc from the position xyz to the position $\xi\eta\zeta$ by means of consecutive rotations about the axes b, a, and c.

In view of the properties of finite rotations, the position of the coordinate system $\xi\eta\zeta$ defined by (182) does not coincide with the position of the coordinate system $\xi\eta\zeta$ defined by (187) for equal angles α, β, and γ.

66

As an example, we shall now derive Table (125) of Chapter II, § 1, which gives the direction cosines of the system $x_1 y_1 z_1$ fixed to the base relative to the system $\xi \eta \zeta$ whose orientation is determined by the moving object.

It is easily seen that if the initial position of the trihedron *abc* coincides with the coordinate system $x_1 y_1 z_1$, then, according to Figures 26 and 27, this trihedron is brought into position $\xi \eta \zeta$ by the following consecutive rotations:

1) through an angle $\beta = -\vartheta_1$ about the axis $b\,(y_1)$;

2) through an angle $\alpha = \psi_1$ about the axis $a\,(\xi_1)$;

3) through an angle $\gamma\,(-(\gamma + \delta)$ in the notation of Chapter II, § 1) about the axis $c\,(\zeta_1)$.

This is a displacement of the second kind, and (187) is applicable.

Replacing in this table x, y, and z by x_1, y_1, and z_1 respectively, and α, β, and γ by ψ_1, $-\vartheta_1$ and $-(\gamma + \delta)$ respectively leads to (125).

Tables (164) and (169), derived in Chapter II, § 2, can be similarly obtained. The first by using the table of the first kind (Table (182)), the second by using the table of the second kind (Table (187)). In both cases the notation of the axes fixed to the rocket body must be changed.

The auxiliary tables (180) and (185) can also be used if the displacement of the trihedron is limited to two finite rotations about any two of its axes. This was the case (see Chapter I, § 1) of the tilting of the gimbal rings of two systems the pivot axes of whose outer rings are mutually perpendicular. Table (3) is identical (except for the notation used) with (185), and Table (6) with (180).

§ 4. Nonholonomic motions of gyroscopic systems

The motions of gyroscopic systems, treated in the precession theory of gyroscopes, can in many cases be considered to occur as if under the influence of nonholonomic constraints.

The simplest example is the motion of a double-gyro frame (Figure 51) in the absence of friction in the bearings of the gyro housings. In this case, the projection of the frame's own angular velocity ω on the frame pivot axis (z-axis) is zero, irrespective of the motion of the base (ship deck, plane, etc.) on which the frame bearings are mounted (cf. Chapter IV, § 5):

$$\omega_z = 0. \tag{188}$$

Another example is the gyro acted upon by correction forces. A moment maintaining the top axis in a position perpendicular to the outer-ring plane $y'z$ is applied to the z-axis by means of a motor M (Figure 52). When these moments are sufficiently large, the top axis is practically perpendicular even when the base is in motion. In the absence of friction in the bearings of the gyro housing, (188) is valid here also, ω being now the angular velocity of the outer gimbal ring.

The precession theory of gyroscopes neglects the so-called inertial terms in the equations of motion of gyroscopic systems (cf. Chapter IV, § 1). These terms contain the equatorial moments of inertia of the tops, and also the moments of inertia of the gimbal rings, housings, and other parts of the gyroscopic system connected with them. The inertial terms are responsible

for the so-called nutational oscillations of a gyroscopic system, which have relatively high frequencies. These oscillations are usually damped rapidly due to the presence of external and internal resistance forces in the system. These last are also often neglected in the equations of motion.

Neglecting inertial terms, the equations of a gyroscopic system contain only the coordinates of the system and their time derivatives. They have, therefore, the same form as the equations of nonholonomic constraints, depending in the general case on time (nonrheonomic equations).
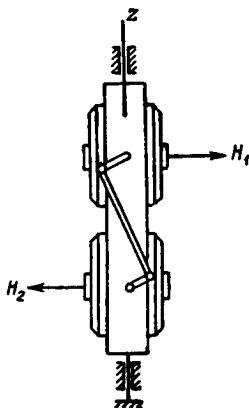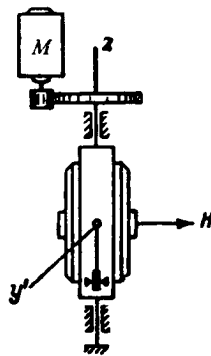
FIGURE 51   FIGURE 52

The motion of a gyroscopic system described by the equations of the (elementary) precession theory of gyroscopes, i.e., without taking into account the inertial terms, is thus in a certain sense a nonholonomic motion whose number of constraints is equal to the number of coordinates.

This approach is useful in many cases arising during the study of certain peculiarities in the behavior of gyroscopic systems mounted on moving bases. In the above example of a gyroscopic frame the equations of the precession theory can be separated into two independent equations. The first of them — equation (188) — has the classical form of the equation of a nonholonomic constraint. The second equation (cf. Chapter IV, § 5) defines the law of the rotations of the housings relative to the frame under the action of external forces. This equation does not have so clear a form of a nonholonomic constraint. When the friction in the bearings of the housings is taken into account, however, this method is sometimes very advantageous.

The motion of the gyro-system base is responsible for the appearance in the equations of terms depending explicitly on time. Any motion of the base thus entails a variation in the orientation of the gyros of the system. If the base returns to its initial position in the course of its motion, the gyros and gimbal rings will not necessarily return to their initial positions (because of the nonholonomic pattern of the motion). This problem is of great practical importance and will be discussed below.

The gyroscopic frame, and the gyro acted upon by correction forces, can, because of (188), be used for the stabilization of a fixed direction in

the horizontal plane, i.e., serve as gyroazimuth (directional gyro). If the frame pivot axis is fixed in a vertical direction, the frame will have an apparent rotation relative to the surface of the Earth. The angular velocity of this rotation is equal and opposite to the vertical component of the angular velocity of the Earth.

In fact, if the angle between the top axis and the north-south line is denoted by x (Figure 53), the projection of the absolute angular velocity of the gyroscopic frame on the local vertical is equal to

$$\omega_z = -\frac{dx}{dt} + U \sin \varphi, \tag{189}$$

where U is the angular velocity of the Earth, and φ, the local latitude.

Inserting (188) into (189) yields

$$\frac{dx}{dt} = U \sin \varphi. \tag{190}$$

If viewed from above, the frame will rotate clockwise in the northern hemisphere.

This rotation can be prevented by applying a suitable moment to the axis of one of the frame's gyro housings. For instance, one resulting from the static unbalance of the gyros, in order to cause a counterclockwise precession of the frame about its pivot axis. Expressed technically the frame is stabilized in azimuth.
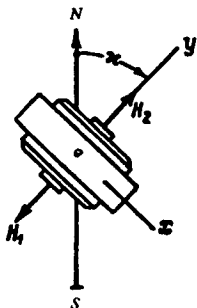
The situation is different if the frame's pivot axis deviates from its vertical direction because of the motion of the base on which the frame bearings are mounted.

If the pivot axis returns to its initial position as a result of the motion of the base, the frame's orientation at the end of the motion will, in the general case, differ from its orientation at the beginning; in other words, the stabilization in azimuth will be lost.

Therefore, a perfect stabilization of the frame pivot axis in the vertical is necessary for an accurate stabilization in azimuth.

FIGURE 53

Consider an arbitrary motion of the trihedron $x^0 y^0 z^0$ fixed to the frame base in such a way that the z^0-axis coincides with the z-axis of the gyroscopic frame (Figure 54).

The translatory motions of the trihedron $x^0 y^0 z^0$ have no influence on what follows. It can therefore be assumed that the z^0-axis of the trihedron passes permanently through some point O, and that the trihedron apex M moves on a stationary sphere of radius R and center O. The direction of the z^0-axis or, which is the same, the position of the point M on the sphere, can be defined by the angles ψ and φ, as the longitude and latitude of a point on the Earth's sphere. For this, the position of a great circle of the sphere — the Equator — and of some initial direction $O\xi$ in its plane must be fixed relative to a Newtonian reference frame.

The position of the trihedron $x^0 y^0 z^0$ in space is fully determined except for a translation by specifying, in addition to the angles ψ and φ, also the angle a formed by the x^0-axis with the tangent to the geographic parallel Mp of the point at which the trihedron apex M is located.

A variation of the angle ϕ corresponds to the rotation of the trihedron $x^0y^0z^0$ about the ζ-axis perpendicular to the equatorial plane (Figure 54). This axis forms an angle $\frac{\pi}{2}-\varphi$ with the z^0-axis.

A variation of the angle φ corresponds to a rotation of the trihedron about Mp perpendicular to the z^0-axis. Finally, a variation of the angle α corresponds to a rotation of the trihedron about the z^0-axis itself. The projection of the angular velocity of the trihedron $x^0y^0z^0$ on its z^0-axis is therefore

$$\omega_{z^0} = \frac{d\psi}{dt}\sin\varphi + \frac{d\alpha}{dt}. \qquad (191)$$

We now fix a trihedron xyz to the gyroscopic frame whose z-axis coincides with the frame pivot axis, and therefore with the z^0-axis. The position of the trihedron xyz relative to the trihedron $x^0y^0z^0$ can be defined by the angle χ

FIGURE 54

between the axes x^0 and x (Figure 55). The relative angular velocity of the trihedron xyz relative to the trihedron $x^0y^0z^0$ is equal to the time derivative of the angle χ and is directed along the z-axis. It follows that the projection of the absolute angular velocity of the frame on its z-axis is, in accordance with the theorems of kinematics,

$$\omega_z = \frac{d\chi}{dt} + \omega_{z^0} = \frac{d\chi}{dt} + \frac{d\psi}{dt}\sin\varphi + \frac{d\alpha}{dt}. \qquad (192)$$

The motion of the gyroscopic frame is such that $\omega_z = 0$ (see (188)). It follows that

$$\frac{d\chi}{dt} + \frac{d\psi}{dt}\sin\varphi + \frac{d\alpha}{dt} = 0, \qquad (193)$$

whence

$$d\chi = -d\alpha - d\psi\sin\varphi. \qquad (194)$$

During the motion of the trihedron $x^0y^0z^0$ (i.e., during the variation of the angles ψ, φ, and α) the angle χ equals

$$\chi = -(\alpha - \alpha_0) - \int_{\psi_0,\,\varphi_0}^{\psi,\,\varphi} \sin\varphi\,d\psi, \qquad (195)$$

where ψ_0, φ_0, α_0 are the values of the angles ψ, φ, and α at the initial position of the trihedron. The initial value of the angle χ is taken as zero.

The value of the right-hand side of (195) depends on the curve described on the sphere by the apex M during the motion of the trihedron.

Let the trihedron $x^0y^0z^0$ return to its initial position. Equation (195) then becomes

$$\chi = -\oint \sin \varphi \, d\psi,$$ (196)

in which the integration is along the closed curve traced on the sphere by the trihedron apex M.

In the general case integral (196) is not zero. The frame is thus oriented differently in space at the end of its motion than at the beginning, in spite of the fact that the z-axis itself has returned to its initial position and that the projection of the absolute angular velocity of the frame on this axis was constantly equal to zero.
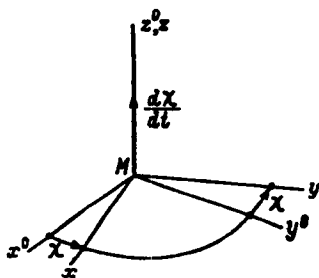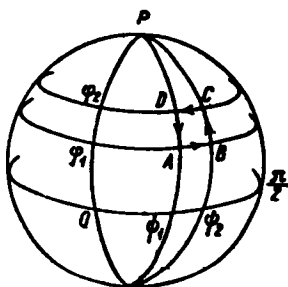
FIGURE 55   FIGURE 56

Consider in particular the motion of the apex of the trihedron $x^0y^0z^0$ along the closed curve formed by two arcs of the parallels AB and CD and two arcs of the meridians BC and DA (Figure 56).

The angle ψ does not vary during motion along the meridians, and therefore $d\psi = 0$. The angle φ does not vary during motion along the parallels, and therefore

$$\oint \sin \varphi \, d\psi = \int_{AB} \sin \varphi \, d\psi + \int_{CD} \sin \varphi \, d\psi = (\sin \varphi_1 - \sin \varphi_2)(\psi_2 - \psi_1),$$ (197)

where φ_1 and φ_2 are the latitudes of points A and C, and ψ_1 and ψ_2 their longitudes.

In this case, therefore.

$$\chi = (\sin \varphi_2 - \sin \varphi_1)(\psi_2 - \psi_1).$$ (198)

In particular, if the trihedron apex traces consecutively three arcs of great circles forming an octant, then

$$\varphi_1 = 0, \quad \varphi_2 = \frac{\pi}{2}, \quad \psi_2 - \psi_1 = \frac{\pi}{2}$$

and therefore

$$\chi = \frac{\pi}{2},$$

i.e., the frame is rotated through 90°; this can also be seen directly.

The right-hand side of (198) represents (as known from the formulas of elementary geometry) the ratio of the area bounded by $ABCD$ to the

71

square of the sphere radius R; in other words, it represents the solid angle Ω subtended by this area. Therefore

$$\chi = \Omega. \tag{199}$$

This formula remains valid for any closed curve on the sphere. Equation (199) can be proved using Green's formula

$$\oint (P\,dx + Q\,dy) = \iint \left(\frac{\partial Q}{\partial x} - \frac{\partial P}{\partial y} \right) dx\,dy. \tag{200}$$

Inserting here

$$P = \sin \varphi, \quad Q = 0, \quad x = \psi, \quad y = \varphi, \tag{201}$$

and taking (196) into account, we obtain

$$\chi = -\oint \sin \varphi \, d\psi = \iint \cos \varphi \, d\psi \, d\varphi. \tag{202}$$

The expression

$$R^2 \cos \varphi \, d\psi \, d\varphi \tag{203}$$

represents a surface element of the sphere bounded by two infinitely close parallels and two infinitely close meridians. Therefore

$$\chi = \frac{S}{R^2}, \tag{204}$$

where S is the part of the sphere's surface bounded by the closed curve. Equation (204) becomes (199) by the definition of the solid angle.

It is thus seen that the angle of rotation of the gyroscopic frame about its pivot axis is equal in value to the solid angle described by the pivot axis in the course of the motion of its base. Therefore the ship's gyroazimuth axis must be stabilized relative to the vertical, since otherwise the ship's roll would lead to additional solid angles being described during the motion by the axis, and therefore to large deviations of the instrument in azimuth*.

A behavior similar to that of the frame is shown by the simple flywheel mounted on a moving shaft in the absence of bearing friction. The initial angular velocity of the flywheel (more exactly its projection on the flywheel axis) must then be zero.

Another case of a nonholonomic constraint in the motion of a rigid body will now be treated by a somewhat different method. Let the rigid body move in such a manner that

$$\omega_\zeta \equiv 0, \tag{205}$$

where ω_ζ is the projection of the instantaneous angular velocity of the body on some fixed direction.

Consider two trihedrons: one, $\xi \eta \zeta$, in space, the other, xyz, fixed to the body. The relative position of these trihedrons can be determined by means of the three angles α, β, and γ in the same way as was done in § 3 of this chapter (p. 63) for displacements of the first kind.

Determine the projections of the angular velocity of the trihedron xyz on the axes ξ, η, and ζ. The vector of angular velocity is equal to the geometric sum of the angular velocities of the trihedron xyz each one of the angles α, β, or γ being varied separately while the other two are kept constant.

* This result, which has a large number of applications, is closely linked with the theory of the parallel transfer of a vector in Riemannian geometry.

It is easily seen (Figure 47) that an increase of the angle γ (the other angles being kept constant) corresponds to a clockwise rotation* about the axis $\zeta(\zeta_1)$ of the trihedron xyz, together with the trihedron $\xi_1\eta_1\zeta_1$ and $x'y'z'$ relative to the trihedron $\xi\eta\zeta$; an increase of the angle β corresponds to a clockwise rotation of the trihedron xyz, together with the trihedron $x'y'z'$, about the axis $\eta_1(y')$ (Figure 46); an increase of the angle α corresponds to a clockwise rotation of the trihedron xyz about the axis $x(x')$ (Figure 45). [In all cases viewed from the positive directions of the axes of rotation.]

It follows that the angular velocity $\frac{d\alpha}{dt}$ is directed toward the negative direction of the x-axis, the angular velocities $\frac{d\beta}{dt}$ and $\frac{d\gamma}{dt}$ toward the negative directions of the axes η_1 and ζ_1 respectively. The following expressions are obtained for the projection of the angular velocity ω on the axes ξ, η, and ζ by using the direction cosines given in (181) and (182):

$$\omega_\xi = -\frac{d\alpha}{dt}\cos\beta\cos\gamma - \frac{d\beta}{dt}\sin\gamma;$$

$$\omega_\eta = -\frac{d\alpha}{dt}(-\cos\beta\sin\gamma) - \frac{d\beta}{dt}\cos\gamma; \qquad (206)$$

$$\omega_\zeta = -\frac{d\alpha}{dt}\sin\beta - \frac{d\gamma}{dt}.$$

The position of the x-axis is determined, in accordance with (182), by the two angles β and γ. The angle α defines the relative position of trihedrons xyz and $x'y'z'$ (Figure 45), the axes x and x' of which coincide.

If the x-axis returns to its initial position in the course of the body's motion, the angles β and γ will likewise assume their initial values. The angle α will, however, in the general case not assume its initial value if a nonholonomic constraint, $\omega_\zeta = 0$, is imposed on the body. The position of the axes y and z will therefore differ from their initial position. In fact, it follows from the third equation (206) that in this case

$$d\alpha = -\frac{d\gamma}{\sin\beta} \qquad (207)$$

and therefore

$$\alpha = -\oint \frac{d\gamma}{\sin\beta}, \qquad (208)$$

where the integration is performed along a closed curve in the $\beta\gamma$ plane, and the initial value of α is taken as zero.

A geometric interpretation can be given to (208), as was done for (196).

Based on similar considerations, the time integral of the projection of the ship's angular velocity on the vertical,

$$\varphi = \int_0^t \omega_\zeta \, dt, \qquad (209)$$

is not the angle of yaw of the ship. In fact, the angle φ may differ from zero in spite of the fact that the ship has after a certain time t_1 returned to its initial course, so that the actual variation of the angle of yaw γ is zero.

---

* In Chapter II, § 3 the trihedron xyz was considered as fixed; as a result, an increase of any of the $\gamma, \alpha,$ or β corresponded to a counterclockwise rotation about the corresponding axis. In this section the trihedron $\xi\eta\zeta$ is fixed, and therefore increases of these angles correspond to clockwise rotations in Figures 45, 46, and 47.

It is seen from the third equation of (206) that

$$\varphi = \int_0^{t_1} \left(-\frac{d\alpha}{dt} \sin\beta - \frac{d\gamma}{dt} \right) dt = -\oint \sin\beta \, d\alpha; \qquad (210)$$

i.e., $\varphi \neq 0$ in the general case.

Chapter III

PHENOMENA CONNECTED WITH THE ELASTICITY
OF GYRO-SYSTEM ELEMENTS

§ 1. Elastic deformations of the gyro rotor under
the influence of centrifugal forces

The accuracy of gyroscopic instruments such as the directional gyro depends to a considerable extent on the accurate location of the rotor's center of gravity relative to the geometric center of the gimbal system. A shift of the order of one μ in the position of the center of gravity causes, as a rule, a deviation of the gyro of the same order as the specified tolerance of the instrument's accuracy.

Take, for instance, a rotor of weight $P = 1200$ g and angular momentum $H = 15,000$ gcm sec; the angular velocity of precession of the directional gyro (Figure 57) caused by a displacement $a = 1\,\mu$ of the center of gravity will then be

$$\frac{da}{dt} = \frac{Pa}{H} = \frac{1200 \cdot 0.0001}{15000} = 0.000008 \text{ sec}^{-1},$$

which is equivalent to 1.65 minutes of an arc per minute of time.

On the other hand, as will be shown below, the elastic deformations of a conventional rotor under the action of centrifugal forces cause a displacement of the center of gravity of the order of one hundredth of a millimeter.
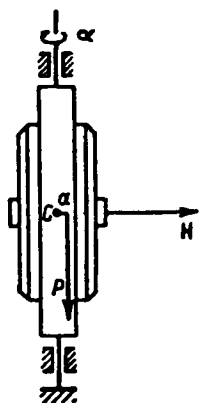
FIGURE 57
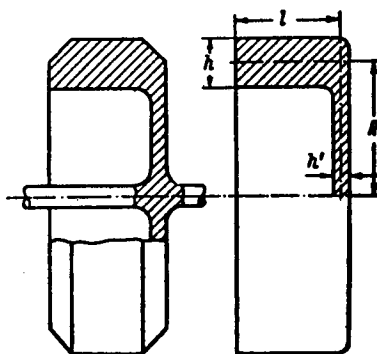
FIGURE 58

This can lead to unacceptable errors in the indications of the gyroscopic instruments during the variation of the rotational speed of the rotor (this variation occurs in many gyroscopic designs).

The rotor of most gyros can be represented schematically by a rela-
tively thin-walled cup revolving about its axis (Figure 58). The cylindrical
part of the cup tends to expand under the action of the centrifugal forces.
This expansion is prevented by the rotor bottom: the cylindrical part bends,
the bottom bulges inward, and, as a result the center of gravity of the rotor
is displaced along its axis (Figure 59).

The centrifugal forces acting on the rotor are considerable: the centri-
fugal force acting on a mass of 1 g situated on the rotor rim at a distance
of 45 mm from the axis of rotation equals 41.3 kg at 30,000 rpm.

The elastic deformations of the cylindrical part of the cup will be de-
termined approximately by the formulas of the axially-symmetrical bend-
ing of a cylindrical shell, and those of its bottom by the formulas of bend-
ing of a plate or disk of constant thickness, neglecting the influence on
bending of the tensile stresses in the median plane of the disk.
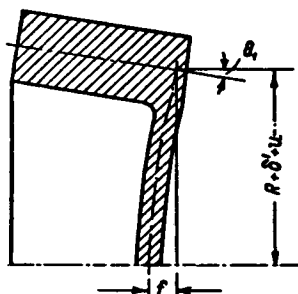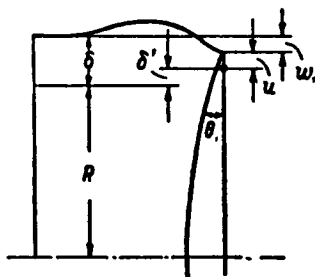
FIGURE 59   FIGURE 60

Let R be the mean radius of the cylindrical shell. Were it not restrained
at the bottom, this radius would increase under the action of the centrifugal
forces by the magnitude*

$$\delta = \frac{\gamma \omega^2 R^3}{g E}.$$

(211)

The influence on the rotor of the pressure of the squirrel cage, also sub-
jected to deformation by the centrifugal forces, is neglected. If necessary,
it can be allowed for by adjusting the value of γ in (211).

On the other hand, as follows from the formulas of the applied theory
of elasticity, the radius R of a disk of constant thickness increases at the
same angular velocity ω by the smaller magnitude

$$\delta' = \frac{(1 - \nu) \gamma \omega^2 R^3}{4 g E}.$$

(212)

In formulas (211) and (212) we have used the following notation:
   γ, specific weight of the material of the rotor;
   g, gravitational acceleration;
   E, modulus of elasticity;
   ν, Poisson's ratio.

* Timoshenko, S. P. Soprotivlenie materialov (Strength of Materials). Vol. II. — GITTL, Moskva-
   Leningrad. 1946; Teoriya uprugosti (Theory of Elasticity). — GTTI, Moskva-Leningrad. 1934.

Since (see Figure 60)

$$\delta > \delta',\qquad (213)$$

the right-hand edge of the shell undergoes, because of the rigid connection between the cylindrical shell and the bottom, an additional deflection w_1 toward the axis of symmetry; at the same time, the disk radius increases by the additional magnitude

$$u = \delta - \delta' - w_1.\qquad (214)$$

At the disk edge there appear distributed tensile stresses of intensity

$$Q' = \frac{Eh'}{1-v}\,\frac{u}{R}\,,\qquad (215)$$

where h' is the thickness of the disk (the cup bottom).

The right-hand edge of the shell also undergoes an angular displacement θ_1 The rigid connection between disk and shell cause an equal angular displacement of the disk edge. As a result, there appears a distributed bending moment at the edge of the disk, given by*

$$M' = \frac{(1+v)\,D'}{R}\,\theta_1,\qquad (216)$$

where

$$D' = \frac{Eh'^3}{12\,(1-v^2)}\,.$$

The deflection of the disk

$$f = \frac{R\theta_1}{2}\,,\qquad (217)$$

since the median surface of the disk bends along the surface of a sphere. The magnitude f is the displacement of the gyro rotor's center of gravity.

The additional deflection w of the cylindrical shell satisfies the following differential equation of the type of the equation of an elastically supported beam:

$$D\frac{d^4 w}{dz^4} + \frac{Eh}{R^2}\,w = 0,\qquad (218)$$

where

$$D = \frac{Eh^3}{12\,(1-v^2)}\,.$$

The bending moment and the shearing force become zero at the left edge of the shell, so that for $z = 0$,

$$\frac{d^2 w}{dz^2} = 0,\qquad \frac{d^3 w}{dz^3} = 0.\qquad (219)$$

The integral of (218) satisfying the boundary conditions (219) is:

$$w = A\,\mathrm{ch}\,x\cos x + B\,\frac{1}{2}\,(\mathrm{ch}\,x\sin x + \mathrm{sh}\,x\cos x),\qquad (220)$$

where

$$x = \beta z;\quad \beta = \sqrt[4]{\frac{3\,(1-v^2)}{R^2 h^2}}\,;\qquad (221)$$

A and B are constants which have to be determined.

The bending moment M and the shearing forces Q at the right end of the

* Timoshenko, S. P. Plastinki i obolochki (Theory of Plates and Shells). — Moskva-Leningrad, Gostekhizdat. 1948.

cylindrical shell can be obtained from

$$M = -\beta^2 D \frac{d^2w}{dx^2}, \quad Q = -\beta^3 D \frac{d^3w}{dx^3} \qquad (222)$$

where
$$x = \beta l,$$

and l is the length of the cylindrical shell.

By Newton's law of action and reaction, the values of M and Q are respectively equal to the corresponding values of M' and Q', for the disk. The following two equations with two unknowns A and B are obtained by equating (215) and (216) to equations (222) and then inserting (214) and (220)

$$-\beta^2 D[-A\,2\,\mathrm{sh}\,\beta l\,\sin\beta l - B(\mathrm{ch}\,\beta l\,\sin\beta l - \mathrm{sh}\,\beta l\,\cos\beta l)] =$$
$$= \frac{(1+\nu)\,D'}{R}\beta[-A(\mathrm{ch}\,\beta l\,\sin\beta l - \mathrm{sh}\,\beta l\,\cos\beta l) + B\,\mathrm{ch}\,\beta l\,\cos\beta l], \qquad (223)$$

$$-\beta^3 D[-A\,2(\mathrm{ch}\,\beta l\,\sin\beta l + \mathrm{sh}\,\beta l\,\cos\beta l) - B\,2\,\mathrm{sh}\,\beta l\,\sin\beta l] =$$
$$= \frac{Eh'}{(1-\nu)R}\Big[\delta - \delta' - A\,\mathrm{ch}\,\beta l\,\cos\beta l -$$
$$- B\,\frac{1}{2}(\mathrm{ch}\,\beta l\,\sin\beta l + \mathrm{sh}\,\beta l\,\cos\beta l)\Big]. \qquad (224)$$

Since
$$\theta_1 = -\frac{dw}{dx}\Big|_{x=l} = \beta[A(\mathrm{ch}\,\beta l\,\sin\beta l - \mathrm{sh}\,\beta l\,\cos\beta l) - B\,\mathrm{ch}\,\beta l\,\cos\beta l], \qquad (225)$$

the displacement of the center of gravity of the rotor can now be found from (217).

Numerical example. Let

$$R = 4.5\ \text{cm}, \quad h = 1.2\ \text{cm}, \quad h' = 0.4\ \text{cm}, \quad \gamma = 0.0078\ \text{kg/cm}^3, \quad l = 3\ \text{cm},$$

$$\omega = 3000\ \text{sec}^{-1}, \quad \nu = 0.3, \quad E = 2100000\ \text{kg/cm}^2.$$

It then follows that

$$\delta = \frac{\gamma\omega^2 R^3}{gE} = 0.00311\ \text{cm}; \quad \delta' = \frac{(1-\nu)\,\gamma\omega^2 R^3}{4gE} = 0.000544\ \text{cm};$$

$$\beta = \sqrt[4]{\frac{3(1-\nu^2)}{R^2 h^2}} = 0.553\ \text{cm}^{-1}; \quad \beta l = 1.660;$$

$$D = \frac{Eh^3}{12(1-\nu^2)} = 332\,000\ \text{kgcm};$$

$$D' = \frac{Eh'^3}{12(1-\nu^2)} = 12\,300\ \text{kgcm}; \quad \frac{1+\nu}{R}D' = 3550\ \text{kg};$$

$$\frac{Eh'}{(1-\nu)R} = 267000\ \text{kgcm}^{-2}.$$

Equations (223) and (224) become
$$-0.306 \cdot 332\,000\,(-5.04A - 2.93B) =$$
$$= 3550 \cdot 0.553\,(-2.93A - 0.243B),$$

$$-0.1691 \cdot 332\,000\,(-4.97A - 5.04B) =$$
$$= 267\,000\,(0.00257 + 0.243A - 1.243B).$$

78

Their solution yields

$$A = -0.000802; \quad B = 0.001396.$$

Inserting these values in (225) and the result in (217), gives

$$\theta_1 = 0.001488, \quad f = \frac{1}{2} R\theta_1 = 0.00335 \text{cm} \cong 33 \, \mu.$$

§ 2. Deformation of the gyro housing

In complex gyroscopic instruments such as the gyroazimuthhorizon, the gimbals and mechanisms are usually mounted on the walls and bottom of the housing. The housing must therefore be sufficiently rigid to avoid seiz-ing due to misalignment.

The danger of misalignment is particularly severe when the housing is mounted on the ship's deck by means of four bolts (Figure 61). A gap of width δ is formed between one foot and the deck because of unavoidable er-rors in the manufacture of the housing base; this gap is frequently closed by strongly tightening the corresponding bolt and the bolt diagonally op-posite; as a result the housing becomes distorted (Figure 62).
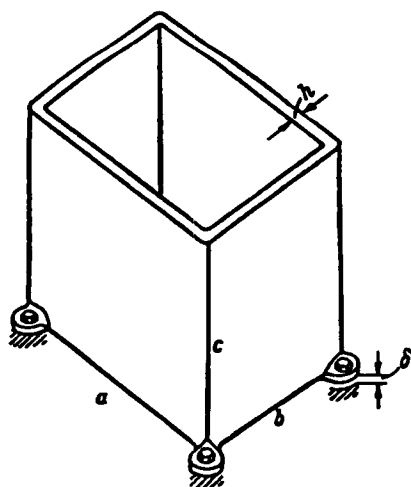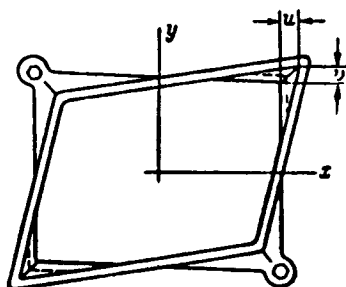
FIGURE 61   FIGURE 62

To find the deformation of the housing and the permissible width of this gap, a model of the housing consisting of four walls and a bottom of constant thickness, similar to a box without lid, will be used. This three-dimen-sional structure is subjected to the action of four concentrated forces P act-ing parallel to the housing center line on the lower corners (Figure 63).

It is evident that if the tensile stresses in the walls and bottom are neg-lected, the housing edges AA', BB', CC', DD', AB, BC, CD, and DA can be as-sumed to remain straight, the trihedrons with apexes at points A, B, C, and D remaining orthogonal.

79

This means that the walls and bottom, which will be considered to be elastic plates, are subjected to pure torsion, by four equal and parallel concentrated forces Q applied to the corners of a rectangular plate (Figure 64).
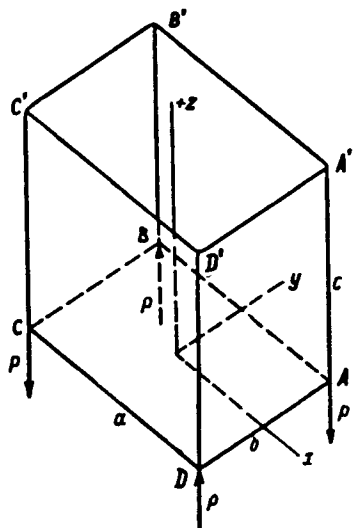
FIGURE 63

The plate deflection for pure torsion* is

$$w = \frac{Qxy}{2(1-\nu)D} .$$ (226)

The deflection w is measured from the plane xy tangent to the plate at its center.
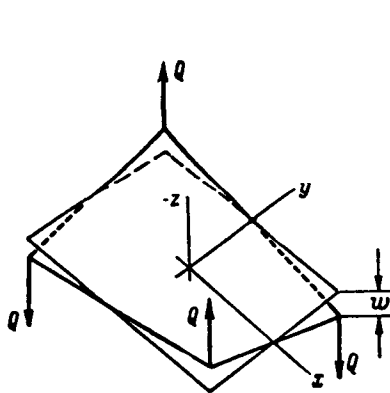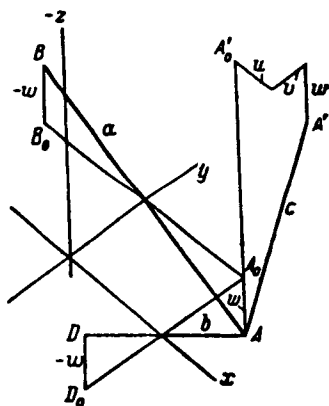
FIGURE 64   FIGURE 65

* Timoshenko, S. P. Plastinki i obolochki (Theory of Plates and Shells). — Moskva–Leningrad, Gostekhizdat. 1948.

We introduce a coordinate system xyz with origin at the center of the housing bottom (Figure 65), z-axis directed along the housing center line, and x- and y-axes parallel to the undeformed bottom edges. We denote by u, v, and w the displacements of the upper corner (point A') in the directions of the axes x, y, and z respectively.

From the assumptions on the absence of tensile stresses in the plates it follows that the displacements of point A of the housing bottom will be respectively

$$u_A = 0, \quad v_A = 0, \quad w_A = w, \tag{227}$$

and those of points B and D

$$u_B = u_D = 0, \quad v_B = v_D = 0, \quad w_B = w_D = -w. \tag{228}$$

The following relationships of orthogonality follow from the perpendicularity of AA' to AB and AD:

$$(AA')_x(AB)_x + (AA')_y(AB)_y + (AA')_z(AB)_z = 0,$$
$$(AA')_x(AD)_x + (AA')_y(AD)_y + (AA')_z(AD)_z = 0, \tag{229}$$

or

$$u \cdot a + v \cdot 0 - 2w \cdot c = 0,$$
$$u \cdot 0 + v \cdot b - 2w \cdot c = 0, \tag{230}$$

where a, b, and c are the lengths of the edges AB, AD, and AA'.

Equations (230) yield

$$u = \frac{2c}{a} w, \qquad v = \frac{2c}{b} w. \tag{231}$$

The potential energy of deformation of the plate $ABCD$ forming the housing bottom is

$$U_0 = \frac{1}{2} 4Qw = \frac{16(1-\nu) D_0 w^2}{ab}. \tag{232}$$

The potential energies of deformation of plates $ABA'B'$ and $ADA'D'$ are, as is easily seen,

$$U_1 = \frac{16(1-\nu) D \left(\frac{1}{2} u\right)^2}{ac},$$
$$U_2 = \frac{16(1-\nu) D \left(\frac{1}{2} v\right)^2}{bc}. \tag{233}$$

Inserting the expressions for u and v from (231) yields the following formula for the total potential energy of the housing:

$$U = U_0 + 2U_1 + 2U_2 = \frac{16(1-\nu) D_0 w^2}{ab}\left(1 + 2\frac{D}{D_0}\frac{bc}{a^2} + 2\frac{D}{D_0}\frac{ac}{b^2}\right). \tag{234}$$

It is known from the theory of elasticity that the potential energy of an elastic system equals half the work done by the external forces along the displacements of the system, i.e.,

$$U = \frac{1}{2} 4Pw. \tag{235}$$

The displacement w is obtained by equating (234) and (235):

$$w = \frac{P}{\frac{8(1-\nu) D_0}{ab}\left(1 + 2\frac{bc}{a^2}\frac{D}{D_0} + 2\frac{ac}{b^2}\frac{D}{D_0}\right)}. \tag{236}$$

81

The forces acting at the housing corners are shown in Figure 66.

The following formulas can be obtained from (226) and (231) and the conditions of equilibrium of the housing walls and bottom:

$$X=Y=\frac{8(1-\nu)D}{ab}w; \quad Z'=2\frac{c}{b}Y; \quad Z''=2\frac{c}{a}X;$$

$$Z=Z'+Z''=P-Q; \quad Q=\frac{8(1-\nu)D_0}{ab}w. \tag{237}$$

Formula (236) could be derived from these equations without using the theorem of the elastic energy.
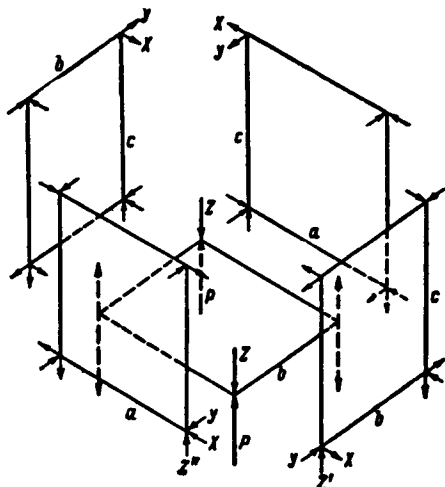
FIGURE 66

N u m e r i c a l   e x a m p l e.   Consider a cube-shaped housing with edges 500 mm long and duraluminum walls ($E=750{,}000$ kg/cm^2, $\nu=0.3$) 10 mm thick. A deflection $\delta=2w=1$ mm is then caused by a tensile force of 40 kg acting on the bolt.

§ 3. The rigidity of the gimbal rings

The gimbal rings of gyroscopic systems, such as the gyroazimuthhorizon, are subjected to considerable loads. At certain instants they carry the entire load due to the rotation of a number of elements linked kinematically with the stabilized parts of the device. The elastic deformations of the gimbal rings may cause erroneous readings of the instruments, or even judder due to friction (cf. § 4 of this chapter).

This section deals with the elastic deformation of gimbal rings and bows for different loading schemes.

1. A ring resting freely on two supports and acted upon by two forces (Figure 67). The deflection f at the points of application of each of the

82

forces and the rotation ϑ of the section at the support are respectively

$$f = PR^3\left(\frac{0.2854}{B} + \frac{0.0708}{C}\right),$$

$$\vartheta = 0.1427\,PR^2\left(\frac{1}{B} + \frac{1}{C}\right). \tag{238}$$

We denote by B the flexural rigidity of the ring or bow, and by C the torsional rigidity.

2. If the pivots are prevented from deflections in the vertical plane (Figure 68), $\vartheta = 0$, and the deflection becomes

$$f^* = PR^3\left(\frac{0.2336}{B} + \frac{0.0190}{C}\right). \tag{239}$$

This case does not occur in practice because of the deformation of the bearings and the unavoidable clearances.
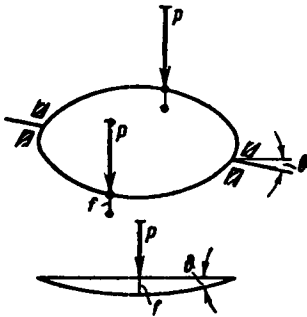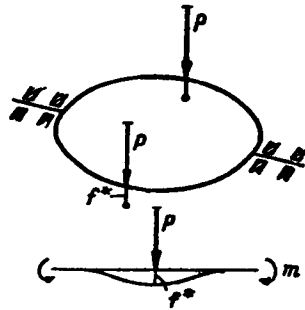
FIGURE 67   FIGURE 68

3. A ring resting freely on two supports and acted upon by a couple (Figure 69); an equilibrating torque acts on one of the pivots. The line connecting the points of application of the forces rotates through the angle

$$\theta_1 = PR^2\left(\frac{0.6263}{B} + \frac{0.0935}{C}\right), \tag{240}$$

relative to the pivot axis. The unloaded pivot rotates through the angle

$$\theta_2 = PR^2\left(\frac{0.7854}{B} + \frac{0.1488}{C}\right), \tag{241}$$

relative to the loaded pivot.

4. The case where one force only acts on the ring (Figure 70) can be obtained from cases 1 and 3. If the section at which the equilibrating torque is applied is considered as rigidly fixed, the deflection f_1 at the point of application of the force P is

$$f_1 = PR^3\left(\frac{0.4558}{B} + \frac{0.0822}{C}\right). \tag{242}$$

The deflection f_2 of the opposite point is less:

$$f_2 = PR^3\left(\frac{0.1705}{B} + \frac{0.0114}{C}\right). \tag{243}$$

83

The rotation θ of one pivot relative to the other is

$$\theta = PR^2\left(\frac{0.3927}{B} + \frac{0.0744}{C}\right). \tag{244}$$

5. If the ring is twisted by opposing torques applied to the pivots (Figure 71), the angle of twist φ of the ring is

$$\varphi = mR\left(\frac{0.7854}{B} + \frac{0.1488}{C}\right). \tag{245}$$

6. The bow is loaded in the center (Figure 72) by a concentrated force P and an equilibrating torque acting at one of the pivots. The deflection w
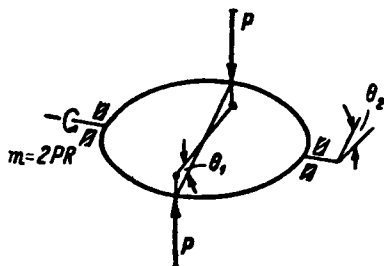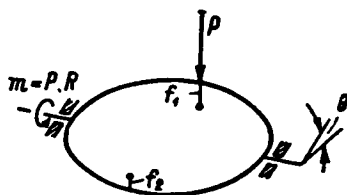
FIGURE 69   FIGURE 70

at the point of application of the force is

$$w = PR^3\left(\frac{0.6781}{B} + \frac{0.4635}{C}\right). \tag{246}$$

One of the pivots rotates relative to the other through the angle

$$\beta = 0.7854\, PR^2\left(\frac{1}{B} + \frac{1}{C}\right). \tag{247}$$

Numerical example. Consider a duraluminum bow $(E = 750,000$ kg/cm^2, $\nu = 0.25)$ of radius $R = 250$ mm loaded by a force $P = 10.0$ kg according to scheme 6 (Figure 72). The dimensions of the bow section are given in Figure 73.
In this case*

$$B = E\,\frac{(a'+\delta)\,(b'+\delta)^3 - (a'-\delta)\,(b'-\delta)^3}{12} =$$

$$= 750\,000 \cdot 25.7 = 19\,270\,000 \text{ kgcm}^2;$$

$$C = G\,\frac{2\,(a'b')^2}{a'+b'}\,\delta = 300\,000 \cdot 31.0 = 9\,300\,000 \text{ kgcm}^2.$$

From (246) we obtain

$$w = 0.0133 \text{ cm} = 0.133 \text{ mm}.$$

---

* Timoshenko, S. P. Soprotivlenie materialov (Strength of Materials). Part II. — GITTL, Moskva-Leningrad. 1946.

If the bow section has the shape shown in Figure 74, then

$$B_1 = 19\,270\,000 \text{ kgcm}^2, \quad C_1 = G\frac{2a' + 2b' - c}{3}\delta^3 =$$

$$= 300\,000 \cdot 0.645 = 193\,500 \text{ kgcm}^2.$$

From (246),

$$w_1 = 0.381 \text{cm} = 3.81 \text{ mm}.$$

In this case the deflection is almost 28 times that of the bow in the previous example.
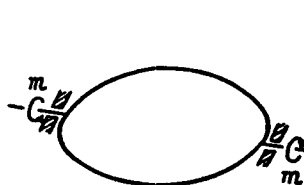
FIGURE 71
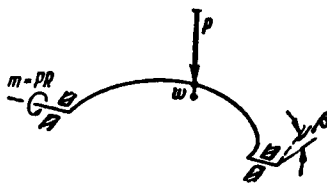
FIGURE 72

The corresponding values of the angle β are, according to (247):

$$\beta = 0.000783 \,(\cong 3') \quad \text{and} \quad \beta_1 = 0.0257 \,(\cong 1°28').$$

An analysis of formulas (238) — (247) shows that the torsional rigidity has a considerable influence on the deformation of the rings. Accordingly, the so-called open (e.g., trough-shaped) profiles should not be used in
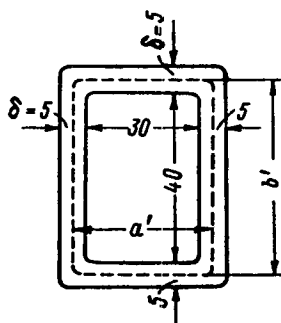
FIGURE 73
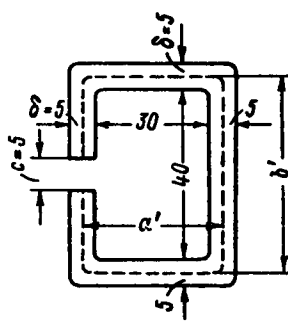
FIGURE 74

gimbal rings; closed profiles should be used instead. Their sections need not be round. It appears that single openings in the walls of closed profiles do not substantially reduce the torsional rigidity, and can therefore be permitted. Unfortunately, the theoretical study of this very important problem is very difficult, while experimental results are not yet available.

§ 4. Discontinuous motion of insufficiently rigid kinematic transmissions

Insufficient rigidity of kinematic chains connecting elements of gyro-scopic instruments and control systems causes not only inaccurate repeat-ing of the required magnitudes, but also loss of transmission smoothness. If, for instance, the gimbal ring rotates relative to the instrument housing sufficiently slowly and uniformly about its axis the rotor of a tachomachine linked to the gimbal ring by a relatively long kinematic chain may move discontinuously.

This phenomenon is known as f r i c t i o n a l   j u d d e r. It results from the laws of friction in the kinematic transmissions, in particular in the link having the greatest mass or moment of inertia. In the case considered this link is the rotor of the tachomachine.

The judder disappears with increasing rotational speed of the gimbal ring or increased rigidity of the transmission between the ring and the rotor.

Many attempts have been made to explain this phenomenon, each attribut-ing different influences to the transmission parameters and the frictional forces.

The theory of judder evolved in 1944 by the author in collaboration with I. V. Kragel'skii is given below. This theory is based on the existence of a relationship between the initial frictional force F and the duration t of the contact between the two bodies, all other conditions being equal (Figure 75).
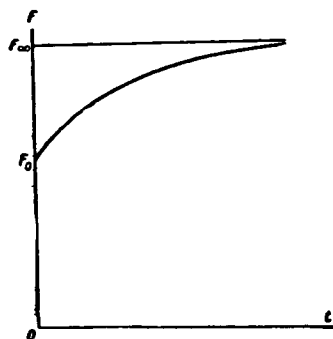
FIGURE 75

This relationship can, on the strength of theoretical considerations, be represented fairly accurately by the formula

$$F = F(t) = F_\infty - (F_\infty - F_0) e^{-at}, \qquad (248)$$

where F_∞ is the initial frictional force for an infinitely long duration of contact between the bodies;

F_0, the frictional force for a very short duration of contact;

a, the coefficient depending on the properties of the two bodies, the condition of their surfaces, lubrication, etc.

Obviously

$$F_\infty > F_0. \qquad (249)$$

86

We assume for the sake of simplicity that the force of dynamic friction is also equal to F_0 and does not depend on the velocity with which one body slides on the other.

FIGURE 76

The following scheme is useful for analyzing the phenomenon of discontinuous motion or judder (Figure 76). A body A, linked to a fixed object by means of a spring C of rate K, lies on the rough surface B. When the surface moves it carries the body with it, pulling on the spring with a force

$$P = Kx, \qquad (250)$$

where x is the displacement of the body from the position at which no force acts on the spring.

The body A will move together with the surface B until the force of the spring C acting on it becomes equal to the starting-friction force for the specified duration of contact between the body and the surface. The displacement x_0 at which the body begins to slide on the surface, when contact is sufficiently long, is given by

$$Kx_0 = F_{\infty}. \qquad (251)$$

This sliding is the result of two forces acting on the body: the contact force of sliding friction F_0 in the direction of motion of the surface, and the elastic force of the spring P, expressed by (250). The subsequent motion of the body under the action of these two forces will be harmonic about the equilibrium position $x = a$ (Figure 77), which is determined by the relationship

$$Ka = F_0. \qquad (252)$$

When sliding begins, the body A has a displacement x_0 and a velocity v. It will therefore continue to move in the same direction as the surface initially, gradually losing speed and lagging behind it. Later the velocity
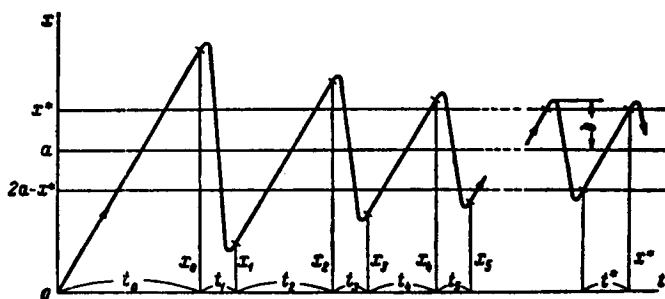
FIGURE 77

becomes zero and changes sign; the body starts moving in the opposite direction with a velocity gradually increasing in absolute value. The absolute value of the velocity attains a maximum at $x = a$, at which the frictional

87

force is equal to the elastic force of the spring, and then begins to decrease until the velocity again becomes zero and changes sign; the body starts moving with increasing speed in the direction of motion of the surface. At $x=x_1$ the body's velocity becomes equal to that of the surface v. Since the body's motion is harmonic, the displacements corresponding to the same value of v are symmetrical about the equilibrium position. Therefore

$$\frac{x_0+x_1}{2}=a, \tag{253}$$

whence

$$x_1=2a-x_0. \tag{254}$$

It is easily seen that the body ceases sliding on the surface B after its velocity has reached the value v, and that its further motion (until sliding sets in again) is in unison with the surface. In fact, the body cannot overtake the surface, since this would mean that the frictional force changes sign and that the force acting on the body in the direction of motion of the surface is

$$-Kx_1-F_0=-K(2a-x_0)-F_0=F_\infty-3F_0. \tag{255}$$

This expression is, however, negative if $F_\infty<3F_0$, so that our assumption is incorrect.

We denote by t_2 the time during which the body A moves together with the surface B after sliding has ceased, and by x_2 the displacement of the body at the instant sliding recommences. The following equation will obviously be satisfied:

$$x_2=x_1+vt_2. \tag{256}$$

On the other hand, sliding recommences at the instant the spring force Kx_2 is equal to the starting-friction force, whose value is determined by the time t_2 during which the point A is in contact with the surface B without sliding. Therefore:

$$Kx_2=K(x_1+vt_2)=F(t_2), \tag{257}$$

from which t_2 and x_2 can be determined if the function $F(t)$ is known.
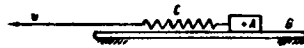
<p align="center">FIGURE 78</p>

The renewed motion will similarly be harmonic and will end at the instant the velocity of the body becomes again equal to that of the surface. The corresponding value of the displacement x_3 is then

$$x_3=2a-x_2, \tag{258}$$

which is similar to (254).

The body A will then again move together with the surface B for a time t_4 at a velocity v until sliding occurs again at $x=x_4$. The time t_4 can be found by solving an equation similar to (257), i.e.,

$$Kx_4=K(x_3+vt_4)=F(t_4). \tag{259}$$

This sliding is again followed by a uniform motion, followed by a third period of sliding etc.

If the durations t_0, t_2, t_4 of joint motion of the body A and the surface B without relative sliding tend toward the nonzero limit t^* then the harmonic motion of the body A (Figure 76) becomes a constant-amplitude periodic oscillation, usually of the relaxation type (which is quite different from a harmonic oscillation).

We now invert this scheme, and let the end of spring C move at constant velocity v, while the surface B remains stationary (Figure 78). The above analysis remains valid also in this case. After a time t_0 the body A will start moving with a succession of stops of respective durations t_2, t_4, ..., in other words, the motion will be discontinuous.

To find the conditions under which discontinuous motion or judder occurs during friction, consider the above scheme (Figure 76) and denote by x^* the limit of the sequence of the displacements x_0, x_2, x_4, ..., at which sliding starts (Figure 77). In the limit the difference $x^* - a$ represents half the distance traveled by the body together with the surface without sliding. Therefore

$$x^* - a = \frac{vt^*}{2},\tag{260}$$

whence

$$x^* = a + \frac{vt^*}{2}.\tag{261}$$

On the other hand, sliding starts at the instant at which the spring force becomes equal to the starting-friction force for the duration t^* of contact without sliding between the body and the surface:

$$Kx^* = F(t^*).\tag{262}$$

Inserting (261) yields

$$K\left(a + \frac{vt^*}{2}\right) = F(t^*).\tag{263}$$

The value t^* can be found from this equation.

Figure 79 represents the starting-friction force $F(t)$ as a function of the duration t of contact without sliding between body and surface. It also shows the spring force $P(t)$

$$P = K\left(a + \frac{vt}{2}\right),\tag{264}$$

at the end of the time t during which the body A remains stationary relative to the moving surface B.

The two curves have a common point at $t = 0$, since

$$Ka = F_0 = F(0).\tag{265}$$

This will be the only common point if the slope of the curve $F = F(t)$ at $t = 0$ is less than the slope of the straight line (264). There are then no relaxation oscillations.

If the starting-friction force is given by (248), then

$$F'(0) = \alpha(F_\infty - F_0).\tag{266}$$

It follows that for no judder the inequality

$$\alpha(F_\infty - F_0) < \frac{Kv}{2},\tag{267}$$

must be satisfied. This will always be the case if the spring stiffness K or the velocity v is sufficiently large.

If inequality (267) is not satisfied (this may happen with a soft spring), the curves in Figure 79 have another intersection point at $t=t^*$. In this case judder is possible. It can be shown that this motion of body A will be stable. The limiting value of v at which inequality (267) becomes an equality will be denoted by v_1.

Consider again the curve $F=F(t)$ of the starting-friction force as a function of the duration of contact without sliding between the body and the surface (Figure 80).
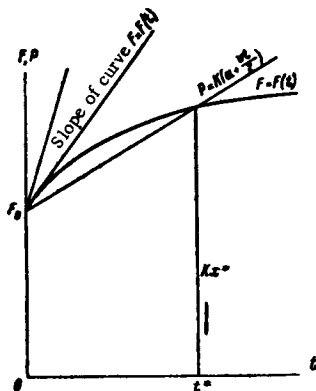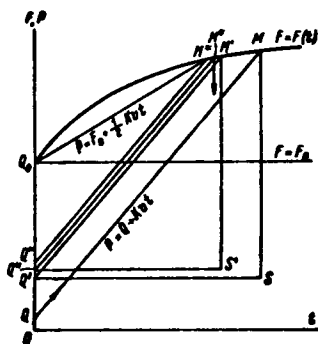
FIGURE 79   FIGURE 80

Draw on the same figure and to the same scale the curve $P=P(t)$ of the spring force as a function of duration t of joint motion without sliding. This curve will be the straight line

$$P=Q+Kvt, \qquad (268)$$

where Q is the spring force at the beginning of the motion in unison. The abscissa of the point M at which the curves $F=F(t)$ and $P=P(t)$ intersect gives the instant at which sliding starts; its ordinate gives the corresponding value of the displacement x of body A, multiplied by the spring rate K.

Mark off a point S symmetrical to M about the line

$$F=F_0, \qquad (269)$$

parallel to the abscissa; also mark off on the ordinate a point Q' having the same ordinate as point S. It is then easy to see that the ordinate of point Q' (or S) represents the value of the spring force at the end of sliding and therefore at the start of a new period of joint motion of body and surface. The spring force will then vary according to the law

$$P=Q'+Kvt, \qquad (270)$$

represented in Figure 80 by the line $Q'M'$, where M' is the intersection of the straight line (270) and the curve $F=F(t)$. The point M' determines the beginning of renewed sliding. Knowing its position, the points S' and Q'' can be found, and plotting can be continued until the sequence M, M', M'',... tends to a limit point M^*. The sequence Q', Q'',... in its turn determines a limit point Q^*. The points M^* and Q^* are located on opposite sides of the line $F=F_0$ at equal distances from it.

90

Mark off on the ordinate a point Q_0 (Figure 80) located at a distance F_0 from the abscissa. The equation of the line Q_0M^* is

$$P = F_0 + \frac{Kvt}{2},$$ (271)

since the slope of the line Q_0M^* is half the slope of Q^*M^*.

By inserting (265) into (271) this last equation becomes identical with (264). The two lines therefore coincide, and the abscissa t^* of point M^* is determined by solving equation (263).

To study the problem of the stability of the interrupted motion, assume that at a certain instant the body A is placed on the surface B to the left of the position corresponding to the end of steady sliding (Figure 81). This corresponds to some point Q located on the ordinate below Q^*. The spring force will vary according to (268) as a straight line of slope Kv up to the intersection with the curve $F = F(t)$ at point M. Sliding starts at this instant.

FIGURE 81   FIGURE 82

The ordinate of point M is larger than the ordinate of M^*, and the displacement of body A from the equilibrium position $x = a$ will therefore be greater at the beginning of sliding than for steady motion.

On the other hand, the ordinate of point M is less than the ordinate of point N at which the straight lines (268) and (271) intersect.

Point N is located at the same distance from the line $F = F_0$ as point Q, as can be easily seen from the similarity of the figures. It follows that point S, symmetrical with point M relative to the line $F = F_0$, will be nearer to this line than point Q. The renewal of joint motion of body and surface is therefore determined by point Q' located between points Q and Q^*. It is seen that the judder amplitude will decrease until a periodic motion is finally established.

It can be similarly shown that if body A is placed on surface B to the right of the position corresponding to the end of sliding at steady motion, the judder amplitude will increase. This case is shown in Figure 82 by points Q_1, M_1, S_1, Q'_1, ... etc.

The amplitude of the steady judder is

$$b = \sqrt{(x^* - a)^2 + \frac{m}{K}v^2},$$ (272)

91

since initially the body's velocity is equal to the velocity v of the surface and the displacement of the body from the equilibrium position is equal to the difference $x^* - a$.

The difference $x^* - a$ decreases with increasing velocity v until it becomes zero for $v = v_1$ (cf. p. 90). Point M^* in Figure 80 approaches point Q_0 until both coincide for $v = v_1$, when the interval t^* becomes zero.

It is thus seen that to point Q_0 (Figure 80) there corresponds a harmonic motion of body A, which slides on the moving surface B continuously (except at the instants in which the velocities of the body and surface become equal).

The limiting value of the amplitude is

$$b_1 = v_1 \sqrt{\frac{m}{K}} . \tag{273}$$

This harmonic motion is unstable if the curve $F = F(t)$ intersects the straight line (264) at a point M^*; it is stable if this straight line lies above the curve $F = F(t)$ and does not intersect it. The proof is similar to the above.

In addition to this harmonic motion, the body A can also perform an infinite number of other harmonic motions of smaller amplitudes. In particular it can be in equilibrium when displaced to a distance $x = a$ (Figure 76) to the right of the position at which no spring force acts. In this case it follows from (265) that the force of dynamic friction F_0 and the spring force P_0 equalize each other, i.e.,

$$P_0 = Ka. \tag{274}$$

This equilibrium is stable. This is, however, different if the force of dynamic friction depends, even slightly, on the relative velocity of sliding.

Let the frictional force have a regressive characteristic, i.e., the frictional force decreases with increasing relative velocity of sliding. In this case the equilibrium becomes unstable; if air resistance is neglected, then for the scheme in Figure 76 either quasi-harmonic oscillations or discontinuous motion will occur, depending on the spring rate C and on the velocity of the surface B.

Regressive friction characteristics are comparatively rare. It follows that the equilibrium at $x = a$ will usually be stable; the resistance of the surrounding medium to the motion of the body also contributes to this stability.

In conclusion, two stationary states are as a rule possible for the scheme in Figure 76 when inequality (267) obtains: a state of rest, and discontinuous motion. The transition from the state of rest to the state of discontinuous motion can be performed only by giving to body A a velocity not less than the velocity v of surface B. The initial joint motion without sliding of body A and surface B, leading to the initial sliding, is a particular case of such an excitation.

The period of the steady motions is the sum of the time during which the body and surface move in unison and the duration of discontinuous motion:

$$T = 2\frac{x^* - a}{v} + \pi \sqrt{\frac{m}{K}} + 2\tau, \tag{275}$$

where the value of τ is found from the ratio

$$\cos\sqrt{\frac{K}{m}}\,\tau = \frac{x^* - a}{b}\,. \tag{276}$$

When the velocity v reaches its limiting value $v = v_1$, $x^* = a$, and therefore

$$T = 2\pi\sqrt{\frac{m}{K}}\,. \tag{277}$$

This case therefore corresponds to harmonic oscillations.

For very small values of v, on the other hand, the first term on the right-hand side of (275) is decisive, and the oscillations exhibit a relaxation pattern.

§ 5. Influence of the rigidity of the gyroscopic-system elements on the frequency of nutations

The elasticity of the elements of the gyros' gimbals and of the various transmissions linked with the gyros is usually neglected when determining the natural frequencies of oscillations of the gyroscopic systems. The frequency of nutations v of the simplest gyroscopic stabilizer (Figure 83)
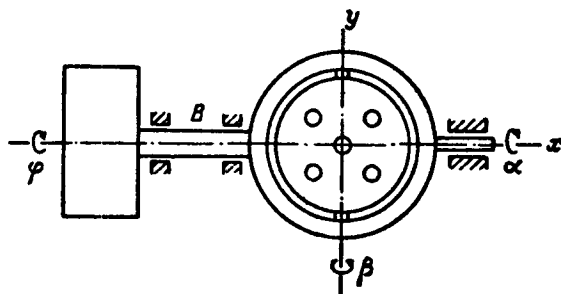
FIGURE 83

is thus determined (Chapter IV, § 1) by the formula

$$v = \frac{H}{\sqrt{(A+J)B}}\,, \tag{278}$$

where H is the angular momentum of the gyrostabilizer;

   A, the moment of inertia of the gyro rotor together with its casing and the outer gimbal ring, referred to the stabilization axis x;

   J, the moment of inertia of the mass to be stabilized, referred to the same axis;

   B, the moment of inertia of the gyro rotor together with its casing, referred to the casing axis y.

Formula (278) is derived under the assumption that the rotor axis forms a small angle with the perpendicular to the xy plane, that all system elements are perfectly rigid bodies, and that there is no friction in the bearings.

93

According to (278) an increase in the angular velocity of the rotor causes a proportional increase in the frequency of nutations ν. In fact

$$H = Cn, \tag{279}$$

where C is the moment of inertia of the gyro rotor about its axis of rotation z. Therefore

$$\nu = \frac{Cn}{\sqrt{(A+J)B}}. \tag{280}$$

The agreement between formula (278) and experimental results is in many cases rather poor. The experimentally determined frequency of nutations is lower than that given by (280), the discrepancy increasing with the angular velocity of the rotor. V.I. Kuznetzov found the cause of this discrepancy in the elasticity of the gyro-system elements.

The influence of the rigidity of the gyroscopic device, shown schematically in Figure 83, on the natural frequencies of its oscillations is analyzed below.

In order to simplify the mathematical treatment, it will be assumed that only the shaft B, connecting the mass to be stabilized with the outer gimbal ring of the gyro, is elastic. The mass of the shaft itself is neglected. The equations of motion of the gyroscopic device are in this case:

$$A \frac{d^2\alpha}{dt^2} - H \frac{d\beta}{dt} = K(\varphi - \alpha),$$

$$B \frac{d^2\beta}{dt^2} + H \frac{d\alpha}{dt} = 0, \tag{281}$$

$$J \frac{d^2\varphi}{dt^2} = K(\alpha - \varphi),$$

where the new symbols introduced have the following meaning:

K, rigidity of the shaft B;

α, angle of tilting of the outer gimbal ring about the stabilization axis;

φ, angle of tilting of the mass to be stabilized about the same axis;

β, angle of tilting of the gyro casing about its axis.

The determinant of the system of auxiliary equations of (281) is

$$D(\lambda) = \begin{vmatrix} A\lambda^2 + K & -H\lambda & -K \\ H\lambda & B\lambda^2 & 0 \\ -K & 0 & J\lambda^2 + K \end{vmatrix} \tag{282}$$

The following equation is obtained by expanding the determinant (282) and equating it to zero:

$$ABJ\lambda^6 + [(A+J)BK + H^2J]\lambda^4 + H^2K\lambda^2 = 0. \tag{283}$$

This equation has a double root $\lambda = 0$. A linear first integral is

$$B \frac{d\beta}{dt} + H\alpha = \text{const.}$$

Introduce the magnitudes

$$\nu^2 = \frac{H^2}{(A+J)B} \quad \text{and} \quad k^2 = \frac{K}{J}. \tag{284}$$

which have simple physical meanings: ν, as already mentioned, is the frequency of nutations of the gyroscopic device, shown in Figure 83, with all its elements including the shaft B perfectly rigid; k is the frequency of

94

the torsional oscillations of the mass to be stabilized, assuming the outer gimbal ring to be fixed and the shaft B to be elastic.

The following biquadratic equation is obtained by simplifying (283) and inserting (284):

$$\frac{A}{A+J}\lambda^4+(k^2+\nu^2)\lambda^2+k^2\nu^2=0.\qquad(285)$$

From this we obtain the two natural frequencies of oscillation of the gyroscopic device.

Using the notation:

$$\alpha=\frac{A}{A+J},\quad x=-\frac{\lambda^2}{k^2},\quad \xi=\frac{\nu^2}{k^2},\qquad(286)$$

equation (285) becomes

$$\alpha x^2-(1+\xi)x+\xi=0,\qquad(287)$$

in which the unknown x is a dimensionless magnitude proportional to the square of the natural frequency of the device. The parameter α is by definition always less than unity. The value of the parameter ξ is a function of the angular velocity of the gyro rotor. The following expression for the parameter ξ is obtained from (279), (284), and (286):

$$\xi=\frac{JC^2n^2}{(A+J)BK}.\qquad(288)$$

Consider the case when ξ is small relative to unity; this case corresponds to a low angular momentum of the gyro or to a high rigidity of the shaft. The roots of (287) can in this case be approximated by the following series expansions:

$$x_1=\xi-(1-\alpha)\xi^2+(1-3\alpha+2\alpha^2)\xi^3+\ldots,\qquad(289)$$

$$x_2=\frac{1}{\alpha}+\frac{1-\alpha}{\alpha}\xi+(1-\alpha)\xi^2+\ldots.\qquad(290)$$

The first terms of these expansions have a simple physical meaning. In fact, inserting (284) and (286) in (289) and (290) yields, when all right-hand terms except the first are neglected:

$$-\lambda_1^2\cong\nu^2=\frac{H^2}{(A+J)B},\qquad(291)$$

$$-\lambda_2^2\cong\frac{k^2}{\alpha}=\frac{(A+J)K}{AJ}.\qquad(292)$$

These are respectively the square of the nutation frequency of the gyroscopic device for a perfectly rigid shaft B, and the square of the frequency of torsional oscillations of two masses having moments of inertia A and J, connected by a shaft of rigidity K (Figure 84).

FIGURE 84

95
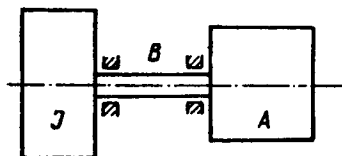
It is thus seen that formula (278) is correct for very small values of ξ, but that for small values of ξ the frequency of nutations increases more slowly with ξ than the angular momentum.

Consider now the case of large values of ξ, corresponding to a very large angular momentum of the gyroscope or to a low rigidity of the shaft **B**. The solution of (287) can in this case be represented as an expansion in powers of $\frac{1}{\xi}$.

$$x_1 = 1 - \frac{1-\alpha}{\xi} + \frac{1-3\alpha+2\alpha^2}{\xi^2} + \ldots \tag{293}$$

$$x_2 = \frac{1}{\alpha}\xi + \frac{1-\alpha}{\alpha} + \frac{1-\alpha}{\xi} + \ldots \tag{294}$$

The first terms of these expansions have likewise a simple physical meaning. In fact, inserting (284) and (286) yields the following approximations:

$$-\lambda_1^2 \cong k^2 = \frac{K}{J}, \tag{295}$$

$$-\lambda_2^2 \cong \frac{\nu^2}{\alpha} = \frac{H^2}{AB}. \tag{296}$$

Formula (296) gives the frequency of nutations of the gyroscopic device when the mass to be stabilized is removed, and (295) gives the frequency of the torsional oscillations of this mass when the outer gimbal ring is fixed [to the ship].

The higher-order terms of expansions (293) and (294) introduce corrections due to the existence of a dynamic linkage between the mass to be stabilized and the gyroscope.

Numerical example. Let

$A = 10 \text{ gcm sec}^2$; $B = 7.2 \text{ gcm sec}^2$; $C = 5 \text{ gcm sec}^2$;
$n = 1500 \text{ sec}^{-1}$; $J = 10 \text{ gcm sec}^2$; $K = 19{,}550{,}000 \text{ gcm}$.

Then

$$\nu^2 = \frac{H^2}{(A+J)B} = 391\,000 \text{ sec}^{-2}; \quad k^2 = \frac{K}{J} = 1\,955\,000 \text{ sec}^{-2};$$

$$\alpha = \frac{A}{A+J} = 0.5; \quad \xi = \frac{\nu^2}{k^2} = 0.2.$$

The following roots are obtained by solving (287):

$$x_1 = 0.180; \quad x_2 = 2.22.$$

The square of the natural frequencies of the gyroscopic device are therefore

$$-\lambda_1^2 = k^2 x_1 = 352\,000 \text{ sec}^{-2}, \quad -\lambda_2^2 = k^2 x_2 = 4\,340\,000 \text{ sec}^{-2}.$$

The value obtained for the frequency of nutations, taking into account the elasticity of shaft **B**, is in this case 5 % less than the value obtained when assuming that all elements of the gyroscopic device are perfectly rigid.

If the angular velocity **n** of the gyro rotor is doubled without altering

its geometric dimensions, the result is

$$\nu^2 = 1\,564\,000 \text{ sec}^{-2}; \qquad \xi = 0.8;$$
$$x_1 = 0.519; \qquad x_2 = 3.08;$$
$$-\lambda_1^2 = 1\,015\,000 \text{ sec}^{-2}, \qquad -\lambda_2^2 = 6\,020\,000 \text{ sec}^{-2}.$$

In this case the difference between the two values obtained for the frequency of nutations is 20%, and a correction has to be introduced in (278).

Curves of the roots of equation (287) as function of ξ have been plotted in Figure 85 for $\alpha = 0.5$.
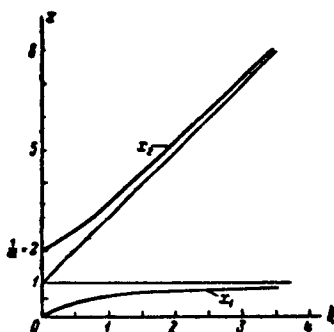
FIGURE 85

It should be noted that a rigidity $K = 19,550,000$ gcm is relatively high; it corresponds to the torsional rigidity of a round steel cylinder 10 mm in diameter and 40 mm long.

The outer gimbal ring, the gyro casing, and the shaft of the gyro rotor have rigidities of this order. Formula (278) is therefore incorrect even for free gyros.

In practice, a correction factor of $0.5 - 0.7$ is introduced into (278),

$$\nu \cong (0.5 - 0.7) \frac{H}{\sqrt{(A + J)B}} \,. \tag{297}$$

The natural frequencies of gyroscopic devices, taking into account the rigidity of the elements, can be similarly obtained. Some of these problems were discussed earlier by G. D. Blyumin. An exact mathematical treatment leads to the determination of the natural frequencies of a mechanical system having an infinite number of degrees of freedom in the presence of gyroscopic forces.

The critical velocity of the rotor shaft must likewise be found taking into account the rigidity and mass of the gimbal elements whose influence can be considerable.

§ 6. The damping of gyroscopic and other devices mounted
on objects moving at high accelerations

The objects on which the gyroscopic devices are mounted often have accelerations of the order of hundreds of g (gravitational acceleration); this is the case when objects dropped from a great height fall into the water.

97

In other cases, these objects are subjected to strong vibrations which produce accelerations of the order of tens of g; this happens when the fuel is burnt during the flight of a missile. The inertia forces caused by these accelerations are undesirable, since they not only affect the accuracy of the gyroscopic instruments, but may also put these out of order.

Large inertia forces can also be caused by careless handling of the instruments. Dampers (shock-absorbers) are used to reduce the inertia forces. However, not only does the damping fail to achieve its aim in may cases, it may even cause an increase in the inertia forces acting on the instruments.

The following rule can be stated:

"The use of shock absorbers is justified only if the distance through which the object containing the instrument to be protected is braked (or accelerated) is not greater than the damping travel."

Gyroscopic or other instruments have frequently been improperly secured through ignorance of this simple rule.

Consider the case of sudden braking of an object having a translatory motion. Let $a(t)*$ be the deceleration of the object, and m the mass of the instrument mounted on the object. Assume that the shock absorber acts in the direction of the object's motion. Denote by A the force developed by the shock-absorber. The equation of motion of the instrument, referred to the object, is then

$$m \frac{d^2z}{dt^2} = ma(t) - A, \qquad (298)$$

where z is the displacement of the instrument from the equilibrium position at steady motion of the object (Figure 86).
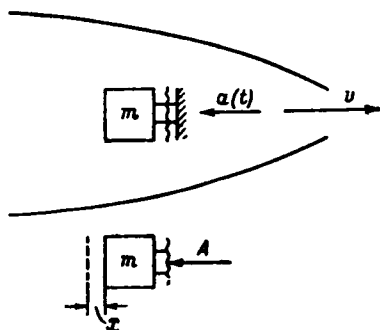
FIGURE 86

If the instrument is connected rigidly to the object, $z \equiv 0$ in (298). This yields

$$A = A_0 = ma(t), \qquad (299)$$

where A_0 is the force with which the object acts on the instrument.

The product $ma(t)$ is thus the inertia force acting on the instrument in the absence of damping.

---

* The damping of vibrations is not discussed, being generally known.

When a shock absorber is used, a force A acts on the instrument. This force is, according to (298),

$$A = ma(t) - m\frac{d^2z}{dt^2}.$$ (300)

The product $ma(t)$ is positive during the entire period that the object is braked. It follows that $A < A_0$ only if the condition

$$\frac{d^2z}{dt^2} > 0$$ (301)

is satisfied during all this time.

It will be shown below that if the damping travel, i.e., the maximum possible displacement of the instrument from its equilibrium position, is much less than the braking distance, then the acceleration $\frac{d^2z}{dt^2}$ is considerably smaller than $a(t)$ when condition (301) is satisfied; it follows that then damping does not attain its aim, since $A \cong ma(t)$.

The initial conditions of the braked motion are

$$z(0) = 0, \qquad \frac{dz(0)}{dt} = 0.$$ (302)

Therefore

$$z = \int_0^{t_1} \left[\int_0^t w(t)\,dt \right] dt,$$ (303)

where t_1 is the duration of braking, and

$$w(t) = \frac{d^2z}{dt^2}.$$ (304)

If the limit of damping travel is denoted by δ, then

$$\int_0^{t_1} \left[\int_0^t w(t)\,dt \right] dt < \delta.$$ (305)

Let the braking distance be s_1, and let the braking reduce the object's velocity by a factor μ; denote by a_{max} the maximum value of the braking deceleration. The following theorem is then true for the conditions stated (including inequality (305)).

T h e o r e m. For every given braking law $s = s(t)$ there exist in the interval $0 \leqslant t \leqslant t_1$ instants t for which $w(t)$ is less than a_{max} if δ is considerably less than s_1.

P r o o f. Introduce the mean value w_* of the acceleration $w(t)$ during the interval $0 \leqslant t \leqslant t_1$. Inequality (305) can then be written

$$w_* \frac{t_1^2}{2} < \delta.$$ (306)

It follows that there are instants for which

$$w(t) < \frac{2\delta}{t_1^2}.$$ (307)

The time during which the object traverses the braking distance $s = s_1$ will be a minimum if the motion is initially unbraked, i.e., at the velocity v_0, the last part of s_1 being traversed at the constant deceleration a_{max} (Figure 87).

Then
$$t_1 \geqslant \frac{s_1 - s_m}{v_0} + \frac{v_0 - v_1}{a_{max}},$$
(308)

where
$$s_m = \frac{v_0^2 - v_1^2}{2a_{max}},$$
(309)

is the minimum braking distance when the condition

$$-\frac{d^2 s}{dt^2} \leqslant a_{max}$$
(310)

is satisfied. In fact
$$s_1 = \lambda s_m$$
(311)

where λ is greater than unity. It is also clear that

$$v_0 = \mu v_1,$$
(312)

where μ is likewise greater than unity.
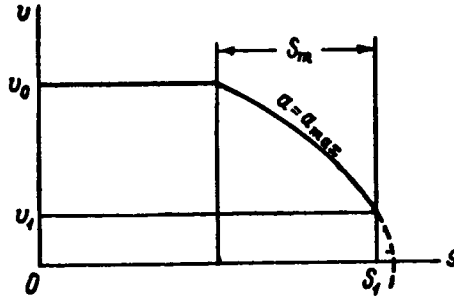
FIGURE 87

Inserting (311) and (312) into (309) yields

$$\frac{s_1}{\lambda} = \frac{\mu^2 - 1}{2a_{max}} v_1^2.$$
(313)

It follows that

$$v_1 = \frac{\sqrt{2s_1 a_{max}}}{\sqrt{\lambda (\mu^2 - 1)}},$$
(314)

$$v_0 = \mu \frac{\sqrt{2s_1 a_{max}}}{\sqrt{\lambda (\mu^2 - 1)}}.$$
(315)

Inserting (311), (314), and (315) into (308) transforms this inequality into

$$t_1 > x \sqrt{\frac{2s_1}{a_{max}}},$$
(316)

where
$$x = \frac{\lambda - 1}{2\mu} \sqrt{\frac{\mu^2 - 1}{\lambda}} + \sqrt{\frac{\mu - 1}{\lambda (\mu + 1)}}.$$
(317)

(For example, if $\lambda = \mu = 2$, then $x = 0.715$.)

100

It follows from (307) and (316) that there exist instants t at which

$$w(t) < \frac{1}{\pi^2} \frac{s}{s_1} a_{max}.$$ (318)

This completes the proof, and also establishes the rule, formulated above, on the cases in which damping of instruments mounted on moving objects is indicated.

If the acceleration of the instrument relative to the object changes sign, then $A > ma(t)$ by (300), and the shock absorber causes an increase of the force acting on the instrument. This is to be expected if the period of natural oscillations of the instrument is shorter than the duration of braking the object. In this case a shock absorber will even be harmful.

Several examples illustrating these considerations will now be given.

1. A spring of rate $K = 150$ kg/cm is used as shock absorber (Figure 88). The instrument weight is $mg = 10$ kg. The object has a constant deceleration $a = 100$ g; the initial velocity of the object is $v_0 = 396$ km/hr, and its final velocity $v_1 = 36$ km/hr.
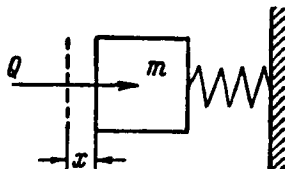
FIGURE 88

The braking distance and time are in this case

$$t_1 = \frac{v_0 - v_1}{a} = 0.1 \text{ sec}, \quad s_1 = \frac{v_0^2 - v_1^2}{2a} = 6 \text{ m}.$$

The equation of motion of the instrument referred to the object is

$$m \frac{d^2x}{dt^2} = -Kx + ma,$$

whence

$$x = \frac{ma}{K} + C \cos \sqrt{\frac{K}{m}} t + D \sin \sqrt{\frac{K}{m}} t,$$

where

$$k = \sqrt{\frac{K}{m}} = 121.3 \text{ sec}^{-1}$$

is the angular velocity of the oscillations of the instrument relative to the object, and C and D are constants which have to be determined.

The initial conditions (302) yield

$$x(0) = \frac{ma}{K} + C = 0,$$

$$\frac{dx(0)}{dt} = kD = 0.$$

Therefore

$$x = \frac{ma}{K} \left(1 - \cos \sqrt{\frac{K}{m}} t \right).$$

101

The maximum displacement of the instrument from the equilibrium position is

$$z_{max} = 2\frac{ma}{K} = 13.3 \, cm,$$

and is reached after a time

$$\frac{T}{2} = \pi\sqrt{\frac{m}{K}} = 0.0259 < 0.1 \, sec,$$

that is long before braking of the object ends.

The maximum force developed by the shock absorber is twice the inertia force

$$A_0 = ma = mg\frac{a}{g} = 1000 \, kg,$$

since in this case

$$A_{max} = Kz_{max} = 2ma = 2000 \, kg.$$

It follows that the shock absorber has a negative influence on the instrument. In addition, the damping travel $\delta > 13.3$ cm would hardly satisfy the design requirements.

2. A noticeable shock-absorber action exists only at excessively large displacements of the instrument relative to the object.

Let, for instance, the spring parameters be such that

$$\frac{T}{4} = \frac{\pi}{2}\sqrt{\frac{m}{K}} > t_1.$$

The following relationships obtain at the instant braking ends:

$$z(t_1) = \frac{ma}{K}\left(1 - \cos\sqrt{\frac{K}{m}}t_1\right),$$

$$\frac{dz(t_1)}{dt} = a\sqrt{\frac{m}{K}}\sin\sqrt{\frac{K}{m}}t_1.$$

Further motion of the instrument is determined by the differential equation

$$m\frac{d^2z}{dt^2} = -Kz$$

with initial conditions

$$z(0) = \frac{ma}{K}(1 - \cos kt_1),$$

$$\frac{dz(0)}{dt} = a\sqrt{\frac{m}{K}}\sin kt_1, \quad k = \sqrt{\frac{K}{m}}.$$

The integral corresponding to these initial conditions is

$$z = \frac{ma}{K}[(1 - \cos kt_1)\cos kt + \sin kt_1 \sin kt].$$

The maximum displacement of the instrument is therefore

$$z_{max} = \frac{ma}{K}\sqrt{(1 - \cos kt_1)^2 + (\sin kt_1)^2} = 2\frac{ma}{K}\sin\frac{kt_1}{2}.$$

The maximum load on the instrument is therefore determined by the formula

$$A_{max} = Kx_{max} = 2ma \sin \frac{kt_1}{2} = 2A_0 \sin \frac{kt_1}{2}.$$

Let

$$\frac{A_{max}}{A_0} = 2 \sin \frac{kt_1}{2} = 0.1.$$

This shows that the force acting on the instrument is only one tenth of the force acting when the instrument is rigidly secured to the object.

Inserting $t_1 = 0.1$ sec:

$$k \cong 1 \sec^{-1}, \quad \frac{K}{m} = k^2 = 1 \sec^{-2}.$$

The corresponding maximum displacement for $a = 100$ g will be almost 100 m.

These calculations show that it is advisable to use shock absorbers when the braking duration t_1 is very short. A very stiff spring can be used in this case causing a comparatively small displacement of the instrument relative to the object.

Let, for instance,

$$t_1 = 0.003 \sec, \quad A_{max} = 0.2A_0, \quad \text{and} \quad a = 10 g.$$

Then

$$\sin \frac{kt_1}{2} = \frac{A_{max}}{2A_0} = 0.1, \quad k = 66.7 \sec^{-1}, \quad x_{max} = \frac{2ma}{K} = \frac{2a}{k^2} = 4.4 \text{cm}.$$

3. Due to space limitations stops are frequently fitted which restrict the deflection of the shock-absorber spring. If the object is sharply braked, the instrument compresses the spring, moves through its entire free travel, and strikes the stop. The impact forces arising at this instant are considerably higher than the forces arising when the instrument is rigidly secured. Such a shock absorber is therefore not recommended.
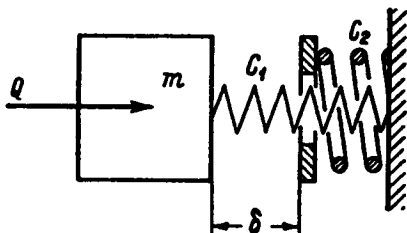
FIGURE 89

A shock absorber with restricted travel can be represented as a combination of two springs compressed by the instrument mass (Figure 89). The spring C_1 has a relatively low rate K; the spring C_2 has a rate B equaling that of the stop.

The compression of spring C_2 starts after spring C_1 has undergone a deflection δ.

Assume for simplicity that the deceleration a of the object is constant and that the duration of braking is longer than the compression time of both

springs; the instrument's motion relative to the object then takes place under the action of the elastic forces of the springs and the constant inertia force

$$Q = ma.$$

Denote by f the maximum deflection of spring C_2. The deflection of spring C_1 is then $f + \delta$, and the potential energy accumulated by the two springs is

$$U = \tfrac{1}{2} K (\delta + f)^2 + \tfrac{1}{2} B f^2.$$

The following equation expresses the law of conservation of energy:

$$\tfrac{1}{2} K (\delta + f)^2 + \tfrac{1}{2} B f^2 = Q (f + \delta).$$

The right-hand side of this equation represents the work done by the force Q along the displacement $f + \delta$. The maximum value of the deflection is therefore

$$f = \frac{Q - K\delta + \sqrt{Q^2 + 2BQ\delta - KB\delta^2}}{K + B}.$$

The maximum value of the force acting on the instrument is

$$A_{max} = K (\delta + f) + B f.$$

Let

$$K = 150 \, \text{kg/cm}, \quad \delta = 5 \, \text{mm}, \quad mg = 10 \, \text{kg}, \quad Q = 1000 \, \text{kg}, \quad \text{and} \quad B = 150\,000 \, \text{kg/cm}.$$

This corresponds to a deformation of the stop amounting to 0.067 mm under the action of a force of one ton.

We obtain in this case

$$f = 0.0864 \, \text{cm}; \quad A_{max} = 13050 \, \text{kg} > 13 Q.$$

If the deflection f of spring C_2 is neglected as being small compared with the deflection δ of spring C_1, we obtain

$$\tfrac{1}{2} (K\delta^2 + Bf^2) \cong Q\delta; \quad f = \sqrt{\frac{2Q\delta - K\delta^2}{B}} = 0.0802 \, \text{cm};$$

$$A_{max} \cong K\delta + Bf = 12\,100 \, \text{kg}.$$

The formula for A_{max} can be simplified still further without great error:

$$A_{max} \cong \sqrt{2BQ\delta} = 12\,240 \, \text{kg}.$$

The physical meaning of the simplifications made in this last formula is that the influence of the shock-absorber spring is neglected after impact against the stop, as is the deflection f relative to δ.

In fact, the force needed to compress spring C_1 by 5 mm is 75 kg. This is considerably less than the inertia force $Q = 1000$ kg.

It is true that an increase of the shock-absorber spring rate reduces the value of A_{max}; this, however, has no great effect, since the force on the instrument is $2Q = 2000$ kg even in the absence of impact against a stop.

Chapter IV

LINEAR THEORY OF GYROSCOPIC SYSTEMS

§ 1. The equations of gyroscopic systems

Gyroscopic phenomena obey strictly the laws of classical mechanics. They provide, together with the motion of celestial bodies, the experimental corroboration of the laws of classical mechanics in a reference frame having its origin at the center of mass of the universe, with axes oriented according to the Newtonian frame (the so-called inertial reference frame).

The equations of motion of the gyros in gyroscopic systems must therefore allow for the angular velocity of the Earth and for the additional rotation of the gyroscopic device, together with the object carrying it, on the curvilinear surface of the Earth.

The forces acting on the gyros are determined by the relative position and motion of the gyro and the other parts of the gyroscopic device, and by the motion of the object on which the gyroscopic system is mounted. The inertia forces arising during the translational motion of the object can affect the gyro considerably, in particular if there are unbalanced parts in the gyroscopic device. The influence of the translational motion is in some cases neutralized by special means (compensation of the accelerations and velocity deviations), while in other cases it is made use of for the measurement of the angular velocity of the object, integration of its linear acceleration, or other measurements.

Euler's dynamic and kinematic equations, widely used in theoretical mechanics in the study of the motion of a rigid body about a fixed point, are not suitable for the study of the gyro's motion, due to the fact (already mentioned in Chapter II, § 3) that the two Euler angles, corresponding to a deviation of the axis of rotation of the rigid body from its initial position, are in general not small. At the same time, the axes of rotation of the gyro's rotors of almost all gyroscopic systems deviate only slightly from some fixed direction in space; in any case, the change in the mean position of the rotor shaft (precessional motion) proceeds at an incomparably slower rate than the rapid motion of the shaft about this mean position (nutational motion). It follows that in order to study the motion pattern it is sufficient to consider only small deviations of the rotor shaft from its initial position during a short time interval.

This shortcoming of the classical equations can be overcome either by using Krylov's system of modified Euler angles* or by using an altogether

---
* Krylov, A. N. and Yu. A. Krutkov. Obshchaya teoriya giroskopov i nekotorykh tekhnicheskikh ikh primenenii (General Theory of Gyroscopes and Some Technical Applications). — Izdatel'stvo Akademiya Nauk SSSR, Leningrad. 1932.

different system of angles, such as the angles representing a finite rotation of the first kind (see Chapter II, § 3).

Let $\xi_0\eta_0\zeta_0$ be a coordinate system oriented according to the Newtonian frame, and xyz a coordinate system characterizing the position which the trihedron abc attains as a result of successive finite rotations about its edges a, b, and c through angles α, β, and γ respectively, the initial position of a, b, and and c coinciding with the axes ξ_0, η_0, and ζ_0, respectively (Figures 90 and 91).
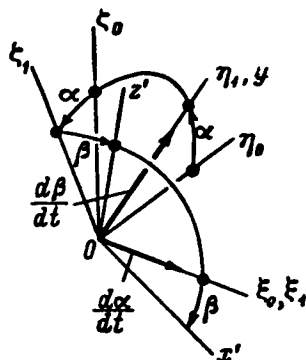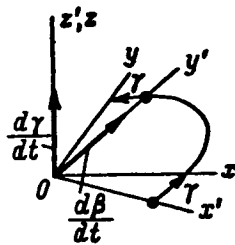
FIGURE 90   FIGURE 91

The direction cosines of the system $\xi_0\eta_0\zeta_0$ relative to the system xyz can be obtained from (182) (see Chapter II, § 3) by interchanging ξ and x, η and y, ζ and z*. The result is:

	x	y	z
ξ_0	$\cos\beta\cos\gamma$	$-\cos\beta\sin\gamma$	$\sin\beta$
η_0	$\sin\alpha\sin\beta\cos\gamma +$ $+\cos\alpha\sin\gamma$	$-\sin\alpha\sin\beta\sin\gamma +$ $+\cos\alpha\cos\gamma$	$-\sin\alpha\cos\beta$
ζ_0	$-\cos\alpha\sin\beta\cos\gamma +$ $+\sin\alpha\sin\gamma$	$\cos\alpha\sin\beta\sin\gamma +$ $+\sin\alpha\cos\gamma$	$\cos\alpha\cos\beta$

$$(319)$$

If the angle α is changed, β and γ remaining constant, the trihedron xyz rotates about the ξ_0-axis with an angular velocity $\frac{d\alpha}{dt}$ (Figure 90) whose projections on the x-, y-, and z-axes are, according to (319),

$$p_\alpha = \frac{d\alpha}{dt}\cos\beta\cos\gamma, \quad q_\alpha = -\frac{d\alpha}{dt}\cos\beta\sin\gamma, \quad r_\alpha = \frac{d\alpha}{dt}\sin\beta. \qquad (320)$$

If the angles α and γ are kept constant, the trihedron xyz revolves about the y'-axis of the system $x'y'z'$ with an angular velocity $\frac{d\beta}{dt}$ ($x'y'z'$ denotes the position of the trihedron abc after the finite rotations through angles α and β about axes a and b have been completed) (Figure 90).

The direction cosines of the system xyz relative to the system $x'y'z'$

* In Chapter II, § 3 the trihedron xyz denotes the initial position of the axes abc, while here it denotes their final position.

106

(Figure 91) are

	x'	y'	z'
x	$\cos\gamma$	$\sin\gamma$	0
y	$-\sin\gamma$	$\cos\gamma$	0
z	0	0	1

(321)

It follows that the projections of the angular velocity $\frac{d\beta}{dt}$ on the axes x, y, and z are respectively

$$p_\beta = \frac{d\beta}{dt}\sin\gamma,$$

$$q_\beta = \frac{d\beta}{dt}\cos\gamma,$$

$$r_\beta = 0.$$

(322)

If, finally, the angle γ is changed with α and β remaining constant, the trihedron xyz rotates about the z-axis with an angular velocity $r_\gamma = \frac{d\gamma}{dt}$ (Figure 91).

The following expressions for the projections of the angular velocity of the trihedron xyz on its edges are obtained through addition:

$$p = \frac{d\alpha}{dt}\cos\beta\cos\gamma + \frac{d\beta}{dt}\sin\gamma;$$

$$q = -\frac{d\alpha}{dt}\cos\beta\sin\gamma + \frac{d\beta}{dt}\cos\gamma$$

$$r = \frac{d\alpha}{dt}\sin\beta + \frac{d\gamma}{dt}.$$

(323)

Assuming that the angles α and β and their time derivatives are small, expressions (323) can be replaced by the following approximate expressions, accurate to second-order terms in α, β, $\frac{d\alpha}{dt}$, and $\frac{d\beta}{dt}$:

$$p = \frac{d\alpha}{dt}\cos\gamma + \frac{d\beta}{dt}\sin\gamma;$$

$$q = -\frac{d\alpha}{dt}\sin\gamma + \frac{d\beta}{dt}\cos\gamma;$$

$$r = \frac{d\gamma}{dt}.$$

(324)

Inserting these formulas into Euler's equations of motion

$$A\frac{dp}{dt} + (C-B)\,qr = M_x,$$

$$B\frac{dq}{dt} + (A-C)\,rp = M_y,$$

$$C\frac{dr}{dt} + (B-A)\,pq = M_z,$$

(325)

[for the meaning of A, B, and C see explanations after (278) and (279)] yields, since $A = B$ (because of the dynamic symmetry of the rotor):

$$A\left(\frac{d^2\alpha}{dt^2}\cos\gamma + \frac{d^2\beta}{dt^2}\sin\gamma\right) + C\frac{d\gamma}{dt}\left(-\frac{d\alpha}{dt}\sin\gamma + \frac{d\beta}{dt}\cos\gamma\right) = M_x,$$

$$A\left(-\frac{d^2\alpha}{dt^2}\sin\gamma + \frac{d^2\beta}{dt^2}\cos\gamma\right) - C\frac{d\gamma}{dt}\left(\frac{d\alpha}{dt}\cos\gamma + \frac{d\beta}{dt}\sin\gamma\right) = M_y,$$

$$C\frac{d^2\gamma}{dt^2} = M_z.$$

(326)

107

We multiply the first equation (326) by $\cos\gamma$ and the second by $-\sin\gamma$ and add them term by term. We then multiply the first equation by $\sin\gamma$, the second by $\cos\gamma$ and add them again term by term. The results are the well-known linear equations of the time derivatives of α and β:

$$A\frac{d^2\alpha}{dt^2} + H\frac{d\beta}{dt} = M_{x'},$$

$$A\frac{d^2\beta}{dt^2} - H\frac{d\alpha}{dt} = M_{y'},$$

(327)

where

$$M_{x'} = M_x\cos\gamma - M_y\sin\gamma,$$

$$M_{y'} = M_x\sin\gamma + M_y\cos\gamma$$

(328)

are the sums of the external moments about the x'- and y'-axes acting on the gyro rotor, and

$$H = C\frac{d\gamma}{dt}$$

(329)

is the angular momentum of the gyro rotor, constant, according to the third equation of (326), if $M_z = 0$.

When the gyro is suspended in gimbals, the moments $M_{x'}$ and $M_{y'}$ also include the moments of the inertia forces on the rotor due to the mass of the gimbal rings (Figure 92). For small angles α and β these are

$$-(I_{\xi_1} + I_{x'})\frac{d^2\alpha}{dt^2}; \quad -I_{y'}\frac{d^2\beta}{dt^2},$$

(330)

where $I_{x'}$ and $I_{y'}$ are the moments of inertia of the inner gimbal ring (or housing) about the x'-, and y'-axes, and I_{ξ_1} is the moment of inertia of the
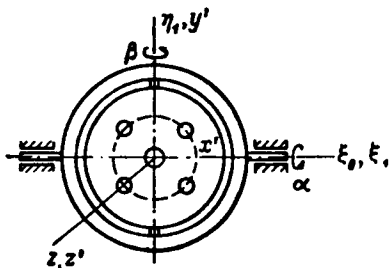
FIGURE 92

outer gimbal ring about the ξ_1-axis; this axis coincides with the ξ_0-axis. We introduce the symbols

$$A_1 = A + I_{\xi_1} + I_{x'}, \qquad B_1 = A + I_{y'}.$$

(331)

Assuming the angle between the x'- and ξ_0-axes to be small, the equations (327) can now be written:

$$A_1\frac{d^2\alpha}{dt^2} + H\frac{d\beta}{dt} = M_{x'} \cong M_{\xi_0},$$

$$B_1\frac{d^2\beta}{dt^2} - H\frac{d\alpha}{dt} = M_{y'}.$$

(332)

Here M_ξ is the sum of the external moments about the axis of the outer gimbal ring acting on the outer and inner gimbal rings and on the gyro rotor, and $M_{y'}$, is the sum of the external moments acting on the rotor and on the inner gimbal ring about the y'-axis [Figure 92].

The moments $M_{\xi'}$ and $M_{y'}$, include the moments due to friction in the gimbals bearings, and the moment of the gravitational force, the moments due to translational inertia forces, the moments of various additional forces (e.g., correction forces), etc.

Equations (332) are widely used in practice for preliminary studies of stability problems in gyroscopic systems.

In deriving (332) terms of second and higher orders in α and β and their time derivatives were neglected. It was also assumed that the moment M_z is zero. For more exact solutions these terms must be included.

Many other simplifying assumptions were also made. The imperfect perpendicularity of the gimbals axes caused by manufacturing errors, the clearances in the bearings, the elasticity of the gimbals elements, the friction in the rotor shaft bearings, etc., were neglected.

There is thus no sense in analyzing the stability of the motion by means of differential equations of higher order than the linear equations (332), without taking into account experimental data.

When the gyroscopic system is known to be stable and the main aim is to study its accuracy, equations (332) can in many cases be considerably simplified by omitting the so-called inertial terms

$$A_1 \frac{d^2\alpha}{dt^2} \quad \text{and} \quad B_1 \frac{d^2\beta}{dt^2}. \tag{333}$$

Equations (332) then become

$$H \frac{d\beta}{dt} = M_\xi,$$
$$-H \frac{d\alpha}{dt} = M_{y'}, \tag{334}$$

The equations obtained can be considered to result from the time averaging of equations (332), with moments M_ξ and $M_{y'}$, varying slowly. In fact, for constant M_ξ and $M_{y'}$, the motion described by equations (332) can be represented as the sum of the solutions of equations (334) and of the set of homogeneous equations

$$A_1 \frac{d^2\alpha}{dt^2} + H \frac{d\beta}{dt} = 0,$$
$$B_1 \frac{d^2\beta}{dt^2} - H \frac{d\alpha}{dt} = 0. \tag{335}$$

Equations (335) represent harmonic oscillations (nutations), usually of high frequency:

$$\nu = \frac{H}{\sqrt{A_1 B_1}}. \tag{336}$$

The average value of the solutions of equations (335) ($\frac{d\alpha}{dt}$ and $\frac{d\beta}{dt}$) is zero.

There is a simple geometric interpretation to equations (334). Draw a plane perpendicular to the ζ_0-axis at unit distance from the origin of the coordinate system $\xi_0\eta_0\zeta_0$ (Figure 93). Denote by G_0 the intersection of this plane with the vector of angular momentum H (or, which is the same, the axis of rotation z of the rotor) drawn from the origin.

Using (319), the following expressions are obtained for the coordinates of point G_0:

$$\xi_0 = OG_0 \cos \xi_0 z = OG_0 \sin \beta,$$

$$\eta_0 = OG_0 \cos \eta_0 z = -OG_0 \sin \alpha \cos \beta, \qquad (337)$$

$$\zeta_0 = OG_0 \cos \zeta_0 z = OG_0 \cos \alpha \cos \beta.$$

Since $\zeta_0 = 1$, by neglecting all terms of higher order than the second in α and β we have

$$\xi_0 = \beta, \quad \eta_0 = -\alpha. \qquad (338)$$

Inserting (338) in (334) yields

$$H \frac{d\xi_0}{dt} = M_{\xi_0}, \qquad (339)$$

$$H \frac{d\eta_0}{dt} = M_{y'}.$$

The derivatives $\frac{d\xi_0}{dt}$ and $\frac{d\eta_0}{d}$ represent the projections on the axes ξ_0 and η_0 of the velocity of point G_0 relative to the system $\xi_0 \eta_0 \zeta_0$, which has a translational motion with axes oriented according to the Newtonian frame.
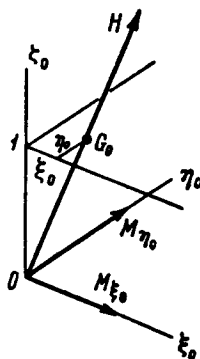
FIGURE 93

The products $H \frac{d\xi_0}{dt}$ and $H \frac{d\eta_0}{dt}$ represent the projections on the axes of the velocity of the end point of the vector H referred to the same coordinate system. The following approximation is valid because of the smallness of the angle α between the axes y' and η_0:

$$M_{y'} \cong M_{\eta_0}. \qquad (340)$$

Equations (339) thus equate the velocity of the end point of the angular momentum vector to the moments acting on the gyro[*]. This follows also from the general theorem on angular momentum if it is remembered that the total angular momentum of the gyro is practically equal to H, represented by a vector always directed along the rotor shaft. Equations (334) or (339) form the basis of the elementary theory of gyroscope precession.

[*] For a more detailed treatment see the author's paper "K teorii giroskopicheskogo mayatnika" (Theory of the Gyroscopic Pendulum). — PMM, Vol. 21, No. 1. 1957.

It is convenient to replace equations (339), which describe the motion of the rotor shaft referred to the system $\xi_0\eta_0\zeta_0$, by

$$Hv_\xi = M_\xi,$$
$$Hv_\eta = M_\eta,$$

(341)

referred to the moving system $\xi\eta\zeta$. The latter is usually partially fixed to the moving object (the ζ-axis may be vertical, while the η-axis is directed along the ship's course line). In (341) v_ξ and v_η are the projections of the "absolute" velocity (relative to system $\xi_0\eta_0\zeta_0$) of point G (defined as the interaction of the axis of rotation of the gyro rotor with the plane parallel to the $\xi\eta$ plane and situated at unit distance from it) on the moving axes ξ and η (Figure 94). It is assumed that the coordinates ξ and η of point G are small compared with unity, and that therefore the angles of deviation of the rotor shaft from the ζ-axis are small; M_ξ and M_η are the sums of the moments about the ξ-and η-axes acting on the gyro rotor, including the moments caused by the reactions of the rotor bearings.
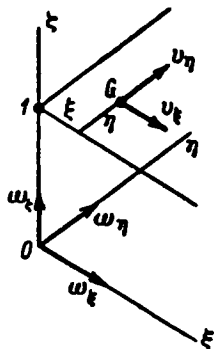
FIGURE 94

The coordinate systems $\xi_0\eta_0\zeta_0$ and $\xi\eta\zeta$ have a common origin at the point of intersection of the rotor shaft and the axis of the inner gimbal-ring pivots or gimbal housing. We denote by ω_ξ, ω_η, ω_ζ the components of the angular velocity of the trihedron $\xi\eta\zeta$ (Figure 94) relative to the coordinate system $\xi_0\eta_0\zeta_0$. The projections of the velocity of point G on the axes ξ and η are:

$$v_\xi = \frac{d\xi}{dt} + 1 \cdot \omega_\eta - \eta\omega_\zeta,$$
$$v_\eta = \frac{d\eta}{dt} + \xi\omega_\zeta - 1 \cdot \omega_\xi.$$

(342)

Equations (341) thus become

$$H\left(\frac{d\xi}{dt} + \omega_\eta - \eta\omega_\zeta\right) = M_\xi;$$
$$H\left(\frac{d\eta}{dt} + \xi\omega_\zeta - \omega_\xi\right) = M_\eta.$$

(343)

These equations have many practical applications.

Equations (334), (339), and (343) can obviously also be obtained by Lagrange's method by writing the equations of motion of the system in generalized coordinates. Lagrange's method is particularly suitable for setting up the equations of motion of complex gyroscopic systems mounted on oscillating and rotating bases. Many relationships that are far from obvious are obtained almost automatically by this method. Its drawback lies in the complicated calculations necessary, since the small terms are eliminated from the equations only at the very end. In addition, the interplay of forces in the gyroscopic system remains obscure.

When the equations of motion of a gyro mounted in gimbals are set up by Lagrange's method, it is first of all necessary to establish an expression for the kinetic energy of the system "rotor-gimbals" in its motion relative to the coordinate system $\xi_0\eta_0\zeta_0$, whose origin is at the gimbals center and which has a translational motion.

Let $\xi\eta\zeta$ be a coordinate system fixed to the moving object, the ξ-axis being the axis of the outer gimbal-ring pivots. The kinetic energy of the outer ring is

$$T_1 = \frac{1}{2}\left[I_{\xi_1}\left(\frac{d\alpha}{dt}+\omega_\xi\right)^2 + I_{\eta_1}(\omega_\eta\cos\alpha+\omega_\zeta\sin\alpha)^2 + \right.$$

$$\left. + I_{\zeta_1}(-\omega_\eta\sin\alpha+\omega_\zeta\cos\alpha)^2\right],\qquad(344)$$

where α is the angle of tilting of the outer ring relative to the coordinate system $\xi\eta\zeta$, and ω_ξ, ω_η, ω_ζ are the projections of the angular velocity of this coordinate system on its axes; I_{ξ_1}, I_{η_1}, I_{ζ_1} are the moments of inertia of the outer ring referred to the coordinate system $\xi_1\eta_1\zeta_1$ (Figure 95) fixed to this ring in such a manner that the ξ_1-axis coincides with the ξ-axis, while the η_1-axis coincides with the y'-axis of the inner ring (or the housing).
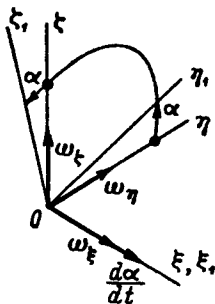
FIGURE 95
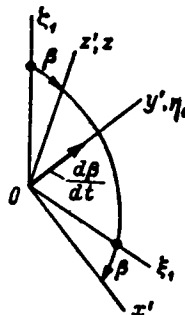
FIGURE 96

It is easily seen from Figure 95 or the table of direction cosines of the coordinate system $\xi_1\eta_1\zeta_1$ relative to the system $\xi\eta\zeta$

	ξ	η	ζ
ξ_1	1	0	0
η_1	0	$\cos\alpha$	$\sin\alpha$
ζ_1	0	$-\sin\alpha$	$\cos\alpha$

(345)

that the expressions

$$\omega^1_{\xi_1} = \frac{d\alpha}{dt}+\omega_{\xi},$$

$$\omega^1_{\eta_1} = \omega_\eta\cos\alpha+\omega_\zeta\sin\alpha,\qquad(346)$$

$$\omega^1_{\zeta_1} = -\omega_\eta\sin\alpha+\omega_\zeta\cos\alpha$$

represent the projections of the angular velocity ω^1 of the outer ring on the axes of the coordinate system $\xi_1\eta_1\zeta_1$ fixed to it.

Let us now find the projections of the angular velocity ω' of the inner ring on the axes of the coordinate system $x'y'z'$ fixed to this ring in such a way (Figure 96) that the z'-axis is directed along the rotor shaft z, while the y'-axis coincides with the η_1-axis of the outer ring. This angular velocity differs from the angular velocity of the outer ring by the vector of the relative angular velocity $\frac{d\beta}{dt}$, directed along the y'-axis. From the

direction cosines of the system $x'y'z'$ relative to the system $\xi_1\eta_1\zeta_1$:

	ξ_1	η_1	ζ_1
x'	$\cos\beta$	0	$-\sin\beta$
y'	0	1	0
z'	$\sin\beta$	0	$\cos\beta$

$$\text{(347)}$$

and from (346), these projections are found to be

$$\omega'_{x'} = \left(\frac{d\alpha}{dt}+\omega_\xi\right)\cos\beta - (-\omega_\eta\sin\alpha + \omega_\zeta\cos\alpha)\sin\beta,$$

$$\omega'_{y'} = \omega_\eta\cos\alpha + \omega_\zeta\sin\alpha + \frac{d\beta}{dt},$$

$$\text{(348)}$$

$$\omega'_{z'} = \left(\frac{d\alpha}{dt}+\omega_\xi\right)\sin\beta + (-\omega_\eta\sin\alpha + \omega_\zeta\cos\alpha)\cos\beta.$$

The kinetic energy of the inner gimbal ring is therefore

$$T_2 = \frac{1}{2}\left\{I_{x'}\left[\left(\frac{d\alpha}{dt}+\omega_\xi\right)\cos\beta - (-\omega_\eta\sin\alpha + \omega_\zeta\cos\alpha)\sin\beta\right]^2 + \right.$$

$$+ I_{y'}\left(\omega_\eta\cos\alpha + \omega_\zeta\sin\alpha + \frac{d\beta}{dt}\right)^2 +$$

$$\left. + I_{z'}\left[\left(\frac{d\alpha}{dt}+\omega_\xi\right)\sin\beta + (-\omega_\eta\sin\alpha + \omega_\zeta\cos\alpha)\cos\beta\right]^2\right\},$$

$$\text{(349)}$$

where $I_{x'}$, $I_{y'}$, $I_{z'}$ are the moments of inertia of the inner gimbal ring referred to the axes x', y', z'.

The kinetic energy of the rotor is

$$T_3 = \frac{1}{2}[A(p^2+q^2)+Cr^2],$$

$$\text{(350)}$$

where the projections p, q, and r of the rotor's angular velocity on the x-, y-, and z-axes fixed to the rotor are

$$p = \frac{d\alpha}{dt}\cos\beta\cos\gamma + \frac{d\beta}{dt}\sin\gamma + \omega_\xi\cos\beta\cos\gamma +$$

$$+ \omega_\eta(\sin\alpha\sin\beta\cos\gamma + \cos\alpha\sin\gamma) +$$

$$+ \omega_\zeta(-\cos\alpha\sin\beta\cos\gamma + \sin\alpha\sin\gamma),$$

$$q = -\frac{d\alpha}{dt}\cos\beta\sin\gamma + \frac{d\beta}{dt}\cos\gamma - \omega_\xi\cos\beta\sin\gamma +$$

$$+ \omega_\eta(-\sin\alpha\sin\beta\sin\gamma + \cos\alpha\cos\gamma) +$$

$$+ \omega_\zeta(\cos\alpha\sin\beta\sin\gamma + \sin\alpha\cos\gamma),$$

$$\text{(351)}$$

$$r = \frac{d\alpha}{dt}\sin\beta + \frac{d\gamma}{dt} + \omega_\xi\sin\beta - \omega_\eta\sin\alpha\cos\beta +$$

$$+ \omega_\zeta\cos\alpha\cos\beta,$$

which differ from the analogous formulas (323) by the presence of terms containing ω_ξ, ω_η, and ω_ζ. These terms are the projections on the axes x, y, z of the angular velocity of the trihedron xyz relative to the system $\xi_0\eta_0\zeta_0$. They are easily found from (182).

Inserting (351) into (350) yields the following final equation for the kinetic

energy of the rotor:

$$T_3 = \frac{1}{2} \left\{ A \left[\left(\frac{d\alpha}{dt} \cos\beta + \omega_\xi \cos\beta + \omega_\eta \sin\alpha\sin\beta - \omega_\zeta \cos\alpha\sin\beta \right)^2 + \right. \right.$$

$$\left. + \left(\frac{d\beta}{dt} + \omega_\eta \cos\alpha + \omega_\zeta \sin\alpha \right)^2 \right] + C \left[\left(\frac{d\alpha}{dt} + \omega_\xi \right) \sin\beta + \right.$$

$$\left. \left. + \frac{d\gamma}{dt} - (\omega_\eta \sin\alpha - \omega_\zeta \cos\alpha) \cos\beta \right]^2 \right\}. \tag{352}$$

The total kinetic energy is equal to the sum of the kinetic energies of the outer gimbal ring (T_1), the inner ring (T_2), and the rotor (T_3):

$$T = T_1 + T_2 + T_3. \tag{353}$$

The generalized coordinates are here the finite rotations α, β, and γ about the axes ξ, y', and z respectively. It follows that the Euler-Lagrange equations can be written in the form

$$\frac{d}{dt} \frac{\partial T}{\partial \left(\frac{d\alpha}{dt} \right)} - \frac{\partial T}{\partial \alpha} = M_\xi,$$

$$\frac{d}{dt} \frac{\partial T}{\partial \left(\frac{d\beta}{dt} \right)} - \frac{\partial T}{\partial \beta} = M_{y'}, \tag{354}$$

$$\frac{d}{dt} \frac{\partial T}{\partial \left(\frac{d\gamma}{dt} \right)} - \frac{\partial T}{\partial \gamma} = M_z,$$

where M_ξ is the sum of the moments about the ξ-axis of all forces acting on the system, including the inertia forces due to the object's motion, $M_{y'}$ is the sum of the moments about the pivot axis y', of the inner gimbal ring of the forces acting on the inner gimbal ring (housing) and rotor, and M_z is the sum of the moments about the rotor's axis of rotation z, of the forces acting on the rotor alone.

If ω_ξ, ω_η, ω_ζ are zero (this is equivalent to the assumption that the motion of the base can be neglected, which is frequently the case when studying problems of the stability of gyroscopic devices), then inserting (344), (349), and (352) into (353) yields,

$$T = \frac{1}{2} \left\{ [I_{\xi_1} + (I_{x'} + A) \cos^2\beta + (I_{z'} + C) \sin^2\beta] \left(\frac{d\alpha}{dt} \right)^2 + \right.$$

$$\left. + (I_{y'} + A) \left(\frac{d\beta}{dt} \right)^2 + C \left(\frac{d\gamma}{dt} \right)^2 + 2C \frac{d\alpha}{dt} \frac{d\gamma}{dt} \sin\beta \right\}. \tag{355}$$

Inserting (355) into (354), the following system of differential equations is obtained after some simplifications:

$$[I_{\xi_1} + (I_{x'} + A) \cos^2\beta + (I_{z'} + C) \sin^2\beta] \frac{d^2\alpha}{dt^2} +$$

$$+ C \sin\beta \frac{d^2\gamma}{dt^2} + C \cos\beta \frac{d\beta}{dt} \frac{d\gamma}{dt} -$$

$$- 2 (I_{z'} - I_{x'} + A - C) \cos\beta \sin\beta \frac{d\alpha}{dt} \frac{d\beta}{dt} = M_\xi, \tag{356}$$

whose axis is made to move together with the axis of symmetry of the gyro-
sphere by an accurate follow-up system. The common axis of the stator
and the supporting cup is linked by means of the latitude carriage K to the
heavy spherical pendulum M suspended in its gimbals. The latitude carriage,
whose function will be explained later, moves the stator axis from the pen-
dulum line in the northern and eastern directions through an angle propor-
tional to the cosine of the local latitude. When the ship turns, the carriage
is automatically rotated by means of a link with the gyrocompass.
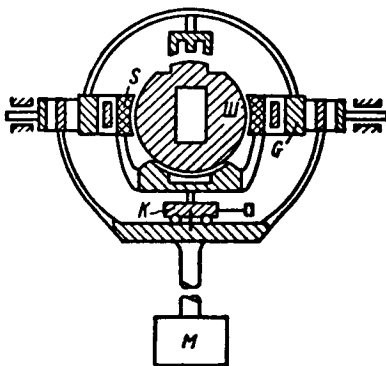
FIGURE 97

This scheme does not make full use of the possibilities of aerodynamic
suspension. Much better results can be obtained through relatively minor
changes; as a result the error in the determination of the true vertical can
be reduced to several minutes of an arc.

The theory of the gyrovertical with aerodynamic suspension, and the
theoretical basis of the alterations that the author proposed already in
1940, are given below.

The gyrosphere is completely stable at normal speed of rotation, and
nutations produced by an external cause such as a shock are rapidly damped.
Accordingly, the equations of the elementary theory of gyroscope precession
should be used for describing the motion of its axis.

By replacing the letters ξ, η, ζ by x, y, z respectively, and H by $-H$ (it is
assumed that the gyrosphere rotates clockwise if viewed from above), equa-
tions (343) become

$$-H\left(\frac{dx}{dt} - \omega_z y + \omega_y\right) = M_x,$$

$$-H\left(\frac{dy}{dt} + \omega_z x - \omega_x\right) = M_y. \tag{357}$$

The coordinate system xyz, with its origin at the geometric center of
the gyrosphere, has its z-axis oriented along the local vertical (Figure 98).
The orientation of the x- and y-axes will be stated in each particular case.

In equations (357) H is the angular moment of the gyro; ω_x, ω_y, ω_z are the
projections of the angular velocity of trihedron xyz on the axes x, y, and z,
oriented according to the Newtonian frame; x and y are the coordinates of point
G (Figure 98) at the intersection of the gyrosphere axis of symmetry with

116

$$(I_{y'} + A)\frac{d^2\beta}{dt^2} + (I_{x'} - I_{z'} + A - C)\cos\beta\sin\beta\left(\frac{d\alpha}{dt}\right)^2 -$$

$$- C\cos\beta\frac{d\alpha}{dt}\frac{d\gamma}{dt} = M_{y'}, \qquad (356)$$

$$C\frac{d^2\gamma}{dt^2} + C\sin\beta\frac{d^2\alpha}{dt^2} + C\cos\beta\frac{d\alpha}{dt}\frac{d\beta}{dt} = M_{z'}.$$

If all terms of higher order than the first in α and β and their time derivatives are neglected and M_z is assumed to be zero, the first two equations are reduced to (332).

Gyroscopic systems are usually connected with electric devices which cause the correcting and stabilizing moments. Lagrange's method of the second kind* can be used for setting up the complete system of equations for such an electromechanical system. The kinetic energy T in this case also includes terms representing the energy of the magnetic and electrical fields, while the number of coordinates of the gyroscopic systems is increased to include the corresponding electric parameters. This method is, however, of limited practical importance, the equations being usually set up by elementary methods.

The equations of small motions of gyroscopic systems are, as already mentioned, linear in the time derivatives of the coordinates. In certain cases a "linearization" of the forces acting on the system is possible; in other words, they can be represented as linear functions of the coordinates, or as linear functions of the coordinates and velocities when viscous friction is taken into account. Only such linear gyroscopic systems will be considered in this chapter. The classical examples of a linear gyroscopic system is the gyrovertical with an aerodynamic suspension (cf. § 2 below). In other cases the linearization is carried out by neglecting dry (Coulomb) friction in systems with ideal (in particular, vibrating) bearings. Some problems concerning the theory of essentially nonlinear gyroscopic systems have been deferred to Chapters V and VI.

§ 2. Theory of the gyrovertical with aerodynamic suspension and its possible improvements

The gyrovertical with aerodynamic suspension of the sensing element is an instrument for the continuous automatic determination of the vertical direction on a ship. The instrument gyro is a steel sphere with internal recesses determining the dynamic axis of symmetry, with a special "head" for controlling the follow-up system. The gyrosphere is driven by a rotating magnetic field on the principle of an asynchronous motor, and has a constant speed of more than 10,000 rpm.

The sphere is supported on an air layer one hundredth of a millimeter thick formed between the rotating sphere and a bronze cup of rather intricate form. The stator S, which creates the rotating magnetic field, and the supporting cup are mounted on the inner gimbal ring. The bearings of the outer gimbal-ring pivots are fitted to the so-called stabilized ring G,

* Bulgakov, B. V. "Kolebaniya" (Oscillations).— Moskva, Gostekhizdat. 1954.

the $x\bar{y}$ plane (the latter is parallel to the xy plane and located at unit distance above it); M_x and M_y are the sums of the moments about the x-and y-axes applied by the stator and cup to the gyrosphere. The x and y coordinates of point G are assumed to be small.

In order to establish the laws to which moments M_x and M_y are subjected, we consider a gyrosphere on a so-called fixed base, i.e., with stator and supporting cup of the instrument fixed relative to the Earth, the axis of the stator and cup being vertical. The motion of the revolving gyrosphere axis following a perturbation will then be such that point G traces a spiral (Figure 99) ending at a fixed point E distinct from point O in which the vertical
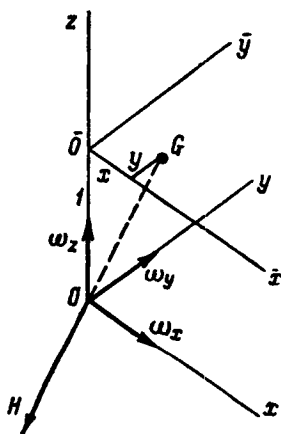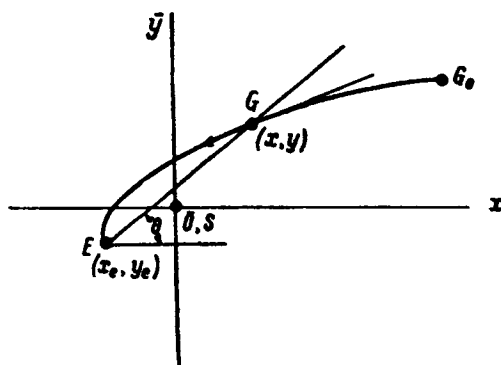
FIGURE 98   FIGURE 99

axis z intersects with the horizontal plane $x\bar{y}$. The distance between G and E decreases in such a way that the ratio between the decrement per unit time and the length $\overline{GE}$ is constant, and that the angle between $\overline{GE}$ and a fixed horizontal direction increases in counterclockwise direction at a constant rate. It follows that point G moves about point E in a logarithmic spiral

$$\rho = \rho_0 e^{-ht}, \qquad \theta = \theta_0 + pt, \tag{358}$$

where ρ_0 is the initial distance of G from E, and θ_0 is the initial angle between EG and some fixed direction in the horizontal plane.

Let the east-west line be this fixed direction. Draw the x-axis of the coordinate system xyz to the east, and the y-axis to the north. Denote by x_e and y_e the coordinates of the fixed point E defining the equilibrium position of the gyrosphere axis. The law of motion of point G can now be represented in the form

$$x = x_e + \rho \cos \theta,$$
$$y = y_e + \rho \sin \theta, \tag{359}$$

where ρ and θ are given by (358).

The projections of the angular velocity on the axes x, y and z linked to the stator fixed relative to the Earth (Figure 100), are

$$\omega_x = 0,$$
$$\omega_y = U \cos \varphi, \tag{360}$$
$$\omega_z = U \sin \varphi,$$

117

where U is the angular velocity of the diurnal rotation of the Earth. $(0.0000729\ \text{sec}^{-1})$, and φ is the local latitude.

The inverse problem of dynamics — determining the forces acting from the known motion — can now be solved by inserting (360) into the differential equations (357). It follows from (359) and (358) that

$$\frac{dx}{dt} = \frac{d\rho}{dt}\cos\theta - \rho\sin\theta\,\frac{d\theta}{dt} =$$

$$= -k\rho_e e^{-kt}\cos\theta - p\rho\sin\theta =$$

$$= -k(x - x_e) - p(y - y_e) \tag{361}$$

and

$$\frac{dy}{dt} = -k(y - y_e) + p(x - x_e). \tag{362}$$

Inserting (361), (362), and (360) into (357) yields

$$M_x = -H\left[-kx - (p + U\sin\varphi)y + kx_e + py_e + U\cos\varphi\right],$$

$$M_y = -H\left[-ky + (p + U\sin\varphi)x + ky_e - px_e\right]. \tag{363}$$

The actual value of the coordinates x_e and y_e of point E or, which is the same, of the angles between the equilibrium position of the gyrosphere
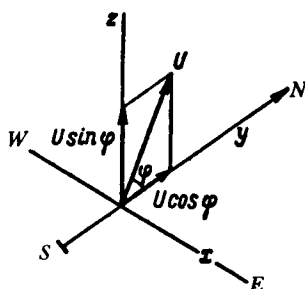
FIGURE 100

axis and the yz and xz planes*, must satisfy:

$$kx_e + py_e + U\cos\varphi = 0,$$

$$ky_e - px_e = 0. \tag{364}$$

Using (364) and neglecting $U\sin\varphi$ which is small in comparison with p (the vertical component of the Earth's angular velocity being much less than p) yields the following formulas determining the motion of the gyrosphere supported on a fixed base with the stator axis vertical:

$$M_x = H(kx + py),$$

$$M_y = H(ky - px). \tag{365}$$

Expressions (365) can be considered as the projections on the x- and y-axes of the geometric sum of vector M_r and vector M_t, each of which is proportional to the angle of deviation of the stator axis from the pendulum line (Figure 101); the proportionality factors are k and p respectively.

* [This is the actual equilibrium position.]

118

The vector M_r is parallel to the straight line connecting S and G and represents the component normal to the gyrosphere axis of the torque M due to the stator's electromagnetic field (Figure 102).

The vector M_t is perpendicular to SG and represents the moment tending to make the sphere's plane of symmetry coincide with the plane of the field. This moment is, inter alia, caused by the magnetic hysteresis of the sphere's material and the properties of the aerodynamic suspension.
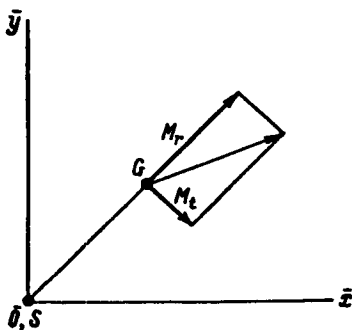
FIGURE 101
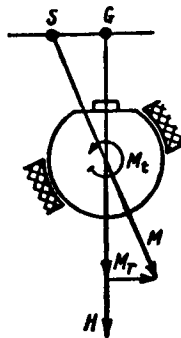
FIGURE 102

The main assumption on which the subsequent analysis is based is the applicability of (365) to the case of a moving base. This assumption cannot lead to serious errors, since the linear velocities of the gyrosphere corresponding to its rotation are much larger than the linear velocities of the points of the stator when the pendulum linked to it oscillates.

On the strength of this assumption the equations of motion of the axis of a gyrosphere supported on a moving base can be written [by inserting (360) and (365) into (357)]

$$-H\left(\frac{dx}{dt} - yU\sin\varphi + U\cos\varphi\right) = kH(x - \xi) + pH(y - \eta),$$
$$-H\left(\frac{dy}{dt} + xU\sin\varphi\right) = kH(y - \eta) - pH(x - \xi), \tag{366}$$

where ξ and η are the coordinates of the point S at the intersection of the stator axis with the horizontal xy plane (the x-axis points eastward as before).

Let

$$\xi = u, \quad \eta = v, \tag{367}$$

where u and v are constants.

Then in accordance with (366), the gyrosphere axis will move toward an equilibrium position whose coordinates x_1 and y_1 satisfy the equations

$$y_1 U\sin\varphi - U\cos\varphi = k(x_1 - u) + p(y_1 - v),$$
$$-x_1 U\sin\varphi = k(y_1 - v) - p(x_1 - u). \tag{368}$$

The following equations have therefore to be satisfied in order that the equilibrium position of the gyro axis be vertical, i.e., that $x_1 = y_1 = 0$:

$$U\cos\varphi = ku + pv,$$
$$0 = pu - kv. \tag{369}$$

119

whence

$$u = \frac{kU \cos \varphi}{k^2 + p^2},$$

$$v = \frac{pU \cos \varphi}{k^2 + p^2}.$$

(370)

The stator axis must (Figure 103) therefore be inclined at an angle u to the east and at an angle v to the north, or which is the same, at an angle

$$s = \sqrt{u^2 + v^2} = \frac{U \cos \varphi}{\sqrt{k^2 + p^2}}$$

(371)

in a direction which forms an angle ψ with the east-west line, where

$$\operatorname{tg} \psi = \frac{v}{u} = \frac{p}{k}.$$

(372)

Assuming $k = 0.01$ sec^{-1}, $p = 0.00436$ sec^{-1}, the values of u, v, s (for a latitude of 60°) and ψ are:

$$u = 0.00305; \quad v = 0.00133; \quad s = 0.00333 \,(11.5');$$

$$\psi = 23°30'.$$

This additional inclination of the stator relative to the pendulum line (the line connecting the center of suspension with the pendulum's center of gravity) is obtained by means of the latitude carriage K (see p. 116).
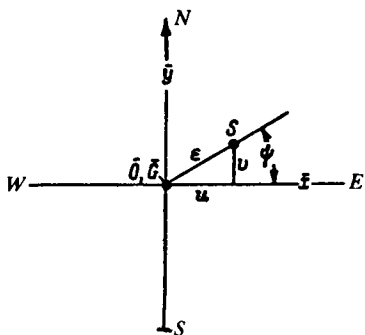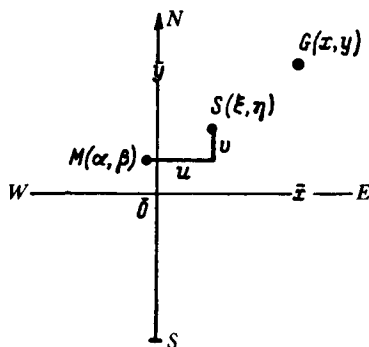
FIGURE 103   FIGURE 104

We denote by α and β the coordinates at the point of intersection M of the pendulum line with the xy plane (Figure 104). The coordinates of S are then

$$\xi = \frac{kU \cos \varphi}{k^2 + p^2} + \alpha,$$

$$\eta = \frac{pU \cos \varphi}{k^2 + p^2} + \beta.$$

(373)

Inserting these expressions into (366) yields (after some transformations)

$$\frac{dx}{dt} + kx + (p - U \sin \varphi) y = k\alpha + p\beta,$$

$$\frac{dy}{dt} + ky - (p - U \sin \varphi) x = k\beta - p\alpha.$$

(374)

120

We multiply the second of equations (374) by $i = \sqrt{-1}$ and add it to the first. Writing

$$z = x + iy \quad \text{and} \quad \gamma = \alpha + i\beta \tag{375}$$

and inserting these expressions into (374), we obtain the following linear differential equation of the first order:

$$\frac{dz}{dt} + [k - i(p - U \sin \varphi)] z = (k - ip) \gamma. \tag{376}$$

The solution of this equation for $\gamma = 0$ (vertically suspended pendulum; $\alpha = \beta = 0$) is

$$z = z_0 e^{-kt} e^{i(p - U \sin \varphi)t}. \tag{377}$$

According to (377), point G moves along a logarithmic spiral from point $z = z_0$ at $t = 0$ to point $\bar{O}$ for which $z = 0$ (Figure 105). In fact, it follows from (377) that in this case

$$|z| = |z_0| e^{-kt}, \quad \arg z = \arg z_0 + (p - U \sin \varphi) t; \tag{378}$$

the length of $\bar{O}z$ and its inclination to the x-axis vary according to a law similar to that given by (358).
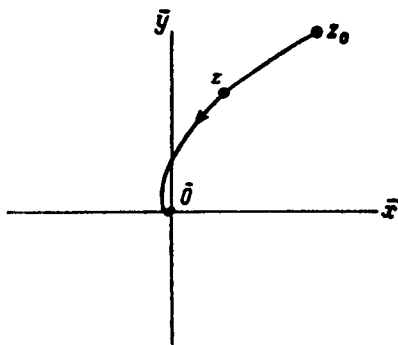
FIGURE 105

Equation (376) can be used for studying the behavior of the gyrosphere during the ship's rolling when on a fixed course.

Let the y-axis be directed along the ship's course line and let the rolling of the ship cause oscillations of the pendulum given by

$$\alpha = \alpha_0 \sin \mu t, \quad \beta \equiv 0, \tag{379}$$

where α_0 is the amplitude of pendulum oscillations relative to the vertical, and μ, the frequency of roll.

Because of the large difference between the period of natural oscillations of the pendulum and the period of roll, it can be assumed that the pendulum is at any moment directed along the apparent vertical. If the center of the pendulum's suspension is located at a distance l from the axis about which the ship rolls with an amplitude θ_0, α_0 is given by

$$\alpha_0 = \frac{\mu^2 l}{g} \theta_0. \tag{380}$$

121

We insert (375) and (379) into (376) and express $\sin \mu t$ by exponential functions. The following equation is obtained after neglecting $U \sin \varphi$ which is small in comparison with p:

$$\frac{dz}{dt} + (k - ip) z = \frac{a_0 (k - ip)}{2i} (e^{i\mu t} - e^{-i\mu t}). \tag{381}$$

It is sufficient to find the forced oscillations of the gyrosphere axis, since its free oscillations are given by (377) and become damped with time. The solution of the differential equation (381) is,

$$z = \frac{a_0 (k - ip)}{2i} \left[\frac{e^{i\mu t}}{k - i(p - \mu)} - \frac{e^{-i\mu t}}{k - i(p + \mu)} \right]. \tag{382}$$

The components in brackets can be interpreted as vectors of different, constant moduli rotating in different directions in the complex plane with equal angular velocities. Solution (382) corresponds therefore to a motion of point G along an ellipse (Figure 106) with semiaxes

$$a = \frac{a_0 \sqrt{k^2 + p^2}}{2} \left[\frac{1}{\sqrt{k^2 + (p - \mu)^2}} + \frac{1}{\sqrt{k^2 + (p + \mu)^2}} \right],$$

$$b = \frac{a_0 \sqrt{k^2 + p^2}}{2} \left[\frac{1}{\sqrt{k^2 + (p - \mu)^2}} - \frac{1}{\sqrt{k^2 + (p + \mu)^2}} \right]. \tag{383}$$

The frequency of roll μ is of the order of $0.5 - 1.0 \text{ sec}^{-1}$, and is therefore much larger than the parameters k and p. Formulas (383) can therefore be replaced by the following approximation:

$$a = \frac{a_0 \sqrt{k^2 + p^2}}{\mu},$$

$$b = \frac{a_0 p \sqrt{k^2 + p^2}}{\mu^2} \ll a. \tag{384}$$

These last formulas could also have been derived directly from (374) by neglecting in them the terms containing x and y. These terms are in fact considerably smaller than the right-hand sides of the equations since the gyro-rotor shaft deviates from the vertical far less than the pendulum line. We thus have

$$\frac{dx}{dt} \cong ka_0 \sin \mu t,$$

$$\frac{dy}{dt} \cong -pa_0 \sin \mu t, \tag{385}$$

whence

$$x \cong -\frac{ka_0}{\mu} \cos \mu t,$$

$$y \cong \frac{pa_0}{\mu} \cos \mu t. \tag{386}$$

These equations define a harmonic motion of point G along a straight line, the amplitude being given by the first of equations (384). Inserting (380) into (384) yields the following final expression for the amplitude of the oscillations about the vertical carried out by the gyrosphere axis caused by the rolling of the ship:

$$a = \frac{\mu l \sqrt{k^2 + p^2}}{g} \theta_0. \tag{387}$$

Numerical example. If $l = 8$ m; $k = 0.0100$ sec^{-1}; $p = 0.00436$ sec^{-1}; $\theta = 0.209$ (12°); and $\mu = 0.6$ sec^{-1} (period of roll about 10 sec), then using (380) and (384) we obtain

$$\alpha_0 = 0.0614 \ (3°31'), \quad a = 0.00112 \ (4'), \quad b = 0.00001 \ (2'').$$

To reduce the error in the instrument indications caused by the rolling of the ship, a special device is used in gyroverticals. This device restricts the pendulum's deviations from the perpendicular to the deck plane to $4 - 6°$.
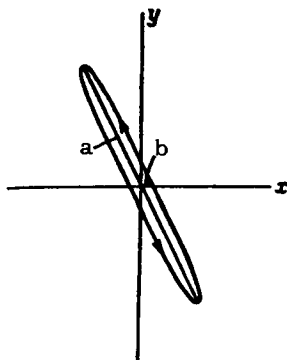
FIGURE 106

Such a device is not always necessary. In the above case, for example, the amplitude of the pendulums angular oscillations is less than 4°. In addition, the pendulum's oscillation on the inclined deck of a listing ship will be asymmetrical, leading to considerable errors. Finally, errors of the type of the phenomena observed by M. I. Zaitsev (Chapter VI, § 1) can occur even with symmetrical oscillations when the pendulum is periodically stopped by the restricting device.

It is therefore desirable not to restrict the sway of the pendulum. This could, however, cause possible large inclinations of the stator and the supporting cup, which could impair the normal functioning of the aerodynamic suspension. The instrument error due to rolling would, in addition, remain considerable.

Both these difficulties are avoided by the following alteration of the instrument.

In the original gyrovertical design the pendulum, suspended on its gimbals, is connected by means of the latitude-carriage pin with the supporting cup and the stator; these have their own suspension. A deviation of the pendulum center line from the instrument axis therefore causes an identical deviation of the stator axis.

Consider a rod-shaped lever one of whose extremities is hinged by means of a ball-and-socket connection G to a stabilized ring (Figure 107) while the other extremity is hinged by means of a sliding ball-and-socket connection K to the pin of the latitude carriage mounted on the pendulum. Let the stator also be hinged to the rod by means of another sliding ball-and-socket connection S. Let the distance between the centers of G and S be $1/n$ times the distance between the centers of G and K.

Draw lines connecting the centers of these points with the center of the gyrosphere, and produce them until they intersect with the horizontal

plane xy (Figure 108). The points of intersection will be designated by the same letters G, S, and K as the corresponding connecting points. The coordinates of point G are obviously x and y, since the stabilized ring follows the motion of the gyrosphere. The coordinates of point S are ξ and η, in accordance with the notation adopted above. The coordinates of point K are denoted by σ and τ.

If the coordinates of point M (the intersection of the pendulum line with the xy plane) are as before denoted by α and β, the following relationships will obtain between the coordinates of points K and M:

$$\sigma = \alpha + u,$$
$$\tau = \beta + v. \tag{388}$$

Here u and v define the position of the latitude carriage pin relative to the pendulum line and enable the infuence of the Earth's rotation on the equilibrium position of the gyrosphere axis to be eliminated.
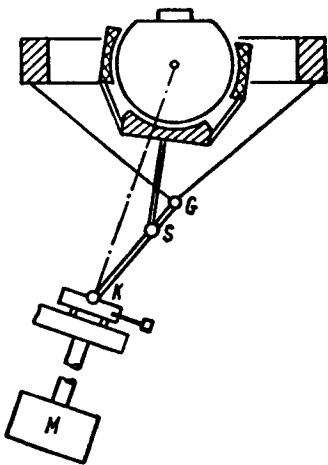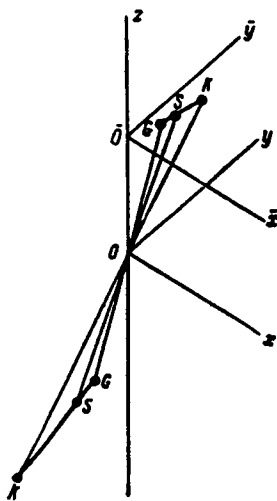
FIGURE 107   FIGURE 108

Points S and K coincide in an instrument without an additional lever system, i.e., $n = 1$, u and v being determined by (370) for the condition that the x-axis points to the east.

The following proportion, accurate to first-order infinitesimals, follows from the theory of similar triangles (Figures 108 and 109):

$$\frac{\xi - x}{\sigma - x} = \frac{\eta - y}{\tau - y} = \frac{SG}{KG} = \frac{1}{n}. \tag{389}$$

Using (389), equations (366) can be written

$$-H\left(\frac{dx}{dt} - yU\sin\varphi + U\cos\varphi\right) = kH\frac{x - \alpha - u}{n} + pH\frac{y - \beta - v}{n},$$

$$-H\left(\frac{dy}{dt} + xU\sin\varphi\right) = kH\frac{y - \beta - v}{n} - pH\frac{x - \alpha - u}{n}. \tag{390}$$

If u and v are chosen so as to satisfy the equations

$$U \cos \varphi = \frac{ku + pv}{n},$$

$$0 = \frac{pu - kv}{n},$$

(391)

then equations (390) can be reduced to

$$\frac{dx}{dt} + \frac{k}{n} x + \left(\frac{p}{n} - U \sin \varphi\right) y = \frac{k}{n} \alpha + \frac{p}{n} \beta,$$

$$\frac{dy}{dt} + \frac{k}{n} y - \left(\frac{p}{n} - U \sin \varphi\right) x = \frac{k}{n} \beta - \frac{p}{n} \alpha.$$

(392)

Equations (392) differ from (374) only in that the parameters k and p have been replaced by magnitudes n times smaller; this is equivalent to saying that the influence of the pendulum's sway on the gyrosphere (the correction) has become less. The instrument error during rolling will obviously be reduced by exactly the same factor, and (387) should be replaced by

$$a = \frac{\mu l \sqrt{k^2 + p^2}}{ng} \theta_0.$$

(393)

If $n = 8$ for the same values of μ, l, k, p, and θ_0 as before, then $a = 0.000140$; this corresponds to an error of about half a minute of arc.
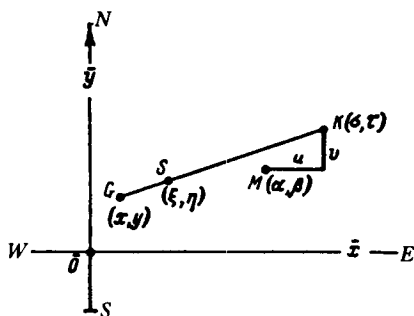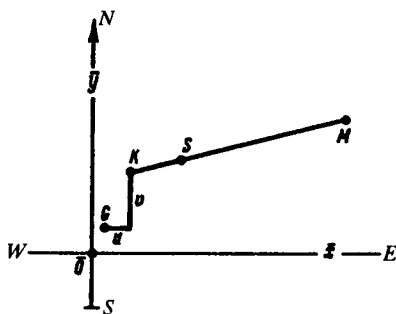
FIGURE 109   FIGURE 110

By comparing (391) and (369) we find that the deviations u and v in the eastern and northern directions must now be n times larger than before. For $n = 8$, the total angle of deviation, ε, where

$$\varepsilon = \frac{nU \cos \varphi}{\sqrt{k^2 + p^2}},$$

(394)

(by analogy to (371)), is about $1.5°$.

To obtain the same result, different lever arrangements could be proposed, all causing a suitable change of u and v. For instance, the latitude carriage could be placed on the stabilized ring or connected to the stator.
If the latitude carriage is placed on the stabilized ring, then (Figure 110)

$$\frac{\xi - \sigma}{\alpha - \sigma} = \frac{\eta - \tau}{\beta - \tau} = \frac{SK}{MK} = \frac{1}{n},$$

(395)

where

$$\sigma = x + u,$$
$$\tau = y + v. \tag{396}$$

The following relationships are easily derived:

$$x - \xi = \frac{x - a}{n} - \frac{n-1}{n} u,$$

$$y - \eta = \frac{y - \beta}{n} - \frac{n-1}{n} v, \tag{397}$$

Using them, equations (366) can be transformed into a form similar to (390), and then, by suitably selecting u and v, into a form similar to (392).

Until now it was assumed that the ship maintains a constant course and, in addition, that the component of the angular velocity of the system xyz, caused by the ship's motion on the curved surface of the Earth, could be neglected. This component is horizontal and directed to port perpendicular to vector V (Figure 111); its value is equal to the ratio of the ship's speed V to the Earth's radius.

Consider now the general case of a ship's motion. Since for $n = 1$ the scheme is equivalent to that of a gyrosphere without additional lever arrangement, we can write the equations of motion for an arbitrary value of n.
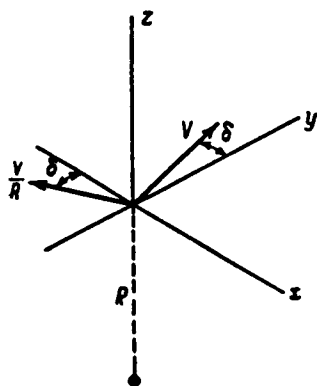
FIGURE 111   FIGURE 112
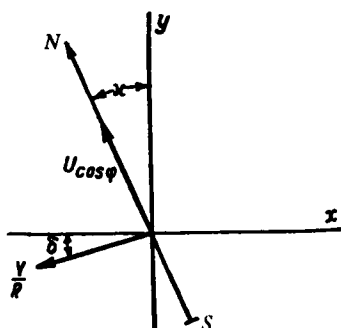
Let x be the ship's course*. The y-axis of the coordinate system xyz is parallel to the ship's course line. The projections of the angular velocity of the trihedron xyz (Figure 112) on the axes x, y, z are respectively,

$$\omega_x = -U \cos \varphi \sin x - \frac{V}{R} \cos \delta,$$

$$\omega_y = U \cos \varphi \cos x - \frac{V}{R} \sin \delta, \tag{398}$$

$$\omega_z = U \sin \varphi + \omega,$$

where δ is the drift angle (Figure 113), and ω, the speed of the ship's

* The ship's course has already been defined in Chapter I, § 1 (see p. 10).

rotation, connected with the course by the relationship

$$\omega = -\frac{dx}{dt}.$$

(399)

The ship's roll has practically no influence on the mean position of the gyrosphere axis. It will therefore be neglected.

The tangential and normal acceleration of the point on the ship at which the instrument is located are (Figure 113):

$$w_\tau = \frac{dV}{dt}$$

(400)

$$w_n = \left(\omega + \frac{d\delta}{dt}\right)V.$$

(401)

The projections of the total translational acceleration of the pendulum's center of suspension on the x- and y-axes are therefore

$$w_x = -\frac{dV}{dt}\sin\delta - \left(\omega + \frac{d\delta}{dt}\right)V\cos\delta,$$

$$w_y = \quad\frac{dV}{dt}\cos\delta - \left(\omega + \frac{d\delta}{dt}\right)V\sin\delta.$$

(402)

Due to inertia, the position of the pendulum deviates from the vertical during translational motion. The coordinates α and β of point M, defining the pendulum's position in the coordinate system xyz, are approximately

$$\alpha = \frac{w_x}{g}, \qquad \beta = \frac{w_y}{g}.$$

(403)

The displacements u and v of the latitude carriage pin, determined by (391), take place in the eastern and northern directions respectively
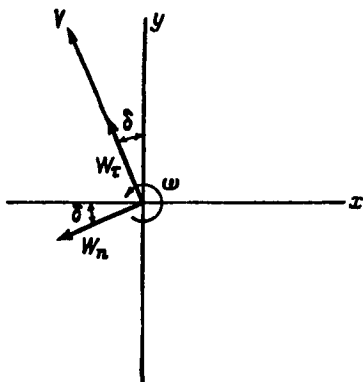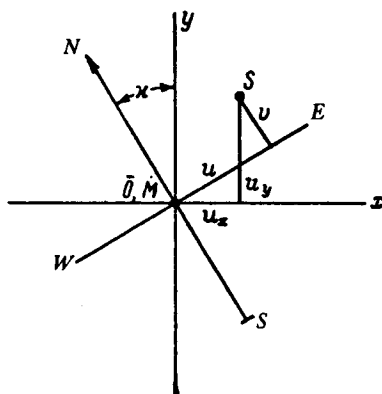
FIGURE 113   FIGURE 114

(Figure 114). The corresponding displacements u_e and u_y in the directions of the x- and y-axes are

$$u_e = u\cos\varkappa - v\sin\varkappa,$$
$$u_y = u\sin\varkappa + v\cos\varkappa.$$

(404)

Using (398), equations (357) can be written in the form

$$-H\left[\frac{dx}{dt}-(\omega+U\sin\varphi)y+U\cos\varphi\cos\varkappa-\frac{V}{R}\sin\delta\right]=M_x,$$

$$-H\left[\frac{dy}{dt}+(\omega+U\sin\varphi)x+U\cos\varphi\sin\varkappa+\frac{V}{R}\cos\delta\right]=M_y. \tag{405}$$

The expressions for M_x and M_y are of the same form as the right-hand sides of (390) if u and v are replaced by u_x and u_y. The following expressions can therefore be written:

$$M_x=H\left[\frac{k}{n}\left(x-\frac{w_x}{g}-u_x\right)+\frac{p}{n}\left(y-\frac{w_y}{g}-u_y\right)\right],$$

$$M_y=H\left[\frac{k}{n}\left(y-\frac{w_y}{g}-u_y\right)-\frac{p}{n}\left(x-\frac{w_x}{g}-u_x\right)\right], \tag{406}$$

in which α and β have been substituted from (403).

We insert (406) into (405). After simplification the following equations are obtained with the aid of (391) and (404):

$$\frac{dx}{dt}+\frac{k}{n}x-\left(\omega+U\sin\varphi-\frac{p}{n}\right)y=\frac{V}{R}\sin\delta+\frac{kw_x}{ng}+\frac{pw_y}{ng},$$

$$\frac{dy}{dt}+\frac{k}{n}y+\left(\omega+U\sin\varphi-\frac{p}{n}\right)x=-\frac{V}{R}\cos\delta+\frac{kw_y}{ng}-\frac{pw_x}{ng}. \tag{407}$$

Using (402), the following differential equations are finally obtained for the motion of the gyrosphere axis with an arbitrary motion of the ship:

$$\frac{dx}{dt}+\frac{k}{n}x-\left(\omega+U\sin\varphi-\frac{p}{n}\right)y=$$

$$=\frac{V}{R}\sin\delta+\frac{k}{ng}\left[-\frac{dV}{dt}\sin\delta-\left(\omega+\frac{d\delta}{dt}\right)V\cos\delta\right]+$$

$$+\frac{p}{ng}\left[\frac{dV}{dt}\cos\delta-\left(\omega+\frac{d\delta}{dt}\right)V\sin\delta\right],$$

$$\frac{dy}{dt}+\frac{k}{n}y+\left(\omega+U\sin\varphi-\frac{p}{n}\right)x=$$

$$=-\frac{V}{R}\cos\delta+\frac{k}{ng}\left[\frac{dV}{dt}\cos\delta-\left(\omega+\frac{d\delta}{dt}\right)V\sin\delta\right]-$$

$$-\frac{p}{ng}\left[-\frac{dV}{dt}\sin\delta-\left(\omega+\frac{d\delta}{dt}\right)V\cos\delta\right]. \tag{408}$$

Only ordinary turns will be considered at this stage. In this case the linear velocity V of the ship, its angular velocity ω, and the drift angle δ are constant. We shall neglect $U\sin\varphi$ as being small compared with ω. Equations (408) then become

$$\frac{dx}{dt}+\frac{k}{n}x-\left(\omega-\frac{p}{n}\right)y=\frac{V}{R}\sin\delta-\frac{k\omega}{ng}V\cos\delta-\frac{p\omega}{ng}V\sin\delta,$$

$$\frac{dy}{dt}+\frac{k}{n}y+\left(\omega-\frac{p}{n}\right)x=-\frac{V}{R}\cos\delta-\frac{k\omega}{ng}V\sin\delta+\frac{p\omega}{ng}V\cos\delta. \tag{409}$$

This system of two differential equations is equivalent to the following

linear differential equation in the complex variable $z = x + iy$

$$\frac{dz}{dt} + \left[\frac{k}{n} + i\left(\omega - \frac{p}{n}\right)\right]z = \left[-i\frac{V}{R} - \frac{k-ip}{ng}\omega V\right]e^{it}$$

(410)

The solution of this equation is

$$z = Ce^{-\left[\frac{k}{n} + i\left(\omega - \frac{p}{n}\right)\right]t} - \frac{i\frac{1}{R} + \frac{k-ip}{ng}\omega}{\frac{k}{n} + i\left(\omega - \frac{p}{n}\right)}Ve^{it}$$

(411)

which consists of two terms. The first is determined by the initial motion and decreases with time, while the second represents the limiting equilibrium position of the gyrosphere axis relative to the coordinate system xyz, rotating about the vertical z-axis together with the ship.

The modulus of this second term

$$\vartheta = \frac{\omega V}{g}\sqrt{\frac{k^2 + \left(p - \frac{ng}{\omega R}\right)^2}{k^2 + (p - n\omega)^2}}$$

(412)

defines the error in the readings of the true vertical during ordinary turns.

The errors for right or left turns at the same absolute angular velocity ω are different. Take for instance $V = 20$ m/sec (about 40 knots) and $|\omega| = 0.01$ sec^{-1} (corresponding to 10.5 min for a 360° turn at a radius of 2000 m). For a left turn $(\omega > 0)$

$$\vartheta = 1°5' \text{ for } n = 1 \quad \text{and} \quad \vartheta = 10' \text{ for } n = 8,$$

for a right turn $(\omega < 0)$

$$\vartheta = 44' \text{ for } n = 1 \quad \text{and} \quad \vartheta = 9' \text{ for } n = 8.$$

The turn for which the steady deviation of the gyrosphere axis from the vertical is a maximum is called resonance turn. The angular velocity ω_r at a resonance turn $(n = 1)$ and the corresponding deviation ϑ_r of the gyrosphere axis from the vertical are approximately

$$\omega_r = \frac{p^2 + k^2}{p},$$
$$\vartheta_r = \frac{p^2 + k^2}{k}\frac{V}{g}.$$

(413)

These values can be obtained from (412) by neglecting the term containing the Earth's radius R, and then finding the maximum for ϑ.

The following results are obtained using the values of p, k, and V assumed before:

$$\omega_r = 0.0274 \text{ sec}^{-1}, \vartheta_r = 1°24'.$$

The error is of the same order of magnitude if the ship's speed is increased or reduced on a straight course. The corresponding equations of motion are obtained by inserting $n = 1$, $\omega = 0$, $\delta = 0$ into (408). The following system of differential equations is obtained by neglecting again $U \sin\varphi$, small in comparison with p, and also the angular velocity $\frac{V}{R}$:

$$\frac{dx}{dt} + kx + py = \frac{p}{g}\frac{dV}{dt},$$

(414)

$$\frac{dy}{dt} + ky - px = \frac{k}{g}\frac{dV}{dt}.$$ (414)

This system is equivalent to the following differential equation in the complex variable z:

$$\frac{dz}{dt} + (k - ip)z = \frac{i(k - ip)}{g}\frac{dV}{dt} \quad (z = x + iy).$$ (415)

Bulgakov's methods of analyzing this equation and of the maximum possible deviation of the gyrosphere axis will not be given in detail here*. Instead, an approximate calculation, assuming that the ship is uniformly accelerated, will be carried out.

If the ship is accelerated at a uniform rate during time T [from a stop] to a maximum velocity V_{max}, the following expression is obtained by intergrating (415) for $t \leqslant T$ with the initial condition $z(0) = 0$:

$$z(t) = \frac{iV_{max}}{gT}[1 - e^{-(k-ip)t}].$$ (416)

It follows that the maximum deviation of the gyrosphere axis is of the same order of magnitude as the deviation of the pendulum

$$\vartheta_m = \frac{V_{max}}{gT}.$$ (417)

For $V_{max} = 20$ m/sec and $T = 2$ min this gives $\vartheta_m = 0.01700$ (58').

These calculations show that if no special measures are taken, the errors in the instrument readings may reach unacceptable values when the ship manoeuvers.

In practice, the so-called "correction elimination" is frequently applied: before the ship begins to manoeuver the gyrovertical pendulum is fixed by clamps relative to the stabilized ring in such a manner that the pendulum line and the axis of the ring coincide.

Experience shows that this procedure causes considerable error.

The lever arrangement described above does reduce the instrument errors during manoeuvers, though not completely. The method of eliminating the instrument errors by artificially inclining the stator axis through an angle proportional to the ship's speed, corrections (also proportional to this speed) being automatically introduced in the instrument readings, is therefore of interest**. The necessity for log readings and the impossibility of completely eliminating the instrument errors without complications due to the drift angle are drawbacks. This is further aggravated by our imperfect knowledge of the laws of variation of the drift angle.

Consider the case when in addition to the displacement undergone by the latitude carriage there is an additional displacement of its pin caused by an attachment connected to the log, so that the coordinates of point K on the xy plane increase by aV and bV respectively (a and b are coefficients that have to be determined).

* Bulgakov, B. V. O nakoplenii vozushchenii v lineinykh kolebatel'nykh sistemakh s postoyannymi parametrami (Cumulative Perturbations in Linear Oscillatory Systems with Constant Parameters). — Doklady Akademii Nauk SSSR, Vol. 51, No. 5. 1946.

** This can be compared with the method of compensating the gyro-pendulum ballistic errors and with the method of introducing an additional gyrohorizon with a variable angular momentum for compensating the inertia forces of the translational motion by gyroscopic forces (cf. below § 3). These methods were proposed by V. I. Kuznetsov, Ya. N. Reutenberg, etc.

The moments M_x and M_y are in this case (by analogy with (406)):

$$M_x = H\left[\frac{k}{n}\left(x - \frac{w_x}{g} - u_x - aV\right) + \frac{p}{n}\left(y - \frac{w_y}{g} - u_y - bV\right)\right],$$
$$M_y = H\left[\frac{k}{n}\left(y - \frac{w_y}{g} - u_y - bV\right) - \frac{p}{n}\left(x - \frac{w_x}{g} - u_x - aV\right)\right]. \tag{418}$$

Inserting (418) into the differential equations (405) yields, after simplifications similar to those made in the derivation of equations (407), the following system of differential equations describing the motion of the gyrosphere axis:

$$\frac{dx}{dt} + \frac{k}{n}x - \left(\omega + U\sin\varphi - \frac{p}{n}\right)y =$$
$$= \frac{V}{R}\sin\delta + \frac{k}{n}\left(\frac{w_x}{g} + aV\right) + \frac{p}{n}\left(\frac{w_y}{g} + bV\right),$$
$$\frac{dy}{dt} + \frac{k}{n}y + \left(\omega + U\sin\varphi - \frac{p}{n}\right)x = \tag{419}$$
$$= -\frac{V}{R}\cos\delta + \frac{k}{n}\left(\frac{w_y}{g} + bV\right) - \frac{p}{n}\left(\frac{w_x}{g} + aV\right).$$

Equations (419) hold, as equations (408), for any law of variation of the ship's speed V and its angular velocity ω.

Assume that the drift angle $\delta = 0$. Equations (402) then become

$$w_x = -\omega V, \qquad w_y = \frac{dV}{dt}. \tag{420}$$

This also follows directly from the formulas on the motion of a particle.

In this case equations (419) become

$$\frac{dx}{dt} + \frac{k}{n}x - \left(\omega - \frac{p}{n}\right)y = \frac{k}{n}\left(-\frac{\omega V}{g} + aV\right) + \frac{p}{n}\left(\frac{1}{g}\frac{dV}{dt} + bV\right),$$
$$\frac{dy}{dt} + \frac{k}{n}y + \left(\omega - \frac{p}{n}\right)x = -\frac{V}{R} + \frac{k}{n}\left(\frac{1}{g}\frac{dV}{dt} + bV\right) + \frac{p}{n}\left(\frac{\omega V}{g} - aV\right). \tag{421}$$

The terms containing the vertical component $U\sin\varphi$ of the Earth's angular velocity have been neglected in (421) for the reasons given above.

Equations (421) form a system of linear differential equations with variable coefficients. The general solution of such a system is the sum of the general solution of the corresponding homogeneous system

$$\frac{dx}{dt} + \frac{k}{n}x - \left(\omega - \frac{p}{n}\right)y = 0,$$
$$\frac{dy}{dt} + \frac{k}{n}y + \left(\omega - \frac{p}{n}\right)x = 0 \tag{422}$$

and of some particular solutions of the nonhomogeneous system (421). The solution of equations (422) can be represented in a complex form similar to (377)

$$z = Ce^{-\frac{k - ip}{n}t}e^{-i\int_0^t \omega\, dt} \qquad (z = x + iy), \tag{423}$$

where C is an arbitrary complex constant.

The modulus of the complex function z tends to zero with time independently of the value of C.

131

It can be shown that

$$x = \frac{p}{ng} V, \qquad y = \frac{k}{ng} V, \tag{424}$$

are a particular solution of the nonhomogeneous system (421), provided the coefficients a and b are suitably selected. In fact, inserting (424) into the left-hand sides of (421) yields

$$2 \frac{pk}{ng} = ka + pb,$$

$$\frac{n}{R} + \frac{k^2 - p^2}{ng} = kb - pa, \tag{425}$$

which can be considered as two equations with two variables a and b. Their solution is

$$a = \frac{p}{ng} \left[1 - \frac{n^2 g}{(k^2 + p^2) R} \right],$$

$$b = \frac{k}{ng} \left[1 + \frac{n^2 g}{(k^2 + p^2) R} \right]. \tag{426}$$

For $n = 1$ and the same values of k and p:

$$a = 0.000438 \, \text{sec/m},$$

$$b = 0.001033 \, \text{sec/m}.$$

At $V = 20$ m/sec (40 knots) the stator is inclined by the following additional angles to starboard (in the positive x-direction) and forward (in the positive y-direction):

$$aV = 0.00876 \, (30'), \qquad bV = 0.0207 \, (1°11').$$

The gyrosphere axis is inclined by the following angles to starboard and forward:

$$\frac{pV}{g} = 0.00888 \, (31'), \qquad \frac{kV}{g} = 0.0204 \, (1°10').$$

It is thus seen that if the values of the angles given by (424) are automatically subtracted from the instrument indications with the aid of an attachment connected to the log, the instrument will indicate the true vertical also when the ship manoeuvers provided the drift angle is zero.

The latitude carriage pin is always displaced under the same angle to the ship's course line.

The attachment to effect this displacement can be located not only on the pendulum, as assumed above, but also on the stator or on the stabilized ring. The values of the coefficients in (424), and of a and b vary accordingly.

Assume that the drift angle is not zero. For a steady turn, even if

$$\cos \delta \cong 1,$$

terms containing $\sin \delta \cong \delta$ will appear on the right-hand sides of (421), as follows from (409), and their influence cannot be neglected. These terms occur because the component of the centrifugal force parallel to the ship's course line acts on the pendulum during the turn. If the drift angle is small, the errors due to these terms will be a fraction of the total error of the instrument during turns without the correction elimination calculated above. Thus the error for a drift angle of 6° is of the order of $6 - 7$ minutes of arc, the linear and angular velocities of the ship being as before.

The error during turns due to drift becomes comparatively small if the instrument is equipped with a lever attachment. In this case, however, the vertical component $U\sin\varphi$ of the Earth's angular velocity in equations (408) can no longer be neglected in comparison with $\frac{p}{n}$ during an increase or reduction of the ship's speed on a straight course. In fact, at 60° latitude and for $n = 8$:

$$U\sin\varphi = 0.0000628 \text{ sec}^{-1}, \quad \frac{p}{n} = 0.000545 \text{ sec}^{-1}.$$

It is thus seen that the influence of the terms in (409) caused by the inertia force is only partially eliminated in the case of drift.

The laws of variation of the drift angle are imperfectly known, as already mentioned, and only certain assumptions can be made about them.

One meriting attention is a direct proportionality

$$\delta = c\omega \tag{427}$$

between the drift angle δ and the angular velocity ω, the coefficient c depending on the hydrodynamic properties of the ship.

Relationship (427) can be used for further improvements of the instrument, such as by an additional rotation of the stator relative to the x- and y-axes depending on the direction of the velocity of the point at which the gyroscopic instrument is located in relation to the ship's course line. In this case the accuracy of eliminating the instrument errors caused by the inertia forces appearing during the ship's manoeuvers will depend only on the accuracy of the log. We will not discuss this point further.

In conclusion, the principle of aerodynamic suspension can be used for developing new gyroscopic devices such as a gyroscopic pendulum with Schuler-Bulgakov period (84.4 min) which is free from so-called ballistic deviations (deviations caused by the inertia forces of the translational motion).

A combination of two such pendulums, with gyrospheres rotating in different directions, makes it possible to eliminate also the velocity deviations during manoeuvers and to determine (at present inaccurately because the instruments do not yet give satisfactory performance) the velocity with which the ship or any other object on the Earth's surface moves (the so-called absolute log).

Since in the absence of a latitude carriage the gyrosphere axis deviates from the vertical in a direction determined by the compass and depending only on the latitude, it is possible in practice to design a gyrolatitude with simultaneous indication of the ship's course.

A perfect directional gyro with horizontal rotation of the gyrosphere can be designed.

§ 3. Gyrovertical with auxiliary gyro

Two contradictory technical problems have to be solved when gyroscopic devices such as the gyrovertical are being designed. The first consists in the selection of sufficiently effective attachments which will orient the gyros in space to a position in which the instruments will indicate the true local vertical.

Without such so-called correcting attachments, the gyros if left to themselves, will change their orientation very rapidly within excessively wide limits, even when suspensions of the highest quality are used. This is mainly due to the friction in the bearings of the gyro suspension during the oscillations of the object on which the gyroscopic device is mounted.

The attachments used are pendulums of various types which either act directly on the gyros, as in the scheme described below, or control solenoids which apply moments to the gyros in the necessary direction. Other correction methods also exist. Obviously the attachments function only so long as the moments which they apply to the gyro are greater than the frictional moments in the bearings of the suspension. In addition, the action of the corrective attachments on the gyro is restricted by the friction in the bearings of the corresponding pendulums. Pendulums with a sufficiently large moment of inertia are to be used in order to overcome the influence of the friction forces.

The second problem is to eliminate the influence of the corrective attachments on the gyros during manoeuvers. In general, the manoeuvering accelerations are small, but due to the duration of manoeuvering the gyros change their orientation considerably because the corrective pendulums react to these accelerations. This influence increases with the moments of inertia of the pendulum in the case of linear-type corrective devices (such as the device described below). Finally, excessive linear correction leads to large instrument errors during rolling. Corrective devices of the nonlinear type have their own shortcomings, in particular during rolling (cf. Chapter VI, § 1).

The availability of a log on the ship and the possibility of feeding its data to the gyroscopic instruments by means of a synchronous link have made it possible to work out schemes for additional attachments so as to avoid the errors of gyroverticals during manoeuvers. The theory of such a device for a gyrovertical with aerodynamic suspension was given in § 2 of this chapter.

Another similar device is described below. Its peculiarity lies in the fact that no corrections proportional to the velocity have to be introduced in the readings of the instrument itself in order to obtain the true vertical. The appearance of a drift angle during turns interferes with the proper functioning of this device.

Consider a gyroscopic system (Figure 115) whose basic gyro has a vertical axis and is suspended in gimbals from a so-called stabilized ring*. The perpendicular to the plane of the stabilized ring is made to move together with the axis of the basic gyro by means of follow-up systems; the ring itself is the inner gimbal ring of a bicardan suspension (Figure 7). The bearings of two upward-turned pendulums, connected by angular levers and hinges to the basic gyro housing, are mounted on the stabilized ring. The

---

* The gimbals of the basic gyro and the stabilized ring are not shown on Figure 115.

function of these pendulums is to force the axis of the basic gyro into the vertical.

The housing of an additional gyro, whose rotor axis is perpendicular to the axis of the basic gyro (and therefore horizontal when the instrument indicates the true vertical), is rigidly connected to the housing of the basic gyro. The function of the additional gyro is to counterbalance the influence on the basic gyro of the corrective pendulums and of the mass of the two gyros during manoeuvers. Thus the axis of the additional gyro rotor is oriented at a specified angle $\phi - \frac{\pi}{2}$ toward the direction y of the ship's course line, and the angular velocity of its rotor is varied in proportion to the ship's speed V.
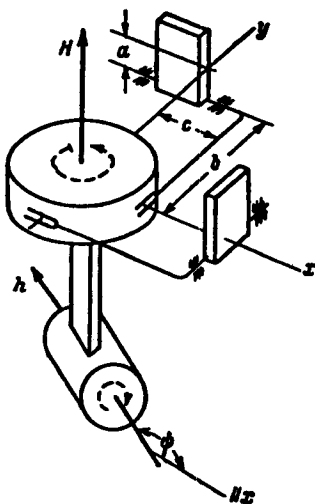
FIGURE 115
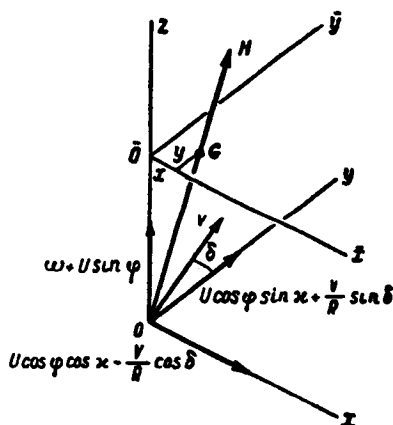
FIGURE 116

To obtain the equations of motion of the gyroscopic device, we introduce a moving reference frame xyz with vertical z-axis, and y-axis parallel to the ship's course line (Figure 116).

As in § 2, a horizontal plane xy lies at unit distance from the center of the gimbal system of the gyros. Let G be the intersection of the axis of the basic gyro with the xy plane, x and y being the abscissa and ordinate of this point respectively.

The equations of motion of the axis of the basic gyro can be written, similarly to (405),

$$H\left[\frac{dx}{dt} - (\omega + U\sin\varphi)y + U\cos\varphi\cos x - \frac{V}{R}\sin\delta\right] = M_x + m_x,$$

$$H\left[\frac{dy}{dt} + (\omega + U\sin\varphi)x + U\cos\varphi\sin x + \frac{V}{R}\cos\delta\right] = M_y + m_y. \qquad (428)$$

Here H is the angular momentum of the basic gyro, directed upward (the rotor of the basic gyro rotates counterclockwise when viewed from above); M_x and M_y are the moments about the x- and y-axes imposed on the housing

135

of the basic gyro by the corrective pendulums together with the frictional moments, the moments of the so-called latitude correction and, in addition, the moments due to gravity and the translational inertia of the gyros (in case their center of mass does not coincide with the center of its gimbal system); m_x and m_y are the moments about the same axes due to the effect of the inertia of the additional gyro on the basic gyro. The remaining notation remains as in § 2 of this chapter. The magnitudes x and y in (428) are small compared with unity.

The frictional moments at the pivots of the basic-gyro gimbals are of the order of several gcm when high-quality bearings are used, and may vary during operation within wide limits due to various random factors (position of the bearing balls, dust, lubrication, temperature, etc).

Under these conditions there is no sense in retaining in equations (428) the terms containing the vertical component $U \sin \varphi$ of the Earth's angular velocity and the angular velocity $\frac{V}{R}$ due to the curvature of the Earth's globe.

Assume the angular momentum of the basic gyro to be $H = 540000$ gcm sec, and let the gyro axis deviate from the vertical by half a degree to the south.
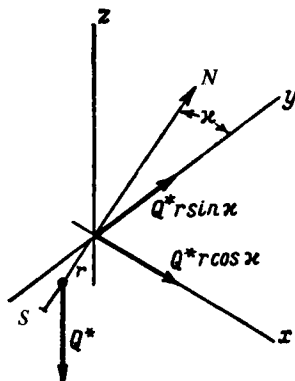
FIGURE 117

It follows that at a latitude of 60°,

$$HUy \sin \varphi = 0.3 \text{ gcm.}$$

If the ship's speed is $V = 20$ m/sec (40 knots), then

$$H \frac{V}{R} = 1.7 \text{ gcm.}$$

These terms are therefore of the order of the accuracy with which the values of the frictional moments are given, and can be neglected in equations (428).

The terms containing the horizontal component $U \cos \varphi$ of the Earth's angular velocity can be eliminated from (428) by adopting special measures for cancelling the effect of this component on the basic gyro. Thus moments

$$M_x^* = HU \cos \varphi \cos x,$$
$$M_y^* = HU \cos \varphi \sin x,$$

(429)

136

can be applied to the housing of the basic gyro by means of a moving load $Q^{\bullet}$ (or by any other means). The load $Q^{\bullet}$ must be placed on the housing of the basic gyro in such a way (Figure 117) that it is always at a distance r to the south of the gimbals center, where

$$Q^{\bullet}r = HU \cos \varphi. \qquad (430)$$

In order to reduce the effect of the load $Q^{\bullet}$ on the basic gyro during manoeuvers, its center of gravity must lie on the perpendicular to the rotor axis, passing through the gimbals center.

This load causes terms equal (up to higher order infinitesimals) to the terms containing the horizontal component $U \cos \varphi$ of the Earth's angular velocity to appear on the right-hand side of (428). These equations thus become

$$H\left(\frac{dx}{dt} - \omega y\right) = M_{x} + m_{x},$$

$$H\left(\frac{dy}{dt} + \omega x\right) = M_{y} + m_{y}, \qquad (431)$$

where M_{x} and M_{y} include only the moments due to gravity and the translational inertia of the gyros, the frictional moments, and the moments imposed on the housing of the basic gyro by the corrective pendulums.

We consider now the behavior of the gyroscopic device when the ship moves on a straight course $(\omega = 0)$ at constant velocity V. In this case, as will be explained below, m_{x} and m_{y} can be taken to be zero. Neglecting for the present the effect of friction in the bearings of the basic gyro and of the corrective pendulums (Figure 115), the following equations are obtained:

$$H\frac{dx}{dt} = Ply - Qa\frac{c}{b}x,$$

$$H\frac{dy}{dt} = -Plx - Qa\frac{c}{b}y, \qquad (432)$$

where P is the weight of the gyros; l, the distance from their center of mass to the gimbals center; Q, the weight of each corrective pendulum; a, the distance of the latter's center of mass from its pivots; b, the distance between the pendulum pivots and the pins of the basic-gyro housing entering into the slot in the angular levers; c, the distance between the gimbals center and the angular levers. The pivots of the two pendulums are located in the plane containing the gimbals center and perpendicular to the x-axis.

Let the basic gyro deviate to starboard (Figure 118). Point G of the $x y$ plane will then move a certain distance x from O in the direction of increasing abscissa (Figure 116). It is obvious that x represents at the same time the angle by which the axis of the basic gyro deviates from the vertical in the xz plane. This deviation produces a moment about the y-axis due to gravity (Figure 118), given by

$$mom_{y}P = - Plx. \qquad (433)$$

The perpendicular to the plane of the stabilized ring moves continuously with the axis of the basic gyro, and the corrective pendulum, whose pivots are parallel to the y-axis, will therefore also incline to starboard. A force

$$Z = \frac{Qax}{b} \qquad (434)$$

137

acts therefore on the gyro-housing pin located on the side of the negative y-axis (Figure 118). This force is directed upward and creates a moment about the x-axis equal to

$$mom_x Z = -Qa\frac{c}{b} x. \tag{435}$$

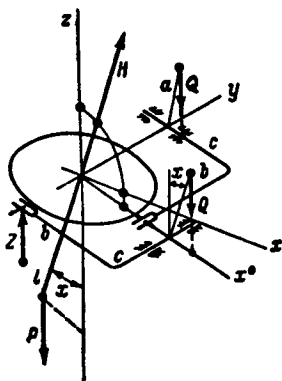The remaining terms of the right-hand sides of equations (432) can be found similarly (Figure 119).
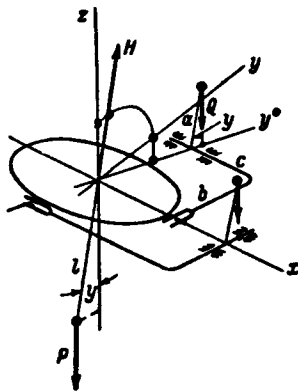

FIGURE 118   FIGURE 119

We introduce the parameters k and p, given by

$$k=\frac{Qac}{bH} \text{ and } p=\frac{Pl}{H}. \tag{436}$$

Inserting these parameters into (432) yields

$$\frac{dx}{dt}+kx-py=0,$$
$$\frac{dy}{dt}+ky+px=0. \tag{437}$$

These equations differ from the similar equations of the preceding section only by the sign of the terms containing p.

The system of differential equations (437) is equivalent to one linear homogeneous equation

$$\frac{ds}{dt}+(k+ip)s=0 \tag{438}$$

of the complex variable

$$s=x+iy. \tag{439}$$

The solution of (438) is

$$s=s_0 e^{-(k+ip)t}, \tag{440}$$

where s_0 is a complex number corresponding to the initial position of G on the $\bar{x}\bar{y}$ plane. According to (440) G moves along a logarithmic spiral (Figure 120) toward the equilibrium position $s = 0$, which determines the vertical position of the basic-gyro axis. In the particular case when the center

138

of mass of the gyros coincides with the gimbals center ($p = 0$), the logarithmic spirals degenerate into straight lines

$$z = z_0 e^{-kt},$$ (441)

passing through the origin (Figure 121).

The influence of the Coulomb friction on the behavior of this gyroscopic system will now be taken into account.

Assume that the values of the frictional moments are identical in the bearings of both gimbals, being equal to F_1. The frictional moment in each bearing of the pendulum suspensions will be denoted by F_2. The signs of the frictional moments in the equations of motion of the system are determined by the direction of the angular velocities of the stabilized ring relative to the basic gyro. These angular velocities are caused by the follow-up systems which constantly align the stabilized-ring axis of symmetry with the axis of the basic gyro. We denote by ξ and η the coordinates of the intersection C between the axis of symmetry of the stabilized ring and the xy plane (Figure 122). The differences

$$\Delta\xi = \xi - x \quad \text{and} \quad \Delta\eta = \eta - y$$ (442)

represent the errors of the follow-up systems. They are essentially determined by the law of motion of the instrument's body or, which is the
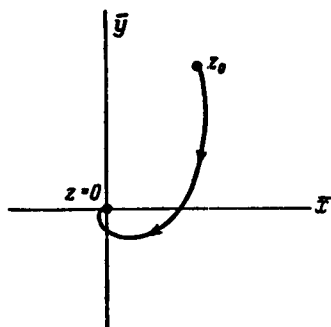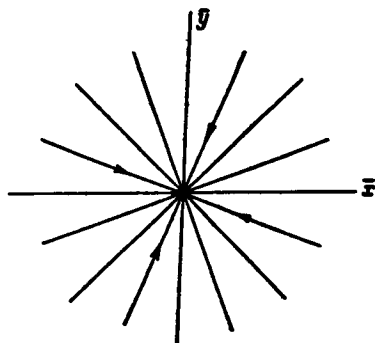

FIGURE 120

FIGURE 121

same, of the ship relative to the frame xyz during rolling. Let point K, located in the xy plane and having the coordinates α and β, determine the position of the instrument's body axis at an arbitrary inclination of the deck. The differences

$$\alpha^* = \alpha - \xi \quad \text{and} \quad \beta^* = \beta - \eta$$ (443)

represent the angles through which the follow-up systems have tilted the stabilized ring relative to the instrument's body at the given instant. The conventional follow-up systems (Chapter VI, § 7) have a so-called velocity (dynamic) error, which can be expressed for comparatively slow motions of the instrument's body caused by the ship's rolling, by

$$\Delta\xi = s \frac{d}{dt}(\alpha - \xi),$$
$$\Delta\eta = s \frac{d}{dt}(\beta - \eta),$$ (444)

where s is one of the parameters of the follow-up system.

139

The values of x and y characterizing the position of the basic-gyro axis
in the frame xyz vary only slowly in comparison with α and β, and can, to a first
approximation, be considered in (442) and (444) as constant.

Equations (444) will not be analyzed here. We only state that the periodic
variation of α and β must be accompanied by a periodic variation of the er-
rors $\Delta\xi$ and $\Delta\eta$. As a result the velocities of the stabilized ring relative to
the basic gyro will vary in phase with the rolling.
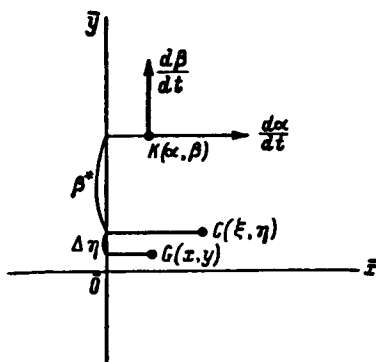
FIGURE 122

Assume the error $\Delta\xi$ to increase. Then, as can be seen from Figure 123,
the stabilized ring, striving to carry with it the basic gyro and the pendulum,
imposes on the housing of the basic gyro moments

$$F_1 \text{ and } F_2 \frac{c}{b}$$

about the y-axis.

If the error $\Delta\eta$ increases (Figure 124), there appear moments

$$-F_1 \text{ and } -F_2 \frac{c}{b}$$

about the x-axis.

Friction in the suspensions thus leads to the appearance of moments

$$M_x^f = -F \, sign \, \frac{d\Delta\eta}{dt},$$

$$M_y^f = F \, sign \, \frac{d\Delta\xi}{dt},$$

(445)

where

$$F = F_1 + F_2 \frac{c}{b}.$$

(446)

In addition to the moments due to friction in the suspensions, for $\Delta\xi$, $\Delta\eta \neq 0$,
the housing of the basic gyro is acted upon by additional moments

$$\Delta M_x = -Qa \frac{c}{b} \Delta\xi + Qa \frac{c^2}{b^2} \Delta\eta,$$

$$\Delta M_y = -Qa \frac{c}{b} \Delta\eta - Qa \frac{c^2}{b^2} \Delta\xi;$$

(447)

140

these are due to the additional deviations of the corrective pendulums from the vertical produced by the tilting of the stabilized ring relative to the basic gyro (Figures 123 and 124). These moments will, however, be neglected because $\Delta\xi$ and $\Delta\eta$ are terms of second and third order and have a mean value of zero.
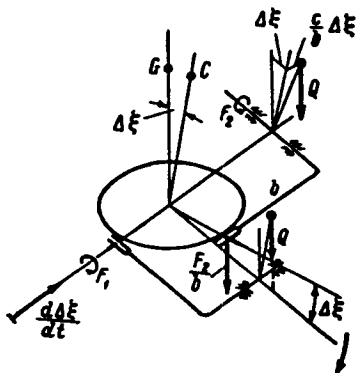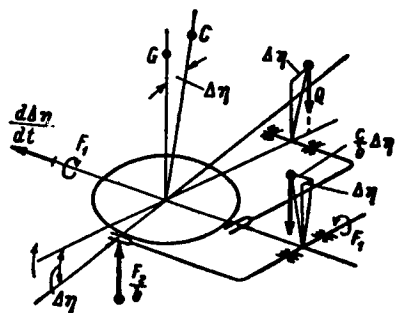

FIGURE 123   FIGURE 124

When friction in the suspensions is taken into account, the following equations are obtained instead of (432):

$$H\frac{dx}{dt} = \quad Ply - Qa\frac{c}{b}x - F\,sign\,\frac{d\Delta\eta}{dt};$$

$$H\frac{dy}{dt} = -Plx - Qa\frac{c}{b}y + F\,sign\,\frac{d\Delta\xi}{dt}. \qquad (448)$$

These can be written in complex form, using (436), as

$$\frac{dz}{dt} + (k+ip)z = (k+ip)f\left(\frac{d\Delta\xi}{dt}, \frac{d\Delta\eta}{dt}\right), \qquad (449)$$

where f is given by the formula

$$f = \frac{iF}{Qa\frac{c}{b}+iPl}\left(sign\,\frac{d\Delta\xi}{dt} + i\,sign\,\frac{d\Delta\eta}{dt}\right). \qquad (450)$$

The complex magnitude f has four possible values

$$\pm[(f_1 - f_2) + i(f_1 + f_2)]; \quad \pm[(f_1 + f_2) - i(f_1 - f_2)], \qquad (451)$$

where

$$f_1 = -\frac{FPl}{\left(Qa\frac{c}{b}\right)^2 + (Pl)^2}, \quad f_2 = \frac{FQa\frac{c}{b}}{\left(Qa\frac{c}{b}\right)^2 + (Pl)^2}, \qquad (452)$$

depending on the sign of the relative angular velocities

$$\frac{d\Delta\xi}{dt} \quad \text{and} \quad \frac{d\Delta\eta}{dt}.$$

141

The points A, B, C, and D corresponding in the xy plane to the four values

	$\dfrac{d\Delta\xi}{dt}$	$\dfrac{d\Delta\eta}{dt}$	$f\left(\dfrac{d\Delta\xi}{dt},\dfrac{d\Delta\eta}{dt}\right)$	
A	>0	>0	$(f_1-f_2)+i(f_1+f_2)$	
B	>0	<0	$(f_1+f_2)-i(f_1-f_2)$	
C	<0	<0	$-(f_1-f_2)-i(f_1+f_2)$	(453)
D	<0	>0	$-(f_1+f_2)+i(f_1-f_2)$	

are the corners of a square (Figure 125).
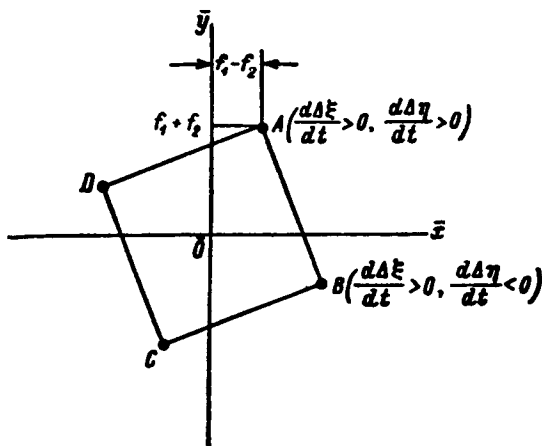
FIGURE 125

The solution of (449) consists of expressions of the form

$$z=C_f e^{-(k+ip)t}+f\left(\frac{d\Delta\xi}{dt},\frac{d\Delta\eta}{dt}\right), \qquad (454)$$

where C_f is a complex constant defined by the initial conditions. Depending on the signs of $\frac{d\Delta\xi}{dt}$ and $\frac{d\Delta\eta}{dt}$, (454) corresponds to the motion of point G along a logarithmic spiral about one of the points A, B, C, or D. Since these signs vary during rolling, point G passes from one logarithmic spiral to another, approaching one of the points A, B, C, or D (Figure 126).

If the gyros are balanced so that $p=0$ in accordance with (436), point G, once inside square $ABCD$, will remain inside. It will generally undergo a random motion along lengths of straight lines passing through the corners of this square (Figure 127).

It follows that if the gyros are mounted together with the pendulums on a fixed base, a point G located inside the square $ABCD$ will correspond in the xy plane to any arbitrary equilibrium position.

Before analyzing the behavior of the gyroscopic device during manoeuvers, we shall find what forces act on the basic gyro due to the additional gyro. Let $x^0 y^0 z^0$ be a reference frame fixed to the stabilized ring (Figure 128),

with the z^0-axis oriented upward, perpendicular to the plane of the ring, and the y^0-axis pointing forward along the pivot axis of gyro's gimbal ring. The axis of the basic-gyro rotor will then be oriented along the z^0-axis if the errors of the follow-up systems are neglected. We denote by ω_{x^0}, ω_{y^0}, ω_{z^0} the projections of the angular velocity of the stabilized ring (or, which is the same in this case, of the angular velocity of the gyros) on the axes x^0, y^0, z^0, by h the angular momentum of the additional gyro, and by ψ the angle between the direction of the rotor axis of the additional gyro and the x^0-axis.

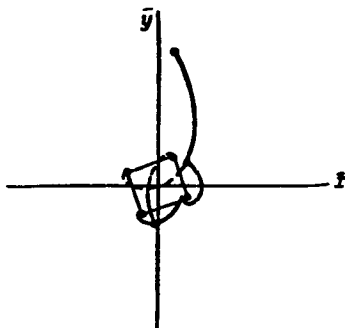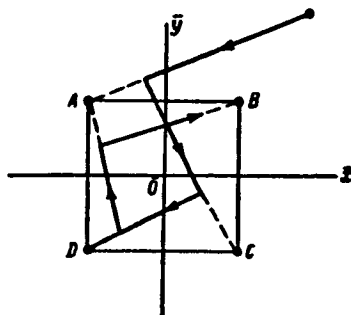FIGURE 126   FIGURE 127

The velocity of the vertex of the vector h [the rate of change of h with respect to time] consists of the vector $\frac{dh}{dt}$, coinciding in direction with the vector h, and of a vector determined by the rotation of the frame $x^0y^0z^0$ relative to which the vector h retains a constant orientation (Figure 129). The projections of this second vector on the axes x^0, y^0, and z^0 are

$$\omega_{y^0}h_{z^0} - \omega_{z^0}h_{y^0} = -\omega_{z^0}h\sin\psi,$$
$$\omega_{z^0}h_{x^0} - \omega_{x^0}h_{z^0} = \omega_{z^0}h\cos\psi,$$
$$\omega_{x^0}h_{y^0} - \omega_{y^0}h_{x^0} = (\omega_{x^0}\sin\psi - \omega_{y^0}\cos\psi)h. \tag{455}$$

According to the theory of gyroscope precession, the following equations are true:

$$-\omega_{z^0}h\sin\psi + \frac{dh}{dt}\cos\psi = -m_{x^0},$$
$$\omega_{z^0}h\cos\psi + \frac{dh}{dt}\sin\psi = -m_{y^0},$$
$$(\omega_{x^0}\sin\psi - \omega_{y^0}\cos\psi)h = -m_{z^0}, \tag{456}$$

where $m_{x^0}, m_{y^0}, m_{z^0}$ are the moments which the additional gyro exerts on the basic gyro. The moment m_{z^0} is balanced by the moment of the gimbals reaction. This moment is directed along the z^0-axis perpendicular to both gimbal rings. The moments m_{x^0} and m_{y^0} are taken up by the basic gyro. Since the angles between the axes of the system $x^0y^0z^0$ and the corresponding axes of the xyz system are small, the following approximations are true:

$$m_{x^0} \cong m_x;$$
$$m_{y^0} \cong m_y, \tag{457}$$

143

and

$$\omega_{z^0} \cong \omega,$$ (458)

where ω is the angular velocity of the ship.

Inserting (456), (457), and (458) into (431) we obtain

$$H\left(\frac{dx}{dt} - \omega y\right) = M_x + \omega h \sin \psi - \frac{dh}{dt} \cos \psi;$$

$$H\left(\frac{dy}{dt} + \omega x\right) = M_y - \omega h \cos \psi - \frac{dh}{dt} \sin \psi.$$ (459)

Expressions for M_x and M_y during manoeuvers of the ship will now be established. This case differs from the preceding in that the gyros and the corrective pendulums are subjected to translational inertia in addition to gravity.
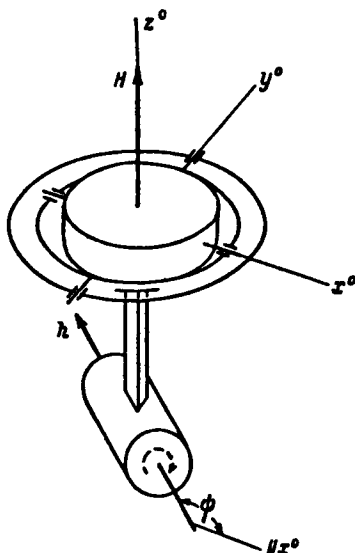

FIGURE 128

We assume that the drift angle is zero at the place where the gyroscopic device is located. In the case of a left turn $(\omega > 0)$ the following forces will act along the x- and y-axes (Figure 130):

$$\frac{P}{g} \omega V \quad \text{and} \quad -\frac{P}{g} \frac{dV}{dt}.$$ (460)

Similar forces will act on the mass of the corrective pendulums (Figure 130).

When these forces, together with gravity and friction, are taken into account, the moments acting (in addition to m_x and m_y) on the basic gyro are (cf. pp. 138 and 140)

$$M_x = Ply - Qa\frac{c}{b}x - \frac{Pl}{g}\frac{dV}{dt} - \frac{Qa}{g}\frac{c}{b}\omega V + M_x';$$

$$M_y = -Plx - Qa\frac{c}{b}y - \frac{Pl}{g}\omega V + \frac{Qa}{g}\frac{c}{b}\frac{dV}{dt} + M_y'.$$ (461)

144

Inserting (461) into (459) yields

$$H\left[\frac{dx}{dt}+kx-(\omega+p)y\right]=-\left(\frac{Pl}{g}\frac{dV}{dt}+\frac{dh}{dt}\cos\psi\right)-$$
$$-\left(\frac{Qa}{g}\frac{c}{b}V-h\sin\psi\right)\omega+M'_x,$$

$$H\left[\frac{dy}{dt}+ky+(\omega+p)x\right]=-\left(\frac{Pl}{g}V+h\cos\psi\right)\omega+ \qquad (462)$$
$$+\left(\frac{Qa}{g}\frac{c}{b}\frac{dV}{dt}-\frac{dh}{dt}\sin\psi\right)+M'_y,$$

where k and p are given by (436). We subject the angular momentum h of the additional gyro and the angle ψ to the following two conditions:

$$h\cos\psi=-\frac{Pl}{g}V;$$
$$h\sin\psi=\frac{Qa}{g}\frac{c}{b}V. \qquad (463)$$

Inserting (463) into (462) yields

$$H\left[\frac{dx}{dt}+kx-(\omega+p)y\right]=M'_x,$$
$$H\left[\frac{dy}{dt}+ky+(\omega+p)x\right]=M'_y. \qquad (464)$$

The physical meaning of (463) is that the moments due to translational inertia are balanced by the gyroscopic moment of the additional-gyro rotor.
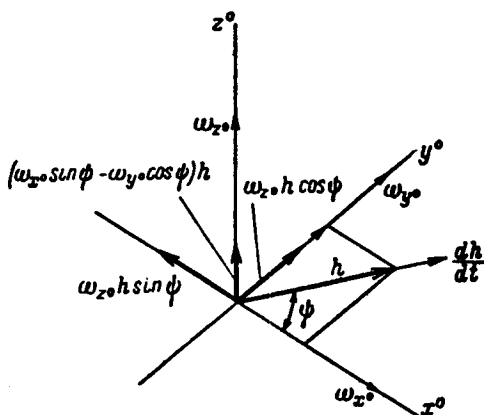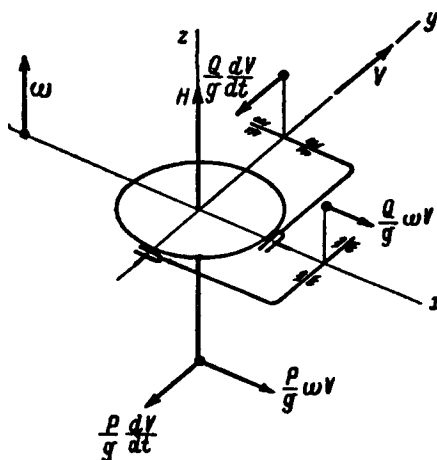

FIGURE 129

FIGURE 130

This balancing is particularly simple when no corrective pendulums are used (Figures 131 and 132). The angle ψ must then be taken as 180°, i.e., the vector h must point to port, perpendicular to the longitudinal axis of the ship.

The moment of the centrifugal inertia force $\frac{Pl}{g}\omega V^*$ is balanced by the gyroscopic moment ωh, and the inertia force $\frac{P}{g}\frac{dV}{dt}$ by the reaction of the gyro

* [This should apparently read $\frac{Pl}{g}\omega V$, which is the Coriolis force. Similar corrections should be applied to other relevant formulas.]

145

rotor. Also,

$$\frac{dh}{dt} = I\frac{d\Omega}{dt},$$ (465)

where I is moment of inertia and Ω is the angular velocity of the additional gyro rotor. Thus

$$h = I\Omega = \frac{Pl}{g}V.$$

In the general case we have, as follows from (463):

$$h = \frac{V}{g}\sqrt{(Pl)^2 + \left(Qa\frac{c}{b}\right)^2},$$

$$\operatorname{tg}\psi = -\frac{Qa}{Pl}\frac{c}{b},$$ (466)

and therefore the angle ψ must be constant, while the angular momentum h must be proportional to the ship's speed.
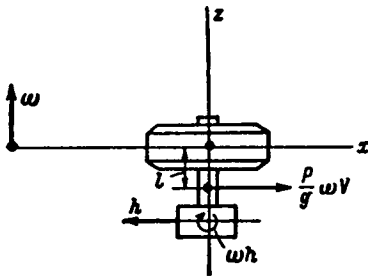

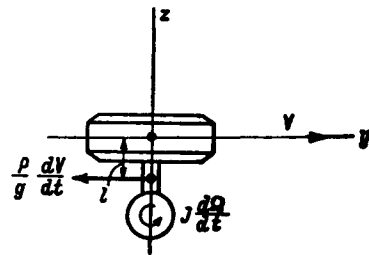FIGURE 131   FIGURE 132

Numerical example. Assume that

$$Pl = 5400\,\text{gcm}, \quad Qa\frac{c}{b} = 4050\,\text{gcm}, \quad V = 20\ \text{m/sec}.$$

It then follows from (466) that

$$h = 13800\,\text{gcm sec}, \quad \operatorname{tg}\psi = -0.750, \quad \psi = 143°10'.$$

Returning to equations (464), it is obvious that they can be written in a complex form, exactly as (448):

$$\frac{dz}{dt} + [k + i(p + \omega)]z = (k + ip)f\left(\frac{d\Delta\xi}{dt}, \frac{d\Delta\eta}{dt}\right),$$ (467)

where f is a complex magnitude defined by (450) and depending on the signs of the rates of change of the error angles in the follow-up systems. In the particular case $\omega = 0$, (467) becomes (449). In the general case $\omega \neq 0$, its solution is similar to (454):

$$z = C_f e^{-[k + i(p + \omega)]t} + \frac{k + ip}{k + i(p + \omega)}f\left(\frac{d\Delta\xi}{dt}, \frac{d\Delta\eta}{dt}\right).$$ (468)

In this case point G, which defines the position of the basic-gyro axis, moves along logarithmic spirals, approaching one of the points

$$f^* = \frac{k + ip}{k + i(p + \omega)}f\left(\frac{d\Delta\xi}{dt}, \frac{d\Delta\eta}{dt}\right),$$ (469)

146

depending on the sign of the derivatives $\frac{d\Delta\xi}{dt}$ and $\frac{d\Delta\eta}{dt}$. These points define a square, just as points A, B, C, D in Figure 125. The sides of this square are rotated relative to the sides of the square $ABCD$. The lengths of the sides of these squares are in the ratio

$$\frac{|f^*|}{|f|}=\sqrt{\frac{k^2+p^2}{k^2+(p+\omega)^2}}\,. \tag{470}$$

The dimensions of the squares characterize to a certain extent the instrument error due to friction in the suspension.

It follows from (470) that the most unfavorable case will be that of a right turn at an angular velocity $\omega=\omega^*$, where;

$$\omega^*=-p. \tag{471}$$

If $k = 0.01$ sec^{-1} and $p = 0.0075$ sec^{-1}:

$$\frac{|f^*|}{|f|}=1.25, \quad \omega^*=-0.0075\ \text{sec}^{-1}.$$

These values correspond to a turning radius equal to 2670 m at $V = 20$ m/sec.

The order of the instrument error during an ordinary turn in the case of drift will now be found. In this case (Figure 133), $\frac{dV}{dt}=0$ must be substituted in (462) and the factor $\cos\delta$ added to all terms containing the ship's speed. In addition, the terms

$$-\frac{Pl}{g}\omega V\sin\delta \quad \text{and} \quad \frac{Q a}{g}\frac{c}{b}\omega V\sin\delta$$

must be added to the right-hand sides, respectively, of the first and second of equations (462). Assuming the drift angle δ to be sufficiently small, the following approximations are valid: $\cos\delta\cong1$, $\sin\delta\cong\delta$. Taking into account (463), the following system of two differential equations is finally obtained [neglecting friction]

$$H\left[\frac{dx}{dt}+kx-(\omega+p)y\right]=-\frac{Pl}{g}\omega V\,\delta;$$

$$H\left[\frac{dy}{dt}+ky+(\omega+p)x\right]=\frac{Qac}{b}\omega V\,\delta. \tag{472}$$

Using the complex variable $z=x+iy$, this system is equivalent to one equation

$$\frac{dz}{dt}+[k+i(\omega+p)]z=i(k+ip)\frac{\omega V}{g}\,\delta. \tag{473}$$

For any initial conditions, the solution of this equation tends to the limit

$$z^*=\frac{i(k+ip)}{k+i(\omega+p)}\frac{\omega V}{g}\delta. \tag{474}$$

The modulus ϑ of the complex number z^* characterizes the order of magnitude of the instrument error caused by the ship's drift during an ordinary turn. It follows from (474) that

$$\vartheta=\sqrt{\frac{k^2+p^2}{k^2+(\omega+p)^2}}\cdot\frac{\omega V}{g}\delta. \tag{475}$$

147

Let $k = 0.001$ sec^{-1}, $p = 0.0075$ sec^{-1}, $\omega = -0.01$ sec^{-1}, $\delta = 12°$ and $V = 20$ m/sec.

Inserting these values into (475) yields

$$\vartheta = 0.0056 \ (19').$$

For an opposite turn

$$\vartheta = 0.0029 \ (10').$$

The large values which are sometimes obtained for ϑ make it necessary to find means to reduce the instrument errors caused by the drift angle. One method was described in § 2 of this chapter.
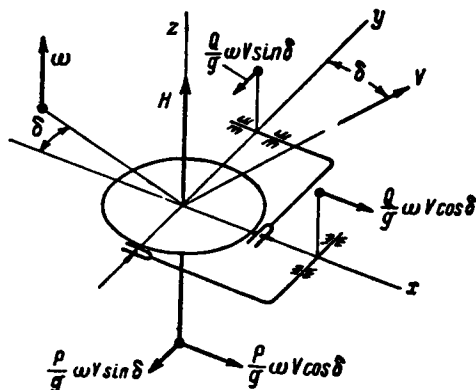

FIGURE 133

We shall not analyze the instrument errors during rolling, the errors caused by inaccuracies in manufacture, or malfunctioning of the follow-up systems (in particular errors in the log indication). Such an analysis is not difficult in the general case and should be conducted for each new instrument design.

§ 4. Theory of the gyroscopic heel equalizer

The preceding two sections of this chapter dealt with the mechanics of measuring gyroscopic systems (systems which do not influence the orientation of the moving object). Such systems determine the orientation of the moving object at any instant, and transmit this information to other devices by means of follow-up systems.

Gyroscopic systems of a different type also exist. Their function is the complete or partial stabilization of the moving object (e.g., the rolling stabilizer and the monorail car) during its rotations about a specified reference frame.

Contemporary systems (in contrast to those mentioned above) use the gyros not as stabilizers, but as control elements for rudders, fins or other components of the moving object. These latter stabilize the object by turning it in the required direction.

The complete system of differential equations describing the operation of such a device must include, in addition to the equations of motion of the gyros, also the equations of motion of the object itself, the equations of motion of the rudders, and in many cases the equations describing the functioning of additional devices (amplifiers, transformers, etc) whose function is to ensure the stability of the system as a whole.

In many cases, however, the complete system of differential equations can be separated into two independent subsystems. In fact, the orientation of the gyros can be considered as constant when studying transient processes and the stability of the object's motion, because of the small angular velocities with which the gyros vary their orientation. Similarly, the object's lag during transient processes (connected with the variation of its orientation caused by the gyros) can be neglected when studying the gyros motion, since the rate at which these variations proceed are incomparably higher than that of the gyros' motion. Thus the motion of the object, of the rudders, and of the additional devices appear in the equations of motion of the gyro system in the form of servomotor constraints. This procedure will be adopted when analyzing the gyroscopic heel equalizer. The function of this device is to reduce the moving object's heel to a minimum by acting on its control system (Figure 134).
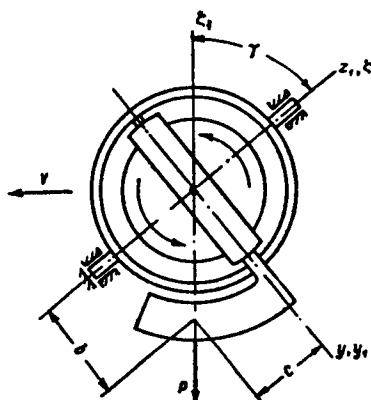

FIGURE 134

The error angle between the plane of the gyro's outer gimbal ring and the object's plane of symmetry will be assumed to be zero (the transient processes occurring during the reduction of this angle to zero are ignored).

In its mean (initial) position the gyro rotor (Figure 134) rotates in the symmetry plane of the moving object in such a way that the velocity of its upper points is directed along the object's motion.

The outer gimbal-ring pivot axis z_1 lies in the plane of symmetry inclined toward the side opposed to the object's motion, forming an angle $\frac{\pi}{2} - \gamma$ with the longitudinal axis of the object.

In the initial position the plane of the outer gimbal ring coincides with the plane of symmetry of the moving object. When the outer ring is tilted through an angle ε relative to its initial position, the control system forces the object to rotate so as to reduce this angle.

In the initial position the plane of the inner gimbal ring is perpendicular to the plane of the outer ring. When the inner ring is tilted through an angle β from its initial position, a correcting moment $K(\beta)$ is applied to the outer ring, which causes a precession of the gyro, tending to reduce the angle β. In particular, this moment can be created by the reaction of air jets discharged from the body of the outer ring impinging on dampers suitably arranged on the inner gimbal ring. If the angle β is small, $K(\beta)$ can be considered as a linear function:

$$K(\beta) = k\beta, \tag{476}$$

where k is a constant.

The linear relationship (476) does not apply when the angle β becomes large.

Assume in the nonlinear case that the curve of the function $K(\beta)$ is of the form represented in Figure 135. The problem does not become too complicated because of this nonlinearity and will be dealt with in this section together with the case of a linear function $K(\beta)$.
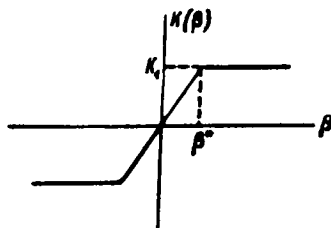

FIGURE 135

The cases of more complex forms of the function $K(\beta)$, leading to different types of motion of the gyroscopic systems, are discussed later (Chapter V, § 1).

The inner gimbal ring of the heel equalizer's gyro rotor is connected rigidly with a weight P (Figure 134). The center of gravity of the weight P lies in the rotor's plane of rotation. It is located at a distance b from the pivot axis of the outer ring axis and at a distance c from that of the inner ring. It will be shown later that when the instrument is correctly adjusted the distances b and c must be connected by the following relationship:

$$b = c \operatorname{tg} \gamma. \tag{477}$$

This also means that the geometric center of the gimbals and the center of gravity of the weight lie on the same vertical, provided, obviously, that the longitudinal axis of the moving object is horizontal and that the heel is zero.

The friction in the gimbals axles will be neglected; this assumption is admissible for this type of device.

When the object turns, its various points have different velocities whose directions in general do not coincide with the longitudinal axis of the object. It will be assumed that there is no drift, so that the direction of the linear velocity of the point where the heel equalizer is located is along the axis of the moving object whenever the latter turns. The Earth's rotation will also be neglected.

150

The equations describing the motion of the heel equalizer will now be established. The following five Cartesian frames, with origins at the gimbals center, will be adopted:

1. The coordinate system $\xi^0\eta^0\zeta^0$ (Figure 136). The ζ^0-axis is directed vertically upward, and the η^0-axis is parallel to the longitudinal axis of the object and directed toward the side opposed to the object's motion (the object's trim is assumed to be zero). This coordinate system is carried by the moving object. Its angular velocity relative to the Earth is equal to the angular velocity ω of the object, the vector being directed along the ζ^0-axis.

It will be assumed that $\omega > 0$ if the object turns to the left (counterclockwise when observed from above).

The rotation of the object causes the centrifugal force $\dfrac{P}{g}\,\omega V$ to act; for $\omega > 0$ it acts on the weight P in the negative direction of the ξ^0-axis.
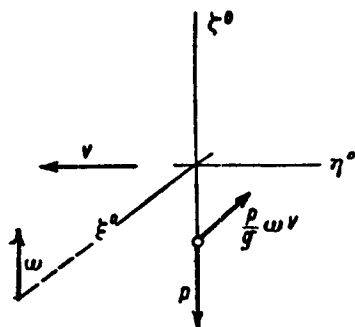

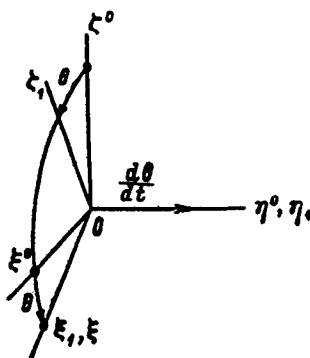FIGURE 136   FIGURE 137

The object's velocity varies during its maneuvers. The inertia force of the weight $\dfrac{P}{g}\,\dfrac{dV}{dt}$ is directed along the negative η^0-axis. It will be assumed that the effect of this force on the heel equalizer is small and can be neglected.

2. The coordinate system $\xi_1\eta_1\zeta_1$ fixed to the moving object (Figure 137). The η_1-axis coincides with the η^0-axis and is therefore parallel to the longitudinal axis of the object. The ζ_1-axis lies in its plane of symmetry.

The angle θ between the axes ζ_1 and ζ^0 is the heel angle of the object. For $\theta > 0$ the object has a heel to port*.

The direction cosines of the system $\xi_1\eta_1\zeta_1$ relative to the system $\xi^0\eta^0\zeta^0$ are:

	ξ^0	η^0	ζ^0	
ξ_1	$\cos\theta$	0	$-\sin\theta$	
η_1	0	1	0	(478)
ζ_1	$\sin\theta$	0	$\cos\theta$	

* This is in contrast to Chapter II, § 1. There the heel to starboard was considered as positive.

151

The angular velocity vector of the object's heel is directed along the $\eta^\bullet$-axis and is equal to $\frac{d\theta}{dt}$.

3. It is convenient to introduce the coordinate system $\xi\eta\zeta$ (Figure 138), also fixed to the object. The ξ-axis of this system coincides with the ξ_1-axis. The ζ-axis deviates from the ζ_1-axis toward the side opposed to the object's motion by the constant angle γ and coincides with the pivot axis z_1 of the gyro's outer gimbal ring (cf. below).

The direction cosines of the system $\xi\eta\zeta$ relative to the system $\xi_1\eta_1\zeta_1$ are:

	ξ_1	η_1	ζ_1
ξ	1	0	0
η	0	$\cos\gamma$	$-\sin\gamma$
ζ	0	$\sin\gamma$	$\cos\gamma$

$$(479)$$

From (478) and (479), the direction cosines of the system $\xi^0\eta^0\zeta^0$ relative to the system $\xi\eta\zeta$ are:

	ξ	η	ζ
ξ^0	$\cos\theta$	$-\sin\gamma\sin\theta$	$\cos\gamma\sin\theta$
η^0	0	$\cos\gamma$	$\sin\gamma$
ζ^0	$-\sin\theta$	$-\sin\gamma\cos\theta$	$\cos\gamma\cos\theta$

$$(480)$$

4. The system $x_1y_1z_1$ fixed to the outer gimbal ring (Figure 139). The z_1-axis is directed along the pivot axis of the outer gimbal ring and coincides with the ζ-axis. The y_1-axis has the same direction as the y-axis (cf. below).
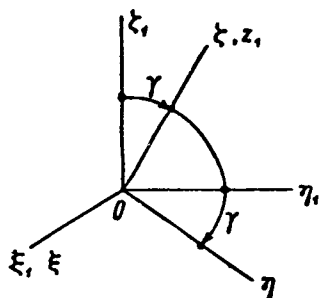

FIGURE 138
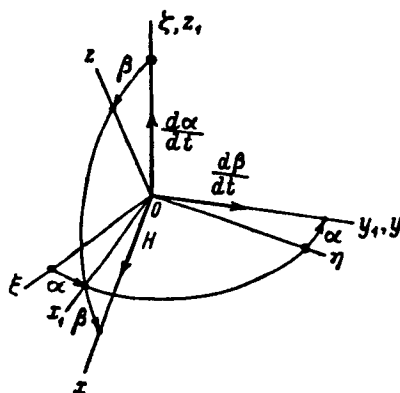
FIGURE 139

The angle of rotation about the z_1-axis of the coordinate system $x_1y_1z_1$ relative to the coordinate system $\xi\eta\zeta$ is denoted by α. This angle α thus defines the position of the outer gimbal ring relative to the instrument body. For $\alpha > 0$, the outer ring is rotated counterclockwise if viewed from above. The vector of the angular velocity of the outer ring relative to the body has the direction of the axis $\zeta(z_1)$ and is equal to $\frac{d\alpha}{dt}$.

152

For $a = 0$, the outer ring lies in the plane of symmetry of the moving object, and the coordinate systems $x_1 y_1 z_1$ and $\xi \eta \zeta$ coincide. In the general case $(a \neq 0)$, the cosines of the two systems are related as follows:

	ξ	η	ζ	
x_1	$\cos a$	$\sin a$	0	
y_1	$-\sin a$	$\cos a$	0	(481)
z_1	0	0	1	

5. Finally, we introduce the coordinate system xyz fixed to the inner gimbal ring (Figure 139). The y-axis, which coincides with the y_1-axis, is directed along the pivot axis of the inner ring. The x-axis is directed along the axis of rotation of the gyro rotor.

In the initial position the plane of the inner ring is perpendicular to the plane of the outer ring, and the xyz and $x_1 y_1 z_1$ coordinate systems coincide. In the general case, the inner ring tilts through an angle β from its initial position. The angle β is positive for counterclockwise tilting of the inner ring about the axis $y(y_1)$ (if viewed from the positive y-axis).

The vector of the angular velocity of the inner relative to the outer ring is directed along the y-axis and is equal to $\frac{d\beta}{dt}$.

The direction cosines of the system xyz relative to the system $x_1 y_1 z_1$ are:

	x_1	y_1	z_1	
x	$\cos \beta$	0	$-\sin \beta$	
y	0	1	0	(482)
z	$\sin \beta$	0	$\cos \beta$	

The direction cosines of the system xyz relative to the system $\xi \eta \zeta$ can now be obtained from (481) and (482):

	ξ	η	ζ	
x	$\cos a \cos \beta$	$\sin a \cos \beta$	$-\sin \beta$	
y	$-\sin a$	$\cos a$	0	(483)
z	$\cos a \sin \beta$	$\sin a \sin \beta$	$\cos \beta$	

It is important to know the direction cosines of the system xyz relative to the system $\xi^0 \eta^0 \zeta^0$; these are found from (480) and (483):

	ξ^0	η^0	ζ^0	
x	$\cos a \cos \beta \cos \theta -$ $- \sin a \cos \beta \sin \gamma \sin \theta -$ $- \sin \beta \cos \gamma \sin \theta$	$\sin a \cos \beta \cos \gamma -$ $- \sin \beta \sin \gamma$	$-\cos a \cos \beta \sin \theta -$ $- \sin a \cos \beta \sin \gamma \cos \theta -$ $- \sin \beta \cos \gamma \cos \theta$	
y	$-\sin a \cos \theta -$ $- \cos a \sin \gamma \sin \theta$	$\cos a \cos \gamma$	$\sin a \sin \theta -$ $- \cos a \sin \gamma \cos \theta$	(484)
z	$\cos a \sin \beta \cos \theta -$ $- \sin a \sin \beta \sin \gamma \sin \theta +$ $+ \cos \beta \cos \gamma \sin \theta$	$\sin a \sin \beta \cos \gamma +$ $+ \cos \beta \sin \gamma$	$-\cos a \sin \beta \sin \theta -$ $- \sin a \sin \beta \sin \gamma \cos \theta +$ $+ \cos \beta \cos \gamma \cos \theta$	

When the rotor rotates as assumed above (the velocities of its upper points are directed along the object's motion), the vector of the gyro rotor's angular momentum H is directed along the positive x-axis (Figures 139 and 140).

The coordinates of the center of gravity of the weight P attached to the inner gimbal ring are, in the xyz system (Figure 140):

$$x=0; \quad y=b; \quad z=-c. \tag{485}$$

In accordance with the theory of gyroscope precession, the equations of motion of the heel-equalizer gyro will be formed by using the theorem on the angular momentum of a system (§ 1 of this chapter).

We denote by p, q, and r the projections of the angular velocity of the frame xyz relative to the Earth. Neglecting the angular velocity of the Earth, and taking into account that the vector H, of constant magnitude, is invariably directed along the z-axis, the following expressions are obtained for the projections on the axes x, y, and z of the velocity of its end point [the components of the time derivative of H] (Figure 140):

$$\begin{aligned} M_x &= 0; \\ M_y &= rH; \\ M_z &= -qH. \end{aligned} \tag{486}$$

In accordance with the angular momentum theorem, the magnitudes M_x, M_y, and M_z represent here the sums of all the moments about the axes x, y, and z acting on the gyro rotor.
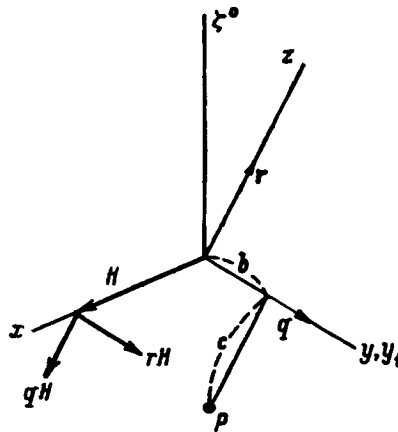

FIGURE 140

The angular velocity of the xyz frame is the vector sum of the angular velocities ω, $\frac{d\theta}{dt}$, $\frac{d\alpha}{dt}$, and $\frac{d\beta}{dt}$, directed along the axes ζ^0, η^0, ζ, and y respectively (cf. Figures 136, 137, and 139).

From (483) and (484), the following expressions are obtained for the projections q and r:

$$q = \omega\,(\sin\alpha\sin\theta - \cos\alpha\sin\gamma\cos\theta) + \frac{d\theta}{dt}\cos\alpha\cos\gamma + \frac{d\beta}{dt},$$

$$r = \omega(-\cos\alpha\sin\beta\sin\theta - \sin\alpha\sin\beta\sin\gamma\cos\theta + \cos\beta\cos\gamma\cos\theta) + \tag{487}$$

$$+ \frac{d\theta}{dt}(\sin\alpha\sin\beta\cos\gamma + \cos\beta\sin\gamma) + \frac{d\alpha}{dt}\cos\beta.$$

154

The angles α, β, and θ will be assumed to be small. Neglecting all terms of higher order than the first in these small magnitudes, (487) becomes

$$q = -\omega \sin \gamma + \frac{d\theta}{dt} \cos \gamma + \frac{d\beta}{dt},$$

$$r = \omega \cos \gamma + \frac{d\theta}{dt} \sin \gamma + \frac{d\alpha}{dt}. \qquad (488)$$

Equations (486) can therefore be written in the form

$$0 = M_x,$$

$$H\left(\omega \cos \gamma + \frac{d\theta}{dt} \sin \gamma + \frac{d\alpha}{dt}\right) = M_y, \qquad (489)$$

$$-H\left(-\omega \sin \gamma + \frac{d\theta}{dt} \cos \gamma + \frac{d\beta}{dt}\right) = M_z.$$

The forces acting on the gyro rotor of the heel equalizer that create the moments M_x, M_y, M_z, consist of the normal reactions of the bearings on the inner gimbal ring, the effect of friction in these bearings and of the rotor in the surrounding air, and the forces caused by the blasts from the nozzles, which tilt the rotor relative to the inner gimbal ring.

The moment M_x is zero at constant angular velocity of the rotor. It follows that the sum of moments about the x-axis due to friction in the bearings of the rotor shaft, the air blast driving the rotor, and the aerodynamic resistance to its rotation is zero.

The normal reactions of the bearings create the moments M_y and M_z, which have to be determined.

Consider now the forces applied to the inner gimbal ring. These forces must balance each other, since the inertia of the mass of the two gimbal rings is not taken into account in the theory of gyroscope precession.
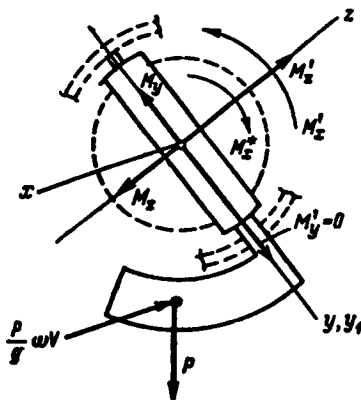

FIGURE 141

The forces and moments which must be taken into account are the normal pressure of the rotor on the bearings in the inner ring which causes moments $-M_y$ and $-M_z$, the moments due to gravity acting on the weight P secured to the inner gimbal ring, the moments due to the centrifugal

force $\dfrac{P}{g}\,\omega V$ acting on this weight during rotation, and the moments due to the reactions M'_x, M'_y, M'_z of the bearings in the outer gimbal ring (Figure 141). The moments due to the reactions of the air jets, the moments caused by friction during the rotations of the rotor in its bearings, and those due to the effect on the inner gimbal ring of the surrounding air that is caused to circulate by the gyro rotor, all act about the x-axis (the rotor axis). The resultant moment $-M^{\bullet}_x$ is generally not zero, since the rotor and the inner gimbal ring are not enclosed in an air-tight casing, so that not all braking forces acting on the rotor originate in the inner gimbal ring.

It follows that the moment $-M^{\bullet}_x$ should be considered as negative, its vector pointing in a direction opposed to that of the angular momentum H (or, which in the same, opposed to that of the rotor's rotational velocity).

The following equilibrium equations of the inner ring are thus obtained:

$$-M^{\bullet}_x + M'_s + mom_s P + mom_s\,\frac{P}{g}\,\omega V = 0;$$

$$-M_y + M'_y + mom_y P + mom_y\,\frac{P}{g}\,\omega V = 0;$$

$$-M_z + M'_z + mom_z P + mom_z\,\frac{P}{g}\,\omega V = 0.$$

(490)

If the moment due to the friction between the inner-ring pivot and the bearings on the outer ring is neglected, then

$$M'_y = 0.$$

(491)

If the moment of inertia of the outer ring referred to its axis of rotation $z_1\,(\zeta)$ is neglected, all the forces acting on it are in equilibrium. It follows that the sum of all the moments about the z_1-axis acting on the outer gimbal ring must be zero.

If friction in the bearings of the outer-ring pivots is neglected, the moments about the outer-ring pivot axis (Figure 142) are due to the action of
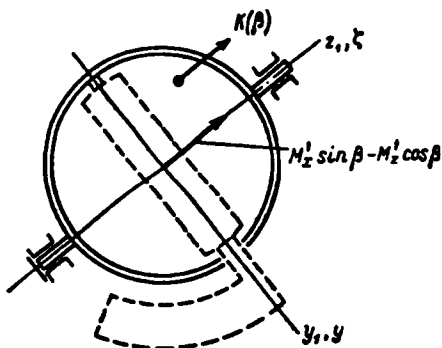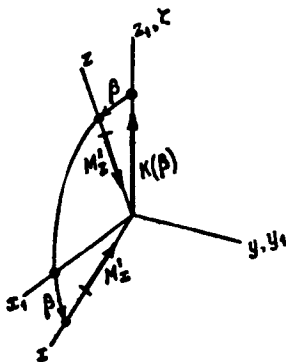

FIGURE 142

FIGURE 143

the inner on the outer ring and to the correcting moment $K(\beta)$ (see below). The former are the moments $-M'_x$ and $-M'_z$. The sum of the projections of these moments on the z_1-axis is (Figure 143):

$$M'_x \sin\beta - M'_z \cos\beta.$$

Therefore

$$K(\beta) + M'_s \sin\beta - M'_z \cos\beta = 0, \tag{492}$$

whence

$$M'_z = M'_s \operatorname{tg}\beta + \frac{K(\beta)}{\cos\beta} \tag{493}$$

or, by the first of equations (490)

$$M'_s = \left(M^\bullet_z - mom_s P - mom_s \frac{P}{g}\omega V\right)\operatorname{tg}\beta + \frac{K(\beta)}{\cos\beta}. \tag{494}$$

Inserting (491) into the second, and (494) into the third of equations (490) yields

$$M_y = mom_y P + mom_y \frac{P}{g}\omega V,$$

$$M_z = mom_z P + mom_z \frac{P}{g}\omega V + \tag{495}$$

$$+ \left(M^\bullet_z - mom_s P - mom_s \frac{P}{g}\omega V\right)\operatorname{tg}\beta + \frac{K(\beta)}{\cos\beta}.$$

Inserting (495) into the second and third of equations (489)

$$H\left(\omega\cos\gamma + \frac{d\theta}{dt}\sin\gamma + \frac{d\alpha}{dt}\right) = mom_y P + mom_y \frac{P}{g}\omega V;$$

$$-H\left(-\omega\sin\gamma + \frac{d\theta}{dt}\cos\gamma + \frac{d\beta}{dt}\right) = mom_z P + mom_z \frac{P}{g}\omega V + \tag{496}$$

$$+ \left(M^\bullet_z - mom_s P - mom_s \frac{P}{g}\omega V\right)\operatorname{tg}\beta + \frac{K(\beta)}{\cos\beta}.$$

The moments about the axes x, y, and z due to gravity and the centrifugal force are:

$$mom_s P = yP_s - zP_y;$$
$$mom_y P = zP_s - xP_s;$$
$$mom_z P = xP_y - yP_s;$$
$$mom_s\left(\frac{P}{g}\omega V\right) = y\left(\frac{P}{g}\omega V\right)_z - z\left(\frac{P}{g}\omega V\right)_y; \tag{497}$$
$$mom_y\left(\frac{P}{g}\omega V\right) = z\left(\frac{P}{g}\omega V\right)_s - x\left(\frac{P}{g}\omega V\right)_z;$$
$$mom_z\left(\frac{P}{g}\omega V\right) = x\left(\frac{P}{g}\omega V\right)_y - y\left(\frac{P}{g}\omega V\right)_s.$$

The coordinates x, y, and z of the center of gravity of the weight P, are given by (485).

The force P is directed along the negative ζ^0-axis, and the centrifugal inertia force $\frac{P}{g}\omega V$ along the negative ξ^0-axis.

From (484) the projections of these forces on the axes x, y, and z are:

$$P_s = -P\left(-\cos\alpha\cos\beta\sin\theta - \sin\alpha\cos\beta\sin\gamma\cos\theta - \right.$$
$$\left. - \sin\beta\cos\gamma\cos\theta\right);$$
$$P_y = -P\left(\sin\alpha\sin\theta - \cos\alpha\sin\gamma\cos\theta\right); \tag{498}$$
$$P_r = -P\left(-\cos\alpha\sin\beta\sin\theta - \sin\alpha\sin\beta\sin\gamma\cos\theta + \right.$$
$$\left. + \cos\beta\cos\gamma\cos\theta\right);$$

$$\left(\frac{P}{g}\,\omega V\right)_x = -\frac{P}{g}\,\omega V\,(\cos\alpha\,\cos\beta\,\cos\theta -$$
$$- \sin\alpha\,\cos\beta\,\sin\gamma\,\sin\theta - \sin\beta\,\cos\gamma\,\sin\theta);$$

$$\left(\frac{P}{g}\,\omega V\right)_y = -\frac{P}{g}\,\omega V\,(-\sin\alpha\,\cos\theta - \cos\alpha\,\sin\gamma\,\sin\theta); \qquad (498)$$

$$\left(\frac{P}{g}\,\omega V\right)_z = -\frac{P}{g}\,\omega V\,(\cos\alpha\,\sin\beta\,\cos\theta -$$
$$- \sin\alpha\,\sin\beta\,\sin\gamma\,\sin\theta + \cos\beta\,\cos\gamma\,\sin\theta).$$

If the angles α, β, and θ are small,

$$P_x = P\,(\theta + \alpha\,\sin\gamma + \beta\,\cos\gamma)$$
$$P_y = P\,\sin\gamma,$$
$$P_z = -P\,\cos\gamma,$$
$$\left(\frac{P}{g}\,\omega V\right)_x = -\frac{P}{g}\,\omega V, \qquad (499)$$
$$\left(\frac{P}{g}\,\omega V\right)_y = \frac{P}{g}\,\omega V\,(\alpha + \theta\,\sin\gamma),$$
$$\left(\frac{P}{g}\,\omega V\right)_z = -\frac{P}{g}\,\omega V\,(\beta + \theta\,\cos\gamma).$$

Inserting (499) and (485) into (497), we obtain

$$mom_x P = (-b\,\cos\gamma + c\,\sin\gamma)\,P,$$
$$mom_y P = -c\,(\theta + \alpha\,\sin\gamma + \beta\,\cos\gamma)\,P,$$
$$mom_z P = -b\,(\theta + \alpha\,\sin\gamma + \beta\,\cos\gamma)\,P,$$
$$mom_x \frac{P}{g}\,\omega V = [-b\,(\beta + \theta\,\cos\gamma) + c\,(\alpha + \theta\,\sin\gamma)]\,\frac{P}{g}\,\omega V, \qquad (500)$$
$$mom_y \frac{P}{g}\,\omega V = c\,\frac{P}{g}\,\omega V,$$
$$mom_z \frac{P}{g}\,\omega V = b\,\frac{P}{g}\,\omega V.$$

Inserting (500) into (496):

$$H\left(\omega\,\cos\gamma + \frac{d\theta}{dt}\,\sin\gamma + \frac{d\alpha}{dt}\right) =$$
$$= -c\,(\theta + \alpha\,\sin\gamma + \beta\,\cos\gamma)\,P + c\,\frac{P}{g}\,\omega V,$$

$$-H\left(-\omega\,\sin\gamma + \frac{d\theta}{dt}\,\cos\gamma + \frac{d\beta}{dt}\right) = -b\,(\theta + \alpha\,\sin\gamma + \beta\,\cos\gamma)\,P + \qquad (501)$$
$$+ b\,\frac{P}{g}\,\omega V + \left\{ M_a^* - (-b\,\cos\gamma + c\,\sin\gamma)\,P - \right.$$
$$\left. - [-b\,(\beta + \theta\,\cos\gamma) + c\,(\alpha + \theta\,\sin\gamma)]\,\frac{P}{g}\,\omega V \right\}\,tg\,\beta + \frac{K(\beta)}{\cos\beta}$$

Neglecting all terms of higher order than the first in α, β, θ, this becomes

$$H\left(\frac{d\theta}{dt}\,\sin\gamma + \frac{d\alpha}{dt}\right) = -c\,(\theta + \alpha\,\sin\gamma + \beta\,\cos\gamma)\,P +$$
$$+ c\,\frac{P}{g}\,\omega V - H\omega\,\cos\gamma, \qquad (502)$$

$$H\left(\frac{d\theta}{dt}\cos\gamma+\frac{d\beta}{dt}\right)=[b(\theta+\alpha\sin\gamma)+c\beta\sin\gamma]P-$$
$$-b\frac{P}{g}\omega V+H\omega\sin\gamma-M_{\alpha}^{\bullet}\beta-K(\beta). \tag{502}$$

This is a system of two differential equations with three unknown functions of time: θ, α, and β. A third equation is given by the rotation of the object about its longitudinal axis:

$$I\frac{d^2\theta}{dt^2}=-D\frac{d\theta}{dt}+M(\alpha), \tag{503}$$

where I is the moment of inertia of the object about its longitudinal axis, $D\frac{d\theta}{dt}$ is the moment due to resistance of the medium to the object's rotation (assumed to be proportional to the rate of variation of the heel angle $\frac{d\theta}{dt}$), and $M(\alpha)$ is the heel-equalizing moment applied to the object by the control system.

Strictly speaking, the moment $M(\alpha)$ is connected with the angle α (the angle between the plane of the outer ring and the object's plane of symmetry) by a more complex relationship; this allows for the action of the control system.

In accordance with the discussion at the beginning of this section, equation (503) will be replaced by the simplified approximate condition of servomotor constraints:

$$\alpha\equiv 0. \tag{504}$$

The physical meaning of (504) is that the object assumes instantaneously the heel specified by the heel equalizer. The motion of the heel-equalizer gyro system is obviously incomparably slower than the rotation of the object about its longitudinal axis.

Inserting (504) into (502) yields

$$H\frac{d\theta}{dt}\sin\gamma=-c(\theta+\beta\cos\gamma)P+\left(c\frac{P}{g}V-H\cos\gamma\right)\omega,$$
$$H\left(\frac{d\theta}{dt}\cos\gamma+\frac{d\beta}{dt}\right)=(b\theta+c\beta\sin\gamma)P- \tag{505}$$
$$-\left(b\frac{P}{g}V-H\sin\gamma\right)\omega-M_{\alpha}^{\bullet}\beta-K(\beta).$$

The terms containing the angular velocity ω represent the perturbation forces acting on the heel equalizer when the moving object turns. They are zero when the following two conditions are simultaneously satisfied:

$$c\frac{P}{g}V=H\cos\gamma, \qquad b\frac{P}{g}V=H\sin\gamma \tag{506}$$

or

$$b=c\,\text{tg}\,\gamma,$$
$$H=\frac{cP}{g\cos\gamma}V. \tag{507}$$

It is easily seen that this method of eliminating the influence of turning is similar to the methods employed in §§ 2 and 3 of this chapter.

The first of conditions (507) is identical with (477), and means that the center of gravity of weight P should be on the same vertical as the gimbals center when heel and trim of the moving object are zero.

The second of conditions (507) means that the angular momentum H of the gyro must be proportional to the linear velocity of the object V. Since the linear velocity of the object varies during turns, the second of conditions (507) can be satisfied only approximately, a mean value of the linear velocity being assumed.

When conditions (507) are satisfied, (505) becomes:

$$H \frac{d\theta}{dt} \sin \gamma = -cP(\theta + \beta \cos \gamma),$$

$$H \left(\frac{d\theta}{dt} \cos \gamma + \frac{d\beta}{dt} \right) = cP(\theta + \beta \cos \gamma) \, tg \, \gamma - M_z^\bullet \beta - K(\beta). \tag{508}$$

In addition, $M_z^\bullet \beta$ can be neglected since its magnitude is considerably less than that of the correcting moment $K(\beta)$.

The case when β is small will be examined first, and expression (476) for $K(\beta)$ will be assumed to be valid. The following equations are then obtained:

$$\frac{H \sin \gamma}{cP} \frac{d\theta}{dt} = -(\theta + \beta \cos \gamma),$$

$$\frac{H}{cP} \left(\frac{d\theta}{dt} \cos \gamma + \frac{d\beta}{dt} \right) = (\theta + \beta \cos \gamma) \, tg \, \gamma - \frac{k}{cP} \beta. \tag{509}$$

To simplify (509), we introduce the dimensionless time

$$\tau = \frac{cP}{H \sin \gamma} t. \tag{510}$$

Then

$$\frac{d\theta}{dt} = \frac{d\theta}{d\tau} \frac{d\tau}{dt} = \frac{cP}{H \sin \gamma} \frac{d\theta}{d\tau}, \quad \frac{d\beta}{dt} = \frac{cP}{H \sin \gamma} \frac{d\beta}{d\tau}. \tag{511}$$

Inserting (511) into (509) gives

$$\frac{d\theta}{d\tau} = -(\theta + \beta \cos \gamma),$$

$$\frac{d\theta}{d\tau} \cos \gamma + \frac{d\beta}{d\tau} = (\theta + \beta \cos \gamma) \frac{\sin^2 \gamma}{\cos \gamma} - \frac{k \sin \gamma}{cP} \beta. \tag{512}$$

We multiply the first of equations (512) by $\cos \gamma$ and add it to the second,

$$\frac{d\beta}{d\tau} = \frac{1}{\cos \gamma} (\theta + \beta \cos \gamma) - \frac{k \sin \gamma}{cP} \beta, \tag{513}$$

and define a new variable

$$\varphi = \beta \cos \gamma. \tag{514}$$

The differential equations (512) then become:

$$\frac{d\theta}{d\tau} = -(\theta + \varphi);$$

$$\frac{d\varphi}{d\tau} = \theta + \varphi - \varkappa \varphi, \tag{515}$$

where

$$\varkappa = \frac{k \sin \gamma}{cP}. \tag{516}$$

System (515) is equivalent to the second-order differential equation

$$\frac{d^2\theta}{d\tau^2} + \varkappa\frac{d\theta}{d\tau} + \varkappa\theta = 0,\tag{517}$$

which is obtained by eliminating the variable φ from the second of equations (515) by means of the substitution

$$\varphi = -\left(\frac{d\theta}{d\tau} + \theta\right),\tag{518}$$

obtained from the first of equations (515).

The general solution of equation (517) is

$$\theta = e^{-\frac{\varkappa}{2}\tau}\left(\theta_0\cos\nu\tau + \frac{2\theta_0' + \varkappa\theta_0}{2\nu}\sin\nu\tau\right).\tag{519}$$

Here θ_0 and θ_0' are the values of θ and $\frac{d\theta}{d\tau}$ for $(\tau = 0)$ and

$$\nu = \frac{1}{2}\sqrt{\varkappa(4 - \varkappa)}.\tag{520}$$

We assume that the inner and outer gimbal rings are freed from the locking device at the instant the heel-equalizer gyro is started, i.e., that

$$\theta_0 \neq 0, \quad \varphi_0 = \beta_0\cos\gamma = 0,\tag{521}$$

where θ_0 is the heel of the moving object at $\tau = 0$.

Thus, from the first of equations (515),

$$\theta_0' = -\theta_0,\tag{522}$$

and (519) becomes

$$\theta = \theta_0 e^{-\frac{\varkappa}{2}\tau}\left(\cos\nu\tau + \frac{\varkappa - 2}{2\nu}\sin\nu\tau\right).\tag{523}$$

From (518) we obtain

$$\varphi = \beta\cos\gamma = \theta_0 e^{-\frac{\varkappa}{2}\tau}\frac{\sin\nu\tau}{\nu}.\tag{524}$$

If $\varkappa < 4$, the parameter ν is real in accordance with (520). In this case (523) and (524) determine the motion of a point S along a spiral approaching the origin of the $\varphi\theta$ plane asymptotically (Figure 144).

The time derivatives of φ and θ are obtained from (515) or by direct differentiation of (523) and (524):

$$\frac{d\varphi}{d\tau} = \theta_0 e^{-\frac{\varkappa}{2}\tau}\left(\cos\nu\tau - \frac{\varkappa}{2\nu}\sin\nu\tau\right);$$
$$\frac{d\theta}{d\tau} = -\theta_0 e^{-\frac{\varkappa}{2}\tau}\left(\cos\nu\tau + \frac{\varkappa}{2\nu}\sin\nu\tau\right).\tag{525}$$

The instants at which φ and θ have maximum magnitudes are obtained by equating the corresponding derivatives to zero. φ, and thus the angle β, is a maximum at instants τ_1 which are roots of the equation

$$\text{tg }\nu\tau_1 = \frac{2\nu}{\varkappa}.\tag{526}$$

The heel angle θ is a maximum at instants τ_2 which satisfy the equation

$$\text{tg }\nu\tau_2 = -\frac{2\nu}{\varkappa}.\tag{527}$$

Each successive maximum of the magnitude of θ (and also of φ) is less than the preceding one by a factor N, where N is given by

$$N = e^{\frac{\pi x}{2v}}.$$

(528)

The dimensionless time interval between successive maxima is

$$\tau_0 = \frac{\pi}{v}.$$

(529)

The corresponding time interval is, by (510),
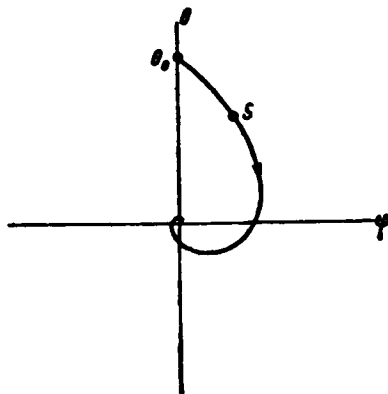
$$t_0 = \frac{H \sin \gamma}{cP}\, \tau_0.$$

(530)

FIGURE 144

Numerical example. Assume that $H = 6420$ gcm sec, $P = 495$ g, $c = 3.7$ cm, $\gamma = 48°$, $k = 3440$ gcm, $\theta_0 = 0.209$ (12°) and $\varphi_0 = 0$. By (510), (514), (516), (520), and (528)—(530);

$$t = \frac{H \sin \gamma}{cP}\, \tau = 2.60 \tau \text{ sec}; \qquad \varphi = \beta \cos \gamma = 0.669\,\beta;$$

$$x = \frac{k \sin \gamma}{cP} = 1.400; \qquad v = \frac{1}{2}\sqrt{x(4-x)} = 0.954;$$

$$\tau_0 = \frac{\pi}{v} = 3.29\,(8.55 \text{ sec}); \qquad N = e^{\frac{\pi x}{2v}} = 9.97.$$

The heel angle decreases to about one tenth during 8.55 sec, while the angle β, which is proportional to φ, becomes again zero.

Equations (526) and (527) yield in this case

$$\text{tg } v\tau_1 = \frac{2v}{x} = 1.363 \quad \text{and} \quad \text{tg } v\tau_2 = -\frac{2v}{x} = -1.363.$$

Their least roots are

$$\tau_1 = 0.984\,(2.56 \text{ sec}), \qquad \tau_2 = 2.31\,(6.00 \text{ sec}).$$

φ is a maximum at $\tau = \tau_1$. The value of this maximum is, by (524),

$$\varphi_1 = 0.423\,\theta_0 = 0.0885 \quad \text{and} \quad \beta_1 = \frac{\varphi_1}{\cos \gamma} = 0.1320\,(7°33').$$

The corresponding value of the heel angle θ_1 is found from (523) or from

the second differential equation (515)

$$\theta_1 = 0.169\,\theta_0 = 0.0353\,(2°\,1').$$

If $\tau = \tau_2$, the heel angle θ is a minimum, its magnitude being a maximum. The corresponding values of θ and φ are, by (523) and (524),

$$\theta_2 = -\,0.169\,\theta_0 = -\,0.0353\,(2°.1'); \quad \varphi_2 = 0.169\,\theta_0 = 0.0353 = -\,\theta_2.$$

The variation of θ and φ is shown in Figures 145 and 146.
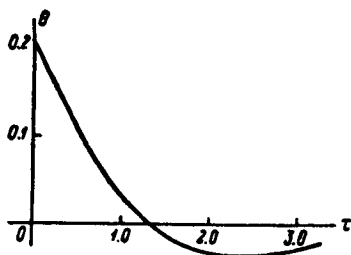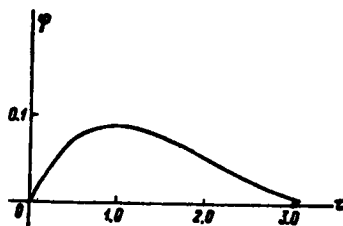

FIGURE 145   FIGURE 146

In the general case, for arbitrary initial values $\theta = \theta_0$ and $\varphi = \varphi_0$ at $\tau = 0$, the solution of equations (515) is

$$\varphi = e^{-\frac{x}{2}\tau}\left[\varphi_0 \cos v\tau - \frac{(x-2)\,\varphi_0 - 2\theta_0}{2v}\sin v\tau\right],$$

$$\theta = e^{-\frac{x}{2}\tau}\left[\theta_0 \cos v\tau + \frac{(x-2)\,\theta_0 - 2\varphi_0}{2v}\sin v\tau\right]. \tag{531}$$

In this case the motion of point S on the $\varphi\theta$ plane has the same spiral pattern as in the motion described by (523) and (524).

If $x > 4$, the value of v is imaginary in accordance with (520). The trigonometric functions in formulas (531) must in this case be replaced by hyperbolic functions:

$$\varphi = e^{-\frac{x}{2}\tau}\left[\varphi_0 \operatorname{ch}\mu\tau - \frac{(x-2)\,\varphi_0 - 2\theta_0}{2\mu}\operatorname{sh}\mu\tau\right],$$

$$\theta = e^{-\frac{x}{2}\tau}\left[\theta_0 \operatorname{ch}\mu\tau + \frac{(x-2)\,\theta_0 - 2\varphi_0}{2\mu}\operatorname{sh}\mu\tau\right], \tag{532}$$

where the parameter μ is given by

$$\mu = \frac{1}{2}\sqrt{x\,(x-4)}. \tag{533}$$

The trajectories of the point S corresponding to (532) are shown in Figure 147. In each of them the point S approaches the origin asymptotically. All trajectories are tangential to the straight line

$$\theta = \lambda_1\varphi, \qquad \lambda_1 = \frac{x}{2} - 1 + \frac{1}{2}\sqrt{x\,(x-4)}, \tag{534}$$

which is itself a trajectory.

The only exception is the straight line (Figure 147):

$$\theta = \lambda_2\varphi, \qquad \lambda_2 = \frac{x}{2} - 1 - \frac{1}{2}\sqrt{x\,(x-4)}. \tag{535}$$

163

This follows directly by analyzing the differential equation

$$\frac{d\theta}{d\varphi} = -\frac{\theta + \varphi}{\theta + (1 - \varkappa)\varphi},$$ (536)

which can be derived from the system of equations (515). Equation (536) has a particular form of an equation studied in the theory of differential equations (case of a mode). The slopes of the straight lines (534) and (535) are roots of the equation

$$\lambda^2 + (2 - \varkappa)\lambda + 1 = 0.$$ (537)

The equations of motion of the gyroscopic heel equalizer will now be solved for the case when the function $K(\beta)$ has the form of a broken line (see Figure 135).
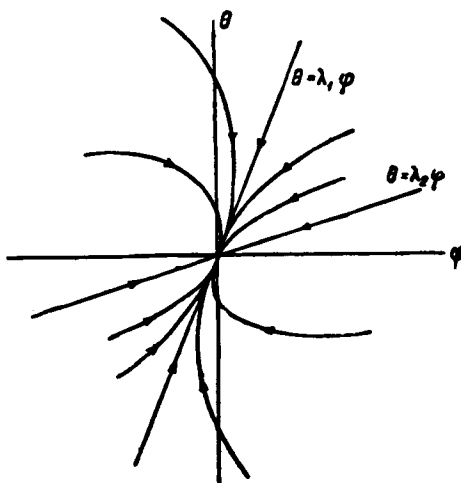

FIGURE 147

In this case by neglecting again the term $M_{zz}^{*}\beta$ in comparison with the corrective moment $K(\beta)$ in (508) and by carrying out similar transformations, we obtain the following equations instead of (515):

$$\frac{d\theta}{d\tau} = -(\theta + \varphi),$$

$$\frac{d\varphi}{d\tau} = \theta + \varphi - m(\varphi),$$ (538)

where $m(\varphi)$ is a function related to $K(\beta)$ by the relationship:

$$m(\varphi) = \frac{K(\beta)}{cP}\cos\gamma\sin\gamma, \qquad \varphi = \beta\cos\gamma.$$ (539)

The curve of $m(\varphi)$ differs only in scale from the curve of $K(\beta)$ (Figure 135).

Let the initial conditions be $\varphi_0 = 0$ and $\theta_0 > 0$, as before. The motion of the heel equalizer will in this case be described at the beginning by the same linear differential equations (515). The solution of these equations is given by (523) and (524).

When φ exceeds φ^{*}, the function $m(\varphi)$ becomes constant and equal to m in accordance with Figure 148. When this happens, the ensuing variations

of φ and θ are described by the equations

$$\frac{d\theta}{d\tau} = -(\theta + \varphi),$$

$$\frac{d\varphi}{d\tau} = \theta + \varphi - m, \tag{540}$$

the initial values being $\varphi = \varphi^*$, $\theta = \theta^*$. The symbol θ^* denotes the magnitude of θ at the instant at which φ attains the value φ^* in accordance with formula (524). The following inequality must be satisfied at this moment:

$$\frac{d\varphi}{d\tau} = \theta^* + \varphi^* - \varkappa\varphi^* > 0, \ (\varkappa\varphi^* = m), \tag{541}$$

since otherwise φ will decrease after this instant, as can easily be shown, and the differential equations (515) will remain valid.

In fact, for $\varphi = \varphi^*$, let

$$\frac{d\varphi}{d\tau} = 0. \tag{542}$$

The subsequent variation of φ is then determined by its second derivative.
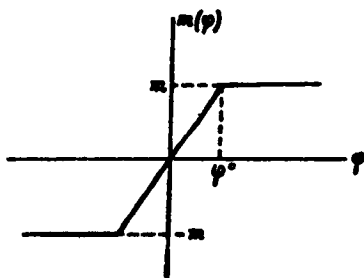
FIGURE 148

By the second equation (515):

$$\theta = \frac{d\varphi}{d\tau} + (\varkappa - 1)\varphi. \tag{543}$$

Inserting (543) into the first of equations (515) gives:

$$\frac{d^2\varphi}{d\tau^2} = -\varkappa\frac{d\varphi}{d\tau} - \varkappa\varphi. \tag{544}$$

Since $\frac{d\varphi}{d\tau} = 0$ and $\varphi = \varphi^* > 0$ by hypothesis, it follows that

$$\frac{d^2\varphi}{d\tau^2} < 0, \tag{545}$$

which means that φ will decrease.

Let inequality (541) be satisfied, so that equations (540) apply. A general solution for any initial conditions of φ and θ is easily obtained. In fact, adding both of equations (540) yields

$$\frac{d\theta}{d\tau} + \frac{d\varphi}{d\tau} = -m, \tag{546}$$

whence

$$\theta + \varphi = -m\tau + \text{const.} \tag{547}$$

We define another zero time so that $\varphi = \varphi^*$, and $\theta = \theta^*$ for $\tau = 0$. The constant in (547) can be found from these initial conditions, and (547)

165

becomes

$$\theta + \varphi = -m\tau + \theta^* + \varphi^*. \tag{548}$$

From the first of equations (540) it follows that

$$\frac{d\theta}{d\tau} = m\tau - (\theta^* + \varphi^*), \tag{549}$$

which after integration yields

$$\theta = \frac{m\tau^2}{2} - (\theta^* + \varphi^*)\,\tau + \text{const.} \tag{550}$$

The constant is again found from the initial condition $\theta = \theta^*$ for $\tau = 0$. Equations (550) and (548) can then be written in the form

$$\theta = \frac{m\tau^2}{2} - (\theta^* + \varphi^*)\tau + \theta^*,$$
$$\varphi = -\frac{m\tau^2}{2} + (\theta^* + \varphi^* - m)\tau + \varphi^*. \tag{551}$$

It is easily seen (cf. Chapter V, § 1) that equations (551) correspond to a motion of the point S along a parabola in the $\varphi\theta$ phase plane.

Differentiating the second of equations (551) gives:

$$\frac{d\varphi}{d\tau} = -m\tau + \theta^* + \varphi^* - m. \tag{552}$$

This derivative is zero at the instant

$$\tau_1 = \frac{\theta^* + \varphi^* - m}{m}, \tag{553}$$

at which φ attains its maximum

$$\varphi_1 = \frac{1}{2m}(\theta^* + \varphi^* - m)^2 + \varphi^*. \tag{554}$$

At this instant the heel angle θ is

$$\theta_1 = \frac{m}{2} - \frac{(\theta^* + \varphi^*)^2}{2m} + \theta^* \tag{555}$$

The derivative $\frac{d\theta}{d\tau}$ in (549) is zero at the instant

$$\tau_2 = \frac{\theta^* + \varphi^*}{m}, \tag{556}$$

at which the angle θ attains its extremum

$$\theta_2 = -\frac{1}{2m}(\theta^* + \varphi^*)^2 + \theta^*, \tag{557}$$

as follows from (551) and (556). The corresponding value of φ is

$$\varphi_2 = -\theta_2 = \frac{1}{2m}(\theta^* + \varphi^*)^2 - \theta^*. \tag{558}$$

It follows from inequality (541) and the second of equations (551) that φ increases at the beginning (for small values of τ). It then decreases again because of the term $-\frac{m\tau^2}{2}$. By inserting $\varphi = \varphi^*$ into the second of equations (551) the following quadratic equation is obtained:

$$-\frac{m\tau^2}{2} + (\theta^* + \varphi^* - m)\tau = 0. \tag{559}$$

166

The first root of this equation is $\tau = 0$; this gives the instant at which φ and θ begin to vary according to the differential equations (540); the second root is

$$\tau_a = \frac{2}{m}(\theta^* + \varphi^* - m) \tag{560}$$

which gives the instant after which the system of differential equations (540) no longer applies. We must then return to the system of differential equations (515) with suitably altered initial conditions, one of which is $\varphi = \varphi^*$. In order to find the initial condition for θ, (560) must be substituted into the first of equations (551); this yields

$$\theta = \theta_a = 2m - \theta^* - 2\varphi^*. \tag{561}$$

The following substitutions must therefore be made in (531):

$$\theta_0 = \theta_a \text{ and } \varphi_0 = \varphi^*. \tag{562}$$

A new time must also be chosen, and the variation of φ must again be found, since (531) is valid only for

$$|\varphi| < \varphi^*. \tag{563}$$

If φ attains the value $-\varphi^*$, then, in accordance with (538) and the curve of $m(\varphi)$ (Figure 148), the system of differential equations

$$\frac{d\theta}{d\tau} = -(\theta + \varphi),$$
$$\frac{d\varphi}{d\tau} = \theta + \varphi + m \tag{564}$$

must be solved under suitable initial conditions in order to find φ and θ.

It can be shown by carrying out the same operations as were used when (551) was derived that the solution of (564) is

$$\theta = -\frac{m\tau^2}{2} - (\theta^0 + \varphi^0)\tau + \theta^0,$$
$$\varphi = \frac{m\tau^2}{2} + (\theta^0 + \varphi^0 + m)\tau + \varphi_0, \tag{565}$$

where $\varphi^0 = -\varphi^*$ and θ^0 are the initial values of φ and θ; the time τ is measured from a new zero.

Equations (565) describe parabolic trajectories of the points S in the $\varphi\theta$ plane.

They are valid as long as φ does not again become equal to $-\varphi^*$; after this equations (515) must be reapplied.

Numerical example. As in the preceding example (cf. p. 162) we assume that

$$x = 1.400; \quad \nu = 0.954; \quad \gamma = 48°; \quad t = 2.6\tau,$$

and let the initial heel of the object be $\theta_0 = 0.209$ (12°) and the initial angle of deviation of the inner gimbal ring from its mean position $\varphi_0 = 0$. We also assume that $\varphi^* = 0.0585$. This corresponds to $\beta^* = 5$ (Figure 135), and

$$m = x\varphi^* = 0.0819.$$

For $0 < \varphi < 0.0585$, φ and θ will vary according to (523) and (524).

167

The following numerical values are obtained:

τ	φ	θ
0.00	0.0000	0.209
0.10	0.0195	0.188
0.20	0.0363	0.168
0.30	0.0500	0.147
0.37	0.0585	0.134

The system of differential equations (515) is valid for $0 < \tau^* \leqslant 0.37$ (0.96 sec) after which system (540) applies. The initial conditions are

$$\varphi^* = 0.0585, \quad \theta^* = 0.134.$$

Formulas (551) then give θ and φ. The dimensionless time τ is measured from a new zero.

Applying (551) the following values are obtained:

τ	φ	θ
0.0	0 0585	0.134
0 4	0.0962	0.063
0.8	0.1208	0.006
1.2	0.1322	—0.038
1.6	0.1307	—0.069
2.0	0.1159	—0.087
2.4	0.0880	—0.092
2.7	0.0585	—0.087

According to (553) φ attains its maximum at the instant

$$\tau_1 = 1.35 \; (3.51 \text{ sec})$$

when, by (554),

$$\varphi_1 = 0.1334.$$

The maximum deviation of the inner gimbal ring from its mean position is

$$\beta_1 = \frac{\varphi_1}{\cos \gamma} = 0.1995 \; (11°26')$$

According to (556), the magnitude of heel θ will be a maximum at the instant

$$\tau_2 = 2.35 \; (6.12 \text{ sec})$$

when, by (557):

$$\theta_2 = -0.093 \; (5°20')$$

To check, we determine by (560) the instant at which φ again becomes equal to φ^*. This happens at

$$\tau_a = 2.70 \; (7.02 \text{ sec}).$$

The corresponding value of θ is found from (561):

$$\theta_a = -0.0874 \; (5°07').$$

The subsequent calculations of φ and θ must again be done by applying (515), taking as initial values in (531)

$$\varphi = 0.0585, \quad \theta = -0.0874.$$

The values obtained for φ and θ are as follows:

τ	φ	θ
0.0	0.0585	−0.0874
0.4	0.0204	−0.0708
0.8	−0.0047	−0.0495
1.2	−0.0183	−0.0289
1.6	−0.0230	−0.0123
2.0	−0.0218	−0.0008
2.4	−0.0174	0.0060
2.8	−0.0120	0.0088
3.2	−0.0069	0.0090
3.29	−0.0059	0.0087

In this case φ does not attain the value $-\varphi^*$. Therefore (531) remains valid for subsequent values of the dimensionless time. The trajectory corresponding to the values of θ and φ as given by these three tables is shown in Figure 149.
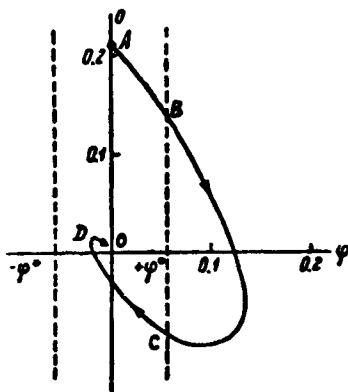

FIGURE 149

Point $A(0.000, 0.209)$ of this curve corresponds to the initial instant $\tau = 0$. Point $B(0.0585, 0.134)$ corresponds to $\tau^* = 0.37$ (0.96 sec). Point $C(0.0585, -0.874)$ corresponds to

$$\tau^* + \tau_a = 3.07 \ (7.99 \, \text{sec}).$$

Lastly, point $D(-0.0059, 0.0087)$ corresponds to

$$\tau^* + \tau_a + \tau_0 = 6.36 \ (16.5 \, \text{sec}).$$

The study of the heel-equalizer motion in the case when the function $K(\beta)$ has a more complex pattern is deferred to Chapter V, § 1, as mentioned at the beginning of this section.

§ 5. The gyroscopic frame

The gyroscopic frame with two gyros (Figure 150) is the basic element of many modern gyroscopic devices with so-called power stabilization.

169

In power stabilization the resistance to rotation of the sensing elements of the transmitting devices and the friction in the kinematic chains are directly taken up by the outer gimbal rings of the gyros. The corresponding moments cause the precession of the gyro to one or the other side from the initial position, this being the position at which the gyro rotor axis is perpendicular to the plane of the outer gimbal ring.

The stabilizing properties of the gyro decrease with increasing angle of deviation of the gyro housing from its initial position, until they vanish when the angle of deviation attains 90°. An electric motor, or some other (e.g., hydraulic) device is therefore used for power stabilization, applying to the outer gimbal ring a moment tending to reduce the angle of precession.
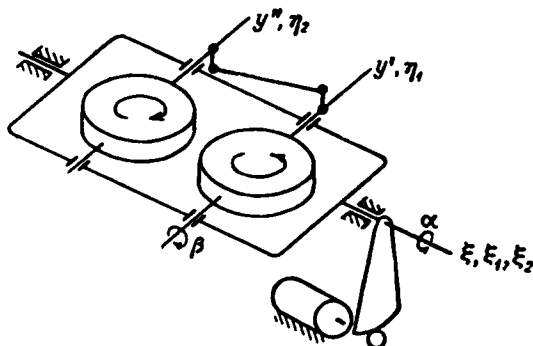

FIGURE 150

The stabilization motor is controlled by a sensing device mounted on the outer gimbal ring, which records the angles at which gyro housing is tilted relative to the outer ring.

Because of gyro precession, the angle of deviation increases when an external moment appears. As a result, an opposing moment acts on the motor shaft, unloading the gyro and stopping its precession. The stabilization motor thus carries out a "supplementary reciprocal aid" for the gyro (term proposed by N.N. Ostryakov).

The stabilization motor and the comparatively large masses fixed to the outer gimbal ring of the gyro are frequently responsible for free oscillations in power-stabilization systems which disturb the normal functioning of the device. Stability problems thus play a decisive part in these systems.

The gyroscopic systems proper of indirect (indicating) stabilization devices (such as were examined in §§ 2 and 3 of this chapter) are completely stable. The device as a whole may, however, be unstable because of free oscillations in the follow-up system.

Some questions of the stability of follow-up systems are examined in Chapter VI, § 7.

This section contains a linear treatment of the stability of gyroscopic frames. A nonlinear treatment of this problem, which takes into account the Coulomb friction, is given in Chapter V, § 2.

The gyroscopic frame can be considered as a system of two gyros whose outer gimbal rings have a common axis ξ—the so-called stabilization axis (Figure 151). The axes y' and y'' of the gyrohousings (or, which is the

same, of their inner gimbal rings) are connected by a four-bar linkage in such a way that they turn through equal and opposite angles (with an accuracy of up to high-order infinitesimals). The rotors of the two gyros rotate in opposite directions.

We now form by Lagrange's method the equations of motion of the gyroscopic frame.
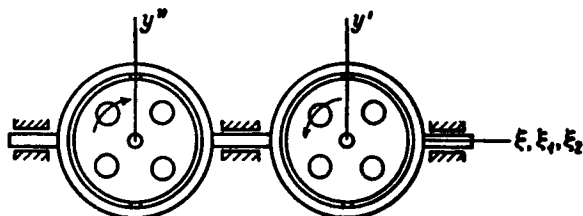

FIGURE 151

We introduce a coordinate system $\xi\eta\zeta$ fixed to the moving object and, as in § 1 of this chapter, denote by ω_ξ, ω_η, ω_ζ the projections of the angular velocity of this coordinate system on its own axes (Figure 152). The ξ-axis is
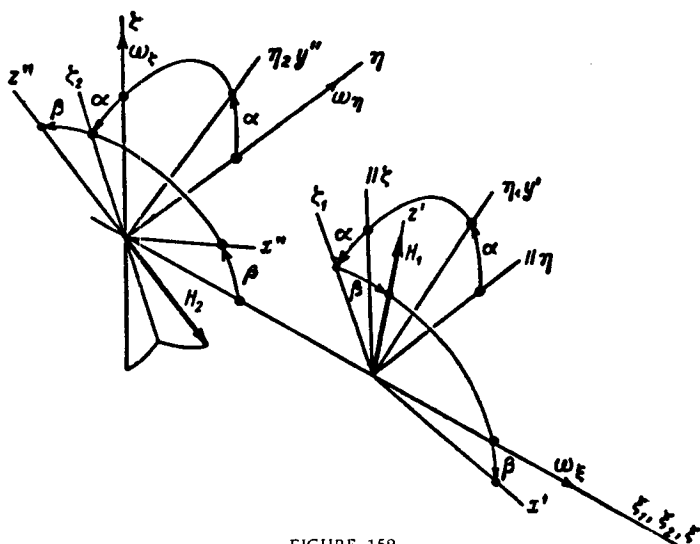

FIGURE 152

the pivot axis of the frame. In the frame itself two coordinate systems $\xi_1\eta_1\zeta_1$ and $\xi_2\eta_2\zeta_2$ are fixed, whose axes are respectively parallel. The ξ_1- and ξ_2-axes coincide with the ξ-axis, while the η_1- and η_2-axes are directed along the axes of the gyrohousings. The coordinate systems $x'y'z'$ and $x''y''z''$ are fixed to the housings, oriented in such a way that the y'-axis coincides with the η_1-axis and the y''-axis with the η_2-axis. The z'- and z''-axes are directed along the corresponding rotor axes.

We denote by α the rotation about the ξ-axis of the coordinate system $\xi_1\eta_1\zeta_1$, and thus also of the coordinate system $\xi_2\eta_2\zeta_2$, relative to the coordinate system $\xi\eta\zeta$ fixed to the moving object.

171

If the rotation about the η_1-axis of the system $x'y'z'$ relative to the co-ordinate system $\xi_1\eta_1\zeta_1$ (i.e., the tilting of the first gyro housing relative to the frame) is denoted by β, the corresponding angle of tilting of the second gyro relative to the frame will obviously be $-\beta$, due to the four-bar linkage.

To express the kinetic energy of the frame relative to a coordinate system having a translational motion (with origin at the gimbals center), we use (344), (349), and (352) obtained in § 1 of this chapter for a single gyro with similar arrangement of the axes.

The expressions for the kinetic energy of the housing and rotor of the second gyro can be obtained from (349) and (352) simply by replacing the letters β and γ by $-\beta$ and $-\gamma$ respectively. The energy of the entire system, including the kinetic energy of the motor, is then

$$T = \left(\tfrac{1}{2} I_{\xi_1} + I_{x'} \cos^2\beta + I_{z'} \sin^2\beta + A\cos^2\beta + C\sin^2\beta\right) \times$$

$$\times \left(\tfrac{da}{dt} + \omega_\xi\right)^2 + (I_{y'} + A)\left(\tfrac{d\beta}{dt}\right)^2 + C\left(\tfrac{d\gamma}{dt}\right)^2 +$$

$$+ 2C\tfrac{d\gamma}{dt}\left(\tfrac{da}{dt} + \omega_\xi\right)\sin\beta + \tfrac{1}{2}\Theta\left(-j\tfrac{da}{dt} + \omega_\xi\right)^2 +$$

$$+ \left(\tfrac{1}{2} I_{\eta_1} + I_{y'} + A\right)\left(\omega_\eta \cos a + \omega_\zeta \sin a\right)^2 + \tfrac{1}{2}\Theta'(\omega_\eta^2 + \omega_\xi^2) +$$

$$+ \left(\tfrac{1}{2} I_{\xi_1} + I_{x'}\sin^2\beta + I_{z'}\cos^2\beta + A\sin^2\beta + C\cos^2\beta\right) \times$$

$$\times \left(-\omega_\eta \sin a + \omega_\zeta \cos a\right)^2. \tag{566}$$

where, in addition to the notation used in § 1, Θ is the moment of inertia of the rotor and the gear, having a transmission ratio j of the power stabilization motor relative to its axis of rotation; Θ' is the moment of inertia of the rotor relative to the axis perpendicular to the axis of rotation.

Terms which do not contain generalized coordinates or velocities have been omitted from (566), since the equations of motion do not depend on them.

Inserting (566) into the Euler-Lagrange equations (354), the following second-order differential equations are obtained when all terms of higher order than the first in a and β and their time derivatives are neglected:

$$(I_{\xi_1} + 2I_{x'} + 2A)\left(\tfrac{d^2a}{dt^2} + \tfrac{d\omega_\xi}{dt}\right) + 2C\tfrac{d^2\gamma}{dt^2}\beta + 2C\tfrac{d\gamma}{dt}\tfrac{d\beta}{dt} +$$

$$+ (-I_{\xi_1} - 2I_{z'} - 2C + I_{\eta_1} + 2I_{y'} + 2A)(\omega_\eta^2 a - \omega_\eta \omega_\zeta - \omega_\zeta^2 a) +$$

$$+ j\Theta\left(j\tfrac{d^2a}{dt^2} - \tfrac{d\omega_\xi}{dt}\right) = M_\xi; \tag{567}$$

$$2(I_{y'} + A)\tfrac{d^2\beta}{dt^2} + 2\beta(I_{x'} - I_{z'} + A - C)(\omega_\xi^2 - \omega_\zeta^2) -$$

$$- 2C\tfrac{d\gamma}{dt}\left(\tfrac{da}{dt} + \omega_\xi\right) = M_{y'};$$

$$2C\tfrac{d^2\gamma}{dt^2} + 2C\tfrac{d(\beta\omega_\xi)}{dt} = M_{z'}.$$

These equations can be considerably simplified if it is assumed that the projections of the angular velocity of the frame ω_ξ, ω_η, ω_ζ are also small, and that the resultant moment M_z acting on the rotors* is zero. This gives

$$I\left(\frac{d^2\alpha}{dt^2}+\frac{d\omega_\xi}{dt}\right)+H\frac{d\beta}{dt}=M_\xi+j(j+1)\Theta\frac{d\omega_\xi}{dt},$$

$$B\frac{d^2\beta}{dt^2}-H\left(\frac{d\alpha}{dt}+\omega_\xi\right)=M_{y'}, \tag{568}$$

$$H=2C\frac{d\gamma}{dt}=\text{const,}$$

where

$$I=I_\xi+2I_{x'}+2A+j^2\Theta;$$
$$B=2(I_{y'}+A). \tag{569}$$

The expression

$$\frac{d\alpha}{dt}+\omega_\xi=\omega_\xi^1 \tag{570}$$

in equations (568) represents the projection of the absolute angular velocity ω^1 of the frame on its stabilization axis ξ. The first two of equations (568) can therefore be written in the form

$$I\frac{d\omega_\xi^1}{dt}+H\frac{d\beta}{dt}=M_\xi+j(j+1)\Theta\frac{d\omega_\xi}{dt}$$
$$B\frac{d^2\beta}{dt^2}-H\omega_\xi^1=M_{y'}. \tag{571}$$

When problems of the accuracy of stabilization are studied in accordance with the theory of gyroscope precession, the so-called inertial terms

$$I\frac{d\omega_\xi^1}{dt} \quad \text{and} \quad B\frac{d^2\beta}{dt^2},$$

must be neglected in equations (571).

In the important case

$$M_{y'}=0, \tag{572}$$

where the resistance to the tilting of the gyro housings relative to the frame can be neglected, the second equation (571) becomes, when $B\frac{d^2\beta}{dt^2}$ is omitted,

$$\omega_\xi^1=0. \tag{573}$$

This means that the projection of the absolute angular velocity of the frame on its stabilization axis ξ is zero when the motion of the frame is slow. It is a relationship of the type of nonholonomic constraints (cf. Chapter II, § 4).

This property of the gyroscopic frame allows it to be used as a directional gyro. In view of the nonholonomic character of (573), angular displacements of the frame, which may lead to considerable errors when it is used as a directional stabilizer, appear at an arbitrary motion of its stabilization axis. This problem was dealt with in detail in Chapter II, § 4

* In order not to complicate the calculations, the equations have been written for gyro rotors linked by a transmission with a ratio of − 1. It can be shown that the same equations (568) would be obtained without this restriction.

on the basis of equation (188), which is, apart from the symbols, identical with equation (573).

If, in particular, the gyroscopic frame is mounted on a ship, then the inclination of the deck relative to the horizontal plane will disturb the stabilization during turns. Let the angular velocity of turning be ω and the inclination of the ξ-axis to the horizontal plane be ϑ (Figure 153). The following expression is then obtained for the projection of the angular velocity of the ship on the frame's axis of tilting (the angular velocity of the Earth is neglected):

$$\omega_\xi = -\omega \sin \vartheta. \tag{574}$$

Inserting (573) and (574) into (570) yields

$$\frac{d\alpha}{dt} = \omega \sin \vartheta. \tag{575}$$

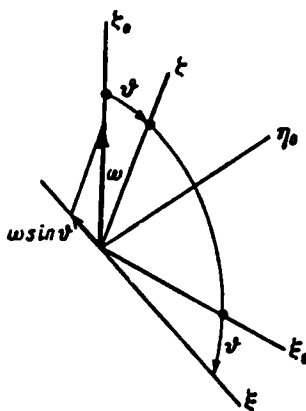The frame will therefore rotate relative to the ship's deck.

FIGURE 153

Gyro horizons are based on a combination of two gyroscopic frames, and gyroazimuthhorizons (Figure 154) on a combination of three gyroscopic frames. In the latter case two frames stabilize the central part of the instument, which is suspended in gimbals, in the horizontal plane. The third frame, whose axis is vertical, ensures stabilization in azimuth.

It is possible to adjust the gyro horizon by means of a gyroscopic pendulum (Figure 155) with simultaneous elimination of the influence of the ship's manoeuvers. The same principle is used as in the device with auxiliary gyro (with variable rotational speed) discussed in § 3 of this chapter.

The deviation of the pendulum from the perpendicular toward the plane of the artificial horizon (the central part of the gyroazimuthhorizon) closes the contact in electromagnets located on the pivots of the gyro-horizon frame housings. This produces moments causing the central part of the instrument to alter its orientation in space in the required direction. The control characteristic of the electromagnets can be similar to that of a relay. As will be shown in Chapter VI, § 1, this fact can cause considerable instrument errors when the ship rolls.

If the amplifier lag is neglected, i.e.,

$$\tau = 0,\tag{579}$$

then the following system of linear differential equations has to be solved:

$$I\frac{d^2\alpha}{dt^2} + H\frac{d\beta}{dt} = \frac{jC}{g}i;$$

$$B\frac{d^2\beta}{dt^2} - H\frac{d\alpha}{dt} = 0;\tag{580}$$

$$L\frac{di}{dt} + jC\frac{d\alpha}{dt} + Ri = -\mu\beta.$$

The characteristic determinant of this system is

$$\Delta(\lambda) = \begin{vmatrix} I\lambda^2 & H\lambda & -\dfrac{jC}{g} \\ -H\lambda & B\lambda^2 & 0 \\ jC\lambda & \mu & L\lambda + R \end{vmatrix}.\tag{581}$$
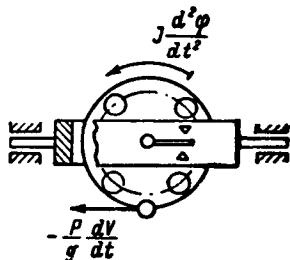
FIGURE 155

The following algebraic equation is obtained by expanding this determinant and equating it to zero:

$$\lambda(a_0\lambda^4 + a_1\lambda^3 + a_2\lambda^2 + a_3\lambda + a_4) = 0,\tag{582}$$

where the following notation has been used:

$$a_0 = BIL;$$

$$a_1 = BIR;$$

$$a_2 = LH^2 + \frac{BI^2C^2}{g};\tag{583}$$

$$a_3 = RH^2;$$

$$a_4 = \frac{\mu HjC}{g}.$$

Equation (582) has a root $\lambda = 0$, due to the fact that α appears in the system of differential equations only in its derivatives and is thus determined except for an arbitrary constant.

The other roots will have negative real parts if the Routh-Hurwitz criterion

$$a_1 a_2 a_3 > a_0 a_3^2 + a_1^2 a_4\tag{584}$$

176

We shall now study the stability of the gyroscopic frame, neglecting the Coulomb friction in the bearings of the gyro housings and of the frame itself*. The moment M_ξ in (568) is then the moment applied to the frame by the stabilizing motor. If the latter is a dc motor with independent excitation, the moment M_ξ is (in kg):

$$M_\xi = j \frac{C}{g} i,$$
(576)

where C is the coefficient of the motor counter emf in v sec, g, the gravitational acceleration $= 9.8$ m sec^{-2}, i, the motor-armature current intensity, in amp.
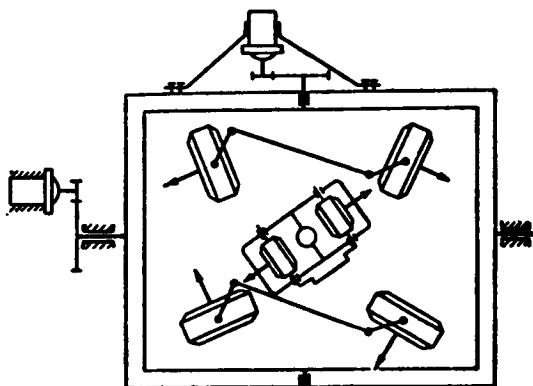

FIGURE 154

The terms in (568) containing the angular velocity ω_ξ represent the perturbation effects on the gyroscopic frame, and can be omitted when considering the stability. When (576) is taken into account, the first two of equations (568) become

$$I \frac{d^2\alpha}{dt^2} + H \frac{d\beta}{dt} = j \frac{C}{g} i;$$

$$B \frac{d^2\beta}{dt^2} - H \frac{d\alpha}{dt} = 0.$$
(577)

The following two equations should be added to this system:

$$v = Ri + L \frac{di}{dt} + jC \frac{d\alpha}{dt},$$

$$\tau \frac{dv}{dt} + v = -\mu\beta.$$
(578)

The first is the equation of the electric circuit of the stabilization motor, and the second, the simplest equation of an amplifier having a time constant τ. Here v is the electromotive force at the amplifier output; R, the ohmic resistance of the armature circuit; L, the self-induction of this circuit; μ, a factor characterizing the amplification of the entire electric device (pick-up — amplifier) creating a tension proportional to the angle β defining the deviations of the gyro housings from their mean position.

* For an analysis of the influence of the Coulomb friction cf. Chapter V, § 2.

is satisfied and if all coefficients a_0, a_1, a_2, a_3, a_4 are positive. The last condition is satisfied in this case. We insert the values of the coefficients, as given by (583), into (584). This yields, after simplifications, the following stability condition of the gyroscopic frame:

$$\frac{jC}{I} > \frac{\mu}{H}. \qquad (585)$$

This condition was obtained in 1943 by V.I. Kuznetsov. Unexpectedly, B, L, and R do not appear. The explanation of this will be given in Chapter V, § 2.

By the first of equations (569):

$$\frac{jC}{I} = \frac{jC}{I_{\xi_1} + 2I_{x'} + 2A + j^2\Theta}. \qquad (586)$$

Therefore the left-hand side of inequality (585) is a maximum if j attains the value

$$j^* = \sqrt{\frac{I_{\xi_1} + 2I_{x'} + 2A}{\Theta}}. \qquad (587)$$

This value was adopted as most advantageous for ensuring the stability of the gyroscopic frame. This conclusion must, however, be qualified, as the calculations in Chapter V, § 2 show. The influence of the parameters B, L, and R on the damping of the free oscillations of the frame will be examined there by means of the energy method employed in studying the stability of gyroscopic systems.

When $\tau \neq 0$, the stability condition of the gyroscopic frame is more complex than that given by (585). It was examined in a general form by Reutenberg.

It is shown in Chapter V, § 2, how approximate frame-stability conditions can be obtained by a simple energy method when the amplifier-lag τ is small.

Numerical example. Assume that $I_{\xi_1} + 2I_{x'} + 2A = 4.75\,\text{kgm sec}^2$; $j = 100$; $\Theta = 2.5 \cdot 10^{-5}\,\text{kgm sec}^2$; $B = 0.05\,\text{kgm sec}^2$; $H = 10\,\text{kgm sec}$; $\mu = 10\,\text{v}$; $C = 0.50\,\text{vsec}$; $R = 10\,\Omega$; $L = 0.1\,\text{h}$.

The first of equations (569) then gives

$$I = I_{\xi_1} + 2I_{x'} + 2A + j^2\Theta = 5.00\ \text{kgm sec}^2.$$

The stability condition (585) is satisfied, since

$$\frac{jC}{I} - \frac{\mu}{H} = 10 - 1 > 0.$$

According to Kuznetsov, the most advantageous transmission ratio j is

$$j^* = \sqrt{\frac{I_{\xi_1} + 2I_{x'} + 2A}{\Theta}} \cong 436.$$

A more precise value will be obtained in Chapter V, § 2 (p.197), where optimum damping will be taken into account. An increasing transmission ratio is, however, accompanied by an increased amplitude of the forced oscillations of the gyroscopic frame during the rolling of its base (cf. Chapter V, § 3, p. 206). As a result, selecting the transmission ratio according to optimum damping will not always be the correct procedure.

Chapter V

NONLINEAR PROBLEMS IN THE THEORY
OF GYROSCOPES

§ 1. Sliding motions of gyroscopic systems

This section gives a strictly [mathematical] treatment, without any geometric assumptions, of the so-called sliding motion of mechanical or similar systems; this is illustrated by the example of the motion of the gyroscopic heel equalizer of any given moving object. Sliding motion appears when the forces acting on the system are defined by discontinuous functions. The point representing the instantaneous position of the system in the phase space (in the phase plane) "sticks" on a surface (or line) of force discontinuity, thus reducing the number of degrees of freedom of the system.

Consider the system of differential equations

$$\frac{d\theta}{dt} = -(\theta + \varphi);$$
$$\frac{d\varphi}{dt} = \theta + \varphi - m(\varphi). \tag{588}$$

which in Chapter IV, § 4 described the motion of the gyroscopic heel equalizer of a moving object. In these equations t is the dimensionless time (previously denoted by τ); θ is the object's heel; φ a magnitude proportional to the angle β through which the inner gimbal ring of the gyro is tilted relative to the outer ring; and $m(\varphi)$ a function defining the law of variation of the corrective moment.

The case of a continuous function $m(\varphi)$ (see Figure 148) was discussed in Chapter IV, § 4. The function $m(\varphi)$ in Figure 156 corresponds to the so-called contact correction without insulating interval; the curve itself represents the limiting case of the curve of Figure 148 for $\varphi^* \to 0$, and therefore for

$$\varkappa = \frac{m}{\varphi^*} \to \infty. \tag{589}$$

The function $m(\varphi)$ in Figure 157 possesses an "insulating interval" $-\varphi^* < \varphi < \varphi^*$ in which the corrective moment is zero. This is the limiting case of the function given in Figure 158 for $\varphi^0 \to \varphi^*$.

Consider first the case when the function $m(\varphi)$ varies according to the curve in Figure 156. The differential equations (588) can in this case be written in the form:

$$\frac{d\theta}{dt} = -(\theta + \varphi),$$
$$\frac{d\varphi}{dt} = \theta + \varphi - m \, sign \, \varphi. \tag{590}$$

where φ is different from zero.

These differential equations are easily solved if one of the inequalities $\varphi > 0$ or $\varphi < 0$ is satisfied; the solution was given in Chapter IV, §4. It is easily seen that for $\varphi > 0$ the solution of system (590) is

$$\theta = \frac{mt^2}{2} - (\theta_0 + \varphi_0)t + \theta_0,$$

$$\varphi = -\frac{mt^2}{2} + (\theta_0 + \varphi_0 - m)t + \varphi_0, \tag{591}$$

where φ_0 and θ_0 are the initial values of φ and θ at $t = 0$. It is obviously assumed that $\varphi_0 > 0$.
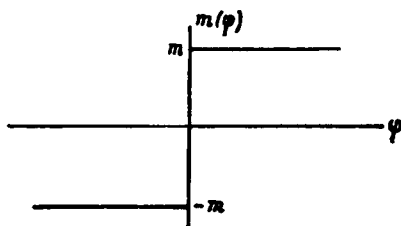

FIGURE 156

If $\varphi_0 < 0$, the sign before m should be reversed in (591).
Assume, for instance, that

$$\varphi_0 = +0. \tag{592}$$

Solution (591) then becomes

$$\theta = \frac{mt^2}{2} - \theta_0 t + \theta_0; $$

$$\varphi = -\frac{mt^2}{2} + (\theta_0 - m)t. \tag{593}$$

This solution is valid only for

$$\theta_0 > m, \tag{594}$$

since otherwise φ would be negative from the very beginning. φ becomes zero at

$$t = t_e = \frac{2(\theta_0 - m)}{m} \tag{595}$$

and is thereafter negative. Solution (593) is therefore invalid for $t > t_e$ and must be replaced by a solution of (590) corresponding to $\varphi < 0$. From the above, such a solution will be of the type

$$\theta = -\frac{mt^2}{2} - \theta_0 t + \theta_0,$$

$$\varphi = \frac{mt^2}{2} + (\theta_0 + m)t, \tag{596}$$

with initial conditions $\theta = \theta_0$, $\varphi = -0$ at instant $t = 0$ of a new time scale. It is, however, meaningful only for

$$\theta_0 < -m, \tag{597}$$

since otherwise φ would immediately become positive for $t > 0$. Comparing (594) and (597) we see that neither (594) nor (596) is valid for initial conditions satisfying the relationships

$$-m < \theta_0 < +m,$$
$$\varphi_0 = 0. \tag{598}$$

It follows that certain additional assumptions must be made in order to solve the problem.

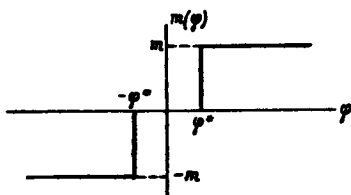<div style="text-align:center">FIGURE 157   FIGURE 158</div>
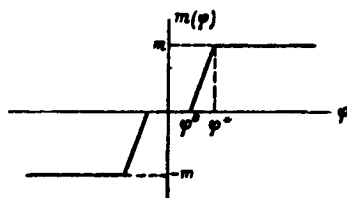
It will be shown below that if the curve in Figure 156 is considered as the limiting case (for $\varphi^* \to 0$) of the curve in Figure 148, then the solution corresponding to initial conditions (598) will be

$$\varphi \equiv 0, \qquad \theta = \theta_0 e^{-t}. \tag{599}$$

In this case the phase point S, having coordinates φ and θ, slides along the ordinate (Figure 159) which separates the regions in which solutions (593) and (596) exist; for this reason the motion defined by (599) is called sliding motion.

The phase trajectories defined by (593) will now be plotted. It will be shown that all phase trajectories are represented by identical parabolas with a common axis forming an angle of 135° with the φ-axis.

It follows from (593) that

$$\theta + \varphi = -mt + \theta_0. \tag{600}$$

The following equation of the phase trajectory is obtained by eliminating the time t from the second equation (593) by means of (600):

$$\varphi = -\frac{1}{2m}(\theta + \varphi - \theta_0)^2 - \frac{\theta_0 - m}{m}(\theta + \varphi - \theta_0). \tag{601}$$

This can be reduced to the canonical form of the equation of a parabola

$$y^2 = 2px, \tag{602}$$

by adopting a new system of coordinates with origin at $\bar{0}$ (the parabola apex) having the coordinates

$$\bar{\varphi} = \frac{\theta_0^2}{2m} - \theta_0 + \frac{3m}{8},$$

$$\bar{\theta} = -\frac{\theta_0^2}{2m} + \theta_0 + \frac{m}{8} \tag{603}$$

and with the x- and y-axes rotated counterclockwise through an angle of

<div style="text-align:center">180</div>

135° relative to the φ- and θ-axes (Figure 160). Then

$$\varphi = \bar{\varphi} - \frac{x+y}{\sqrt{2}},$$ (604)

$$\theta = \bar{\theta} + \frac{x-y}{\sqrt{2}}$$

and

$$p = \frac{m}{2\sqrt{2}}.$$ (605)

It follows from (603) that

$$\bar{\varphi} + \bar{\theta} = \frac{m}{2}.$$ (606)

For $\theta_0 > m$, $(\varphi_0 = +0)$, the apex of parabola (601) thus lies on the straight line (606), while the parabola itself always has the shape defined by (602).

It is thus seen that all phase trajectories in the $\varphi\theta$ plane can be plotted by using the same template in accordance with (602) and (605).

The motion of the phase points on any of these trajectories starts from $(\theta_0 > m$, $\varphi_0 = +0)$ in the direction of increasing φ and decreasing θ.

At the instant

$$t_1 = \frac{\theta_0 - m}{m},$$ (607)

φ attains its maximum,

$$\varphi_1 = \frac{(\theta_0 - m)^2}{2m},$$ (608)

in accordance with the second equation (593).

The corresponding value of θ is obtained from the first equation (593):

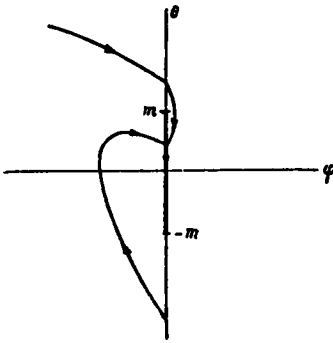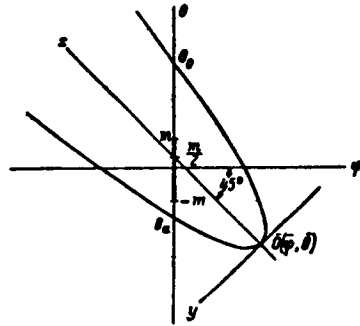$$\theta_1 = \theta_0 - \frac{\theta_0^2}{2m} + \frac{m}{2}.$$ (609)

FIGURE 159

FIGURE 160

Also, at the instant

$$t_2 = \frac{\theta_0}{m},$$ (610)

by the first equation (593), the angle θ reaches its minimum

$$\theta_2 = \theta_0 - \frac{\theta_0^2}{2m}.$$ (611)

The corresponding value of φ is

$$\varphi_2 = -\theta_0 + \frac{\theta_0^2}{2m} = -\theta_2. \tag{612}$$

Lastly, as already stated (p. 179), φ again becomes zero at the instant

$$t_a = \frac{2(\theta_0 - m)}{m},$$

the corresponding value of θ being, by the first equation (593),

$$\theta_a = -\theta_0 + 2m. \tag{613}$$

It is easily seen that for $\theta_0 > 3m$,

$$|\theta_a| > m; \tag{614}$$

for $m < \theta_0 < 3m$ the corresponding trajectory ends on the ordinate section

$$-m < \theta < m. \tag{615}$$

This last observation is very important for plotting the trajectories of the phase points in the region of negative values of φ. In this case, i.e., for $\varphi < 0$, the system of differential equations

$$\frac{d\theta}{dt} = -(\theta + \varphi),$$
$$\frac{d\varphi}{dt} = \theta + \varphi - m, \tag{616}$$

which is valid for $\varphi > 0$, should be replaced by the system

$$\frac{d\theta}{dt} = -(\theta + \varphi),$$
$$\frac{d\varphi}{dt} = \theta + \varphi + m. \tag{617}$$

The system of differential equations (617) becomes identical with system (616) if φ and θ are replaced by new variables

$$\bar{\varphi} = -\varphi \quad \text{and} \quad \bar{\theta} = -\theta. \tag{618}$$

All the trajectories in the region $\varphi < 0$ are therefore obtained from the trajectories of the region $\varphi > 0$ by two successive mirror transformations about the φ- and θ-axes or, which is the same, by rotating the semi-infinite plane $\varphi > 0$ through 180° about the origin.

A trajectory for which

$$\bar{\theta}_0 > 3m, \quad \bar{\varphi}_0 = 0, \tag{619}$$

ends, according to (613), at the point

$$\bar{\theta}_a = 2m - \bar{\theta}_0 < -m, \quad \bar{\varphi}_a = 0, \tag{620}$$

and can therefore be continued into the region of positive φ, if

$$\theta_0 = -(2m - \bar{\theta}_0), \quad \varphi_0 = 0; \tag{621}$$

if (619) is taken into account, it is found that $\theta_0 > m$.

All the trajectories starting from points

$$m < \bar{\theta}_0 < 3m, \quad \bar{\varphi}_0 = 0, \tag{622}$$

182

will end on the section $-m < \theta < m$ of the ordinate, and cannot be continued into the region of positive φ. This is because trajectories (593), located in the region of positive φ and starting at points

$$m < \theta_0 < 3m, \ \varphi_0 = 0,$$

end on this section.

The motion of the phase point S in the $\varphi\theta$ plane is as follows: The point S moves clockwise along a spiral curve (Figure 161) consisting of parts of parabola (602), cutting off sections on the ordinate that successively decrease by the magnitude $2m$. The motion along the spiral continues until the last parabolic arc ends at a point of the section $-m < \theta < m$ of the ordinate.
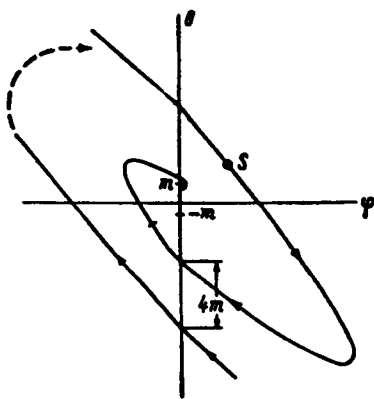
FIGURE 161

As already mentioned the subsequent motion requires a special study. Solution (599) can be obtained formally by substituting $\varphi \equiv 0$ in the first of equations (616) or (617). In this case

$$\frac{d\theta}{dt} = -\theta, \tag{623}$$

and therefore

$$\theta = \theta_0 e^{-t}, \tag{624}$$

i.e., the heel angle of the moving object will tend asymptotically to zero for $|\theta_0| < m$.

A strict reasoning, leading to the same result, starts by considering the motion defined by equations (590) as the limiting case of the motions satisfying the equations

$$\frac{d\theta}{dt} = -(\theta + \varphi),$$
$$\frac{d\varphi}{dt} = \theta + \varphi - m(\varphi), \tag{625}$$

where $m(\varphi)$ is a function of the type shown in Figure 148; in addition it is assumed that the "linearity zone" of the curve, i.e., the interval $(-\varphi^*, \varphi^*)$, tends to zero.

183

Since the function $m(\varphi)$ is continuous, the solution of system (625) de-fines on the plane $\varphi\theta$ (Figure 162) continuous curves with continuously vary-ing tangents. Each curve is a trajectory of the phase point S having co-ordinates φ and θ; they define the instantaneous tilting angle of the inner gimbal ring of the instrument and the object's heel for given values φ_0 and θ_0 at $t=0$.

With increasing t, the point S tends to the coordinate origin for any initial conditions. This motion was discussed in detail in Chapter IV, § 4.
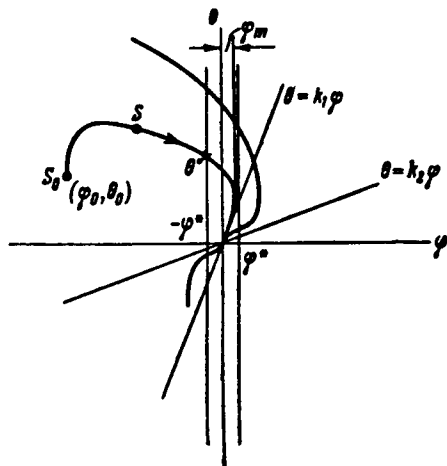
FIGURE 162

Let the initial values φ_0 and θ_0 be such that point S lies to the left of the straight line $\varphi=-\varphi^*$ (Figure 162). Then, as follows from (591) after re-placing m by $-m$, point S will move along the parabola

$$\varphi=\frac{mt^2}{2}+(\theta_0+\varphi_0+m)\,t+\varphi_0,$$

$$\theta=-\frac{mt^2}{2}-(\theta_0+\varphi_0)\,t+\theta_0 \tag{626}$$

and will after a certain time reach the straight line $\varphi=-\varphi^*$, where θ as-sumes the value θ^0.

The subsequent motion of point S will satisfy the linear differential equa-tions (515) considered in Chapter IV, § 4; after substituting t for τ these equations can be written in the form

$$\frac{d\theta}{dt}=-(\theta+\varphi),$$

$$\frac{d\varphi}{dt}=\theta+\varphi-\varkappa\varphi, \tag{627}$$

where

$$\varkappa=\frac{m}{\varphi^*}. \tag{628}$$

184

The system of differential equations (627) will be solved under the assumption $\varkappa \to \infty$. The solution will therefore be of the form (532), and contain hyperbolic functions. It is easily seen that the solution corresponding to the initial conditions $\theta = \theta^\circ$, $\varphi = -\varphi^*$ is

$$\varphi = e^{-\frac{\varkappa}{2}t}\left[-\varphi^* \operatorname{ch}\mu t + \frac{(\varkappa - 2)\varphi^* + 2\theta^\circ}{2\mu}\operatorname{sh}\mu t\right],$$

$$\theta = e^{-\frac{\varkappa}{2}t}\left[\theta^\circ \operatorname{ch}\mu t + \frac{(\varkappa - 2)\theta^\circ + 2\varphi^*}{2\mu}\operatorname{sh}\mu t\right], \tag{629}$$

where

$$\mu = \frac{1}{2}\sqrt{\varkappa(\varkappa - 4)}. \tag{630}$$

Two cases are then possible depending on the initial value θ°: either the point S remains in the zone of linearity $-\varphi^* < \varphi < \varphi^*$ and attains the origin at $t \to \infty$, or the trajectory of the point S intersects the straight line $\varphi = \varphi^*$, the subsequent motion being described by (591) after a suitable change in the time origin (Figure 162).

The instant $t = t_0$ at which φ becomes zero and the phase trajectory intersects the ordinate is found, according to the first of equations (629), by solving the transcendental equation

$$\operatorname{th}\mu t_0 = \frac{2\mu\varphi^*}{(\varkappa - 2)\varphi^* + 2\theta^\circ}, \tag{631}$$

which has a positive root $t_0 > 0$ if the inequality

$$2\mu\varphi^* < (\varkappa - 2)\varphi^* + 2\theta^\circ \tag{632}$$

is satisfied or, which is the same, if

$$\theta^\circ > \left(\mu - \frac{\varkappa - 2}{2}\right)\varphi^*. \tag{633}$$

If (633) is not satisfied, it can be shown that φ increases monotonically, with zero as limit, so that the point remains not only in the zone of linearity $-\varphi^* < \varphi < \varphi^*$, but even in the left-hand semi-infinite plane $\varphi < 0$.

Assume that inequality (633) is satisfied. It is then obvious that the point S will leave the zone of linearity $-\varphi^* < \varphi < \varphi^*$ if (Figure 162)

$$\varphi_m > \varphi^*, \tag{634}$$

where φ_m is the maximum value of φ during its variation according to the first of equations (629).

The maximum of φ is obtained by equating its time derivative to zero; this is, by (629) and (630),

$$\frac{d\varphi}{dt} = e^{-\frac{\varkappa}{2}t}\left\{[(\varkappa - 1)\varphi^* + \theta^\circ]\operatorname{ch}\mu t - \frac{(\varkappa^2 - 3\varkappa)\varphi^* + \varkappa\theta^\circ}{2\mu}\operatorname{sh}\mu t\right\}. \tag{635}$$

Putting $\frac{d\varphi}{dt} = 0$, we obtain

$$\operatorname{th}\mu t_m = a, \tag{636}$$

where

$$a = 2\mu\frac{(\varkappa - 1)\varphi^* + \theta^\circ}{(\varkappa^2 - 3\varkappa)\varphi^* + \varkappa\theta^\circ}. \tag{637}$$

The roots of (636) determine the instants at which φ is a maximum. It is easily seen that a positive root t_m always exists: it is sufficient to prove

that $\operatorname{th} \mu t_m < 1$. This last condition is satisfied, since the inequality

$$2\mu[(x-1)\,\varphi^* + \theta^\circ] < (x^2 - 3x)\,\varphi^* + x\theta^\circ \tag{638}$$

is equivalent to (633), as can be shown by the identity

$$\mu - \frac{x-2}{2} = \frac{2\mu\,(x-1) - (x^2 - 3x)}{x - 2\mu}. \tag{639}$$

By substituting (630) into this equation, it can easily be seen that it is an identity.

The following expression is obtained for the maximum of φ by substituting $t = t_m$ in the first of formulas (629):

$$\varphi_m = e^{-\frac{xt_m}{2}} \operatorname{ch} \mu t_m \left[-\varphi^* + \frac{(x-2)\varphi^* + 2\theta^\circ}{2\mu} \operatorname{th} \mu t_m \right]. \tag{640}$$

It is known that hyperbolic functions satisfy the following equations:

$$\operatorname{ch} \mu t_m = \frac{1}{\sqrt{1-a^2}}, \quad \operatorname{sh} \mu t_m = \frac{a}{\sqrt{1-a^2}}, \quad e^{-\mu t_m} = \sqrt{\frac{1-a}{1+a}}, \tag{641}$$

$$(a = \operatorname{th} \mu t_m).$$

Condition (634) can therefore be written in the form

$$\frac{\varphi_m}{\varphi^*} = (1-a)^{\frac{x}{4\mu} - \frac{1}{2}} (1+a)^{-\frac{x}{4\mu} - \frac{1}{2}} \left[a\left(\frac{x-2}{2\mu} + \frac{\theta^\circ}{\mu\varphi^*} \right) - 1 \right] > 1. \tag{642}$$

For large values of x, the ratio $\frac{x}{2\mu}$ can be expanded in a series in powers of $\frac{1}{x}$:

$$\frac{x}{2\mu} = \frac{x}{\sqrt{x^2 - 4x}} = \left(1 - \frac{4}{x}\right)^{-\frac{1}{2}} = 1 + \frac{2}{x} + \frac{6}{x^2} + \cdots. \tag{643}$$

Similarly

$$\frac{2\mu}{x} = \left(1 - \frac{4}{x}\right)^{\frac{1}{2}} = 1 - \frac{2}{x} - \frac{2}{x^2} - \cdots \tag{644}$$

Inserting φ^* from (628) and (644) into (637), the expression obtained for a can be expanded in the series

$$a = 2\mu \frac{(x-1)\,\varphi^* + \theta^\circ}{(x^2 - 3x)\,\varphi^* + x\theta^\circ} =$$

$$= \left(1 - \frac{2}{x} - \frac{2}{x^2} - \cdots\right)\left[1 + \frac{\frac{2}{x}m}{\left(1 - \frac{3}{x}\right)m + \theta^\circ}\right] =$$

$$= 1 - \frac{2\theta^\circ}{m + \theta^\circ} \frac{1}{x} + \frac{b}{x^2} + \cdots, \tag{645}$$

where b depends on m and θ°.

Inserting (643), (644), (645), and the value of φ^* from (628) into (642)

186

gives

$$\frac{\varphi_m}{\varphi^*}=\left(\frac{2\theta^\circ}{m+\theta^\circ}\frac{1}{\varkappa}+\ldots\right)^{\frac{1}{\varkappa}+\cdots}\left(2-\frac{2\theta^\circ}{m+\theta^\circ}\frac{1}{\varkappa}+\ldots\right)^{-1-\frac{1}{\varkappa}-\cdots}\left[\frac{1-\frac{2}{\varkappa}}{1-\frac{2}{\varkappa}-\frac{2}{\varkappa^2}-\ldots}\left(1-\right.\right.$$

$$\left.\left.-\frac{2\theta^\circ}{m+\theta^\circ}\frac{1}{\varkappa}+\ldots\right)+\frac{\theta^\circ}{m}\left(2+\frac{4}{\varkappa}+\ldots\right)\left(1-\frac{2\theta^\circ}{m+\theta^\circ}\frac{1}{\varkappa}+\ldots\right)-1\right] \quad (646)$$

The limit of

$$z=\left(\frac{2\theta^\circ}{m+\theta^\circ}\frac{1}{\varkappa}+\ldots\right)^{\frac{1}{\varkappa}+\cdots} \quad (647)$$

for $\varkappa\to\infty$ is unity, since

$$\lim_{\varkappa\to\infty}\ln z=\lim_{\varkappa\to\infty}\left[\frac{1}{\varkappa}\left(\ln\frac{2\theta^\circ}{m+\theta^\circ}-\ln\varkappa\right)\right]=0. \quad (648)$$

It follows that

$$\lim_{\varkappa\to\infty}\frac{\varphi_m}{\varphi^*}=\frac{\theta^\circ}{m}. \quad (649)$$

The maximum of φ thus satisfies the inequality $\varphi_m>\varphi^*$ for $\theta^\circ>m$ and sufficiently large values of $\varkappa$. This means that in this case point S enters in the zone of nonlinearity $\varphi>\varphi^*$.

The time which it takes for the point S to pass through the zone of linearity $-\varphi^*<\varphi<\varphi^*$ is the shorter, the larger $\varkappa$, i.e., the narrower the zone. In fact, this time is less than t_m, which by (641) is

$$t_m=-\frac{1}{\mu}\ln\sqrt{\frac{1-a}{1+a}}. \quad (650)$$

Similar calculations show that this expression is zero when $\varkappa\to\infty$.

For $\theta^\circ<m$, the phase point S remains in the zone of linearity. In this case $\varphi_m<\varphi^*$ according to (649). If (633) is not satisfied, so that φ has no maximum, the point S will move toward the origin with φ increasing continuously (Figure 162).

To find the law according to which the point S moves in the zone of linearity, consider the limiting case of (629) for $\varkappa\to\infty$, replace the hyperbolic functions by exponential functions, and substitute (628) and (630):

$$\varphi=\frac{m}{2\varkappa}\left\{\left(\frac{\varkappa-2}{\varkappa\sqrt{\varkappa(\varkappa-4)}}+\frac{2\varkappa\theta^\circ}{m\sqrt{\varkappa(\varkappa-4)}}-1\right)e^{\left[-\frac{\varkappa}{2}+\frac{1}{2}\sqrt{\varkappa(\varkappa-4)}\right]t}-\right.$$

$$\left.-\left(\frac{\varkappa-2}{\varkappa\sqrt{\varkappa(\varkappa-4)}}+\frac{2\varkappa\theta^\circ}{m\sqrt{\varkappa(\varkappa-4)}}+1\right)e^{\left[-\frac{\varkappa}{2}-\frac{1}{2}\sqrt{\varkappa(\varkappa-4)}\right]t}\right\},$$

$$\theta=\frac{\theta^\circ}{2}\left\{\left(1+\frac{\varkappa-2}{\sqrt{\varkappa(\varkappa-4)}}+\frac{2m}{\theta^\circ\varkappa\sqrt{\varkappa(\varkappa-4)}}\right)e^{\left[-\frac{\varkappa}{2}+\frac{1}{2}\sqrt{\varkappa(\varkappa-4)}\right]t}+\right. \quad (651)$$

$$\left.+\left(1-\frac{\varkappa-2}{\sqrt{\varkappa(\varkappa-4)}}-\frac{2m}{\theta^\circ\varkappa\sqrt{\varkappa(\varkappa-4)}}\right)e^{\left[-\frac{\varkappa}{2}-\frac{1}{2}\sqrt{\varkappa(\varkappa-4)}\right]t}\right\}.$$

Since

$$\lim_{x \to \infty} \left[-\frac{x}{2} + \frac{1}{2}\sqrt{x(x-4)} \right] = -1, \tag{652}$$

the following formulas are obtained from (651) when $x \to \infty$:

$$\theta = \theta^0 e^{-t}, \quad \varphi = 0. \tag{653}$$

The same result could have been obtained directly from the differential equations (627). In fact,

$$\lim_{x \to \infty} \varphi = \lim_{x \to \infty} \frac{\theta - \frac{d\varphi}{dt}}{x-1} = 0, \tag{654}$$

and therefore in the limit

$$\frac{d\theta}{dt} = -\theta,$$
$$\varphi = 0, \tag{655}$$

whence we again obtain formulas (653). This derivation presupposes, how-ever, that the limit of the solution of a system of differential equations is
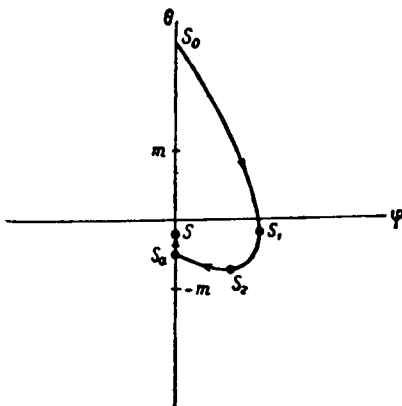
FIGURE 163

identical with the solution of the limit system of the same differential equa-tions. The derivation given in this paragraph is therefore more rigorous.

Numerical example. Let the function $m(\varphi)$ vary according to Figure 156, where

$$m = 0.0818, \quad \varphi_0 = 0, \quad \theta_0 = 0.209 \, (12°).$$

Since $\theta_0 > m$, the point S will, according to (593), move along the para-bola $S_0 S_1 S_2 S_3$ (Figure 163), the function φ reaching its maximum

$$t_1 = \frac{\theta_0 - m}{m} = 1.555$$

at the instant

$$\varphi_1 = \frac{(\theta_0 - m)^2}{2m} = 0.0989.$$

188

The following system of differential equations will describe the motion in the second region of the phase plane:

$$\frac{d\theta}{dt} = -(\theta + \varphi),$$

$$\frac{d\varphi}{dt} = \theta + \varphi. \tag{657}$$

Adding these two equations gives

$$\frac{d\theta}{dt} + \frac{d\varphi}{dt} = 0. \tag{658}$$

whence

$$\theta + \varphi = \text{const.} \tag{659}$$

The phase curves in the so-called "insulation interval" $-\varphi^* < \varphi < \varphi^*$ are therefore straight lines having a negative slope of 45° (Figure 164).

FIGURE 164

Divide the $\varphi\theta$ plane into two by the straight line AC

$$\theta + \varphi = 0. \tag{660}$$

This line bisects the second and fourth quadrants of the phase plane. The motion of a phase point will be from left to right above AC, and from right to left below this line. The points of the bisector are equilibrium points, since by (657),

$$\frac{d\varphi}{dt} = \frac{d\theta}{dt} = 0.$$

Except for $A(\varphi^*, -\varphi^*)$, and C $(-\varphi^*, \varphi^*)$, all these points are points of unstable equilibrium, as is easily seen from Figure 164. Strictly speaking even the equilibrium at A and C is unstable; it has, however, certain peculiarities which will be examined below.

The sections AB and CD, each of length m, are sliding lines. In fact, the straight parts of the phase trajectories of the region $-\varphi^* < \varphi < \varphi^*$ end on one side of AB, since it lies above AC. On the other hand, it lies below the line $\theta = m - \varphi$ containing, according to (608) and (609), the points of parabolas (601) most remote from the ordinate. Therefore the parabolic parts of the phase trajectories of the $\varphi > \varphi^*$ region also end on AB. Thus when the phase point reaches AB, it remains there.

The heel angle at that instant is

$$\theta_1 = \theta_0 - \frac{\theta_0^2}{2m} + \frac{m}{2} = -0.0171.$$

At the instant

$$t_2 = \frac{\theta_0}{m} = 2.55,$$

the magnitude θ of the object's heel reaches its maximum

$$\theta_2 = \theta_0 - \frac{\theta_0^2}{2m} = -0.0580.$$

The corresponding value of φ is

$$\varphi_2 = -\theta_0 + \frac{\theta_0^2}{2m} = -\theta_2 = 0.0580.$$

Finally, φ again becomes zero at the instant

$$t_4 = \frac{2(\theta_0 - m)}{m} = 3.11.$$

The corresponding value of θ is

$$\theta_4 = -\theta_0 + 2m = -0.0454.$$

Since the values $\varphi_4 = 0$, $\theta_4 = -0.0454$ define a point inside the section $-m < \theta < m$ of the ordinate, the subsequent motion satisfies the law

$$\theta = \theta_4 e^{-t}, \qquad \varphi \equiv 0.$$

It follows that the heel angle at $t = 1.00$ will be

$$\theta = \theta_4 e^{-1.00} = -0.0168\,(58').$$

In this given case the heel angle θ decreases from $\theta_0 = 0.209$ to $\theta = -0.0168$ during a dimensionless time

$$t = 3.11 + 1.00 = 4.11$$

and continues to decrease after this.

Consider now the case when the corrective moment varies according to Figure 157.

The function $m(\varphi)$ in the system of differential equations (588) is defined in this case by the following equations (Figure 156):

$$\varphi > \varphi^*, \quad m(\varphi) = \quad m;$$
$$-\varphi^* < \varphi < \varphi^*, \quad m(\varphi) = \quad 0;$$
$$\varphi < \varphi^*, \quad m(\varphi) = -m. \tag{656}$$

The $\varphi\theta$ plane consists therefore of three regions:

$$\varphi > \varphi^*; \quad -\varphi^* < \varphi < \varphi^*; \quad \varphi < -\varphi^*.$$

In the first region, $\varphi > \varphi^*$, the system of differential equations is of the type studied above. The phase curves are the parabolas (601) whose common axis is the straight line (606).

The phase curves in the third region are polar-symmetrical to the phase curves of the first region, as in the case discussed on p. 182.

189

. A detailed study can be made of the problem of the sliding motion along **AB** as limit, taking into account that the curve in Figure 157 can be considered as the limiting case of the curve in Figure 158 for $\varphi^0 \to \varphi^*$.

This study is carried out in the same way as above but is analytically simpler.

The motion of a phase point along **AB** takes place according to the first of equations (588), in which we put $\varphi = \varphi^*$:

$$\frac{d\theta}{dt} = -(\theta + \varphi^*), \tag{661}$$

whence

$$\theta = -\varphi^* + (\theta_0 + \varphi^*) e^{-t}, \tag{662}$$

where θ_0 is the value of θ at the beginning of the phase point's motion along **AB**.

Point **A**, having coordinates $\varphi = \varphi^*$, $\theta = -\varphi^*$, is the limit for the motion described. It defines an equilibrium position of a peculiar character: the phase point **S** returns to this position after a small deviation from it provided that this deviation is inside the curvilinear sector $I - I$ (Figure 164). When the deviations are outside this sector, the phase point moves to the region $-\varphi^* < \varphi < \varphi^*$ and then approaches point **C** asymptotically. Deviations along **AC** are exceptions, since all points on it are, as already mentioned, unstable equilibrium points.

It is thus seen that point **A** (and also point **C**) represents a "semistable" equilibrium position of the system.
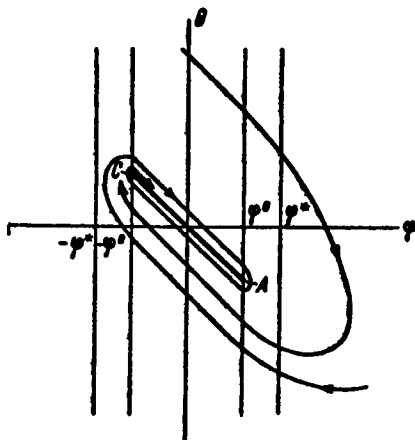

FIGURE 165

We now compare the various nonlinear corrections of the heel-equalizer gyro. If $m(\varphi)$ is of the type shown in Figure 148 or 156, the object's heel tends to zero at the limit. In the case just considered (Figure 157), where an "insulation interval" exists, the instrument does not bring the moving object into a position in which its heel is absolutely zero.

Due to the existence of various disturbances, the phase point will be "knocked out" of the semistable equilibrium positions **A** and **C** and move

forward and back near AC; the object's heel will therefore vary in the interval $-\varphi^* < \theta < \varphi^*$.

If the corrective moment obeys a more complex law, such as that represented in Figure 158, without discontinuities in variation of φ, the general pattern of motion of the phase point remains nearly the same. Sliding motion is in this case replaced by motion along spiral arcs about the points A and C, which now cease to be even "semistable".

The phase trajectory "coils" around AC (Figure 165), each point of which is an unstable equilibrium point. These points are characterized, however, by a certain peculiarity which unstable equilibrium points usually do not possess: At small deviations of the phase point from any equilibrium position on AC, the phase point bypasses one of the extreme equilibrium positions A or C and approaches again the "lost" equilibrium position; these "approaches" are then repeated to infinity, the phase trajectory approaching AC asymptotically.

§ 2. Energy method for investigating the stability of gyroscopic systems

The most common causes of instability in gyroscopic systems are the so-called artificial forces caused by stabilization motors, corrective devices, and various amplifiers. In contrast to friction, which as a rule contributes to the damping of the natural oscillations of the gyroscopic systems, the artificial forces can "rock" the system by increasing its kinetic energy.

When the parameters of the gyroscopic system approach those values at which it becomes unstable, the natural oscillations of the systems are usually similar to nutation-type harmonic oscillations. The work of the artificial forces and the work of the forces damping the gyroscopic system have opposite signs and balance each other. The gyroscopic system behaves as if it were unaffected by external forces, undergoing oscillations similar to undampened nutations. It can therefore be assumed with sufficient accuracy that the frequency of oscillations of the gyroscopic system at the stability threshold equals the frequency of nutations.

These considerations lie at the base of the so-called energy method for investigating the stability of gyroscopic systems; the application of the method is illustrated below by the example of the motion of a gyroscopic frame (or monoaxial gyroscopic stabilizer) when the Coulomb friction is taken into account. A similar procedure can easily be followed also for other nonlinear forces acting on the gyroscopic systems.

Consider first the problem of the stability of motion of a gyroscopic frame in the presence of Coulomb friction in its simplest formulation, namely when the counter emf of the stabilization motor and the transient processes in the circuit of its armature are neglected together with friction in the bearings of the gyro housings. When Coulomb friction in the stabilization axis* is taken into account, the equations of motion of the gyroscopic frame (Chapter IV, § 5) can then be written in the form

$$I\frac{d^2\alpha}{dt^2} + H\frac{d\beta}{dt} = -M_s sign\frac{d\alpha}{dt} - k\beta, \tag{663}$$

* Unlike the notation used in Chapter IV, § 5, the stabilization axis is denoted now by s.

192

$$B \frac{d^2\beta}{dt^2} - H \frac{d\alpha}{dt} = 0. \tag{663}$$

where I is the total moment of inertia of the frame, rotors, and housings of the gyros with respect to the stabilization axis x, together with the moments of inertia of the motor rotor and the transmission parts linked kinematically with the frame, referred to the same axis; B is twice the moment of inertia of each gyro (housing and rotor) with respect to the housing axis, together with the referred moments of inertia of the gyro coupling, solenoids, pick-ups, and other parts of the frame connected to the gyro housings; H, twice the angular momentum of the gyro rotor; α, the angle through which frame tilts about x-axis; β, the angle of deviation of gyros from the mean position; M_s, moment of Coulomb friction in the bearings of the stabilization axis; k, factor of proportionality between β and the moment applied to the frame by the stabilization motor (slope of stabilization-moment characteristic).

Multiplying the first of equations (663) by $\frac{d\alpha}{dt}$, the second by $\frac{d\beta}{dt}$, and adding:

$$I \frac{d^2\alpha}{dt^2} \frac{d\alpha}{dt} + B \frac{d^2\beta}{dt^2} \frac{d\beta}{dt} = -M_s \frac{d\alpha}{dt} \, sign \, \frac{d\alpha}{dt} - k\beta \frac{d\alpha}{dt}. \tag{664}$$

The kinetic energy of the frame less the constant kinetic energy due to the rotation of the rotors, is

$$T = \frac{1}{2}\left[I \left(\frac{d\alpha}{dt}\right)^2 + B\left(\frac{d\beta}{dt}\right)^2\right]. \tag{665}$$

Equation (664) can be written in the form;

$$\frac{dT}{dt} = -M_s \frac{d\alpha}{dt} \, sign \, \frac{d\alpha}{dt} - k\beta \frac{d\alpha}{dt}. \tag{666}$$

The stability is therefore determined by the behavior of the right-hand side of (666). Its first term always satisfies the inequality,

$$-M_s \frac{d\alpha}{dt} \, sign \, \frac{d\alpha}{dt} < 0, \tag{667}$$

i.e., friction in the bearings of the frame suspension tends to reduce the kinetic energy of the frame and therefore contributes to the damping of its oscillations. On the other hand, as will be shown below, the second term on the right-hand side of (666) contributes to the increase in the kinetic energy, i.e., causes "rocking" of the frame.

As a first approximation it can therefore be assumed that the motion of the frame is mainly determined by the system of equations

$$I \frac{d^2\alpha}{dt^2} + H \frac{d\beta}{dt} = 0,$$

$$B \frac{d^2\beta}{dt^2} - H \frac{d\alpha}{dt} = 0. \tag{668}$$

In other words, it is similar in form to the periodic motion described by

$$\alpha = a \cos(\nu t + \delta),$$
$$\beta = b \sin(\nu t + \delta), \tag{669}$$

where ν is the angular frequency of nutation of the frame free from friction in the suspension bearings and from the action of the "artificial" generalized force $k\beta$. This frequency is

$$\nu = \frac{H}{\sqrt{BI}}. \tag{670}$$

193

The oscillation amplitudes of frame and housings are connected by the equation

$$b = a\sqrt{\frac{I}{B}},\tag{671}$$

as is shown by inserting (669) and (670) into (668).

The influence of the forces $k\beta$ and $-M_s sign \frac{d\alpha}{dt}$ during a comparatively short period, such as one nutation period

$$T = \frac{2\pi}{\nu}\tag{672}$$

can be assessed by means of (669), in which the amplitudes a and b are assumed to be constant. Inserting (669) into (666) yields, after omitting δ,

$$\frac{dT}{dt} = M_s \nu a \sin \nu t \, sign \, (-\nu a \sin \nu t) + k a b \nu \sin^2 \nu t.\tag{673}$$

It follows that ΔT, the variation of the kinetic energy during one nutation period, is given by

$$\Delta T = \int_0^{\frac{2\pi}{\nu}} [-M_s \nu a \sin \nu t \, sign \, (\nu a \sin \nu t) + k a b \nu \sin^2 \nu t]\, dt.\tag{674}$$

Integrating this expression gives

$$\Delta T = -4 a M_s + \pi a b k.\tag{675}$$

If the amplitude b satisfies the inequality

$$b > \frac{4 M_s}{\pi k},\tag{676}$$

we conclude that the kinetic energy of the frame and the oscillation amplitude increase; otherwise, the oscillations are damped. It follows that

$$b^* = \frac{4 M_s}{\pi k}\tag{677}$$

is the approximate value of the amplitude of unstable periodic motion.

The gyroscopic frame will therefore be stable if the amplitude of the oscillations of β, caused by any disturbance, does not exceed the value b^*. Such a disturbance may be a constant moment M about the stabilization axis, suddenly applied to the frame. In order to find the initial amplitude of the oscillations caused by these moments, friction and the moment caused by the stabilizing motor will be neglected. The equations of motion of the gyroscopic frame are then

$$I \frac{d^2\alpha}{dt^2} + H \frac{d\beta}{dt} = M,$$
$$B \frac{d^2\beta}{dt^2} - H \frac{d\alpha}{dt} = 0.\tag{678}$$

The solution of these equations for the initial conditions

$$\alpha = \beta = 0, \quad \frac{d\alpha}{dt} = \frac{d\beta}{dt} = 0,\tag{679}$$

194

is of the form

$$a = \frac{BM}{H^2} (1 - \cos vt),$$

$$\beta = \frac{M}{H} t - \frac{M}{vH} \sin vt. \qquad \qquad (680)$$

It follows from these equations that

$$b = \frac{M}{vH}, \qquad \qquad (681)$$

is the initial oscillation amplitude of the tilting angle of the housings, caused by the sudden application of a moment M. In accordance with (676), the frame oscillations will therefore increase if the inequality

$$\frac{M}{vH} > \frac{4M_e}{\pi k}, \qquad \qquad (682)$$

is satisfied. The magnitude

$$M^* = \frac{4H^2 M_e}{\pi k \sqrt{BI}} \qquad \qquad (683)$$

thus characterizes in a certain sense the frame stability following disturbances by constant moments.

It is possible to draw conclusions from (675) not only on the stability, but also on the variation with time of the oscillation amplitude of β. The following approximation of the kinetic energy of the gyroscopic frame is obtained by inserting (669) into (665) and using (671):

$$T = \frac{1}{2} (Ia^2 v^2 \sin^2 vt + Bb^2 v^2 \cos^2 vt) = \frac{1}{2} Bv^2 b^2. \qquad \qquad (684)$$

The variation ΔT of the kinetic energy during one nutation period is therefore approximately

$$\Delta T \cong \frac{dT}{dt} \frac{2\pi}{v} = Bv^2 b \frac{db}{dt} \frac{2\pi}{v}. \qquad \qquad (685)$$

The amplitude b is assumed to be a slowly varying function of time (the variation of b during a nutation period has till now been neglected in this section).

The following differential equation is obtained by equating the right-hand sides of (685) and (675) and expressing a by (671):

$$2\pi Bvb \frac{db}{dt} = b \sqrt{\frac{B}{I}} (-4M_e + \pi kb). \qquad \qquad (686)$$

Inserting (670) yields after simplifications

$$\frac{db}{dt} = \frac{-4M_e + \pi kb}{2\pi H}. \qquad \qquad (687)$$

The variation of b with time can be determined by integrating (687).

We shall now study the gyroscopic frame stability in a more general way, taking into account transient processes in the circuit of the stabilization motor armature, its counter emf, and friction in the gyro-housings bearings. The corresponding differential equations can be obtained by adding to (580) (Chapter IV, § 5) terms representing the moments due to Coulomb friction acting about the stabilization axis of the frame and the axes of the gyro

housings. The following system of equations is then obtained:

$$I \frac{d^2 a}{dt^2} + H \frac{d\beta}{dt} = \frac{jC}{g} i - M_s \text{sign} \frac{da}{dt},$$

$$B \frac{d^2 \beta}{dt^2} - H \frac{da}{dt} = -M_y \text{sign} \frac{d\beta}{dt}, \tag{688}$$

$$L \frac{di}{dt} + Ri + jC \frac{da}{dt} = -\mu\beta.$$

In addition to the notation already defined, M_y is the moment due to Coulomb friction in the bearings of the gyro housings.

Assume, as before, that in this case too the motion is determined mainly by the system of equations (688), i.e., that motion of the frame during one or two periods is similar to the harmonic motion described by

$$a = a \cos vt,$$
$$\beta = b \sin vt. \tag{689}$$

Formulas (689) differ from (669) only by the constant δ which determines the time origin.

Inserting (689) into the third of equations (688) gives

$$L \frac{di}{dt} + Ri = (vajC - \mu b) \sin vt. \tag{690}$$

Assuming that the initial transient process in the armature circuit has already come to an end, we have

$$i = \frac{vajC - \mu b}{\sqrt{R^2 + v^2 L^2}} \sin(vt - \epsilon), \tag{691}$$

where

$$\cos \epsilon = \frac{R}{\sqrt{R^2 + v^2 L^2}}, \quad \sin \epsilon = \frac{vL}{\sqrt{R^2 + v^2 L^2}}. \tag{692}$$

The validity of (691) is easily shown by direct substitution into (690), using (692).

As before, we multiply the first two of equations (688) by $\frac{da}{dt}$ and $\frac{d\beta}{dt}$ respectively and add, thus obtaining

$$\frac{dT}{dt} = -M_s \frac{da}{dt} \text{sign} \frac{da}{dt} - M_y \frac{d\beta}{dt} \text{sign} \frac{d\beta}{dt} + \frac{jC}{g} i \frac{da}{dt}, \tag{693}$$

where T is the kinetic energy determined by (665). It follows from (689) and (691) that

$$\int_0^{\frac{2\pi}{v}} \frac{da}{dt} \text{sign} \frac{da}{dt} dt = \int_0^{\frac{2\pi}{v}} (-va \sin vt) \text{sign} (-va \sin vt) dt = 4a,$$

$$\int_0^{\frac{2\pi}{v}} \frac{d\beta}{dt} \text{sign} \frac{d\beta}{dt} dt = \int_0^{\frac{2\pi}{v}} vb \cos vt \text{sign} (vb \cos vt) dt = 4b, \tag{694}$$

$$\int_0^{\frac{2\pi}{v}} i \frac{da}{dt} dt = \int_0^{\frac{2\pi}{v}} \frac{vajC - \mu b}{\sqrt{R^2 + v^2 L^2}} (\sin vt \cos \epsilon - \cos vt \sin \epsilon) \times$$

$$\times (-va \sin vt) dt = \frac{\pi a R (\mu b - vajC)}{R^2 + v^2 L^2}.$$

·Integrating (693) and subsituting (694) gives the following expression for the variation of the kinetic energy ΔT during one nutation period:

$$\Delta T = -4aM_z - 4bM_y + \frac{\pi a j C R\,(\mu b - v a j C)}{g\,(R^2 + v^2 L^2)}.$$ (695)

Inserting (670) and (671) into (695) yields

$$\Delta T = -4\left(M_z\,\sqrt{\frac{B}{I}} + M_y\right)b + \frac{\pi b^2 j C R}{g\,(R^2 + v^2 L^2)}\left(\mu - \frac{jCH}{I}\right)\sqrt{\frac{B}{I}}.$$ (696)

The value of ΔT is always negative, and the gyroscopic frame is therefore always stable, if

$$\mu - \frac{jCH}{I} < 0,$$

which is identical with the stability condition (585) obtained in Chapter IV, § 5 for the case $M_z = M_y = 0$. If condition (585) is not satisfied, then, by analogy with the above, frame oscillations with small amplitudes will be damped, and those with large amplitudes will increase.

It follows from (696) and (685) that the natural oscillations of the gyro housings will be damped, according to the law

$$\frac{1}{b}\frac{db}{dt} = -\frac{2}{\pi H b}\left(M_z + M_y\sqrt{\frac{I}{B}}\right) -$$

$$-\frac{jCR}{2g\,(R^2 + v^2L^2)}\left(\frac{jC}{I} - \frac{\mu}{H}\right).$$ (697)

Numerical example. Assume, in accordance with the data for the example given in Chapter IV, § 5 (p. 275): $I = 5\,\mathrm{kgm\,sec^2}$; $B = 0.05\,\mathrm{kgm\,sec^2}$; $H = 10\,\mathrm{kgm\,sec}$; $j = 100$; $C = 0.50\,\mathrm{v\,sec}$; $R = 10\,\Omega$; $L = 0.1\,\mathrm{h}$; $\mu = 10\,\mathrm{v}$. Assume the following values for the moments due to Coulomb friction: $M_z = 0.5\,\mathrm{kgm}$, $M_y = 0.001\,\mathrm{kgm}$.

When friction and motor torque are neglected, the frequency of nutations of the system is by (670)

$$v = \frac{H}{\sqrt{BI}} = 20\,\mathrm{sec^{-1}}.$$

It follows from (697) that

$$\frac{1}{b}\frac{db}{dt} = -\frac{0.0324}{b} - 2.21.$$

For $b > 0.0146$ (50'), the counter emf of the motor plays the main role in the damping; for $b < 0.0146$, on the contrary, Coulomb friction is decisive.

From (696) and (685) the influence of the parameters B, L, and R on frame stability can also be determined when $M_z = M_y = 0$. This problem remained unsolved in Chapter IV, § 5, since these parameters did not appear in the stability condition (585). In this case

$$2\pi B v b\,\frac{db}{dt} = -\frac{\pi b^2 j C R H}{g\,(R^2 + v^2 L^2)}\left(\frac{jC}{I} - \frac{\mu}{H}\right)\sqrt{\frac{B}{I}},$$ (698)

whence, by (670):

$$\frac{1}{b}\frac{db}{dt} = -\frac{jCR}{2g\,(R^2 + v^2 L^2)}\left(\frac{jC}{I} - \frac{\mu}{H}\right).$$ (699)

The frame oscillations are damped more rapidly the larger the right-hand side of (699).

197

When the stability conditions (585) are satisfied, the parameters $B, L,$ and R enter into the expression for the damping decrement of the natural oscillations of the gyroscopic frame.

According to the first of equations (569) (Chapter IV, § 5):

$$I = I_{t_1} + 2I_{s'} + 2A + j^2\Theta,$$

where Θ is the moment of inertia of the stabilization-motor rotor with respect to its axis of rotation; $I_{t_1} + 2I_{s'} + 2A$ is the moment of inertia of the frame together with the gyros with respect to the stabilization axis.

The right-hand side of (699) is thus a fairly complex function of the transmission ratio j. The selection of the most advantageous transmission ratio according to (587) has therefore to be reconsidered. If, for instance, $CH = 5\mu I$, $I = 2 \cdot 10^5 \Theta$, then the strongest damping will occur at a transmission ratio 2.4 times larger than that given by (587).

The right-hand side of (699) contains the factor

$$\frac{R}{R^2 + v^2 L^2}, \tag{700}$$

which enables us to study the influence of the resistance R of the electric-motor armature circuit, the self-inductance L of this circuit, and the moment of inertia B of the gyro housings, none of which appears in stability condition (585), on the damping rate of the frame oscillations.

An increase of the self-inductance L reduces the factor (700) and thus also the damping. For $L = \text{const}$, damping is improved when R increases from zero to

$$R^* = vL, \tag{701}$$

becoming worse with any further increase of R.

The total moment of inertia of the gyro housings B appears in (700) in terms of the frequency v of nutational gyroscopic-frame oscillations, given by (670)

$$v = \frac{H}{\sqrt{BI}}.$$

An increase of B can improve the damping slightly, since L is usually small, the inductive reactance vL of the armature circuit being less than the ohmic resistance R.

An increase of B is undesirable from another point of view. It follows from the first of equations (680) that when a moment M is suddenly applied to the gyroscopic frame, the amplitude b of the frame's angular oscillations about the stabilization axis is proportional to the moment of inertia B. It is important to note that the amplitude of the forced oscillations of the frame about the stabilization axis, caused, for instance, by the ship's rolling, also increases with the moment of inertia B, as will be shown in § 3 of this chapter. An excessive transmission ratio j is undesirable for the same reasons.

Lastly, we shall analyze the influence of the time constant in the circuit of the amplifier which supplies to the stabilizer motor a voltage depending on the angle of deviation from the mean position of the gyro housings. When the influence of this factor is taken into account, the third of equations (688)

$$L\frac{di}{dt} + Ri + jC\frac{d\alpha}{dt} = -\mu\beta$$

has to be replaced by (578):

$$L\frac{di}{dt} + Ri + jC\frac{da}{dt} = v;$$ (702)

$$\tau\frac{dv}{dt} + v = -\mu\beta.$$ (703)

Here τ is the time constant of the amplifier, usually comparatively small, and v is the voltage at the amplifier output.

Ignoring the processes encountered in a system with high frequencies, (703) can be approximated to

$$v = -\mu\beta - \tau\frac{dv}{dt} \cong -\mu\left(\beta - \tau\frac{d\beta}{dt}\right),$$ (704)

since for low frequencies $v \cong -\mu\beta$.

The third of equations (688) can therefore be written:

$$L\frac{di}{dt} + jC\frac{da}{dt} + Ri = -\mu\left(\beta - \tau\frac{d\beta}{dt}\right).$$ (705)

When (689) is inserted into (705), a differential equation is obtained whose integration yields an analytic expression for the current i. Inserting this expression into the energy equation (693), the stability condition $\Delta T < 0$ becomes for $M_x = M_y = 0$

$$\frac{jC}{I} - \frac{\mu}{H}\left(1 + \frac{H\tau}{\sqrt{BI}}\right) > 0.$$ (706)

This result can also be obtained from the Routh-Hurwitz criterion if the time constant is assumed to be small; Reutenberg derived it in this way.

The fact that loss of stability in gyroscopic and other mechanical systems is accompanied by the appearance of steady increasing oscillations, similar to harmonic oscillations, makes it possible in many cases to give a simple approximate solution of comparatively difficult problems in the theory of stability. This is done principally by establishing a correspondence between the given mechanical system, which is at the stability threshold, and another system, having one degree of freedom, described by a linear differential equation of the second order with constant coefficients,

$$A\frac{d^2x}{dt^2} + B\frac{dx}{dt} + Cx = 0.$$ (707)

The coefficients A, B, and C are selected so as to render the corresponding motion as similar as possible to the motion of the mechanical system considered. The stability depends on the sign of B.

Consider the problem of the stability of a mechanical system described by a third-order differential equation with positive constant coefficients:

$$a_0\frac{d^3x}{dt^3} + a_1\frac{d^2x}{dt^2} + a_2\frac{dx}{dt} + a_3x = 0.$$ (708)

Assume that near the stability threshold the motion can for a short time (one or two periods) be approximated by the harmonic law

$$x = a\cos(\omega t + \delta),$$ (709)

so that

$$\frac{d^3x}{dt^3} \cong -\omega^2\frac{dx}{dt}.$$ (710)

199

For stability investigations (708) can then be replaced by the following second-order equation:

$$a_1 \frac{d^2z}{dt^2} + (a_2 - \omega^2 a_0) \frac{dz}{dt} + a_3 z = 0. \tag{711}$$

The condition of asymptotic stability of the motion described by (711) is,

$$a_2 - \omega^2 a_0 > 0. \tag{712}$$

At the stability threshold the coefficient of the first derivative in (711) is small, and therefore hardly influences the oscillation frequency ω; thus

$$\omega^2 = \frac{a_3}{a_1}. \tag{713}$$

Inserting (713) into (712) yields the well-known stability condition

$$a_1 a_2 > a_0 a_3. \tag{714}$$

Similarly, when the stability of a mechanical system described by a fourth-order differential equation

$$a_0 \frac{d^4z}{dt^4} + a_1 \frac{d^3z}{dt^3} + a_2 \frac{d^2z}{dt^2} + a_3 \frac{dz}{dt} + a_4 z = 0, \tag{715}$$

is being investigated, it may be assumed that

$$\frac{d^4z}{dt^4} = -\omega^2 \frac{d^2z}{dt^2}, \quad z = -\frac{1}{\omega^2} \frac{d^2z}{dt^2}, \tag{716}$$

so that the problem is reduced to that of the stability of a mechanical system described by the differential equation

$$a_1 \frac{d^3z}{dt^3} + \left(a_2 - \omega^2 a_0 - \frac{1}{\omega^2} a_4\right) \frac{d^2z}{dt^2} + a_3 \frac{dz}{dt} = 0. \tag{717}$$

In this case the stability condition is

$$a_2 - \omega^2 a_0 - \frac{1}{\omega^2} a_4 > 0. \tag{718}$$

As in (713), the frequency can be represented by the formula

$$\omega^2 = \frac{a_3}{a_1}.$$

Inserting this value into (718) yields the stability condition for a fourth-order linear differential equation:

$$a_1 a_2 a_3 > a_0 a_3^2 + a_1^2 a_4. \tag{719}$$

[This is the Routh-Hurwitz criterion.]

Consider now the problem of stability in the Mathieu equation

$$\frac{d^2z}{dt^2} + (\mu + \nu \cos 2\omega t) z = 0. \tag{720}$$

Changing the time origin, this equation can be written

$$\frac{d^2z}{dt^2} + \mu z = -\nu \cos (2\omega t + \varepsilon) z. \tag{721}$$

Assume as above that the law of variation of z at the stability threshold is approximately

$$z = a \sin \omega t. \tag{722}$$

Inserting (722) into the right-hand side of (721) gives

$$\frac{d^2x}{dt^2} + \mu x = -\frac{va}{2}\sin(3\omega t + \epsilon) + \frac{va}{2}\sin(\omega t + \epsilon). \qquad (723)$$

According to (722) the following relationship is valid:

$$a\sin(\omega t + \epsilon) = a\sin\omega t\cos\epsilon + a\cos\omega t\sin\epsilon = x\cos\epsilon + \frac{1}{\omega}\frac{dx}{dt}\sin\epsilon. \qquad (724)$$

Using this relationship, equation (723) can be reduced to the form

$$\frac{d^2x}{dt^2} - \frac{v}{2\omega}\frac{dx}{dt}\sin\epsilon + \left(\mu - \frac{v}{2}\cos\epsilon\right)x = -\frac{va}{2}\sin(3\omega t + \epsilon). \qquad (725)$$

The solution of (725) is unstable if

$$\sin\epsilon > 0. \qquad (726)$$

On the other hand, it must be assumed in accordance with (725) and (722) that [near the stability threshold]

$$\mu - \frac{v}{2}\cos\epsilon = \omega^2. \qquad (727)$$

Equation (727) has a root $0 \leqslant \epsilon \leqslant \pi$, and therefore inequality (726) is possible if

$$\omega^2 - \frac{v}{2} < \mu < \omega^2 + \frac{v}{2}. \qquad (728)$$

In accordance with (728) the instability region in the μv plane (Figure 166), is the area between the straight lines

$$\mu \pm \frac{v}{2} = \omega^2. \qquad (729)$$

These lines are tangential to the precise boundaries of the instability region, which were established by Ince*.

In accordance with the general theory of Mathieu equations, for $v > 0$, stability (or the so-called phenomenon of parametric resonance) obtains inside a continuous range of frequencies ω, bounded by the inequalities

$$\omega_1^2 \leqslant \omega^2 \leqslant \omega_2^2, \qquad (730)$$

where

$$\omega_1^2 \cong \mu - \frac{v}{2};$$
$$\omega_2^2 \cong \mu + \frac{v}{2}. \qquad (731)$$

If a term corresponding to linear damping in a mechanical system is added to the Mathieu equation, we obtain

$$\frac{d^2x}{dt^2} + a\frac{dx}{dt} + (\mu + v\cos 2\omega t)x = 0. \qquad (732)$$

The following equation then takes the place of (725):

$$\frac{d^2x}{dt^2} + \left(a - \frac{v}{2\omega}\sin\epsilon\right)\frac{dx}{dt} + \left(\mu - \frac{v}{2}\cos\epsilon\right)x =$$
$$= -\frac{va}{2}\sin(3\omega t + \epsilon). \qquad (733)$$

The boundary of the instability region in the μv plane (Figure 167) is in this

* McLachlan, N. W. Theory and Applications of Mathieu Functions. — Clarendon Press, Oxford. 1947. [Translated into Russian. 1953.]

case a hyperbola whose equation is obtained by eliminating the angle of
phase shift ε between the relationships

$$\alpha - \frac{v}{2\omega} \sin \varepsilon = 0,$$

$$\mu - \frac{v}{2} \cos \varepsilon = \omega^2.$$

(734)

In this case the instability region is narrower than for $\alpha = 0$, and disappears altogether when v is small (Figure 167).

The above examples corresponded to linear differential equations of motion for the mechanical systems. The same method can, however, also be applied to nonlinear systems.
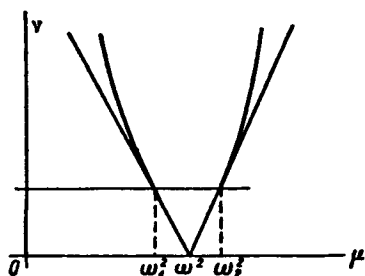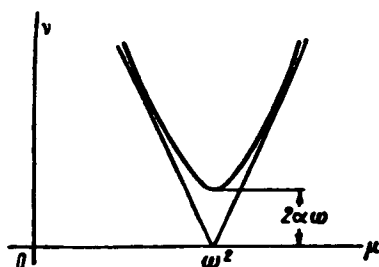

FIGURE 166   FIGURE 167

Consider, for instance, the Duffin-Bulgakov* equation

$$\frac{d^2x}{dt^2} + f(x) = P \sin \omega t, \quad f(+x) = -f(-x).$$

(735)

Inserting into this equation

$$x = a \sin \omega t,$$

(736)

we obtain the approximation

$$\frac{d^2x}{dt^2} + \frac{A_1(a) - P}{a} x = R(t),$$

(737)

where $A_1(a)$ is the coefficient of $\sin \omega t$ when the function $f(a \sin \omega t)$ is expanded in a trigonometric series; $R(t)$ is the remainder of the series [after the first term]. Formula (736) is a solution of the differential equation

$$\frac{d^2x}{dt^2} + \omega^2 x = 0.$$

(738)

The following equation is obtained by comparing (737) and (738):

$$A_1(a) - P = a\omega^2.$$

(739)

The possible amplitudes of the steady oscillations defined by (735) can be approximately determined from this equation.

---

* Bulgakov, B. V. K zadache o vynuzhdennykh kolebaniyakh psevdolineinykh sistem (The Problem of Forced Oscillations of Pseudolinear Systems). — PMM, No. 1. 1943.

The following equation for determining the amplitude a is obtained[*] from (739) by substituting for $A_1(a)$ its expression as a function of $f(a \sin \omega t)$:

$$P + \omega^2 a = \frac{1}{\pi} \int_{-\pi}^{+\pi} f(a \sin \varphi) \sin \varphi \, d\varphi. \tag{740}$$

Equations of the type

$$\frac{d^2 x}{dt^2} + \epsilon f\left(x, \ \frac{dx}{dt}\right) \frac{dx}{dt} + k^2 x = 0, \tag{741}$$

in which ϵ is so small ("small parameter") that the solution differs only little from the harmonic motion, can be similarly investigated.

From the mathematical point of view the above method is one of non-linear mechanics. The strict theory of such approximate methods has been given by Krylov and Bogolyubov.

In some cases the differential equations describing the behavior of a complex mechanical or electromechanical system must be simplified, i.e., their order must be reduced.

In many cases the higher-order derivatives correspond to rapidly decaying transient processes of no great importance. In gyroscopic systems of the indicator type these are the so-called inertial terms, which, because of the unavoidable friction, cause rapidly damped nutations. When the order of a system of differential equations is increased by allowing for secondary phenomena, the accuracy of the result is not always improved. In fact, the differential equations describing the system contain inaccuracies both in the description of the functional behavior of the system's elements and in the values of the various parameters. These inaccuracies increase with the order of the system, and can cause excessive errors in solving the equations.

Experience shows that in many cases equations of the fifth or sixth order describe in the best way possible the behavior of the mechanical system, and any further increase of the order of the equations is undesirable.

Experiments and observations usually show which terms of the equations determine the fundamental oscillation frequency of the system. By using relationships of the type of (710) and (716), the study of the stability of such a system can be reduced to that of a differential equation of the second order.

§ 3. Forced oscillations of a gyroscopic frame
(monoaxial stabilizer)

By considering the forced oscillations of gyroscopic systems we can determine the part played by parameters which are of secondary importance from the point of view of stability, and to select values for these parameters which will not cause excessive forced oscillations of the gyros.

Consider first the motion of a gyroscopic frame when the base on which it is mounted oscillates according to the law

$$\theta = \theta_0 \cos(pt + \delta) \tag{742}$$

[*] [Cf. footnote on preceding page.]

about an axis parallel to the frame-stabilization axis ξ. We use equations (571) describing the motion of the gyroscopic frame

$$I \frac{d\omega'_\xi}{dt} + H \frac{d\beta}{dt} = M_\xi + j(j+1)\theta \frac{d\omega_\xi}{dt},$$

$$B \frac{d^2\beta}{dt^2} - H \omega'_\xi = M_{y'},$$

which were obtained in Chapter IV, § 5. The projection ω_ξ of the angular velocity of the base on the frame axis is in this case

$$\omega_\xi = \frac{d\theta}{dt} = -p\theta_0 \sin(pt + \delta). \tag{743}$$

The projection ω'_ξ of the angular velocity of the gyroscopic frame on the ξ-axis can be written

$$\omega'_\xi = \frac{d\theta}{dt} + \frac{d\alpha}{dt} = \frac{d\psi}{dt}, \tag{744}$$

where, as in Chapter IV, § 5, α is the tilting angle of the gyroscopic frame relative to its base and ψ is the tilting angle of the frame relative to the Earth. The angular velocity of the latter will be neglected.

If, in addition, the Coulomb friction in the bearings of the frame suspension and the torque developed by the stabilization motor are taken into account, (571) must be written in the form

$$I \frac{d^2\psi}{dt^2} + H \frac{d\beta}{dt} = -M_s \, sign \, \frac{d\alpha}{dt} + \frac{jC}{\xi} i -$$

$$- j(j+1)\theta p^2\theta_0 \cos(pt + \delta), \tag{745}$$

$$B \frac{d^2\beta}{dt^2} - H \frac{d\psi}{dt} = -M_y \, sign \, \frac{d\beta}{dt}.$$

Here, in contrast to Chapter IV, § 5, the frame-stabilization axis is denoted again by x and the axis of one of the gyro housings by y; M_s, M_y are the sums of moments due to Coulomb friction in the bearings of the stabilization axis and the axes of the gyro housings respectively.

The angular velocity $\frac{d\psi}{dt}$ of the frame is small compared with the angular velocity $\frac{d\theta}{dt}$ at which the base rolls. Therefore, (744) leads to

$$sign \, \frac{d\alpha}{dt} \cong - sign \, \frac{d\theta}{dt}. \tag{746}$$

To system (745) we add the equation of the motor-armature electric circuit, which has the form of the third of equations (580) (Chapter IV, § 5):

$$L \frac{di}{dt} + Ri + jC \frac{d\alpha}{dt} = -\mu\beta. \tag{747}$$

Inserting the value of $\frac{d\alpha}{dt}$ from (744) gives

$$L \frac{di}{dt} + Ri + jC \frac{d\psi}{dt} = jC \frac{d\theta}{dt} - \mu\beta. \tag{748}$$

Substituting θ from (742) into (748) and inserting (746) into the first of equations (745), the following system of equations defining the motion of the gyroscopic frame is obtained:

$$I \frac{d^2\psi}{dt^2} + H \frac{d\beta}{dt} = M_s \, sign \, \frac{d\theta}{dt} + \frac{jC}{\xi} i -$$

$$- j(j+1)\theta p^2\theta_0 \cos(pt + \delta), \tag{749}$$

$$B \frac{d^2\beta}{dt^2} - H \frac{d\psi}{dt} = -M_y \, sign \frac{d\beta}{dt} \, ,$$

$$L \frac{di}{dt} + Ri + jC \frac{d\psi}{dt} = -\mu\beta - jCp\theta_0 \sin(pt + \delta).$$

(749)

In order to assess the influence of the Coulomb friction on the amplitude of the forced oscillations of the gyroscopic frame, we assume first that $M_z = M_y = 0$. The corresponding equations are then

$$I \frac{d^2\psi}{dt^2} + H \frac{d\beta}{dt} = \frac{jC}{\epsilon} i - j(j+1) \theta p^2\theta_0 \cos(pt+\delta),$$

$$B \frac{d^2\beta}{dt^2} - H \frac{d\psi}{dt} = 0$$

(750)

$$L \frac{di}{dt} + Ri + jC \frac{d\psi}{dt} = -\mu\beta - jCp\theta_0 \sin(pt+\delta).$$

Since these equations are linear, the forced oscillations of the frame are harmonic, having a frequency p. The constant δ in (750) can therefore be chosen so that the following conditions are satisfied:

$$\psi = \psi_0 \cos pt, \quad \psi_0 > 0,$$

(751)

where ψ_0, which has to be determined, is the amplitude of the forced oscillations of the gyroscopic frame about the stabilization axis.

It follows from the second of equations (750) that

$$\beta = \beta_0 \sin pt,$$

(752)

where

$$\beta_0 = \frac{H}{pB} \psi_0.$$

(753)

Furthermore, by the first of equations (750), using (751) − (753):

$$\frac{jC}{\epsilon} i = j(j+1) \theta p^2\theta_0 \cos(pt+\delta) + \left(\frac{H^2}{B} - p^2I\right) \psi_0 \cos pt.$$

(754)

Using (751) − (754), the third of equations (750) can be written in the form:

$$[a \sin(pt+\delta) + b \cos(pt+\delta)] \theta_0 = (c \sin pt + d \cos pt) \psi_0,$$

(755)

where

$$a = pjC - \frac{(j+1) p^3\theta_g L}{C} \, ,$$

$$b = \frac{(j+1) p^2\theta_g R}{C} \, ,$$

$$c = pjC + \frac{p_g L}{jC} \left(\frac{H^2}{B} - p^2I\right) - \frac{\mu H}{pB} \, ,$$

(756)

$$d = -\frac{g R}{jC} \left(\frac{H^2}{B} - p^2I\right).$$

The following two equations are necessary in order that (755) be satisfied:

$$(a \cos \delta - b \sin \delta) \theta_0 = c \psi_0,$$

$$(a \sin \delta + b \cos \delta) \theta_0 = d \psi_0.$$

(757)

From these equations we obtain

$$(a^2 + b^2) \theta_0 \cos \delta = (ac + bd) \psi_0,$$

$$(a^2 + b^2) \theta_0 \sin \delta = (ad - bc) \psi_0$$

(758)

205

so that

$$\psi_0 = \frac{a^2 + b^2}{\sqrt{(ac + bd)^2 + (ad - bc)^2}}\,\theta_0,\qquad(759)$$

or

$$\psi_0 = \sqrt{\frac{a^2 + b^2}{c^2 + d^2}}\,\theta_0.\qquad(760)$$

This result can also be obtained directly from (755).

The angle of phase shift δ is found from (758).

It follows from (760) that the amplitude of the forced oscillations ψ_0 increases inversely to c and d.

In accordance with (670),

$$\frac{H^2}{B} = v^2 I,\qquad(761)$$

and since usually $v > p$, it follows that

$$\frac{H^2}{B} - p^2 I > 0.\qquad(762)$$

It follows from the fourth of formulas (756) that d decreases in magnitude inversely to the moment of inertia B.

The same is true for c, since the last term in the third of equations (756),

$$-\frac{\mu H}{pB},$$

is much larger than the sum of the remaining terms.

It was shown in the last section that the damping of the natural oscillations of the gyroscopic frame can be improved by increasing the moment of inertia B of the gyro housings; this, however, causes an increase in the amplitude of the forced oscillations of the gyroscopic frame during rolling.

If as a first approximation the frequency p of the roll of the base is neglected in comparison with the frequency v of the natural oscillations of the frame, and if it is assumed in addition that $L \cong 0$, then (756) becomes

$$a = jCp,$$

$$b = \frac{(j + 1)\,p^2\theta_g R}{C},$$

$$c = pjC - \frac{\mu H}{pB},\qquad(763)$$

$$d = -\frac{g R H^2}{jCB},$$

and the following approximate expression is obtained from (760) for the amplitude ψ_0 of the forced oscillations:

$$\psi_0 = \theta_0 \sqrt{\frac{p^2 j^2 C^2 + \left[\dfrac{(j+1)\,p^2\theta_g R}{C}\right]^2}{\left(pjC - \dfrac{\mu H}{pB}\right)^2 + \left(\dfrac{g R H^2}{jCB}\right)^2}}.\qquad(764)$$

This expression can be simplified still further. In fact, the product $p^2 j^2 C^2$ is considerably larger than the term

$$\left[\frac{(j+1)\,p^2\theta_g R}{C}\right]^2.$$

206

(This will be shown below in a numerical example.) However, the ratio

$$\frac{pH}{pB}$$

is many times larger than the term pjC in the denominator. Expression (764) can therefore be replaced in a first approximation by

$$\phi_0 = \frac{p^2 j^2 C^2 B}{H \sqrt{(\mu j C)^2 + (g R p H)^2}} \theta_0. \tag{765}$$

This formula is suitable and convenient for preliminary calculations.

Coulomb friction in the bearings of the frame suspension and the gyro housings will now be taken into account. It can be assumed with sufficient accuracy that if Coulomb friction is not excessive the forced oscillations of the frame will remain almost harmonic if the ship's roll obeys (742). Consider, for instance, the moment about the axes of the gyro housings due to friction:

$$-M_y \, sign \, \frac{d\beta}{dt}. \tag{766}$$

We assume that the following expression can be written for β:

$$\beta = \beta^0 \sin(pt + \delta), \quad \frac{d\beta}{dt} = p\beta^0 \cos(pt + \delta), \quad \beta^0 > 0. \tag{767}$$

Since the function

$$sign \, \frac{d\beta}{dt} = sign \, [p\beta^0 \cos(pt + \delta)] = sign \, [\cos(pt + \delta)] \tag{768}$$

is periodic, it can be represented as a trigonometric series

$$sign \, [\cos(pt + \delta)] = \frac{4}{\pi} \left[\cos(pt + \delta) - \frac{\cos 3(pt + \delta)}{3} - \cdots \right]. \tag{769}$$

The following approximation is obtained from (767) and (769) by retaining only the first term of the series:

$$-M_y \, sign \, \frac{d\beta}{dt} \cong -\frac{4M_y}{\pi p \beta^0} \frac{d\beta}{dt}. \tag{770}$$

The Coulomb friction in the bearings of the gyro housings can therefore be approximated by an equivalent viscous friction, the viscosity depending on the frequency and amplitude of the forced oscillations.

The case of the moment due to friction in the bearings of the frame itself (the stabilization axis) is different since the angular velocity of the journal relative to the bearing is mainly determined by the tilting of the frame base about the stabilization axis. The motion of the frame relative to the Earth, which is of the order of several minutes of arc per minute of time, can be neglected. For this reason the friction in the stabilization-axis bearings is given in (749) by the term $M_z \, sign \, \frac{d\theta}{dt}$, and not $-M_z \, sign \, \frac{d\epsilon}{dt}$ as would follow from the more accurate equations (745).

The following approximation is obtained by calculations similar to the above, assuming harmonic rolling of the frame base according to (742):

$$M_z \, sign \, \frac{d\theta}{dt} \cong \frac{4M_z}{\pi p \theta_0} \frac{d\theta}{dt} = -\frac{4M_z}{\pi} \sin(pt + \delta). \tag{771}$$

It follows from (770) and (771) that equations (749) can be replaced by

the following equations:

$$I \frac{d^2\psi}{dt^2} + H \frac{d\beta}{dt} - \frac{jC}{g} i = - \frac{4M_z}{\pi} \sin(pt + \delta) -$$
$$- j(j+1)\Theta p^2 \theta_0 \cos(pt + \delta);$$

$$B \frac{d^2\beta}{dt^2} - H \frac{d\psi}{dt} = - \frac{4M_y}{\pi p \theta_0} \frac{d\beta}{dt} ; \tag{772}$$

$$L \frac{di}{dt} + Ri + jC \frac{d\psi}{dt} + \mu\beta = -pjC\theta_0 \sin(pt + \delta).$$

These equations can be solved as follows. First, M_z and M_y are assumed to be zero, the amplitudes ψ_0 and β_0 are determined by the method given by (760) and (753), and the phase-shift angle δ from (758). The value obtained for β_0 is then substituted in the right-hand side of the second of equations (772), and the problem of forced oscillations in the presence of a moment (770) due to friction and an additional perturbation moment (771) is solved. If the values ψ_1 and β_1 obtained for the amplitudes differ considerably from ψ_0 and β_0, the calculation is repeated.

The numerical solution of system (772) is most simple when complex numbers are used. We transfer the time origin so that $\delta = 0$, and replace $\cos pt$ and $\sin pt$ by the exponential functions e^{ipt} and $- ie^{ipt}$ whose real parts they represent. Lastly we replace the variables in (772) by the complex variables

$$\psi \to X e^{ipt};$$
$$\beta \to Y e^{ipt}; \tag{773}$$
$$i \to Z e^{ipt},$$

the complex numbers X, Y, Z being the new unknowns. Here i denotes the current intensity in the armature circuit, previously denoted by i.

Inserting (773) into (772), the following three algebraic equations in the three unknowns X, Y, Z are obtained when the common factor e^{ipt} is omitted:

$$-p^2 I X + ipHY - \frac{iC}{g} Z = -i \frac{4M_z}{\pi} - j(j+1)\Theta p^2 \theta_0,$$

$$-ipHX + \left(-p^2 B + i \frac{4M_y}{\pi\theta_0}\right)Y = 0, \tag{774}$$

$$ipjCX + \mu Y + (R + ipL)Z = ipjC\theta_0.$$

Since some of the coefficients in (774) are complex numbers, it is simplest to solve by means of determinants:

$$X = \frac{1}{\Delta} \begin{vmatrix} i \frac{4M_z}{\pi} - j(j+1)\Theta p^2 \theta_0 & ipH & -\frac{iC}{g} \\ 0 & -p^2 B + i \frac{4M_y}{\pi\theta_0} & 0 \\ ipjC\theta_0 & \mu & R + ipL \end{vmatrix} \tag{775}$$

$$Y = \frac{1}{\Delta} \begin{vmatrix} -p^2 I & i\frac{4M_z}{\pi} - j(j+1)\Theta p^2 \theta_0 & -\frac{iC}{g} \\ -ipH & 0 & 0 \\ ipjC & ipjC\theta_0 & R + ipL \end{vmatrix} \tag{776}$$

208

$$Z = \frac{1}{\Delta} \begin{vmatrix} -p^2 I & ipH & i\frac{4M_s}{\pi} - i(j+1)\theta p^2\theta_0 \\ -ipH & -p^2 B + i\frac{4M_y}{\pi\beta_0} & 0 \\ ipjC & \mu & ipjC\theta_0 \end{vmatrix} \qquad (777)$$

where

$$\Delta = \begin{vmatrix} -p^2 I & ipH & -\frac{jC}{g} \\ -ipH & -p^2 B + i\frac{4M_y}{\pi\beta_0} & 0 \\ ipjC & \mu & R + ipL \end{vmatrix} \qquad (778)$$

Let X_1, Y_1, Z_1 be the real parts and X_2, Y_2, Z_2 the imaginary parts of the complex magnitudes X, Y, and Z. It can be shown that the solution of (772) is then,

$$\psi = X_1 \cos pt - X_2 \sin pt,$$
$$\beta = Y_1 \cos pt - Y_2 \sin pt, \qquad (779)$$
$$i = Z_1 \cos pt - Z_2 \sin pt.$$

The amplitude and phase of the variables ψ, β, and i can now be found. Assume, for instance, that

$$\beta = \beta_1 \cos(pt + \epsilon). \qquad (780)$$

It then follows that

$$\beta_1 = \sqrt{Y_1^2 + Y_2^2},$$
$$\cos \epsilon = \frac{Y_1}{\sqrt{Y_1^2 + Y_2^2}}, \quad \sin \epsilon = \frac{Y_2}{\sqrt{Y_1^2 + Y_2^2}}. \qquad (781)$$

Similar formulas can be obtained also for ψ and i.

If the value of β_1 differs considerably from β_0 obtained from (753) and (760), β_1 is substituted for β_0 in the second of equations (772) and the calculation repeated.

The terms containing L, M_y, I, and Θ in the determinants (775) $-$ (778) and the term containing B in the determinant (778), can be neglected without greatly reducing the accuracy of the calculations, as will be shown in an example. The following approximate formulas for ψ_1 and β_1 are then obtained:

$$\psi_1 = \frac{p^2 B \left(j^2 C^2 - \frac{4gRM_s}{\pi\theta_0 p} \right)}{H \sqrt{(\mu j C)^2 + (gRpH)^2}} \, \theta_0; \qquad (782)$$

$$\beta_1 = \frac{H}{pB} \, \psi_1. \qquad (783)$$

For $M_s = 0$, (782) becomes (765), while (783) is similar to (753).
Numerical example. Let

$$I = I_{\xi'} + 2I_{s'} + 2A + j^2\Theta = 5 \, \text{kgm sec}^2; \quad j = 100;$$
$$B = 0.05 \, \text{kgm sec}^2; \quad \Theta = 2.5 \cdot 10^{-5} \, \text{kgm sec}^2;$$
$$H = 10 \, \text{kgm sec}; \quad M_s = 0.5 \, \text{kgm}; \quad M_y = 0.001 \, \text{kgm};$$

209

$$C = 0.50 \text{ vsec}; \mu = 10 \text{ v}; \quad R = 10 \Omega; \; ; \quad L = 0.1 \text{ h};$$
$$\theta_0 = 0.2 \; (\sim 12°); \quad g = 9.8 \text{ m/sec}^2;$$
$$p = 0.6 \text{ sec}^{-1} \text{ (period of roll 10.47 sec)}.$$

The amplitudes of the forced oscillations obtained assuming that $M_x = M_y = 0$, i.e., by (760) and (753), are

$$\psi_0 = \theta_0 \sqrt{\frac{a^2 + b^2}{c^2 + d^2}} = 0.001174 \, (4'),$$

$$\beta_0 = \frac{H}{pB} \, \psi_0 = 0.391 \, (22° \, 25').$$

By (756)

$$a = jpC - \frac{gL \, (j+1) \, p^3 \theta}{C} = 30.0 - 0.00107;$$

$$b = \frac{(j+1) \, \theta p^2 g R}{C} = 0.1783;$$

$$c = pjC + \frac{pgL}{jC} \left(\frac{H^2}{B} - p^2 I \right) - \frac{\mu H}{pB} = 30.0 + 23.6 - 3333;$$

$$d = -\frac{gR}{jC} \left(\frac{H^2}{B} - p^2 I \right) = -3920.$$

The phase shift angle δ is found using (758):

$$\delta = 229°45'.$$

If it is assumed, in accordance with (742), that

$$\theta = \theta_0 \cos \, (pt + \delta) = 0.2 \; \cos \, (pt + 229°45'),$$

then by (751) and (752)

$$\psi = \psi_0 \cos \, pt = 0.001174 \cos \, pt,$$
$$\beta = \beta_0 \sin \, pt = 0.391 \sin \, pt.$$

The approximate formulas (764) and (765) give the following values for ψ_0:

$$\psi_0 = \theta_0 \sqrt{\frac{p^2 j^2 C^2 + \left[\frac{(j+1) \, \theta p^2 g R}{C} \right]^2}{\left(pjC - \frac{\mu H}{pB} \right)^2 + \left(\frac{gRH^2}{jCB} \right)^2}} = 0.001168,$$

or

$$\psi_0 = \frac{p^2 j^2 C^3 B}{H \sqrt{(\mu jC)^2 + (gRpH)^2}} \, \theta_0 = 0.001165.$$

To allow for Coulomb friction in the suspension we must use (775) — (778). In a first approximation for $\beta_0 = 0.391$, these become:

$$\begin{vmatrix} -p^2 I & ipH & -\dfrac{jC}{g} \\[2mm] -ipH & -p^2 B + i \dfrac{4M_y}{\pi \beta_0} & 0 \\[2mm] ipjC & \mu & R + ipL \end{vmatrix} = \Delta = -360 + i \, 301$$

210

$$\begin{vmatrix} i\,\dfrac{4M_{\varepsilon}}{\pi} - j\,(j+1)\,\Theta p^2\theta_0 & ipH & -\dfrac{iC}{\mathscr{g}} \\[4pt] 0 & -p^2B + i\,\dfrac{4M_y}{\pi\beta_0} & 0 \\[4pt] ipjC\theta_0 & \mu & R + ipL \end{vmatrix} = -0.116 - i0.666$$

$$\begin{vmatrix} -p^2I & i\,\dfrac{4M_{\varepsilon}}{\pi} - j\,(j+1)\,\Theta p^2\theta_0 & -\dfrac{iC}{\mathscr{g}} \\[4pt] -ipH & 0 & 0 \\[4pt] ipjC & ipjC\theta_0 & R + ipL \end{vmatrix} = -222 - i\,1.32$$

$$X = -0.000720 + i0.00125; \quad Y = 0.361 + i\,0.305.$$

Furthermore, by (779),

$$\psi = -0.000720 \cos pt - 0.00125 \sin pt,$$

$$\beta = 0.361 \cos pt - 0.305 \sin pt.$$

When Coulomb friction is allowed for in the suspension, the amplitudes in a first approximation are:

$$\psi_1 = 0.00144, \quad \beta_1 = 0.473.$$

These values differ only little from ψ_0 and β_0, and a second approximation is therefore unnecessary.

The approximate formulas (782) and (783) give

$$\psi_1 = 0.00141, \quad \beta_1 = 0.470.$$

Similar calculations for the current intensity i in the armature circuit of the stabilizing motor lead to the following result:

$$i = -0.357 \cos pt - 0.301 \sin pt.$$

§ 4. Behavior of a directional gyro on a rolling base

Approximate solutions such as those given above, based on the assumption that the motion of the gyroscopic system is harmonic, are often insufficient. In such cases it is customary to use successive approximations, based on treating the separate terms of the differential equations describing the given gyroscopic system as external forces. The laws of variation of these forces with time gain in accuracy with each subsequent approximation. From the mathematical point of view this method represents a variant of the small-parameter method.

Since as a rule far-reaching simplifying assumptions are made when setting up the differential equations of motion of the system, the question of the convergence of the successive approximations has hardly any meaning. In particular, there is no sense in continuing with further approximations when the difference between successive solutions lies within the limits of the accuracy with which the coefficients of the differential equations or the functional expressions of physical laws (friction, virtual forces, etc) appearing in these equations have been given.

211

The suitability of the approximate solutions is usually determined by comparing them with the results of corresponding measurements on gyroscopic devices operating under laboratory conditions.

The method of successive approximations is used in this section to investigate the causes of azimuthal motion of a directional gyro assembled as shown in Figure 168. This motion was so large when this particular directional gyro was tested on a rolling base that it became necessary to abandon the design. It will be shown below that a satisfactory performance can only be expected from such a device if the axis of the gyro's outer gimbal ring is stabilized in the vertical direction.
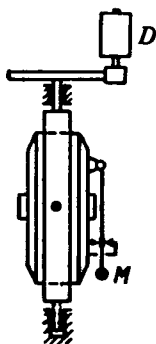
We set up the equations of motion of the directional gyro, assuming that the base on which it is mounted rolls about the horizontal axis ξ of the fixed coordinate system $\xi\eta\zeta$, and that a corrective moment of constant magnitude is applied to the pivot axis of the outer ring by an electric motor D. The sign of the moment is determined by the position of the corrective pendulum M mounted on the gyro housing (Figure 168).

The Earth's rotation will be neglected, since the apparent motion of the directional gyro produced by the vertical component of its angular velocity can be made to vanish by means of a special weight secured to the gyro housing. The moment about the gyro-housing axis due to this weight must be such as to make the angular velocity of precession about the outer-ring pivot axis caused by the weight equal to the vertical component of the Earth's angular velocity. The horizontal component of this velocity can be neglected since it is small compared with the angular velocities relative to the Earth of the base, the outer ring, and the gyro housing. The angular velocity of the housing is mainly determined by the torque of the stabilization motor, the inertia of its rotor, and the friction in the bearings of the outer-ring pivots.

Fix a moving coordinate system $\xi'\eta'\zeta'$ to the base of the device (Figure 169) in such a way that the ξ'-axis passes through the center of the gyro gimbals and is parallel to the ξ-axis about which the base rolls, the ζ'-axis being parallel to the outer-ring pivot axis $\mathbf{s'}$. The vertical ζ-axis of the fixed system $\xi\eta\zeta$ and the ζ_1-axis of the auxiliary system $\xi_1\eta_1\zeta_1$ lie in the "rolling plane" $\eta'\zeta'$; the ξ_1-axis of the auxiliary system is horizontal and coincides with the ξ'-axis.

Let ψ denote the angle which the base plane makes with the horizontal plane (ψ is the angle formed by the ζ'-axis with the vertical axis ζ_1 of the $\xi_1\eta_1\zeta_1$ coordinate system moving translationally). Fix a coordinate system $x'y'z'$ to the outer ring of the gyro in such a way that the x'-axis is parallel to the gyro housing axis and the z'-axis parallel to the outer-ring pivot axis (as already mentioned above).

Let θ be the angle between the x'- and ξ'-axes (Figure 169). For $\psi = 0$ the angle θ defines the gyro position in azimuth.

The velocity of the coordinate system $x'y'z'$ can be considered to consist of an angular velocity $\frac{d\theta}{dt}$ relative to the $\xi'\eta'\zeta'$ system and an angular velocity $\frac{d\psi}{dt}$ jointly with this latter system. Since the vector of angular velocity $\frac{d\theta}{dt}$ is directed along the ζ'-axis (parallel to the z'-axis), and that of $\frac{d\psi}{dt}$ along the

ζ'-axis (Figure 169), the projections on its axes of the total angular velocity of the $x'y'z'$ system are respectively

$$\frac{d\psi}{dt}\cos\theta, \quad -\frac{d\psi}{dt}\sin\theta, \quad \frac{d\theta}{dt}. \tag{784}$$

Fix now a coordinate system xyz to the gyro housing, with y-axis parallel to the rotor's axis of rotation and in the direction of the angular momentum vector H, the x-axis being parallel to the x'-axis (Figure 170). Let φ (Figure 170) denote the angle between the y- and y'-axes, thus defining the tilting of the housing relative to the outer ring. The absolute angular velocity
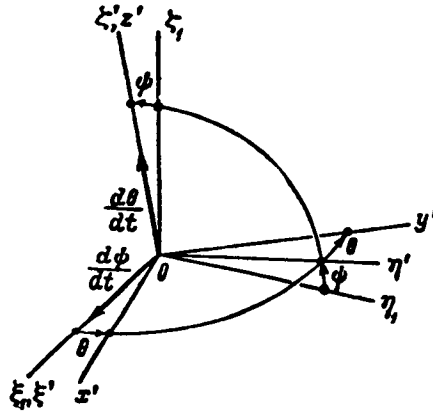
FIGURE 169

of the gyro housing is equal to the geometric sum of the absolute angular velocity of the coordinate system $x'y'z'$ and the angular velocity $\frac{d\varphi}{dt}$ of the housing relative to this system, whose vector is directed along the x-axis which coincides with the x'-axis. The projections of the angular velocity of the system $x'y'z'$ on the axes x, y, and z are equal to the sums of the projections on these axes of the components directed along the axes x', y', and z' (Figure 170). These sums are respectively

$$\frac{d\psi}{dt}\cos\theta, \quad -\frac{d\psi}{dt}\sin\theta\cos\varphi + \frac{d\theta}{dt}\sin\varphi,$$
$$\frac{d\psi}{dt}\sin\theta\sin\varphi + \frac{d\theta}{dt}\cos\varphi. \tag{785}$$

It follows that the projections of the angular velocity of the coordinate system xyz on its own axes are

$$p = \frac{d\psi}{dt}\cos\theta + \frac{d\varphi}{dt},$$
$$q = -\frac{d\psi}{dt}\sin\theta\cos\varphi + \frac{d\theta}{dt}\sin\varphi, \tag{786}$$
$$r = \frac{d\psi}{dt}\sin\theta\sin\varphi + \frac{d\theta}{dt}\cos\varphi.$$

Since the angular momentum H of the gyro rotor is of constant magnitude and its vector is directed along the y-axis, the projections of the velocity of

213

its vertex on the axes x, y, and z (Figure 171) are respectively

$$-rH, \quad 0, \quad pH. \tag{787}$$

These projections are equal (cf. Chapter IV, § 1) to the sums of the moments about the corresponding axes due to the forces acting on the gyro housing. The moments about the x-axis are due to friction in the bearings of the housing spindle. This friction being very small, it can be assumed with an accuracy sufficient for our investigations that

$$-rH = -\left(\frac{d\psi}{dt}\sin\theta\sin\varphi + \frac{d\theta}{dt}\cos\varphi\right)H = 0, \tag{788}$$

whence

$$\frac{d\theta}{dt} = -\frac{d\psi}{dt}\sin\theta\,\mathrm{tg}\,\varphi. \tag{789}$$

Let N be the sum of the moments about the z-axis due to the forces applied to the gyro housing by the outer ring. It follows that

$$pH = \left(\frac{d\psi}{dt}\cos\theta + \frac{d\varphi}{dt}\right)H = N. \tag{790}$$

Let N' denote the sum of the moments about the z'-axis due to all the forces except the housing reaction acting on the outer ring. When the
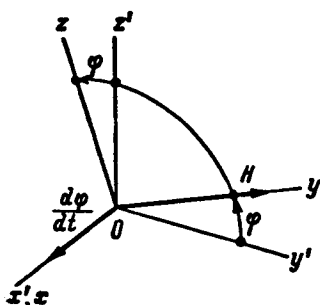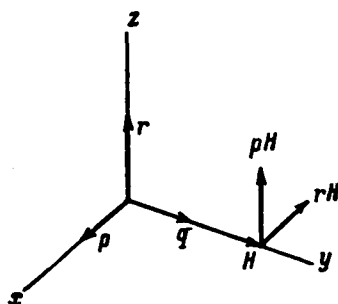

FIGURE 170

FIGURE 171

inertia of this ring is neglected, it is found that the sum of the moments about the z'-axis due to the forces acting on the ring (Figure 172) is zero.

$$N' - N\cos\varphi = 0. \tag{791}$$

The moment N' consists mainly of the moments due to inertia of the rotating parts linked kinematically with the ring (stabilization motor rotor, follow-up system pick-up, etc) and friction in the bearings of these parts (referred to the outer-ring pivot axis), and also the stabilizing moment exerted by the stabilization motor:

$$N' = -I\frac{d^2\psi}{dt^2} - F\,\mathrm{sign}\,\frac{d\theta}{dt} \pm K, \tag{792}$$

where I is the moment of inertia of the whole system about the outer ring axis, F is the moment due to friction, and K is the stabilizing moment whose sign depends on the position of the corrective pendulum fixed to the gyro housing.

214

. Assuming φ to be small, the following approximation is true:

$$N' = N, \qquad (793)$$

so that by (790),

$$\left(\frac{d\psi}{dt} \cos \theta + \frac{d\varphi}{dt} \right) H = -I \frac{d^2\theta}{dt^2} - F \operatorname{sign} \frac{d\theta}{dt} \pm K. \qquad (794)$$

We introduce the notation

$$a = \frac{I}{H}, \quad \mu = \frac{F}{H}, \quad \nu = \frac{K}{H}. \qquad (795)$$

The following two differential equations describing the motion of the directional gyro are then obtained from (789) and (794):

$$\frac{d\theta}{dt} = -\frac{d\psi}{dt} \sin \theta \, \operatorname{tg} \varphi,$$

$$\frac{d\varphi}{dt} + \frac{d\psi}{dt} \cos \theta = -a \frac{d^2\theta}{dt^2} - \mu \operatorname{sign} \frac{d\theta}{dt} \pm \nu. \qquad (796)$$

The corrective pendulum is mounted in such a way that the moment exerted by the stabilization motor when the base is immobile and the rotor axis not horizontal, tends to restore the rotor axis to the horizontal position. In particular, on a horizontal base ($\psi = 0$), the sign of ν in the second of equations (796) must be opposite to the sign of φ. For instance if $\varphi > 0$, the left-hand contacts of the corrective pendulum are closed (Figure 172);
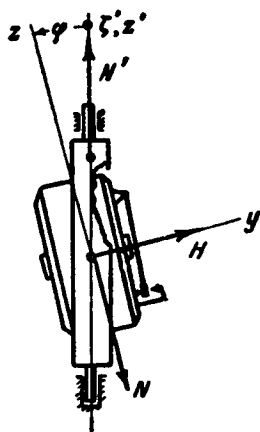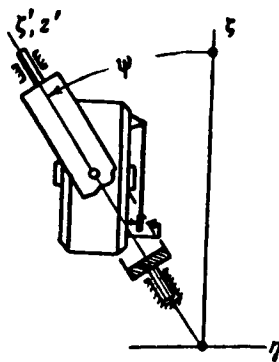

FIGURE 172

FIGURE 173

when the friction in the outer-ring pivot bearings is neglected, (796) becomes

$$\frac{d\theta}{dt} = 0,$$

$$\frac{d\varphi}{dt} = -\nu. \qquad (797)$$

During rolling, the pendulum will close its contacts alternately, depending on the direction of the inertia forces due to the translational motion of the instrument.

It is easily seen (Figure 173) that when

$$-\frac{\pi}{2} < \theta < \frac{\pi}{2}, \tag{798}$$

the inertia forces due to translational motion are directed to the left when $\psi > 0$ (Figure 173), if the gyro housing is viewed from the positive ζ-axis, and if it is assumed that rolling obeys the law

$$\psi = \psi_0 \sin pt, \tag{799}$$

where ψ_0 is the amplitude of rolling, and p its frequency.

In fact, in this case the projection of the translational acceleration on the η-axis is positive. The projection of the inertia force, on the other hand, is negative. It follows that when $\psi > 0$ and φ is small, the pendulum will press mainly against the left contact, so that the sign of v in (796) must be negative. When rolling takes place, the equations of motion (796) of the directional gyro must be written in the form

$$\frac{d\theta}{dt} = -\frac{d\psi}{dt} \sin \theta \, \mathrm{tg}\, \varphi,$$

$$\frac{d\varphi}{dt} + \frac{d\psi}{dt} \cos \theta = -a \frac{d^2\theta}{dt^2} - \mu \, sign \, \frac{d\theta}{dt} - v \, sign \, \psi, \tag{800}$$

where ψ is defined by (799) and θ is within the limits given by (798).

It is very difficult to solve these equations accurately. Accordingly, the influence of each of the terms on the right-hand side of the second equation on the azimuthal motion of the gyro will be analyzed approximately and independently of the other terms: only the influence of inertia forces $\left(-a \frac{d^2\theta}{dt^2} \right)$, friction $\left(-\mu \, sign \, \frac{d\theta}{dt} \right)$, or the corrective pendulum $(-v \, sign \, \psi)$ will be taken into account.

Since the angle θ changes comparatively slowly, the functions $\sin \theta$ and $\cos \theta$ in (800) can be considered as constants in the calculation of $\frac{d\theta}{dt}$ and $\frac{d\varphi}{dt}$. In addition, the expression

$$\mathrm{tg}\, \varphi \cong \varphi, \tag{801}$$

can be inserted into these equations since φ is small, and all terms after the first in the Fourier series for $sign \, \psi$ [cf. (769)],

$$sign \, \psi = sign \, (\psi_0 \sin pt) = \frac{4}{\pi} \sin pt + \frac{4}{3\pi} \sin 3 pt + \ldots \tag{802}$$

can be neglected.

It follows from (800) and from the assumptions just made that the following differential equations account for the influence of the corrective pendulum only:

$$\frac{d\theta}{dt} = -\frac{d\psi}{dt} \varphi \sin \theta,$$

$$\frac{d\varphi}{dt} + \frac{d\psi}{dt} \cos \theta = -\frac{4v}{\pi} \sin pt. \tag{803}$$

The approximate integration of the second of equations (803) (assuming $\theta = \mathrm{const}$) gives

$$\varphi = a + \frac{4v}{\pi p} \cos pt - \psi \cos \theta. \tag{804}$$

216

As first approximation we neglect the term $-a\frac{d^2\theta}{dt^2}$. Integrating the second, of equations (809) yields

$$\varphi = a - \psi \cos \theta. \tag{810}$$

Inserting this expression into the first of equations (809) leads to

$$\frac{d\theta}{dt} = -\frac{d\psi}{dt}\,(a - \psi \cos \theta) \sin \theta. \tag{811}$$

As second approximation the term $-a\frac{d^2\theta}{dt^2}$ is retained in the second of equations (809). Using (811), integration yields

$$\varphi = a - \psi \cos \theta - a\frac{d\theta}{dt} =$$

$$= a - \psi \cos \theta + a\frac{d\psi}{dt}\,(a - \psi \cos \theta) \sin \theta. \tag{812}$$

Inserting this expression into the first of equations (809) gives the second approximation for $\frac{d\theta}{dt}$:

$$\frac{d\theta}{dt} = -\frac{d\psi}{dt} \sin \theta \left(a - \psi \cos \theta + a\frac{d\psi}{dt} a \sin \theta - a\psi\frac{d\psi}{dt}\sin\theta\cos\theta \right). \tag{813}$$

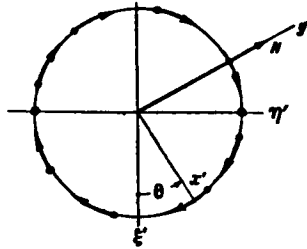Substituting the expression $\psi_0 \sin pt$ for ψ, the following equation is then

FIGURE 175

obtained for the angular velocity of deviation in azimuth of the outer gimbal ring:

$$\frac{d\theta}{dt} = -p\psi_0 a \sin \theta \cos pt + p\psi_0^2 \cos \theta \sin \theta \cos pt \sin pt -$$

$$- ap^2\psi_0^2 a \sin^2\theta \cos^2 pt + ap^2\psi_0^3 \cos^2 pt \sin pt \cos \theta \sin^2 \theta, \tag{814}$$

which can be reduced to

$$\frac{d\theta}{dt} = -p\psi_0 a \sin \theta \cos pt + \frac{1}{2} p\psi_0^2 \cos \theta \sin \theta \sin 2pt +$$

$$+ \frac{a}{4} p^2\psi_0^3 \cos \theta \sin^2 \theta\,(\sin pt + \sin 3pt) -$$

$$- \frac{a}{2} p^2\psi_0^2 a \sin^2\theta \cos 2pt - \frac{a}{2} p^2\psi_0^2 a \sin^2 \theta. \tag{815}$$

All terms in (815) except the last are periodic functions of time and do not therefore influence the continuous deviation in azimuth of the gyro.

The integration constant α is equal to the mean value of the angle between the gyro-rotor axis and the horizontal plane, and also, by virtue of (799), to the mean value of φ.

Inserting (804) into the first of equations (803) gives

$$\frac{d\theta}{dt} = - \frac{d\psi}{dt}\left(\alpha + \frac{4v}{\pi p}\cos pt - \psi \cos \theta\right)\sin \theta, \qquad (805)$$

which by virtue of (799) is transformed into

$$\frac{d\theta}{dt} = -pa\psi_0 \cos pt \sin \theta + p\psi_0^2 \cos pt \sin pt \cos \theta \sin \theta - $$

$$- \frac{4v}{\pi}\psi_0 \cos^2 pt \sin \theta, \qquad (806)$$

or,

$$\frac{d\theta}{dt} = -pa\psi_0 \sin \theta \cos pt + \frac{1}{4}p\psi_0^2 \sin 2\theta \sin 2pt - $$

$$- \frac{2v}{\pi}\psi_0 \sin \theta \cos 2pt - \frac{2v}{\pi}\psi_0 \sin \theta. \qquad (807)$$

The first three terms on the right-hand side of (807) define a periodic variation of θ while the base rolls. The last term defines a continuous azimuthal deviation of the gyro at an angular velocity

$$- \frac{2v}{\pi}\psi_0 \sin \theta. \qquad (808)$$

If the leads of the pendulum contacts are reversed, the gyro's deviation in azimuth must change direction. This has been confirmed experimentally.
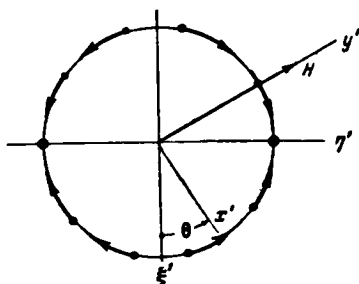

FIGURE 174

Figure 174 shows the motion in azimuth of the gyro in different quadrants under the influence of the stabilization motor, controlled by the corrective pendulum. The rotor axis tends by the shortest path to attain the rolling plane $\eta'\zeta'$ perpendicular to the ξ-axis about which the gyro base rolls.

Consider now the influence of inertia on the azimuthal motion when the outer gimbal ring tilts about its axis. Replacing the term $-\frac{4v}{\pi}\sin pt$ in the second of equations (803) by $-a\frac{d^2\theta}{dt^2}$, we obtain

$$\frac{d\theta}{dt} = -\frac{d\psi}{dt}\varphi \sin \theta, \qquad (809)$$

$$\frac{d\varphi}{dt} + \frac{d\psi}{dt}\cos \theta = -a\frac{d^2\theta}{dt^2}.$$

217

This motion is determined by the last term alone, i.e.,

$$-\frac{a}{2}\,p^2\psi_0^2\alpha\sin^2\theta. \tag{816}$$

The gyro's deviation in azimuth during rolling, caused by the inertia of the outer gimbal ring, is shown in Figure 175 $(a>0)$.

It remains to investigate the influence of friction in the outer-ring pivot bearings on the azimuthal motion of the gyro.

The relevant differential equations are

$$\frac{d\theta}{dt}=-\frac{d\psi}{dt}\,\varphi\sin\theta,$$

$$\frac{d\psi}{dt}\cos\theta+\frac{d\varphi}{dt}=-\mu\,sign\frac{d\theta}{dt}. \tag{817}$$

If instead of the Coulomb friction in (817) we substitute viscous friction characterized by a suitable viscosity coefficient η we can expect that the results will not be altered significantly. The following equations will therefore be considered:

$$\frac{d\theta}{dt}=-\frac{d\psi}{dt}\,\varphi\sin\theta,$$

$$\frac{d\psi}{dt}\cos\theta+\frac{d\varphi}{dt}=-\eta\frac{d\theta}{dt}. \tag{818}$$

As a first approximation neglect the influence of friction on the gyro motion, and assume, as before, that θ is a slowly varying function of time. An expression identical with (810) is then obtained:

$$\varphi=\alpha-\psi\cos\theta.$$

Using it, we again obtain (811)

$$\frac{d\theta}{dt}=-\frac{d\psi}{dt}\,(\alpha-\psi\cos\theta)\sin\theta.$$

Integrating this expression under the assumption $\theta=$ const yields

$$\theta=-\alpha\psi\sin\theta+\frac{1}{2}\,\psi^2\sin\theta\cos\theta+\beta, \tag{819}$$

where β is a constant.

The following expression is obtained from (818) and (819) as a second approximation:

$$\varphi=\alpha-\psi\cos\theta-\eta\theta=\alpha-\psi\cos\theta+\eta\alpha\psi\sin\theta-$$

$$-\frac{1}{2}\,\eta\psi^2\sin\theta\cos\theta, \tag{820}$$

so that

$$\frac{d\theta}{dt}=-\frac{d\psi}{dt}\,\varphi\sin\theta=$$

$$=-\frac{d\psi}{dt}\sin\theta\left(\alpha-\psi\cos\theta+\eta\alpha\psi\sin\theta-\frac{1}{2}\,\eta\psi^2\sin\theta\cos\theta\right). \tag{821}$$

Inserting (799) finally reduces this expression to the form

$$\frac{d\theta}{dt}=-p\psi_0\alpha\sin\theta\cos pt+\frac{1}{2}\,p\psi_0^2(\sin\theta\cos\theta-\eta\alpha\sin^2\theta)\sin 2pt+$$

$$+\frac{1}{8}\,\eta p\psi_0^3\sin^2\theta\cos\theta(\cos pt-\cos 3pt). \tag{822}$$

All terms on the right-hand side of this expression are periodic func-
tions of time whose mean values are zero.

It follows that friction does not cause the deviation in azimuth of the
directional gyro during rolling. The main causes of this deviation are the
influence of inertia when the outer gimbal ring is tilted relative to the
instrument body, and the moment applied to the outer ring by the stabiliza-
tion motor when the latter is controlled by the corrective pendulum.

It can be shown that although the problem is nonlinear, the total angular
velocity of deviation in azimuth of the directional gyro is approximately

$$\frac{d\theta}{dt} \cong -\frac{a}{2} p^2 \psi_0^2 a \sin^2 \theta - \frac{2\nu}{\pi} \psi_0 \sin \theta. \qquad (823)$$

It follows that the angular velocity of deviation is zero when $\theta=0$ and
$\theta=\pi$, i.e., when the angular momentum vector is perpendicular to the
axis of roll ξ. For other values of θ the second term is either added to,
or subtracted from the first. It may therefore happen that the angular
velocity of gyro deviation is excessive, or that it is almost zero. This is
the main reason why this design was abandoned.

Numerical example. Assume that

$$H = 500\,000\ \text{gcm sec}; \quad I = 25000\ \text{gcm sec}^2; \quad K = 5000\ \text{gcm};$$

$$\psi_0 = 0.2\ (\sim 12°); \quad a = 0.05\ (\sim 3°);$$

$$\theta = 90°; \quad p = 1.0\ \text{sec}^{-1}.$$

In this case

$$a = \frac{I}{H} = 0.05\ \text{sec}; \quad \nu = \frac{K}{H} = 0.01\ \text{sec}^{-1};$$

$$\frac{a}{2} p^2 \psi_0^2 a \sin^2 \theta = 0.00005\ \text{sec}^{-1} \cong 0.17°/\text{min};$$

$$\frac{2\nu}{\pi} \psi_0 \sin \theta = 0.001275\ \text{sec}^{-1} \cong 4.33°/\text{min}.$$

The calculated values of the deviations of the directional gyros are near
to the experimental results.

It follows that the directional gyro must either be mounted on a stabilized
base, or the parameter a (which characterizes the moment of inertia of the
outer gimbal ring and the parts linked kinematically to it) and the corrective
coefficient ν considerably reduced.

Designs of directional gyros exist in which the stabilization motor is
controlled by a special contact device connected with the housing spindle
(Figure 191). In this case the motor develops a torque moment of such a
sign that the gyro precession caused by it tends to move the axis of the gyro
rotor into a position perpendicular to the plane of the outer gimbal ring. It
can be shown that in this case the behavior of the directional gyro is similar
to that of a double-gyro frame used as gyro azimuth. The need to stabilize
the vertical axis of the frame suspension in order to avoid large deviations
in azimuth due to the so-called additional solid angle was indicated in
Chapter II, § 4. The same will obviously be true for a similar monogyro
gyroazimuth design.

It is easily seen that when rolling is not excessive

$$\gamma = \frac{w}{g} - x, \tag{825}$$

where w is the horizontal component of the acceleration of the point at which the instrument is located (caused by the ship roll), and g, the gravitational acceleration*. Assume that

$$\frac{w}{g} = \alpha \sin(pt + \delta) + \beta \sin(qt + \epsilon). \tag{826}$$

This is the case of complex rolling, in which the motion of the dynamic vertical represents the superposition of two periodic oscillations of different frequencies p and q, usually with different amplitudes α and β and phase angles δ and ϵ.

For most instruments the functional relationship $K(\gamma)$ has the form shown in Figure 176.

The region of linearity, $-\gamma_1 \leqslant \gamma \leqslant \gamma_1$, in which the corrective moment K is proportional to γ, is usually small, vanishing in certain instruments. We shall therefore assume that the corrective moment is under a so-called contact control, defined by

$$K(\gamma) = K_1 \, sign \, \gamma, \tag{827}$$

i.e.,

$$K = -K_1, \quad \text{for} \quad \gamma < 0$$

and

$$K = +K_1, \quad \text{for} \quad \gamma > 0. \tag{828}$$

Introduce the notation

$$U \cos \varphi = \mu, \tag{829}$$

$$\frac{K_1}{H} = \nu, \tag{830}$$

$$\xi = \frac{w}{g}. \tag{831}$$

Using also (825) and (827), equation (824) can be written in the following form:

$$\frac{dx}{dt} = \mu + \nu \, sign \, (\xi - x). \tag{832}$$

An elementary analysis of (832) was given by Zaitsev for simple rolling, defined by

$$\xi = \alpha \sin pt. \tag{833}$$

The large errors predicted by the theory were confirmed by experiments made by Zaitsev under laboratory conditions.

Great difficulties arise when applying Zaitsev's method to the solution of equation (832) in the case of complex rolling. The problem is therefore approached in this section in a quite different way, applying probability considerations. A remarkable result of the theory confirmed by tests of a gyrohorizon under operating conditions, is that the errors during complex rolling are much smaller than the errors during simple rolling of the same amplitude.

Consider first the elementary solution of (832) [by Zaitsev's method]. Plot a curve corresponding to equation (833) (Figure 177). Let the value

* More exactly, $\gamma = arctg \dfrac{w}{g - w'} - x$, where w' is the vertical component of this acceleration.

Chapter VI

VARIOUS PROBLEMS IN GYRO-SYSTEM MECHANICS

§ 1. Application of probability methods to determining the
errors of a gyrohorizon with contact correction
during rolling

The orientation in space of gyro axes may change due to various factors,
e.g., friction in the suspension, inertia, the Earth's rotation, imbalance,
etc (see Chapter IV). When gyros are used to stabilize a horizontal plane
on a rolling ship (or any other moving object), it becomes necessary to apply
suitable corrective moments in order to return them to their initial position.
These corrective moments are created by devices reacting to changes in
the direction of the dynamic vertical to the ship's deck*.

The rolling and pitching of the ship cause a continuous change in the
direction of the dynamic vertical, and therefore a continuous variation of
the gyros' orientation through the action of the corrective moments. This
leads to errors in the determination of the horizontal plane.

In order not to complicate the analysis, we assume that only rolling oc-
curs with zero yaw and pitch, and that the ship does not turn. The apparent
motion of the gyros will then be due to the angular velocity of the Earth and
to the action of the corrective moments. The influence of the angular veloc-
ity of the ship due to its motion along the curved surface of Earth can usually
be ignored.

Let the gyrohorizon consist of only one gyro with a vertically oriented
vector of angular momentum**, and let the axes of its gimbals be respec-
tively parallel to the longitudinal and transversal axes of the ship. Denote
by x the angle of deviation of the gyro's angular momentum vector from the
[true] vertical to port in the transverse plane of the ship, and assume that
the ship's bow points in the north-south direction. The gyro motion will
then be described by the equation

$$H\left(\frac{dx}{dt} - U\cos\varphi\right) = K(\gamma).$$ (824)

Here U is the angular velocity of Earth; φ, the local latitude; $K(\gamma)$, the
magnitude of the corrective moment; and γ, the angle between the dynamic
vertical at the point where the instrument is located and the angular mo-
mentum vector H of the gyro rotor.

* The dynamic vertical is the direction of the geometric sum of the gravitational acceleration vector
  and a vector equal and opposite in sign to the translational acceleration vector of the point at which the
  instrument is located. It is the direction of a pendulum whose period of natural oscillations is small
  compared with the period of the ship's roll.
** Different gyrohorizon designs are analyzed in the same way.

of x for $t=0$ be $x_0 > 0$ (different initial conditions are treated in the same way). In this case x will be greater than ξ at $t=0$ and for a certain time after this, and therefore

$$\xi - x < 0. \tag{834}$$

It follows then from (832) that

$$\frac{dx}{dt} = \mu - \nu. \tag{835}$$

Integrating (835), we have

$$x = x_0 - (\nu - \mu) t. \tag{836}$$

This equation is represented in Figure 177 by the straight line **AB**. It is easily seen that a condition necessary for the proper functioning of the instrument is

$$\nu > \mu; \tag{837}$$

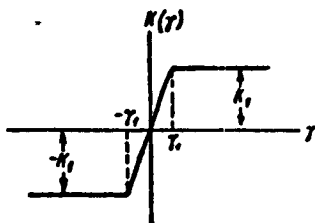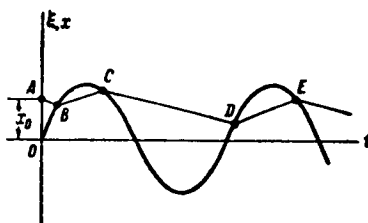this means that the corrective moment K_1 must be sufficiently large.

FIGURE 176

FIGURE 177

The line (836) intersects the curve (833) at point **B** at which the angle

$$\gamma = \xi - x \tag{838}$$

becomes zero, and then changes its sign.

From that point on x will vary (as seen from (832)) according to the law:

$$\frac{dx}{dt} = \mu + \nu. \tag{839}$$

The integral of this equation is represented in Figure 177 by the straight line **BC** having a positive slope. Point **C** corresponds to the next change in sign of the angle γ; the variation of x after this point will again be given by (835), etc.

The function $x = x(t)$ is thus represented by the broken line **ABCDE...**, whose break points lie on the sinusoid (833), and whose slope is alternately positive and negative, depending upon whether it lies below or above the sinusoid. If point **B** lies near the maximum of sinusoid (833), it may happen that at this point

$$\frac{d\xi}{dt} < \mu + \nu. \tag{840}$$

An analysis similar to that in Chapter V, § 1 shows that the line **BC** must in this case be replaced by part of the sinusoid, the position of point **C** being determined by the equation

$$\frac{d\xi}{dt} = \mu - \nu. \tag{841}$$

The function $x=x(t)$ beyond this point is as given above. This plotting method can obviously be used for any shape of the curve $\xi=\xi(t)$, including the case of complex rolling according to (826); in the latter case, however, it is difficult to draw conclusions on the position of the broken line parts.

For a sinusoid the solution of the problem is simple, since it is obvious that the broken line rapidly becomes a periodic function whose period equals that of the sinusoid (833).

Consider three consecutive break points of the line (Figure 178). Let t_1, t_2, t_3 be the abscissae and x_1, x_2, x_3 the ordinates of these points. It follows from (839) and (835) that

$$\frac{x_2-x_1}{t_2-t_1}=\mu+\nu, \tag{842}$$

$$\frac{x_3-x_2}{t_3-t_2}=\mu-\nu. \tag{843}$$

Because of the periodicity,

$$x_3=x_1, \tag{844}$$

$$t_3-t_1=\frac{2\pi}{p}. \tag{845}$$

Lastly, since the break points lie on the sinusoid (833):

$$x_1=a\sin pt_1, \tag{846}$$
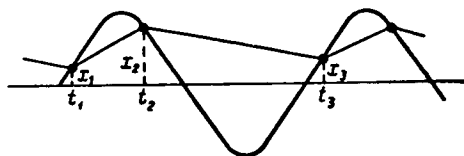
$$x_2=a\sin pt_2. \tag{847}$$

FIGURE 178

Relationships (842)—(847) form a system of six equations with six unknowns, these being the coordinates of the three break points. Equation (842) can be written

$$(x_2-x_1)=(\mu+\nu)(t_2-t_1). \tag{848}$$

Eliminating x_3 and t_3 from (843) by means of (844) and (845) yields:

$$(x_2-x_1)=(\nu-\mu)\left(\frac{2\pi}{p}+t_1-t_2\right). \tag{849}$$

It follows from (848) and (849) that

$$p(t_2-t_1)=\frac{\nu-\mu}{\nu}\pi, \tag{850}$$

and therefore

$$x_2-x_1=\frac{\nu^2-\mu^2}{p\nu}\pi. \tag{851}$$

On the other hand, by (846), (847), and (850),

$$x_2-x_1=2a\cos\left(\frac{\nu-\mu}{2\nu}\pi+pt_1\right)\sin\frac{\nu-\mu}{2\nu}\pi. \tag{852}$$

224

Thus, by (851) and (852):

$$\frac{v^2 - \mu^2}{pv}\pi = 2a \cos\left(\frac{v - \mu}{2v}\pi + pt_1\right)\sin\frac{v - \mu}{2v}\pi, \qquad (853)$$

from which t_1 can be determined.

Of particular interest is the mean deviation of the gyro axis from the [true] vertical:

$$x_{av} = \frac{z_1 + z_2}{2}. \qquad (854)$$

It follows from (846) and (847) that

$$x_{av} = a \sin p\frac{t_1 + t_2}{2}\cos p\frac{t_1 - t_2}{2}. \qquad (855)$$

Inserting (850) this expression becomes

$$x_{av} = a \sin\left(\frac{v - \mu}{2v}\pi + pt_1\right)\cos\frac{v - \mu}{2v}\pi. \qquad (856)$$

It follows from (853) that

$$\sin\left(\frac{v - \mu}{2v}\pi + pt_1\right) = \sqrt{1 - \left[\frac{(v^2 - \mu^2)\pi}{2pva\sin\frac{v - \mu}{2v}\pi}\right]^2}, \qquad (857)$$

so that (856) becomes

$$x_{av} = a \cos\frac{v - \mu}{2v}\pi \cdot \sqrt{1 - \left[\frac{\pi(v^2 - \mu^2)}{2pva\sin\frac{v - \mu}{2v}\pi}\right]^2}. \qquad (858)$$

If $\mu = 0$, i.e., if the influence of the Earth's rotation on the instrument is eliminated in some way (for instance, by a compensating moment), (858) shows, as was to be expected, that

$$x_{av} = 0. \qquad (859)$$

As is easily seen from (830), v represents the angular velocity of the correction; it is usually considerably larger than the horizontal component μ of the Earth's angular velocity. The following approximations can therefore be employed:

$$\cos\frac{v - \mu}{2v}\pi = \sin\frac{\mu\pi}{2v} \cong \frac{\mu\pi}{2v}, \qquad (860)$$

$$\sin\frac{v - \mu}{2v}\pi = \cos\frac{\mu\pi}{2v} \cong 1. \qquad (861)$$

Inserting (860) and (861) into (858) and neglecting μ^2, small compared with v^2, yields:

$$x_{av} = \frac{a\mu}{v}\cdot\frac{\pi}{2}\sqrt{1 - \left(\frac{v\pi}{2pa}\right)^2}. \qquad (862)$$

The product pa represents the angular velocity with which the dynamic vertical deviates from the true vertical. This velocity is much larger than the angular velocity v of the correction. The radical in (862) can therefore be replaced by unity. This leads to the following approximate formula first derived by Zaitsev:

$$x_{av} \cong \frac{a\mu}{v}\cdot\frac{\pi}{2}. \qquad (863)$$

225

The following numerical example will show how large the mean deviation of the angular momentum vector from the vertical can become during rolling. Assume that

$$\frac{w}{g} = a \sin pt, \quad a = 0.1, \quad p = 1.0 \sec^{-1},$$

$$\mu = 10 \ '/min, \quad \nu = 100 \ '/min.$$

It follows then from (863) that

$$x_{av} = \frac{a\mu}{\nu} \cdot \frac{\pi}{2} = 0.0157 \ (54'),$$

which represents a considerable error in the instrument indication. The exact formula (858) gives

$$x_{av} = 0.01564.$$

The second method of investigation is based on the assumption that the range of variation of x is small compared with the corresponding range of variation of ξ. In other words, it is assumed that during simple or complex rolling the deviation from the vertical of the angular momentum vector varies negligibly compared with the range deviation of the dynamic vertical. This is true for time intervals of the order of the roll period.

Integrating the equation (832), i.e.,

$$\frac{dx}{dt} = \mu + \nu \, sign \, (\xi - x),$$

from $t = 0$ to $t = T$ yields

$$\frac{x(T) - x(0)}{T} = \mu + \frac{\nu}{T} \int_0^T sign \, (\xi - x) \, dt. \tag{864}$$

The left-hand side of (864) can be neglected for sufficiently large values of T. For a steady periodic motion of the gyroscopic instrument during simple rolling of the ship, the left-hand side of (864) vanishes if T is the period of roll. Thus

$$\frac{\mu}{\nu} + \frac{1}{T} \int_0^T sign \, (\xi - x) \, dt = 0. \tag{865}$$

The magnitude x in the integrand of (865) can be considered as constant in accordance with the above assumption so that

$$\int_0^T sign \, (\xi - x) \, dt = T_2 - T_1, \tag{866}$$

where T_1 is the sum of the time intervals during which the curve $\xi = \xi(t)$ lies below the line $\xi = x = const$, and T_2 is the sum of the time intervals during which the reverse is true.

For complex rolling characterized by an equation of the type of (826), it can be expected that

$$\lim_{T \to \infty} \frac{T_1 - T_2}{T} = f(x), \tag{867}$$

where $f(x)$ is a function depending on the specific form of (831) for the function $\xi = \xi(t)$.

226

In order to solve this problem under the above assumptions, it is sufficient to find the limit of $T_2 : T$ when $T \to \infty$, T_2 being as above, the sum of the time intervals during which $\xi(t) > x$ (see p. 226).

If p and q are incommensurable, $\xi(t)$ can be considered as the sum of two random independent variables[*]:

$$\eta(t) = \alpha \sin(pt + \delta) \text{ and } \zeta(t) = \beta \sin(qt + \epsilon). \tag{877}$$

The probability that η will lie in the interval $(\eta, \eta + d\eta)$ is

$$\frac{1}{\pi} \frac{d\eta}{\sqrt{\alpha^2 - \eta^2}}. \tag{878}$$

In fact, (878) represents the fraction of the period during which a point whose motion is given by

$$\eta = \alpha \sin(pt + \delta), \tag{879}$$

is situated in the interval $(\eta, \eta + d\eta)$, since differentiating (879) yields:

$$d\eta = p\alpha \cos(pt + \delta) dt = \sqrt{\alpha^2 - \eta^2} \, p \, dt, \tag{880}$$

or

$$dt = \frac{d\eta}{p\sqrt{\alpha^2 - \eta^2}}, \tag{881}$$

where dt is the time taken by the point to pass through the interval $d\eta$. During one period the point passes twice through this interval. The fraction of the period during which it is within the interval $d\eta$ is therefore

$$\frac{2dt}{\frac{2\pi}{p}} = \frac{d\eta}{\pi\sqrt{\alpha^2 - \eta^2}}. \tag{882}$$

Similarly, for the random magnitude $\zeta(t)$ the probability is

$$\frac{1}{\pi} \frac{d\zeta}{\sqrt{\beta^2 - \zeta^2}}. \tag{883}$$

The probability that η and ζ will simultaneously lie within the specified intervals $(\eta, \eta + d\eta)$, $(\zeta, \zeta + d\zeta)$ is

$$\frac{1}{\pi^2} \frac{d\eta d\zeta}{\sqrt{(\alpha^2 - \eta^2)(\beta^2 - \zeta^2)}}. \tag{884}$$

To find for what part of a sufficiently long time interval T, η and ζ remain within a given region S (Figure 180), this expression must be integrated over the region S:

$$\iint_S \frac{1}{\pi^2} \frac{d\eta d\zeta}{\sqrt{(\alpha^2 - \eta^2)(\beta^2 - \zeta^2)}}. \tag{885}$$

In our case the region of compatible values of η and ζ in the $\eta\zeta$ plane is a rectangle with vertexes $(\pm\alpha, \pm\beta)$. It is easily seen that

$$\frac{1}{\pi^2} \int_{-\alpha}^{+\alpha} \int_{-\beta}^{+\beta} \frac{d\eta d\zeta}{\sqrt{(\alpha^2 - \eta^2)(\beta^2 - \zeta^2)}} = 1; \tag{886}$$

this was to be expected. Compatible values of η and ζ are impossible outside this region. The condition

$$\xi \geqslant x \tag{887}$$

[*] Gnedenko, B.V. Kurs teorii veroyatnostei (A Course in the Theory of Probability). — Fizmatgiz. 1961.

·It follows from (865) − (867) that

$$f(x) = \frac{\mu}{\nu}.$$ (868)

The roots of this equation have to be found in order to solve the problem.
In the case of simple rolling according to (833),

$$\xi = \alpha \sin pt,$$

it can be assumed, as already mentioned, that T is equal to the roll period:

$$T = \frac{2\pi}{p}.$$ (869)

On the diagram of the sinusoid (833) draw a straight line parallel to the abscissa and at a distance x_0 above it (Figure 179). It is immediately seen that

$$T_2 = \frac{T}{2} - 2t_1,$$

$$T_1 = \frac{T}{2} + 2t_1,$$ (870)

so that

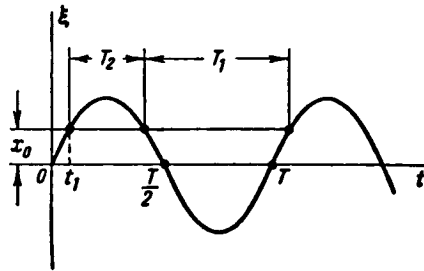$$\frac{T_1 - T_2}{T} = \frac{4t_1}{T} = \frac{2pt_1}{\pi}.$$ (871)

FIGURE 179

Here t_1 is the least root of the equation

$$\alpha \sin pt = x_0.$$ (872)

When x_0 is small compared with α, (872) can be replaced by the approximation

$$\frac{x}{\alpha} = \sin pt_1 \cong pt_1$$ (873)

whence

$$\frac{T_1 - T_2}{T} = \frac{2x}{\pi\alpha}.$$ (874)

The following relationship is obtained from (865), (866), and (874):

$$\frac{\mu}{\nu} - \frac{2x}{\pi\alpha} = 0.$$ (875)

This again leads to (863).

Consider now the case of complex rolling, for which the deviation of the dynamic vertical from the true vertical is given by (826):

$$\xi(t) = \frac{w}{g} = \alpha \sin(pt + \delta) + \beta \sin(qt + \epsilon).$$ (876)

227

corresponds to that part of the rectangle (Figure 181) to the right and above the straight line

$$\eta + \zeta = x. \tag{888}$$

The ratio $T_2 : T$ which we shall denote by $f_2(x)$, thus represents a double integral over this region.

For $x > 0$ the region $\zeta > x$ may be either triangular or trapezoidal, depending upon whether $\alpha - \beta$ is larger or smaller than x. For $\alpha = \beta$ the region can only be triangular. Usually the region is trapezoidal; only this
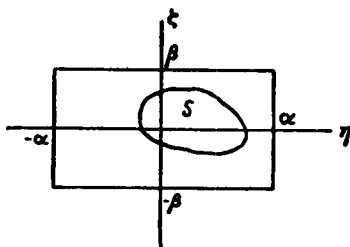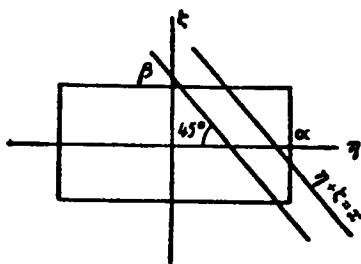

FIGURE 18C   FIGURE 181

case will therefore be discussed. Let us assume that $\alpha > \beta$. In this case ζ has to be integrated from $-\beta$ to β, and η from $x - \zeta$ to α. Therefore

$$\lim_{T \to \infty} \frac{T_2}{T} = f_2(x) = \frac{1}{\pi^2} \int_{-\beta}^{+\beta} \left\{ \int_{x-\zeta}^{\alpha} \frac{d\eta}{\sqrt{\alpha^2 - \eta^2}} \right\} \frac{d\zeta}{\sqrt{\beta^2 - \zeta^2}}. \tag{889}$$

The value of the indefinite inner integral is $\arcsin \frac{\eta}{\alpha}$. Therefore

$$\lim_{T \to \infty} \frac{T_2}{T} = \frac{1}{\pi^2} \int_{-\beta}^{+\beta} \left(\frac{\pi}{2} - \arcsin \frac{x-\zeta}{\alpha} \right) \frac{d\zeta}{\sqrt{\beta^2 - \zeta^2}} =$$

$$= \frac{1}{2} - \frac{1}{\pi^2} \int_{-\beta}^{+\beta} \arcsin \frac{x-\zeta}{\alpha} \frac{d\zeta}{\sqrt{\beta^2 - \zeta^2}}. \tag{890}$$

Since

$$T_1 = T - T_2, \tag{891}$$

it follows that

$$\lim_{T \to \infty} \frac{T_1 - T_2}{T} = \lim_{T \to \infty} \left(1 - 2\frac{T_2}{T} \right) = \frac{2}{\pi^2} \int_{-\beta}^{+\beta} \arcsin \frac{x-\zeta}{\alpha} \frac{d\zeta}{\sqrt{\beta^2 - \zeta^2}}. \tag{892}$$

Inserting (892) and (868) into (867) gives

$$\frac{2}{\pi^2} \int_{-\beta}^{+\beta} \arcsin \frac{x-\zeta}{\alpha} \frac{d\zeta}{\sqrt{\beta^2 - \zeta^2}} = \frac{\mu}{\nu}, \tag{893}$$

229

which by the substitution

$$\zeta = \beta \sin \theta \qquad (894)$$

is reduced to the form

$$\int_{-\frac{\pi}{2}}^{+\frac{\pi}{2}} \arcsin \frac{x - \beta \sin \theta}{\alpha}\, d\theta = \frac{\pi^2}{2}\,\frac{\mu}{\nu}. \qquad (895)$$

Therefore

$$\frac{x}{\alpha} = \varphi \left(\frac{\beta}{\alpha},\ \frac{\mu}{\nu} \right), \qquad (896)$$

where φ, being a function of two variables, can be plotted with the aid of numerical calculations.

An approximate solution of (895) is easily obtained by assuming that $x \ll \beta$. The integrand can then be replaced by the first two terms of a Maclaurin expansion:

$$\arcsin \left(\frac{x}{\alpha} - \frac{\beta}{\alpha} \sin \theta \right) = - \arcsin \left(\frac{\beta}{\alpha} \sin \theta \right) +$$

$$+ \frac{x}{\alpha}\, \frac{1}{\sqrt{1 - \left(\frac{\beta}{\alpha} \sin \theta \right)^2}} + \cdots \qquad (897)$$

The function $\arcsin \left(\frac{\beta}{\alpha} \sin \theta \right)$ being odd,

$$\int_{-\frac{\pi}{2}}^{+\frac{\pi}{2}} \arcsin \left(\frac{\beta}{\alpha} \sin \theta \right) d\theta = 0, \qquad (898)$$

so that (895) can be replaced by the following approximation:

$$\frac{x}{\alpha} \int_{-\frac{\pi}{2}}^{+\frac{\pi}{2}} \frac{d\theta}{\sqrt{1 - \left(\frac{\beta}{\alpha} \sin \theta \right)^2}} = \frac{\mu}{\nu}\, \frac{\pi^2}{2}, \qquad (899)$$

whence

$$x = \frac{\pi^2}{4} \cdot \frac{\alpha}{K \left(\frac{\beta}{\alpha} \right)} \cdot \frac{\mu}{\nu}, \qquad (900)$$

where $K \left(\frac{\beta}{\alpha} \right)$ is a complete elliptic integral of the first kind[*]. It is remarkable that in the case of simple rolling ($\beta = 0$) (900) becomes identical with (863). This happens because

$$K(0) = \frac{\pi}{2}. \qquad (901)$$

In the general case

$$K \left(\frac{\beta}{\alpha} \right) = \frac{\pi}{2} \left[1 + \frac{1}{4} \left(\frac{\beta}{\alpha} \right)^2 + \cdots \right] > \frac{\pi}{2}. \qquad (902)$$

---

[*] Smirnov, V. I. Kurs vysshei matematiki (A Course of Higher Mathematics). Vol. III, Part 2. —GITTL, 1949.

It follows that the instrument error during complex rolling, defined by (876), is smaller than during simple harmonic rolling which is one of the components of complex rolling.

This is probably the reason why in the case of contact correction the gyrohorizon error on a rolling ship is smaller than is apparent from (863). In fact, the maximum deviation during rolling of the dynamic vertical, defined by (876), is $\alpha+\beta$. Consider now simple rolling with an amplitude $\alpha+\beta$; by (863) the error will be:

$$x^{*}=\frac{(\alpha+\beta)\mu}{v}\frac{\pi}{2}. \tag{903}$$

This exceeds the value of x given by (900) by a factor

$$2\frac{\alpha+\beta}{\pi\alpha}K\left(\frac{\beta}{\alpha}\right). \tag{904}$$

If, for instance, $\alpha = 0.06$ and $\beta = 0.04$, then

$$2\frac{\alpha+\beta}{\pi\alpha}K\left(\frac{\beta}{\alpha}\right)=1.86,$$

so that in the example on p. 226 the error will be 29' instead of 54', which was the value obtained in the case of simple rolling with an amplitude of deviation of the dynamic vertical equal to $0.06 + 0.04$.

The numerical solution of the exact equation (895) gives the following value for the gyrohorizon error:

$$x=0.0077\ (26°5').$$

The approximate formula (900) is thus quite adequate.

It may be expected that complex rolling consisting of three or more harmonic components will cause an even smaller error of the gyrohorizon.

This analysis remains valid also if the corrective moment is asymmetric (Figure 182):

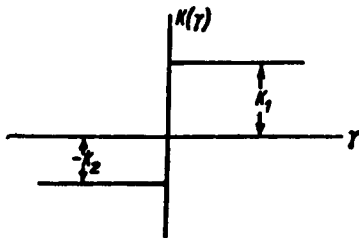$$K=K_2 \text{ for } \gamma>0,$$
$$K=-K_1 \text{ for } \gamma<0, \tag{905}$$

FIGURE 182

with $K_1 \neq K_2$. In this case

$$\mu=\omega\cos\varphi+\frac{K_2-K_1}{2H}, \tag{906}$$

and therefore an error remains during rolling even when the effect of the Earth's rotation on the instrument is fully compensated.

§ 2. The effect of the ship's yaw on the accuracy of the gyrohorizon readings

A plane physical pendulum whose axis is perpendicular to the ship's diametral plane, or a physical pendulum suspended in gimbals, have a deviation toward the ship's bow during yawing of the order of one degree. It would therefore appear that such pendulums are unsuitable for the correction of gyrohorizons and similar instruments when the latter are located at a considerable distance from the ship's center.

In fact this is not so. Firstly the deviation of the gyrohorizon toward the ship's bow during yaw is incomparably smaller than the corresponding deviation of the plane pendulum. Secondly, and this is most important, there exists no deviation of the gyrohorizon if its motion is referred to a coordinate frame oriented by the points of the compass, i.e., if the frame does not participate in the ship's yaw.

To prove these two assertions consider the simplest scheme of a gyrohorizon consisting of an astatic gyro* with a vertical axis and the scheme of two corrective pendulums. The pendulum axes are both parallel to the ship's deck and respectively parallel to the longitudinal and transverse sections of the ship.

In order not to complicate the problem, we shall arbitrarily assume that heel and trim are permanently zero, so that only the effect of the ship's yaw on the gyrohorizon has to be examined.

Assume further for the sake of simplicity that the so-called linear law of radial correction obtains: the moments applied to the gyro are proportional to the angles of deviation of the corrective pendulums from their mean position. Thus, a deviation of the pendulum whose axis is parallel to the ship's longitudinal section will cause a moment proportional to this deviation and acting about the axis parallel to the transverse section of the ship to be applied to the gyro.

Under these assumptions, small motions of the gyro about the vertical will be described (Chapter IV, § 1) by the following equations:

$$H\left[\frac{dx}{dt} - \omega(t)y\right] = K(\alpha - x),$$

$$H\left[\frac{dy}{dt} + \omega(t)x\right] = K(\beta - y); \qquad (907)$$

the friction in the suspension is neglected.

Here H is the angular momentum of the gyro; x and y are small angles of deviation of the gyro axis from the vertical to starboard and toward the bow respectively; α and β are the angles of deviation of the corresponding corrective pendulums from the vertical; K is the so-called curvature of the correction characteristic; $\omega(t)$ is the angular velocity of yawing.

We can simplify the problem still further by assuming that the angular velocity of yawing varies according to a harmonic law

$$\omega(t) = \omega_0 \cos pt, \qquad (908)$$

and that, in addition, one of the points of the ship's longitudinal axis (the center of yaw) has a uniform straight motion.

---

* A gyro is called astatic if the center of gravity of the system housing rotor coincides with the center of the gimbals and if the center of gravity of the outer ring lies on its pivot axis.

If the instrument is located in the foreship near the diametral plane at a distance l from said point, the angles of deviation of the pendulums from the vertical will be determined by the equations

$$\frac{d^2\alpha}{dt^2} + \frac{g}{l_1}\alpha = -\frac{l}{l_1}\frac{d\omega}{dt} = \frac{\omega_0 p l}{l_1}\sin pt,$$

$$\frac{d^2\beta}{dt^2} + \frac{g}{l_1}\beta = -\frac{l}{l_1}\omega^2(t) = -\frac{\omega_0^2 l}{l_1}\cos^2 pt, \tag{909}$$

where l_1 is the length of each pendulum, and α and β are assumed to be small. Assuming that the natural oscillation frequency of the pendulum is many times greater than the yaw frequency, the natural oscillations of the pendulums will be neglected. We can then approximately write

$$\alpha = \frac{\omega_0 p l}{g}\sin pt,$$

$$\beta = -\frac{l\omega_0^2}{g}\cos^2 pt = -\frac{l\omega_0^2}{2g} - \frac{l\omega_0^2}{2g}\cos 2pt. \tag{910}$$

The mean values of α and β, representing the mean deviations of the pendulums to starboard and toward the bow, are by (910)

$$\alpha_{av} = 0 \quad \text{and} \quad \beta_{av} = -\frac{l\omega_0^2}{2g}. \tag{911}$$

Inserting (908) and (910) into (907) yields

$$H\left[\frac{dx}{dt} - \omega_0 y \cos pt\right] = K\left(\frac{l\omega_0 p}{g}\sin pt - x\right),$$

$$H\left[\frac{dy}{dt} + \omega_0 x \cos pt\right] = K\left(-\frac{l\omega_0^2}{g}\cos^2 pt - y\right). \tag{912}$$

The functions $x(t)$ and $y(t)$, which determine the deviation of the gyro axis from the vertical, can be obtained by solving (912).

It is easily seen that the general solution of (912) for the initial conditions

$$x(0) = x_0, \quad y(0) = y_0 \tag{913}$$

tends to a harmonic function of frequency p.

In fact, the general solution is the sum of the general solution of the homogeneous system

$$H\left[\frac{dx}{dt} - \omega_0 y \cos pt\right] = -Kx,$$

$$H\left[\frac{dy}{dt} + \omega_0 x \cos pt\right] = -Ky, \tag{914}$$

and of a particular solution of (912).

Any solution of (914) tends to zero with increasing t. To prove this, we multiply the second equation by $i = \sqrt{-1}$, add it to the first, and introduce the complex function of t

$$z(t) = x(t) + iy(t). \tag{915}$$

This yields the following differential equation:

$$\frac{dz}{dt} + (\varkappa + i\omega_0 \cos pt)z = 0. \tag{916}$$

233

Its integral is

$$z(t) = Ce^{-\varkappa t - i\frac{\omega_0}{p}\sin pt}, \tag{917}$$

which tends to zero with increasing t, since

$$\varkappa = \frac{K}{H} > 0. \tag{918}$$

It can be shown that among the particular solutions of (912) there exists one periodic solution which will be the limit for any solution of this system.

An approximation of this periodic solution can be obtained by substituting

$$x = a_0 + a_1 \cos pt + b_1 \sin pt,$$
$$y = c_0 + c_1 \cos pt + d_1 \sin pt, \tag{919}$$

in (912) and equating the free terms and the coefficients $\cos pt$ and $\sin pt$ on the left- and right-hand sides (higher harmonics are neglected).

The following equations for the determination of the coefficients a_0, a_1, b_1, c_0, c_1, d_1 are then obtained:

$$-\frac{\omega_0 H}{2}c_1 = -Ka_0; \qquad \frac{\omega_0 H}{2}a_1 = -K\frac{l\omega_0^2}{2g} - Kc_0;$$

$$pHb_1 - \omega_0 Hc_0 = -Ka_1; \qquad pHd_1 + \omega_0 Ha_0 = -Kc_1; \tag{920}$$

$$-pHa_1 = K\frac{l\omega_0 p}{g} - Kb_1; \qquad -pHc_1 = -Kd_1.$$

Equations (920) can be separated into two independent systems, one of which is homogeneous. Their solution gives

$$a_0 = 0, \quad a_1 = -\frac{l\omega_0^2}{2g} \cdot \frac{2K}{\omega_0 H} \cdot \frac{\left(p^2 + \frac{\omega_0^2}{2}\right)H^2}{K^2 + \left(p^2 + \frac{\omega_0^2}{2}\right)H^2},$$

$$b_1 = \frac{l\omega_0 p}{g} \cdot \frac{K^2}{K^2 + \left(p^2 + \frac{\omega_0^2}{2}\right)H^2}, \tag{921}$$

$$c_0 = -\frac{l\omega_0^2}{2g} \cdot \frac{K^2}{K^2 + \left(p^2 + \frac{\omega_0^2}{2}\right)H^2}, \quad c_1 = 0, \quad d_1 = 0.$$

Note that the second of expressions (911)

$$\beta_{av} = -\frac{l\omega_0^2}{2g},$$

represents, as mentioned above, the mean deviation toward the bow of one of the corrective pendulums caused by ship yawing according to (908).

At the same time, the corresponding mean deviation c_0 of the gyro axis toward the bow is, according to (921), only a fraction of β_{av}.

Numerical example. Let the yaw amplitude be $\varphi = 0.05$ (3°) and the yaw period $T = 6.28$ sec, i.e., $p = 1$ sec^{-1}; then

$$\omega = p\varphi_0 \cos pt = 0.05 \cos t,$$

and therefore

$$\omega_0 = 0.05 \text{ sec}^{-1}.$$

If $l = 50$ m, then

$$|\beta_{av}| = \frac{l\omega_0^2}{2g} = 0.0064.$$

The mean deviation from the vertical of the corrective pendulum is thus considerable (about 0.4°).

On the other hand, even with a strong correction, for which

$$\frac{K}{H} = \varkappa = 0.01 \text{ sec}^{-1},$$

(921) gives the practically negligible value

$$c_0 = -\frac{l\omega_0^2}{2g} \frac{K^2}{K^2 + \left(p^2 + \frac{\omega_0^2}{2}\right)H^2} = -0.00000063 \ (0.002'),$$

though a_1 is larger

$$a_1 = 0.00255 \ (8.7').$$

The coefficient b_1 is also negligible (about 0.08').

In this case, the gyrohorizon motion can be approximated fairly accurately to periodic oscillations of the gyro axis in the ship's transverse plane, in synchronism with the forced oscillations of the corrective pendulum in the same plane.

Consider now the gyrohorizon motion in the $\xi\eta\zeta$ frame oriented by the points of the compass.

It is convenient to interpret the small angles formed by the gyro axis with the $\xi\zeta$ and $\eta\zeta$ coordinate planes as the coordinates ξ and η of a point G lying on said axis, for which $\zeta = z = 1$ (Chapter IV, § 1, Figure 94).

Assume for the sake of simplicity that the ship's course is along the η-axis. Then

$$\xi = x \cos\varphi - y \sin\varphi,$$
$$\eta = x \sin\varphi + y \cos\varphi, \tag{922}$$

where φ is the yaw angle, and x and y are the coordinates of point G in the xy coordinate system fixed to the ship, with the x-axis directed to starboard and the y-axis toward the bow.

The coordinate x is, with an accuracy of up to third-order infinitesimals, equal to the angle between the gyro axis and the ship's longitudinal plane, and the coordinate y is with the same accuracy, equal to the angle between the gyro axis and the ship's transverse plane. The angle between the y- and η-axes, or, which is the same, between the x- and ξ-axes, is the yaw angle.

Equations (907) can be written

$$H\left(\frac{dx}{dt} - y\frac{d\varphi}{dt}\right) = K(a - x),$$
$$H\left(\frac{dy}{dt} + x\frac{d\varphi}{dt}\right) = K(\beta - y), \tag{923}$$

where

$$\frac{d\varphi}{dt} = \omega(t). \tag{924}$$

Differentiating (922) with respect to time yields

$$\frac{d\xi}{dt} = \frac{dx}{dt}\cos\varphi - \frac{dy}{dt}\sin\varphi - x\frac{d\varphi}{dt}\sin\varphi - y\frac{d\varphi}{dt}\cos\varphi,$$

$$\frac{d\eta}{dt} = \frac{dx}{dt}\sin\varphi + \frac{dy}{dt}\cos\varphi + x\frac{d\varphi}{dt}\cos\varphi - y\frac{d\varphi}{dt}\sin\varphi. \qquad (925)$$

Multiply the first of equations (923) by $\cos\varphi$, the second by $-\sin\varphi$, and add. Also multiply the first of equations (923) by $\sin\varphi$, the second by $\cos\varphi$, and add. When (922) and (925) are taken into account, the result is

$$H\frac{d\xi}{dt} + K\xi = K(\alpha\cos\varphi - \beta\sin\varphi),$$

$$H\frac{d\eta}{dt} + K\eta = K(\alpha\sin\varphi + \beta\cos\varphi). \qquad (926)$$

Equations (926) can also be obtained directly.

The natural frequency of the pendulums will, as before, be considered considerably larger than the frequency of yawing. It is then easily seen that

$$\alpha = -\frac{l}{g}\frac{d^2\varphi}{dt^2}, \quad \beta = -\frac{l}{g}\left(\frac{d\varphi}{dt}\right)^2, \qquad (927)$$

since the deviation angles of the pendulums are determined respectively by their centrifugal and tangential accelerations during the yawing.

If the expressions

$$\varphi = \varphi_0 \sin pt \quad \text{and} \quad p\varphi_0 = \omega_0, \qquad (928)$$

are substituted in (927), we obtain (910).

Since

$$\frac{d^2\varphi}{dt^2}\cos\varphi - \left(\frac{d\varphi}{dt}\right)^2\sin\varphi = \frac{d}{dt}\left(\frac{d\varphi}{dt}\cos\varphi\right),$$

$$\frac{d^2\varphi}{dt^2}\sin\varphi + \left(\frac{d\varphi}{dt}\right)^2\cos\varphi = \frac{d}{dt}\left(\frac{d\varphi}{dt}\sin\varphi\right), \qquad (929)$$

inserting (927) into (926) yields

$$H\frac{d\xi}{dt} + K\xi = -K\frac{l}{g}\frac{d}{dt}\left(\frac{d\varphi}{dt}\cos\varphi\right),$$

$$H\frac{d\eta}{dt} + K\eta = -K\frac{l}{g}\frac{d}{dt}\left(\frac{d\varphi}{dt}\sin\varphi\right). \qquad (930)$$

System (930) consists of two independent nonhomogeneous linear equations. The solutions of the corresponding homogeneous equations tend to zero with increasing t. It is therefore sufficient to find a particular solution of each equation. If $\varphi = \varphi(t)$ is a periodic-function given by (928), one of the particular solutions will be periodic and can be represented as a Fourier series. The particular solutions of the two equations (930) are:

$$\xi = a_0' + a_1'\cos pt + b_1'\sin pt + \dots \qquad (931)$$

$$\eta = c_0' + c_1'\cos pt + d_1'\sin pt + \dots \qquad (932)$$

It is easily seen that $a_0' = c_0' = 0$. In fact, since the functions ξ, η, and φ

are periodic,

$$\int_0^T \frac{d\xi}{dt}\, dt = 0 \text{ and } \int_0^T \frac{d}{dt}\left(\frac{d\varphi}{dt}\cos\varphi\right) dt = 0 \quad \left(T = \frac{2\pi}{p}\right), \tag{933}$$

and it follows from the first of equations (930) that

$$\frac{1}{2\pi}\int_0^T \xi\, dt = a_0' = 0. \tag{934}$$

It is similarly shown that $c_0' = 0$. This proves that during yawing the mean deviation of the gyrohorizon relative to a reference frame oriented by the points of the compass is zero.

An elementary explanation of this result can be given. The angles of deviation α and β of the pendulums are proportional to the corresponding components of the absolute acceleration of the point at which the gyro-horizon is located on the ship. A spherical pendulum suspended at this point would have the same angles of deviation to starboard and toward the bow provided the frequency of its natural oscillations was, as in the case of the corrective pendulums, considerably higher than the frequency of yawing. Since the mean deviation of the point of suspension from the center of yaw is zero, the average acceleration, the average velocity, and the average displacement of the pendulum itself, referred to a reference frame oriented by the points of the compass and having its origin in the center of yaw, will also be zero.

On the other hand, the mean deviation of this spherical pendulum referred to a moving reference frame fixed to the ship will differ from zero because of motion of this frame.

The case of uniform rotation of the stationary ship about the center of yaw is the simplest example. In such a rotation the pendulum deviates by a constant angle toward the bow; in a nonrotating frame, however, the pendulum axis will describe a cone, and its mean position will therefore be the true vertical.

The same is true for the gyrohorizon, which in a certain sense takes up the above-mentioned mean position of the pendulum.

In conclusion, the exact periodic solution of (912) is

$$x + iy = \varkappa e^{-\varkappa t - i\frac{\omega_0}{p}\sin pt}\int_{-\infty}^t e^{\varkappa t + i\frac{\omega_0}{p}\sin pt} f(t)\, dt, \tag{935}$$

where

$$f(t) = \frac{l\omega_0 p}{g}\sin pt - i\frac{l\omega_0^2}{g}\cos^2 pt.$$

To carry out calculations with (935), it is necessary to apply the theory of Bessel functions.

§ 3. The gyro top bow

The name top bow is given to the angle of deviation (Figure 183) of the inner gimbal ring of the gyro suspension from its mean position at which

the axis of the top is perpendicular to the pivot axis of the outer ring.

The top bow of a free gyro without corrective devices (except for compensation of the influence of the Earth's rotation) varies inversely with its speed. It has also been noted that the bow decreases with time during rotation of the top, except when the gyro housings have no openings.

A theoretical explanation of this phenomenon is given in this chapter. In order to simplify the investigation, the influence of friction in the gimbal bearings (usually very small) and of the angular velocity of the Earth's rotation on the gyro will be neglected. With a vertically disposed outer-ring pivot axis the Earth's rotation can be neutralized by means of a weight secured to the inner ring and by orienting the top axis along the north-south line.

This study will remain within the framework of the elementary theory of gyroscope precession (cf. Chapter IV, § 1); nutations will therefore be neglected.

Let a be the angle of tilting of the outer gimbal ring relative to its (arbitrary) initial position and β the top bow (cf. above). The corresponding angular velocities are $\frac{da}{dt}$ and $\frac{d\beta}{dt}$.
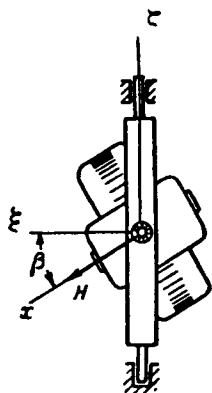
Fix to the inner gimbal ring a reference frame xyz, with the x-axis oriented along the top axis and the y-axis along the inner-ring pivot axis (Figure 184). Let the orientation of the z-axis be such that the top rotates

FIGURE 183

counterclockwise when viewed from its positive direction. Assume that positive values of β correspond to a counterclockwise tilting of the inner ring relative to the outer gimbal ring when viewed from the positive direction of the y-axis. It is easily seen (Figure 184) that the projections $p, q,$ and r of the inner ring's angular velocity on the x-, y-, and z-axes, when the instrument base is fixed, are

$$p = -\frac{da}{dt} \sin \beta, \quad q = \frac{d\beta}{dt},$$

$$r = \frac{da}{dt} \cos \beta. \tag{936}$$

The direction of the angular velocity $\frac{da}{dt}$ is chosen so that the outer ring tilts counterclockwise when viewed from the positive direction of the z-axis if $-90° < \beta < 90°$. If $\beta = 0$, the z-axis coincides with the outer-ring pivot axis ζ.

The angular momentum vector of the gyro is, in accordance with the above, directed along the positive x-axis. Its magnitude according to the theory of gyroscope precession, is

$$H = C\omega, \tag{937}$$

where C is the moment of inertia of the gyro top about its axis of rotation (the x-axis) and ω is the angular velocity of the top relative to the inner ring.

Let us find the projections of the time rate of change of H on the x-, y-, and z-axes. The projection on the x-axis represents the variation of H in magnitude and is therefore

$$C \frac{d\omega}{dt}. \tag{938}$$

238

. The projections on the y- and z-axes represent the change of the orientation of H together with the xyz coordinate system (i.e., together with the inner gimbal ring). It is easily seen (Figure 185) that they are respectively

$$rH \text{ and } -qH, \qquad (939)$$
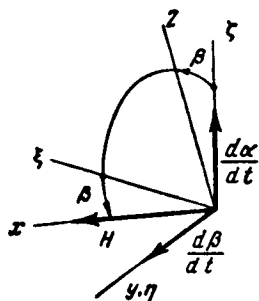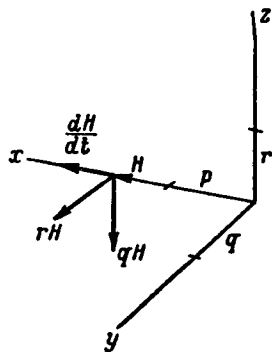
as shown in Chapter IV, § 4.

FIGURE 184

FIGURE 185

The angular momentum theorem of a mechanical system states that the components of the rate of change of H are equal to the moments M_x, M_y, M_z acting on the top about the corresponding axes. It follows therefore from (938) and (939) that

$$C \frac{d\omega}{dt} = M_x;$$
$$rH = M_y; \qquad (940)$$
$$-qH = M_z.$$

The moment M_x consists, as shown in Chapter IV, § 4, of the sum of the moments due to two systems of forces:

1) those originating in the inner ring, including both the torque driving the top* and the resistance due to the inner ring. The latter includes aerodynamic drag in addition to friction in the bearings of the top shaft;

2) the remaining aerodynamic forces not due to the inner ring.

The total moment about the top axis (the x-axis) due to the forces of the second system opposes the top rotation. Assuming that $\omega > 0$, the moment M_x is therefore

$$M_x = K - L, \quad L > 0, \qquad (941)$$

where K is the sum of moments of the forces of the first system, and L, the sum of moments of the second system.

K is positive during acceleration and at constant speed and negative during deceleration.

The moments M_y and M_z are the sums of the moments about the corresponding axes, caused by the reactions in the top shaft bearings. They may also include moments due to aerodynamic drag; these, however, can be ignored.

* If the torque driving the top acts at the outer ring, certain changes will have to be made in the following discussion.

The forces which act on the inner gimbal ring originate in the top and. the outer gimbal ring.

The sums of the moments about the x- y-, and z-axes caused by the first system of forces are, according to Newton's law of action and reaction, respectively

$$-K, \quad -M_y, \quad -M_z. \tag{942}$$

The sums of the moments about these same axes caused by forces originating in the outer gimbal ring are respectively

$$-M'_x, \quad -M'_y, \quad -M'_r. \tag{943}$$

The moments acting on the outer ring and originating in the inner ring are equal and of opposite signs:
$$M'_x, \quad M'_y, \quad M'_s. \tag{944}$$

If the inertia of the inner ring is neglected in accordance with the theory of gyroscope precession, it must be assumed that the sum of the moments acting on the inner ring is zero:

$$-K - M'_z = 0,$$
$$-M_y - M'_y = 0, \tag{945}$$
$$-M_s - M'_s = 0.$$

Note that

$$M'_y = 0, \tag{946}$$

since M'_y represents the friction in the bearings of the inner-ring pivots which is assumed to be zero.

The second of equations (945) yields therefore

$$M_y = 0. \tag{947}$$

Consider now the second of equations (940). Inserting the third of equations (936) in the left- and (947) in the right-hand side yields

$$rH = H \frac{d\alpha}{dt} \cos \beta = 0, \tag{948}$$

whence

$$\alpha = \text{const.} \tag{949}$$

This means that the outer gimbal ring is stationary.

If the inertia of the outer ring is similarly neglected, the sum of the moments about the ζ-axis (and also about the other axes) acting on this ring must be zero. Since friction in the bearings of the ring pivots is neglected, the equation of equilibrium of the moments about the ζ-axis (Figure 186) is

$$-M'_z \sin \beta + M'_s \cos \beta = 0. \tag{950}$$

Aerodynamic drag has been neglected here.

Inserting the first and third of equations (945) into (950) gives

$$M_s = K \operatorname{tg} \beta. \tag{951}$$

Since according to (941) and the first of equations (940)

$$K = M_s + L = C \frac{d\omega}{dt} + L, \tag{952}$$

and since according to the third of equations (940) and the second of equations (936)

$$M_z = -qH = -H\frac{d\beta}{dt},\qquad(953)$$

we may write (951) in the form

$$-H\frac{d\beta}{dt} = \left(C\frac{d\omega}{dt} + L\right)\operatorname{tg}\beta.\qquad(954)$$

It may be assumed that the torque during acceleration and deceleration

$$M_z = C\frac{d\omega}{dt}$$

considerably exceeds the moment of external drag L, so that the latter can be neglected in (954). Using (937), we may write (954) in the form

$$H\frac{d\beta}{dt} = C\omega\frac{d\beta}{dt} = -C\frac{d\omega}{dt}\operatorname{tg}\beta,\qquad(955)$$

whence

$$\omega\cos\beta\,d\beta + \sin\beta\,d\omega = d(\omega\sin\beta) = 0\qquad(956)$$

or, integrating,

$$\omega\sin\beta = \omega_0\sin\beta_0 = \mathrm{const},\qquad(957)$$

where ω_0 and β_0 are respectively the angular velocity and bow of the top at the initial instant.

It follows from (957) that the top bow (the angle β) varies inversely with the angular velocity ω of the top.
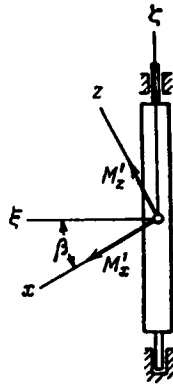

FIGURE 186

The instant at which the top starts rotating should not be taken as the initial instant, since friction, which was neglected, plays an important part at the beginning of rotation (i.e., at low angular velocities of the top), for which the theory of gyroscope precession is not valid.

During steady rotation of the top

$$\frac{d\omega}{dt} = 0.\qquad(958)$$

In addition, the moment of external drag (not originating in the inner gimbal

ring) can be assumed constant. Equation (954) then becomes

$$-H\frac{d\beta}{dt}=L\,\text{tg}\,\beta. \tag{959}$$

Integrating this equation under the assumption H = const yields

$$\sin\beta=\sin\beta_0 e^{-\frac{L}{H}t}, \tag{960}$$

where β_0 is the top bow at $t=0$.

It follows from (960) that the top bow must gradually decrease during steady top rotation. For tops with completely enclosed housings $L=0$, so that this phenomenon will not be observed.

The results given by (957) and (960) can be obtained far more simply by direct application of the angular momentum theorem to the mechanical system containing the top and the two gimbal rings. In fact, the forces of interaction between the gimbal rings, and between the rings and the top, are
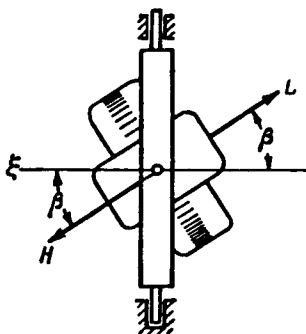

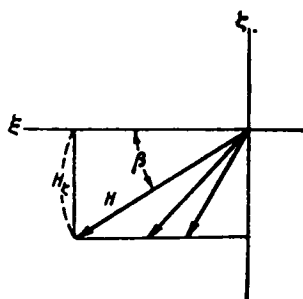FIGURE 187   FIGURE 188

internal forces in this system and therefore do not affect its angular momentum. If the influence of friction in the bearings of the outer-ring pivots is neglected, the only external moment about the ζ-axis (Figure 187) will be the projection of L on this axis:

$$M_\zeta=L\sin\beta. \tag{961}$$

On the other hand (Figure 188), the projection of the angular momentum vector on the ζ-axis is (under the assumptions of the elementary theory of gyroscope precession),

$$H_\zeta=-H\sin\beta. \tag{962}$$

The angular momentum theorem states that

$$\frac{d}{dt}H_\zeta=M_\zeta. \tag{963}$$

Inserting (961) and (962) into this equation yields

$$-\frac{d}{dt}(H\sin\beta)=L\sin\beta. \tag{964}$$

When the rate of variation of H is large, such as when the top is started or stopped, the right-hand side of (964) can be taken as zero. Inserting (937) into (964) leads in this case to the result given by (957).

242

· The geometric meaning of this is that the projection of H on the ζ-axis has a constant value. Obviously, the greater the magnitude of the vector H (Figure 188), i.e., the greater the angular velocity ω of the top, the smaller is the angle β, i.e., the top bow.

During steady rotation of the top

$$H = C\omega = \text{const.} \tag{965}$$

Using this expression, the integration of (964) leads to (960).

The more difficult derivation at the beginning of this section was given in order to expose the interplay of forces in the gyro gimbals. A similar derivation may be useful in other cases of gyroscopic systems; in particular such a method was used for setting up the equations of motion of the heel equalizer in Chapter IV, § 4.

§ 4. The errors of the gyroscopic apparent-velocity meter

This short section analyzes an instrument used on moving objects for the measurement of the so-called apparent velocity. This analysis will illustrate how second-order infinitesimals are allowed for in the theory of gyroscopes.
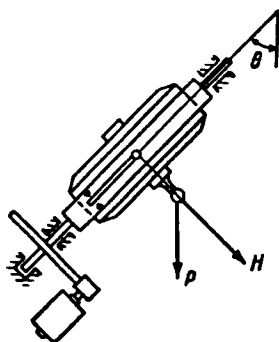

FIGURE 189
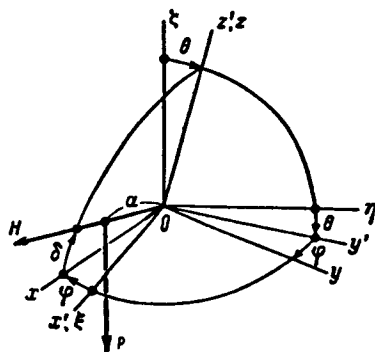
FIGURE 190

The instrument gyro (Figure 189) has a statical unbalance relative to the housing axis. A torque which maintains the rotor axis perpendicular to the plane of the outer ring is applied by means of an electric motor to the outer-ring pivot axis. The motor is controlled by means of a contact device located on the housing axis. The gyro has a precession about the outer-ring pivot axis caused by gravity and the inertia of the moving object. The corresponding tilting angle is one of the input data of the system controlling the object's motion.

When the instrument was tested on a stationary inclined base, it was found that the constant angle between the gyro axis and the perpendicular to the plane of the outer ring has a considerable influence on the precession period.

This phenomenon is easily explained theoretically. Let θ be the angle of deviation of the outer-ring pivot axis z from the vertical ζ, and introduce a coordinate system $x'y'z'$ fixed to the instrument base (Figure 190); the z'-axis is oriented along the z-axis of the outer gimbal ring, the x'-axis lying in a horizontal plane perpendicular to the vertical plane containing the ζ- and z'-axes.

Let a coordinate system xyz be fixed to the outer gimbal ring, the z-axis coinciding with the z'-axis, the y-axis being directed along the pivot axis of the gyro housing. The angle between the x- and x'-axes is denoted by φ. Lastly, let δ be the angle of deviation of the gyro rotor axis from the x-axis, i.e., from the perpendicular to the plane of the outer gimbal ring.

The precession about the outer-ring pivot axis causes a moment about the housing axis (the y-axis) due to gravity. This moment is given by

$$M_y = z P_x - x P_z, \qquad (966)$$

where x and z are the coordinates in the xyz system of the gyro's center of gravity, and P_x and P_z are respectively the projections on these axes of the force of gravity. Obviously

$$x = a \cos \delta \quad \text{and} \quad z = a \sin \delta, \qquad (967)$$

where a is the distance from the gyro's center of gravity to the geometric center of the gimbals.

To find the projections of the force of gravity on the axes x, y, z, we note that its components along the axes x', y', z' are respectively (Figure 190)

$$0, \qquad P \sin \theta, \qquad -P \cos \theta. \qquad (968)$$

The last of these is also the projection of P on the z-axis. In order to find the projection of the force of gravity on the x-axis, it is necessary to project on this axis its component along the y'-axis; the following expression is then obtained:

$$P_x = -P \sin \theta \sin \varphi. \qquad (969)$$

The moment M_y, given by (966), can therefore be expressed in the form

$$M_y = Pa \, (\cos \delta \cos \theta - \sin \delta \sin \theta \sin \varphi). \qquad (970)$$

According to the theory of gyroscope precession, the moment M_y is equal to the y-component of the rate of change of the gyro's angular momentum, given by

$$H \cos \delta \, \frac{d\varphi}{dt}. \qquad (971)$$

The following differential equation is obtained by equating (970) to (971):

$$H \cos \delta \, \frac{d\varphi}{dt} = Pa \, (\cos \delta \cos \theta - \sin \delta \sin \theta \sin \varphi). \qquad (972)$$

Separating the variables and integrating:

$$t = \frac{H}{Pa} \int_{\varphi_0}^{\varphi} \frac{\cos \delta \, d\varphi}{\cos \delta \cos \theta - \sin \delta \sin \theta \sin \varphi}. \qquad (973)$$

The period of precession T is obtained by integrating between the limits

$\varphi_0 = 0$ and $\varphi = 2\pi$; this gives, for constant angles θ and δ:

$$T = \frac{H}{Pa\cos\theta} \int_0^{2\pi} \frac{d\varphi}{1 - \mathrm{tg}\,\delta\,\mathrm{tg}\,\theta\,\sin\varphi} = \frac{H}{Pa\cos\theta} \cdot \frac{2\pi}{\sqrt{1 - (\mathrm{tg}\,\delta\,\mathrm{tg}\,\theta)^2}}. \qquad (974)$$

The result is a generalization of the well-known formula for the precession period of a heavy top. In fact, when $\theta = 0$ (vertical axis of precession)

$$T_0 = \frac{2\pi H}{Pa}, \qquad (975)$$

which is independent of δ.

For $\theta \neq 0$, the precession period increases with δ irrespective of its sign, as was found experimentally.

The following series expansion can be substituted with sufficient accuracy into (974):

$$\frac{1}{\sqrt{1 - \mathrm{tg}^2\,\delta\,\mathrm{tg}^2\,\theta}} \cong 1 + \frac{1}{2}\,\mathrm{tg}^2\,\delta\,\mathrm{tg}^2\,\theta \cong 1 + \frac{1}{2}\,\delta^2\,\mathrm{tg}^2\,\theta. \qquad (976)$$

The result obtained by this substitution can also be derived with the aid of the binomial theorem:

$$\int_0^{2\pi} \frac{d\varphi}{1 - \mathrm{tg}\,\delta\,\mathrm{tg}\,\theta\,\sin\varphi} \cong \int_0^{2\pi} [1 + \mathrm{tg}\,\delta\,\mathrm{tg}\,\theta\,\sin\varphi + (\mathrm{tg}\,\delta\,\mathrm{tg}\,\theta\,\sin\varphi)^2]\,d\varphi =$$

$$= 2\pi + \pi\,\mathrm{tg}^2\,\delta\,\mathrm{tg}^2\,\theta. \qquad (977)$$

Numerical example. Assume $\theta = 45°$ and $\delta = 0.07$ ($\sim 4°$); the precession period is then obtained from (974), (975), and (976):

$$T = \left(1 + \frac{1}{2}\,\delta^2\,\mathrm{tg}^2\,\theta\right)\frac{2\pi H}{Pa\cos\theta} = 1.0024\,\frac{T_0}{\cos\theta}.$$

The error when δ is assumed zero is thus only 0.25%.

Therefore, to ensure proper functioning of the instrument, the range of variation of δ should be small.

The instrument error can be similarly found when the center of gravity of the system housing top does not lie on the axis of rotation of the top.

§ 5. Precessional oscillations of a gyroscope
acted upon by a load

Monogyro systems with a stabilizing motor (Figure 191) are widely used for stabilizing various devices about an axis. The gyro housing of such a system is free to rotate with minimum friction in the outer-ring bearings. When the gyro deviates from its mean position in which the rotor axis is perpendicular to the plane of the gimbal ring, an electric motor connected to the gimbal-ring pivot is started by means of a contact device. The torque developed by the motor is directed so as to cause the precession induced by it to return the gyro to its mean position.

Periodic oscillations of the gyro housing relative to the gimbal ring are observed in such gyroscopic systems. The frequency and amplitude of these oscillations depend to a considerable extent on the so-called destabilizing or load moment applied to the outer gimbal ring.

245

The frequency is considerably less than that of the nutational oscillations of the system, which is of the order of the angular velocity of the rotor. In the theoretical study of such phenomena, it thus suffices to consider the precessional oscillations within the limits of the elementary gyroscope theory.
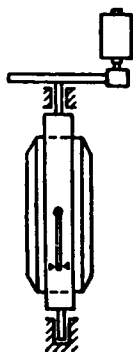
In addition, clearances in the transmission from the motor to the gimbal ring, friction in the bearings of the gyro housing and the gimbal ring, extra currents in the contact devices, and other secondary factors may also be neglected.

The motion of the gyro housing relative to the outer ring is in this case given by the following differential equation:

$$H \frac{dx}{dt} = M - K,$$ (978)

where H is the angular momentum of the gyro; x is the angle of deviation* of the gyro housing from its mean position; M is the magnitude of the destabilizing moment, assumed to be constant; and K is the torque applied to the gimbal ring by the electric motor.

FIGURE 191

Since the motor is of the squirrel-cage type, it can be assumed that the torque K varies according to a specified law [during the transient process of switching-on]

$$K = \varphi(t).$$ (979)

The time origin $t = 0$ corresponds to the instant at which the contact device is triggered. The torque of the motor becomes zero when the contact is opened if the breaking extra current is neglected.

It will be assumed that the transient process of switching-on is mainly determined by the inductive resistance of the motor armature. In this case

$$\varphi(t) = K_1 \left(1 - e^{-\frac{R}{L}t}\right),$$ (980)

where K_1 is the steady motor torque under short-circuit conditions, R is the ohmic resistance, and L the self-inductance of the motor armature circuit.

When the intermediate relays and amplifiers have considerable lag times, the function $\varphi(t)$ will have a more complex form. This does not, however, render the determination of the frequency and amplitude of the gyro oscillation more difficult.

According to (978), (979), and (980), the following equation will apply during the time the contact device is closed:

$$H \frac{dx}{dt} = M - K_1 (1 - e^{-at}),$$ (981)

where

$$a = \frac{R}{L}.$$ (982)

Integrating (981) yields

$$Hx = -(K_1 - M)t - \frac{K_1}{a} e^{-at} + C.$$ (983)

The contact device is triggered in the mean position of the gyro housing. It follows that $x = 0$ at $t = 0$. Inserting these initial conditions into (983)

* [Apparently about the outer-ring pivot axis.]

246

gives
$$C = \frac{K_1}{a}. \tag{984}$$

Inserting (984) into (983) leads to
$$\frac{aH}{K_1} x = 1 - e^{-at} - (1 - \mu) at, \tag{985}$$

where
$$\mu = \frac{M}{K_1}. \tag{986}$$

Equation (985) defines the gyro motion up to the instant $t = t_1$ at which the angle x becomes again zero. It is easily seen that the precession period can be determined from
$$\frac{1 - e^{-\tau_1}}{\tau_1} - 1 + \mu = 0, \tag{987}$$

where
$$\tau_1 = at_1. \tag{988}$$

In fact, the motor torque becomes instantaneously zero (if the circuit-breaking extra current is neglected) immediately after the contacts are opened, and the gyro starts moving under the action of the destabilizing moment M in the direction of increasing angle x. The contacts are rapidly closed again, and the action is repeated.

An interesting fact is that the period t_1 is independent of the gyro's angular momentum H, and is determined only by the parameters
$$\mu = \frac{M}{K_1} \quad \text{and} \quad a = \frac{R}{L}.$$

These characterize the relative load on the motor due to the destabilizing moment (K_1 is the maximum torque which the motor can develop) and the electric properties of the armature circuit.

The maximum deviation x_m of the gyro from its initial mean position is obtained at an instant $t = t_m$ at which the speed of precession becomes zero.

The following equation is obtained from (981) for determining t_m:
$$M - K_1(1 - e^{-at_m}) = 0, \tag{989}$$

whence follows, using (986),
$$t_m = -\frac{1}{a} \ln(1 - \mu). \tag{990}$$

Inserting (990) into (985) gives the following expression for the maximum deviation of the gyro:
$$x_m = \frac{K_1}{aH} [\mu + (1 - \mu) \ln(1 - \mu)]. \tag{991}$$

Table (993) gives the values of
$$\tau_1 = at_1, \quad \tau_m = at_m, \quad \xi_m = \frac{aH}{K_1} x_m \tag{992}$$

calculated from (990) and (991) and by numerical solution of (987) for different values of μ ($0 < \mu < 1$). Curves representing these values are given in Figures 192 and 193.

μ	τ_1	τ_m	ξ_m
0.05	0.103	0.051	0.0013
0.10	0.213	0.105	0.0052
0.20	0.464	0.223	0.0215
0.30	0.762	0.357	0.0501
0.40	1.126	0.511	0.0935
0.50	1.594	0.693	0.153
0.60	2.231	0.916	0.234
0.70	3.197	1.204	0.339
0.80	4.965	1.609	0.478
0.90	10.0	2.303	0.670
0.95	20.0	2.996	0.800

$$(993)$$

The following approximations are true for small values of μ:

$$\xi_m = \frac{\mu^2}{2} + \frac{\mu^3}{6},$$

$$\tau_1 = 2\mu + \frac{4}{3}\mu^2.$$

$$(994)$$
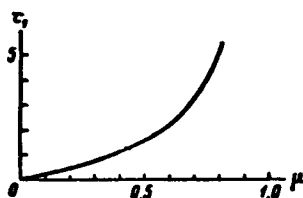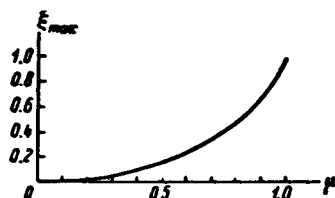

FIGURE 192

FIGURE 193

Numerical example. Assume that $H = 5000$ gcm sec, $M = 40$ gcm, $K_1 = 50$ gcm, $a = 5$ sec^{-1}; it follows then from (986) that

$$\mu = \frac{M}{K_1} = 0.8$$

and therefore, according to Table (993)

$$\tau_1 = 4.965, \quad \tau_m = 1.609, \quad \xi_m = 0.478.$$

It follows from (992) that

$$x_m = \frac{K_1}{aH} \xi_m \cong 0.000956\,(3.3'), \qquad t_1 = \frac{\tau_1}{a} \cong 1 \text{ sec}.$$

In the given case the gyroscopic stabilizer will undergo about one oscillation per second.

Figure 194 gives curves of the gyro motion in the $\xi\tau$ plane for several values of the parameter μ. These curves represent to a scale of $1 : \frac{K_1}{aH}$ the angle x defining the deviation of the gyro from its mean position and to the scale of $1 : \frac{L}{R}$ the time t.

In the general case, in which after the closing of the contacts the motor develops a torque according to an arbitrary law (979)

$$K = \varphi(t),$$

248

the integral

$$f(t) = \int_0^t \varphi(t)\, dt \qquad\qquad (995)$$

has to be plotted and a straight line of slope M to be drawn through the origin. It follows from (978), that the difference between the ordinates of the curve and the straight line represents Hx, and is therefore at every instant proportional to the angle of deviation of the gyro. The abscissa of the intersection of these lines determines the period of the precessional oscillations of the gyro.
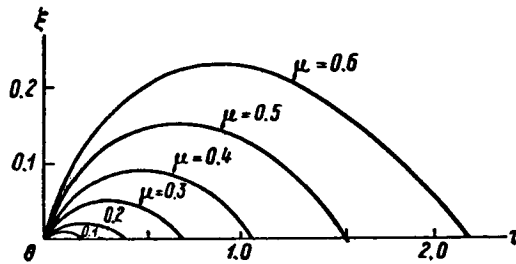

FIGURE 194

When the gyro housing is tilted in relation to the outer ring, friction in the bearings of the housing pivots causes a precession of the gyro about the outer-ring pivot axis. Let F be the moment due to Coulomb friction in the housing bearings. Its direction varies together with the precessional velocity $\frac{dx}{dt}$ of the gyro about the outer-ring pivot axis.

It follows that the outer ring will tilt to one side by an angle

$$\frac{F}{H}\, t_m \qquad\qquad (996)$$

in the time interval $(0, t_m)$, and to the other side by an angle

$$\frac{F}{H}\, (t_1 - t_m) \qquad\qquad (997)$$

in the time interval (t_m, t_1).

The expression

$$\frac{d\psi}{dt} = \frac{F}{H} \cdot \frac{2t_m - t_1}{t_1} = \frac{F}{H} \cdot \frac{2\tau_m - \tau_1}{\tau_1} \qquad\qquad (998)$$

represents the mean angular tilting velocity of the outer ring. The instants t_m and t_1 are determined by the destabilizing moment. The angular tilting velocity of the outer ring thus depends on the load acting on the gyro (Z. M. Tsetsior).

249

§ 6. Influence of vibrations on the accuracy of
gyroscopic instrument readings

Systematic errors are sometimes observed in the indications of gyro-scopic devices tested on a vibrating base. This contradicts the widely-held opinion that vibrations have a positive influence on the operation of gyroscopic instruments, since they reduce friction in the gimbals of the sensing elements, replacing vibrating or revolving bearings frequently used for this purpose.

It will be shown below that vibrations can greatly reduce the accuracy of gyroscopic instruments. This is due to the elasticity of the gimbal element and the housing cover, and to the almost unavoidable clearances in the rotor bearings.

Due to the component of inertia forces, directed along the rotor axis, the center of gravity of the gyro deviates periodically from the geometric center of the gimbals; the other components cause spurious precessional moments which lead to gyro wander.

To illustrate this phenomenon, consider the wander of a directional gyro caused by the vibrations of its base (Figure 195).
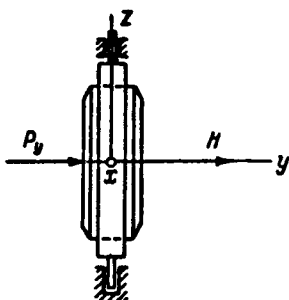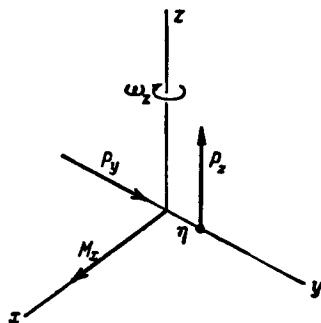

FIGURE 195   FIGURE 196

Fix to the outer gimbal ring of the gyro a coordinate system xyz (Figure 196), the z-axis lying along the ring pivot axis, the x-axis along the housing pivot axis, and the y-axis perpendicular to the two.

Let the vibrations of the base be such that if the gimbals were absolutely rigid their geometric center would undergo harmonic oscillations along a straight line. This motion can be resolved into three harmonic motions along the axes x, y, and z. The accelerations of these component motions are respectively

$$w_x = -\omega^2 a \cos \omega t,$$

$$w_y = -\omega^2 b \cos \omega t, \qquad\qquad (999)$$

$$w_z = -\omega^2 c \cos \omega t,$$

where a, b, and c are the amplitudes of the component oscillation motions, and ω, the frequency.

250

· These accelerations determine the inertia forces of translation:

$$P_x = -mw_x, \quad P_y = -mw_y, \quad P_z = -mw_z. \tag{1000}$$

The force P_x does not affect the gyro readings. The force P_y causes a periodic variation of the position of the rotor's center of gravity relative to the pivot axis of the housing. If the mass of the housing and the elasticity of its pivots are neglected, only the rigidity of the cover being taken into account*, the axial shift of the center of gravity of the rotor will be

$$\eta = \frac{\omega^2}{n^2 - \omega^2}\, b \cos \omega t, \tag{1001}$$

where n is the frequency of the rotor's natural oscillations in the axial direction, determined by the elasticity of the housing cover (all the other gimbal elements are assumed to be absolutely rigid and the axial clearance to be zero). Formula (1001) follows from the differential equation of the axial vibrations of the rotor:

$$m \frac{d^2\eta}{dt^2} + K\eta = P_y = m\omega^2 b \cos \omega t. \tag{1002}$$

Here m is the rotor mass and K, the spring of the housing walls together with the rotor bearings at axial displacements of the rotor. Obviously

$$K = n^2 m. \tag{1003}$$

When the rotor's center of gravity is displaced (Figure 196), a moment

$$M_z = \eta P_z = mbc\, \frac{\omega^4}{n^2 - \omega^2} \cos^2\omega t, \tag{1004}$$

appears due to the force P_z, causing precession of the gyro about the vertical axis at a mean angular velocity

$$\omega_z = \frac{mbc}{2H} \frac{\omega^4}{n^2 - \omega^2}, \tag{1005}$$

where H is the gyro's angular momentum.

The precession is in one direction for $n > \omega$, and in the opposite direction for $n < \omega$. This was found experimentally.

Clearances in the axial direction of the rotor bearings has a quantitative influence on the phenomenon; essentially, however, it remains the same.

We thus see that rigid construction of the gyros and their gimbals and proper assembly are very important for obtaining high-accuracy in gyroscopic systems.

§ 7. Theory of follow-up systems

Contemporary control instruments are complex systems of gyroscopic and computing units having many additional devices; important among them are the follow-up systems.

The function of follow-up systems is to reproduce with satisfactory accuracy the angle of rotation (or the shift) indicated by an instrument (in particular gyroscopic) without applying to it forces liable to affect its readings.

---

* It can be shown that there is no gyro wander during vibrations when the rotor is equally elastic in the y and z directions.

A poorly functioning follow-up system can greatly reduce the accuracy of gyroscopic precision systems. It is therefore necessary to analyze the processes occuring in follow-up systems and in their components; this requires a suitable mathematical theory.

Some simplifying assumptions regarding electrical and mechanical processes taking place in the follow-up system and the laws governing them have to be made; the correctness of these assumptions has to be determined experimentally.

In spite of the extensive literature dealing with the general theory of follow-up systems, it is useful to outline such a system (Figure 197).
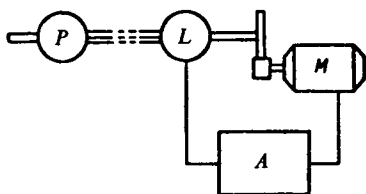

FIGURE 197

The pick-up P feeds to the amplifier A a voltage u which is a function of the angle of misalignment of the system

$$\varphi_1 - \theta_1, \tag{1006}$$

where φ_1 is the angle of rotation of the pick-up P and θ_1 the angle of rotation of the load L. [Actually it is the comparator (or mixer) which feeds the voltage.]

The voltage v obtained at the amplifier output is fed to an electric motor M in such a way as to make the armature rotate in the direction of decreasing misalignment angles.

For small misalignment angles a linear relationship between the latter and the input voltage

$$u = k_1 (\varphi_1 - \theta_1), \tag{1007}$$

can be assumed.

The angle of rotation of the motor armature is related to θ_1 by the equation

$$\theta = j\theta_1, \tag{1008}$$

where j is the transmission ratio (usually $j \gg 1$).

Expression (1007) can be written

$$u = k (\varphi - \theta), \tag{1009}$$

where

$$\varphi = j\varphi_1, \quad k_1 = jk. \tag{1010}$$

The relationship between the input and output voltages can be represented as a first approximation by the following differential equation

$$\tau \frac{dv}{dt} + v = \mu u, \tag{1011}$$

where v is the amplifier output voltage, τ, the so-called time constant of the amplifier, and μ, the constant-voltage (static) amplification factor.

When a constant voltage $u = u_0$ is applied to the amplifier input, a constant voltage $v = v_0 = \mu u_0$ is obtained at its output at the end of a transient process during which the voltage increases according to (1011) by the exponential law

$$v = v_0 \left(1 - e^{-\frac{t}{\tau}} \right). \tag{1012}$$

If u varies according to the harmonic law

$$u = u^0 \sin pt, \tag{1013}$$

integration of (1011) will give the following law of variation for the output voltage:

$$v = v^0 \sin (pt - \varepsilon), \tag{1014}$$

where

$$v^0 = \frac{\mu u^0}{\sqrt{1 + p^2 \tau^2}}, \quad \operatorname{tg} \varepsilon = p\tau. \tag{1015}$$

It is thus seen that the output voltage v varies according to the same sinusoidal law as the input voltage u, but with a time lag

$$t_1 = \frac{\varepsilon}{p}. \tag{1016}$$

The time lag t_1 between the input and output voltages decreases with increasing frequency p; the phase shift ε tends toward the value $\frac{\pi}{2}$, and the amplification toward zero. The following approximation is valid for low frequencies p (more precisely, for small values of the product $p\tau$):

$$p\tau = \operatorname{tg} \varepsilon \cong \varepsilon \tag{1017}$$

whence

$$t_1 \cong \tau, \quad v \cong v^0 \sin p(t - \tau). \tag{1018}$$

The relationships between input and output voltages u and v in the amplifiers used in practice are considerably more complex than equation (1011), which is nevertheless sufficient in many cases involving narrow ranges of variation of the frequencies p.

After v^0 and ε have been determined experimentally, the parameters μ and τ can be obtained from

$$\mu = \frac{v^0}{u^0 \cos \varepsilon}, \quad \tau = \frac{1}{p} \operatorname{tg} \varepsilon, \tag{1019}$$

which follow from (1015).

If the motor M is a dc separately-excited motor, the equation of the electric circuit of its armature is (neglecting the armature self-induction)

$$v = Ri + C \frac{d\theta}{dt}, \tag{1020}$$

where R is the ohmic resistance of the circuit, C, the coefficient of the motor counter emf, and θ the angle of rotation of the armature.

Since the torque of a separately excited dc motor is proportional to the armature current i, it follows that

$$I \frac{d^2\theta}{dt^2} = \frac{C}{g} i - N, \tag{1021}$$

where I is the moment of inertia of all revolving parts of the follow-up system referred to the motor axis; N, the moment of resistance to the

253

armature rotation due to the load and friction; g, the gravitational ac-
celeration.

The resistance moment N is practically independent of the armature
angular velocity $\frac{d\theta}{dt}$, but is determined by its sign. If the pick-up P rotates
in the same direction at constant speed, load L also rotates without chang-
ing direction when the follow-up system functions smoothly. It can then be
assumed that

$$N = \text{const.} \tag{1022}$$

Under these assumptions the operation of the follow-up system is de-
scribed by the following equations:

$$u = k(\varphi - \theta);$$

$$\tau \frac{dv}{dt} + v = \mu u;$$

$$v = Ri + C \frac{d\theta}{dt}; \tag{1023}$$

$$I \frac{d^2\theta}{dt^2} = \frac{C}{g} i - N.$$

The following equations are obtained by eliminating u from the first two and
the current intensity i from the last two of equations (1023):

$$\tau \frac{dv}{dt} + v = k\mu (\varphi - \theta),$$

$$RI \frac{d^2\theta}{dt^2} + \frac{C^2}{g} \frac{d\theta}{dt} = \frac{C}{g} v - NR. \tag{1024}$$

If the pick-up rotates uniformly, that is if

$$\varphi = \omega t, \tag{1025}$$

the load will rotate after attenuation of the transient process according to
the law

$$\theta = \theta^0 + \omega t. \tag{1026}$$

Assume that during the transient process the load rotates without chang-
ing direction, so that (1022) remains valid.

Also assume

$$v = v^0 + \bar{v}, \quad \theta = \omega t + \theta^0 + \bar{\theta}, \tag{1027}$$

where v^0 and θ^0 are given by

$$v^0 = -k\mu\theta^0,$$

$$\frac{C^2}{g} \omega = \frac{C}{g} v^0 - NR. \tag{1028}$$

Inserting (1027) and (1025) into (1024) and using (1028):

$$\tau \frac{d\bar{v}}{dt} + \bar{v} = -k\mu\bar{\theta},$$

$$RI \frac{d^2\bar{\theta}}{dt^2} + \frac{C^2}{g} \frac{d\bar{\theta}}{dt} = \frac{C}{g} \bar{v}. \tag{1029}$$

These equations define the time variation of $\bar{v}$ and $\bar{\theta}$; these magnitudes re-
present the deviations of v and θ from their limiting steady values

$$v = v^0, \quad \theta = \theta^0 + \omega t. \tag{1030}$$

It follows from (1028) that

$$v^0 = C\omega + \frac{gRN}{C},$$

$$\theta^0 = -\frac{v^0}{k\mu} = -\frac{1}{k\mu}\left(C\omega + \frac{gRN}{C}\right). \tag{1031}$$

The magnitude θ^0 represents the error of the follow-up system at steady operating conditions. It consists of the so-called velocity error [the steady-state velocity lag]

$$\theta_1^0 = -\frac{C}{k\mu}\omega, \tag{1032}$$

which is proportional to the angular velocity of the pick-up, and of the static error

$$\theta_2^0 = -\frac{gRN}{k\mu C}, \tag{1033}$$

which is determined by the resistance moment N.

The follow-up system will function satisfactorily only if v and θ tend to zero for any initial conditions. The system is called stable if this condition is satisfied.

The determinant of the set of differential equations (1029) is

$$\begin{vmatrix} \tau\lambda + 1 & k\mu \\ -\dfrac{C}{g} & RI\lambda^2 + \dfrac{C^2}{g}\lambda \end{vmatrix} = a_0\lambda^3 + a_1\lambda^2 + a_2\lambda + a_3 = 0, \tag{1034}$$

where

$$a_0 = \tau RI; \quad a_1 = RI + \frac{\tau C^2}{g}; \quad a_2 = \frac{C^2}{g}; \quad a_3 = \frac{k\mu C}{g}. \tag{1035}$$

A necessary and sufficient condition for the decrease with time of all solutions of (1029), and therefore for the stability of the follow-up system, is (for positive coefficients (1035)) that the stability condition

$$a_1 a_2 > a_0 a_3, \tag{1036}$$

be satisfied.

Inserting the values of the coefficients given by (1035) into (1036) yields

$$\left(RI + \frac{\tau C^2}{g}\right)\frac{C^2}{g} > \tau RI\,\frac{k\mu C}{g}, \tag{1037}$$

which can be reduced to

$$\tau\left(\frac{k\mu}{C} - \frac{C^2}{gRI}\right) < 1. \tag{1038}$$

If the left-hand side of (1038) is negative, i.e., if

$$C^3 > k\mu gRI, \tag{1039}$$

the system will be stable for any value of τ. This condition is, however, almost unattainable.

In fact, it follows from (1032) that in order to ensure a sufficiently low velocity error of the follow-up system the coefficient C must not be excessive, since the product $k\mu$ is limited by the amplifier output voltage v^0.

Actually, fulfillment of stability condition (1038) necessitates a time constant τ so small that it can sometimes be attained only by means of

additional amplifier circuits (this is the case with magnetic amplifiers, as in the numerical example below). These additional circuits (the so-called feedbacks) may cause unstable operation of the amplifier itself, and usually require very careful adjustment.

Numerical example. Assume that $I = 1\,\text{gcm sec}^2 = 0.00001\,\text{kgm sec}^2$; $C = 0.25\,\text{v sec}$; $R = 35\,\Omega$; $k\mu = 16$ v (the amplifier output voltage is 115 v for a misalignment angle $\varphi_1 - \theta_1 = 0.002$ and a transmission ratio $j = 3600$).

For these values
$$\frac{k\mu}{C} - \frac{C^2}{gRI} = 64 - 18.2 = 45.8$$

Stability condition (1038) is satisfied if
$$\tau < 0.022\,\text{sec}.$$

The time constant of a magnetic amplifier is considerably larger (of the order of $0.1 - 0.2$ sec).

A method for reducing the amplifier time-constant will now be considered. It consists in applying the amplifier output voltage v to the primary of a transformer T, the voltage obtained from its secondary being applied to the amplifier input (see Figure 198).
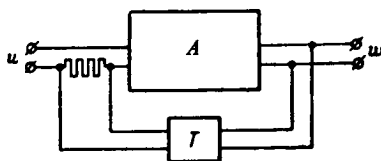

FIGURE 198

The influence of the amplifier input circuit on the transformer secondary can be neglected, so that the magnetic leakage flux need not be taken into account; the equations of the transient processes in the transformer primary and the secondary are then respectively:

$$v = R_1 i_1 + n_1 \frac{d\Phi}{dt}, \tag{1040}$$
$$0 = R_2 i_2 + n_2 \frac{d\Phi}{dt},$$

where
$$\Phi = M (n_1 i_1 + n_2 i_2). \tag{1041}$$

Here

i_1, is the current intensity in primary;

n_1, the number of turns of primary;

R_1, the ohmic resistance of primary circuit;

i_2, the current intensity in secondary;

n_2, the number of coils of secondary;

R_2, the ohmic resistance of secondary circuit;

Φ, the magnetic flux (when an air gap exists in the magnetic circuit of the transformer);

M, the mutual inductance.

Multiply the first of equations (1040) by n_2, the second by n_1, and subtract the second from the first. The result is

$$vn_2 = n_2 R_1 i_1 - R_2 n_1 i_2. \tag{1042}$$

Inserting (1041) into the second of equations (1040) yields

$$R_2 i_2 + n_2 M \frac{d}{dt} (n_1 i_1 + n_2 i_2) = 0. \tag{1043}$$

Substituting the expression for i_1 obtained from (1042) we obtain

$$\sigma \frac{di_2}{dt} + i_2 = -h \frac{dv}{dt}, \tag{1044}$$

where

$$\sigma = M \left(\frac{n_1^2}{R_1} + \frac{n_2^2}{R_2} \right), \quad h = \frac{M n_1 n_2}{R_1 R_2}. \tag{1045}$$

Let R be the resistance of the load on the transformer secondary. The additional voltage fed to the amplifier input is then

$$u' = -R i_2, \tag{1046}$$

if the terminals of the transormer secondary are suitably connected.

When this feedback exists, (1011) is replaced by the following two equations:

$$\tau \frac{dv}{dt} + v = \mu (u - R i_2),$$
$$\sigma \frac{di_2}{dt} + i_2 = -h \frac{dv}{dt}. \tag{1047}$$

Eliminating i_2 between these two equations reduces them to the following second-order differential equation

$$\sigma\tau \frac{d^2v}{dt^2} + (\sigma + \tau - a) \frac{dv}{dt} + v = \mu \left(u + \sigma \frac{du}{dt} \right), \tag{1048}$$

where a denotes the parameter

$$a = \mu R h = \frac{\mu R M n_1 n_2}{R_1 R_2}. \tag{1049}$$

Replace the second of equations (1023) by (1048). The following two differential equations are obtained in the same way as (1029):

$$\sigma\tau \frac{d^2\bar{v}}{dt^2} + (\sigma + \tau - a) \frac{d\bar{v}}{dt} + \bar{v} = -k\mu \left(\sigma \frac{d\bar{\theta}}{dt} + \bar{\theta} \right),$$
$$R l \frac{d^2\bar{\theta}}{dt^2} + \frac{C^2}{g} \frac{d\bar{\theta}}{dt} = \frac{C}{g} \bar{v}. \tag{1050}$$

These equations describe small perturbations of the steady motion of the follow-up system, given by (1030).

In the case of feedback, the first of equations (1050) is called the amplifier equation and the second the motor equation.

When

$$\sigma + \tau = a, \tag{1051}$$

undamped oscillations of frequency

$$q = \frac{1}{\sqrt{\sigma\tau}}, \tag{1052}$$

257

can appear in the amplifier circuits if the influence of the right-hand side of the first of equations (1050) is small.

This is in fact, usually the case, since q is relatively large so that the torsional vibrations of the motor shaft are almost unnoticeable; the clearances prevent the transmission of vibrations to the load.

These oscillations of the follow-up system are e l e c t r i c a l   o s c i l l a -
t i o n s.   When

$$a > \sigma + \tau, \tag{1053}$$

oscillations of a frequency close to q are established in the system.

Another type of oscillation, m e c h a n i c a l   o s c i l l a t i o n s, is characterized by large amplitudes of the torsional vibrations of the motor shaft and by a considerably lower frequency p. This frequency can be determined approximately by neglecting all transient processes in the amplifier circuit and writing

$$v \cong -\mu k \dot{\theta}. \tag{1054}$$

Inserting this into the second of equations (1050) gives the frequency if the term containing the first derivative of θ is neglected,

$$p = \sqrt{\frac{k\mu C}{gRI}}. \tag{1055}$$

The condition for the absence of mechanical oscillations can be obtained by means of the following considerations.

When the frequency p is relatively low, the term in the first of equations (1050) containing the second time derivative of v can be neglected. In addition, when σ is small, the following relationship is obtained:

$$(\tau - a)\frac{dv}{dt} + v = -k\mu\dot{\theta}. \tag{1056}$$

This equation differs from the first of equations (1029) only in that the time constant τ has been reduced by a. The stability condition (1038) can now be replaced by the following approximation:

$$(\tau - a)\left(\frac{k\mu}{C} - \frac{C^2}{gR}\right) < 1. \tag{1057}$$

If this condition is satisfied, no mechanical oscillations occur.

If the amplifier has a relatively large time constant τ, the magnitude of a should be close to that of τ in order to ensure the stability of the follow-up system, i.e., in order to satisfy (1057).

Since σ is usually small, a small variation of a may cause (1053) to become true, leading to electric instability.

The permissible range of variation of a is thus very narrow, a fact which makes adjustment of the follow-up system difficult.

Both types of oscillations are easily observed during this adjustment.

The values of the frequencies of these oscillations at their discontinuity boundary can serve to determine the various parameters of the follow-up system, and also as a check of the validity of the simplifying assumptions made above.

A stricter treatment of the same problem requires a study of the stability condition of (1050).

Expanding the determinant of this system:

$$\lambda^4 + \frac{\sigma\tau + \tau\rho + \rho\sigma - \sigma\rho}{\rho\sigma\tau}\lambda^3 + \frac{\sigma + \tau + \rho - \sigma}{\rho\sigma\tau}\lambda^2 +$$

$$+ \frac{1 + \sigma m}{\rho\sigma\tau}\lambda + \frac{m}{\rho\sigma\tau} = 0, \tag{1058}$$

where

$$\rho = \frac{I g R}{C^2} \tag{1059}$$

(the so-called mechanical time constant) and

$$m = \frac{k\mu}{C}. \tag{1060}$$

The Routh-Hurwitz criterion for (1058) is:

$$f(a) = a^2 + \frac{s_2(1 + \sigma m - 2\rho m) + \rho s_1(1 + \sigma m)}{\rho^2 m - \rho - \rho\sigma m}a +$$

$$+ \frac{(1 + m\sigma)^2 s_3 - s_1 s_2(1 + m\sigma) + s_2^2 m}{\rho^2 m - \rho - \rho\sigma m} < 0, \tag{1061}$$

where

$$\begin{aligned} s_1 &= \rho + \sigma + \tau; \\ s_2 &= \sigma\tau + \tau\rho + \rho\sigma; \\ s_3 &= \rho\sigma\tau. \end{aligned} \tag{1062}$$

If (1061) is satisfied, the follow-up system is stable.
If the quadratic equation for a

$$f(a) = 0 \tag{1063}$$

has two real roots a_1 and a_2, undamped oscillations of the follow-up system, corresponding to each root, are possible at the stability limit. Mechanical harmonic oscillations of the system, of frequency p, correspond to the smaller root, while electrical oscillations of frequency q correspond to the larger root.

If equation (1063) has no real roots, the follow-up system cannot be stable for any value of a. In order to obtain stability in this case it is necessary either to vary other parameters of the system or to use different feedback schemes.

The values of ρ and m in the example given above (p. 256) are

$$\rho = \frac{I g R}{C^2} = 0.0549, \qquad m = \frac{k\mu}{C} = 64.$$

Let the amplifier time constant be $\tau = 0.05$ and the feedback circuit time constant $\sigma = 0.001$.

For these values equation (1063) has the roots

$$a_1 = 0.0295 \text{ and } a_2 = 0.0509.$$

The follow-up system will therefore be stable

$$0.0295 < a < 0.0509.$$

It follows from (1057) and (1051) that

$$\tau - \frac{1}{\frac{k\mu}{C} - \frac{C^2}{g R}} < a < \sigma + \tau,$$

259

or
$$0.0282 < a < 0.0510.$$

The following pairs of imaginary roots are obtained from (1058) for a equal to a_1 and a_2 respectively:

$$\lambda_{1,2} = \pm i29.4; \quad \lambda_{3,4} = \pm i137.6.$$

The first pair of roots corresponds to the frequency of mechanical oscillations

$$p = 29.4 \, \text{sec}^{-1},$$

the second, to the frequency of electrical oscillations

$$q = 137.6 \, \text{sec}^{-1}.$$

The approximations (1055) and (1052) gives the following values:

$$p = \sqrt{\frac{k\mu C}{gRI}} = \sqrt{\frac{m}{\rho}} = 34 \, \text{sec}^{-1}, \quad q = \frac{1}{\sqrt{\sigma\tau}} = 141 \, \text{sec}^{-1}.$$

This numerical example thus confirms the correctness of the approximations made above.

The methods used in this section to simplify the equations describing the behavior of follow-up systems can also be applied, exactly as the methods used in Chapter V, § 2, in the study of other oscillatory processes.

260

Appendix 1

THEORY OF COMPLEX GYROSCOPIC
STABILIZATION SYSTEMS*

The equations of motion of complex gyroscopic systems are usually es-
tablished by the Lagrange method of the second kind**. While this method
has its undoubted advantages, it is very cumbersome and frequently obscures
the physical meaning of the equations obtained.

On the other hand, with a certain amount of practice it is comparatively
easy to form the equations of motion of complex gyroscopic devices by ap-
plying the angular momentum theorem successively to the mechanical sys-
tem of the device as a whole and to its separate components. The present
paper is devoted to a description of this method, using as an example the
study of a system of power gyro stabilization.

1. After attenuation of a transient process, the motion of gyroscopic
systems used for stabilization usually becomes a slow change in the orienta-
tion of the gyros' axes relative to the Newtonian frame. This is usually
called precessional motion.

The angular momentums of the gyroscopic-system suspension elements
and of the housings of its gyros, the equatorial components of the angular
momentums of the rotors themselves, and the angular momentums of the
motor armatures can be neglected in the study of a precessional motion.
The polar angular momentum components (directed along the axis of rota-
tion of the gyro), can be taken as the product of the axial moment of inertia
of the gyro rotor and its angular velocity relative to its housing.

The above-mentioned assumptions lead to the so-called elementary
theory of gyroscope precession. The equations describing the motion of
the gyroscopic system are considerably simplified when these assumptions
are made: in particular, their order is reduced. At the same time, the
accuracy of the results obtained by the elementary theory is completely
adequate, except in special cases when the influence of the gimbal-ring
inertia must be taken into account.

Transient processes in gyroscopic systems can be investigated only if
the angular momentums of all parts are taken into account; the equations
of the elementary theory are insufficient for this.

2. When the angular momentum theorem is used to obtain the differ-
ential equations of motion of a gyroscopic device, the composition of the
mechanical system to which it is to be applied must first be stipulated
clearly.

The angular momentum and its derivative must be determined relative to a reference frame $\xi^* \eta^* \zeta^*$ having a translational motion; this frame must also be clearly defined. We shall call it the basic reference frame. The forces of inertia due to translational motion acting on the mechanical system considered, have to be calculated relative to this basic frame. These forces can be replaced by their resultant. Its line of action passes through the center of gravity of the mechanical system, and its direction is opposed to that of the acceleration of the basic reference frame relative to the so-called absolute reference frame $\xi_a^* \eta_a^* \zeta_a^*$. The origin of the latter is located at the center of mass of the Universe, and its axes are oriented according to the Newtonian frame.

The resultant of the inertia forces is obviously equal in magnitude to the product of the mass of the mechanical system and the acceleration of the basic reference frame.

In the general case, the basic reference frame may be any frame $\xi \eta \zeta$, not necessarily having a translational motion. However, if this basic frame $\xi \eta \zeta$ rotates relative to the absolute frame $\xi_a^* \eta_a^* \zeta_a^*$ the problem of allowing for the inertia due to translational motion is greatly complicated. Coriolis forces then appear which must be considered as external forces acting on the system. Coriolis forces occur when the basic reference frame has a translational motion.

3. Let a given reference frame $\xi^* \eta^* \zeta^*$ be selected as basic reference frame, and let G be the angular momentum of the mechanical system considered relative to this frame which has a translational motion. It follows from the angular momentum theorem that

$$\frac{dG_{\xi^*}}{dt} = M_{\xi^*}, \quad \frac{dG_{\eta^*}}{dt} = M_{\eta^*}, \quad \frac{dG_{\zeta^*}}{dt} = M_{\zeta^*}. \tag{1}$$

The left-hand sides of these expressions represent respectively, the time derivatives of the projections of the angular momentum vector G on the ξ^*-, η^*-, and ζ^*-axes while the right-hand sides represent the sums of all external moments acting on the mechanical system considered about these same axes. The moments due to forces of inertia arising out of the translational motion are included in these sums.

Equations (1) are inconvenient because of the unwieldy expressions obtained. The calculations can be considerably simplified by projecting the angular momentum derivative on the axes of a moving reference frame, whose motion is in a certain way related to that of the mechanical system considered.

Let xyz be such a reference frame; it will be called the auxiliary frame. Let ω be the angular velocity of this frame relative to the basic frame $\xi^* \eta^* \zeta^*$, and let the origins of both coincide. The projections of the time rate of change of the angular momentum vector on the x-, y-, and z-axes are

$$\frac{dG_x}{dt} + \omega_y G_z - \omega_z G_y, \quad \frac{dG_y}{dt} + \omega_z G_x - \omega_x G_z, \quad \frac{dG_z}{dt} + \omega_x G_y - \omega_y G_x, \tag{2}$$

where G_x, G_y, G_z are the projections of the angular momentum vector on these axes, and ω_x, ω_y, ω_z, the components of the angular velocity of the reference frame xyz relative to the basic frame $\xi^* \eta^* \zeta^*$ or, which is the same, relative to the absolute reference frame $\xi_a^* \eta_a^* \zeta_a^*$.

In accordance with the angular momentum theorem, the components (2) are equal to the sums of the moments due to all external forces acting on

the mechanical system considered and to the translational motion of the basic reference frame $\xi^*\eta^*\zeta^*$. (The frame xyz was only introduced because it is simpler to calculate the angular momentum derivative relative to it than relative to the basic frame $\xi^*\eta^*\zeta^*$.) The following equations are obtained by denoting these sums of moments by M_x, M_y, M_z:

$$\frac{dG_x}{dt} + \omega_y G_z - \omega_z G_y = M_x, \quad \frac{dG_y}{dt} + \omega_z G_x - \omega_x G_z = M_y,$$
$$\frac{dG_z}{dt} + \omega_x G_y - \omega_y G_x = M_z. \tag{3}$$

These relationships are equivalent to (1).

4. The external forces acting on mechanical systems include the unknown constraining forces between them and the base (usually moving) on which they are mounted. Gyroscopic systems are usually mounted on the base by means of gimbals. When the mechanical system consists of several elements of the gyroscopic device, for instance of the entire system less the outer ring, or of a single gyro with its housing and rotor, the constraining element is usually a simple hinge. In many cases it can be assumed approximately that friction in the hinge is independent of the constraining force of the bearing on the pivot. If the pivot axis coincides with one of the axes of the reference frame xyz, the equation of system (3) will contain no unknown constraining forces.

In the more general case when the pivot axis does not coincide with the x-, y-, or z-axes, the equation of motion of the gyroscopic system, which contains no constraining forces, is

$$\left[\frac{dG_x}{dt} + \omega_y G_z - \omega_z G_y\right]\cos x\nu + \left[\frac{dG_y}{dt} + \omega_z G_x - \omega_x G_z\right]\cos y\nu +$$
$$+ \left[\frac{dG_z}{dt} + \omega_x G_y - \omega_y G_x\right]\cos z\nu = M_\nu. \tag{4}$$

$\cos x\nu$, $\cos y\nu$, $\cos z\nu$ are the direction cosines of the pivot axis ν relative to the frame xyz, and M_ν is the sum of the moments about the pivot axis due to the external forces acting on the mechanical system. M_ν includes also the moment due to friction in the hinge, the torque transmitted to the pivot by means of, e.g., an electric motor, and the moments about the ν-axis, due to inertia forces caused by the translational motion of the basic reference frame $\xi^*\eta^*\zeta^*$

$$M_\nu = M_x \cos x\nu + M_y \cos y\nu + M_z \cos z\nu. \tag{5}$$

If the friction in the hinge depends on the constraining forces, an equation of motion not containing these unknowns is far more difficult to obtain. All three relationships (3) have to be used in this case. It would then also be very difficult to establish the equations of motion of a gyroscopic system by the method of Lagrange multipliers.

5. Consider as an illustration the determination of the equations of motion of a three-dimensional triaxial gyroscopic power stabilizer* (Figure 1).

The pivot ξ- (x'-) axis of the gimbal frame K of platform P is mounted in bearings on the moving base carrying the stabilizer. The platform P can tilt about the axis y' (y) lying in the plane of frame K and forming a right angle with the axis ξ (x'). Two gyros, I and II, are mounted on the platform; their housings can tilt about the z_1- and z_2-axes which are perpendicular to the plane of the platform.

* Such a system was developed in 1957 for the Academy of Sciences of the Ukrainian SSR for the stabilization of electric measuring frames on a moving base (helicopter).

The body *B* which has to be stabilized can also tilt together with gyro III about the *z-* (*ž-*) axis which is also perpendicular to the plane of platform *P*. The *y₃-* (*ỹ-*) axis (the housing pivot axis of gyro III) is parallel to the plane of platform *P*.
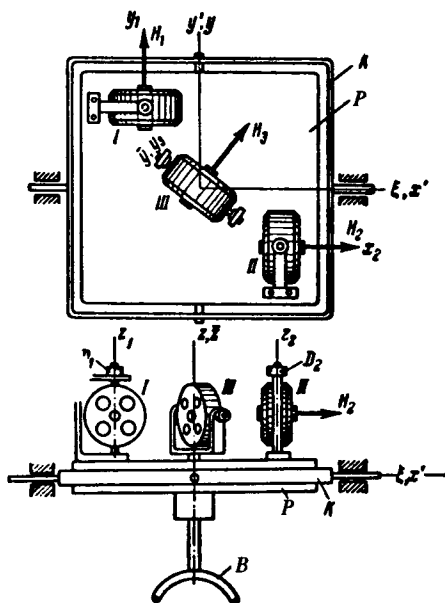

FIGURE 1

Introduce the right-handed coordinate systems $\xi\eta\zeta$, $x'y'z'$, xyz, and $x\tilde{y}\tilde{z}$, fixed respectively to the moving base, the frame *K*, the platform *P*, and the body to be stabilized *B*. The reference frame *xyz* will be considered as basic frame in all subsequent calculations. The ξ-axis of the coordinate system $\xi\eta\zeta$ coincides with the longitudinal axis of the moving object (the moving base), and the η-axis with its transversal axis. The *x'-* and *y'-*axes of the coordinate system $x'y'z'$ lie in the plane of frame *K*; the *x'*-axis coincides with the ξ-axis and is the axis about which the frame *K* tilts (Figure 2). Let *α* be the tilting angle of the frame relative to the object. The coordinate systems $x'y'z'$ and $\xi\eta\zeta$ coincide when *α* = 0. When *α* > 0 the frame tilts counterclockwise if viewed from the positive ξ- (or the *x'-*) axis.

The coordinate system *xyz* is fixed to the platform *P* (Figure 3). Its *y*-axis coincides with the *y'*-axis and forms the tilting axis of platform *P*. Let β be the tilting angle. The *x*-axis of the coordinate system *xyz* lies in the plane of the platform, the *z*-axis being perpendicular to it. The planes of platform *P* and frame *K*, and therefore the corresponding axes of the systems *xyz* and *x'y'z'*, coincide when β = 0. When β > 0, the platform *P* tilts counterclockwise when viewed from the positive *y*- (or *y'-*) axis.

Lastly, the coordinate system $x\tilde{y}\tilde{z}$ is fixed to the body *B* which has to be stabilized. The *ž*-axis coincides with the *z*-axis of the coordinate system *xyz* fixed to platform *P*. Let ψ be the angle of rotation of the system $x\tilde{y}\tilde{z}$ relative to the system *xyz* (Figure 4). The *x*- and *ẋ*-, *y*- and *ỹ*-axes coincide

respectively when $\psi = 0$. When $\psi > 0$, body B is rotated counterclockwise relative to its initial position when viewed from the positive z- ($\mathbf{z}$-) axis.
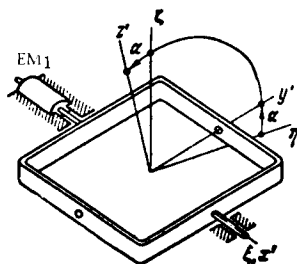
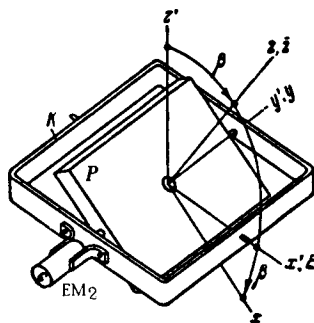Let γ_1 and γ_2 be the tilting angles of the housings of gyros I and II relative to platform P (Figure 5). When $\gamma_1 = 0$, the axis of rotation of gyro I is parallel to the y-axis; the axis of rotation of gyro II is similarly parallel to the
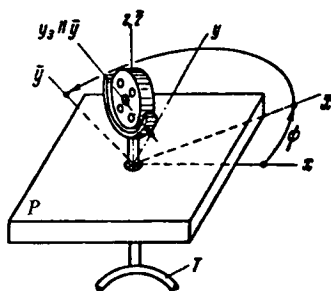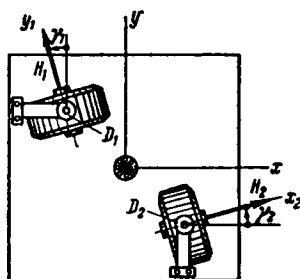
x-axis when $\gamma_2 = 0$. The signs of γ_1 and γ_2 are determined in a similar way to the sign of ψ.

Lastly let δ be the angle between the axis of rotation of gyro III and the plane of the platform (Figure 6). Choose the positive direction of δ in such a way that the projection of the angular momentum vector of gyro III on the z- ($\mathbf{z}$-) axis is positive when $0 < \delta \leqslant {}^1\!/_2\pi$.

6. To ensure continuous stabilization of body B, the device described must include, in addition to the gyros, also elements applying to frame K, platform P, and body B torques of magnitudes and directions determined by γ_1, γ_2, and δ. These elements may be the electric motors EM_1, EM_2, and EM_3 (Figures 2, 3, and 6). The frame of motor EM_1 is secured to the moving base; it develops a torque $M_{x'}$, applied to the gimbal frame K about the ξ- (x'-) axis. The motor is controlled by means of an amplifier, whose input voltage is supplied by the pick-up D_1 mounted on the housing pivot of gyro I. The torque applied to gyro I by the motor EM_1 causes a precession of the gyro which tends to reduce the angle γ_1. If the torque is sufficiently

large, γ_1 will never attain the value $\frac{1}{2}\pi$ at which the stabilization is disturbed. This could happen due to a rotation about the z-axis of the device together with the moving base, or by some other cause (gravity, friction, inertial loads, etc).

The motor EM_2, which applies to platform P, a torque M_y about the y'- (y-) axis, is mounted on frame K. It is controlled through the pick-up D_2, which records the angle γ_2.

Lastly, the motor EM_3, mounted on the platform P, tends to rotate the body B about the z- ($\tilde{z}$-) axis by developing a torque whose magnitude and direction are determined by δ (Figure 6).
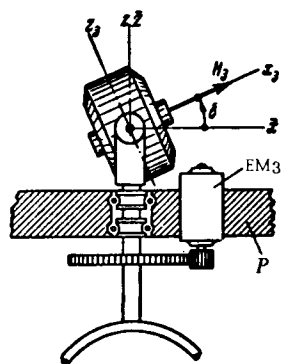

FIGURE 6

The body B can vary its orientation only as a result of the action of moments applied about the pivot axes of the housings of gyros I, II, and III. These may be due to friction which causes the specified orientation of body B to be altered. In order to restore this orientation, torques are caused to act about the pivot axes of the housings of the gyros by means of solenoids, and in many cases by utilizing the force of gravity*.

7. Six mechanical systems will be examined successively in order to establish the equations describing the behavior of this complex gyroscopic device: 1) the device as a whole, comprising the frame K, the platform P, the body B, and all three gyros with all the additional elements linked to them kinematically; 2) the device without the frame K; 3) the body B with gyro III; 4) the gyro I; 5) the gyro II; 6) the gyro III.

Each of these systems is linked to the others or to the moving base by a plane hinge. The torque about the hinge pivots due to external forces acting on the relevant system is assumed to be known.

* Torques created by small additional weights are capable of bringing the platform into the horizontal position, and of creating a precession of gyro III so that body B will not rotate relative to the Earth. For this latter purpose, a suitable weight, creating a torque about the y_3-axis, has to be mounted on the housing of gyro III. In order to bring the platform P into the horizontal position, it is sufficient to fix additional weights to one side of the housings of gyros I and II. When the platform is inclined, these weights create torques about the pivot axes of the housings, causing the precession of gyros I and II. When the weights are fixed to the correct sides of the housings, the platform returns to the horizontal position. Such a correction system is called mechanical. It is simpler than the so-called electric correction, in which the required torques are caused by solenoids. The magnitudes and directions of the torques are in this case determined by the deviations of pendulums mounted on platform P.

The angle of rotation of the pivot relative to the bearing is one of the generalized coordinates of the device; this is in fact the reason for selecting the above-mentioned mechanical systems.

A reference frame having its origin at the geometric center of the gimbals, i.e., at the common origin of the coordinate systems $\xi\eta\zeta$, $x'y'z'$, xyz, and xyz (fixed respectively to the moving base, the frame K, the platform P, and the body B), is taken as the basic frame $\xi^*\eta^*\zeta^*$ for the first three mechanical systems. The origins of the basic reference frames for the last three mechanical systems (the individual gyros) coincide in each case with the intersection of the housing-pivot and rotor axes of the corresponding gyro.

The same reference frame xyz, fixed to the platform P, is used in all cases as auxiliary frame. The angular velocity of this frame (or, which is the same, of the platform P) relative to the basic reference frame $\xi^*\eta^*\zeta^*$ will be denoted by ω, and its projections on the x-, y-, and z-axes by ω_x, ω_y, ω_z. The projections ω_x and ω_y are determined by the precession of gyros I and II, and must therefore be small; since ω_z is determined by the motion of the base carrying the stabilizer, its magnitude can be arbitrary.

8. Let M' be the resultant moment of the external forces acting on the first mechanical system*.

The angular momentum G' of the first mechanical system is (within the limits of the elementary theory) equal to the sum of the angular momentums of gyros I, II, and III. Its projections on the axes of the auxiliary reference frame xyz will respectively be

$$G'_x = H(-\sin \gamma_1 + \cos \gamma_2 + \cos \delta \cos \psi),$$
$$G'_y = H(\cos \gamma_1 + \sin \gamma_2 + \cos \delta \sin \psi), \qquad (6)$$
$$G'_z = H \sin \delta,$$

as is easily seen from Figures 5 and 7. The angular momentum of each gyro is assumed to be $H = $ const.

The following relationships, similar to (3), are obtained by applying the angular momentum theorem to the first mechanical system:

$$\frac{dG'_x}{dt} + \omega_y G'_z - \omega_z G'_y = M'_x,$$
$$\frac{dG'_y}{dt} + \omega_z G'_x - \omega_x G'_z = M'_y, \qquad (7)$$
$$\frac{dG'_z}{dt} + \omega_x G'_y - \omega_y G'_x = M'_z.$$

It is seen from Figure 3 that (exactly as for (5)) the expression

$$M'_x \cos \beta + M'_z \sin \beta = M'_{x'} \qquad (8)$$

represents the sum of the moments about the x'- (ξ-) axis due to the forces acting on the first mechanical system, i.e., the complete stabilizer. This sum does not contain the moments due to the bearings constraints.

---

* Within the limits of the elementary theory of gyroscope precession the resultant vector of all these forces is equal to zero; they are therefore equivalent to a couple of moment M'.

We obtain

$$\left[\frac{dG'_z}{dt}+\omega_y G'_z-\omega_z G'_y\right]\cos\beta+\left[\frac{dG'_z}{dt}+\omega_z G'_y-\omega_y G'_z\right]\sin\beta=M'_{z'}, \quad (9)$$

by subsituting in (8) for M'_z and M'_z their expressions from (7). This represents therefore the equation of motion of the gyrostabilizer. It does not contain the moments due to the unknown constraints in the pivot bearings of frame K^*.

Inserting (6) into (9) yields

$$H\left\{\cos\beta\frac{d}{dt}\left(-\sin\gamma_1+\cos\gamma_2\right)-\cos\beta\cos\delta\sin\psi\left(\omega_z+\frac{d\psi}{dt}\right)-\right.$$
$$-\left(\cos\beta\sin\delta\cos\psi-\sin\beta\cos\delta\right)\frac{d\delta}{dt}+\omega_y\left[\cos\beta\sin\delta-\right.$$
$$-\sin\beta\left(-\sin\gamma_1+\cos\gamma_2+\cos\delta\cos\psi\right)]+$$
$$+\left(\omega_z\sin\beta-\omega_z\cos\beta\right)\left(\cos\gamma_1+\sin\gamma_2\right)+$$
$$\left.+\omega_z\sin\beta\cos\delta\sin\psi\right\}=M'_{z'}. \quad (10)$$

The torque $M'_{z'}$ includes, in addition to the moments due to friction and to the torque developed by the electric motor EM_1, also the moments due to gravity acting on the moving parts and to the inertia forces caused by the translational motion of the basic frame $\xi^*\eta^*\zeta^*$ (whose origin is at the geometric center of the gimbals).
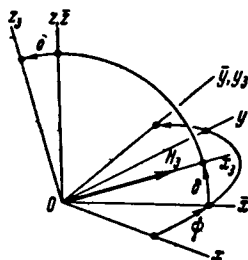

FIGURE 7

9. Equation (10) is one of the six differential equations which describe the motion of the gyroscopic stabilizer. In order to obtain the second of these equations, consider a mechanical system which includes all components of the stabilizer except the frame K. Since the angular momentum of frame K is neglected in the elementary theory of gyroscopes, the total angular momentum G of this system is equal to the total angular momentum G' of the system which includes the frame:

$$G_z=G'_z, \quad G_y=G'_y, \quad G_z=G'_z, \quad (11)$$

where G_z, G_y, and G_z are the projections of the angular momentum of the new mechanical system on the axes x, y, and z, and G'_z, G'_y and G'_z are given by (6).

In this system the constraints acting between platform P and frame K are external and must be taken into account in the equations derived from the

* It is assumed that friction in all gimbal bearings is independent of the constraining forces.

268

angular momentum theorem. These equations are similar to (3). The only equation (3) which contains no constraining forces is the second, since the y- (y'-) axis is the pivot axis of platform P whose bearings are rigidly fixed to frame K.

The following equation is obtained from (6), (7), and (11):

$$H\left[\frac{d}{dt}(\cos\gamma_1+\sin\gamma_2)-\sin\delta\sin\psi\frac{d\delta}{dt}+\left(\omega_z+\frac{d\psi}{dt}\right)\cos\delta\cos\psi+\right.$$
$$\left.+\omega_z(-\sin\gamma_1+\cos\gamma_2)-\omega_x\sin\delta\right]=M_y. \tag{12}$$

The torque M_y includes the moment due to friction of the platform pivot in its bearings, the torque of motor EM_2, and the moments due to gravity and the inertia forces caused by the translational motion of all elements of the stabilizer except the frame K.

10. Consider now the third mechanical system — the body B with gyro III (Figure 4). Its angular momentum is the angular momentum $\vec{G}$ of gyro III. It follows (Figure 7) that the projections of the vector $\vec{G}$ on the axes of the auxiliary reference frame xyz are equal to

$$\vec{G}_x=H\cos\delta\cos\psi, \qquad \vec{G}_y=H\cos\delta\sin\psi, \qquad \vec{G}_z=H\sin\delta. \tag{13}$$

In this case the third equation (3) has to be used, since the other two contain the unknown constraints in the bearings of the body B. These are external forces with respect to this particular mechanical system. The following equation is therefore obtained with the aid of (13):

$$H\left(\cos\delta\frac{d\delta}{dt}+\omega_x\cos\delta\sin\psi-\omega_y\cos\delta\cos\psi\right)=\tilde{M}_z. \tag{14}$$

Here $\tilde{M}_z$ is the moment about the z- (z-) axis due to all external forces acting on the third mechanical system consisting of the body B, and the housing and rotor of gyro III. This includes friction, the torque applied by motor EM_3, and also the moments due to inertia and gravity. The inertia forces are those due to the translational motion of the basic reference frame $\xi^*\eta^*\zeta^*$ whose origin is at the geometric center of the stabilizer suspension.

11. When the last three mechanical systems — the gyros I, II, and III — are being considered, the corresponding basic reference frames $\xi_1^*\eta_1^*\zeta_1^*$, $\xi_2^*\eta_2^*\zeta_2^*$ and $\xi_3^*\eta_3^*\zeta_3^*$ have to be chosen so that their origins will lie at the intersections of the housing-pivot axis with the rotor spindles of the corresponding gyros. They will have different accelerations relative to the absolute reference frame $\xi_a^*\eta_a^*\zeta_a^*$. This difference is due to the angular velocity ω of the platform P and, in the case of the basic frame $\xi_3^*\eta_3^*\zeta_3^*$, also to the relative angular velocity $\frac{d\psi}{dt}$ of body B relative to platform P.

Due to the small dimensions of the gyroscopic stabilizer and to the low values of ω_x, ω_y, ω_z and $\frac{d\psi}{dt}$ this difference between the accelerations of the frames $\xi_1^*\eta_1^*\zeta_1^*$, $\xi_2^*\eta_2^*\zeta_2^*$, $\xi_3^*\eta_3^*\zeta_3^*$ and the acceleration of the basic frame $\xi^*\eta^*\zeta^*$ is small and usually can be neglected.

The following equation, similar to the third relationship (3), is obtained by applying the angular momentum theorem to the mechanical system consisting of the rotor and housing of gyro I:

$$\frac{d}{dt}G_z^I+\omega_xG_y^I-\omega_yG_z^I=M_{z_1}^I. \tag{15}$$

This equation does not contain the unknown constraining forces at the housing bearings. Here (Figure 5),

$$G_x^I = -H \sin \gamma_1, \quad G_y^I = H \cos \gamma_1, \quad G_z^I = 0 \qquad (16)$$

are the projections of the angular momentum G^I of this system (equal to the angular momentum of gyro I) on the axes of the auxiliary reference frame xyz.

The magnitude $M_{z_1}^I$ represents the sum of the moments about the z_1-axis due to the forces acting on the housing and rotor of this gyro. These forces are due to friction in the bearings of the housing suspension, gravity, the translational motion, the elasticity of the electric wires, and the reactions of the pick-ups.

Inserting (16) into (15) yields

$$H \left(\omega_x \cos \gamma_1 + \omega_y \sin \gamma_1 \right) = M_{z_1}^I. \qquad (17)$$

This is the fourth equation of motion of the gyroscopic stabilizer.

Similar calculations for gyro II yield the fifth equation:

$$H \left(\omega_x \sin \gamma_2 - \omega_y \cos \gamma_2 \right) = M_{z_1}^{II}. \qquad (18)$$

The moment $M_{z_1}^{II}$ is analogous to the moment $M_{z_1}^I$; it represents the sum of the moments about the z_2-axis due to the forces acting on the housing and rotor of gyro II.

Equations (17) and (18) do not contain the unknown constraining forces at the bearings of the gyro housings.

12. Consider finally the sixth mechanical system, consisting of the housing and rotor of gyro III (Figure 6). Inserting into (3) the projections

$$G_x^{III} = H \cos \delta \cos \psi, \quad G_y^{III} = H \cos \delta \sin \psi, \quad G_z^{III} = H \sin \delta \qquad (19)$$

of the angular momentum of gyro III yields

$$H \left[\frac{d}{dt} (\cos \delta \cos \psi) + \omega_y \sin \delta - \omega_z \cos \delta \sin \psi \right] = M_x^{III},$$

$$H \left[\frac{d}{dt} (\cos \delta \sin \psi) + \omega_z \cos \delta \cos \psi - \omega_x \sin \delta \right] = M_y^{III}, \qquad (20)$$

$$H \left[\frac{d}{dt} \sin \delta + (\omega_x \sin \psi - \omega_y \cos \psi) \cos \delta \right] = M_z^{III}.$$

M_x^{III}, M_y^{III}, M_z^{III} are the sums of the moments about axes respectively parallel to the x- y-, and z-axes, but passing through the geometric center of the gimbals of gyro III, due to forces acting on the housing and rotor of gyro III.

These forces include also the constraining forces at the bearings of the gyro housing, located in body B. To eliminate these unknown forces, form the expression

$$-M_x^{III} \sin \psi + M_y^{III} \cos \psi = M_{y_3}^{III}, \qquad (21)$$

being the sum of the moments about the y_3-axis due to the forces acting on gyro III. It contains no constraining forces. Substitution of the values of M_x^{III} and M_y^{III} from (20) yields

$$H \left[\left(\omega_z + \frac{d\psi}{dt} \right) \cos \delta - (\omega_x \cos \psi + \omega_y \sin \psi) \sin \delta \right] = M_{y_3}^{III}. \qquad (22)$$

270

, Note that different auxiliary reference frames may be used to derive (17), (18), and (22); thus, (22) can be obtained by using the frame xyz fixed. to body B (Figure 4).

Equation (22) completes the set of six equations describing the behavior of the gyrostabilizer and its components both relative to each other and relative to the Newtonian frame.

13. Let (10), (12), (14), (17), (18), and (22) form a set. The following equations describing the motion of a triaxial power gyrostabilizer are obtained:

$$H\left\{\cos\beta\left[\frac{d}{dt}(-\sin\gamma_1+\cos\gamma_2)-\cos\delta\sin\phi\left(\omega_z+\frac{d\psi}{dt}\right)+\omega_y\sin\delta\right]-\right.$$

$$-(\cos\beta\sin\delta\cos\phi-\sin\beta\cos\delta)\frac{d\Omega}{dt}+\sin\beta[\omega_z\cos\delta\sin\phi-$$

$$-\omega_y(-\sin\gamma_1+\cos\gamma_2+\cos\delta\cos\phi)]+$$

$$\left.+(\omega_z\sin\beta-\omega_x\cos\beta)(\cos\gamma_1+\sin\gamma_2)\right\}=M'_{x'};$$

$$H\left[\frac{d}{dt}(\cos\gamma_1+\sin\gamma_2)-\sin\delta\sin\psi\frac{d\Omega}{dt}+\left(\omega_z+\frac{d\psi}{dt}\right)\cos\delta\cos\phi+\right.$$

$$\left.+\omega_z(-\sin\gamma_1+\cos\gamma_2)-\omega_s\sin\delta\right]=M_{y};$$

(23)

$$H\left(\cos\delta\frac{d\Omega}{dt}+\omega_z\cos\delta\sin\phi-\omega_y\cos\delta\cos\phi\right)=\bar{M}_{z};$$

$$H(\omega_z\cos\gamma_1+\omega_y\sin\gamma_1)=M^I_{z_1};$$

$$H(\omega_z\sin\gamma_2-\omega_y\cos\gamma_2)=M^{II}_{z_1};$$

$$H\left[\left(\omega_z+\frac{d\psi}{dt}\right)\cos\delta-(\omega_z\cos\phi+\omega_y\sin\phi)\sin\delta\right]=M^{III}_{y_1}.$$

14. Several important conclusions can be drawn from these equations. Let

$$M^I_{z_1}=M^{II}_{z_1}=M^{III}_{y_1}=0. \tag{24}$$

This means that no torques are applied to the pivot axes of the gyro housing. This can in practice be approximated by reducing friction in bearings and strain in the electric wires to a minimum and by mounting the stabilizer so that by careful balancing the center of gravity of each mechanical system housing rotor is made to lie on the housing pivot axis.

The fourth and fifth equations (23) then yield:

$$\omega_z\cos\gamma_1+\omega_y\sin\gamma_1=0, \quad \omega_z\sin\gamma_2-\omega_y\cos\gamma_2=0. \tag{25}$$

It follows that

$$\omega_z=\omega_y=0 \tag{26}$$

unless

$$\gamma_2=\gamma_1\pm\frac{1}{2}\pi, \tag{27}$$

which means that the axes of rotation of gyros I and II are parallel. Thus if γ_1 and γ_2 are maintained smaller than 45° by the action of the electric motors EM_1 and EM_2, the platform P will be partially stabilized when the first two of conditions (24) are satisfied. The perpendicular to the platform (the z-axis) does not alter its orientation relative to the Newtonian frame.

Inserting (24) and (26) into the sixth of equations (23) yields

$$\omega_z + \frac{d\psi}{dt} = 0;\qquad (28)$$

provided, of course, that

$$\delta \neq \pm \frac{1}{2}\pi.\qquad (29)$$

The left-hand side of (28) represents the projection on the z- ($\tilde{z}$-) axis of the angular velocity of body B relative to the basic reference frame $\xi^*\eta^*\zeta^*$. The projections of this angular velocity on the x- and y-axes coincide with the corresponding projections of the angular velocity of platform P and are equal to zero because of (26). Therefore, when no torques are applied to the pivot axes of the housings of the three gyros, i.e., when condition (24) is satisfied, the body B is stabilized relative to the Newtonian reference frame.

Inserting (26) and (28) into the first three of equations (23) yields,

$$-H\cos\beta\left[\frac{d}{dt}(\sin\gamma_1 - \cos\gamma_2) + (\sin\delta\cos\psi - \cos\delta\,\mathrm{tg}\,\beta)\frac{d\delta}{dt} + \right.$$
$$\left. + \omega_z(\cos\gamma_1 + \sin\gamma_2)\right] = M'_{x'},$$
$$H\left[\frac{d}{dt}(\cos\gamma_1 + \sin\gamma_2) - \sin\delta\sin\psi\frac{d\delta}{dt} + \omega_z(-\sin\gamma_1 + \cos\gamma_2)\right] = M_y, \qquad (30)$$
$$H\cos\delta\frac{d\delta}{dt} = \tilde{M}_z.$$

15. Assume that no torques are applied to frame K, platform P, and body B, and that there is no friction in their bearings:

$$M'_{x'} = M_y = \tilde{M}_z = 0.\qquad (31)$$

If condition (24) is also satisfied, and if the angular velocity of the base is such that

$$\omega_z = 0,\qquad (32)$$

then equations (30) will be satisfied when γ_1, γ_2, and δ are constant.

Let the electric motors EM_1, EM_2, and EM_3 be controlled in such a manner that the torques applied by them to the pivot axes of frame K, platform P, and body B are proportional to the tilting angles of the housings of the corresponding gyros, and assume that there is no friction in the gimbal bearings. In this case

$$M'_{x'} = k\gamma_1,\quad M_y = -k\gamma_2,\quad \tilde{M}_z = -k\delta,\qquad (33)$$

where k is a proportionality factor.

Equations (30), together with condition (32), have in this case a solution:

$$\gamma_1 = 0,\quad \gamma_2 = 0,\quad \delta = 0.\qquad (34)$$

It is easily seen that the equilibrium position of the gyrostabilizer, defined by (34), is stable (within the limits of the elementary theory). In fact, if γ_1, γ_2, and δ are small, their trigonometric functions in (30) can be replaced by the zero- and first-order terms of their series expansions. Taking into account (32) and (33), equations (30) become

$$-H\cos\beta\frac{d\gamma_1}{dt} = k\gamma_1 - H\sin\beta\frac{d\delta}{dt},\quad H\frac{d\gamma_2}{dt} = -k\gamma_2,\qquad (35)$$
$$H\frac{d\delta}{dt} = -k\delta.$$

It follows that γ_1, γ_2, and δ will tend to zero irrespective of the law of variation of β determined by the motion of the base; of course $\beta < 90°*$.

In the general case the right-hand sides of (30), i.e., the torques $M'_{x'}$, M_y, and $\tilde{M}_z$, include in addition to the torques of the electric motors, also the moments due to friction in the suspension bearings of the frame K, platform P, and body B, determined by the relative angular velocities $d\alpha/dt$, $d\beta/dt$, and $d\psi/dt$. In addition, when the mechanical system and its separate parts are insufficiently balanced, $M'_{x'}$, M_y, and $\tilde{M}_z$ include also the moments due to gravity and the inertia forces caused by the translational motion.

Assume that $\omega_z \neq 0$. Then, assuming that γ_1, γ_2, and δ are small, equations (30) can be written

$$-H\cos\beta\left[\frac{d\gamma_1}{dt} - \operatorname{tg}\beta\frac{d\delta}{dt} + \omega_z(1+\gamma_2)\right] = M'^{\bullet}_{x'} + M(\gamma_1),$$

$$H\left[\frac{d\gamma_2}{dt} + \omega_z(1-\gamma_1)\right] = M^{\bullet}_y + M(\gamma_2), \qquad (36)$$

$$H\frac{d\delta}{dt} = \tilde{M}^{\bullet}_z + \tilde{M}(\delta),$$

where $M'^{\bullet}_{x'}$, $M^{\bullet}_y$, and $\tilde{M}^{\bullet}_z$ are the sums of the moments due to friction, inertia, gravity, etc, acting respectively on the following mechanical systems:
1) frame K— platform P — body B and gyros I, II, III; 2) platform P— body B and gyros I, II, III; 3) body B and gyro III.

$M(\gamma_1)$, $M(\gamma_2)$, and $\tilde{M}(\delta)$ are the torques applied to these mechanical systems by the motors EM_1, EM_2, and EM_3 respectively.

The torque produced by each electric motor cannot exceed a certain limit imposed by motor and motor transmission. Figure 8 shows a fairly common type of functional relationship between the motor torque M for the case of a short-circuited squirrel-cage motor (rotor at rest) and the angle γ for the corresponding gyro. The so-called stepped relationship, is shown in Figure 9.
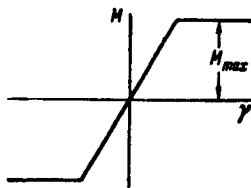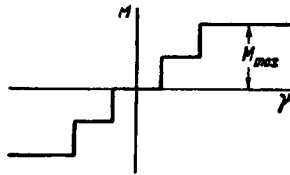

FIGURE 8   FIGURE 9

Satisfactory performance of the stabilizer requires that for any motion of the object, the maximum torque M_{max} exceed the corresponding destabilizing moment $M'^{\bullet}_{x'}$, $M^{\bullet}_y$, or $\tilde{M}^{\bullet}_z$. Similarly, the maximum torque of motors EM_1 and EM_2 should exceed by a margin the product

$$(\omega_z)_{max} H, \qquad (37)$$

* It is possible that when the motors are switched in the transient processes mentioned in §1 are not damped, leading to oscillations of the gyroscopic platform (primarily about the x-axis). To study these oscillations and the means for damping them, it is necessary to take into account the moments of inertia of the gyroscopic-device elements and transient processes in the electric circuits of the motors and the feedback circuits of the amplifiers. The influence of the motion of the base itself on the oscillations is usually negligible because of their high frequency. The analysis of these oscillations of the gyrostabilizer forms the subject of a separate study.

where $(\omega_z)_{max}$ is the maximum value of the angular velocity of the platform about the z-axis, caused by the object's rotation. In the contrary case, the housings of gyros I and II will lag behind the platform during its rotation, and γ_1 and γ_2 may increase infinitely.

The conditions under which the body B is stabilized relative to a Newtonian frame are given above. They require that the sum of the moments about the pivot axes of the corresponding housings due to the forces acting on each of the three mechanical-system housing rotors be separately equal to zero. This can be achieved only if friction in the bearings of the housing pivots is completely eliminated, if the center of gravity of the system housing rotor is accurately located on the housing pivot axis, etc.

In many cases it is required that the body B be stabilized relative to a reference frame linked to the local vertical and the compass points; such a frame is usually called a geographic reference frame, and its axes are directed to the east, the north, and the zenith respectively. When the base is stationary, the angular velocity of body B must be equal to the angular velocity of the Earth. If the base moves, the angular velocity of body B must be equal to the sum of the angular velocity of the Earth and the angular velocity relative to the Earth of the geographic reference frame.

In this case, torques $M_{z_1}^I$, $M_{z_2}^{II}$, and $M_{y_3}^{III}$, causing precession of the gyros, and, as a result, the required angular velocity of body B, have in accordance with the last three of equations (23) to be applied to the pivot axes of the housings of gyros I, II, and III. It is very difficult to realize this technically.

Appendix 2

THEORY OF THE GYROHORIZONCOMPASS*

1. This appendix gives a rigorous treatment of the precessional theory of a gyrohorizoncompass having as sensitive element a device similar to the so-called gyrosphere of the "New Anschütz" gyrocompasses**.

This sensitive element can be considered as a set of two gyros whose housings have parallel pivot axes with bearings rigidly mounted on the same frame; this frame will be called the gyro frame (Figure 1).   In the
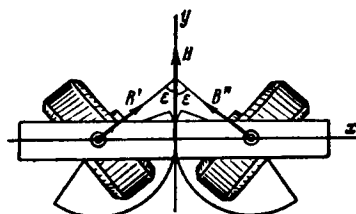

FIGURE 1

double-gyrocompass this frame is enclosed in a spherical shell and immersed in a liquid.   An almost frictionless suspension is thus obtained (Figure 2).
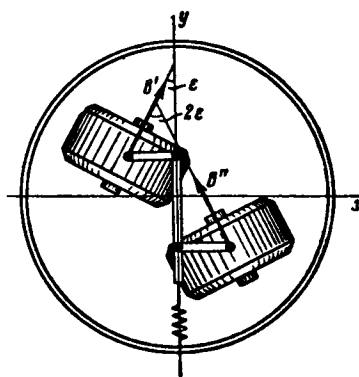

FIGURE 2

275

It will be assumed that the center of the frame suspension moves along a sphere S of radius R which encloses the Earth, and that the force of gravity acting on the frame is a single force F applied at the center of gravity of the frame and gyros, in a direction normal to the sphere.

It will also be assumed that the sphere S does not participate in the Earth's rotation and does not alter its orientation relative to a Newtonian reference frame. The translational motion of the sphere due to the Earth's rotation about the Sun can be neglected since the gravitational gradient is very small. The center of sphere S can therefore be considered as stationary.

It is convenient to study the gyro-frame motion relative to the sphere S*.

Friction in the suspension of the frame and in the bearings of the gyro-housing pivot axes, and the unavoidable assembly inaccuracies (e.g., axial and radial clearance in the bearings, residual unbalance about the suspension axes), will be neglected.

It will be assumed that the housings of the two gyros are tilted through equal and opposite angles relative to the frame (or, which is the same, relative to the sensitive element of the double-gyrocompass) by gears or link mechanisms (Figures 1 and 2).

2. In accordance with the elementary theory of gyroscope precession, it will be assumed that the total angular momentum H of the gyro frame as a whole is equal to the geometric sum of the angular momentums B' and B'' (of equal magnitude) of the two gyros. Let 2ε be the angle between the axes of the gyro rotors (Figure 1). Thus

$$H = 2B \cos \varepsilon \quad (B = B' = B'').\tag{1}$$

The vector of the total angular momentum H, is directed along the bisector of the angle 2ε; because of the above-mentioned gear [or linkage], the vector H has a constant position relative to the frame.

Let a coordinate system xyz be fixed to the gyro frame with origin at the center of suspension, y-axis parallel to the vector H, and z-axis parallel to the pivot axes of the gyro housings. This defines uniquely the position of the x-axis (Figure 3).
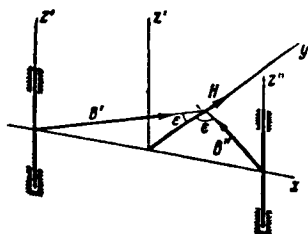

FIGURE 3

Let ω_x, ω_y, and ω_z be the projections on the axes of this system of the frame's angular velocity relative to the sphere S (or, which is the same,

* Ishlinskii, A. Yu. Ob otnositel'nom ravnovesii fizicheskogo mayatnika s podvizhnoi tochkoi opory (The Relative Equilibrium of a Physical Pendulum with a Moving Point of Support). — PMM, Vol. 20, No. 3. 1956.

relative to a Newtonian reference frame). The expressions

$$\frac{dH_x}{dt} + \omega_y H_z - \omega_z H_y,$$

$$\frac{dH_y}{dt} + \omega_z H_x - \omega_x H_z,$$

$$\frac{dH_z}{dt} + \omega_x H_y - \omega_y H_x$$

(2)

represent the projections of the time rate of change of the angular momentum H on the x-, y-, and z-axes.

According to the angular momentum theorem, these projections are respectively equal to the sums of the moments acting on the frame about these axes. These moments will be denoted by M_x, M_y, and M_z.

The frame's angular momentum vector is directed along the y-axis. Therefore,

$$H_x = 0, \quad H_y = H = 2B \cos \varepsilon, \quad H_z = 0.$$

The following three equations result from this:

$$-\omega_z H = M_x, \quad \frac{dH}{dt} = M_y, \quad \omega_x H = M_z. \tag{3}$$

The gyro frame thus represents a mechanical system having four degrees of freedom, and therefore a fourth equation, containing the projection of the angular velocity ω_y, has to be added to (3) in order to define the motion completely. The z-components of the time rate of change of the gyros' angular momentums are

$$\omega_x B'_y - \omega_y B'_x = M'_z, \quad \omega_x B''_y - \omega_y B''_x = M''_z. \tag{4}$$

Here M'_z and M''_z are the sums of the moments acting on the housings of each gyro about the pivot axes of these housings, and B'_x, B'_y, B''_x, B''_y are the projections on the x- and y-axes of the angular momentums B' and B'' of the gyros. Obviously (Figure 3):

$$B'_x = -B''_x = B \sin \varepsilon, \quad B'_y = B''_y = B \cos \varepsilon. \tag{5}$$

In accordance with the elementary theory of gyroscope precession only the angular momentums of the gyro rotors enter into the equations of motion. The remaining angular momentums and their time variations are neglected. It is therefore assumed that the forces acting directly on the frame are in equilibrium. In particular

$$M_z - M'_z - M''_z = 0. \tag{6}$$

Here $-M'_z$ and $-M''_z$ are the moments of the couples counteracting the moments M'_z and M''_z applied by the frame.

When (4) is inserted into (6) and (1) and (5) are taken into account, the third of equations (3) is obtained.

Let N be the difference between the moments M'_z and M''_z. It then follows from (4) and (5) that

$$N = M'_z - M''_z = -\omega_y 2B \sin \varepsilon. \tag{7}$$

A moment N can be created by means of a spring device.

By virtue of (3), (7), and (1), the motion of the gyro frame is determined by the following four equations:

$$-\omega_x 2B \cos \varepsilon = M_x; \qquad \omega_z 2B \cos \varepsilon = M_z;$$
$$\frac{d}{dt}(2B \cos \varepsilon) = M_y; \qquad -\omega_y 2B \sin \varepsilon = N. \tag{8}$$

3. The parameters characterizing the gyro frame, and in particular the relationship between N and ε, can be chosen so that for certain initial conditions the z-axis will remain always normal to the sphere S, irrespective of the motion of the frame suspension point on it.

To prove this, it suffices to find the conditions under which equations (8) become identities.

Introduce a moving reference frame $\xi^*\eta^*\zeta^*$ having its origin at the point of gyro-frame suspension and whose axes are oriented by a Newtonian reference frame. The equations of motion of the gyro frame relative to this coordinate system are given by (8).

The forces acting on the gyro frame also include, in addition to gravity and the suspension constraints, the inertia forces due to the translational motion together with frame $\xi^*\eta^*\zeta^*$. These inertia forces form a single force Q acting at the center of gravity of the gyro frame. The projections of this force on the x-, y-, and z-axes are

$$Q_x = -mw_x, \quad Q_y = -mw_y, \quad Q_z = -mw_z. \tag{9}$$

Here m is the mass of the frame together with the housings and rotors of the gyros, and w_x, w_y, w_z are the projections on the x-, y-, z-axes of the acceleration of the frame suspension point.

Therefore [*]

$$w_x = \frac{dv_x}{dt} + \omega_y v_z - \omega_z v_y, \quad w_y = \frac{dv_y}{dt} + \omega_z v_x - \omega_x v_z,$$
$$w_z = \frac{dv_z}{dt} + \omega_x v_y - \omega_y v_x, \tag{10}$$

where v_x, v_y, v_z are the projections of the velocity of the frame suspension point, and ω_x, ω_y, ω_z the projections of the angular velocity of the gyro frame (and therefore of the coordinate system xyz) relative to the sphere S.

The z axis must be normal to the sphere S, and therefore [**]

$$v_x = \omega_y R, \quad v_y = -\omega_x R, \quad v_z = 0. \tag{11}$$

Using (9), (10), and (11), the projections of the force Q on the axes of the system xyz can now be written in the form

$$Q_x = -mR\left(\frac{d\omega_y}{dt} + \omega_z \omega_x\right), \quad Q_y = -mR\left(-\frac{d\omega_x}{dt} + \omega_z \omega_y\right),$$
$$Q_z = -mR(-\omega_x^2 - \omega_y^2). \tag{12}$$

Let the frame's center of gravity be located on the negative z-axis at a distance l from the suspension point. In this case the force of gravity is

[*] Suslov, K. G. Teoreticheskaya mekhanika (Theoretical Mechanics). — Gostekhizdat. 1944. [cf: Goldstein Classical Mechanics. p. 135. —Addison-Wesley Press. 1951.]

[**] Ishlinskii, A. Yu. Ob otnositel'nom ravnovesii fizicheskogo mayatnika s podvizhnoi tochkoi opory (The Relative Equilibrium of a Physical Pendulum with a Moving Point of Support). — PMM, Vol. 20, No. 3. 1956.

directed along the z-axis, and its moment about the suspension point is therefore zero. The same is true of the component Q_z of the inertia force due to translational motion and of the reaction of the link. In order to determine the moments M_x, M_y, and M_z, it suffices therefore to find the moments about the x-, y-, and z-axes due to the forces Q_x and Q_y. The following expressions are then obtained:

$$M_x = lQ_y, \quad M_y = -lQ_x, \quad M_z = 0. \tag{13}$$

Inserting these expressions into (8), and using (12) in the resulting equations, yields

$$-\omega_z 2B \cos \varepsilon = mlR\left(\frac{d\omega_x}{dt} - \omega_y\omega_z\right), \qquad \omega_x 2B \cos \varepsilon = 0,$$

$$\frac{d}{dt}(2B \cos \varepsilon) = mlR\left(\frac{d\omega_y}{dt} + \omega_x\omega_z\right), \quad -\omega_y 2B \sin \varepsilon = N. \tag{14}$$

It remains to determine the conditions under which these equations become identities.

It follows from the third of equations (14) (except for the exceptional case $\varepsilon = \frac{1}{2}\pi$) that:

$$\omega_x = 0. \tag{15}$$

It is now easily seen that the first two of equations (14) are satisfied if

$$2B \cos \varepsilon = H = mlR\omega_y. \tag{16}$$

Eliminating ω_y from the fourth of equations (14) by means of (16) yields

$$N = -\frac{4B^2}{mlR} \cos \varepsilon \sin \varepsilon. \tag{17}$$

It follows from (15) and the second of equations (11) that

$$v_y = 0. \tag{18}$$

The x-axis must therefore be initially tangent to the trajectory of the suspension point in its motion on the sphere S (Figure 4), but it will remain so
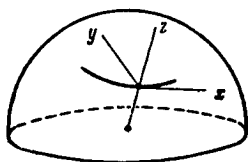
FIGURE 4
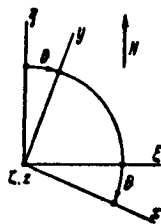
FIGURE 5

throughout the motion only if the other initial conditions, given below, are likewise satisfied.

Since by (11) and (15) $v_y = v_z = 0$, $v = v_x = \omega_y R$, where v is the velocity of the frame suspension point relative to the sphere S. Equation (16) therefore becomes

$$2B \cos \varepsilon = mlv. \tag{19}$$

If the initial velocity is v_0, the initial angle ε_0 will be given by

$$\cos \varepsilon_0 = \frac{mlv_0}{2B}. \tag{20}$$

Equation (19) will then be satisfied throughout the motion of the suspension point, as can be seen by inserting (15) into the second of equations (14).

Lastly, the z-axis must initially be normal to the sphere S.

When these conditions are satisfied, the moment N given by (17) will be such that the component ω_y of the angular velocity of the frame, determined by it, will satisfy the first of equations (11), as can be seen by inserting (16) and (17) into the fourth of equations (14).

If conditions (18) and (20) are nearly satisfied initially and the z-axis deviates by a small angle from the normal to the sphere S, the motion of the frame can be analyzed by studying the small perturbations of the motion which would strictly satisfy the initial conditions. This problem will be discussed under 6.

4. The gyro-frame motion relative to the Earth will now be examined under the assumption that the Earth is a sphere of radius R and that all the conditions under 3 are rigorously satisfied.

Introduce a moving reference frame $\xi\eta\zeta$ (a geographical trihedron), with the ξ-axis directed to the east and tangent to the parallel, η-axis to the north and tangent to the meridian, and ζ-axis directed upward along the Earth's radius; let the origin be located at the frame suspension point.

Let U be the angular velocity of the Earth, φ, the local latitude (strictly speaking the geocentric latitude), and V_ξ and V_η, the eastern and northern components of the velocity relative to the Earth of the origin of the system $\xi\eta\zeta$. The projections on the ξ- and η-axes of the velocity of the origin relative to the sphere S are

$$v_\xi = V_\xi + UR \cos \varphi, \quad v_\eta = V_\eta. \tag{21}$$

Replacing the subscripts x and y in (11) by ξ and η respectively, and using (21), we have

$$u_\xi = -\frac{V_\eta}{R}, \quad u_\eta = \frac{V_\xi}{R} + U \cos \varphi \tag{22}$$

where u_ξ and u_η are the projections of the angular velocity of the trihedron $\xi\eta\zeta$ relative to the Newtonian reference frame $\xi^*\eta^*\zeta^*$. The projection of this angular velocity on the ζ-axis is

$$u_\zeta = \frac{V_\xi}{R} \operatorname{tg} \varphi + U \sin \varphi. \tag{23}$$

Let ϑ be the angle between the y- and η-axes, measured as shown in Figure 5. It is easily seen that the projections on the x-, y-, and z-axes of the angular velocity of the reference frame xyz fixed to the gyro frame are

$$\omega_x = u_\xi \cos \vartheta - u_\eta \sin \vartheta, \quad \omega_y = u_\xi \sin \vartheta + u_\eta \cos \vartheta,$$

$$\omega_z = u_\zeta - \frac{d\vartheta}{dt}. \tag{24}$$

In accordance with (15) the x component of this angular velocity is equal to zero. Inserting (22) into the first of equations (24) yields

$$\operatorname{tg} \vartheta = -\frac{V_\eta}{RU \cos \varphi + V_\xi}. \tag{25}$$

The y-axis, which is linked to the gyro frame, thus deviates from the northern direction by an angle ϑ determined by (25). This is the so-called velocity deviation of the gyrocompass.

* Bulgakov, B. V. Prikladnaya teoriya giroskopov (Applied Theory of Gyroscopes). — Moskva, Gostekhizdat. 1955.

Consider now relationship (19) between the angular momentum of the gyro frame and the velocity of its suspension point on the sphere S. Inserting (21) into it yields[*],

$$H = 2B \cos \epsilon = ml \sqrt{(RU \cos \varphi + V_E)^2 + V_r^2} \qquad (26)$$

The above discussion shows that if (26) is satisfied the gyrocompass deviation will be strictly according to (25), provided only the relationship between N and ϵ, given by (17), and the initial conditions under 3 are observed. Note that the z-axis, linked to the gyro frame, is in this case directed toward the center of the Earth, and therefore forms with the vertical a small angle depending on the local latitude.

5. Form a Darboux trihedron $x^0 y^0 z^0$ with apex at the gyro-frame suspension point, and with the x^0-axis (edge) lying in the direction of the velocity relative to the sphere S of the frame suspension point, and the z^0-axis normal to the sphere; the direction of the y^0-axis is then uniquely determined. If the initial conditions of motion stated under 3 are observed, the x-, y-, and z-axes linked to the gyro frame will always coincide with the x^0-, y^0-, and z^0-axes for any displacement of the trihedron on the sphere S.

Consider now the initial conditions in the general case and form the equations of the gyro-frame motion relative to the trihedron $x^0 y^0 z^0$.

The position of the coordinate system xyz relative to the trihedron $x^0 y^0 z^0$ is defined by the three angles α, β, γ (see Figures 6 and 7). The angle α defines the rotation about the z'-axis, which coincides with the z^0-axis, of the auxiliary coordinate system $x'y'z'$ relative to the system $x^0 y^0 z^0$; the angle β defines the rotation about the x''-axis, which coincides with the x'-axis, of the auxiliary system $x''y''z''$ relative to the system $x'y'z'$; lastly, the angle γ defines the rotation about the y-axis, which coincides with the y''-axis, of the coordinate system xyz relative to the system $x''y''z''$. The direction cosines of the system xyz relative to the system $x^0 y^0 z^0$ are

	x^0	y^0	z^0
x	$\cos\alpha\cos\gamma - \sin\alpha\sin\beta\sin\gamma$	$\sin\alpha\cos\gamma + \cos\alpha\sin\beta\sin\gamma$	$-\cos\beta\sin\gamma$
y	$-\sin\alpha\cos\beta$	$\cos\alpha\cos\beta$	$\sin\beta$
z	$\cos\alpha\sin\gamma + \sin\alpha\sin\beta\cos\gamma$	$\sin\alpha\sin\gamma - \cos\alpha\sin\beta\cos\gamma$	$\cos\beta\cos\gamma$

$$(27)$$

In order to obtain the projections of the angular velocity of the coordinate system xyz on its own axes, it is necessary to take the sum of the projections on these axes of the angular velocity of trihedron $x^0 y^0 z^0$ and of the relative angular velocities $d\alpha/dt$ of the system $x'y'z'$ relative to the system $x^0 y^0 z^0$, $d\beta/dt$ of the system $x''y''z''$ relative to the system $x'y'z'$, and $d\gamma/dt$ of the system xyz relative to the system $x''y''z''$.

The vector of the angular velocity $d\alpha/dt$ is directed along the z^0-axis, that of $d\gamma/dt$ along the y''-axis, and that of $d\beta/dt$ along the x'-axis. The x'-axis, which coincides with the x''-axis, is the intersection of the planes $x^0 y^0$ and zx; it forms angles γ, $^1/_2\pi$, and $^1/_2\pi - \gamma$ respectively with the axes of the coordinate system xyz.

---

* Such a relationship was obtained earlier by Zheleznov in his improvement on the well-known Schuler condition $H = mlRU\cos\varphi$ in the approximate theory of gyrocompasses. When the Schuler condition is satisfied, the deviation of the gyrocompass is to a certain extent independent on of the ship's velocity and acceleration and is mainly determined by (25). Other scientists (Sleeve, Roitenberg) improved Schuler's condition (for the case of high latitudes) by taking into account only the eastern component V_E of the ship's velocity; this led to the expression $H = ml(RU\cos\varphi + V_E)$.

The following expressions for these projections are thus obtained from (27):

$$\omega_x = \omega_{x^0}^0 (\cos\alpha \cos\gamma - \sin\alpha \sin\beta \sin\gamma) +$$
$$+ \omega_{y^0}^0 (\sin\alpha \cos\gamma + \cos\alpha \sin\beta \sin\gamma) +$$
$$+ \left(\omega_{z^0}^0 + \frac{d\alpha}{dt}\right)(-\cos\beta \sin\gamma) + \frac{d\beta}{dt}\cos\gamma;$$

$$\omega_y = \omega_{x^0}^0 (-\sin\alpha \cos\beta) + \omega_{y^0}^0 \cos\alpha \cos\beta + \left(\omega_{z^0}^0 + \frac{d\alpha}{dt}\right)\sin\beta + \frac{d\gamma}{dt}; \qquad (28)$$

$$\omega_z = \omega_{x^0}^0 (\cos\alpha \sin\gamma + \sin\alpha \sin\beta \cos\gamma) +$$
$$\omega_{y^0}^0 (\sin\alpha \sin\gamma - \cos\alpha \sin\beta \cos\gamma) +$$
$$\left(\omega_{z^0}^0 + \frac{d\alpha}{dt}\right)\cos\beta \cos\gamma + \frac{d\beta}{dt}\sin\gamma.$$
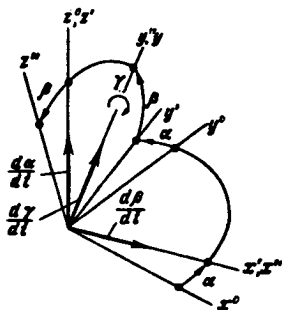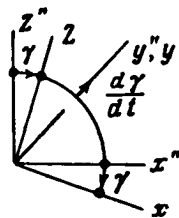

FIGURE 6

FIGURE 7

Here $\omega_{x^0}^0$, $\omega_{y^0}^0$, $\omega_{z^0}^0$ are the projections of the angular velocity of the trihedron $x^0 y^0 z^0$ on its own edges. It follows from (11) that

$$\omega_{x^0}^0 = -\frac{v_{y^0}^0}{R}, \quad \omega_{y^0}^0 = \frac{v_{x^0}^0}{R}, \qquad (29)$$

where $v_{x^0}^0$ and $v_{y^0}^0$ are the projections of the velocity of the trihedron apex on the x^0- and y^0-axes. However

$$v_{y^0}^0 = 0, \qquad (30)$$

since by assumption the velocity of the trihedron apex is along the x^0-axis. Inserting (29) and (30) into (28) yields:

$$\omega_x = \frac{v}{R}(\sin\alpha \cos\gamma + \cos\alpha \sin\beta \sin\gamma) +$$
$$+ \left(\omega + \frac{d\alpha}{dt}\right)(-\cos\beta \sin\gamma) + \frac{d\beta}{dt}\cos\gamma;$$

$$\omega_y = \frac{v}{R}\cos\alpha \cos\beta + \left(\omega + \frac{d\alpha}{dt}\right)\sin\beta + \frac{d\gamma}{dt}; \qquad (31)$$

$$\omega_z = \frac{v}{R}(\sin\alpha \sin\gamma - \cos\alpha \sin\beta \cos\gamma) +$$
$$+ \left(\omega + \frac{d\alpha}{dt}\right)\cos\beta \cos\gamma + \frac{d\beta}{dt}\sin\gamma.$$

Here

$$v = v_{x^0}^0, \quad \omega = \omega_{x_0}^0 \qquad (32)$$

are respectively the velocity of the trihedron apex relative to the sphere S

and the projection of the angular velocity of the trihedron apex on the normal to the sphere. The expressions for $\omega_x, \omega_y, \omega_z$ have to be inserted into the left-hand sides of (8).

We now find the right-hand sides of (8). The force of gravity F is, in accordance with the assumption under 3, directed toward the center of the sphere S and acts on the center of gravity of the frame. It is almost parallel to the z^0-axis. In accordance with (27), the projections of F on the x-, y-, and z-axes linked to the gyro frame are

$$F_x = F \cos \beta \sin \gamma, \quad F_y = -F \sin \beta, \quad F_z = -F \cos \beta \cos \gamma. \tag{33}$$

In order to find the corresponding projections of the inertia force Q due to translational motion, we use (12), which, with the aid of (29), (30), and (32), can be rewritten

$$Q_{x'} = -m \frac{dv}{dt}, \quad Q_{y'} = -m\omega v, \quad Q_{z'} = m \frac{v^2}{R}. \tag{34}$$

The same result could have been obtained directly by taking into account that

$$w_t = \frac{dv}{dt}, \quad w_g = \frac{v^2}{\rho_g}, \quad w_n = -\frac{v^2}{R} \tag{35}$$

represent the projections of the acceleration of a point moving on the sphere on the edges of the Darboux trihedron moving along the trajectory of this point. The radius of geodesic curvature ρ_g of the trajectory*, the angular velocity ω of the Darboux trihedron about the normal to sphere S (about the z^0-axis), and the velocity of its apex v are connected by the relationship

$$v = \omega \rho_g \tag{36}$$

The following expressions for the projections of the inertia force Q on the x-, y-, and z-axes linked to the gyro frame are obtained from (34) and (27):

$$Q_x = -m \frac{dv}{dt}(\cos \alpha \cos \gamma - \sin \alpha \sin \beta \sin \gamma) -$$
$$- m\omega v(\sin \alpha \cos \gamma + \cos \alpha \sin \beta \sin \gamma) + m \frac{v^2}{R}(-\cos \beta \sin \gamma);$$

$$Q_y = -m \frac{dv}{dt}(-\sin \alpha \cos \beta) - m\omega v \cos \alpha \cos \beta + m \frac{v^2}{R} \sin \beta; \tag{37}$$

$$Q_z = -m \frac{dv}{dt}(\cos \alpha \sin \gamma + \sin \alpha \sin \beta \cos \gamma) -$$
$$- m\omega v(\sin \alpha \sin \gamma - \cos \alpha \sin \beta \cos \gamma) + m \frac{v^2}{R} \cos \beta \cos \gamma.$$

The center of gravity of the gyro frame has the following coordinates in the system xyz: $x_c = y_c = 0$, $z_c = -l$.

The moments M_x, M_y, M_z of the forces acting on the gyro frame are therefore

$$M_x = l(F_y + Q_y) + M_x^\bullet, \quad M_y = -l(F_x + Q_x) + M_y^\bullet, \quad M_z = M_z^\bullet, \tag{38}$$

where $M_x^\bullet$, $M_y^\bullet$, $M_z^\bullet$ are the moments about the x-, y-, and z-axes due to all forces except gravity and inertia forces acting on the gyro frame.

The reaction at the frame suspension point, or forces due to fluid pressure on the gyrosphere in an Anschütz gyrocompass give rise to moments about the x-, y-, and z-axes which are separately equal to zero. Substituting

* Rashevskii, P. K. Kurs differentsial'noi geometrii (A Course in Differential Geometry). — Gostekhizdat, 1956.

in (38) for F_x, F_y, Q_x, and Q_y their expressions from (33) and (37) yields .

$$M_x = l\left[-m\frac{dv}{dt}(-\sin\alpha\cos\beta) - m\omega v\cos\alpha\cos\beta + \left(m\frac{v^2}{R} - F\right)\sin\beta\right] + M_x^*,$$

$$M_y = -l\left[-m\frac{dv}{dt}(\cos\alpha\cos\gamma - \sin\alpha\sin\beta\sin\gamma) - \right.$$

$$- m\omega v(\sin\alpha\cos\gamma + \cos\alpha\sin\beta\sin\gamma) + \quad\quad (39)$$

$$\left. + \left(m\frac{v^2}{R} - F\right)(-\cos\beta\sin\gamma)\right] + M_y^*,$$

$$M_z = M_r^*.$$

These expressions have to be inserted into (8) together with (31). The following equations of motion of the gyro frame relative to the Darboux trihedron are obtained as a result:

$$-\left[\frac{v}{R}(\sin\alpha\sin\gamma - \cos\alpha\sin\beta\cos\gamma) + \left(\omega + \frac{d\alpha}{dt}\right)\cos\beta\cos\gamma + \right.$$

$$\left. + \frac{d\beta}{dt}\sin\gamma\right]2B\cos\varepsilon = ml\frac{dv}{dt}\sin\alpha\cos\beta - ml\omega v\cos\alpha\cos\beta + $$

$$+ \left(ml\frac{v^2}{R} - lF\right)\sin\beta + M_x^*;$$

$$\frac{d}{dt}2B\cos\varepsilon = ml\frac{dv}{dt}(\cos\alpha\cos\gamma - \sin\alpha\sin\beta\sin\gamma) + $$

$$+ ml\omega v(\sin\alpha\cos\gamma + \cos\alpha\sin\beta\sin\gamma) + \quad\quad (40)$$

$$+ \left(ml\frac{v^2}{R} - lF\right)\cos\beta\sin\gamma + M_y^*;$$

$$\left[\frac{v}{R}(\sin\alpha\cos\gamma + \cos\alpha\sin\beta\sin\gamma) - \right.$$

$$\left. - \left(\omega + \frac{d\alpha}{dt}\right)\cos\beta\sin\gamma + \frac{d\beta}{dt}\cos\gamma\right]2B\cos\varepsilon = M_z^*;$$

$$-\left[\frac{v}{R}\cos\alpha\cos\beta + \left(\omega + \frac{d\alpha}{dt}\right)\sin\beta + \frac{d\gamma}{dt}\right]2B\sin\varepsilon = N(\varepsilon).$$

Equations (40) hold for any gyro frame. By inserting into them

$$M_x^* = M_y^* = M_z^* = 0, \quad\quad (41)$$

and expression (17) for the moment $N(\varepsilon)$, the equations of motion of a gyro-compass having the properties described under (3) are obtained. As was to be expected in this case equations (40) become identities if

$$\alpha = \beta = \gamma = 0, \qu\quad (42)$$

and if ε satisfies (19). The functions $v = v(t)$ and $\omega = \omega(t)$, which define the motion of the gyro-frame suspension point on the sphere S, are in this case arbitrary.

When (42) and (19) are satisfied, the gyro frame will move in the manner described under 3 and 4: its angular momentum vector, directed along the y-axis, will throughout remain perpendicular to the vector of the velocity relative to sphere S of the suspension point; the z-axis, which is parallel to the pivot axes of the gyro frame housings, will always pass through the center of sphere S, and therefore also through the center of the Earth.

6. The equations of motion (40) of the gyro frame about the x^0-, y^0-, z^0-axes of the Darboux trihedron moving along the trajectory of the suspension point are too complex in a general study of the motion of the gyro frame. Only small motions of the gyro frame in relation to this trihedron will therefore be considered; accordingly, only first-order terms in α, β, γ and their time derivatives will be retained in (40).

Using (41) and (17), we therefore obtain

$$-\left(\frac{d\alpha}{dt} - \frac{v}{R}\beta + \omega\right)2B\cos\epsilon = l\left[m\frac{dv}{dt}\alpha - \left(F - m\frac{v^2}{R}\right)\beta - m\omega v\right],$$

$$\frac{d}{dt}(2B\cos\epsilon) = l\left[mv\omega\alpha - \left(F - m\frac{v^2}{R}\right)\gamma + m\frac{dv}{dt}\right],$$

$$\left(\frac{d\beta}{dt} + \frac{v}{R}\alpha - \omega\gamma\right)2B\cos\epsilon = 0,$$

$$-\left(\frac{d\gamma}{dt} + \frac{v}{R} + \omega\beta\right)2B\sin\epsilon = -\frac{4B^2}{mlR}\cos\epsilon\sin\epsilon.$$

(43)

These equations determine the perturbations of the motion of the compass gyro frame relative to the basic motion for which α, β, γ, and ϵ are given by (42) and (19). If for the basic motion ϵ is denoted by $\sigma(t)$, then

$$\epsilon = \sigma(t) + \delta,$$

(44)

where δ is the same order of magnitude as α, β, and γ.

Inserting (44) into (43), neglecting all terms of higher order than the first in α, β, γ, δ and using

$$2B\cos\sigma(t) = mlv(t),$$

(45)

which follows from (19), lead to the following equations describing the perturbations of the motion of the gyro frame:

$$-mlv\frac{d\alpha}{dt} - ml\frac{dv}{dt}\alpha + lF\beta = -\omega\, 2B\,\delta\sin\sigma,$$

$$-\frac{d}{dt}(2B\,\delta\sin\sigma) + l\left(F - \frac{mv^2}{R}\right)\gamma = \omega\, mlv\,\alpha,$$

$$\frac{d\beta}{dt} + \frac{v}{R}\alpha = \omega\,\gamma,$$

$$\frac{d\gamma}{dt} + \frac{2B\,\delta\sin\sigma}{mlR} = -\omega\,\beta.$$

(46)

Let the velocity of the apex of the Darboux trihedron and its angular velocity ω about the normal to the sphere S be constant. System (46) then becomes a homogeneous system with constant coefficients. Inserting into it the approximation:

$$F - \frac{mv^2}{R} \cong F \cong mg,$$

(47)

where g is the gravitational acceleration, gives the following roots of the expanded determinant of system (46):

$$\pm i(v + \omega), \quad \pm i(v - \omega).$$

(48)

Here $\nu = \sqrt{\frac{g}{R}}$ is the frequency corresponding to the Schuler period

$$T = 2\pi \sqrt{\frac{R}{g}}. \tag{49}$$

According to the approximate theory of the space gyrocompass developed by Geckeler*, the perturbations of the motion of a gyro frame consist of two independent oscillations, each having a period equal to the Schuler period. In one mode only α and β vary, in the other only γ and δ. It is seen from the above discussion that Geckeler's theory is rather inaccurate, although in general it leads to correct expressions similar to (17) and (19) for the characteristic parameters of the sensitive element of a gyrocompass whose xy plane remains throughout tangential to the sphere S (Geckeler considered this plane to be almost horizontal).

7. If (47) is valid, equations (46) can also be integrated when v and ω are variables, i.e., for an arbitrary motion of the suspension point on the sphere S.

In fact, inserting (47) and $\nu = \sqrt{\frac{g}{R}}$, equations (46) become

$$\frac{d}{dt} \frac{v\alpha}{\sqrt{gR}} - \nu\beta = \omega \frac{2B\delta \sin \sigma}{ml \sqrt{gR}}, \qquad \frac{d}{dt}\left(\frac{2B\delta \sin \sigma}{ml \sqrt{gR}}\right) - \nu\gamma = -\omega \frac{v}{\sqrt{gR}}\alpha,$$

$$\frac{d\beta}{dt} + \nu \frac{v}{\sqrt{gR}} \alpha = \omega\gamma, \qquad \frac{d\gamma}{dt} + \nu \frac{2B\delta \sin \sigma}{ml \sqrt{gR}} = -\omega\beta, \tag{50}$$

We now define the following two complex functions of the real argument t:

$$\varkappa(t) = \frac{v\alpha}{\sqrt{gR}} + i\beta, \quad \mu(t) = \gamma - i\frac{2B\delta \sin \sigma}{ml \sqrt{gR}}. \tag{51}$$

Using them, system (50) can be replaced by the two equations

$$\frac{d\varkappa}{dt} + i\nu\varkappa = i\omega\mu, \qquad \frac{d\mu}{dt} + i\nu\mu = i\omega\varkappa. \tag{52}$$

This system can be separated into two independent equations:

$$\frac{d}{dt}(\varkappa + \mu) + i(\nu - \omega)(\varkappa + \mu) = 0,$$

$$\frac{d}{dt}(\varkappa - \mu) + i(\nu + \omega)(\varkappa - \mu) = 0, \tag{53}$$

which are easily integrated. The result is

$$\varkappa + \mu = (\varkappa_0 + \mu_0) exp\left[-i \int_0^t (\nu - \omega)\, dt\right],$$

$$\varkappa - \mu = (\varkappa_0 - \mu_0) exp\left[-i \int_0^t (\nu + \omega)\, dt\right], \tag{54}$$

where $\varkappa_0$ and μ_0 are the values of $\varkappa(t)$ and $\mu(t)$ for $t = 0$.

Using (54) and (51), the variables α, β, γ, δ can now be given explicitly as functions of their initial values α_0, β_0, γ_0, δ_0 and of the time t.

* Grammel, R. Der Kreisel. Vol. II. — F. Vieweg, Braunschweig. 1920. [Translated into Russian. 1952.]

When $\omega = $ const, equations (50) become linear differential equations with constant coefficients in which the variables are $v\alpha/\sqrt{gR}$, β, γ, and $2B\,\delta \sin \sigma/ml\,\sqrt{gR}$. $\sin \sigma$ is determined in accordance with (45) by

$$\sin \sigma = \sqrt{1 - \left(\frac{mlv}{2B}\right)^2}.$$ (55)

In accordance with (23), (24), and (32),

$$\omega = U \sin \varphi + \frac{V_K}{R} \, \mathrm{tg}\, \varphi - \frac{d\vartheta}{dt},$$ (56)

where ϑ is given by (25).

In particular the angular velocity ω is constant when the suspension point moves uniformly along the Equator or any parallel.

8.   The above theory of small motions of a gyro frame about the moving axes of the Darboux trihedron moving along the trajectory of the suspension point shows that undamped oscillations are likely to occur.   The problem of the stability of the motion defined by the nonlinear equations (40) requires further investigation.

Introducing in the gyro frame's mechanical system a damping similar to that used in Anschütz double-gyrocompasses causes ballistic deviations, i.e., additional variations of α, β, γ, and δ, determined by the laws governing the acceleration of the suspension point in its motion on the sphere S. A special analysis is needed to calculate these deviations.

We shall determine further on the perturbations introduced in the motion of the sensitive element of the double-gyrocompass by the deviation of the Earth's shape from a perfect sphere.

Appendix 3

DETERMINING THE POSITION OF A MOVING OBJECT
BY GYROS AND ACCELEROMETERS*

The problem of the so-called autonomous determination (i.e., a determination which uses no external reference points) of the position of a moving object (inertial navigation) is of great practical importance.

Because of the insufficient accuracy of the sensitive elements available, namely Newton-meters (accelerometers), gyros, and integrators, no practical solution to this problem existed until recently. However, instruments developed recently** make it possible to solve this problem with a satisfactory accuracy, provided the duration of the object's motion is comparatively short.

This appendix considers the theory of one method of autonomous determination of the position of a moving object, i.e., of inertial navigation.

The important problem of evaluating the inaccuracy in determining position, caused by the so-called instrumental errors of the integrators, Newton-meters, gyros, and other elements of the system, is outside the scope of this study. It will therefore be assumed that the above-mentioned elements are perfect, i.e., operate without errors. The electromechanical system on which solution of the problem is based, will therefore be treated under the assumption that all its parameters correspond exactly to their theoretical values, and that there are no mechanical faults (such as inaccurate assembly and lost motion in the transmissions). The initial conditions of the system's motion are arbitrary.

1. We begin by solving the problem of the autonomous position determination of an object moving along an arc of a great circle of a nonrotating sphere S whose center coincides with that of the Earth (Figure 1). In the simplest case this corresponds to a motion at constant height above the Equator. The determination of the object's position relative to the Earth itself thus becomes simply a determination of the duration of motion.

Let two coordinate systems xy and $\xi^*\eta^*$ with a common origin be fixed at some point of the moving object (Figure 1). We shall call this point the

---

object center. The x-axis of the coordinate system xy is directed along the object's velocity vector v. The y-axis is the prolongation of the Earth's radius to the moving object's center. The axes of the Newtonian coordinate system $\xi^*\eta^*$ have a fixed orientation relative to the sphere S.

Let the two coordinate systems coincide at $t=0$. Subsequently, the coordinate system xy will rotate through an angle φ, varying with time, relative to the system $\xi^*\eta^*$ which has a translational motion. This angle is related to the distance $s=s(t)$ traveled by the object center from the initial point:

$$\varphi = \frac{s}{R}.\tag{1}$$

Here R is the radius of the great-circle arc along which the object center moves.
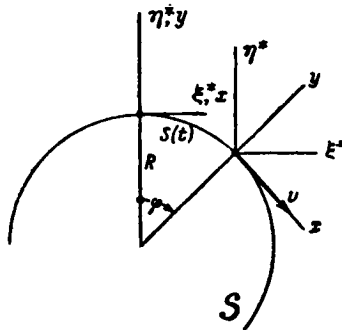

FIGURE 1

Let a platform (1), stabilized by gyros, be mounted on the object (Figure 2). In the simplest case this platform is oriented by follow-up systems in such a way that it is always perpendicular to the angular momentum vector of a precision gyro. The pivot bearings of this gyro's outer ring are mounted on the stabilized platform.

Let the angular momentum H of the gyro lie in the $\xi^*\eta^*$ plane, and let a moment $M = M(t)$ be applied to the pivot axis of its outer gimbal ring (Figure 2). In this case the precession of the gyro also takes place in the $\xi^*\eta^*$ plane. Following the gyro, the stabilized platform will rotate at an angular velocity

$$\frac{d\psi}{dt} = \frac{M(t)}{H},\tag{2}$$

where ψ is the angle between the vector H and the η^*-axis.

Let a Newton-meter (2) be mounted in the plane of the stabilized platform (1) (Figure 2), and denote by $a = a(t)$ its instantaneous reading. If the sensitivity axis of the Newton-meter does not coincide with the x-axis, the reading $a(t)$ of the meter (Figure 3) will be:

$$a(t) = \left(j - \frac{v^2}{R}\right)\sin\alpha + \frac{d^2s}{dt^2}\cos\alpha.\tag{3}$$

Here j is the gravitational acceleration, and

$$\alpha = \varphi - \psi\tag{4}$$

the angle of deviation of the stabilized platform from the horizontal direction

(more accurately, from the direction perpendicular to the Earth's radius).
If the function $a(t)$ obtained as the Newton-meter output is fed to an integrating unit, a new function

$$K \int_0^t a(t)\,dt + m, \tag{5}$$

is obtained, where K and m are constants whose values will be determined below.
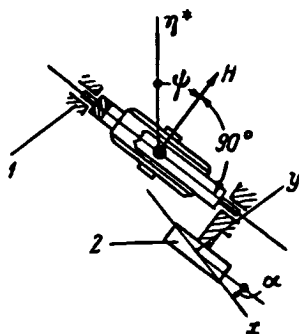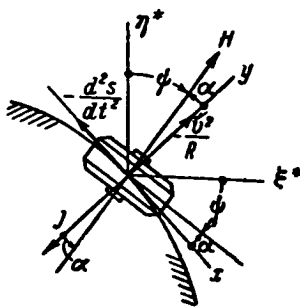

FIGURE 2

FIGURE 3

The function (5) can be reproduced as a moment $M(t)$ acting on the gyro. Substituting this expression for $M(t)$ in (2) and integrating yields

$$\psi = \frac{K}{H} \int_0^t \int_0^t a(t)\,dt^2 + \frac{m}{H}\,t + \psi_0, \tag{6}$$

where ψ_0 is the angle of inclination of the stabilized platform to the horizontal plane (more exactly, to the x-axis or the ξ^*-axis coinciding with the latter at that instant) for $t=0$.

Inserting (1) and (6) into (4) yields

$$\alpha = \frac{s}{R} - \frac{K}{H} \int_0^t \int_0^t a(t)\,dt^2 - \frac{m}{H}\,t - \psi_0, \tag{7}$$

from which a differential equation for the function $\alpha = \alpha(t)$ and its initial conditions can be established. In fact, substituting $t=0$ in (7) gives, since $s(0)=0$,

$$\alpha(0) = -\psi_0, \tag{8}$$

which could obviously also have been obtained directly from (4). Differentiating both sides of (7) with respect to time, we have

$$\frac{d\alpha}{dt} = \frac{1}{R}\frac{ds}{dt} - \frac{K}{H}\int_0^t a(t)\,dt - \frac{m}{H}. \tag{9}$$

It follows that the initial value of the time derivative of $\alpha(t)$ is

$$\frac{d\alpha(0)}{dt} = \frac{v(0)}{R} - \frac{m}{H}, \tag{10}$$

where $v(0)$ is the initial value of the velocity $\frac{ds}{dt}$ of the object center relative to the sphere S.

A second differentiation of both sides of (7) yields, after subsituting (3) for $a(t)$,

$$\frac{d^2a}{dt^2} + \frac{K}{H}\left(j - \frac{v^2}{R}\right)\sin a = \left(\frac{1}{R} - \frac{K}{H}\cos a\right)\frac{d^2s}{dt^2}. \tag{11}$$

When the function $s = s(t)$ is given, this is a second-order differential equation for determining the angle of inclination $a = a(t)$ of the stabilized platform relative to the horizontal plane. The initial conditions for this differential equation are given by (8) and (10).

2. The differential equation (11) has the particular integral

$$a \equiv 0, \tag{12}$$

if the equality

$$\frac{1}{R} = \frac{K}{H}, \tag{13}$$

is satisfied, and if the initial conditions are such that

$$a(0) = 0, \qquad \frac{da(0)}{dt} = 0. \tag{14}$$

Equation (13) defines the parameter K. The first of conditions (14), together with (8), state that for $t = 0$ the stabilized platform will be parallel to the horizontal plane, i.e.,

$$\psi_0 = 0. \tag{15}$$

The second of conditions (14), together with (10), yield

$$\frac{v(0)}{R} = \frac{m}{H}. \tag{16}$$

This defines the value which the parameter m must take in the device for which (5) is true.

Thus when (15), (16), and (13) are satisfied, the stabilized platform will remain horizontal (more exactly, perpendicular to the Earth radius) throughout any arbitrary motion $s = s(t)$ of the moving object.

Let $a \equiv 0$. Inserting this into (3) yields $a(t) = \frac{d^2s}{dt^2}$. Substituting this expression together with (16) and (13) into (5) yields:

$$K\left[\int_0^t \frac{d^2s}{dt^2}dt + v(0)\right] = Kv(t). \tag{17}$$

It follows that in this case the function (5) represents, except for the constant factor K, the instantaneous value of the object's velocity $v = v(t)$ relative to the sphere S. If the value of (5) is fed to a second integrating unit, the distance $s(t)$ traveled by the object from its initial position will be obtained as output (omitting the factor K).

3. In the general case $a \not\equiv 0$, the magnitude

$$\int_0^t \left[K\int_0^t a(t)dt + m\right]dt, \tag{18}$$

computed by the integrating units, will differ from $Ks(t)$. In accordance

291

with (7) and (13) the difference between these two magnitudes is

$$\Delta s = s(t) - \frac{1}{K} \int_0^t \left\{ \int_0^t K a(t)\, dt + m \right\} dt = R a(t) + R \psi_0. \tag{19}$$

The error Δs in the determination of the distance $s(t)$ by this method is therefore

$$\Delta s = R[a(t) - a(0)], \tag{20}$$

where $a(t)$ is obtained from (11) and the initial conditions (8) and (10) when condition (13) is satisfied.

The angle of inclination $a(t)$ of the stabilized platform to the x-axis can be assumed to be small, so that all terms in (11) of higher order than the first in a can be neglected. Using (13), equation (11) then becomes the homogeneous linear differential equation

$$\frac{d^2 a}{dt^2} + \frac{1}{R}\left(j - \frac{v^2}{R}\right) a = 0. \tag{21}$$

The following approximation holds for low velocities:

$$j - \frac{v^2}{R} \cong g \cong \text{const}, \tag{22}$$

where g is the gravitational acceleration in the region of motion of the object. In this case the solution of (21) is a harmonic function

$$a(t) = a(0)\cos vt + \frac{1}{v}\frac{da(0)}{dt}\sin vt \qquad \left(v^2 = \frac{g}{R}\right), \tag{23}$$

whose period is

$$T = 2\pi \sqrt{R/g} \cong 84.4 \text{ min}$$

known in the theory of gyroscopes as the Schuler period.

It thus follows from (20) and (23) that in the general case the error in the autonomous determination of the object's position has an oscillatory pattern.

4. Other methods exist for determining the position of an object moving along the arc of a great circle. These usually lead to similar results.

Let the platform be stabilized so that it remains parallel to the $\xi\eta$-axis during the object's motion. This can be obtained by means of free gyros or by following the stars (astronavigation)[*]. In this case

$$\chi = \frac{1}{R}\int_0^t\int_0^t a(t)\, dt^2 + \frac{v(0)}{R} t. \tag{24}$$

When certain equations similar to those above are satisfied, the following relationship is obtained:

$$s = R\chi. \tag{25}$$

Ingenious devices exist which carry out the necessary double integration in one step instead of two (the Bojkov integrator[**]).

---

[*] Wrigley, W., R.B. Woodbury, and J. Hovorka. Inertial Guidance. — Preprint No.698. Institute of Aeronautical Sciences, New York. 1957.

[**] Bojkov, J.M. Einrichtung zum Messen von Wegstrecken. — Deutsch. Patent No.661822, Kl.42, Siemens Apparate und Maschinen, G.m.b.H. Berlin. 2 June, 1938.

5. We shall now discuss the problem of determining the position of an object whose center moves arbitrarily on the Earth's sphere. We assume that a platform is stabilized by gyros in such a way that angular velocities

$$\omega_x = \frac{M_2}{H}, \qquad \omega_y = \frac{M_1}{H}, \qquad \omega_z = \frac{M_3}{H} \tag{26}$$

about the x- and y-axes lying in the plane of the platform and about the z-axis normal to this plane are caused by three torques M_1, M_2, M_3.
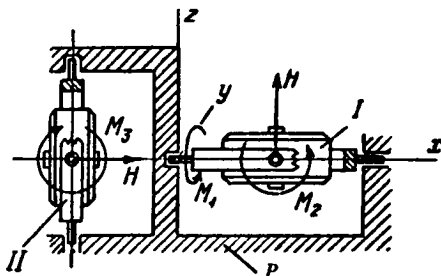

FIGURE 4

Figure 4 gives one possible way of obtaining such a stabilization. Platform P, mounted on the object in gimbals (not shown on the drawing) is continuously maintained perpendicular to the axis of rotation of gyro I by means of follow-up systems. The outer gimbal ring of gyro I is carried in bearings mounted on the stabilized platform in such a way that its pivot axis lies in the plane of the platform. When the follow-up systems work perfectly, the inner-ring pivot axis or, which is the same, the pivot axis of the gyro housing, lies in the same plane.

Let M_1 and M_2 be the torques applied respectively to the pivot axes of the outer gimbal ring and of the housing. Denote these axes by x and y respectively. The torques M_1 and M_2 cause precession of the gyro and, consequently, rotation of the platform about the x- and y-axes at angular velocities ω_x and ω_y given by the first two of equations (26).

The outer gimbal ring of gyro II (Figure 4) which has the same angular momentum H as gyro I, is carried in bearings mounted on platform P in such a way that its pivot axis is perpendicular to the plane of the platform. A corrective torque is applied to this axis so as to cause the axis of rotation of gyro II to take up a position parallel to the plane of the platform. The x-axis, fixed rigidly to the stabilized platform, is made to coincide continuously with the axis of rotation of gyro II, by means of a follow-up system.

The torque M_3, applied to the pivot axis of the second gyro housing, causes a precession of the gyro and, as a result, a rotation of the platform at an angular velocity ω_z about the z-axis. This axis is perpendicular to the plane of the platform and forms together with the x- and y-axes a Cartesian coordinate system xyz, fixed to the platform. It will be assumed that the origin of this system coincides with the object center. The magnitudes M_3 and ω_z are related by the third of equations (26).

Two Newton-meters (not shown in Figure 4), whose sensitivity axes are directed along the x- and y-axes, are mounted on the stabilized platform in the vicinity of the origin of the coordinate system xyz.

293

Let the object center move arbitrarily on the Earth, and let the torques M_1 and M_2 be related to the readings a_x and a_y of the corresponding Newton-meters by the formulas:

$$M_1 = K \int_0^t a_x dt + m_2, \qquad M_2 = -K \int_0^t a_y dt - m_1. \qquad (27)$$

Integrating units must be provided to create the torques M_1 and M_2.

The values of the torque M_3 and of the parameters K, m_1, and m_2 in (27), required to maintain the platform in a horizontal plane will now be found.

The projections on the x-, y-, and z-axes of the acceleration of the system xyz relative to the sphere S are*

$$w_x = \frac{dv_x}{dt} + \omega_y v_z - \omega_z v_y,$$

$$w_y = \frac{dv_y}{dt} + \omega_z v_x - \omega_x v_z, \qquad (28)$$

$$w_z = \frac{dv_z}{dt} + \omega_x v_y - \omega_y v_x,$$

where v_x, v_y, and v_z are respectively the projections on these axes of the velocity of the coordinate origin relative to the sphere S.

The projections of the force of gravity on the x- and y-axes vanish in this case. It follows that the Newton-meters measure the accelerations w_x and w_y directly. The following equations are therefore obtained in accordance with (26) and (27), taking into account that $v_z \equiv 0$:

$$\omega_x = -\frac{K}{H} \int_0^t \left(\frac{dv_y}{dt} + \omega_z v_x \right) dt - \frac{m_1}{H},$$

$$\omega_y = \frac{K}{H} \int_0^t \left(\frac{dv_x}{dt} - \omega_z v_y \right) dt + \frac{m_2}{H}. \qquad (29)$$

Since the plane of platform P must remain horizontal throughout the object's motion, and since the z-axis is directed along the Earth's radius, the following equations** must be substituted into (29):

$$v_x = \omega_y R, \qquad v_y = -\omega_x R. \qquad (30)$$

Expressing ω_x and ω_y in (29) by means of (30) yields

$$v_x = \frac{KR}{H} \int_0^t \left(\frac{dv_x}{dt} - \omega_z v_y \right) dt + \frac{R}{H} m_2,$$

$$v_y = \frac{KR}{H} \int_0^t \left(\frac{dv_y}{dt} + \omega_z v_x \right) dt + \frac{R}{H} m_1. \qquad (31)$$

These equations must be satisfied for any arbitrary variation of v_x and v_y, i.e., they must be identities. This is, however, only possible if the

---

* Suslov, G. K. Teoreticheskaya mekhanika (Theoretical Mechanics). — Gostekhizdat. 1944. [cf. Goldstein, Classical Mechanics. p. 135. — Addison-Wesley. 1951.]

** Ishlinskii, A. Yu. Ob otnositel'nom ravnovesii fizicheskogo mayatnika s podvizhnoi tochkoi opory (The Relative Equilibrium of a Physical Pendulum with a Moving Point of Support). — PMM, Vol. 20, No. 3. 1956.

following conditions are satisfied:

$$\frac{KR}{H}=1: \qquad \omega_r \equiv 0; \qquad m_1 = Kv_y(0); \qquad m_2 = Kv_x(0). \tag{32}$$

The first of these conditions is identical with (13), the second leads, in accordance with the third of equations (26), to

$$M_2 = 0. \tag{33}$$

Finally, the last two conditions connect the projections on the x- and y-axes of the initial velocity relative to the sphere S of the moving object center with the parameters m_1 and m_2 of the integrating units.

6. The substitution of (27) and (33) in (26) shows that the projections ω_x and ω_y of the angular velocity of the stabilized-platform are transformed by the integrators into known time functions. In addition, $\omega_s \equiv 0$, and the z-axis is directed along the Earth's radius. This makes possible in principle the continuous determination of the object's position on the Earth and of its course.
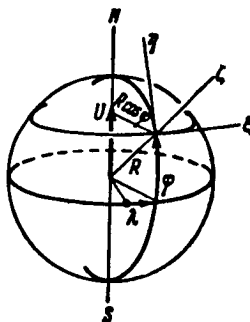

FIGURE 5

Consider the so-called geographic trihedron $\xi\eta\zeta$ (Figure 5), whose apex coincides with the origin of the coordinate system xyz (i.e., with the object center). The ξ-axis is directed to the east, the η-axis to the north, and the ζ-axis upward along the Earth's radius. The projections of the absolute angular velocity u of this trihedron (i.e., of the angular velocity relative to the sphere S), are*

$$u_\xi = -\frac{V_N}{R}, \quad u_\eta = \frac{V_E}{R} + U\cos\varphi, \quad u_\zeta = \frac{V_E}{R}\,\mathrm{tg}\,\varphi + U\sin\varphi. \tag{34}$$

Here U is the angular velocity of the Earth, φ is the latitude, V_E and V_N are respectively the eastern and northern components of the velocity of the object center relative to the Earth. Obviously

$$V_E = R\cos\varphi\,\frac{d\lambda}{dt}, \qquad V_N = R\,\frac{d\varphi}{dt}, \tag{35}$$

where λ is the longitude.

* Bulgakov, B.V. Prikladnaya teoriya giroskopov (Applied Theory of Gyroscopes).— Moskva, Gostekhizdat. 1955. [English translation, IPST. 1960.]

The ζ-axis coincides in this case with the z-axis. The projections ω_x, ω_y, ω_z are therefore related to u_ξ, u_η, and u_ζ as follows:

$$\omega_x = \quad u_\xi \cos \chi + u_\eta \sin \chi,$$

$$\omega_y = - u_\xi \sin \chi + u_\eta \cos \chi, \tag{36}$$

$$\omega_z = \quad u_\zeta + \frac{d\chi}{dt},$$

where χ is the angle between the ξ- and x-axes (Figure 6).

We note that $\omega_z \equiv 0$, and that $\omega_x = \omega_x(t)$ and $\omega_y = \omega_y(t)$ are known functions of time. Then inserting (34) and (35) into (36) leads to the following system of three differential equations with three unknown functions $\varphi(t)$, $\lambda(t)$, and $\chi(t)$:

$$-\frac{d\varphi}{dt} \cos \chi + \left(U + \frac{d\lambda}{dt} \right) \cos \varphi \sin \chi = \omega_x(t);$$

$$\frac{d\varphi}{dt} \sin \chi + \left(U + \frac{d\lambda}{dt} \right) \cos \varphi \cos \chi = \omega_y(t); \tag{37}$$

$$\left(U + \frac{d\lambda}{dt} \right) \sin \varphi + \frac{d\chi}{dt} = 0.$$

When the initial conditions $\varphi(0)$, $\lambda(0)$, and $\chi(0)$ are known, i.e., when data on the object's position and orientation at $t = 0$ are available, equations (37) can be solved by a computer. For this it is convenient to write them in an explicit form with respect to the derivatives:

$$\frac{d\varphi}{dt} = - \omega_x(t) \cos \chi + \omega_y(t) \sin \chi,$$

$$\frac{d\lambda}{dt} = - U + \frac{\omega_x(t) \sin \chi + \omega_y(t) \cos \chi}{\cos \varphi}, \tag{38}$$

$$\frac{d\chi}{dt} = - [\omega_x(t) \sin \chi + \omega_y(t) \cos \chi] \, \mathrm{tg}\, \varphi.$$

Having determined the functions $\varphi(t)$ and $\chi(t)$, it is possible to find the object's course, i.e., the angle $\varkappa$ between the vector of its velocity relative
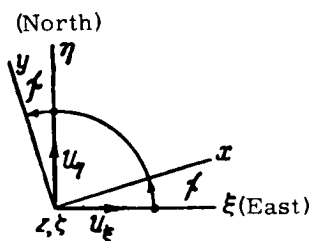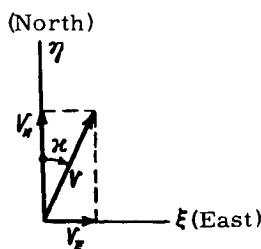

(North)

FIGURE 6

(North)

FIGURE 7

to the Earth and the local meridian (Figure 7). In accordance with (35) and (38), $\varkappa$ is determined by the equation:

$$\mathrm{tg}\, \varkappa = \frac{V_E}{V_N} = \frac{U \cos \varphi - \omega_x(t) \sin \chi - \omega_y(t) \cos \chi}{\omega_x(t) \cos \chi - \omega_y(t) \sin \chi}. \tag{39}$$

. We shall now study the perturbations of the motion of platform P, assuming that its plane is not strictly horizontal at $t=0$, and that conditions (32), determining the parameters m_1 and m_2, are satisfied within a small error. It will however be assumed that the first two of conditions (32) are rigorously fulfilled.

Introduce a Darboux trihedron $x^0 y^0 z^0$ with x^0- and y^0-axes tangential to the Earth's sphere*, and therefore also to the nonrotating sphere S. The x^0-axis is directed along the vector $\boldsymbol{v}$ of the velocity of the trihedron apex relative to sphere S. The trihedron $x^0 y^0 z^0$ will be called the natural Darboux trihedron. Let its apex be at the center of the moving object, i.e., at the origin of the coordinate system xyz fixed to the stabilized platform. The projections of the angular velocity $\boldsymbol{\omega}^0$ of the natural Darboux trihedron on the x^0-, y^0-, and z^0-axes are

$$\omega_{x^0}^0 = 0, \qquad \omega_{y^0}^0 = \frac{v}{R}, \qquad \omega_{z^0}^0 = \tilde{\omega}. \qquad (40)$$

For a given velocity $\boldsymbol{v}=\boldsymbol{v}(t)$, the function $\tilde{\omega}=\tilde{\omega}(t)$ defines** the geodesic curvature of the trajectory of the Darboux trihedron apex on the sphere S.
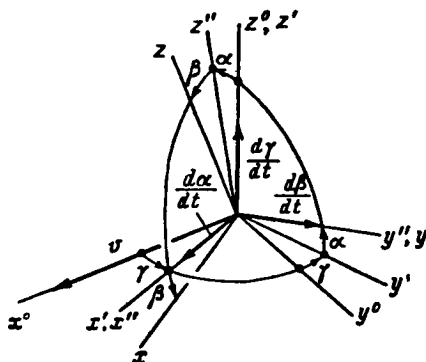

FIGURE 8

The projections on the x^0-, y^0-, and z^0-axes of the apex acceleration relative to the sphere S are

$$w_{x^0} = \frac{dv}{dt}, \qquad w_{y^0} = \tilde{\omega}v, \qquad w_{z^0} = -\frac{v^2}{R}. \qquad (41)$$

The direction cosines of the system xyz relative to trihedron $x^0 y^0 z^0$ are:

	x^0	y^0	z^0
x	$\cos\gamma\cos\beta - \sin\gamma\sin\alpha\sin\beta$	$\sin\gamma\cos\beta + \cos\gamma\sin\alpha\sin\beta$	$-\cos\alpha\sin\beta$
y	$-\sin\gamma\cos\alpha$	$\cos\gamma\cos\alpha$	$\sin\alpha$
z	$\cos\gamma\sin\beta + \sin\gamma\sin\alpha\cos\beta$	$\sin\gamma\sin\beta - \cos\gamma\sin\alpha\cos\beta$	$\cos\alpha\cos\beta$

(42)

The angles α, β and γ determine the orientation of the coordinate system xyz relative to the trihedron $x^0 y^0 z^0$ (Figure 8). The angle γ is the angle through which the auxiliary coordinate system $x'y'z'$, whose z'-axis coincides with the z^0-axis, is rotated relative to the Darboux trihedron; the

* Cf. Appendix 2, p. 281.
** Cf. Appendix 2, p. 284.

297

rotation is counterclockwise if viewed from the positive z'-axis, and is intended to make the x'-axis lie in the zx plane. The angle α is similarly determined by the relative position of the coordinate system $x'y'z'$ and the auxiliary coordinate system $x''y''z''$, whose x'- and x''-axes coincide. The z'-axis of the latter coordinate system is likewise made to lie in the zx plane, as a result of which the y''-axis coincides with the y-axis.

For $\alpha > 0$, the rotation of the system $x''y''z''$ relative to the system $x'y'z'$ is counterclockwise if viewed from the z'-axis (or, which is the same, from the positive x''-axis).

Lastly, the angle β is the angle between the x- and x''-(x'-) axes of the coordinate systems xyz and $x''y''z''$. The sign of β is determined in a similar way to that of γ and α.

The angular velocity ω of the coordinate system xyz relative to the sphere S represents the geometric sum of the angular velocity ω^0 of the natural Darboux trihedron relative to this sphere and of the three relative angular velocities $d\gamma/dt$, $d\alpha/dt$, and $d\beta/dt$. The latter are respectively the angular velocities of the coordinate system $x'y'z'$ relative to the trihedrom $x^0y^0z^0$, of the system $x''y''z''$ relative to the system $x'y'z'$ and, finally, of the system xyz (the stabilized platform) relative to the system $x''y''z''$.

The vector of the relative angular velocity $d\gamma/dt$ is directed along the z^0-axis, that of the angular velocity $d\beta/dt$ along the y-axis, and that of the angular velocity $d\alpha/dt$ along the x'-axis. The x'- and x^0-axes coincide when $\gamma = 0$; this makes it possible to find from (42) the direction cosines of the angular velocity $d\alpha/dt$ relative to the coordinate system xyz (Figure 8). Thus, the projections ω_x, ω_y, and ω_z of the angular velocity of the stabilized platform on the axes of the coordinate system xyz are

$$\omega_x = \frac{v}{R}(\sin\gamma\cos\beta + \cos\gamma\sin\alpha\sin\beta) +$$
$$+ \left(\bar{\omega} + \frac{d\gamma}{dt}\right)(-\cos\alpha\sin\beta) + \frac{d\alpha}{dt}\cos\beta;$$

$$\omega_y = \frac{v}{R}\cos\gamma\cos\alpha + \left(\bar{\omega} + \frac{d\gamma}{dt}\right)\sin\alpha + \frac{d\beta}{dt};$$

$$\omega_z = \frac{v}{R}(\sin\gamma\sin\beta - \cos\gamma\sin\alpha\cos\beta) +$$
$$+ \left(\bar{\omega} + \frac{d\gamma}{dt}\right)\cos\alpha\cos\beta + \frac{d\alpha}{dt}\sin\beta. \tag{43}$$

By (42) and (41), the projections w_x, w_y, and w_z of the acceleration of the origin of the system xyz are:

$$w_x = \frac{dv}{dt}(\cos\gamma\cos\beta - \sin\gamma\sin\alpha\sin\beta) + \bar{\omega}v(\sin\gamma\cos\beta +$$
$$+ \cos\gamma\sin\alpha\sin\beta) - \frac{v^2}{R}(-\cos\alpha\sin\beta),$$

$$w_y = \frac{dv}{dt}(-\sin\gamma\cos\alpha) + \bar{\omega}v\cos\gamma\cos\alpha - \frac{v^2}{R}\sin\alpha,$$

$$w_z = \frac{dv}{dt}(\cos\gamma\sin\beta + \sin\gamma\sin\alpha\cos\beta) + \bar{\omega}v(\sin\gamma\sin\beta -$$
$$- \cos\gamma\sin\alpha\cos\beta) - \frac{v^2}{R}\cos\alpha\cos\beta. \tag{44}$$

In contrast to 6, the projections of the force of gravity on the x- and y-axes differ from zero. As a result, a Newton-meter whose sensitivity

axis is directed along the x-axis will now measure the difference between the acceleration w_x and the projection on the x-axis of the gravitational acceleration j, which is directed along the z^0-axis toward the Earth's center.

It follows from (44) and (42) that the readings a_x and a_y of the Newton-meters must be expressed by the formulas

$$a_x = \frac{dv}{dt}(\cos\gamma\cos\beta - \sin\gamma\sin\alpha\sin\beta) + \bar{\omega}v(\sin\gamma\cos\beta +$$

$$+ \cos\gamma\sin\alpha\sin\beta) + \left(j - \frac{v^2}{R}\right)(-\cos\alpha\sin\beta),$$

$$a_y = \frac{dv}{dt}(-\sin\gamma\cos\alpha) + \bar{\omega}v\cos\gamma\cos\alpha + \left(j - \frac{v^2}{R}\right)\sin\alpha. \tag{45}$$

The torques M_1 and M_2 are given by (27), it being assumed that M_3 is zero. Substituting these values in (26) yields

$$\omega_x = -\frac{K}{H}\int_0^t a_y dt - \frac{m_1}{H},$$

$$\omega_y = \frac{K}{H}\int_0^t a_x dt + \frac{m_2}{H}, \tag{46}$$

$$\omega_z = 0.$$

The left-hand sides of these equations are given by (43), and the integrands by (45). Inserting these into (46) for given functions $v(t)$ and $\bar{\omega}(t)$ yields a system of equations for determining the time functions $\alpha(t)$, $\beta(t)$, and $\gamma(t)$.

Time differentiation of the first two of equations (46) yields

$$\frac{d\omega_x}{dt} + \frac{K}{H}a_y = 0, \qquad \frac{d\omega_y}{dt} - \frac{K}{H}a_x = 0, \qquad \omega_z = 0. \tag{47}$$

Assuming that α and β in (43) and (45) are small, terms of second and higher order in these variables can be neglected. Thus (43) and (45) become

$$\omega_x = \frac{v}{R}\sin\gamma - \left(\bar{\omega} + \frac{d\gamma}{dt}\right)\beta + \frac{d\alpha}{dt},$$

$$\omega_y = \frac{v}{R}\cos\gamma + \left(\bar{\omega} + \frac{d\gamma}{dt}\right)\alpha + \frac{d\beta}{dt},$$

$$\omega_z = \frac{v}{R}(\beta\sin\gamma - \alpha\cos\gamma) + \bar{\omega} + \frac{d\gamma}{dt},$$

$$a_x = \frac{dv}{dt}\cos\gamma + \bar{\omega}v\sin\gamma - \left(j - \frac{v^2}{R}\right)\beta, \tag{48}$$

$$a_y = -\frac{dv}{dt}\sin\gamma + \bar{\omega}v\cos\gamma + \left(j - \frac{v^2}{R}\right)\alpha.$$

Since $\omega_z \equiv 0$, it follows from the third of equations (48) that

$$\bar{\omega} + \frac{d\gamma}{dt} = \frac{v}{R}(\alpha\cos\gamma - \beta\sin\gamma). \tag{49}$$

Thus the terms

$$\left(\bar{\omega} + \frac{d\gamma}{dt}\right)\alpha, \quad \left(\bar{\omega} + \frac{d\gamma}{dt}\right)\beta, \tag{50}$$

299

in the first two of equations (48) are of the second order in α and β and can therefore be neglected. Therefore, up to first-order infinitesimals:

$$\omega_x = \frac{v}{R} \sin \gamma + \frac{d\alpha}{dt}, \quad \omega_y = \frac{v}{R} \cos \gamma + \frac{d\beta}{dt}. \tag{51}$$

Inserting the value of $\bar{\omega}$ given by (49) into the last two of equations (48) yields:

$$a_x = \frac{d}{dt}(v \cos \gamma) + \frac{v^2}{R}(\alpha \cos \gamma - \beta \sin \gamma) \sin \gamma - \left(j - \frac{v^2}{R}\right)\beta;$$

$$a_y = -\frac{d}{dt}(v \sin \gamma) + \frac{v^2}{R}(\alpha \cos \gamma - \beta \sin \gamma) \cos \gamma + \left(j - \frac{v^2}{R}\right)\alpha. \tag{52}$$

Inserting (51), (52), and (13), into the first two of equations (47) yields

$$\frac{d^2\alpha}{dt^2} + \frac{j}{R}\alpha = \frac{v^2}{R^2}(\alpha \sin \gamma + \beta \cos \gamma) \sin \gamma;$$

$$\frac{d^2\beta}{dt^2} + \frac{j}{R}\beta = \frac{v^2}{R^2}(\alpha \sin \gamma + \beta \cos \gamma) \cos \gamma. \tag{53}$$

Together with (49) these two equations form a system of differential equations for determining the functions $\alpha(t)$, $\beta(t)$, and $\gamma(t)$*.

We define two new variables ξ and η as follows:

$$\xi = \alpha \cos \gamma - \beta \sin \gamma,$$
$$\eta = \alpha \sin \gamma + \beta \cos \gamma. \tag{54}$$

Substituting these variables for α and β in (49) and (53) yields:

$$\frac{d^2\xi}{dt^2} + 2\frac{d\gamma}{dt}\frac{d\eta}{dt} + \eta\frac{d^2\gamma}{dt^2} - \xi\left(\frac{d\gamma}{dt}\right)^2 + \frac{j}{R}\xi = 0;$$

$$\frac{d^2\eta}{dt^2} - 2\frac{d\gamma}{dt}\frac{d\xi}{dt} + \xi\frac{d^2\gamma}{dt^2} - \eta\left(\frac{d\gamma}{dt}\right)^2 + \left(\frac{j}{R} - \frac{v^2}{R^2}\right)\eta = 0; \tag{55}$$

$$\frac{d\gamma}{dt} + \bar{\omega} - \frac{v}{R}\xi = 0.$$

Substitute in the first two of these equations the values of $\frac{d\gamma}{dt}$ and $\frac{d^2\gamma}{dt^2}$ obtained from the third. Neglecting second-order terms in ξ, η, and also their time derivatives, leads to a system of two linear differential equations with variable coefficients, which define the small oscillations of the stabilized platform.

8. Putting aside the problem of integrating (55) for an arbitrary motion of the object on the Earth, we shall restrict ourselves to the case $\bar{\omega} = \text{const}$ and $v = \text{const}$, which corresponds to a motion at constant velocity along a great-circle arc on the sphere S. The motion relative to the Earth will in the general case be along an irregular trajectory at a variable relative velocity. Motion of an object at constant velocity relative to the Earth along a parallel or along the Equator is an exception.

---

* For small oscillations of the stabilized platform equations (53) are identical with the equations of small oscillations of a physical pendulum whose point of support moves on the sphere S. The equilibrium conditions of this pendulum relative to the natural Darboux trihedron are given in the author's paper: Ob otnositel'nom ravnovesii fizicheskogo mayatnika s podvizhnoi tochkoi opory (The Relative Stability of a Physical Pendulum with a Moving Point of Support). — PMM, Vol. 20, No. 3, 1956.

, If $\tilde{\omega}$ and v are constant, system (55) reduces in a first-order approximation, after the variable γ has been eliminated, to the following form:

$$\frac{d^2\xi}{dt^2} - 2\tilde{\omega}\frac{d\eta}{dt} + \left(\frac{j}{R} - \tilde{\omega}^2\right)\xi = 0,$$

$$\frac{d^2\eta}{dt^2} + 2\tilde{\omega}\frac{d\xi}{dt} + \left(\frac{j}{R} - \tilde{\omega}^2 - \frac{v^2}{R^2}\right)\eta = 0. \tag{56}$$

This is a system of linear differential equations with constant coefficients.

For $\tilde{\omega} = 0$ and $v = \text{const}$ (motion along a great-circle arc), system (56) can be separated into two independent equations:

$$\frac{d^2\xi}{dt^2} + \frac{j}{R}\xi = 0,$$

$$\frac{d^2\eta}{dt^2} + \left(\frac{j}{R} - \frac{v^2}{R^2}\right)\eta = 0. \tag{57}$$

The first of these corresponds to angular oscillations of the platform about the y^0-axis of the natural Darboux trihedron, the second to oscillations about the x^0-axis (which lies in the direction of the velocity vector v).

These oscillations have similar frequencies, if the velocity v is not too large (i.e., considerably lower than the velocity of points on the Equator due to the diurnal rotation of the Earth). The period is approximately equal to the Schuler period (84.4 min).

9. When the stabilized platform undergoes small oscillations, i.e., when α and β differ from zero, equations (30) will not be strictly satisfied. In addition, equations (31) on which this method is based, will not be exact identities, since the readings a_x and a_y of the Newton-meters include the corresponding projections of the gravitational acceleration j.

When conditions (32) are satisfied, it can be expected that the errors caused by these factors when determining the latitude and longitude of the moving object and its course will have an oscillatory pattern. Further studies are, however, necessary in order to determine the time variation of these errors accurately.

10. It was assumed above that the object's center moves on the sphere S so that $v_z = 0$ in (28). We shall now show how to eliminate this restriction and solve the problem of inertial navigation in the case of an arbitrary object motion about the Earth.

Let a platform stabilized by gyros move in such a way that its plane remains perpendicular to the Earth's radius. This again necessitates the fulfillment of (30), in which v_x and v_y are, as above, the projections on the x- and y-axes of the velocity v of the center of the platform gimbals relative to the sphere S, and ω_x and ω_y are the projections of the angular velocity ω on these axes. The following equations must therefore hold:

$$\omega_x = -\frac{v_y}{R}, \quad \omega_y = \frac{v_x}{R}. \tag{58}$$

In contrast to (30), however, here $R = R(t)$ is variable, being the distance between the platform gimbal center and the center of sphere S.

The angular velocities ω_x and ω_y are caused by precessional torques M_1 and M_2 defined by the first two of equations (26). Substituting (58) in them leads to the following expressions for the torques:

$$M_2 = -\frac{H}{R}v_y, \quad M_1 = \frac{H}{R}v_x. \tag{59}$$

Assume that in the vicinity of the gimbal center two Newton-meters are mounted whose sensitivity axes are respectively directed along the x- and y-axes lying in the plane of the platform. Their readings $a_x(t)$ and $a_y(t)$ will not contain the projections of the gravitational acceleration j on the x- and y-axes, since by assumption the stabilized platform remains throughout its motion perpendicular to the line connecting the gimbal center to the center of the Earth. The following expressions can therefore be written:

$$a_x(t) = w_x = \frac{dv_x}{dt} + \omega_y v_z - \omega_z v_y, \quad a_y(t) = w_y = \frac{dv_y}{dt} + \omega_z v_x - \omega_x v_z. \qquad (60)$$

In contrast to the previous case, v_z is not zero:

$$v_z = \frac{dR}{dt}. \qquad (61)$$

Assuming as before that $M_3 = 0$, it again follows from the third of equations (26) that $\omega_z \equiv 0$, i.e., that the platform will have no angular velocity ω component along the z-axis directed along a radius of the sphere S. Because of this and of (58) and (61), equations (60) can be written in the form

$$a_x(t) = \frac{dv_x}{dt} + \frac{v_x}{R} \frac{dR}{dt}, \quad a_y(t) = \frac{dv_y}{dt} + \frac{v_y}{R} \frac{dR}{dt}. \qquad (62)$$

These relationships can be considered as differential equations. If their solutions $a_x(t)$, $a_y(t)$, and $R(t)$ are known, the functions $v_x(t)$ and $v_y(t)$, which are required for determining the torques M_1 and M_2 which control the orientation of the platform, can be found.

Equations (62) can be solved by quadratures:

$$v_x = \frac{1}{R(t)} \left[\int_0^t R(t) a_x(t) \, dt + R(0) v_x(0) \right],$$

$$v_y = \frac{1}{R(t)} \left[\int_0^t R(t) a_y(t) \, dt + R(0) v_y(0) \right]. \qquad (63)$$

It follows from (59) and (63) that the torques M_1 and M_2 are functions of the readings $a_x(t)$ and $a_y(t)$ of the Newton-meters:

$$M_1 = \frac{H}{R^2(t)} \left[\int_0^t R(t) a_x(t) \, dt + R(0) v_x(0) \right];$$

$$M_2 = -\frac{H}{R^2(t)} \left[\int_0^t R(t) a_y(t) \, dt + R(0) v_y(0) \right]. \qquad (64)$$

This means that units capable of multiplying and dividing the instantaneous values must be introduced in the inertial navigation system.

The variable $R = R(t)$ in (64) is assumed to be known in advance. The availability of a third Newton-meter, whose sensitivity axis is parallel to the z-axis (the Earth's radius), permits the independent determination of this function. The readings of this Newton-meter are

$$a_z = w_z + j = \frac{dv_z}{dt} + \omega_x v_y - \omega_y v_x + j. \qquad (65)$$

where

$$j = j_0 \frac{R_0^2}{R^2} \tag{66}$$

is the gravitational acceleration, which decreases inversely with the distance from the Earth's center, and j_0 is the value of this acceleration on the surface of the Earth whose radius is R_0.

Inserting (58), (61), and (66) into (65) leads to the following differential equation for the function $R(t)$:

$$\frac{d^2R}{dt^2} - \frac{v_x^2 + v_y^2}{R} + j_0 \frac{R_0^2}{R^2} = a_z(t). \tag{67}$$

The unit which integrates this differential equation must be included in one system with the integrators which reproduce the torques M_1 and M_2, because of the relationships between the latter and $R(t)$. As (59) shows, these torques differ only by a constant factor from $v_x(t)$ and $v_y(t)$; it is seen from (67) and (63) that v_x and v_y appear in the equation for $R(t)$, while $R(t)$ appears in the equations for v_x and v_y.

The next step in determining the position of a moving object is the integration of system (38), $\omega_x(t)$ and $\omega_y(t)$, because of (58), (59), and (63), being known functions of time.

The problem of the stability of this inertial navigation system (allowing for small oscillations of the stabilized platform) requires further study.

BIBLIOGRAPHY

Publications in Russian

ANDRONOV, A. A., A. A. VITT, and S. E. KHAIKIN. Teoriya kolebanii (Theory of Oscillations).—Moskva, Fizmatgiz. 1959.

BOICHUK, O. F. and M. E. TEMCHENKO. Do teoriyi tryvisnoho hiroskopichnoho stabilizatora (Theory of Three-Axis Gyroscopic Stabilizer).— "Avtomatyka", No. 3, Kiev. 1959. [In Ukrainian.]

BOICHUK, O. F. and M. E. TEMCHENKO. Sposib usunennya balistychnykh deviatsii tryvisnoho hiroskopichnoho stabilizatora (A Method of Elimination of Ballistic Deviations of a Three-Axis Gyroscopic Stabilizer).— "Automatyka", No. 2, Kiev. 1961. [In Ukranian.]

BOICHUK, O. F. Pobudova adiabatychnoyi vertykali za dopomohoyu hirohoryzonta z tyahartsevoyu korektsiyeyu (Construction of the Adiabatic Vertical by Means of a Gyrohorizon with Gravitational Correction).—DAN USSR, No. 6. 1962. [In Ukrainian.]

BORISENOK, I. T. Uluchshenie dinamicheskikh kharakteristik girostabilizatora pri pomoshchi korrektiruyushchikh konturov (Improving the Dynamic Characteristics of a Gyrostabilizer by Means of Corrective Contours).— Izvestiya AN SSSR, OTN, No. 5. 1958.

BORISENOK, I. T. Uluchshenie perekhodnykh protsessov v girostabilizatore pri pomoshchi korrektiruyushchikh konturov (Improving the Transient Processes in a Gyrostabilizer by Means of Corrective Contours).—Vestnik Moskovskogo Universiteta, Series I, "Matematika, Mekhanika", No. 1. 1960.

BULGAKOV, B. V. K zadache o vynuzhdennykh kolebaniyakh psevdolineinykh sistem (The Problem of Forced Oscillations of Pseudolinear Systems).—PMM*, Vol. 7, No. 1. 1943.

BULGAKOV, B. V. O nakoplenii vozmushchenii v lineinykh kolebatel'nykh sistemakh s postoyannymi parametrami (The Accumulation of Disturbances in Linear Oscillatory Systems with Constant Parameters).—DAN SSSR, Vol. 51, No. 5. 1946.

BULGAKOV, B. V. and Ya. N. ROITENBERG. K teorii silovykh giroskopicheskikh gorizontov (The Theory of Power Gyrohorizons).—Izvestiya AN SSSR, OTN, No. 3. 1948.

BULGAKOV, B. V. Prikladnaya teoriya giroskopov (Applied Theory of Gyroscopes).— Moskva, Gostekhizdat. 1955.

BULGAKOV, B. V. Kolebaniya (Oscillations).—Moskva, Gostekhizdat. 1954.

CHETAEV, N. G. Ustoichivost' dvizheniya (Stability of Motion).—Moskva, GITTL. 1955.

* [For this and other abbreviations appearing in this bibliography see Explanatory List, p. 311.]

CHETAEV, N. G. O giroskope v kardanovom podvese (Gyros in Gimbal Suspensions). — PMM, Vol. 22, No. 3. 1958.

FEODOS'EV, V. I. and G. B. SINYAREV. Vvedenie v raketnuyu tekhniku (Introduction to Rocket Technology). — Moskva, Oborongiz. 1961.

GANTMAKHER, F. R. Lektsii po analiticheskoi mekhanike (Lectures on Analytical Mechanics). — Moskva, Fizmatgiz. 1960.

GANTMAKHER, F. R. Teoriya matrits (Theory of Matrices). — Moskva, GITTL. 1953.

GNEDENKO, B. V. Kurs teorii veroyatnostei (A Course in the Theory of Probability). — Gostekhizdat. 1951.

GOLUBEV, V. V. Lektsii po integrirovaniyu uravnenii dvizheniya tyazhelogo tverdogo tela okolo nepodvizhnoi tochki (Lectures on Integrating the Equations of Motion of a Heavy Rigid Body about a Stationary Point). — Moskva, GITTL. 1953.

ISHLINSKII, A. Yu. and I. V. KRAGEL'SKII. O skachkakh pri trenii (Judder during Friction). — ZhTF, Nos. 4—5. 1944.

ISHLINSKII, A. Yu. Ob otnositel'nom ravnovesii fizicheskogo mayatnika s podvizhnoi tochkoi opory (The Relative Equilibrium of a Physical Pendulum with a Moving Point of Support). — PMM, Vol. 20, No. 3. 1956.

ISHLINSKII, A. Yu. K teorii giroskopicheskogo mayatnika (The Theory of the Gyroscopic Pendulum). — PMM, Vol. 21, No. 1. 1957.

ISHLINSKII, A. Yu. Teoriya dvukhgiroskopicheskoi vertikali (Theory of the Double-Gyro Vertical). — PMM, Vol. 21, No. 2. 1957.

ISHLINSKII, A. Yu. Ob avtonomnom opredelenii mestopolozheniya dvizhushchegosya ob"ekta posredstvom prostranstvennogo giroskopicheskogo kompasa, giroskopa napravleniya i integriruyushchego ustroistva (The Autonomous Determination of the Position of a Moving Object by Means of a Spatial Gyrocompass, a Directional Gyro and an Integrating Unit). — PMM, Vol. 23, No. 1. 1959.

ISHLINSKII, A. Yu. Giroskop (The Gyroscope). — Fizicheskii Entsiklopedicheskii Slovar', Vol. I, Izdatel'stvo BSE. 1960.

ISHLINSKII, A. Yu. Giroskopa uravneniya dvizheniya (The Gyroscope, Its Equations of Motion). — Fizicheskii Entsiklopedicheskii Slovar', Vol. I, Izdatel'stvo BSE. 1960.

ISHLINSKII, A. Yu. Ob uravneniyakh pretsessionnoi teorii giroskopov v forme uravnenii dvizheniya izobrazhayushchei tochki v kartinnoi ploskosti (The Equations of the Precessional Theory of Gyroscopes in the Form of the Equation of Motion of an Imaginary Point in the Plane of the Paper). — PMM, Vol. 23, No. 5. 1959.

KALINOVICH, V. N. Pro vidozminy inertsial'noyi systemy navihatsiyi hirohoryzont-kompas — hiroskop napryamku — lichyl'no-rozv'yazuval'nyi prystrii (Changes in Navigation. The Gyrohorizoncompass as a Simple Gyroscope and as a Calculating Device). — DAN USSR, No. 5. 1962. [In Ukrainian.]

KALINOVICH, V. N. Pro vplyv sukhoho tertya v pidshypnykakh osei kozhukhiv hiroskopiv hirohoryzontkompasa na kharakter ioho rukhu i na tochnist' avtonomoho vyznachennya (The Influence of Dry Friction in Bearings of Gyroscope Housings of the Gyrohorizoncompass on Its Motion and on the Precision of the Autonomous Location). —DAN USSR, No. 6. 1960. [In Ukrainian.]

KLIMOV, D. M. Zatukhanie sobstvennykh kolebanii giroskopa v kardanovom podvese s sukhim treniem (Damping the Natural Oscillations of a Gyro in Gimbals with Dry Friction). —DAN SSSR, Vol. 123, No. 3. 1958.

KLIMOV, D. M. O dvizhenii giroskopa v kardanovom podvese s neaksial'no nasazhennym rotorom (The Motion of a Gyro in Gimbals with Nonaxially Fitted Rotor). — DAN SSSR, Vol. 124, No. 3. 1959.

KLIMOV, D. M. O dvizhenii astaticheskogo giroskopa v kardanovom podvese s sukhim treniem (The Motion of an Astatic Gyro in Gimbals with Dry Friction). — PMM, Vol. 24, No. 4. 1960.

KHARLAMOV, S. A. O dvizhenii giroskopa v kardanovom podvese pri nalichii momenta vokrug osi sobstvennogo vrashcheniya (The Motion of a Gyro in Gimbals in the Presence of a Torque Applied to its Axis of Rotation). —DAN SSSR, Vol. 139, No. 2. 1961.

KHARLAMOV, S. A. O dvizhenii giroskopa, ustanovlennogo na sharikovykh podshipnikakh v kardanovom podvese (The Motion of a Gyro Mounted in Ball-Bearing Gimbals). —PMM, Vol. 26, No. 2. 1962.

KHARLAMOV, S. A. O vliyanii uprugosti opor osi vneshnego kol'tsa kardanova podvesa na nutatsionnye kolebaniya i ukhod giroskopa (The Influence of the Elasticity of the Outer Gimbal-Ring Pivot Bearings on the Nutational Oscillations and Wander of the Gyro). —DAN SSSR, Vol. 142, No. 5. 1962.

KOSHLYAKOV, V. N. K teorii girokompasov (The Theory of Gyrocompasses). — PMM, Vol. 23, No. 5. 1959.

KOSHLYAKOV, V. N. O privodimosti uravnenii dvizheniya girogorizontkompasa (The Reductibility of the Equations of Motion of the Gyrohorizoncompass). — PMM, Vol. 25, No. 5. 1961.

KOSHLYAKOV, V. N. Ob ustoichivosti girogorizontkompasa pri nalichii dissipativnykh sil (The Stability of the Gyrohorizoncompass in the Presence of Dissipative Forces). —PMM, Vol. 26, No. 3. 1962.

KRYLOV, A. N. and Yu. A. KRUTKOV. Obshchaya teoriya giroskopov i nekotorykh tekhnicheskikh ikh primenenii (General Theory of Gyroscopes and some Technical Applications). — Leningrad, Izdatel'stvo AN SSSR. 1932.

KRYLOV, N. M. and N. N. BOGOLYUBOV. Vvedenie v nelineinuyu mekhaniku (Introduction to Nonlinear Mechanics). — Izdatel'stvo AN USSR. 1937.

KUDREVICH, B. I. Izbrannye trudy (Selected Works). — Leningrad. 1959. (Izdanie upravleniya nachal'nika gidrograficheskoi sluzhby VMF).

KUZOVKOV, N. T. O dvizhenii girostabilizirovannoi platformy, ustanovlennoi v bikardanovom podvese (The Motion of a Gyrostabilized Platform Mounted in a Bicardan Suspension). — Izvestiya AN SSSR, OTN, No. 7. 1958.

KUZOVKOV, N. T. Odnoosnyi silovoi girostabilizator s kosym raspolozheniem osi kozhukha (The Monoaxial Power Gyrostabilizer with Obliquely Mounted Housing Pivot Axis). — Izvestiya AN SSSR, OTN, No. 11. 1958.

LUNTS, Ya. L. O dvizhenii po inertsii giroskopa v kardanovom podvese (The Inertial Motion of a Gyro in Gimbals). — Leningrad, Izvestiya Vysshikh Uchebnykh Zavedenii, "Priborostroenie", Vol. 2, No. 3. 1959.

LUR'E, A. I. Nekotorye nelineinye zadachi teorii avtomaticheskogo regulirovaniya (Nonlinear Problems in the Theory of Automatic Control). — Gostekhizdat, 1951.

LUR'E, A. I. Analiticheskaya mekhanika (Analytical Mechanics). — Moskva, GITTL. 1961.

LYAPUNOV, A. M. Obshchaya zadacha ob ustoichivosti dvizheniya (The General Problem of the Stability of Motion). — Moskva-Leningrad, ONTI. 1935.

MAGNUS, K. Ob ustoichivosti dvizheniya tyazhelogo simmetrichnogo giroskopa v kardanovom podvese (The Stability of Motion of a Heavy Symmetrical Gyroscope in Gimbals). — PMM, Vol. 22, No. 2. 1958.

MERKIN, D. R. Giroskopicheskie sistemy (Gyroscopic Systems). — Moskva, GITTL. 1956.

MERKIN, D. R. Ob ustoichivosti dvizheniya giroramy (The Stability of Motion of the Gyro Frame). — PMM, Vol. 25, No. 6. 1961.

METELITSYN, I. I. Giroskop (The Gyroscope). — Tekhnicheskaya Entsiklopediya, Vol. 5, Moskva. ONTI, NKTP SSSR. 1937.

METELITSYN, I. I. K voprosu o giroskopicheskoi stabilizatsii (The Problem of Gyroscopic Stabilization). — DAN SSSR, Vol. 86, No. 1. 1952.

METELITSYN, I. I. Giroskopicheskie sistemy s neideal'nymi svyazyami (Gyroscopic Systems with Nonideal Constraints). — Izvestiya AN SSSR, OTN. Mekhanika i Mashinostroenie, No. 1. 1959.

METELITSYN, I. I. Giroskopicheskie pribory (Gyroscopic Instruments). — Fizicheskii Entsiklopedicheskii Slovar', Vol. I, Izdatel'stvo BSE. 1960.

NEMYTSKII, V. V. and V. V. STEPANOV. Kachestvennaya teoriya differentsial'nykh uravnenii (A Qualitative Theory of Differential Equations). — Moskva-Leningrad, Gostekhizdat. 1949.

NIKOLAI, E. L. O dvizhenii uravnoveshennogo giroskopa v kardanovom podvese (The Motion of a Balanced Gyro in Gimbals). — PMM, Vol. 3, No. 4. 1939.

NIKOLAI, E. L. Teoriya giroskopov (Gyroscope Theory). — Moskva-Leningrad, Gostekhizdat. 1948.

PAVLOV, V. A. Sistematicheskii dreif giroskopa v kardanovom podvese, obuslovlivaemyi faktorami, porozhdayushchimi kolebaniya sistemy (The Systematic Drift of a Gyro in Gimbals Caused by the Factors which Start Oscillations in the System). — Izvestiya Vysshikh Uchebnykh Zavedenii, "Priborostroenie", No. 6. 1961.

PEL'POR, D. S. Svobodnoe dvizhenie giroskopa, zaklyuchennogo v kardanovom podvese (The Free Motion of a Gyro Enclosed in Gimbals). — Nauchnye Doklady Vysshei Shkoly, Mashinostroenie i Priborostroenie, No. 3. 1958.

RASHEVSKII, P. K. Kurs differentsial'noi geometrii (A Course of Differential Geometry). — Gostekhizdat. 1956.

RESHETNIKOV, V. I. Deyaki pytannya dynamiky kardanovoho pidvisu tryvisnoi stabilizovanoyi platformy (Some Problems of the Dynamics of Gimbal Suspensions of a Platform Stabilized in Three Axes). — "Prikladna Mekhanika", Vol. 7, No. 2. 1961. [In Ukrainian.]

RIVKIN, S. S. Primenenie metodov teorii matrits k analizu geometrii giroskopicheskikh ustroistv (Application of the Methods of the Theory of Matrices to the Analysis of the Geometry of Gyroscopic Devices). — "Voprosy prikladnoi giroskopii", No. 2, NTO Priborproma. Leningrad, Sudpromgiz. 1960.

ROITENBERG, Ya. N. Mnogogiroskopnaya vertikal' (The Multigyro Vertical). — PMM, Vol. 10, No. 1. 1946.

ROITENBERG, Ya. N. Avtokolebaniya giroskopicheskikh stabilizatorov (Free Oscillations of Gyroscopic Stabilizers). — PMM, Vol. 11, No. 2. 1947.

ROITENBERG, Ya. N. Ob uskorennom privedenii giroskopicheskogo kompasa v meridian (The Accelerated Aligning of the Gyrocompass to the Meridian). — PMM, Vol. 23, No. 5. 1959.

ROITENBERG, Ya. N. O privedenii giroskopicheskogo kompasa v meridian vo vremya razgona rotorov giroskopov (Aligning the Gyrocompass to the Meridian during Acceleration of the Gyro Rotors). — PMM, Vol. 24, No. 1. 1960.

ROITENBERG, Ya. N. Nekotorye voprosy teorii silovykh giroskopicheskikh stabilizatorov (Some Problems in the Theory of Power Gyrostabilizers). — Izvestiya AN SSSR, OTN, Mekhanika i Mashinostroenie, No. 4. 1962.

RUMYANTSEV, V. V. Ob ustoichivosti dvizheniya giroskopa v kardanovom podvese (The Stability of Gyro Motion in Gimbals). — PMM, Vol. 22, No. 3. 1958.

RUMYANTSEV, V. V. Ob ustoichivosti dvizheniya giroskopa v kardanovom podvese (2) (The Stability of Gyro Motion in Gimbals, Part 2). — PMM, Vol. 22, No. 4. 1958.

SKIMEL', V. N. Nekotorye zadachi dvizheniya i ustoichivosti tyazhelogo giroskópa (Problems of the Motion and Stability of a Heavy Gyro). — Trudy Kazanskogo Aviatsionnogo Instituta, Vol. 38. 1958.

SUSLOV, G. K. Teoreticheskaya mekhanika (Theoretical Mechanics). — Moskva, Gostekhizdat. 1944.

TIKHMENEV, S. S. K voprosu ob "uvode" giroskopa na kardanovom podvese pri ego nutatsii (The Problem of Gyro "Wander" in Gimbals during Nutation). — Izvestiya Vysshikh Uchebnykh Zavedenii", "Priborostroenie", No. 5. 1959.

TIMOSHENKO, S. P. Kolebaniya v inzhenernom dele (Oscillations in Engineering). — Moskva, Fizmatgiz. 1959.

TIMOSHENKO, S. P. Teoriya uprugosti (Theory of Elasticity). — Moskva-Leningrad, GITTL. 1934. [Translated into English. McGraw-Hill. 1951.]

TIMOSHENKO, S. P. Plastinki i obolochki (Theory of Plates and Shells). — Moskva-Leningrad, Gostekhizdat. 1948. [Translated into English. McGraw-Hill. 1959.]

TIMOSHENKO, S. P. Soprotivlenie materialov (Strength of Materials), Vols. I and II. — Moskva-Leningrad, GITTL. 1946. [Translated into English. Van Nostrand. 1956.]

ZHBANOV, Yu. K. Girogorizontkompas na vibriruyushchem osnovanii (A Gyrohorizon-compass on a Vibrating Base). —PMM, Vol. 25, No. 5. 1961.

ZHBANOV, Yu. K. Issledovanie svobodnykh kolebanii v sisteme avtonomnogo opredeleniya koordinat dvizhushchegosya ob"ekta (A Study of Free Oscillations in a System Intended for the Autonomous Determination of the Coordinates of a Moving Object). — PMM, Vol. 24, No. 6. 1960.

Publications in other languages

DRAPER, C. S., W. WRIGLEY, and J. HOVORKA. Inertial Guidance. — Pergamon, New York. 1960.

GECKELER, J. W. Kreisselkompass und Schiffmänover. — Ingenieur-Archiv, t. IV, Heft 4, Berlin. 1935.

GECKELER, J. W. Kreiselmechanik des Annschütz-Raumkompasses. — Ingenieur-Archiv, t. VI, Heft 4, Berlin. 1935.

Gyroscope: Theory and Design. With Applications to Instrumentation, Guidance and Control. — McGraw-Hill, New York, 1961.

GLITSCHER, K. Die Kompensation störender Horizontalbeschleunigungen an Pendeln und Kreiselpendeln auf fahrzeugen. — Wissenschaftlich Veröffentlichungen aus den Siemens-Werken, XIX Band, Zweites Heft (abegeschlossen am 14 März 1940).

GRAMMEL, R. Der Kreisal, Vols. I and II. — Springer, Berlin. 1950.

GOODMAN, L. E. and A. R. ROBINSON. Influence of Finite Rotations on Gyroscopic Sensitive Elements. — In "Mekhanika", Collection of papers translated into Russian, Vol. 5, No. 57. 1959.

CANNON, R. H. Kinematic Wander of a Gyro with Two Degrees of Freedom. — In "Mekhanika", Collection of papers translated into Russian, Vol. 1, No. 59. 1959.

MACMILLAN, W. D. Rigid Body Dynamics. — IL Publishing House, Moskva. 1951. [In Russian translation.]

MAGNUS, K. Auswanderungserscheinungen an schwingenden Kreiseln in Kardanischer Lagerung. — Advances Aeronaut. Sci., Vol. 1, pp. 507—533. Pergamon, New York. 1957.

MAGNUS, K. Beiträge zur Dynamik des kraftefreien, kardanisch gelagerten Kreisels. — ZAMM, Band 35, Heft 1—2. Januar – Februar, 1955.

McLACHLAN, N. W. Theory and Applications of Mathieu Functions. — Clarendon Press, Oxford, 1947. [Translated into Russian. 1953.]

PITMAN, GEORGE R. (ed.). Inertial Guidance. — Pergamon, New York. 1962.

PLYMALE, B. T. and R. GOODSTEIN. Nutation of the Free Gyro Subjected to an Impulse. — Journal of Applied Mechanics. Transactions of the Americal Society of Mechanical Engineers, Vol. 22, No. 3. 1955.

SCARBOROUGH, J. B. The Gyroscope. Theory and Applications. — Interscience, New York. 1958. [Translated into Russian. 1961.]

SCHULER, M. Der Kreiselkompass unter Einfluss der Schiffsschwingungen. — Zeitschrift für angewandte Mathematik und Mechanik, t. 2, Heft 4, Berlin. 1922.

SCHULER, M. Die Störung von Pendel und Kreiselapparanten durch die Beschleunigung des Fahrzeuges. — Physikalische Zeitschrift, t. 24, No. 16, Leipzig. 1923.

EXPLANATORY LIST OF ABBREVIATED NAMES OF USSR INSTITUTIONS, ORGANIZATIONS, AND JOURNALS APPEARING IN THIS TEXT

Abbreviation	Full name (transliterated)	Translation
AN SSSR	Akademiya Nauk SSSR	Academy of Sciences of the USSR
DAN SSSR	Doklady Akademii Nauk SSSR	Proceedings of the Academy of Sciences of the USSR
OTN	Otdel tekhnicheskikh nauk	Department of Technical Sciences (of the Academy of Sciences of the USSR)
PMM	Prikladnaya matematika i mekhanika	Applied Mathematics and Mechanics
VMF	Voenno-morskoi flot	Navy
ZhTF	Zhurnal teoreticheskoi fiziki	Journal of Theoretical Physics